

**APPLICATION OF ADVANCED NON-
DESTRUCTIVE TESTING METHODS ON
BRIDGE HEALTH ASSESSMENT AND
ANALYSIS**

GÖKHAN KILIÇ

A thesis submitted in partial fulfilment of the
requirements of the University of Greenwich
for the Degree of Doctor of Philosophy

November 2012

DECLARATION

“I certify that this work has not been accepted in substance for any degree, and is not concurrently being submitted for any degree other than that of Doctor of Philosophy being studied at the University of Greenwich. I also declare that this work is the result of my own investigations except where otherwise identified by references and that I have not plagiarised the work of others.”

Gökhan KILIÇ

Candidate

Supported By:

Professor Amir M. Alani

Supervisor

To my fiancé and family, whom I love more than everything

ACKNOWLEDGEMENTS

It would not have been possible to write this doctoral thesis without the help and support of the kind people around me, to only some of whom it is possible to give particular mention here.

First of all I would like to express my deepest gratitude to my supervisor, Prof Amir M. Alani for his support, guidance, great inspiration, and encouragement during my PhD studies in University of Greenwich. The completion of this thesis would not have been possible without his enthusiasm for the ideas and concepts developed in this thesis. I also give my thanks to my supervisor team Dr Morteza Aboutalebi and Dr Huapeng Chen for their constant support and help.

I express my thanks to the School of Engineering and the University of Greenwich for providing me with a productive work environment and supporting my study with a research bursary.

I would like to thank Mr Kevin Banks and other members of staff in the IDS Limited collaborative company for their support and advice.

I wish to thank my colleagues at the University of Greenwich in particular Miss Ruth Queen, Mr Luc Tidy and Dr Asaad Faramarzi for their supports throughout my study.

These words are too short to express my deep love for my fiancé Özlem Öner. Her support, encouragement, quiet patience and unwavering love were undeniably the bedrock upon which the past year of my life has been built. Her tolerance of my occasional vulgar moods is a testament in itself of her unyielding devotion and love.

At last but not least I would like to thank my parents Mr Cemil Kılıç and Mrs Nevin Kılıç who have loved me and supported me through my life. I am deeply indebted to my brother Mr Tahir Uğur Kılıç and his dearest wife Mrs Melisa Kılıç, who always have encouraged me and supported me during my studies. Indeed, they have been the greatest inspiration of my life.

LIST OF PUBLICATIONS

Journals

- Gökhan Kılıç, Amir M. Alani, Morteza Aboutalebi “Damage Detection and Health Monitoring of Pentagon Road Bridge Using IBIS-S and Finite Element Method” *Journal of Structural Concrete*, 2012, (ISSN 1464-4177) (Submitted)
- Amir M. Alani, Morteza Aboutalebi, Gökhan Kılıç “A Parametric Assessment of the Cracked Pentagon Road Bridge Using the Finite Element Method” *The Baltic Journal of Road and Bridge Engineering*, 2012, (no-no1747-1567) (Submitted).
- Morteza Aboutalebi, Amir M. Alani, Gökhan Kılıç “FE Modelling For Bridge Assessment Based On Actual and Simulated Data” *Journal of Structure and Infrastructure Engineering*, 2012, (ISSN 1744-8980) (Accepted).
- Amir M. Alani, Morteza Aboutalebi, Gökhan Kılıç “Applications of Ground Penetrating Radar (GPR) in Bridge Deck Monitoring and Assessment”, *Journal of Applied Geophysics*, 2012, (ISSN 0926-9851), (Submitted).

Conferences

- Amir M. Alani, Gökhan Kılıç, Morteza Aboutalebi “Applications of Ground Penetrating Radar in Bridge Health Monitoring Using Different Frequency Antennae Systems” *EGU GA - Civil Engineering Applications of Ground Penetrating Radar*, 22-27 April 2012, Wien, Austria
- Amir M. Alani, Morteza Aboutalebi, and Gökhan Kılıç. 2012. Health Assessment of Bridge Structures Adopting Inverse Parametric Approach. *XXII International Scientific and Technical Conference STARODUBOVSKIY CHTENIYA*, 19–20 April 2012, Prydniprov's'ka State Academy, Dnipropetrovs'k, Ukraine.
- Gökhan Kılıç, Amir M. Alani, Pentagon Road Bridge Health Assessment and Analysis, University of Greenwich, School of Engineering, 11th School Research Conference (2011) (Oral / poster).
- Amir M. Alani, Gökhan Kılıç, Kevin Banks, "Applications of Ground Penetrating Radar in Bridge Health Monitoring and Assessment, *XXI International Scientific and Technical Conference – Starodubov's Reading, PSACEA* ,Dnepropetrovsk, Ukraine 19-21 April 2011.
- Gökhan Kılıç, Amir M. Alani, Application of Advanced Non-Destructive Testing Methods on Bridge Health Assessment and Analysis, University of Greenwich, School of Engineering, 10th School Research Conference (2010) (Oral / poster).

ABSTRACT

Bridge structures have an important role in economic, social and environmental aspects of society life. Bridges are also subject to a natural process of deterioration of construction materials, as well as natural and environmental events such as flooding, freezing, thawing etc. Health monitoring and assessment of the structural integrity of bridges have been the focus of engineers and researchers for decades. Currently, the various aspects of bridge health are monitored separately. However, measuring these aspects independently does not give the overall health of the bridge and crucial indicators of structural damage can be neglected. Generally, bridge health assessments take the form of individual NDT (non-destructive techniques) detecting individual defects. However value can be added to these results by combining and comparing the findings of several different NDT surveys. By completing this, a more accurate assessment of bridge health is obtained. This increases confidence in the decision as to whether remedial action is necessary. In this thesis an integrated bridge health monitoring approach is proposed which applies several NDT specifically chosen for bridge health assessments, thus achieving this added value. This method can be used as a part of a comprehensive bridge monitoring strategy as an assessment tool to evaluate the bridges structural health. This approach enables the user of this approach to obtain a detailed structural report on the bridge with all the necessary information pertaining to its' health, allowing for a fully educated decision to be made regarding whether remedial action is necessary.

This research presents the results of the applications of such methods on case studies utilising Ground Penetrating Radar (GPR), IBIS-S technology / system (deflection and vibration detection sensor system with interferometric capability) and Accelerometer sensors. It also evaluates the effectiveness of the adopted methods and technologies by comparing and validating the yielded results with conventional methods (modelling and visual inspection). The research presents and discusses processed data obtained by the above mentioned methods in detail and reports on challenges encountered in setting up and materialising the assessment process.

This work also reports on Finite Element Modelling (FEM) of the main case study (Pentagon Road Bridge) using specialist software (SAP2000 and ANSYS) in order to simulate the perceived movement of the bridge under dynamic and static conditions.

The analytical results output were compared with results obtained by the applications of the above non-destructive methods. Thus by using these techniques the main aim of this thesis is to develop an integrated model/approach for the assessment and monitoring of the structural integrity and overall functionality of bridges.

All the above methods were validated using preliminary case studies (GPR), additional equipment (accelerometers for IBIS-S validation) and additional techniques and information (SAP 2000 and ANSYS were compared to one another and IBIS-S results). All of these techniques were applied on the Pentagon Road Bridge. This bridge was chosen as no information was available regarding its structural composition. Visual inspection showed the external defects of the structure: cracking, moisture ingress and concrete delamination was present in one of the spans of the bridge. The GPR surveys gave the position of the rebars and also signs of moisture ingress at depths of 20cm (confirmed using velocity analysis). IBIS-S gave results for the deflection of the structure. FEM was used to model the behaviour of the bridge assuming no defects. To achieve additional model accuracy the results of the rebar position were input in to the model and it was calibrated using IBIS-S data. The deflection results from the model were then compared to the actual deflection data to identify areas of deterioration. It was found that excessive deflection occurred on one of the spans. It was thus found that all NDT indicated that a particular span was an area of significant deterioration and remedial action should be completed on this section in the near future. Future prediction was also completed by running simulations in ANSYS for increasing crack lengths and dynamic loading. It was found that if there is no remedial action excessive beam bending moments will occur and eventual collapse.

The results of this research demonstrated that GPR provided information on the extent of the internal structural defects of the bridge under study (moisture ingress and delamination) whilst IBIS-S technology and Accelerometer sensors permitted measurement of the magnitude of the vibration of the bridge under dynamic and static loading conditions. The results depicted similarities between the FEM results and the adopted non-destructive methods results in location and pattern. This work can potentially contribute towards a better understanding of the mechanical and physical behaviours of bridge structures and ultimately assess their life expectancy and functionality.

TABLE OF CONTENTS

Chapter 1: Introduction	1
1.1 Background to Research	2
1.2 Layout of the Thesis	5
1.3 Justification and Scope.....	6
1.4 Aims and Objectives	11
1.5 Collaboration.....	12
1.6 Limitations to Approach	12
1.7 Summary	13
Chapter 2: Literature Review and Background Studies.....	14
2.1 Introduction	15
2.2 Bridge Health Monitoring	16
2.3 Non-Destructive Methods	17
2.4 Visual Inspection.....	20
2.5 Ground Penetrating Radar (GPR) Technique	24
2.5.1 Introduction and Background.....	24
2.5.2 General Principles	26
2.5.3 GPR Role in Bridge Assessment.....	27
2.5.4 GPR Antenna Signal Factors	29
2.5.4.1 Antenna Types, Orientation and Selection	30
2.5.4.2 The Transmitting and Receiving Antenna	32
2.5.4.3 Dielectric Constant or Permittivity	32
2.5.4.4 Conductivity	33
2.5.4.5 Attenuation.....	34
2.5.4.6 Moisture	35
2.5.5 Radar Stratigraphy	39
2.5.6 Velocity	41
2.5.6 Advantages and Disadvantages of GPR.....	44
2.6 IBIS-S Interferometric Radar Monitoring Technology.....	47
2.6.1 Introduction	47
2.6.2 General Principles	48
2.6.3 SAR technique	53
2.6.4 Interferometric Technique.....	54
2.6.5 Static and Dynamic Monitoring of a Bridge Structure	54
2.7 Accelerometers.....	57
2.7.1 Introduction	57
2.7.2 General Principles	59
2.7.3 Monitoring of a Bridge Structure Using Accelerometers	61
2.8 Other Non-Destructive Techniques.....	62
2.8.1 Wireless Sensor Networks	62
2.8.2 Laser Scanner	63
2.8.3 Infrared Thermography	64
2.8.4 X-Ray Radiography	64
2.8.5 Gamma (γ) Ray Radiography/Radiometry.....	64
2.8.6 Ultrasonic Testing	65
2.8.7 Acoustic Emission (AE).....	65

2.8.8	Sonic Techniques	66
2.8.9	Impact Echo (IE)	66
2.8.10	Resistivity Measurement	66
2.8.11	Half Cell Potential	67
2.8.12	Magnetic Induction	67
2.8.13	Magnetic Flux Exclusion	68
2.9	Summary of NDT Findings	68
2.10	Structural Theories of Concrete Bridges	77
2.10.1	Introduction	77
2.10.2	Structural Loading Theories	79
2.11	Application of Numerical Methods in Bridge Health Monitoring	81
2.11.1	Introduction	81
2.11.2	ANSYS, SAP2000 Commercial Software and Crack Modelling	84
2.11.2	Finite Element Modelling of Bridge Superstructures	85
2.12	Summary	89
Chapter 3: Research Methodology		91
3.1	Introduction	92
3.2	Step 1: Determine the most appropriate NDT for bridge health monitoring	94
3.3	Step 2: Acquire necessary knowledge of NDT	95
3.3.1	Visual Inspection	95
3.3.2	Ground Penetrating Radar	96
3.3.3	IBIS-S Interferometric Radar	100
3.3.4	Validation IBIS-S	101
3.4	Step 3: Carry out detailed surveys on the main case study (Pentagon Road Bridge)	101
3.5	Step 4: Develop FEM	103
3.6	Step 5: Develop an Integrated mechanism for bridge health monitoring	104
3.7	Summary	106
Chapter 4: Results and Analysis		107
4.1	GPR Trials	108
4.2	Preliminary Case Studies	109
4.2.1	Forth Road Bridge	110
4.2.2	St Marys Island Lifting Bridge	116
4.2.3	Darvel Road Bridge	120
4.2.4	Historic Rochester Bridge	124
4.2.5	Summary and Significant of Preliminary Case Studies	128
4.3	Main Case Study: Pentagon Road Bridge	129
4.3.1	Introduction	129
4.3.2	Visual Inspection	130
4.3.2.1	Inspection	131
4.3.2.2	Main Findings of Visual Inspection	136
4.3.3	IBIS-S Monitoring	138
4.3.3.1	Introduction	138
4.3.3.2	IBIS-S Results	143
4.3.3.3	Summary of IBIS-S Results	147
4.3.4	Validation of Measurements	150
4.3.4.1	Introduction	150
4.3.4.2	Wireless Sensor Network Monitoring	152
4.3.4.3	Accelerometer Sensors Monitoring	153
4.3.4.4	Validation Results	154
4.3.5	Ground Penetrating Radar (GPR) Survey	156
4.3.5.1	Introduction	157

4.3.5.2	Setting out GPR Survey	157
4.3.5.3	GPR Results	159
4.3.5.4	Summary of GPR Results	174
4.3.6	Analysis of GPR data: Wave Propagation Velocity Determination	176
4.3.6.1	Introduction	176
4.3.6.2	Wave Propagation Velocity Determination Results	178
4.3.6.3	Summary Wave Propagation Velocity Determination.....	184
4.4	Summary	185
Chapter 5: Parametric Study		188
5.1	Introduction	189
5.2	Modelling Precedures.....	190
5.2.1	SAP2000 Modelling Procedure.....	190
5.2.2	ANSYS Modelling Procedure.....	191
5.3	FE Modelling Assumptions	193
5.4	Moving Load.....	198
5.5	Modelling with SAP2000.....	200
5.5.1	Introduction	200
5.5.2	Calibration of connections with IBIS-S monitoring results.....	202
5.5.3	Results	206
5.6	Modelling with ANSYS	214
5.6.1	Introduction	214
5.6.2	ANSYS Crack Modelling	215
5.6.3	Finite Element Model Specifications	216
5.6.4	Studied Parameters and their Range of Change.....	218
5.6.5	Numerical Results	219
5.6.6	Discussion on Numeric Results	221
5.7	Summary	225
Chapter 6: Discussion		227
6.1	Discussion	228
6.1.1	Advanced Non-Destructive Testing.....	229
6.1.2	Analysis.....	232
6.1.3	Future Prediction.....	233
6.1.4	Integrated Health Mechanism	234
6.2	Contribution to Knowledge.....	237
Chapter 7: Conclusion and Further Work		239
6.1	Conclusion	240
6.2	Recommendations for Future Research	248
References		249
Appendix A: IBIS-S		266
Appendix B: GPR.....		279
Appendix C: Validation Results		295
Appendix D: Pentagon Road Bridge		300
Appendix E: List of Publications.....		319

LIST OF FIGURES

Figure 1.1	– Schematic Depiction of the Integrated Approach	10
Figure 2.1	– GPR operating principles (Highway Agency BA/8606 Section 3, 2006)	26
Figure 2.2	– GPR operation on Pentagon Road Bridge (photos from Gokhan Kilic, 2010).....	27
Figure 2.3	– Wave view for different material from radar diagram (EuroGPR, 2010)	29
Figure 2.4	– Summary of GPR antenna frequency	31
Figure 2.5	– GPR attenuation paths (EuroGPR, 2010)	34
Figure 2.6	– Reflection view of the deck (Rhazi J., 2002).....	35
Figure 2.7	– Diagrammatic view of steel corroding in cracked concrete (Digest 444 part1, 2000)	37
Figure 2.8	– Drawing of a moisture depiction view (Gokhan Kilic, 2011)	38
Figure 2.9	– Electromagnetic Spectrum (NASA, 2011)	40
Figure 2.10	– Propagating Electromagnetic Wave (www.sciencejunkies.com, 2010)	40
Figure 2.11	– The GPR principle in layer thickness. (Highway, 2010).....	41
Figure 2.12	– Three views of radar trace profiles in homogenous material. (Lester and Bernold, 2007)	43
Figure 2.13	– Common depth point method of depth estimation, (Daniels, 1996).....	44
Figure 2.14	– View of IBIS-S system (photos from Gokhan Kilic, 2010)	47
Figure 2.15	– IBIS-S Horn Antenna (IDS Manual, 2010)	48
Figure 2.16	– Examples of corner reflectors (Photos from Gokhan Kilic, 2010).....	48
Figure 2.17	– Projection of displacement data (IDS Manual, 2010).....	49
Figure 2.18	– Schematic diagram of the antenna beam (IDS Manual, 2010).....	49
Figure 2.19	– The principle of interferometric measurement. (Ids ltd., 2010).....	50
Figure 2.20	– Radial displacement vs. projected displacement (Bernardini et al., 2007)	51
Figure 2.21	– Example of a spatial resolution grid (Albaa et al, 2008)	54
Figure 2.22	– Dynamic monitoring of a full-scale bridge with IBIS-S (Ids ltd., 2012)	55
Figure 2.23	– IBIS-S calibration on Pentagon Road Bridge (Gokhan Kilic, 2011)	56
Figure 2.24	– Sample of 20g Accelerometers (Meggitt Sensing Systems, 2010).....	58
Figure 2.25	– Hand-Held Shaker (PCB Group, 2012)	58
Figure 2.26	– Typical Constructions of Commonly-Used Accelerometers (Judd, 2008)..	60
Figure 2.27	– WSN System Kit (Oracle, 2012)	63
Figure 2.28	– NDT Framework.....	69
Figure 2.29	– Loads on bridges (Kim, 2005)	79
Figure 2.30	– Typical finite element geometries in one through three dimensions (Barton and Rajan, 2000)	83
Figure 3.1	– Aims and Objectives Research Design Framework	92
Figure 3.2	– Five Stage Research Design Framework	93
Figure 3.3	– Visual Inspection Procedure	95
Figure 3.4	– GPR Survey Procedure	96
Figure 3.5	– GPR Hi BriT GPR Antenna (Photos from Gokhan Kilic, 2010).....	98
Figure 3.6	– GPR Hi BriT GPR Antenna (Photos from Gokhan Kilic, 2010).....	98
Figure 3.7	– UTSI GPR Antenna (Photos from Gokhan Kilic, 2010)	99
Figure 3.8	– IBIS-S Monitoring Procedure	100

Figure 3.9	– Integrated approach for bridge health monitoring	105
Figure 4.1	– GPR trials on a concrete slab	108
Figure 4.1	– GPR Trials radargram	109
Figure 4.3	– Location of the Forth Road Bridge. (Google Maps, 2010).....	110
Figure 4.4	– General view of the Forth Road Bridge (Forth Estuary Transport Authority, 2010)	110
Figure 4.5	– Areas of Investigation of the Forth Road Bridge. (GoogleMaps, 2010)	111
Figure 4.6	– The b-scan with identified section	112
Figure 4.7	– Expansion of the moisture affected area 1(Data processed by Gokhan Kilic, 2010).....	114
Figure 4.8	– Area of visible rebar (Photo taken by Kevin Banks, 2010).....	115
Figure 4.9	– Location of the St Marys Island Bridge. (Google Maps, 2010)	116
Figure 4.10	– The St Marys Island Bridge before (left) and previous view (right). (Chatham Maritime House, 2010).....	116
Figure 4.11	– GPR Survey on the St Marys Island Lifting Bridge. (photo taken by Gokhan Kilic, 2010)	117
Figure 4.12	– Pavement GPR B-Scan 20cm depth Result	118
Figure 4.13	– GPR Radargram results	118
Figure 4.14	– Location of the Darvel Road Bridge. (Google Maps and Wikipedia, 2010).....	120
Figure 4.15	– Historic and recent view of the Darvel Road Bridge. (Wikipedia and Picture by Gokhan Kilic, 2010).....	120
Figure 4.16	– Heavy vegetation view side of the bridge (photo taken by Gokhan Kilic, 2010).....	121
Figure 4.17	– Water ponding on north side of the bridge (photo taken by Gokhan Kilic, 2010).....	121
Figure 4.18	– GPR Survey on the Darvel Road Bridge. (photo taken by Gokhan Kilic, 2010).....	122
Figure 4.19	– GPR Radargram 600 MHz.....	122
Figure 4.20	– Area 1 GPR b-Scan 20cm depth Result.....	123
Figure 4.21	– Beams locations shown on an AutoCAD Plan (Drawn by Gokhan Kilic, 2010).....	123
Figure 4.22	– Location of the Historic Rochester Bridge. (Google Maps, 2010).....	124
Figure 4.23	– Rochester Bridge (The Rochester Bridge Trust, 2010)	124
Figure 4.24	– Bridge deck to be surveyed by GPR (photos by Gokhan Kilic, 2010)..	125
Figure 4.25	– GPR Survey areas	125
Figure 4.26	– GPR Processed Data	126
Figure 4.27	– GPR Radargram	127
Figure 4.28	– View of Pentagon Road Bridge (Photos from Gokhan Kilic, 2010)	129
Figure 4.29	– Non-destructive testing timeline on Pentagon Road Bridge.....	130
Figure 4.30	– General Visual Inspection.....	132
Figure 4.31	– Concrete deterioration between Spans three and four	133
Figure 4.32	– Apparent cracks, Rebar deterioration and concrete degradation.	135
Figure 4.33	– Corner reflectors. (Photos from Gokhan Kilic, 2010)	139
Figure 4.34	– Test Layout (Photos from Gokhan Kilic, 2010)	140
Figure 4.35	– Test Layout plan (Gokhan Kilic, 2010).....	142
Figure 4.36	– View from IBIS – Reflector Positions (Photos from Gokhan Kilic, 2010)	144
Figure 4.37	– IBIS-S 7 th November 2010 20 MHz Monitoring Results	145
Figure 4.38	– IBIS-S 11 th of March 2012 20 MHz Monitoring Results	145
Figure 4.39	– IBIS-S 11 th of March 2012 200 MHz Monitoring Results	145

Figure 4.40 – Comparison of IBIS-S Monitoring Results (November 2010 – 20MHz, March 2012 – 20MHz, March 2012 – 200MHz).....	145
Figure 4.41 – IBIS-S 7 th November 2010 20 MHz Monitoring Results	146
Figure 4.42 – IBIS-S 11 th of March 2012 20 MHz Monitoring Results	146
Figure 4.43 – IBIS-S 11 th of March 2012 200 MHz Monitoring Results	146
Figure 4.44 – Comparison of IBIS-S Monitoring Results (November 2010 – 20MHz, March 2012 – 20MHz, March 2012 – 200MHz).....	148
Figure 4.45 – Mode of Vibration of the Bridge for a given period of time	148
Figure 4.46 – Pointing the results in aerial and depiction view	149
Figure 4.47 – IBIS-S Reflector, Wireless Sensor Node and Accelerometer Sensor (Photos from Gokhan Kilic, 2010).....	151
Figure 4.48 – Diagram of the wireless nodes system.....	154
Figure 4.49 – Accelerometer node 1 and IBIS-S results.....	155
Figure 4.50 – IBIS-S 7 th November 2010 20 MHz Monitoring Results	155
Figure 4.51 – IBIS-S 7 th November 2010 20 MHz Monitoring Results	153
Figure 4.52 – GPR Survey zones	158
Figure 4.53 – 3D Volume processed data	160
Figure 4.54 – Zone 5- 2D tomography data 40cm below the surface.....	161
Figure 4.55 – 2GHz Vertical Sliced processed data (left) and 600MHz Vertical Sliced processed data (right).....	163
Figure 4.56 – GPR Zone 5 Radar Gram.....	164
Figure 4.57 – (a) Radargram displays upper and lower rebars, (b) Upper and Lower rebar depth (d) zone 5 location, (e) view of zone 5, (f) the B-Scan slice position taken from zone 5.....	165
Figure 4.58 – (a) RIS Hi BriT (2 GHz) Radargram processed data, Winter 2011, (b) RIS Hi BriT (2 GHz) Radargram processed data, summer 2011, (c) zone 5 location, (d) view of zone 5, (e) the B-Scan slice position taken from zone 5.....	167
Figure 4.59 – (a) RIS Hi BriT (2 GHz) Radargram processed data, Winter 2011, (b) UTSI (1.5 GHz) Radargram processed data, summer 2011, (c) zone 5 location, (d) view of zone 5, (e) the B-Scan slice position taken from zone 5.....	169
Figure 4.60 – (a) RIS Hi BriT (2 GHz) Radargram processed data, summer 2011, (b) RISMFI-HI-MOD (200-600 MHz) Radargram processed data (c) zoom output from identified area (red box).....	170
Figure 4.61 – Depiction and Aerial view of GPR a-b lane	171
Figure 4.62 – 600MHz Antenna cross section a-b lane radargram.....	172
Figure 4.63 – 1GHz Antenna cross section a-b lane radargram.....	172
Figure 4.64 – 1.5 GHz Antenna cross section a-b lane radargram.....	172
Figure 4.65 – 2GHz Antenna cross section a-b lane radargram.....	173
Figure 4.66 – 4GHz Antenna cross section a-b lane radargram.....	173
Figure 4.67 – Zone 5 GPR Radargram and Rebar Location	174
Figure 4.68 – Zone 5 and 6 GPR results	175
Figure 4.69 – Principle of GPR (Adopted from Gokhan Kilic, 2010).....	177
Figure 4.70 – Radargram velocity analyses	178
Figure 4.71 – Radargram lower rebar velocity analyses	179
Figure 4.72 – Calculate depth	179
Figure 4.73 – Velocity.....	180
Figure 4.74 – Zone 5 plan	181
Figure 4.75 – Depth of the lower rebar	182
Figure 4.76 – Dielectric constant	183
Figure 4.77 – GPR Output	184

Figure 4.78	– Combination of Visualisation, IBIS-S, and GPR Results	187
Figure 5.1	– SAP2000 Modelling Procedure	191
Figure 5.2	– ANSYS Modelling Procedure	192
Figure 5.3	– Rebar position from GPR radargram	194
Figure 5.4	– Rebar diameter measurement from a radargram.....	195
Figure 5.5	– Rebar position in ANSYS modelling	196
Figure 5.6	– Geometry of SHELL181 element in ANSYS.....	197
Figure 5.7	– Geometric detail of BEAM4 element in ANSYS.....	198
Figure 5.8	– Cherry Picker	199
Figure 5.9	– Plan, Elevation and the 3-D view of SAP model.....	201
Figure 5.10	– Inverse Problem Methodology	203
Figure 5.11	– Inverse problems flow chart	203
Figure 5.12	– View of Bearing Connections between Abutment and Bridge Deck ..	204
Figure 5.13	– Normalised deflections from Rigid and simple connected bridge deck and IBIS-S monitoring.	205
Figure 5.14	– SAP200 Mid-Point Span 1 Result	207
Figure 5.15	– IBIS-S Results- Mid-point Span 1 with four passes	207
Figure 5.16	– IBIS-S Results- SAP2000 Span 1 Comparison (Lorry speed 25MPH).	208
Figure 5.17	– SAP2000 Mid-Point Span 2 Result.	208
Figure 5.18	– IBIS-S Results- Mid-point Span 2 with four passes	209
Figure 5.19	– IBIS-S Results- SAP2000 Span 2 Comparison (Lorry speed 25MPH).	209
Figure 5.20	– SAP2000 Cantilever Zone Result.	210
Figure 5.21	– IBIS-S Results- Cantilever Zone with four passes	210
Figure 5.22	– IBIS-S Results- SAP2000 Cantilever Zone (Lorry speed 25MPH)	211
Figure 5.23	– IBIS-S and SAP2000 Conclusion.....	213
Figure 5.24	– ANSYS Beam Design.....	214
Figure 5.25	– Beam Alignment in span 4.....	215
Figure 5.26	– Areas depicting the geometry of the bridge.....	217
Figure 5.27	– Beam and Shell elements.....	217
Figure 5.28	– Maximum deflection in the cantilever zone.	221
Figure 5.29	– Maximum bending stress in the beam supporting the cantilever slab ...	222
Figure 5.30	– Maximum bending stress in the cantilever slab zone.	222
Figure 5.31	–46 Tonne Moving Load	224
Figure 6.1	– Development Integrated Approach.....	228
Figure 7.1	– Integrated approach on Pentagon Road Bridge.	246
Figure 7.2	– Development Integrated Mechanism.....	247

LIST OF TABLES

Table 2.1 – IBIS-S operational characteristics (Bernardini et al., 2007)	52
Table 2.2 – NDT information	70
Table 2.3 – Summary of NDT	71
Table 4.1 – Visual Inspection	131
Table 4.2 – The IBIS-S Monitoring	138
Table 4.3 – Moving load crossing time	141
Table 4.4 – The GPR assessments	157
Table 4.5 – Depth of the lower rebar	181
Table 4.6 – Dielectric constant	183
Table 5.1 – Pentagon Road Bridge FE Modelling Assumptions	193
Table 5.2 – Comparison of deflections from FE models to IBIS-S results to find actual Young’s modulus	206
Table 5.3 – Selected beam for the parametric study	219
Table 5.4 – Maximum structural responses in the cantilever region	220
Table 5.5 – Maximum beam stress in the cantilever region	223
Table 6.1 – Correlation of the FE models	235

LIST OF ABBREVIATIONS

c	Speed of light
cm	Centimetres
CMP	Common Depth Point
CRC	Continuous Reinforced Concrete
d	Depth of the feature
Db	Decibels
DW	Direct wave
f	Frequency
f_c	Concrete compressive strength
FFT	Fast Fourier Transform
GHz	Gigahertz
GPR	Ground Penetrating Radar
HA	Highway Agency
Hz	Hertz
K	Dielectric Constant of material
km	Kilometre
km/h	Kilometre per hour
L	Axle load of vehicle
Ls	Standard axle
m	Metres
MHz	Megahertz
mm	Millimetres
NDT	Non-destructive testing
ns	Nanoseconds
SB	Sub-base
SR	Surface reflection
r	Resistivity
R	Resistor
RX	Receiver X
S	Optimum antenna separation
SR	Surface Reflection
TRL	Transport Research Laboratory
TX	Transmitter X
V	Velocity
μm	micrometre
ϵ_r	Relative permittivity of a medium
ϵ_0	Permittivity of free space
ϵ'	Reel part of the complex permittivity
α	Attenuation coefficient (in nepers per metre)
α'	Attenuation coefficient (in decibels)
ω	Angular frequency
μ_r	Relative magnetic permeability
μ_0	Magnetic permeability of free space
σ	Conductivity
λ	Wavelength

Chapter 1

INTRODUCTION

This chapter provides a foundation for this thesis, detailing the field of research, emphasizing research gaps and stating the main objectives of this project. The research aim has been justified, an outline of the main points given and the structure of the thesis outlined. The scope of the research has been defined, in order to provide focus for the literature review.

1.1 Background to Research

Bridges represent a major part of British infrastructure, comprising of thousands of structures that often vary in their construction; owing to their placement and purpose. Due to the demanding conditions and individualistic needs of bridge design a common choice of material became reinforced concrete throughout the midsection of the 20th century. The primary reason behind this choice is the capacity of concrete to be cast into a large range of shapes and sizes and also its apparent high durability in early years of construction. This was the school of thought until the 1970s when it became apparent that concrete structures were deteriorating at a quicker rate than originally predicted (Mawson and Lark, 2009).

Since the construction of these reinforced bridges, investigations into better construction methods have led to designs that are more able to cope with modern requirements, however their existing legacy needs to be addressed. Older bridges can have major problems both apparent (cracks, delamination) and unapparent (moisture ingress). These can have a significant impact on the structural performance of the bridge leading to a possible collapse. A large amount of the research relating to the use-case scenarios for these older bridges did not consider modern requirements, and given that they are being used for modern activity, many require action to be taken. The exact course of action, however, is not often clear with original plans either non-existent, or the exact effect of environmental and operational conditions able to be quantified.

The impact of a bridges health in the UK is enormous with approximately 81,000 bridges managed by various agencies and authorities (based on the 2000 bridge census provided by Imran, 2005). The financial stakes are also high with the Highways Agency alone controlling a bridge stock of 15,600 structures valued at £22 billion, of which nearly 50% contain concrete as the primary structural material and are thus susceptible to these problems (Imran, 2005).

The problems posed by aging concrete bridges are not limited to the UK alone with 29% of bridges in the US being classed as functionally deficient needing \$10.6 billion per year over the next decade to correct (ASCE, 2011).

Similar problems are encountered in many bridges throughout the world with aging infrastructure, typically built in the 1950's and 1960's, needing health monitoring to prevent avoidable financial expenditure. The risks involved with bridge health monitoring are not purely monetary with personal safety being of paramount importance, with bridge collapses occurring to this day, during the monsoons just before the Commonwealth Games in September 2010 the footbridge connecting a car park with the Games' main stadium collapsed and at least 23 construction workers were injured. With the risks being so high, a large area of research has been devoted to developing techniques whereby the health of the bridge can be assessed before it deteriorates enough to require high cost remedial work or even collapse (Walker, 2000).

Methods which assess bridge health have often been extremely costly in terms of time and money. However recent advances in Non-Destructive Techniques (NDT) have considerable advantages which decrease the time and financial costs required to determine these parameters, and utilization these techniques has gained great momentum in recent years. The use of NDT has proven to be successful in discovering possible defects on specific aspects of a bridge's structural components. These are techniques where sections of a bridge structure do not need to be removed (or destroyed) in order to carry out an assessment. NDT have been employed since the 19th century (Walker, 2000) however; in recent years these have employed advanced technologies, such as Ground Penetrating Radar (GPR), Interferometric Radar, and Accelerometer Sensors. This is then combined with more traditional surveying methods, such as visual inspection. The information gathered from these methods are then able to inform engineers regarding what course of action, if any, they need to take in order to ensure the longevity of the bridge; as replacement is often costly, and failure can lead to consequences; including the loss of life.

However there are two major problems that have been identified with the way in which NDT are exploited:

- As bridge structures are vulnerable to an array of potential sources of deterioration such as delamination of beams and moisture ingress, as such addressing of these sources globally cannot be carried out by one single method (Yu et al., 2011). Currently, NDT are applied singularly to determine specific

problem areas however, no particular method can identify all structural defects. For example too often GPR is used as a method to identify structural anomalies however there is no way of telling with GPR whether the defects found are having an adverse effect on the structural integrity of the bridge. This is a serious oversight on behalf of the research community as it is impossible to tell the level of displacement (which is a measurement of bridge health) without more detailed testing. However with the large amount of NDT available today, no large scale studies have been completed into which techniques integrate well together.

- An additional problem not tackled by traditional techniques is that fact that often crucial structural reports and drawings are missing (as is the case with the main case study in this thesis - Pentagon Road Bridge) with older bridges which results in important information such as the position of rebar, supports and other design details being unknown. Lack of vital information of this nature, no doubt, will limit the capability of structural and design engineers in order to be able to model and simulate structural behaviour of such bridges reliably and accurately using numerical methods. This will also result in the inability of NDT results to be compared with initial bridge behaviour.

As eluded to it earlier, applications of NDT methods in assessing structures such as bridges within the context of health monitoring of structures is not a new concept. Significant advancements have been made by design engineers and practitioners in this field in recent years. The most important advancements probably are: improvement in surveying and monitoring techniques as well as equipment and data processing software. However, it is fair to say that, there is a noticeable lack of an established integrated approach that utilises results of NDT applications in order to develop a reliable numerical model for simulating the structural behaviour of i.e., bridge structures under different loading conditions (static and dynamic). Development of such models and approaches are essential in assessing reliability and integrity of bridge structures and their functions in future.

These are the identified gaps in literature that this thesis seeks to partially address by assessing the effectiveness of different NDT. Application of NDT and parametric

studies results in conjunction with one another in order to formulate a bridge health assessment strategy. This strategy is then discussed, detailing the constituent elements and describing how these can come together in order to increase the valid information, and therefore the confidence. Of those who carry out bridge health assessment when making decisions regarding the status of a bridge, and whether any remedial action is required in order to prevent dangerous, or catastrophic, events occurring; potentially leading to the saving of lives and money.

1.2 Layout of the Thesis

This research work comprises of an abstract and the following chapters and appendices:

Chapter 1: Introduction: This chapter gives an introduction to the research domain and states the Aim, Objectives and Scope of the research project. It also presents a brief summary of the contents of each chapter.

Chapter 2: Literature Review: This chapter includes a review of the available literature concerning bridge health and assessment techniques and systems. As well as different types of technique and their capabilities related to health monitoring, it is important to choose a system for the bridge's needs. Moreover, it identifies bridges as an important part of the infrastructure asset and heritage of any society. Finally, it also represents the finite element analysis which is then used to model the structural behaviour of bridges. Areas for further research are also identified.

Chapter 3: Research Methodology: This chapter details the development of an integrated approach to assess and monitor the structural integrity and overall functionality of bridges.

Chapter 4: Results and Analyses: This chapter examines the results collected for the preliminary and major case studies. The obtained results are presented in this thesis.

Chapter 5: Parametric Study: This chapter details the development of finite element model of main case study for the structural behaviour and integrity and overall functionality of main case study.

Chapter 6: Discussion: This chapter discuss the finding and explain the limitations and problems encountered during this research work and how they have been solved.

Chapter 7: Conclusion and Further Work: This chapter summarises the objectives mentioned in chapter 1 and is based on the results derived from the study leading to the final conclusions of the research so far. Further work is also defined.

Appendix A: Contains figures analysing Pentagon Road Bridge IBIS-S results.

Appendix B: Contains figures analysing Pentagon Road Bridge GPR results.

Appendix C: Contains figures validation of Pentagon Road Bridge IBIS-S and Accelerometer results.

Appendix D: Contains detailed drawings, visualisation for the Pentagon Road Bridge.

Appendix E: Contains abstract of peer reviewed journals and international conferences.

1.3 Justification and Scope

Health monitoring is of crucial importance to maintain the structural integrity of bridges in use today. Bridges are an important part of the infrastructure asset and the heritage of any society, and are subject to a natural process of deterioration of construction materials which can have massive financial implications and in worst cases can cause fatalities.

With over 25% of the bridges in the UK today being of reinforced concrete composition an effective method of providing an integrated health monitoring technique is needed which addresses the current problems with non-destructive testing (NDT) identified in section 1.1. Unfortunately no such mechanism exists. Currently, the various aspects of bridge health are monitored separately using strain gauges (Liu et al, 2009), tell tails for crack monitoring and visual inspections. However these methods used independently do not give an overall description of the health of the bridge and potentially can lead to crucial indicators of structural damage being missed. This thesis can be considered as a

significant contribution towards improvement of current assessment practices of bridge structures. In this study, a number of NDT methods were considered with direct applications to actual case studies. The results have clearly demonstrated the appropriateness of applications of these methods in combination in bridge health monitoring and assessment.

The proposed mechanism of utilisation of non-destructive methods in combination and in association with available commercial bridge modelling software is applicable to different types of bridge structures. Nevertheless, the applicability of the proposed mechanism should be considered on a case by case basis. That is to say, applications of NDT methods may not be appropriate in the assessment and monitoring of certain bridge structures. In summary, the proposed mechanism can be considered as a novel approach in the assessment and monitoring of bridge structures that either can be used in combination with other practices or on a stand-alone basis.

Currently, bridge monitoring strategies and assessment comprise of several main types of inspection (Rashidi & Gibson, 2011; Vaghefi et al. 2012):

- Initial Inspection

This form of inspection is performed on newly built bridges and provides the basis for all future inspections.

- Routine Inspection

Routine inspection occurs at regular defined intervals, for example every 15 months. It is often based on subjective visual investigations by the bridge inspectors. During this form of inspection, no major structural deterioration is expected to be found and the work falls within the range of maintenance.

- Detailed Inspection

Here, several NDT methods are applied to a selected area of the bridge, the aim being to identify any structural defects which may lead to future problems. According to the outcome of this assessment, several consequences may arise such as the organisation of a structural assessment, the preparation of a list of remedial actions to be taken or the establishment of a medium-term maintenance plan. The period recommended for a detailed inspection is five years.

- Structural assessment

This is normally the result of the identification of a major structural or functional defect during a routine or detailed inspection. Here, as well as extensive application of NDT, static and dynamic loading may be applied along with laboratory testing if possible. The results obtained from this assessment are the quantification of structural defects, their location on the bridge and an evaluation of its present load-bearing capacity.

Other forms of inspection such as special investigations and underwater investigations may be necessary in particular circumstances.

There are problems associated with this programme of inspections that this thesis serves to address. Firstly, often bridges are not appropriately assessed when newly built, thus there is no benchmark to compare routine and detailed assessment results with. This is remedied by the creation of a finite element model (FEM) using structural information from the bridge and using it to model the static and dynamic behaviours of the bridge as new providing this benchmark for comparison.

The approach proposed by this thesis falls under the “mandate” of structural assessment. However, it improves on it by providing a set list of techniques to be applied to the bridge which can evaluate its structural integrity comprehensively, thus eliminating the objectivity which is often deemed a problem with bridge health monitoring assessments (Vaghefi et al. 2012). This approach also provides additional information, such as identification of rebar position and other anomalies within the structure (internal cracks, delamination, ingress of moisture and the existence of cavities), which otherwise is not readily available. This information no doubt can be used in developing a more accurate numerical model of the structure. The developed model then can be used for further numerical modelling within the context of predicting future structural behaviour.

In addition to the above, this approach has multiple advantages over current practices including:

- Direct identification of the most effective/appropriate NDT method for bridge monitoring.
- Identification of previously unknown bridge parameters using suitable NDT.
- Comparison of FEM (which simulates the bridge as new using the parameters obtained by NDT) with actual NDT results giving a more complete picture of the bridge's deterioration since construction.
- Comparing the results of all the above to determine the key locations of structural failings within the bridge deck.

The research scope is defined as collecting, processing and interpretation of relevant data in order to assess the health and perform analysis of appropriate bridges. It is of paramount importance to have an integrated approach of structural monitoring solutions, within the context of using NDT, application systems and assessment technology to support preventative maintenance. This has the potential to not only save money, but lives as well.

Figure 1.1 demonstrates the approach used in the research in order to achieve the set objectives of this research programme.

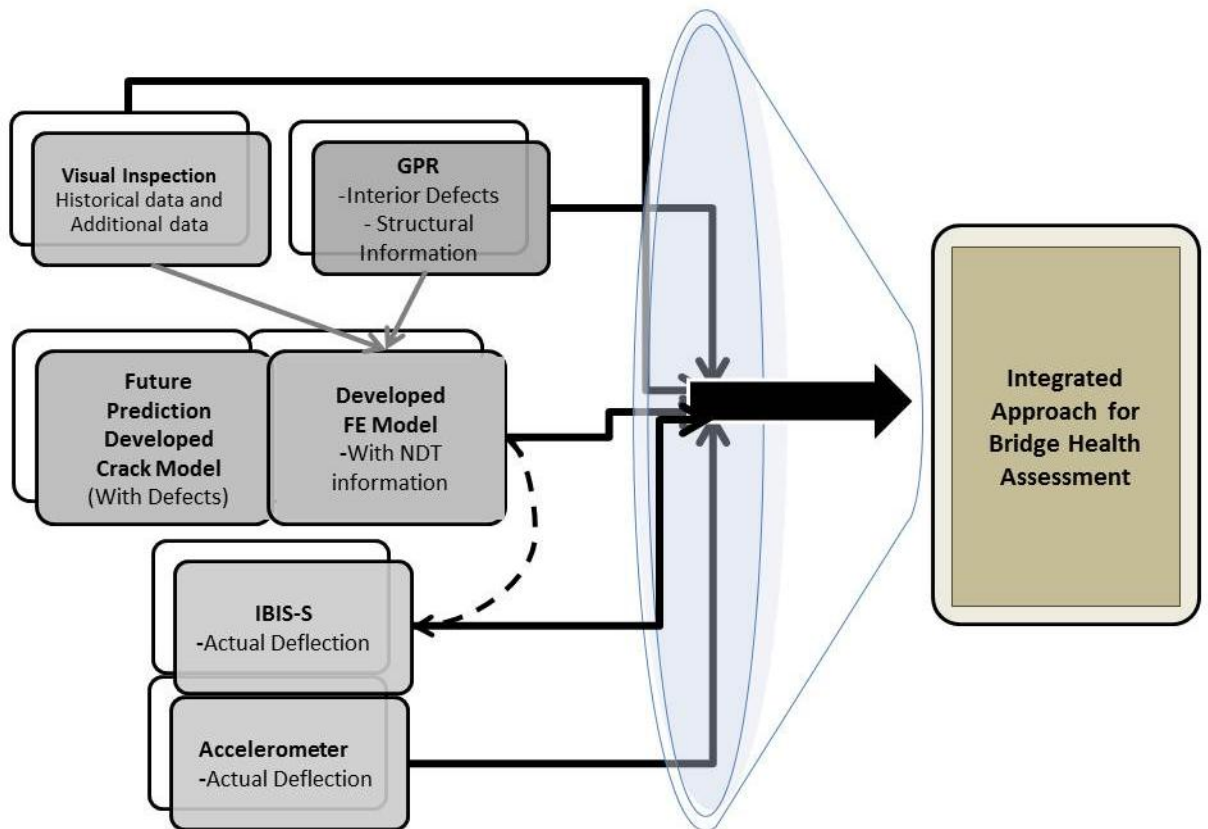


Figure 1.1 – Schematic Depiction of the Integrated Approach

This mechanism has the potential strength to become a fundamental practice in bridge health engineering and in the future could become a popular step by step method of determining the health of bridge structures.

1.4 Aims and Objectives

The aim of this research is to develop an integrated approach for the assessment of the structural integrity of bridges. In order to achieve the above aim, the following objectives have been set:

1. To acquire necessary knowledge of operation, collection, processing and interpretation of complex data compiled by advanced structural monitoring equipment, such as GPR, Accelerometers and IBIS-S (a radar based technology with interferometric capability Technology, measuring vibration and structural movement) and specialist FE software.
2. To establish the effectiveness and applicability of non-destructive testing methods and technology in structural monitoring and assessment of bridge structures.
3. To establish detailed monitoring data on the extension of structural defects and identification of structural and non-structural features which increases understanding of anomalies within the bridge structure. This includes the interpretation of GPR data to identify moisture ingress by means of velocity analysis.
4. To develop Finite Element modelling of bridge structures using specialist software (SAP2000, ANSYS) for simulation purposes.
5. To develop an integrated mechanism bringing together the obtained knowledge and information about defects and mechanical behaviour of bridges within the context of health monitoring and integrity of structures.

1.5 Collaboration

The research programme sought and put in place in this thesis was collaborated with relevant industry. This research programme has received the full support of the IDS Ltd (an Italian ground radar development company based in the UK). IDS has provided the research team with the state of the art GPR and IBIS-S technology as well as supporting the programme with their expert knowledge and supervision of data collection activities. This research programme has also received some support from the XODUS GROUP Europe (an independent, international consultancy providing a uniquely integrated package of solutions company based in the UK). The research programme has also received the support of the Medway City Council (Energy Division) in terms of accessibility to the main case study, facilitating and managing the traffic control and acquiring subcontractor for installation of sensors detecting reflectors and the previous report and information on the bridge. The overall domain, Aim, and Objectives of the project were devised and refined in collaboration with relevant industry.

1.6 Limitations to Approach

While completing this thesis, the focus was to create a process whereby the health of a bridge could be assessed without the need for costly and disruptive destruction techniques. While every care was taken to provide a solution that was both appropriate and viable several weaknesses in the methodology have been identified as follows:

The main focus on this project was to assess the health of reinforced concrete bridges only. Thus this method is not appropriate for other bridge types such as steel bridges. Some of the techniques examined however are suitable for all bridge types i.e. IBIS-S for monitoring deflection. So it is possible that with adaptation this method could be used to assess all bridges by adding additional NDT specific to bridge types.

It was not possible to use methods which physically touch the deteriorated cracked area such as tell-tail crack monitoring due to the health and safety issues highlighted by Medway Council. Thus it was only feasible to monitor the

increase in the dimensions of these cracks by non-invasive means i.e. photography and visual inspections (Parameswaran et al., 2008).

It would have been beneficial to apply additional methods of NDT such as laser scanning. A laser scan would have provided an accurate 3D image of the bridge which could have been used to design the FEM, this would have given a more accurate assessment of its behaviour under loading. However, the addition of another piece of equipment would make this process more costly and time-consuming both these aspects would have a negative effect on the overall goal of the project to provide a bridge health assessment technique which is cost effective with minimal disruption.

Another criticism is the choice of only one main case study, examining further bridges in as detailed a manner as was achieved with the Pentagon Road Bridge would have proven the repeatability and appropriateness of the proposed bridge health monitoring technique. However, examining further bridges would have diverted time and resources away from the Pentagon Road Bridge's assessment which would have resulted in more case studies but in less detail thus overall undermining the strength of the project.

1.7 Summary

This section has provided a foundation for the thesis, detailing the field of research, emphasizing the research gaps and stating the main Objectives of this study. The research Aim has been justified, an outline of the main methodologies given and the structure of the thesis outlined. The limitations of the research have been established and justified hence allowing the research to continue with a detailed literature review.

Chapter 2

Literature Review and Background Studies

This chapter describes the theories related to bridge health assessment techniques and systems. Comprehensive desk-top research was undertaken, including academic journal papers, books and a range of websites to support research for finding earlier publications. The review is broadly divided into three parts:

- Firstly, it will discuss different types of technique capabilities related to health monitoring, and demonstrate the importance of choosing a system for the bridge's needs.
- Secondly, it will discuss structural loading theories concerning concrete bridges.
- Thirdly, it will also review application of numerical methods in bridge health monitoring.

Theories of Bridge Health Assessment

2.1 Introduction

Bridges are key elements of the infrastructure network, and are critical to a society's economic and industrial prosperity. As such, regular maintenance inspections and assessments are vital in order to prevent the costly and potentially disastrous consequences of them failing and for them to achieve their maximum serviceable life span. Environmental corrosion, traffic and wind loading, earthquakes and aging all impact on the structural vulnerability of bridges and new testing techniques are in demand.

Two distinct causes of deterioration in reinforced and pre-stressed concrete bridges are identified by Cope (1987): chemical and physical environmental effects on the concrete and corrosion of embedded steel. He also describes how the testing of concrete properties is probably necessary to allow this information to be contrasted with specifications. This could then be introduced when calculating serviceability and loading capacity, in the evaluation of likely resilience and in planning for future maintenance.

There are many difficulties facing bridge authorities, including increased traffic use and safeguarding against natural disasters; such as earthquakes and flooding. In an effort to build structures which are more able to withstand these kinds of conditions, new sensing technologies and analytical methods are being pursued by engineers, which could automatically follow a structure's degradation by the use of damage detection algorithms in conjunction with structural monitoring systems. The role of bridge inspectors must also be seen as vital in identifying developing issues before they become too problematic or costly.

It can be seen therefore that, due both to the key role bridges play in a society's infrastructure, as well as the vulnerability of bridge structures worldwide to a great many environmental and manmade hazards, the use and further evolution of structural health monitoring techniques is vital.

2.2 Bridge Health Monitoring

The structural health monitoring of bridges is currently in immense demand and much research is taking place.

Live, dynamic and environmental loads to bridges, such as vehicular traffic and weather conditions, all have a negative effect on the structural integrity of bridge structures and maintenance will therefore be required. These kinds of load-carrying requirements must be taken into account at the bridge's design stage and, whilst calculation errors are always a possibility, realistically any small errors are outweighed by safety factors on the live load and in the material strength, meaning that miscalculation is rarely the central reason for bridge collapse. Bridge collapses play a key role in the continued accumulation of structural knowledge and advancement of assessment techniques.

Chae et al., (2012) describe how the relatively recent introduction of real-time monitoring into the structural health monitoring field is becoming more commonplace. It monitors real-time structural behaviour in terms of appraising structural performance under varied loads and identifying structural damage or deterioration. It also ensures continued structural safety and informs bridge management plans. It corroborates new structural design in terms of validating construction outputs and facilitates the quick detection of any problems.

Researchers and engineers have several bridge monitoring methods and technologies available to them and selection of the technique to be used depends on the construction type, its material composition, the element of the structure under test and the suitability of the method being employed. It is also clear that, in order to facilitate the impartial evaluation of structural performance for that structure's effective maintenance, a wide-ranging knowledge of structural behaviour is a prerequisite and it is likely that the gathering of information relating to structural behaviour will be improved upon with modern technological advances (Nagayama et al., 2001).

In foreseeing bridge deterioration, maintenance work can be carried out to avoid possible structural failure and, therefore, being able to predict bridge condition based on

regular inspections is crucial. In order to predict future condition accurately, some 60% of bridge maintenance strategies rely on regular bridge inspection data. The five typical steps involved in bridge health assessment strategies are (Pan et al., 2009):

- condition assessment;
- predication of deterioration;
- agreeing a suitable maintenance programme;
- prioritising maintenance;
- making the most of available resources.

2.3 Non-Destructive Methods

Non-destructive testing (NDT) is a method of discovering faults, flaws, structural defects and the structural composition of a structure without affecting the tested object, making it a valuable and widely used technology for bridge health monitoring. Having said this, in its application to concrete some methods do require localised surface damage whilst causing no harm to the remainder of the structure. There are several such examples, known sometimes as ‘partially-destructive’. As there is no breaking out, coring or partial demolition required, no consideration is necessary in relation to post tensioned or pretension cables or highly reinforced areas of the deck; and without remedial repairs of demolished parts required, a survey of the entire deck can be completed to obtain a full representation of the health of the bridge. This furthermore indicates that NDT is a more sustainable choice and a more cost effective solution in the long term. Techniques which necessitate the removal of a sample for analysis are however not typically classified as non-destructive (Cope, 1987).

Whilst no one NDT method can give a complete picture, each method has been proven successful in certain applications and so it is important to choose the right NDT technique related to the particular bridge health monitoring need, by the undertaking of a prior feasibility study to appraise the appropriateness of the proposed technique. There is an array of NDT methods available for concrete testing, some broad in potential usage and others highly specialised. These include infrared thermography, GPR, acoustic impact (sounding), ultrasonic pulse-velocity, ultrasonic pulse-echo and impact echo, all of which (apart from the first two) rely on stress wave propagation

(Highway Agency BA 86/06 Section 3, 2006). In deciding which method of NDT will be most suitable for a particular project, the following requirements will typically be considered: depth of structural penetration, vertical and lateral resolution for the anticipated targets, contrast in physical properties between the target and its surroundings, signal to noise ratio for the physical property measured at the structure under investigation and knowledge of the construction methods used (McCann and Forde, 2001).

A recent development in NDT is remote monitoring whereby recording devices pick up vibration in real-time in attempting to accurately determine bridge condition and enable early detection of developing problems. In combination with automated imaging techniques, remote monitoring can drastically reduce bridge maintenance costs by reducing physical attendance by bridge inspectors, minimising any safety risk and providing on-going information on bridge deterioration.

The purpose of this literature review is to identify the various methods of NDT, including technologies needed to accomplish that specific method, and then summarise its findings in a table listing the method, its application and what can be expected from the results. Of fundamental importance is that a systematic and holistic investigation of the structure is undertaken which could proceed as shown in the following steps (Anon, 1997):

- Visual inspection.
- Scrutiny of load carrying capacity.
- Further investigate or, if unnecessary, return to routine visual inspection schedule. If further investigation is necessary, continue with the below points.
- Conduct a study to research the history of the bridge, e.g. its designer, its builder and its style of construction (e.g. soil backfill or cellular).
- Select the most appropriate and cost-effective strategy for further investigation. NDT may be chosen when (a) physical measurement was inadequate or expensive; and (b) extension of a limited physical investigation is necessary (Gangone et al., 2008).

This literature review will also look into the varying methods and technologies available for monitoring and assessing bridges using NDT methods, leading to an in-depth study of the use of GPR, IBIS-S interferometric radar and accelerometer sensors to identify the practicability and usefulness of these technologies (Highway Agency BA 86/06 Section 3, 2006).

This section will also describe the theory behind each NDT technique, including any limits in the applications, possible advantages and disadvantages, what the technique measures and how it is applied in health monitoring applications. The techniques are:

2.4 Visual Inspection

2.5 GPR - Ground Penetrating Radar

2.6 IBIS-S Interferometric Radar

2.7 Accelerometers

2.8 Other Non-Destructive Techniques

2.8.1 Wireless Network

2.8.2 Laser Scanning

2.8.3 Infrared Thermography

2.8.4 X-Ray Radiography

2.8.5 Gamma (γ) Ray Radiography/Radiometry

2.8.6 Acoustic Emission (AE)

2.8.7 Ultrasonic Testing

2.8.8 Sonic Techniques

2.8.9 Impact Echo (IE)

2.8.10 Resistivity Measurement

2.8.11 Half Cell Potential

2.8.12 Magnetic Induction

2.8.13 Magnetic Flux Exclusion

2.4 Visual Inspection

Visual inspection is a conventional method of structural inspection and is still in use despite advances in other methods of structural health monitoring. Visual inspection is not entirely adequate as it is limited to visible surface defects and is subject to human judgement, so leading to possible errors (Basharat et al., 2005).

Gros (2001) explains how visual examination remains popular due to its low cost and its speed in identifying obvious defects. The purpose of visual inspection is to find flaws early enough to ensure the continued operation of the structure. However, the inspection is superficial in the sense that only surface area defects are immediately apparent. Visual inspection provides the most natural form of structural assessment and means simply using the eye. Whilst visual inspection is amongst the simplest method, damage which occurs beneath the surface is not easily picked up by the human eye and, even when picked up, detail may not be easily identified. On a large scale structure, the visual method of inspection is inadequate (Kessler, 2002).

Gangone et al., (2008) explain that, although many USA transportation agencies use visual inspection techniques, this method of inspection alone is not always adequate since it is subjective and provides an incomplete picture. It also produces difficulties in terms of the possible inaccessibility of parts of the structure as well as time constraints and therefore a more vigorous system of monitoring also becomes necessary. Levels of visual inspections vary from a principal inspection which examines the structure thoroughly, noting all defects and possible remedies, right down to a superficial inspection where an overall assessment is made and only large defects noted.

Clearly, an examiner needs to be an individual who has the necessary knowledge to carry out an inspection adequately, although visual inspections can include the implementation of apparatus such as endoscopes to access unseen elements and CCTV for areas with poor access. This method has cost saving benefits over other inspection methods and so is often used as a first step in the inspection process, before applying other NDT methods. Visual inspection examines and evaluates structures with the use of mechanical devices such as magnifiers but also by use of the senses. The acts of

looking, listening, feeling, smelling, shaking, and twisting the structure and its components, in conjunction with the operator's structural knowledge, provides the basis of this method (Spencer, 1996). A current shortage of personnel qualified to carry out these inspections is also proving a challenge (Zhu et al., 2010).

Visual inspection is a slow and possibly hazardous method but inspection is vital in the management of bridges, and transportation agencies must develop adequate inspection programmes encompassing inspection frequency, the nature of observations and measuring equipment. Factors may influence which method of inspection is selected and the timing of such inspections include the condition of the bridge, its age, traffic density, personnel availability, geographic location and construction method, all of which can affect a bridge's deterioration rate (Abudayyeh et al., 2004).

Roberts et al., (2006) consider that the recent failure of several bridges around the world can be put down to inadequate testing brought about by the complexity of the operational conditions of those bridges making inspection difficult, which verifies how crucial rigorous inspections are. Visual inspection is time consuming, inexpensive and labour intensive and provides inadequate information on surface flaws only at timed intervals (Meng et al., 2011).

Inspections consist of visual observations and assessments of the condition of the bridge elements, including its columns, abutments, decks/slabs and girders. Bridge inspection is an expensive but essential element of bridge management and involves various components of the bridge being examined visually by trained inspectors, in providing a condition rating (Abudayyeh et al., 2004).

During such a visual inspection, the inspector is making an assessment, based on his knowledge, of the condition of the bridge. Despite the fact that inspectors have an array of tools to help provide accurate and reliable information, still visual inspection is the most commonly used method of bridge assessment (Phares et al., 2000). Kijevski-Correa et al., (2006) consider that major research is required into the methods of visual inspection and automated monitoring techniques in the area of civil infrastructure maintenance.

Prior to inspection, the inspector will make preparatory note templates and sketches, following which an overall inspection plus an examination of existing flaws will be carried out. The inspector will be looking out for such defects as cracks, loss of cover and spalling and corrosion (Zhu et al., 2010).

Effective bridge, road and highways infrastructure monitoring and maintenance would have to take account of the following:

- A crucial aspect of road and highway management consists of inspection and maintenance.
- This effective management forms an important element of society, both for road users and beyond.
- An effective networked regime in understanding the procedures necessary to protect the condition of the highway infrastructures must be in place.
- The concept both of network safety and sustainability and safe working practice in working on the highway is vital.
- An effective assessment and maintenance programme should be in place. (Highway Agency BA 86/06 Section 2.3, 2006)

Pan et al., (2009) describe the noted observations of visual inspection to consist of both `fuzzy` and `crisp` data. They describe fuzzy data as being that information submitted in the subjective language of the inspector, such as “The condition of this pier is very good” whereas data relating to traffic load or bridge geometry will be numerical and therefore crisp.

This method is a subjective method, leading sometimes to great variance in the condition ratings of bridges given by various inspectors (Abudayyeh et al., 2004). This inconsistency in judgement is not just true from person to person but an individual can also visually perceive differently from day to day. To avoid mistakes, only experienced operatives should perform the inspection, and great care must be taken over inspection ratings and parameters must be prepared as objectively as possible (Caner et al., 2006).

The traditional visual inspection method of monitoring the structural condition of bridge structures is certainly still in common use today but, as discussed this method has distinct disadvantages such as being subjective to the individual engineer and is purely an indication of the external damage which may or may not be internal also. Great strides have been made in the world of non-destructive structural health monitoring in modern times and each of the currently available methods will now be examined in more detail.

2.5 Ground Penetrating Radar (GPR) Technique

“... ground penetrating radar (GPR) is an advanced, non-invasive sub-surface imaging technique that typically uses short pulses of electromagnetic energy to ‘see’ into the ground. GPR can image through soil, concrete, tarmac, rock, wood, ice and even water. It is quick, easy to use and inexpensive in comparison to other investigation methods. It is capable of probing down to a few tens of metres (depending on the system type & ground conditions) and provides the user with a ‘cross-sectional’ image of the sub-surface”

(EuroGPR ,2010)

2.5.1 Introduction and Background

In the above extract from the EuroGPR (2010) web site, GPR is identified as a complex non-destructive imaging technique which utilizes electromagnetic waves to identify subsurface anomalies and objects. It is able to map underlying objects to a few tens of metres depending on antenna and conditions and then produces radargrams of these hidden objects. This technique can be used in a variety of different applications including in this case bridge health monitoring and has numerous advantages such as its ease of use and low-cost when compared to other methods. In this section, the most recent and well known research studies on GPR techniques and particularly its use for bridge health assessment are presented. The choice of material to include was based on the limitations, advantages and disadvantages of GPR in the assessment and monitoring of bridge health.

Although GPR has existed since the early twentieth century in military applications it is only in the last couple of decades that it has been implemented as a research tool (Thumm, 2006). In recent years employment of GPR has become broadly respected by various professionals and it has been effectively put into practice and implemented to solve complex engineering and scientific challenges. The extent to which the use of GPR has increased in recent years is largely due to its rise in credibility owing to new progress in GPR technology (equipment and software), recognition by scientists and engineers of its efficiency and its wide range of applications. At the moment GPR is used by a variety of scientists and engineers including Civil Engineers, Archaeologists, Geologists, Geotechnical Engineers, Glaciologists, Forensic Investigators,

Environmental Scientists and Hydrologists in order to obtain solutions to the most challenging of problems.

In structural engineering, GPR has become an established non-invasive, continuous, high-speed tool to inspect civil engineering structures, such as tunnels, concrete structures and bridges. In bridges health assessment this technique allows the maintaining agencies to obtain detailed information of their bridge structures. It has been consistently shown that GPR gives information regarding bridge deck delaminations and the position of underground utilities (Lagarde-Forest, 2007).

However the uses of GPR in structures such as transport infrastructure, including the evaluation and examination of bridges and tunnels, are not a recent concept. The results of GPR are widely accepted with GPR being effectively applied to monitor bridge decks within the context of identification and integrity assessment of rebar, rebar cover length, depth of cracks, settlement, ingress of moisture and delamination, layers of materials, cavities, location of rebar and other structural features (beams and columns) as well as bridge abutments (leakage, cracks and settlement). (Parrillo and Roberts, 2006), (Benmokrane et al., 2004), (Rhazi et al., 2003), (Lubowiecka et al., 2009).

In conclusion, in the past GPR has been used in a diverse range of functions from military applications to archaeology. It was chosen for use in these fields due to a combination of its simplicity, ease of use, cost, depth of penetration, accuracy and durability, all factors which are of crucial importance to bridge health assessment. This therefore makes GPR an obvious choice as a non-destructive technique for further studies as it can identify and quantify underlying anomalies in the bridge deck quickly and easily, with an output which can be further analysed away from the bridge area. Thus fulfilling several of the key objectives of this thesis (Objectives 2-3) by further examining the functionality of GPR will be completed in this chapter, objective one which relates to acquiring necessary knowledge regarding appropriate structural monitoring equipment, will be partially completed.

In further sections, the general principles of its operation will be explained along with key aspects of its functionality such as antenna type, orientation and selection, velocity

of the wave and others. These key aspects have great bearing on the quality and extent to which underlying images are captured by the scanner and will be greatly explored in both the preliminary and main case studies which form an integral part of this thesis.

2.5.2 General Principles

Various GPR principles have been described by different authors such as (Pérez-Gracia et al., 2009a), (Sussmann et al., 2003), (Forde et al., 1999), (Diamanti et al., 2008). They have concluded that GPR is an advanced non-destructive technology and its basic principles are well established.

The GPRs' basic principle is based on the transmission of electromagnetic pulses into the subsurface, partly transmitted into deeper layers and partly reflecting at subsurface interfaces, and the measuring, recording and display of this reflected energy.

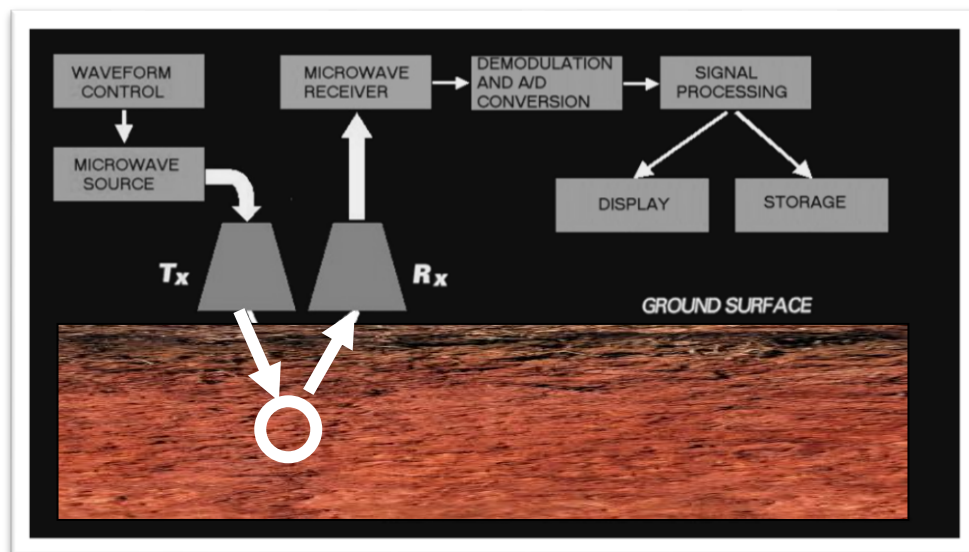


Figure 2.1 – GPR operating principles (Highway Agency BA 86/06 Section 3, 2006)

Above, Figure 2.1 shows how GPR works by emitting an electromagnetic wave from the transmitter antennae and measuring the time it takes for the signal to rebound back to the receiver antennae, where the data is transmitted to a laptop or any other data processing device. The data is then interpreted by software as a two dimensional image of the ground's cross section, showing details of the layering, composition,

moisture content and location of metal bars/pipes/fragments (Olhoeft and Smith III, 2000).

2.5.3 GPR Role in Bridge Assessment

In recent years the popularity of GPR as a method of bridge health assessment has grown partially due to the advantages of quick and easy data collection (Cagnoli and Russell, 2000) but the application of this technique to bridge assessment and integration with other techniques is not always simple. Huston et al., (2000) agrees with Cagnoli and Russell, (2000) that GPR is a functional and reliable non-destructive technique in assessing the damage of a bridge under continual loading, environmental stress, and weather conditions. Damage such as corrosion, cracks and delamination can be hidden inside the bridge deck because it is not always shown on the surface unless it is at an advanced stage. GPR gives a potentially reliable, powerful, effective assessment of bridge health in terms of hidden damage. Forde et al., (1999) also studied this area and represents an increasing awareness of bridge damage and failure over the past decade in the US, Europe and the UK. Bridge assessment has large problems in terms of the inspection and evaluation of the condition of bridge decks. To avoid bridge collapsing, an assessment must be conducted to determine if a concrete deck needs to be replaced due to the fact that bridge decks deteriorate more rapidly than any other bridge section.

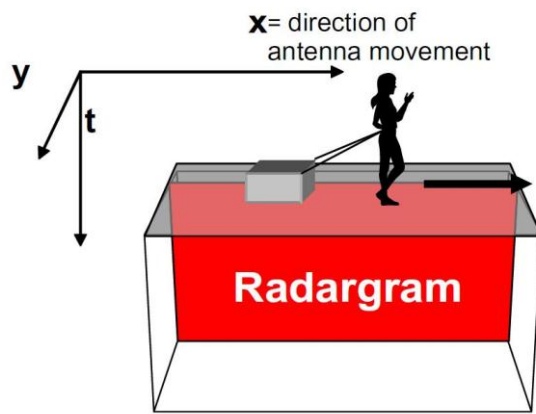


Figure 2.2 – GPR operation on Pentagon Road Bridge (photos from Gokhan Kilic, 2010)

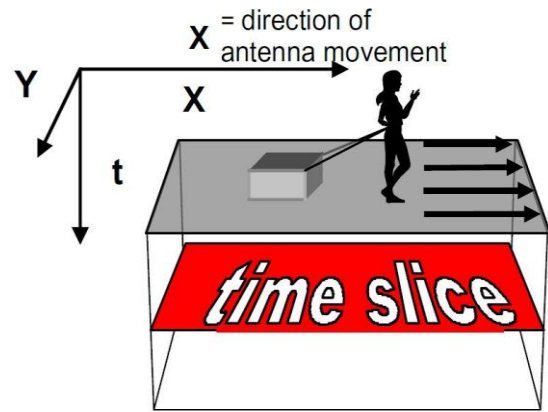
Industry and research have concentrated on developing a multichannel high-frequency GPR system for bridge health assessment survey. In terms of the bridge deck, Maser (2009) suggests that when traditional methods are limited for bridge surveying then GPR can be used. The dielectric properties and attenuation of the concrete provides a measure of concrete bridge deck deterioration. Concrete bridge decks with cracks, corrosion and freeze-thaw damage and with a high moisture and chloride content, can cause high variations in the dielectric permittivity in the concrete under the overlay. In studies, Hugenschmidt, (2002) also identified that recently GPR has become an essential advanced non-destructive technique for assessing a bridge and has advantages according to traditional techniques. Figure 2.2 represent the 2 GHz GPR antenna used on the Pentagon Road Bridge.

Further research was conducted by Jol, (2009) who specifies the use of GPR in the assessment of bridge pavement and layer thickness, location of damage, position and spacing between re-bars (reinforcement bars) and tendons or tendon ducts, concrete and pavement properties.

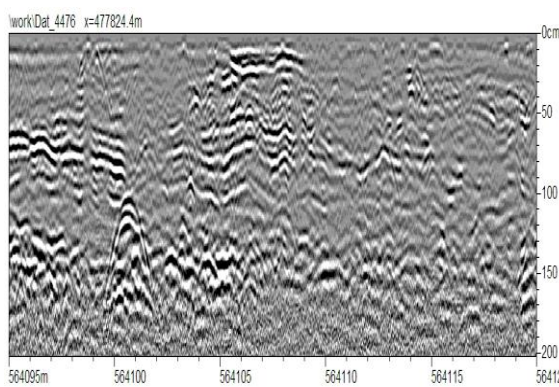
GPR data can be displayed on-screen in different configurations, as radargrams and as time slices. In Figure 2.3 (a), the radargrams acquisition position is shown, where the GPR system is moved in the x-direction and the reflected signals record continuously via computer. In Figure 2.3 (b) the time slice displays on the computer screen the data acquired on a surface along several parallel lines. In Figure 2.3 (c) radargrams record in the x-direction and display on the computer screen. When the survey is completed on the planned area with all parallel lines, Figure 2.3 (d) represents slices from different times/depths. This diagram provides a good example for Hugenschmidt and Mastrangelo, (2006)'s argument relating to the quality of the results. It is obvious that having the choice of a high frequency device ensures high quality results.



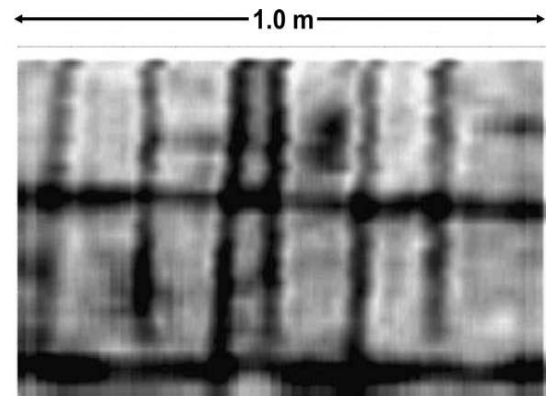
(a) – Schematic sketch of a radargram



(b) – Schematic sketch of a time slice.



(c) – Example of a radargram from concrete floor.



(d) – Example of time slice from concrete floor.

Figure 2.3 – Wave view for different material from radar diagram (EuroGPR, 2010)

There are many factors which affect the acquisition of GPR data and these are discussed in sections 2.5.4 and 2.5.5.

As can be seen GPR can accurately establish detailed information regarding actual functional defects and anomalies of a bridge structure thus aiding in the fulfilment of objective three of this thesis. However in order to accurately quantify these defects the many factors which affect the GPRs electromagnetic waves must be examined.

2.5.4 GPR Antenna Signal Factors

As stated previously the ability to obtain applicable and correct data from the GPR relating to the position of buried objects etc. is affected by a number of significant

factors. These factors are identified and discussed below and include antenna type, dielectric constant, conductivity and attenuation.

2.5.4.1 Antenna Types, Orientation and Selection

It is useful to discuss the antenna types before any GPR survey in relation to the features investigation. GPR antennae can be used to transmit energy, receive energy or both. GPR techniques use the signals of electromagnetic waves to present the subsurface structure images. These wide-band electromagnetic signals are centre frequencies generated by transmitting antennae and a high power pulse generator (Cagnoli and Russell, 2000).

Also Narayanan et al., (2004) and Berard and Maillol, (2007) agree that this technology uses radar pulses with different frequencies to image the subsurface. Low frequency signals obtain poor quality resolution but penetrate deeper and better, while high frequency signals obtain high quality resolution but are not able to penetrate deeper into the subsurface. Using both of them can provide better resolution and deeper penetration, simultaneously.

As detailed by Hugenschmidt et al., (2010) and Jol (2009), the GPR electric field is a component of the EM pulse, this is created by the dipole and used to gather information relating to underlying objects such as pipes and rebars. The reception of the reflected energy is affected by this electric field which is polarised along the main axis of the dipole.

On the other hand Clark et al., (2003) concentrates on the importance of the use of the antennae for surveying and on choosing a certain antenna orientation in relation to the survey. According to He et al., (2009) the most common GPR antennas are dipole antennas which radiate linearly polarised energy along the long axis of the dipole. Most commercial GPR antennas are devoted to purposefully polarise the dielectric field parallel to the long axis. Dipole antennas are commonly used in the Parallel Broadside (PL-BD) to get a 2D cross section because they have a larger footprint in the "broadside" direction than in the "end fire" direction. When the GPR scanner is parallel

to buried objects, the electric magnetic field is perpendicular to these objects which scatters the electric field and makes them difficult to identify. The optimum angle for detection depending on the direction of the buried object which is typically unknown, necessitating both L and T scans of the bridge deck.

Thus, underlying objects within the bridge deck which lie parallel to the dipole receiver (perpendicular to the movement of the GPR scanner) are easily detected as they do not affect the polarisation of the electric field. Objects which lie perpendicular to the dipole scan direction (parallel to the movement of the GPR scanner) will effectively scatter the electric field and be more difficult to identify. This results in the necessity for both Longitudinal (L) and Transversal (T) scans, so that buried objects can be successfully identified regardless of the angle at which they are laid. The information gathered by both the L and T scans combines in the data processing software to produce a complete 2D or 3D radargram of all buried objects.

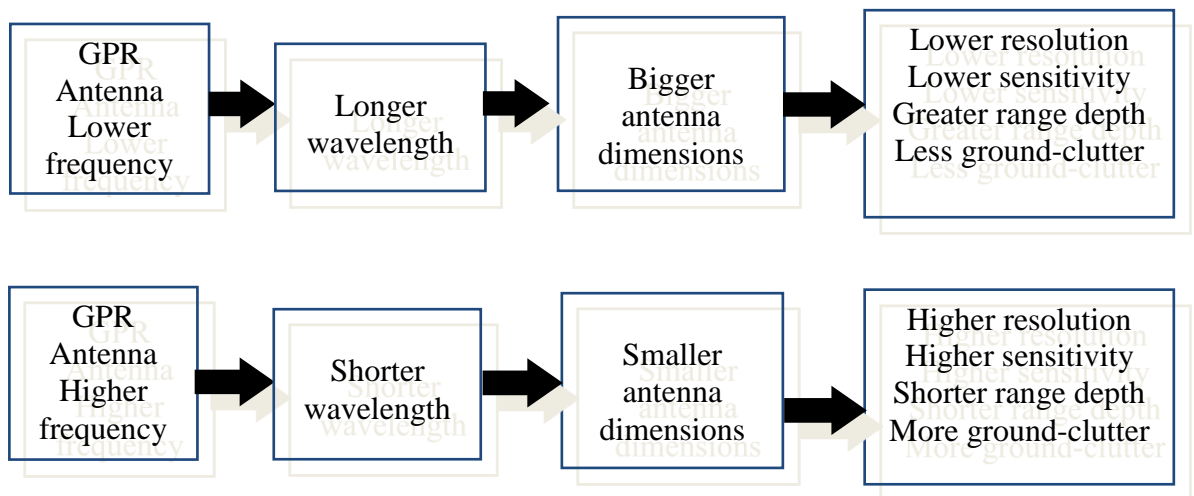


Figure 2.4 – Summary of GPR antenna frequency

Figure 2.4 shows the relationship between resolution and penetration depth in GPR antenna with both low and high frequency. The resolution is dependent on the frequency of the antenna, with high frequencies creating higher resolution which results in a lower penetration depth. As can be seen from Figure 2.4, the frequency affects the resolution as higher frequencies produce shorter wavelengths which give a more accurate representation of the bridge deck but do not have the same ability as longer wavelengths to penetrate deeper.

It is of crucial importance to select the correct antenna to obtain the correct results. It is highly recommended given the information above that two antennas be used (one of a higher and lower frequency) so that both the specifications of accuracy and depth penetration are fulfilled.

2.5.4.2 The Transmitting and Receiving Antenna

The transmitting antenna generates the electromagnetic wave, which travels through the material with a velocity determined primarily by the permittivity of the material, and then displays the buried object on a radargram. The transmitting antenna is a combination of a transmitter and a transmitting dipole. The total transmitting power of the antenna is a few milliWatts (Daniels, 2007).

The receiving antenna monitors the waves reflected back from the surface of the buried object and records the information on a digital storage device for processing and interpretation. The receiving antenna is a combination of a receiver and a receiving dipole. (Manacorda et al, 2009)

2.5.4.3 Dielectric Constant or Permittivity

Chang et al., (2008) defines the Dielectric Constant, also known as Relative Dielectric Permittivity, as the capability of a material to store, and allow passage of, electromagnetic energy when a field is imposed on it. This affects GPR results, as different materials affect attenuation of electromagnetic radar waves in different magnitudes; for example some materials attenuate the whole radar wave resulting in minimal reflection. Perez-Gracia et al., (2009a) and Loizos and Plati, (2007) agree that the stronger the contrast between the material's dielectric constants, the stronger the reflection will be and therefore a clear intersection of the pulses path is seen. For example in relation to GPR, concrete and metal piping will have differing dielectric constants so the reflection from a pipe encased in concrete will be identifiable from a GPR scan. On the other hand Perez-Gracia et al., (2008) and EuroGPR, (2010) point out that dielectric constant may change with frequency. Therefore, materials with similar dielectric constants result in weaker signal reflection and this makes differentiating

between the boundaries of these materials more complex. This can affect the identification of areas of moisture present in the bridge deck being scanned. A table is available which lists a selection of dielectric constants for various materials from Daniels (2007).

2.5.4.4 Conductivity

Perez-Gracia et al., (2008) states that the Electrical Conductivity is an additional aspect which directly influences the transmitted and received EM pulse, and this can change the reduction in the pulse as it travels through the material. The electrical conductivity of a material is a measure of the capacity of this material to conduct an electrical current, with higher values indicating a more conductive substance.

Manacorda G., (2009) and Jol, (2009) also state that when the EM pulse travels through the material under investigation, it transfers a current into the material. The larger the value of conductivity within the material, the greater the amount of energy absorbed from the EM pulse and hence there is necessity to diminish the intensity of the pulse. Metal completely reflects the radar energy, so when a radar wave hits a metal object, no penetration occurs and the transmitted pulse is reflected entirely back to the receiver. Thus rebars are shown as very defined on GPR radargrams for this reason. Because of the spacing and positions of rebars when compared to that of a metal sheet, the EM pulse is not totally reflected, resulting in features below the rebars being visible providing the spacing between them is not too small. If the spacing is minimal, the rebars react in a similar fashion to a metal sheet, reflecting the EM pulse totally back to the receiver and not permitting any penetration below them. A table is available from EuroGPR (2010) which provides a record of materials along with their corresponding electrical conductivity. As the conductivity in soils is directly connected to water content, especially water which contains free chloride ions, the greater the water content, typically, the higher the conductivity.

Hence, high water content can impede particular factors in bridge deck assessment, such as rebar positioning or depth of cover.

2.5.4.5 Attenuation

Attenuation is defined as the loss in energy of the EM pulse in relation to the signal amplitude as it passes through a medium; its unit is decibels per metre (dB/m). Various frequencies attenuate at various rates, with larger frequencies being subject to greater attenuation when compared with those of lesser frequencies (Jol, 2009).

Hence, if attenuation does not occur, in theory there is no limitation to the depth of penetration that can be reached, although in practice this is not the case.

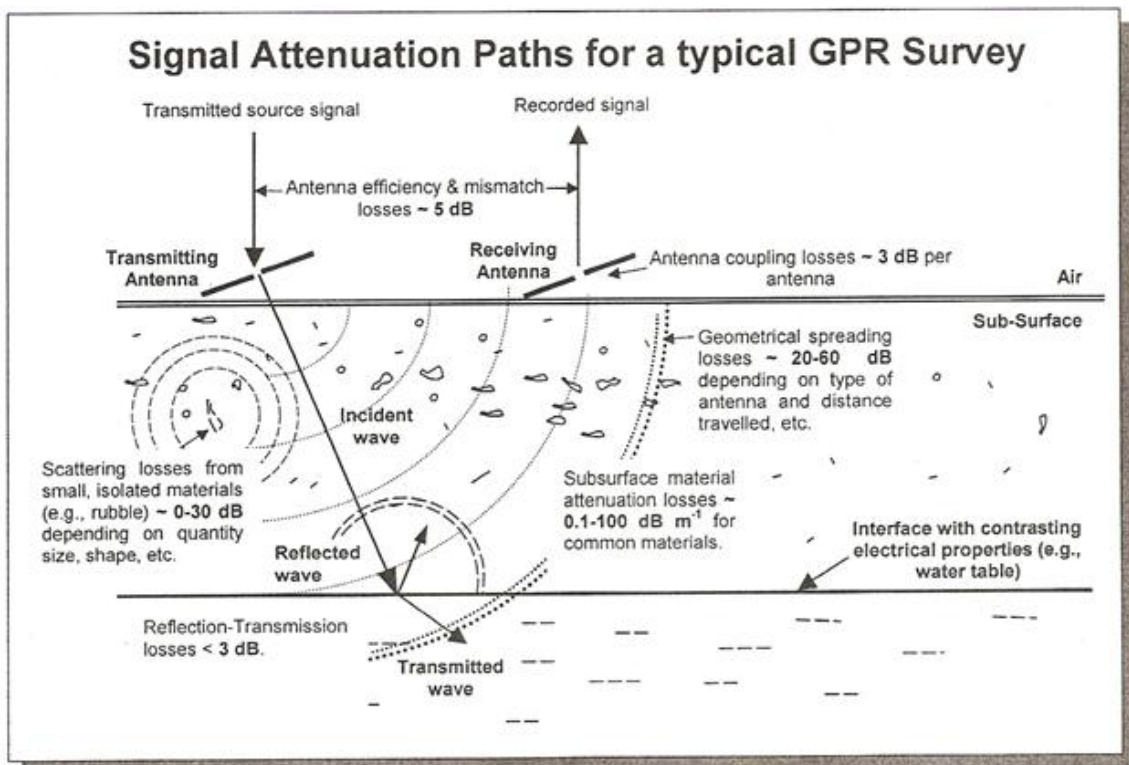


Figure 2.5 – GPR attenuation paths (EuroGPR, 2010)

Several aspects can impact penetration depth, and these are illustrated in Figure 2.5. However the dominant factor on penetration depth is attenuation losses. Figure 2.5 also shows the source of increased attenuation. It also includes the following aspects of GPR attenuation paths (EuroGPR, 2010):

- Frequency of the EM pulse. The greater the frequency, the greater the resolution achievable which results in clearer radargram images.

- EM pulse spread.
- Boundary interface reflections.
- Scattering of the pulse.
- Antenna position in relation to the ground.
- Losses which differ from one GPR system to another are also present with attenuation apparent due to material properties relating to conductivity.

2.5.4.6 Moisture

As stated earlier, GPR is a very useful, comparatively quick to use, non-destructive tool in the investigation of bridge decks.

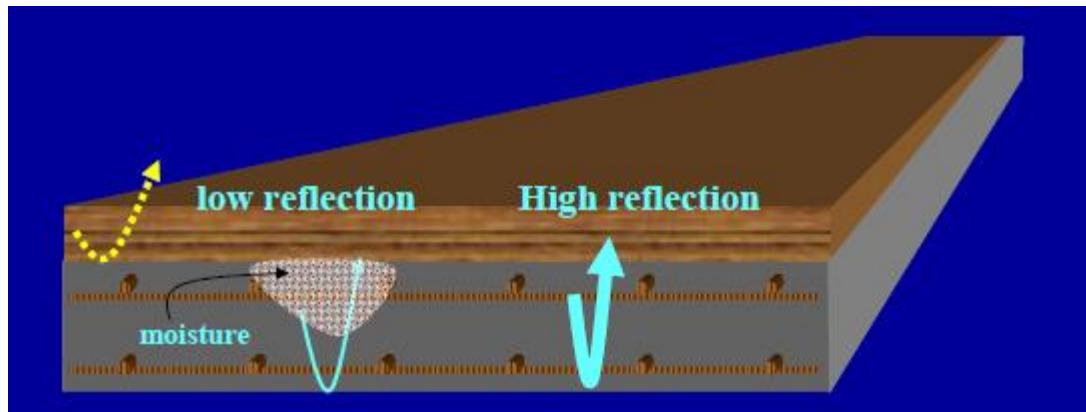


Figure 2.6 – Reflection view of the deck (Rhazi J., 2002) (Evans et al., 2008)

GPR's apparent sensitivity to moisture makes its use promising in the detection of factors such as the corrosion of reinforcing steel, alkali silica reaction and freeze/thaw damage; the main causes of bridge deck deterioration (Figure 2.6).

Moisture in the bridge deck is a very serious issue as it can potentially lead to the structural weakening of the rebars. There are four phases in the transport of moisture in concrete (Digest 491, 2004):

- Adsorption

In dry initial conditions, the moisture which enters the concrete attaches to the walls of the pores. A thin moisture coating may remain even subsequent to the drying process.

- Condensation

In general, concrete pores are filled with a continuous vapour phase. This moisture can be diffused throughout the concrete owing to pressure differentials.

- Liquid and vapour transport

As humidity increases, the moisture present in the vapour phase condenses causing a layer of liquid to form. This is in addition to the vapour layer discussed above.

- Liquid Transport

In a saturated environment, the liquid phase becomes continuous.

As well as these mechanisms a further transport process is present for cases of excessive cracking. Cracking causes preferential pathways through the cover allowing for water to be transported into the centre of the concrete.

This causes corrosion to the rebars in the form of: carbonation, moisture, and chloride ion ingress (Barnes and Trottier, 2000). Concrete carbonation and the chloride ions in a solution damage the normally alkaline environment of concrete in which a passive oxide layer exist. This passive layer generally prevents further oxidation of the steel reinforcement (Barnes and Trottier, 2000). Additionally, chloride ions create anodic and cathodic areas on the reinforcement causing oxidation of the steel at the anode and a transfer of electrons at the cathode, forming hydroxyl cations. As ferric oxide forms, volume increases, causing internal stress to increase leading to the debonding of concrete cover from the reinforcement layer (Barnes and Trottier, 2000).

The impact of cracking on carbonation and rebar corrosion is highly variable with crack width less important to corrosion than crack frequency, cover depth and concrete quality. Figure 2.7 shows the corrosion of a rebar in cracked concrete (Digest 444 part 1, 2000).

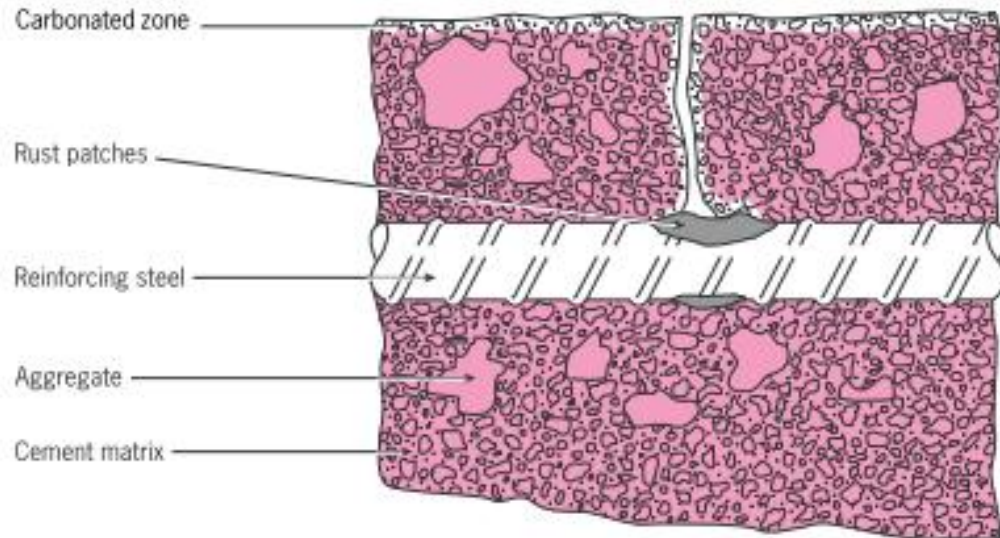


Figure 2.7 – Diagrammatic view of steel corroding in cracked concrete (Digest 444 part1, 2000)

For these reasons, it is important to quantify areas of significant moisture in the bridge deck, as this moisture can lead to the corrosion of rebars in this area.

Early studies using ground-coupled systems were carried out to identify delamination in concrete bridge decks - data analysis was supported by qualitative investigation of the radargram produced by GPR (Loulizi, 2001).

Furthermore, a commonly used method of assessing deck condition is to map using the reflection amplitudes from layer interfaces and the top rebar. The presence of longitudinal reinforcement bars has proved problematic in data collection using air coupled antennas but Romero and Roberts (2004) have studied a special dual polarisation horn antenna setup and processing technique which eradicates this. In assessing the accuracy of GPR results on bridge decks, Shin and Grivas (2003) concluded that rebar reflection data detects defects with 75% accuracy. Surface dielectric value did not distinguish defects from the decks. There is debate over the reliability of GPR testing, particularly in the testing of bridge decks, partly due to resolution issues, and hence higher frequency antennas are recommended for use in these surveys (Huston et al., 2002).

On the other hand, the strength and deformation of road structures and subgrade soils is significantly affected by moisture content. As such, it is important in highway design (in areas with expansive clay, and in assessing the vulnerability of soils to frost) to gain knowledge of the moisture content of the subgrade soil to approximate its stability and compressibility (Saarenketo and Scullion., 2000). This applies to bridge decks also with moisture significantly affecting the yield strength of the concrete and causing cover delamination's. It is thus crucial to quantify its presence on the bridge deck so its detrimental effects can be mitigated.

It is valuable to have measurements of the dielectric properties of various materials, which can be affected by GPR frequencies, temperature and moisture. In investigating the dielectric properties of asphalt samples in the range of 100Hz to 12GHz, Jaselskis et al., (2003) found that the dielectric constant of asphalt samples increased with both temperature and moisture (greatly at low frequencies and slightly at higher frequencies) (Evans et al., 2008).

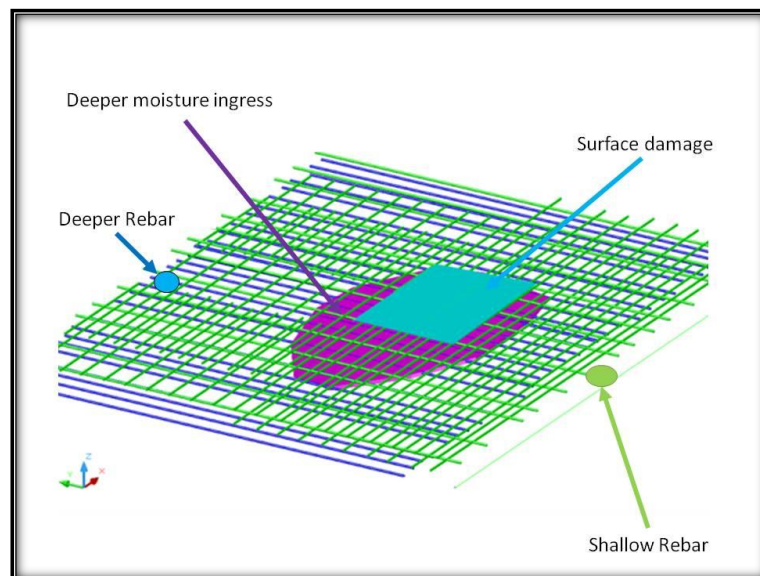


Figure 2.8 – Drawing of a moisture depiction view (Gokhan Kilic, 2011)

Daniels (2007) found that water has a dielectric constant of around 80 and that just a small rise in moisture (Figure 2.8) can significantly alter the bulk dielectric constant of asphalt materials (with a dielectric constant of approximately 2-12 ϵ_r). This correlation

between moisture and dielectric constant lies behind the “time domain reflectometry” method in assessing soil moisture content (Evans et al., 2008).

GPR requires high electrical resistivities and good contrast in dielectric constants and is possible because the void zone is made up of various materials. Pavement has layers of various properties and so cannot be applied here. The ground water table must be visible on the radargram and therefore a longer time is taken for improved depth penetration, which leads to diminished resolution on the top of the pavement. Some of the layers will not be visible and only the variation of the visible layer will be shown. GPR also does not take account of the fact that the dielectric material is different for each layer initially making it impossible to establish from the visible layer, which layer contains more moisture (Loulizi, 2001).

It is crucial to quantify the existence of moisture in a bridge deck as it can lead to structural damage.

2.5.5 Radar Stratigraphy

The main purpose of radar stratigraphy is to characterise radar features and correlate them to specific depositional environments (Vandenberghe and van Overmeeren, 1999). Also Ékes and Hickin, (2001) reviewed that radar reflection signal configurations from different types of element reflections can give very similar results; as a result the interpreter’s observation is quite important. Furthermore, GPR radar systems can determine with different depths the shape, extent and position of features but to image features depends on the frequency. Higher frequency GPRs can image moderately scaled features (cm to tens of cm) but only within the first few metres of the subsurface. Lower frequency GPR signals can penetrate deeper (tens of m) but can only image larger-scale features of a metre or more in size (Figure 2.9).

Electromagnetic Spectrum

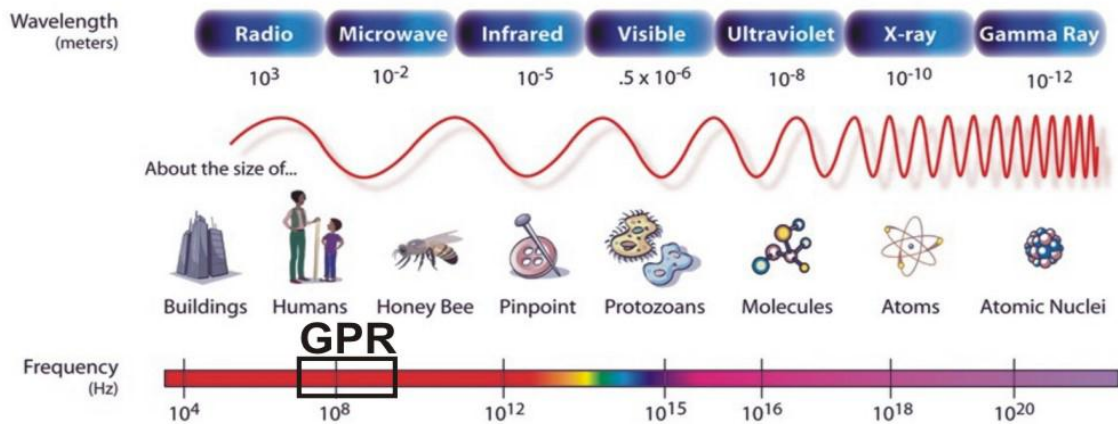


Figure 2.9 – Electromagnetic Spectrum (NASA, 2011)

Daniels, (1996) also describes how the GPR radar signal is dispersed and attenuated by the absorption, scattering, geometrical spread and moisture content of the objects.

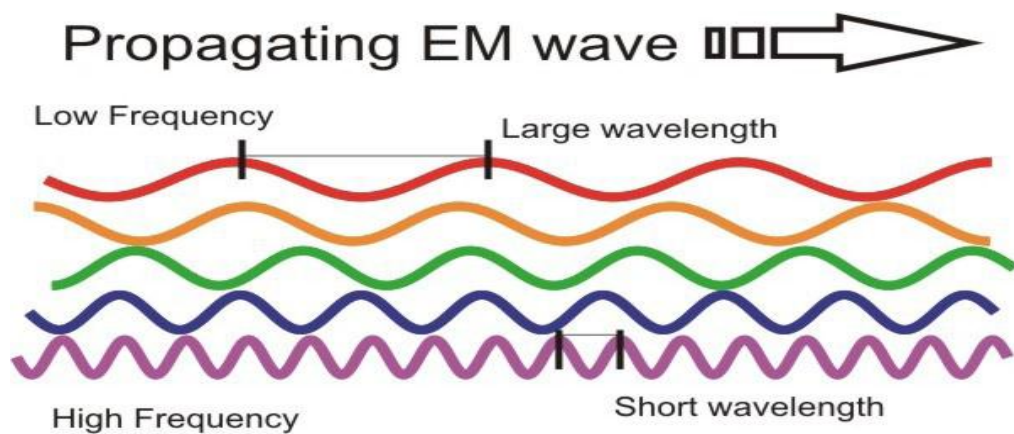


Figure 2.10 – Propagating Electromagnetic Wave (www.sciencejunkies.com, 2010)

The attenuation and velocity of GPR radar waves are dependent on the dielectric and conductivity properties of the object. The signal propagation affects wavelength and increases with depth, the signal becomes weaker and there is less signal energy to be reflected (Figure 2.10) (Davis and Annan, 1989).

However, GPR signals cannot penetrate in wet, clay-rich conditions or with saline objects because any specific frequency velocity of the materials also affects the wavelength. So, wavelength and, therefore, target resolution is determined by material

velocity and frequency. In high velocity materials at low frequencies (e.g., dry sands, concrete, etc) target resolution is poor, whilst low velocity materials (saturated sands) at high frequencies give good target resolution.

2.5.6 Velocity

The velocity of GPR is utilised in assessing the depth of layers or features. The velocity is influenced by the water content and change in materials and their ability to absorb and reflect back energy (Saarenketo and Scullion, 2000). Loizos and Plati, (2007) point out that the energy reflections depend on the velocity of the GPR waves' propagation by the properties and depth of different layers as a function of the dielectric constant. The dielectric properties of water content layers depend on the compaction during the GPR measurements which are only valid for a few days.

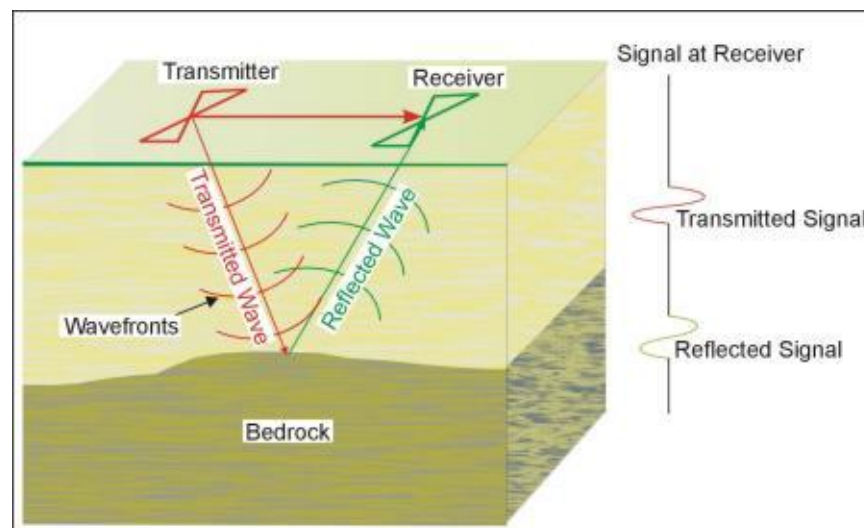


Figure 2.11 – The GPR principle in layer thickness. (Highway CFL, 2010)

Figure 2.11 shows a visual representation of how the GPR sends signals and then receives its signals, and a simplified version of result data from the scan.

Therefore the velocity of GPR can be measured (equation 2.1) by carrying out calculations (Common Depth Point estimation or Wide angle reflection), by means of direct measurement of the depth of cores, and by using pre-determined velocities from the literature (Loizos and Plati, 2007).

$$V_r = \frac{c}{\left\{ \left(\frac{\epsilon_r \mu_r}{2} \right) * [(1 + P^2) + 1] \right\}^{\frac{1}{2}}} \quad (2.1)$$

V_r : The speed of radio waves in a material

c: speed of light (m/s)

ϵ_r : relative permittivity or dielectric constant of the material

μ_r : relative magnetic permeability (=1 for non-magnetic materials)

P: the loss factor,

$$P = \tan \delta = \frac{\sigma}{\omega \epsilon}$$

On the other hand, GPR techniques are often applied to low loss materials ($\tan \delta < 1$) due to the radio frequencies at which it operates. As a result ($P=0$, $\mu_r=1$) and the velocity propagation of the wave is simplified to (equation 2.2):

$$V_r = \frac{c}{\sqrt{\epsilon_r}} \quad (2.2)$$

V_r : velocity propagation of the radar signal (m/s)

c: speed of light (m/s)

ϵ_r : relative permittivity or dielectric constant of the medium (Fm^{-1})

However, in most situations, the travel time and reflection amplitude measurement from a short electromagnetic pulse transmitted then partly reflected off electrical interfaces through a structure depends on impulse GPR techniques. These electrical interface differences come from the GPR waves' reactions to changes in moisture content or material density (Saarenketo and Scullion, 2000). Morganti et al., (2007) agrees with Saarenketo and Scullion, (2000) that the velocity propagation capacity of radar electromagnetic waves depends on electrochemical, geometries, dielectric properties and water saturation.

Jol (2009) described in greater depth how GPR works and the speeds at which electromagnetic waves travel through different mediums, for example in air they travels

300mm/ns, in asphalt between 130-175mm/ns and in water at 33mm/ns. A list of materials along with corresponding dielectric constant value (relative permittivity) and electrical conductivity is available from Eurogpr (2010).

Although high water content can hamper some parts of bridge deck assessment such as rebar positioning or depth of cover, it can be advantageous in some aspects as it detects failures in the waterproofing by identifying areas of unusually high signal absorption in the processed data when compared with surrounding areas.

Figure 2.12 shows three different views of a GPR result – these radar images show black and white bands in various forms and shapes, which split and join at all angles with sands, clays, gravel, and are mixed with stones, tree roots, construction debris, and utilities of all kinds. (Lester and Bernold, 2007)

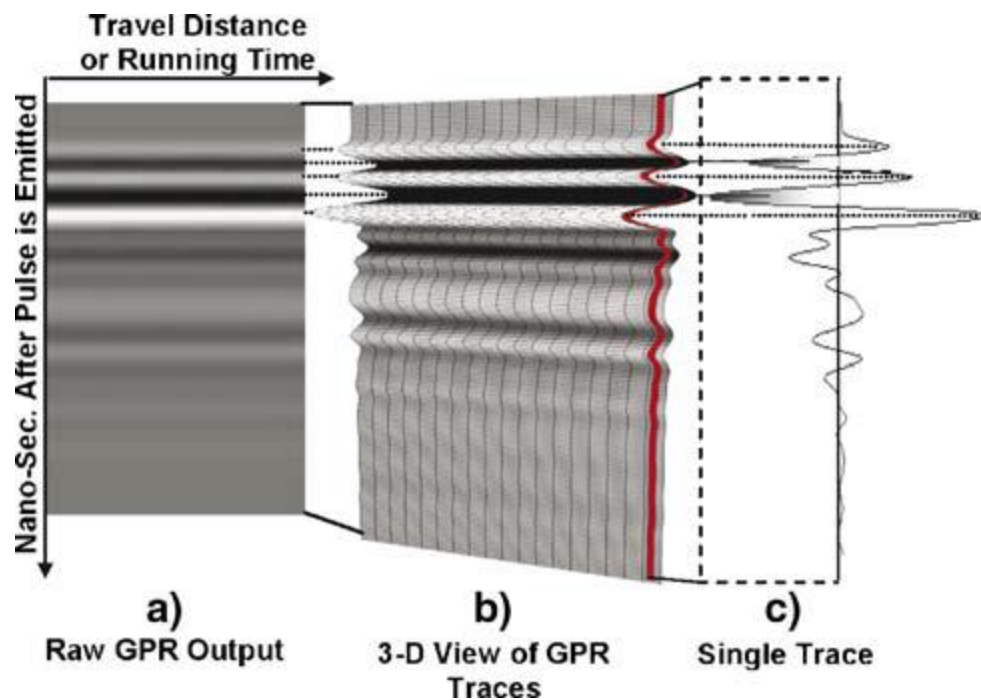


Figure 2.12 – Three views of radar trace profiles in homogenous material. (Lester and Bernold, 2007)

The two way travel time is the radar signal transmitted to the target, and reflected and received by the antenna. The velocity or depth can be resolved with equation (2.3).

$$d = v_r * \frac{t_r}{2} \quad (2.3)$$

d : depth of the target

V_r : velocity propagation of the radar signal (m/s)

t_r : two way travel time

In Figure 2.13 the Common Centre Point technique depends on the GPR transmitter and receiver, if both moved equal distances from the common centre point.

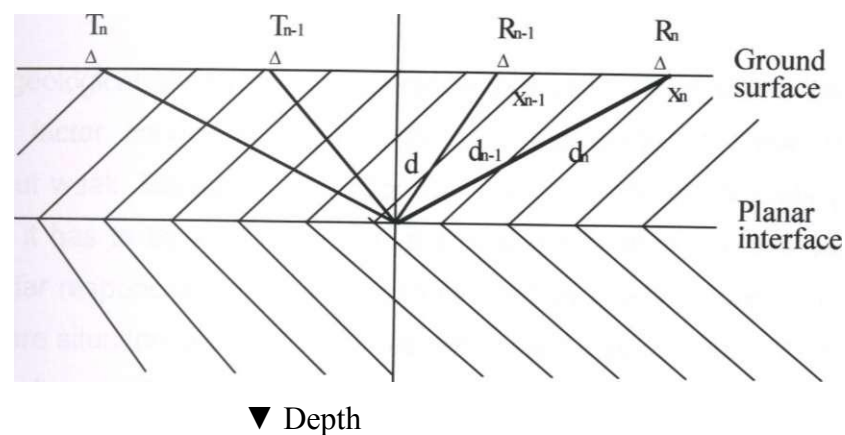


Figure 2.13 – Common depth point method of depth estimation, (Daniels, 1996)

2.5.7 Advantages and Disadvantages of GPR

Lester and Bernold (2007) identified that GPR is able to detect buried utilities such as polyethylene water and gas pipes as well as utilities such as fibre-optic cables which are a subsurface infrastructure worldwide. It prevents damage to underground utilities because digging and trenching into the ground can easily damage close utilities.

Bungey (2004) represents the advantages of GPR as an advanced non-destructive investigating technique which can be used quickly and effectively in a large area. GPR equipment staffs are light, portable and easy to operate on survey areas. GPR has the sensitivity and potential to detect defects and display the results as a radargram. GPR investigations can be conducted anywhere and provide records or process the signals

immediately. McMechan et al., (1998) identifies that another advantage of GPR on geometry and inside materials is to provide spatial constraints on examination by adding the third spatial dimension to outcrop data. GPR has the potential to detect concrete delamination and near-surface voids before they are visible at the bridge surface and reported by visual survey.

On the other hand there are also disadvantages of GPR discussed by several researchers. Schrott and Sass, (2008) and Bungey, (2004) believe one of the disadvantages of GPR to be its sensitivity which causes the device to receive other unwanted signals such as mobile phone signals, radio signals and any electromagnetic waves which can affect the data. GPR performance can be affected by heavy rain or snow. Experienced individuals and experts are required to produce effective GPR surveys but it does not give much detailed information such as grain size/aggregate quality.

These disadvantages may have an impact on the results obtained from this survey, however the advantages are seen too far outweigh the drawbacks of this technique.

In summary, the use of GPR technology in bridge health monitoring and assessment has gained popularity in the last decade. It has proven to be a valuable tool in identifying certain aspects of bridges' structural components such as:

- Asphalt and concrete slab thickness measurement
- Deck slab and protective concrete damage location
- Drainage and other buried pipes mapping
- Rebar condition and depth measurement
- Delamination detection
- Moisture damage detection

This identified it as an advanced structural monitoring technique applicable to bridge health monitoring, thus more knowledge was gathered regarding it. This information included factors which affect signal transfer which is of crucial importance and also problems with the detection and identification of moisture. This has proven to be

problematic in the cases of complex compositions such as bridge decks, as factors such as voids and porosity can have a similar appearance on a radargram, this has helped partially fulfil objective one. This objective will be completed by operating, collecting and processing GPR equipment at my preliminary case studies (Forth Road Bridge, St Marys Island Lifting Bridge, Darvel Road Bridge and Rochester Bridge) and main case study (the Pentagon Road Bridge).

In the above section many sources have been cited which confirm the effectiveness and applicability of this NDT demonstrating its usefulness as a bridge health monitoring tool, partially fulfilling objective two. Its ability to establish detailed structural information has also been shown which applies to objective three. Finally the structural information such as rebar position obtained from GPR results can be used to create more accurate FEM which include actual bridge dimensions which aids in the completion of objective four.

This thesis will concentrate on GPR techniques in the detection and measurement of the main defects of bridge deck. This will include the investigation, through modelling, of the effect of rebar positions, layers, moisture and voids on bridge deck to clarify whether the GPR can be relied upon in terms of in moisture identification. Further information on GPR can be found at EuroGPR website (www.eurogpr.org).

2.6 IBIS-S Interferometric Radar Monitoring Technology

2.6.1 Introduction

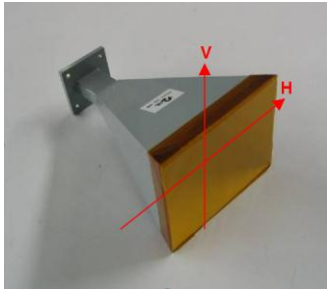
The IBIS-S interferometric radar system is an advanced and sensitive non-destructive technique which measures dynamic or static displacement and vibration of structures such as bridges, towers, buildings, and dams with accuracy of up to a hundredth of a millimetre. Dei et al., (2009) show that it can follow the displacements of a structure, provided that vertical bending movements are predominant with respect to torsional ones and that the interferometric sensor module is transmitting, receiving and operating electromagnetic waves based on the principle of electromagnetic interference between coherent waves. There is a lack of research relating to the measuring of moving vehicle behaviour partly due to difficulties in simultaneously monitoring both the dynamics of the bridge and a moving vehicle.

IBIS-S consists of a radar unit with two horn antennas (Figure 2.14 - b), affixed to a tripod with a rotating head (Figure 2.14 – a). The radar is controlled by IBIS software running on a standard laptop (Figure 2.14 – c) and is powered by a single 12V, 12Ah battery (Figure 2.14 – d).



Figure 2.14 – View of IBIS-S system (photos from Gokhan Kilic, 2010)

Figure 2.15 shows the system consists of a yellow radar unit with two horn antennas, affixed to a tripod with a rotating head.



The IBIS-S horn antenna following characteristics are:

- Maximum gain of 23.5 dBi;
- Horizontal antenna beam width at -3dB: 11deg.
- Vertical antenna beam width at -3dB: 10deg.

Figure 2.15 – IBIS-S Horn Antenna (IDS Manual, 2010)

Most structures have enough natural reflectors to make it possible to perform a measurement without the installation of corner reflectors (Figure 2.16) but their use is recommended.

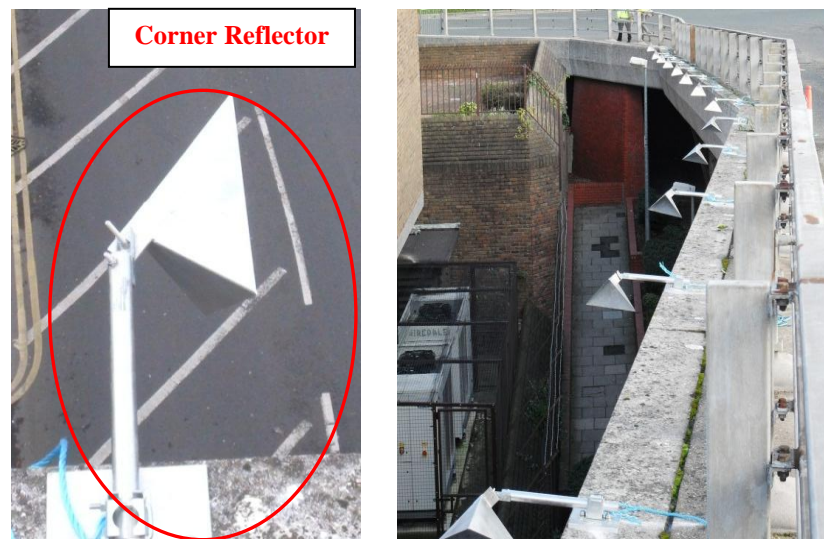


Figure 2.16 – Examples of corner reflectors (Photos from Gokhan Kilic, 2010)

2.6.2 General Principles

The technique calculates displacements along the ideal line linking the sensor to the examination point (radial displacement) and so if the real displacement transpires in a different direction, the displacement must be projected on the basis of geometrical considerations, as shown in Figure 2.17 (IDS manual, 2010).

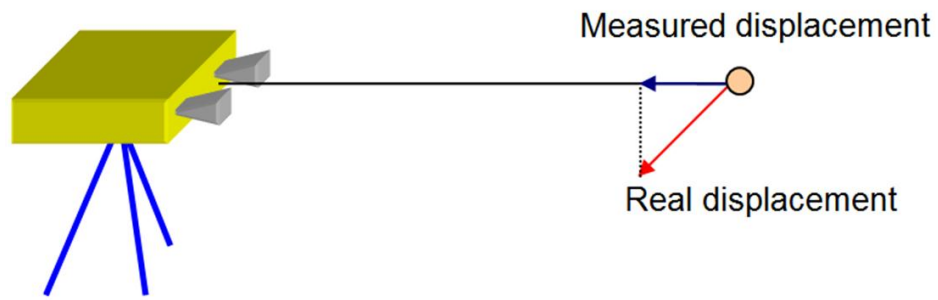


Figure 2.17 – Projection of displacement data (IDS Manual, 2010)

The base of the chief lobe of an antenna can be illustrated as a truncated cone with an elliptic base. The apex of the cone is aligned with the antenna. The base of the cone is elliptical as the lobes of antennas usually have different angular amplitudes in the elevation (V) and azimuth (H) planes as shown in Figure 2.18 (IDS manual, 2010).

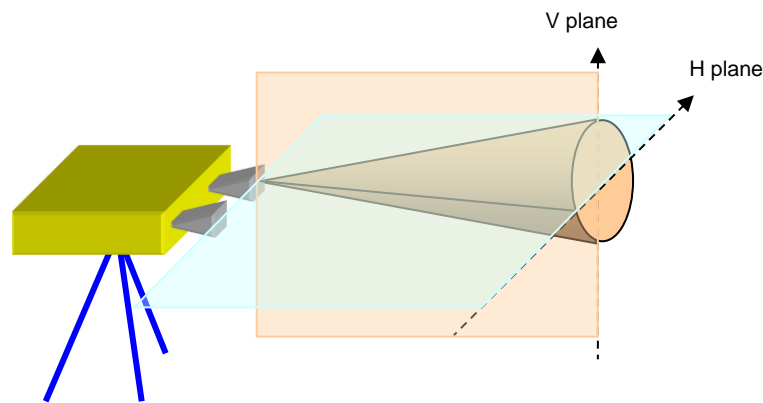


Figure 2.18 – Schematic diagram of the antenna beam (IDS Manual, 2010)

Gentile et al., (2008) point out that the IBIS-S statistical distribution of the displacement and dynamic signals provide information such as any vehicle movement over the bridge. IBIS-S interferometric radar has an excellent performance because it transmits continuous electromagnetic waves at a bandwidth rate ranging up to 100 Hz.

The interferometric investigation supplies information on object displacement by equating phase data, gathered in various time intervals, of waves reflected from the object, giving a measure of the displacement with a precision of less than 0.01mm (intrinsic radar accuracy in the order of 0.001mm) (IDS Limited presentation, 2010). Equation (2.4) determines displacement in the direction of wave propagation (Kocierz et al., 2011). Using trigonometric functions, data on the radial displacement allows for calculation of the displacement in an appropriate coordinate system (Figure 2.19).

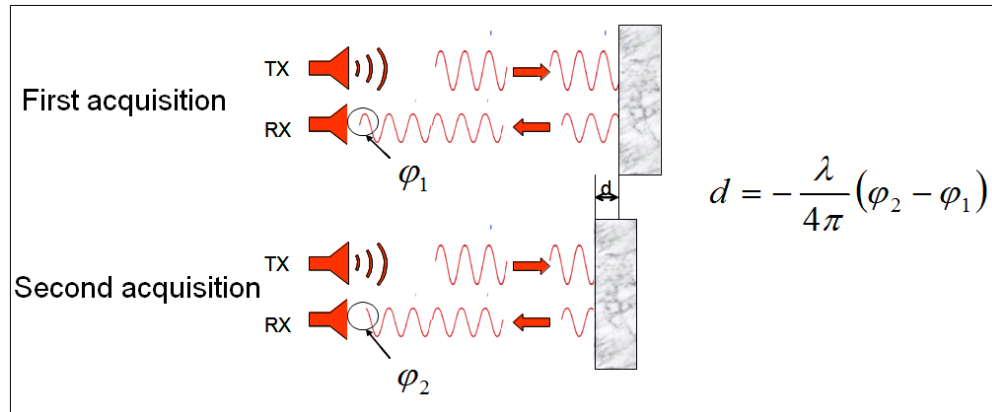


Figure 2.19 – The principle of interferometric measurement. (Ids ltd., 2010)

$$dp = \frac{\lambda}{4\pi} \cdot \Delta\varphi \quad (2.4)$$

where $dp = \text{measured displacement}$

$\lambda = \text{wavelength}$

$\Delta\varphi = \text{carrier wave phase shift}$

As described by Mayer et al., (2009), once the displacement response of several points has been identified at discrete acquisition times, the response of each point is assessed using the differential interferometry method, which contrasts the phase information of the back-scattered electromagnetic waves collected at the various times.

IBIS-S sends and receives the electromagnetic waves of a target displacement to determine the phase shift measured by sensor modules at the discrete acquisition times. The equation (2.4) for radial displacement (dp), the phase shift ($\Delta\varphi$) and electromagnetic signal wavelength (λ) are shown equation (2.5),

$$dp = \alpha \frac{\lambda}{4\pi} \Delta\varphi \quad (2.5)$$

Typically, when a target surface is displaced, a phase shift measured between the radar signals reflected by the target surface at the discrete acquisition times occurs. The radial displacement d_r (i.e. the displacement along the route of wave propagation) and the

phase shift $\Delta\phi$ are linked by equation (2.5) where λ is the wavelength of the electromagnetic signal.

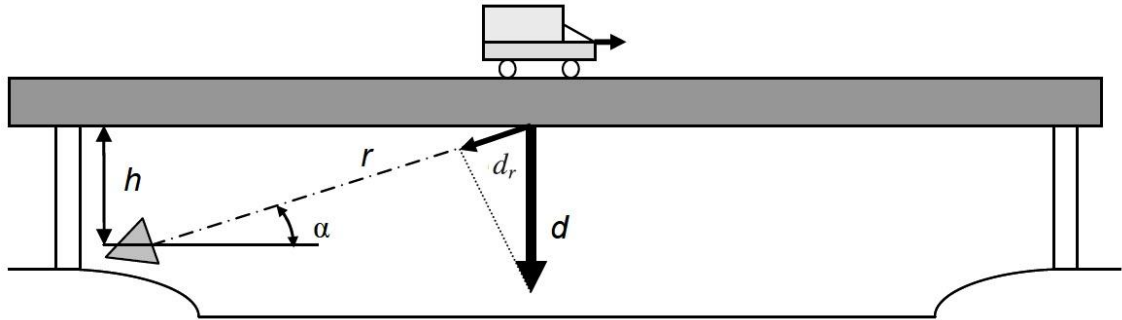


Figure 2.20 – Radial displacement vs. projected displacement. (Bernardini et al., 2007)

Successions of electromagnetic waves are emitted from the sensor module throughout the measurement stage. Phase information is processed at intervals of up to 5 milliseconds in order to identify any developing displacement. The interferometric technique gives a radial displacement measurement of all the structural reflections illuminated by the antenna beam. When the radial displacement d_r has been appraised, the vertical displacement d is established by way of geometric projection, as shown in Figure 2.20 and equation (2.6) (Mayer et al., 2009).

$$d = \frac{d_r}{\sin(\alpha)} \quad \rightarrow \quad \sin(\alpha) = \frac{h}{R} \quad \rightarrow \quad d = d_r \cdot \frac{R}{h} \quad (2.6)$$

Albaa et al., (2008) describe how the stepped frequency continuous wave (SF-CW) enables a range resolution of up to 0.5m. Rather than transmitting a short pulse of time duration with a large bandwidth in the frequency domain, IBIS transmits a burst of N monochromatic pulses with identical and increasing frequency (with set frequency step of Δf) within a bandwidth B , as shown in equation (2.7)

$$B = (N - 1)\Delta f \quad (2.7)$$

The system uses the SF-CW technique to provide range resolution. From this SF-CW technique the radar sweeps a large bandwidth (Equation 3) (Lee et al., 2002), (Bernardini et al., 2007), (Gentile et al., 2008).

IBIS-S can distinguish between different targets, which require use of the Stepped-Frequency Continuous Wave (SF-CW) technique. To attain high range resolution, pulse radars use short time duration pulses. The range resolution Δr correlates to the pulse duration t as follows equation (2.8):

$$\Delta r = \frac{ct}{2} \quad (2.8)$$

where c is the speed of light in free space. $t = 1/B$, the range resolution; as shown in equation (2.9)

$$\Delta r = \frac{c}{2B} \quad (2.9)$$

As the frequency bandwidth of a transmitted electromagnetic wave increases, range resolution increases, as illustrated in Equation (2.6). This means that targets in close proximity can be distinguished along the radar's line of sight (Mayer et al., 2009). Like a short pulse with a large bandwidth B , N monochromatic pulses sample the situation in the frequency domain. The signal source of a SF-CW radar hesitates at each frequency for a duration sufficient to allow the echoes to be received back to each receiver, meaning that the time taken for every single pulse (T_{pulse}) is indicative of the maximum distance (R_{max}) to be observed, as shown in equation (2.10)

$$T_{pulse} \geq \frac{2R_{max}}{c} \quad (2.10)$$

Also IBIS-S system operational characteristics are summarised in Table 2.1. (Bernardini et al., 2007)

Table 2.1 – IBIS-S operational characteristics. (Bernardini et al., 2007)

Parameter	
Maximum operational distance (for minimum 40Hz sampling frequency)	500.00 m
Maximum sampling frequency	100.00 Hz
Displacement sensitivity (accuracy)	0.01 mm
Operative weather condition	All

Figure 2.20 shows a model range profile achieved when the radar transmitting beam illuminates a succession of targets at various distances and angles from the sensor. The range profile refers to N target points at 0.50 m intervals. When more than one object with scatter properties that are alike lie in the same range bin (here with a depth of 0.50 m) the outcome is a distinctive radar echo. In this example, no discrimination between displacements of different points can be made, but the echo will provide a depiction of all mean changes of all scatters (Albaa et al., 2008). For the positioning and identification of displacement, the use of three radar techniques is necessary (Alba et al., 2008). Stepped-frequency continuous wave modulation (SF-CW) is implemented in the detection of the surface of objects situated at various distances from the apparatus (Kocierz et al., 2011).

The response of the samples acquired in the frequency domain is reconstructed in the time domain of the radar by taking their Inverse Discrete Fourier Transform (IDFT). The amplitude of each sample of the IDFT of the acquired vector samples is then acquired in order to find the amplitude range profile of the radar echoes so that a one dimensional map of scattering objects in the viewable space in function of their relative distance from the equipment can be acquired (Albaa et al., 2008).

2.6.3 SAR Technique

The Synthetic Aperture Radar (SAR) method permits radars with wide physical antenna beam width to attain high angular resolution in azimuth. The coherent composition of the acquisitions allows for the obtaining of a synthetic antenna with an inverse beam width proportional to the relative movement between the scenario and the radar (Ferretti et al., 2007).

In uniting the SF-CW and SAR techniques, the radar image is arranged into pixels with dimensions of 0.5 m in range and $4.5, 10-3r$ m in crossrange, where r is the distance from radar to target.

Figure 2.21 represents a resolution grid for a system with a distance resolution of 5 m and angular resolution of 5.2 mrad. The object shape under examination is essential in

allowing discrimination between exact observed points. If the range and crossrange directions in the horizontal plane are taken into account, and if the object has a vertical surface, the amount of scatteres will be insignificant but, if the object has a tilted surface, the amount of scatter points will increase significantly (Albaa et al., 2008).

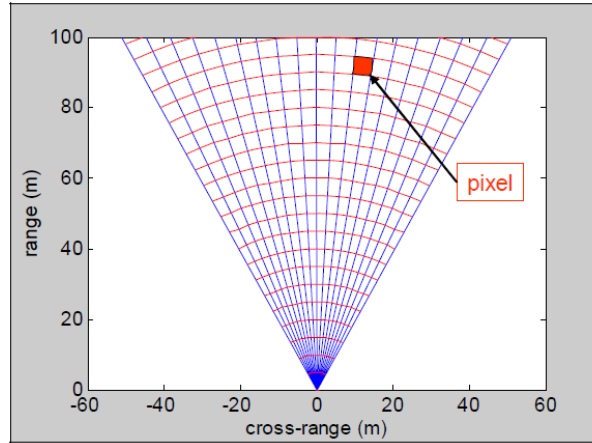


Figure 2.21 – Example of a spatial resolution grid (Albaa et al., 2008)

2.6.4 Interferometric Technique

The Interferometric technique is used with radars on the ground, which allow the illumination of precise areas with a very high range resolution. On determining a 2-D map of a structure at uniform sampling intervals, the displacement response of every pixel is assessed allowing the displacement of a scattering object to be appraised by contrasting the phase information of the electromagnetic waves reflected by the object at various time instants (Albaa et al., 2008). Any displacement is identified by the phase shift gauged by the radar sensor at the discrete acquisition times. The LoS (Line of Sight) displacement (i.e. the displacement along the route of wave propagation) and the phase shift $\Delta\phi$ are related as follows in equation (2.11):

$$d_{LOS} = \alpha \frac{\lambda}{4\pi} \Delta\phi \quad (2.11)$$

2.6.5 Static and Dynamic Monitoring of a Bridge Structure

IBIS-S is capable of monitoring vibrations of up to 100Hz and line of sight deformations of less than 0.01mm. The maximum range is approximately 500m and it

produces a one dimensional image with a range resolution of up to 0.5m. Dei et al., (2009) show that dynamic testing with interferometric radar is able to provide dynamic images with a sampling rate high enough to track the movements of structures such as bridges (Figure 2.22).



Figure 2.22 – Dynamic monitoring of a full-scale bridge with IBIS-S (Ids ltd., 2012)

The IBIS-S equipment calibrates using its own internal calibration software (IDS Manual, 2010). The calibration can be performed while the cherry picker was moving across the bridge during a pre-test as shown on Pentagon Road Bridge IBIS-S survey (Figure 2.23).

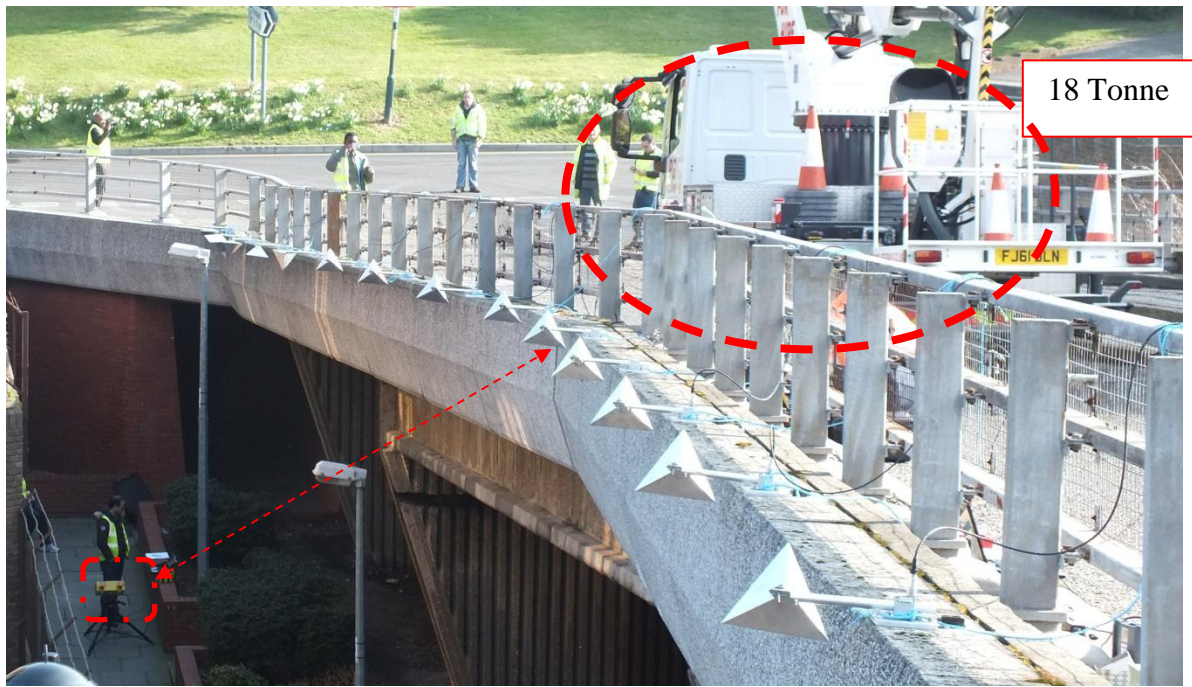


Figure 2.23 – IBIS-S calibration on Pentagon Road Bridge (Gokhan Kilic, 2011)

In Summary, IBIS-S is a new assessment interferometric radar technique of structures, with significant advantages over other techniques such as the remote sensing at a large number of points (Gentile and Bernardini, 2008). With the exception of placing corner reflectors, IBIS-S monitoring is quick and easy to use but is not mobile. It can provide practically permanent monitoring of the static and dynamic displacements of the entire structure during all weather conditions. IBIS-S interferometric techniques can be used to detect either static or dynamic displacements in real time, although trees, water, fences, wires and other features below can block electromagnetic waves.

Gentile and Bernardini (2008) apply a new IBIS-S interferometer to examine the effects of traffic induced dynamic response on a full scale bridge. They also used accelerometers to verify their results in a similar fashion to the approach used in this thesis.

Gentile and Bernardini (2008) describe the advantages of IBIS:

- It is easy to use and no interruption in bridge use is required for the testing to take place, which is necessary as the traffic itself forms part of the conditions.

- The most ideal loading condition is a load moving over the structure, where it will load the bridge at numerous points, thereby exciting all modes sensitive to vertical loading.
- There is increasing availability of computerised data acquisition and storage systems.

IBIS-S radar is used to assess structural displacement under dynamic, live and static loads. The transceiver is positioned in such a location that the majority are line of sight. Upon applying a load such as a vehicle of known weight to the deck, the radar calculates the deck's deflection by contrasting the received and transmitted signals.

The main limitation of IBIS-S is its suitability to inaccuracies due to covering of the area between the radar and the reflectors. It thus must be ensured that no objects enter this area during the surveying time. IBIS-S also does not have the capability of flaw detection but it does measure the structure's behaviour under load, which is in itself a feature of the structure and this feature depends on its defects. Although not sufficient of itself in terms of structural health monitoring, in using it in conjunction with other non-destructive testing methods, it is useful in ascertaining how identified defects influence bridge behaviour under load. Further information on IBIS-S can be found at Ids ltd (Ids ltd., 2010).

2.7 Accelerometers

2.7.1 Introduction

Accelerometers (Figure 2.24) are a style of sensor used in Structural Health Monitoring (SHM) that measure structural vibration including the vibration of hanger cables, pylons, stiffening trusses etc. Depending on the use to which they will be put, there is an array of accelerometer sensors to choose from, chosen on the basis of range of measurement, range and resolution so as to ensure the appropriate type is chosen for the structure (Chae et al., 2012).

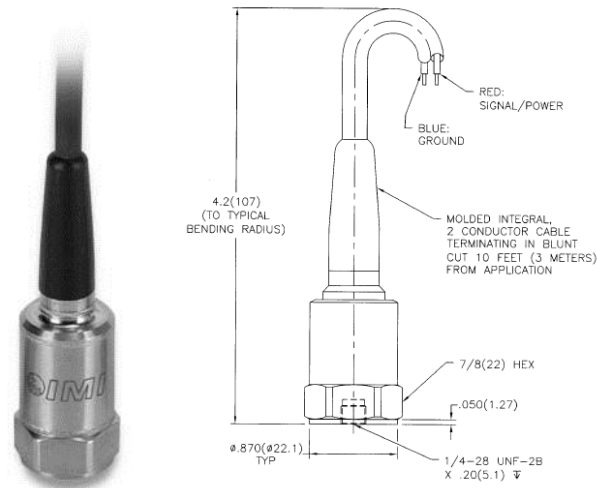


Figure 2.24 – Sample of 20g Accelerometers (Meggitt Sensing Systems, 2010)

Accelerometers are rugged, stainless steel vibration monitoring sensors for predictive maintenance applications. They are hermetically sealed and case isolated. Also accelerometer sensors interface directly with handheld data collectors for both permanent mount and route based applications (PCB Group, 2012).

Accelerometer calibrator is the Model 699A02 Hand Held Shaker is a small, handy, completely self-contained vibration reference source. It is intended for rapid checking of vibration measurement, monitoring and recording systems using piezoelectric accelerometers as well as other types of vibration transducer (see Figure 2.25) (PCB Group, 2012).

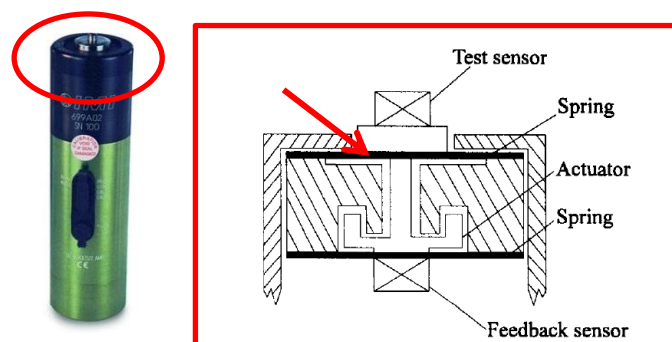


Figure 2.25 – Hand-Held Shaker (PCB Group, 2012)

Many maintenance decisions relating to machinery or structures are carried out pursuant to a condition monitoring process. Condition monitoring has become common practice, enabling organisations to enhance availability, lower maintenance expenses and ensure

safety. One of the methods used on this basis is vibration based condition monitoring as vibration measurement is a vital element in the detection and diagnoses of the development of anomalies (Albarbar et al., 2009).

Gangone et al., (2008) describe how research in the area of structural monitoring has become a common topic. The method utilises a network of data collecting sensors and interpretive software in conjunction with data analysis methodologies. In using accelerometers sensors, structural behaviour under various loading conditions can be recorded and analysed. The purpose of accelerometers is to identify the dynamic characteristics of a structure under ambient and forced vibrations in the determination of modal properties (mode shapes, damping ratio and natural frequencies).

González (2011) describes how, along with strain gauges, accelerometers are the most commonly used sensors within SHM. The accelerometer is attached to a frame and, as this frame accelerates, the inaction of the mass leads to deformities. These deformities create electrical currents which are measurable and can be interpreted back to acceleration.

2.7.2 General Principles

As its name implies, an accelerometer is used to measure how quickly speed changes. Accelerometers have the ability to sense acceleration which can be applied very usefully to many elements of projects and design (Lindsay, 2005).

Accelerometers are also known as motion sensors and they can operate by taking a three-way measurement of the acceleration of the structure and using it to calculate deflection. Judd (2008) details the wide use of accelerometers in measuring the vibrations of rotating machinery, moving vehicles, aircraft and structures.

The use of conventional piezoelectric accelerometers in vibration measurements is well established but this is an expensive method owing to the high price of the apparatus and related signal conditioning circuits. (Albarbar et al., 2009).

In using piezoelectric sensors to measure the acceleration of a mass, Newton's Second Law ($F = ma$) and the piezoelectric effect are utilised. Inside a piezoelectric accelerometer is a "seismic mass" – when that mass has force applied, the movement of its mounting "squeezes" a natural quartz crystal or manmade piezoelectric ceramic measuring element (Judd, 2008).

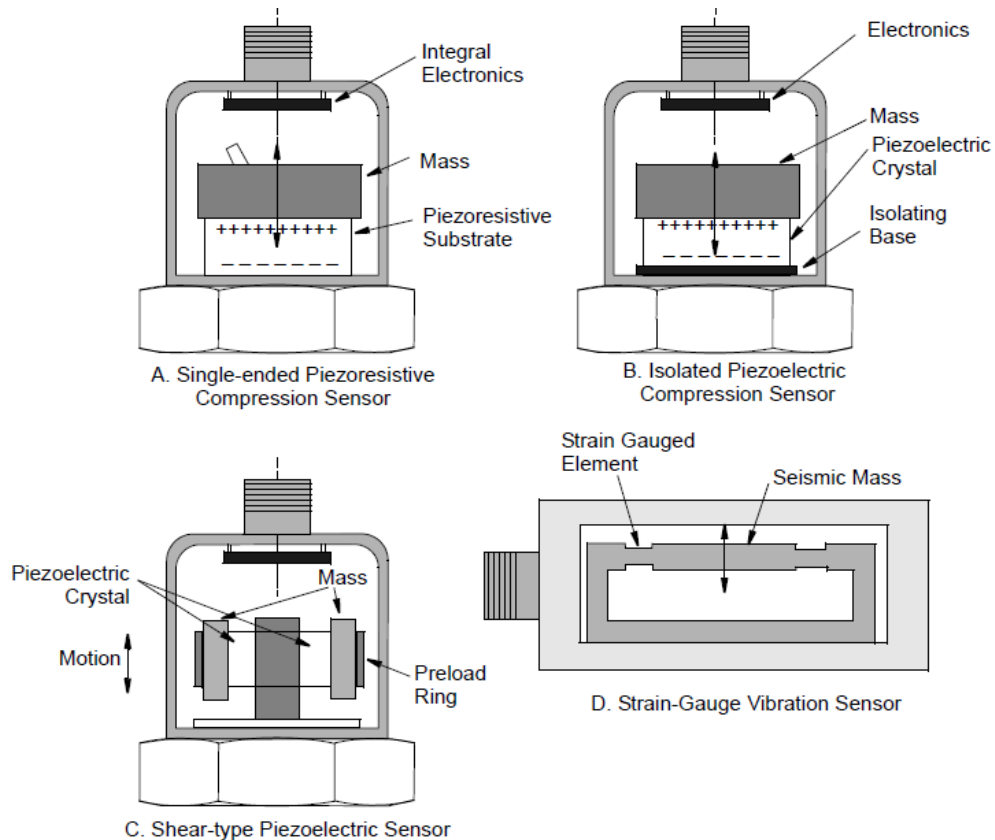


Figure 2.26 – Typical Constructions of Commonly-Used Accelerometers (Judd, 2008)

In contrast, piezoresistive accelerometers use a piezoresistive substrate rather than a piezoelectric crystal, as illustrated in Figure 2.26 A and B. When force is created by the seismic mass it alters the resistance of the strain gauge elements of a Wheatstone bridge engraved on the substrate, which yields a signal which correlates to acceleration. Piezoresistive sensors have the advantage over piezoelectric sensors of the capacity to precisely calculate acceleration at zero frequency, providing a true static measurement (Judd, 2008).

Figure 2.26 C and D illustrates the typical use in current strain gauge accelerometers of a silicon or foil strain gauge bonded to a component that deforms upon the movement of

a seismic mass. This strain is identified by a bridge circuit. Strain gauge sensors can also be utilised in identifying static measurements at 0Hz (Judd, 2008).

2.7.3 Monitoring of a Bridge Structure Using Accelerometers

Accelerometers have been used widely for bridge dynamic monitoring to analyse and determine resolution time histories of acceleration. The load testing of bridges has become an extensively accepted method to estimate the load capacity. Accelerometers are also widely used in testing on reinforced concrete bridges. Gastineau et al., (2009) has also proposed that accelerometer analysis results represent an estimate of the displacement and stress levels of the bridge structure. Also, accelerometer processing data can provide useful measurements to generate an accurate picture of deflection (Moschas and Stiros, 2011).

Meng et al., (2011) explain how triaxial accelerometers are used in the management of short to medium span bridges and other structures including high-rise buildings, in detecting the dynamics of these structures. Typically, accelerometers cannot reliably identify such a slow bridge motion but they do have the advantage of being able to pick up high vibrations of bridges.

In carrying out onsite load testing of bridges, it is accepted that a fair approximation of the load capabilities of that bridge can be ascertained. The use of accelerometers has the advantage over some other analytical methods of capturing the full extent of those variables with the greatest effect on bridge load capacity. The variables most often captured in the case of bridge testing are: live load distribution, live load dynamic effect (or 'impact') and composite deck action (Chowdhury and Ray, 2003).

In Summary, the most beneficial use of accelerometers has been shown to be in the testing of reinforced concrete bridges. Vigilance should be exercised in the placement of the accelerometers as concrete bridges are highly likely to have at least some degree of cracking and the effects of these cracks need to be analysed. Quite apart from the presence of cracks, accelerometers can comprehensively record the behaviour of beams as well as providing useful measurement information of vehicle–bridge dynamic

interaction, resulting in improved estimations of vehicle impact factors (Chowdhury and Ray, 2003).

Accelerometers have the advantage of providing information on the integrated response of bridges as well as information relating to their deflection and rotation by integrating the measured acceleration data. They are deemed simple to install. A downside to the technique includes the huge power requirement for transmitting large quantities of data from the main station by cellular modem (Briaud et al., 2010).

Therefore, application of the accelerometer technique is quick and low-cost. On the other hand, structure frequency and mass loading compromise is necessary. The main limitation of the accelerometer technique is resolution. Because of resistive noise, they are only suitable for low and medium frequencies. Supply voltage is required.

2.8 Other Non-Destructive Techniques

2.8.1 Wireless Sensor Networks

The Wireless Sensor Network (WSN) technique is gaining popularity within structural health monitoring and has the potential to completely take over from wired monitoring methods. WSN gives the freedom of wireless technology, is quick to instal and reconfigure and is low maintenance. However, there are restrictions relating to damage detection reliability, the requirement for wireless models, computer compatibility and limitations in the range and speed of data communication. Also, when used with concrete and steel, radio wave reflection and absorption can occur. Further information can be found relating to a study by Kim and Lynch (2011) into the interaction between bridge and vehicle using wireless monitoring.

Wireless technologies represent a cost-effective solution for densely populated large-scaled networks and sensors systems. The sensor communication board is designed based on IEEE 802.15.4 radio over the 2.4 GHz frequency band (Oracle, 2012) (see the Figure 2.27).



Figure 2.27 – WSN System Kit (Oracle, 2012)

Figure 2.27 also shows wireless sensor/actuator device, with a demo sensor board on top, the main processor and radio board in the middle, and a battery board on the bottom.

2.8.2 Laser scanner

Laser scanning allows for the collection of data to enable the accurate measurement and 3D modelling of bridge structures for the purpose of structural analysis. The technique collects dense 3D point clouds of geometric data of objects situated up to 50 m away with no requirement for physical contact. It works by emitting a laser beam onto the structure and recording travel time from emission of the beam to it reaching the structure's surface. Potential downsides include instrumental errors, complications caused by weather conditions, interfering radiation, the necessity for training of personnel in collecting and interpreting the data and the inadequate resolution of data when investigating, for example, breaklines of cracks or surface types. Laser scanning can be used alongside other techniques such as GPR and IBIS-S, for increased accuracy. However, overall the effectiveness of laser scanning as a method of structural analysis has increased greatly over the past 20 years and further material can be found by Al-Khader et al., (2009).

2.8.3 Infrared Thermography

Infrared thermography (IT) is a quick, portable, medium cost technique which can be used to detect surface and internal (although this requires surface contact) defects and anomalies in structures. Its portability is particularly useful for bridge assessment as it minimises the necessity for traffic disruption. All objects absorb and emit infrared energy and the spectral characteristics of this radiation can be picked up with an infrared camera and produced as an easily interpreted colour coded image. Non-uniformities, inclusions, delamination, debonding and cracks can all be picked up using IT, although the method can be affected detrimentally by weather conditions such as wind, direct sunlight and rain. Although the literature suggests that GPR is more accurate than IT at greater penetration depths, it is possible that the technique could be integrated with GPR and IBIS-S to increase data available for comparison and validation.

2.8.4 X-Ray Radiography

Radiographic and X-ray inspection methods can detect flaws in materials by penetration of high energy photons, thickness or material composition being determined by the level of energy passing through the structure. The denser the material, the more energy is absorbed. The x-ray radiography used in bridge assessment is more powerful than that used in a medical setting and all on-site x-ray inspections involve stringent safety precautions (McCann and Forde, 2001). The method is relatively expensive but is highly sensitive in many situations, including in the detection of reinforcement in concrete, voids around post tensioned cables in concrete, porous concrete and changes in the composition of the test element. Downsides include a 1 m penetration depth limitation, transportation difficulties, the fact that it cannot be used in the detection of corrosion of reinforcement and the strict safety precautions surrounding use of the equipment.

2.8.5 Gamma (γ) Ray Radiography/Radiometry

Gamma ray (γ -ray) radiography uses a decaying radioisotope to generate a small amount of γ radiation. The method is useful in locating the position, size and condition of reinforcement, voids in concrete or grouting of post-tensioned construction and

compaction variations. On applying the radiation to concrete, some of it passes straight through, some is absorbed and the remainder is scattered upon impact with electrons present in the concrete, which scatter allows examination of the properties of material near the surface (Bungey, 2004). This is an expensive method of assessment and is only useful for concrete thicknesses of less than 0.5m. Other downsides include the fact that access is required to both sides of the sample, development of the image takes longer than with the x-ray method, strict guidelines govern its use, the isotope cannot be switched off and isotopes fluctuate in strength and eventually die. Again, it is possible for the technique to be integrated with other techniques, such as GPR or IBIS-S.

2.8.6 Ultrasonic Testing

Ultrasonic testing is a relatively inexpensive, commonly used testing method, useful in the detection of voids, cracks, corrosion, rods and pipes. Ultrasonic waves are transmitted into a material and then reflected back. The transmission of signal strength through the material, and the disturbance of these waves, accurately depicts the material composition and the presence of any defects, so providing data on specimen thickness, non-uniformity, modulus of elasticity and 3D mapping. The presence of metal articles in the sample can cause faults within the data and there is a requirement for the application of a conductive solution in between the transceiver and the sample. Also, data analysis can cause difficulties and so skilled operators are necessary. A further downside is the fact that the sample's surface must be ground smooth and clean before use. Overall, its usefulness in bridge structure applications is limited and it offers no greater accuracy than GPR in providing information on bridge health assessment.

2.8.7 Acoustic Emission (AE)

Acoustic Emission (AE) is widely used for structural assessment and gives a real time assessment of the behaviour of materials deforming under stress. The method uses piezoelectric sensors to detect small amounts of energy in monitoring the integrity of structure and components. AE is useful for long term temperature monitoring, has a low/medium cost and is a straightforward technique but it is dependent on environmental conditions. Also, this technique requires training and a specialised

operator. It is possible that AE could be integrated with techniques such as GPR or IBIS-S to increase confidence in making a judgment about bridge health. Several researchers have reviewed the technique of AE in bridge health monitoring and integrity assessment including Nair and Cai (2010).

2.8.8 Sonic Techniques

There are several sonic techniques: Sonic Transmission, Sonic Tomography, Sonic Resonance and Sonic Reflection/Transmission, all of which have limitations for bridge health assessment. For example, they are not entirely successful for blind interrogation of structures and they are only able to project 2D slices. Each sonic technique is relatively cheap, but they are highly operator dependent and require training and experience.

2.8.9 Impact Echo (IE)

Impact Echo (IE) is a low/medium cost technique which is useful in the detection of flaws in concrete and works by scrutinising the surface of the sample following a short duration mechanical impact. These stress waves circulate throughout the structure, reflecting back when coming into contact with interfaces such as delaminations, voids, cracks and large steel bars or with a boundary (Kruger, 2005). Downsides to IE include a reduction in signal due to material deformation when struck, a lack of sensitivity of the receiver and the fact that concrete's heterogeneous nature can cause difficulties in detecting the returning signal as scattering arises at material boundaries such as aggregate, causing ghosting or noise on the receiving end. Also, great proficiency in acoustics is required in its use and it has difficult systems and unclear instructions. The method does not allow deep penetration into the bridge deck structure and therefore GPR can provide greater information on bridge deck condition.

2.8.10 Resistivity Measurement

Having the ability to detect moisture in an RC element is very important as defects in RC structures are often related to corrosion, which high moisture levels can lead to. The

level of water content of a structure determines the resistivity of an RC element to the flow of electrons, ie low resistivity indicates a high water content (as in the case of concrete) and a high resistivity indicates a low water content. The resistivity can be measured with a “Wenner array” which is made up of electrodes placed into small drilled holes in the deck of the RC structure. The structure’s resistivity is measured by passing an AC current through the outer electrodes and measuring the voltage between the inner electrodes (McCann and Forde, 2001). This technique has been widely used to assess concrete structures to determine specific defects but it does have limitations for bridge health assessment. It is moderately cheap but is highly operator dependent, requiring training and experience.

2.8.11 Half Cell Potential

The Half Cell Potential technique is a quick, cheap and easy method of identifying corrosion and/or areas at high risk of corrosion in bridge deck reinforcement. It does not give a direct indication of the presence of delamination but rather it can be inferred that areas identified as actively corrosive will delaminate.

2.8.12 Magnetic Induction

The Magnetic Induction technique is used to accurately identify bar location and depth in concrete reinforcement. An iron ‘U’ shaped core has a coil wound around each end, one of which is connected to AC power. The current creates a magnetic field in this coil whilst creating a magnetic field and inducing a current in the other. The current within the second coil alters when the magnet travels over steel and this alteration has a non-linear connection with the rebar depth (cover of concrete) and the bar diameter (McCann and Forde, 2001). This method is susceptible to inaccuracies where salt is present and so it requires training and a specialised operator. It could be used in conjunction with GPR to give more accurate information when assessing bridge health.

2.8.13 Magnetic Flux Exclusion

The Magnetic Flux Exclusion method can pick up the presence of any stray magnetic fields in the deck of an RC structure by the application of a magnetic field using an inverted “U” electro-magnet, with a magnetic field sensor attached between the poles. The presence of any such stray fields would indicate defects such as corrosion or ruptures within the hidden rebar or tensioning cables (Krause et al., 2002). This method has the disadvantage of also picking up the location of tie wires and stirrups. Experienced engineers are required to interpret results accurately and the depths of pressurised elements, as well as other rebar, must be considered in data interpretation. It is possible that defects can be concealed behind shallower, mild distribution steel or be hidden amongst pre-stressed cables, leading to the necessity for sensitive equipment. This method is not appropriate to this thesis’s preliminary and main case studies because it cannot give a broad picture of the health of bridge structures.

2.9 Summary of Non-Destructive Techniques

It is evident from the literature review that there is no individual technique of NDT existing which is able to identify every fault or defect that an engineer may require. At present it is general routine to use a mixture of inspections which go together with one another to gather all data required for bridge health monitoring and assessment. Bridges are the lifeblood of modern society. It is therefore imperative to monitor their structural integrity to ensure failure does not occur.

In order to accomplish this several key health indicators of bridges have been identified. It is crucial to monitor these indicators as they can denote bridge deterioration. These indicators have been identified as visual cracking, moisture ingress and deflection (Ryall et al. 2003; Jol 2009). It is also important to quantify unknown structural parameters such as rebar position which can be used to model the bridge if necessary. Thus several NDT have been selected which can monitor all the parameters need and an NDT framework has been created as illustrated by Figure 2.28.

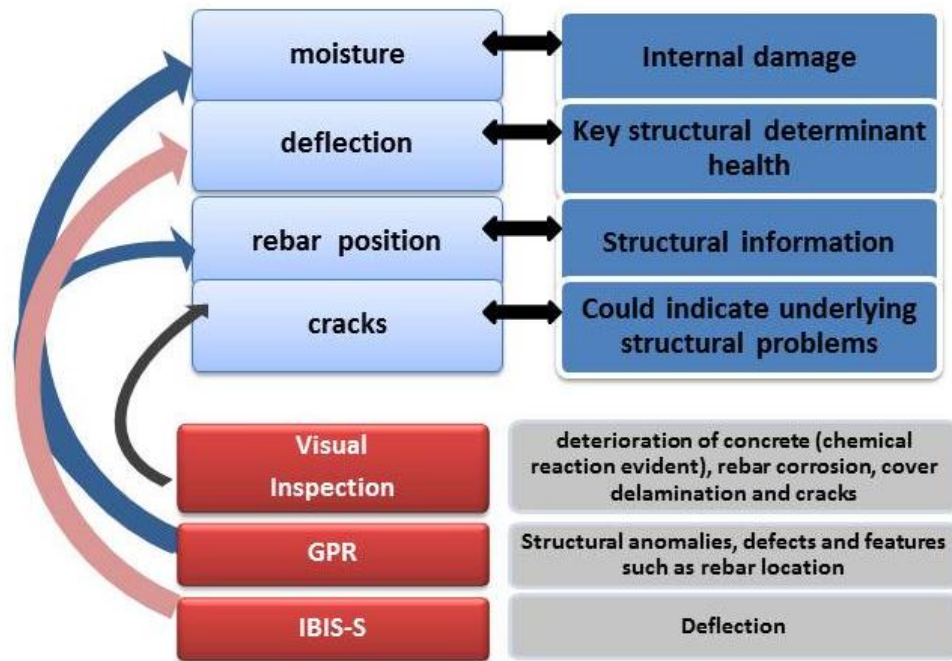


Figure 2.28 –NDT Framework

The techniques employed depend on specific data obtained from a visual inspection and the most applicable NDT techniques are chosen based on this information. Even though a visual inspection can identify faults which have already spread to the surface of the structure, it can determine areas which may profit from other NDT testing techniques owing to particular considerations relating to the elements of the bridge under inspection.

The use of GPR in bridge health assessment application is growing quickly to obtain the investigations damages such as voids, corrosion, cracks and delamination can be hidden inside the bridge deck. However, during the investigations of the literature survey, limited research was carried out with GPR on the detection of moisture. In a complicated stage to determine moisture such as the bridge deck including porosity, voids, material and state of compaction which GPR could detects promising results consisting in the determination of the velocity under control condition. Therefore, GPR determines in order to be located the moisture and voids within bridge deck assessment.

Each of the IBIS-S and Accelerometer monitoring techniques are an effective product to use on the deck of bridges, either of slab and girder section for evaluation of natural

frequencies through the measurement of displacement in reflective points. IBIS-S is a new technology and therefore a real case study needs to be carried out, including collecting data with corner reflectors placing, which is more effective with reflectors on the deck of bridges. The information given by the techniques was crucial in order to successfully obtain a complete picture of the structural health of the bridge. This information is shown in Table 2.2.

Table 2.2 – NDT Information

NDT	Notes	Information given
Visual Inspection	Identifies defects which can be further examined with additional NDT	deterioration of concrete (chemical reaction evident), rebar corrosion, cover delamination and cracks
GPR	Can provide information for FEM	Structural anomalies, defects and features such as rebar location
IBIS-S	Validated with accelerometer. Results compared with as new bridge model in FEM	Deflection
Accelerometer	Validation of IBIS-S results	Deflection
FEM	Implant GPR data IBIS-S data which was used as a comparison for the FEM	Dynamic behaviour

Table 2.3 summarise all of these techniques have been discussed by McCann and Forde, (2001; Mori et al., (2002); Jol, (2009) in their application to bridge health assessment. Also these techniques cannot give a complete answer but they all have been proven successful in certain applications and their limitations have been identified. The parameter measures, identifiable data, acquisition and interpretation of data, advantages, disadvantages and cost of each NDT technique (Highway Agency BA 86/06 Section 3, 2006).

Table 2.3 - Summary of NDT

Inspection method	Parameter measures	Identifiable data	Acquisition & interpretation of data	Advantages	Disadvantages	Cost
2.4 Visual Inspection	Condition of the exterior structure such as beams and supports.	Any visible surface anomaly such as cracks, moisture etc.	Basic Knowledge of bridge and concrete engineering.	Cost effective, not time consuming, only basic knowledge needed.	Gives limited information about the interior faults which may be more serious than the results of this method suggest.	Low
2.5 GPR - Ground Penetrating Radar	EM wave velocity	Rebar size & location, thickness of element, delamination, water ingress, composition of element under inspection, possible corrosion locations	Relatively quick survey time, data interpretation requires some skill, experience and preliminary training	Time effective, data is easy to visualise, accurate,	Penetration depth dependant on material properties & antenna used, interpretation can be difficult, Homogenous materials affect results. Some parameters such as moisture can be hard to identify High Cost	High
2.6 IBIS-S Interferometric Radar	EM wave velocity	Deflection of structure under dynamic , static & imposed loads	Reflectors can need fixing to the element under test, data displayed graphically	Able to see how structure behaves, ease of processing	Fixing reflectors to elements, line of sight needed for detection of deflection. Licence needed for Radar use, non-conclusive	High

					data is used by itself High cost	
2.7 Accelerometers	Vibrations of structures	Investigates deflection of structural	Modest skill required and needs experience	Measures static acceleration and easy and cheap manufacturing and application.	Supply voltage required and resistive noise causes limited resolution. Needs to be calibrated using additional equipment.	Moderate
2.8.1 Wireless Network	Radio Wave velocity	Investigates movement of structure	Modest skill required and needs experience and training	Measures structural behaviour	Weather conditions can affect the accuracy, battery life is low	Low to moderate
2.8.2 Laser Scanner	Laser light	Complete measure 3D model and detailed views of a structure	High skills required and needs experience	Completes 3D speed and accuracy measurements and model for structural assessment and analyses which cannot be achieved by traditional methods.	Weather conditions can affect the accuracy and structure components, cracks, surface types and patterns are difficult to define. Very expensive.	High

2.8.3 Infrared Thermography	Temperature differences	Spalls, delamination	moderate skill required in application, data displayed visually	Can detect temperature differences down to 0.08°C, Surface contact not needed	Only detects delamination and spalls, the weather can increase or decrease the temperature of the structure, Clear line of site necessary	Low to moderate
2.8.4 X-Ray Radiography	Radiation penetration & absorption	Interior anomalies such as , cracks, voids, moisture, rebar location and size	High skill, licence required for acquisition of data. Interpretation is relatively simple	High energy produces almost instant results, can be switched off	Large exclusion zone imposed, safety issues, large & heavy equipment necessary, up to 1m penetration only. Very inconvenient and expensive	High
2.8.5 Gamma (γ) Ray Radiography/Radiometry	Radiation penetration & absorption	Internal defects, cracks, voids, porosity, rebar location and size	High skill, licence required for acquisition of data. Interpretation is relatively simple	Lower energy so smaller exclusion zone required, smaller equipment, easy of transportation	Exclusion zone imposed, licence required, 0.5m penetration, safety issues, low resolution due to weak energy, constantly on Very inconvenient and expensive	High
2.8.6 Acoustic Emission (AE)	Wave velocity	Continuous monitoring of	Modest skill required and needs experience	Detects onset of failure, locates	Expensive test to run, used only when	Low to

		structure and monitoring performance of structure during proof testing.		source of possible failure and equipment is portable and easy to operate	structure is loaded and needs experienced operator	mode rate
2.8.7 Ultrasonic Testing	Wave velocity	Voids, cracks, uniformity of concrete across deck	Experience and skill required when applying method and interpreting data	More accurate than sonic transmission	Contact fluid necessary for transmission of ultrasound wave, locations of rebar necessary	Low to mode rate
2.8.8 Sonic Techniques						
Sonic Transmission	Wave velocity	Voids, cracks, compressive strength	moderate skill required in interpretation	Identifies useful information	Does not give location or extent of defects, surface contact needed	Low
Sonic Tomography	Wave velocity, tomographic cross-section	Voids, cracks	Relatively high skill required	Locates defects and their extent	Very slow, errors can be introduced in processing, surface contact needed	Low
Sonic Reflection Method	Wave velocity	Internal dimensions, properties of fill material, voids, cracks	Interpreting data requires skill to distinguish useful information	Only access to one side of element necessary	Poor resolution with low frequency energy, difficult to process, surface contact needed	Low
Sonic Resonance Method	Resonance of element under test	Delamination, cavities	Relatively easy to perform, modest skill required	Quick and cheap to perform.	Does not give depth of defect, surface contact needed	Low

				modest skills required		
2.8.9 Impact Echo (IE)	Wave velocity	Voids, cracks, internal defects	Data acquired needs detailed processing, relatively high skill required	Defect depth is obtainable, plate like structures are ideal candidate, access needed to one side only	Scattering of waves due to heterogeneous nature of concrete, impedes data processing, surface contact needed	Low
2.8.10 Resistivity Measurement	Electrical Resistivity	Detecting moisture content and possible waterproofing defects	Relatively quick acquisition, processing requires skill and further investigation	Ability to map areas of low resistivity, potential areas of corrosion of rebar	Holes in the surface of the element necessary for electrodes. Needs to be used in conjunction with other methods, lack of accuracy locating of defects	Low
2.8.11 Half Cell Potential	Electrochemical potential differences	Possible locations of Local chloride induced corrosion, Deterioration rate	Precise knowledge on mechanism of corrosion & experience in half cell mapping & interpretation necessary	Rapid assessment technique in detecting areas susceptible to corrosion	Does not predict or identify actual areas of corrosion, or corrosion rate. A direct electrical contact is required with the reinforcement within concrete.	Low

					Compensation of results may be needed for improved accuracy	
2.8.12 Magnetic Induction	Magnetic field	Rebar location and depth	Quick and simple data acquisition, interpretation requires modest skill	Quick and accurate	Water containing chlorides can yield false readings, corrosion of rebar not detectable, limited information gathered	Low
2.8.13 Magnetic Flux Exclusion	Stray Magnetic fields	Cracks, ruptures and corrosion locations in tensioning cables	Detailed processing required to eliminate errors, moderate to high skill required	Accurate results can be obtained	Location of tensioning cables need to be known, stirrups and tie wire can yield errors	Low

2.10 Structural Theories of Concrete Bridges

2.10.1 Introduction

The earliest bridges were simple structures which spanned a gap with timber or rope. However these were inappropriate for spanning larger breaches and thus the evolution of bridge design began. Initially with different materials such as stone and wood and then with different practices such as the arch developed by the Romans (Mondorf, 2006).

Up until the beginning of the 20th century, the dominant materials in bridge construction were either masonry or steel, their popularity owing to their high bearing capacities. However the use of reinforced concrete grew rapidly upon its introduction to the discipline during the early part of the 20th century due to its versatility, design flexibility and natural durability (CBDG, 2012). Chen and Duan (2003) explain how concrete is widely viewed as the most reliable of bridge construction materials and is the only material which is made on-site. At its highest quality, it will meet all structural and aesthetic requirements over a sustained period at minimal cost, will be easy to work with in its fresh condition, will accord with design in terms of strength and specification, will have durability, volume stability, be blemish-free in terms of scaling etc., be impermeable and aesthetically pleasing. Well designed and fabricated concrete can remain free of cracks under normal loads but also under modest overload which is a desirable feature for structures situated in an especially corrosive environment.

The advent of pre-stressed concrete both during and after the Second World War increased its choice as a suitable material to replace the many bridges destroyed both in the U.K and across Europe (CBDG, 2012). Due to the functionality and cost effectiveness of concrete bridges, they have become popular with the highways agency for use while constructing motorway networks. It is estimated that at least 75% of the Highways Agency concrete bridge stock has been built since 1960 (CBDG, 2012). At present there are over 10,000 concrete bridges in the UK of which over 50% are

reinforced concrete, 28% are pre-stressed concrete and a further 13% are steel-concrete composite structures (Neild , 2001).

As a large number of reinforced concrete bridges have been in use since the midpoint of the 20th century, they are at a point in their lifecycle whereby they require monitoring to ensure their structural integrity. It is also noted that during the past 50 years vehicular traffic has increased immensely so the original bearing capacity estimates for these bridges may be surpassed. Bridges are constantly open to the elements and to ever-increasing vehicular volume and many are ageing and, therefore, possibly in a state of deterioration. Consequences of this deterioration include a lessening of comfort for vehicle drivers and increased vulnerability in terms of its structural condition, with associated maintenance costs and even possible closure. An inadequate maintenance programme leads to a deteriorating bridge and common defects include cracking, surface distortion, rebar corrosion, expansion joint damage, waterproof deterioration and foundation erosion (Pan et al., 2009). Because of the important role they play in the transportation system, the maintenance of bridges is essential in assuring the necessary service and reliability of networks (Pan et al., 2009).

With the development of health and safety conciseness the monitoring of bridge health has become a major research area. However at the same time bridge accidents continue to happen, one major cause of which is natural disaster. During the monsoons just before the Commonwealth Games were held in Delhi, India, in September 2010 the footbridge connecting a car park with the Games' main stadium collapsed and at least 23 construction workers were injured. According to the authorities the accident happened when labourers were applying a concrete layer (Walker, 2010), (Guardian News and Media Limited, access date 27.12.2010). It is thus of utmost importance to develop bridge health monitoring systems for reinforced concrete bridges owing to their popularity and use in situations of heavy loading (highways bridges).

2.10.2 Structural Loading Theories

Different types of bridges support different predominant loads such as dead load (the weight of the bridges themselves) and the weight and stresses of the vehicles on the bridge. On the other hand there are other factors including wind, earthquakes, snow, temperature and construction on bridges. (see Figure 2.29) (Kaszynska et al., 2005).

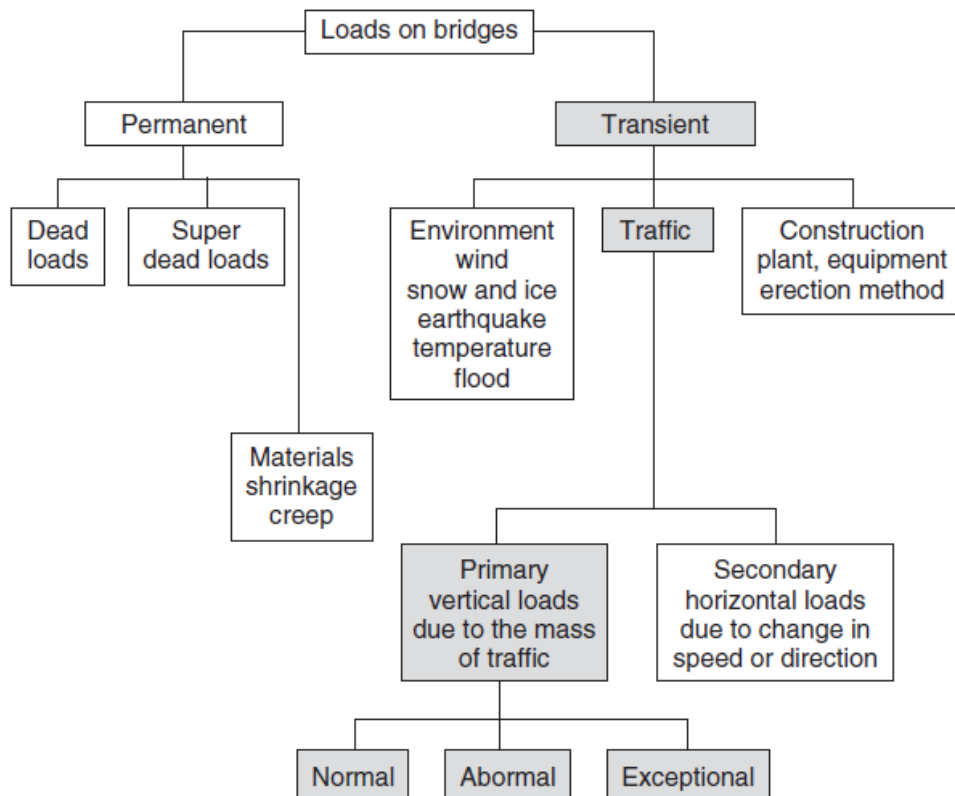


Figure 2.29 – Loads on bridges (Kim , 2005)

Hejll (2007) found that loads can be separated into the following categories:

- Deterministic, which is a known load in terms of location and magnitude over time (eg water pressure acting on dams)
- Stochastic, which is an assumed load of the future (eg probable future traffic trends which must take into account loads, position and geometry of the loads and a model based on the load effects).

Before the engineering revolution most bridges were single- or multiple-span masonry arch bridges. Also before the industrial revolution the live traffic loads were not important for design because they were carrying no more than pedestrians, herds of

animals and horse and carts. The development of industry changed vehicle weights, numbers and speeds. Therefore all new bridge designs have to consider vehicle specifications (Nguyen , 2006).

Today the main reasons for bridge collapse can be classified into categories. Significant numbers of bridges will need repairs upon reaching a certain age. Repairs have advantages such as minimising the cost of necessary maintenance, minimising related traffic disruption, and the protection of service utilities. If a bridge has an insufficient load-carrying capacity, bears heavier than assumed loads, if the strength of the material to be used is miscalculated or if calculation errors occur, failure of the bridge could occur. Even the most famous of designers are fallible, as was the case of Norman Foster's London Millennium Footbridge over the River Thames. The bridge opened on 10th June 2000 but during the opening day unexpected substantial loading effects occurred when pedestrians crossed the bridge (Fitzpatrick et al, 2001).

Dead loads (permanent loads) include all structural parts such as surface, parapets, all services, kerbs, footways and electric materials. Besides this deformations such as settlement and loads imposed due to shrinkage and creep are defined as dead loads (Kim, 2005).

Bridge design guidance provides more detail on dynamic loadings in any country. Decisions must be made on loading limits for systems used by the public. In optimising workload, hauliers benefit from transporting larger amounts of goods fewer times, thereby increasing single weight loads. However, in the interests of bridge health, restrictions must be enforced by bridge owners in terms of allowable weight. These weight restrictions are higher in Sweden and Finland than in any other European country, probably due to long transportation distances for timber (Hejll, 2007).

Loads can also be separated into further groups such as dynamic, which are usually known as live loads, and static (usually in civil structures the only static load considered in design is the dead load) (Bergmeister, 2002).

Hejll (2007) represents that commonly for structures the loads can be divided into:

- Dead loads, meaning the weight of both structural and non-structural elements which are deterministic.
- Super-imposed dead loads, meaning the weight of non-structural elements which are considered stochastic.
- Live loads, meaning, eg, wind loads, collisions and water pressure loads which are considered stochastic.
- Secondary loads, meaning issues such as thermal effects, friction forces, settlement forces etc, which are considered to be stochastic (Eurocode 1 BS EN 1990, BS EN 1991).

Another consideration is as to the position of the load on the bridge. However, in terms of vehicular traffic using a bridge, this is relatively straight-forward as the behaviour of drivers driving over, or queuing on, a bridge is quite predictable. Therefore, the position of loads is assumed normally to be deterministic (Hejll, 2007).

In summary, bridge designers formulate structure for safely supporting the loads of heavy vehicles and to withstand the often unpredictable forces of wind and water. Parke et al., (2008) has also proposed that the design of bridge structures can themselves be the cause of danger due to, for example, incorrect analysis, the inappropriate use of materials, and poor construction methods. Bridge structures are designed to carry highways, railways, deep valleys and other transportation routes to provide continuous passage over an obstacle. Bridges also provide utility services such as water, electricity and power cables or house telecommunications lines. Therefore, bridges are the lifeblood of modern society.

2.11 Application of Numerical Methods in Bridge Health Monitoring

2.11.1 Introduction

Simulation techniques and analysis such as the finite element method (FEM) are now widely used in industries, such as, aerospace, structural engineering and geotechnical

engineering. Numerical analysis works by creating a model which can be manipulated with various pieces of data to predict the behaviour that would occur in a real structure. In producing reliable results from this method, it is crucial to start with a model which accurately reflects the material properties of the structure being studied.

The FEM or the practical application, finite element analysis (FEA), is a numerical technique for solving partial differential (PDE) and integral equations. Various researchers have assisted in the development of finite element analyses for bridges. One of the researchers, Dixit (2008), represents that the FEM method essentially consists of assuming the piecewise continuous function for the solution and obtaining the parameters of the functions in a method that approaches the error in the solution.

The finite element method is a well-regarded tool, used in a vast array of engineering analysis areas. It is the case however that the analytical predictions produced by this method are often not identical to the results from a real structure. The reason for this is that the finite element model is based on ideal engineering knowledge rather than being representative of actual physical structures. In updating certain parameters of the model (e.g. of materials or boundary conditions) a more accurate prediction may be realised (Ren and Chen, 2010).

At the point of design, finite element analyses of highway bridges are performed in order to establish structural behaviour. There are some difficulties with this however in the sense that elements such as materials, boundary conditions and section properties incorporated into these analyses are sometimes altered later in the process. Workers can make mistakes during construction and loads which are not adequately included in the analyses may become common elements in the use of the bridge. In this case, the performance of the bridge must be monitored by field testing or experimental measurements (Altunisik et al., 2011).

Schlune et al., (2011) explain how, in combining finite element analysis and on-site measurement through finite element model updating, a potential improvement in estimates of structural parameters can be achieved but care must be taken as simplified initial models and insufficient measurements may instead provide inaccuracies.

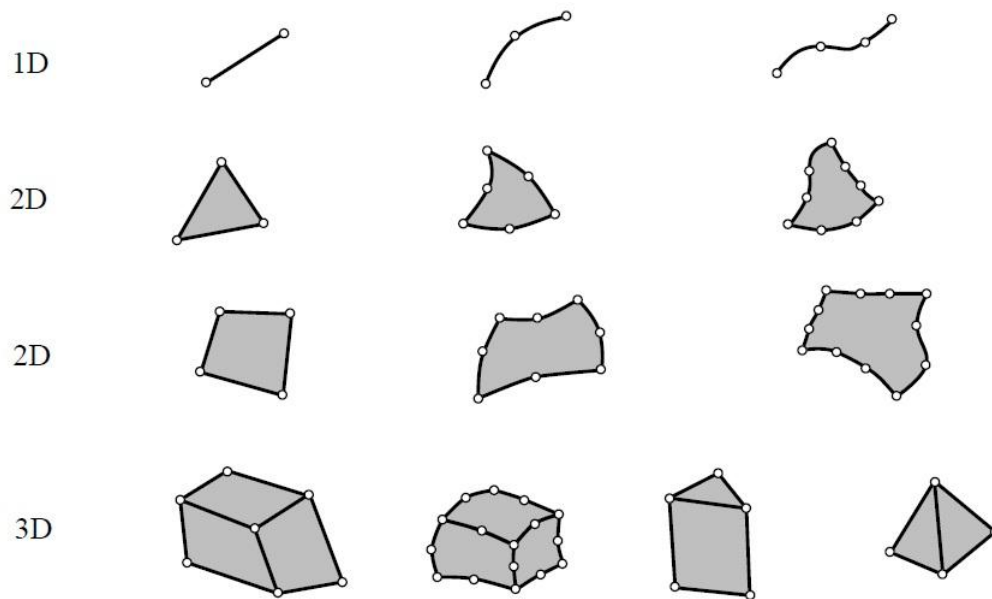


Figure 2.30 – Typical finite element geometries in one through three dimensions (Barton and Rajan, 2000).

Figure 2.30 introduces that the basic concept in the physical interpretation of the FEM is to divide structure into pieces, assemble the elements at the nodes to form an approximate system of equations for the whole structure to solve the system of equations involving unknown quantities at the nodes which can be displacements, then calculate strains and stresses at selected elements.

Solving the FEM with differential equations of the mathematical model into simple geometric shapes is disjointed, meaning non-overlapping components of simple geometry, called finite elements or elements for short. Element response in the way of finite number of degrees of freedom characterised as the value of an unknown function, or functions, at a set of nodal points (Barton and Rajan, 2000).

However, whilst FEM is an exceptionally successful tool, it does have its critics. Such criticisms include the fact that practitioners are applying the method whilst having inadequate knowledge of structural behaviour, that no critical evaluation of results is carried out and that a further lack of knowledge exists in terms of the actual limitations and possibilities of the method. Therefore only engineers fully trained in FEM and structural mechanics are able to make a full and accurate analysis using this method (Hartmann and Katz, 2007).

Chan et al., (2011) describe the limitations of finite element modelling in the cases of large civil infrastructure and the importance of the model being adjusted to take account of initial flaws and deterioration. In evaluating these structures, a global finite element model is first used to determine critical locations, followed by local analysis to determine stress distribution risk, typically understood as being fundamental information for condition assessment. A mixed dimensional coupling method is implemented to overcome the different scales of the structural behaviour and to enable one-step analysis, by integrating a characteristic detailed joint geometry model into the global model.

2.11.2 ANSYS, SAP2000 Commercial Software and Crack Modelling

The ANSYS software is a competent FE based tool commonly used in analysing a vast variety of structures (Padmarajaiah and Ramaswamy, 2002 and Dahmani, Khennane and Kaci, 2010). Zhou (2004) uses ANSYS to analysis the decks of single span slab-on-girders bridges. They use ANSYS to study the effects of the flexibility of the bridge superstructure on the strength of the concrete slab. The ANSYS software is equipped with numerous elements capable of modelling large or small strains and displacements and concrete cracking under various loading conditions such as static and transient load cases. SAP2000 (Computers and Structures, 2011), structural analysis program, is used to model the structure. It is capable of modelling 3D structures under moving loads. ANSYS (ANSYS, 2011) requires a set of static loads, in a database, in order to derive a dynamic load. SAP2000 has the capability of modelling the variable load due to passing vehicles without this intermediary step.

The crack modelling of concrete structures was a crucial subject for researchers such as Wilson et al. (1973). Modelling the plastic nonlinear brittle behaviour of concrete was too complicated for the elementary Finite Difference or Finite Element based software of that time. Most research was only based on theoretical models providing a reasonable presentation of the realities of the concrete behaviour beyond the first cracking moment (Willam and Warnke, 1975). However, any state-of-the-art software capable of modelling cracks in concrete is based on nonlinear fundamentals such as the ones presented by Taylor et al. (1976) Experimental investigations of cracks, such as those

conducted by NASA (Newman and Raju, 1979), have played a key role in providing a suitable basis for evaluation of the new FE techniques such as the solution methods of Rhee and Salama (1987). The science of fracture mechanics has now branched into a diversity of state-of-the-art topics investigated by a wide variety of scientific specialists, with investigation results being applied to a broad range of problems. (Anderson, 2005) Based on these invaluable findings, FE computer packages provide the opportunity of solving problems such as stress concentration in a cracked surface in a fraction of a second (Kamaya, 2006).

2.11.3 Finite Element Modelling of Bridge Superstructures

In the bridge engineering design process, load combinations include dead load, live loads, traffic loads, braking forces, load on the road embankment, additional surfacing and earth pressure. All these loads, forces and pressures are significant factors in the design of any structure. In research terms, the purpose of structural numerical analysis is to ascertain a baseline finite element model of the structure. FEM is crucial for studies on structural health monitoring and condition assessment, wind and earthquake resistance etc. Therefore, many researchers focus on FEM, revising studies based on measurement data in attaining a suitable baseline model, which has in turn led to the introduction of many updating methods in mechanical, aerospace and civil engineering. (Wang et al., 2010)

There are three different dimensional FEM techniques available for bridge modelling. These techniques include a mixture of different types of elements for different parts of the bridge structure. The upkeep and replacement of bridges is expensive and disruptive to traffic and so it must be concluded that accurate information relating to the condition of these structures is vital. However, many current approaches use simplified structural models which may have detrimental effects on the resulting analysis. Structural models should be verified, refined, and tuned in relation to actual measurements in order to improve on maintenance decisions and much research has been carried out in relation to this (Schlune, 2009).

Barton and Rajan (2000) agree that FEM has many important advantages to the design engineer, such as its easy application to steady-state, time dependent and eigenvalue problems, and its applicability to linear and nonlinear problems, including problems in solid mechanics, fluid mechanics, chemical reactions, electromagnetics, etc. They also point out that FEM has advantages at simulation such as identifying problems in designs before tooling is connected, optimising performance before modelling and noticing design problems before processing, giving more time for design engineers to use their judgment, and avoiding reduced testing and redesign costs so limiting the product development time. Experience and judgment are compulsory in order to develop and analyse a good finite element model (Barton and Rajan, 2000).

In overcoming the limitations, often only dynamic information such as the natural frequencies and mode shapes are introduced to the updating model. This means that the inert response of the structure is not taken into account and therefore inaccuracies in the static response of the updated model may subsist. By incorporating the measured static information into the updating model, the input information is augmented and accuracy of the model is assured in terms of both dynamic and static properties. In addition, the ability of the optimal search techniques is restricted in terms of the amount of possible candidate parameters and a progressive model updating approach, including dealing with parameters individually, could allow the revision of more parameters and thereby improve reliability of the updated model (Wang et al., 2010).

Bapat (2009) also identified that professionals and researchers have developed more advanced computational methods, such as FEM, which have become more accepted with advances in computer technology. Recently, most engineers and researchers prefer to use three-dimensional finite element analysis over line girder analysis and grillage analysis. Three-dimensional FEA introduces the ability to overcome the limitations imposed by line girder analysis and grillage analysis.

Whilst studies into the effect of vehicular traffic have been ongoing for over 100 years, researchers can now perform analyses of the interaction between moving vehicles and bridges (Ju and Lind, 2007). Finite element analyses for three-dimensional bridge idealisations introduce some geometric errors and incompatibilities in the structure

system, which affect their ability to capture the actual response of the bridge (Bapat, 2009).

Fatigue and the impact of moving vehicular traffic are two of the many factors which cause damage to bridges. Structural damage has the potential to cause effects such as stiffness and damping which in turn have an effect on the dynamic responses and characteristics of the bridge. In using vibration-based non-destructive damage detection, use is made of these alterations in the dynamic responses and characteristics at intervals over the lifetime of the structure for damage assessment (Lu and Liu, 2011).

Knowledge in terms of the age of a structure, its usage and its reliability are important factors for consideration in the prevention of disastrous events. Bridges are constructed with the expectation that they will have a long lifespan but they are constantly subjected to variations of vehicular traffic, service loads, environmental and accidental actions, all of which can cause damage. For these reasons, a constant programme of health monitoring of important bridges is essential for the quick detection of developing defects (Chan et al., 2011).

The FE modelling process, which is the dynamic and statistical response of the structure, is required to be interpreted. The analysis process utilises a design that considers load combinations of the structure, and their dead load, live loads, traffic loads, braking forces, load on the road embankment, additional surfacing and earth pressure. All these loads, forces and pressures are significant for designing the structure. The third factor is the end-user's knowledge requirement of each technique which is included in the engineering judgment process, because all results are based on the user's requirements in the Integrated Approach development. Therefore, these three factors will be investigated in the real health assessment.

In Summary, it is clear the finite element analysis has become a popular modelling tool in recent times primarily owing to the occurrence of powerful computers over the last few decades. Recently, simulation techniques and particularly the finite element method (FEM) have been extensively and successfully used as a robust tool in the analysis of a wide range of bridge engineering.

The main advantage of this method over other conventional structural analyses is that it can be used for statistically unknown irregular-shaped structures and complex boundary conditions. Another advantage is that FEM software is available at a reasonable cost, and can be readily applied on microcomputers, including workstations and PCs. FEM can also be coupled to CAD programs to simplify the modelling and mesh technics. On the other hand a powerful computer and reliable FEM software are sometimes necessary to input and output data which may be large and tedious to prepare and interpret.

FEM is particularly suited for simulating the behaviour of a bridge structure as it can solve complex geometry problems and complex analysis types such as vibration, transients, nonlinear heat transfer and fluids. It can also be easily applied to complex loading such as point loads (node-based loading), element-based loading (pressure, thermal, inertial forces), time or frequency dependent loading and every element in the model could be assigned a different set of material properties. At the same time, FEM software packages have numerical problems such as the fact that computers will only carry a finite number of significant digits, round off and error accumulation and assist the condition by not attaching small elements to large elements.

The most appropriate FEM software was found to be SAP2000 (Computers and Structures, 2011) and ANSYS (2011) as these are the most frequently used commercial and research appropriate software on the market to date. The identification and analysis of these FEM tools fulfils objective one. Their applicability and success as NDT was also determined fulfilling objective two. It was determined that this software can identify weak points in the structure fulfilling objective four. Objective four will be also further completed by the results gathered were input into a finite-element model in both ANSYS and SAP2000. The information gathered from the visual inspection and all GPR, IBIS-S and Accelerometer results indicated that a particular area of the bridge had a significant structural health problem. This correlated with the findings of the finite-element model developed and compared with the information given by the non-destructive techniques. Therefore this successfully demonstrated the effectiveness and applicability of non-destructive techniques.

2.12 Summary

This chapter reviewed a number of non-destructive technologies for bridge health assessment. Its general purpose was to partially fulfil objective one (To acquire necessary knowledge of operation, collection, processing and interpretation of complex data compiled by advanced structural monitoring equipment). In order to achieve this many NDT were analysed, the review indicated that each technique has its own advantage, disadvantages and limitations.

Prior efforts to implement several NDT together have been detailed (Lubowieka et al. (2009), Barnes et al., (2008), Sevim et al., 2011, Gentile and Bernardini (2008)) however the most notable attempt being that Lubowieka et al. (2009) which evaluated a masonry bridge using GPR, Laser Scanner and FEM software. In this paper, a three stage approach was outlined involving a geometric data collection (using laser scanning), internal structure description (using GPR) and structural analysis (using FEM). This structural analysis comprised of establishing the Young's modulus of the bridge. This thesis however includes all the elements detailed by Lubowieka et al (2009) (Although the geometric data collection was achieved using an independent report and visual inspection not a laser scanner) and further information such as structural response (IBIS-S and accelerometer), detailed internal composition i.e. rebar position (GPR), and detail structural modelling i.e. crack propagation (ANSYS). This, therefore results in a far more accurate assessment of the bridge health than that found by Lubowieka et al (2009). It is also worth noting that reinforced concrete is a far wider used bridge construction material than masonry and therefore the mechanism described in this thesis is appropriate for a greater number of structures.

In order to determine the most appropriate NDT for bridge structures a comprehensive literature survey was completed. GPR and IBIS-S were identified as the most suitable equipment. GPR can identify both defects such as cracking and moisture ingress and also structural features such as rebar positioning which can be incorporated into FEM. It is suitable for bridge deck surveying as it is rugged and lightweight, it also takes a relatively short amount of time to complete a survey. GPR does not give detailed information about the behaviour of the structure however hence IBIS-S is used to

monitor deflection. IBIS-S is easy to set up and accurate to 0.01mm (IDS Ltd., 2011). Visual inspection was also identified as a simple method to determine exterior defects. Other methods were examined such as laser scanner, infrared thermography etc. but these were discounted for numerous reasons detailed in this chapter.

FEM will be used to model the behaviour of the bridge. The FEM software chosen was SAP2000 and ANSYS as it has been used previously to model bridge behaviour. ANSYS also has crack modelling capabilities whereby the impact of growing cracks on bridge behaviour can be modelled.

These NDT will be incorporated into a methodology to achieve the main aim of this thesis and this will be detailed in Chapter 3.

Chapter 3

Research Methodology

This chapter presents the research methodology used in this project. It utilises five stages that reflect the objectives outlined in chapter one, and successfully provides a research design framework for completion of this thesis. This chapter also presents the advanced non-destructive techniques, along with illustrative examples to demonstrate certain procedures and compare the performance, advantages, disadvantages and limitations of different approaches. This chapter also introduces the equipment used along with preliminary and main case studies:

- Forth Road Bridge
- St Mary's Island Lifting Bridge
- Darvel Road Bridge
- Rochester Bridge
- Pentagon Road Bridge

3.1 Introduction

Bridge health assessment poses an ever present problem to the engineering community. Destructive methods can be costly and time consuming and, therefore, non-destructive testing methods were researched in the following way. This chapter details the work undertaken during the three years study and provides an overview of the approach taken. This research develops a FE model using specialist software for improving its accuracy and an integrated approach for assessment and monitoring of the structural integrity and overall functionality of bridges. The aim of this approach is to gather a more comprehensive knowledge of the conditions of bridge structures. This will give a more realistic picture of the bridge health, and increased confidence when making a judgment regarding remedial action. The Aim and Objectives research design framework is presented in Figure 3.1:

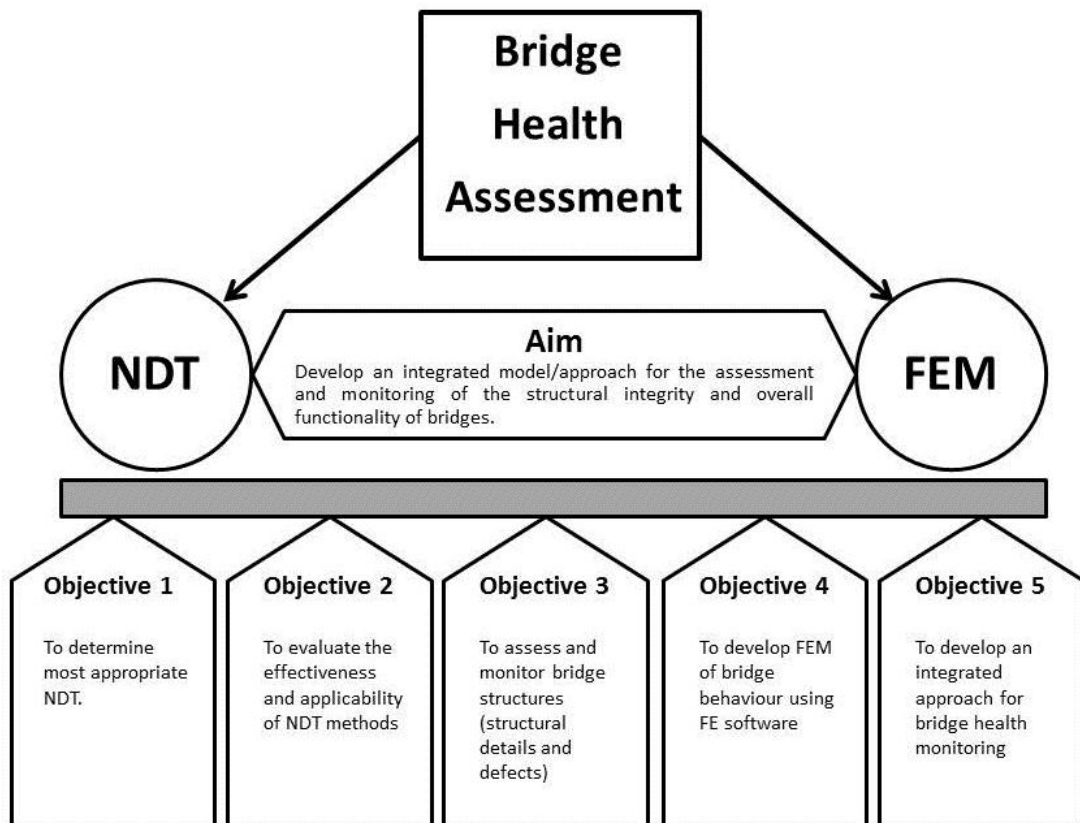


Figure 3.1 – Aim and Objectives Research Design Framework

In order to achieve the set objectives, as highlighted in chapter one, a series of five methods and measures were put in place. The five-stage research design framework is presented in Figure 3.2:

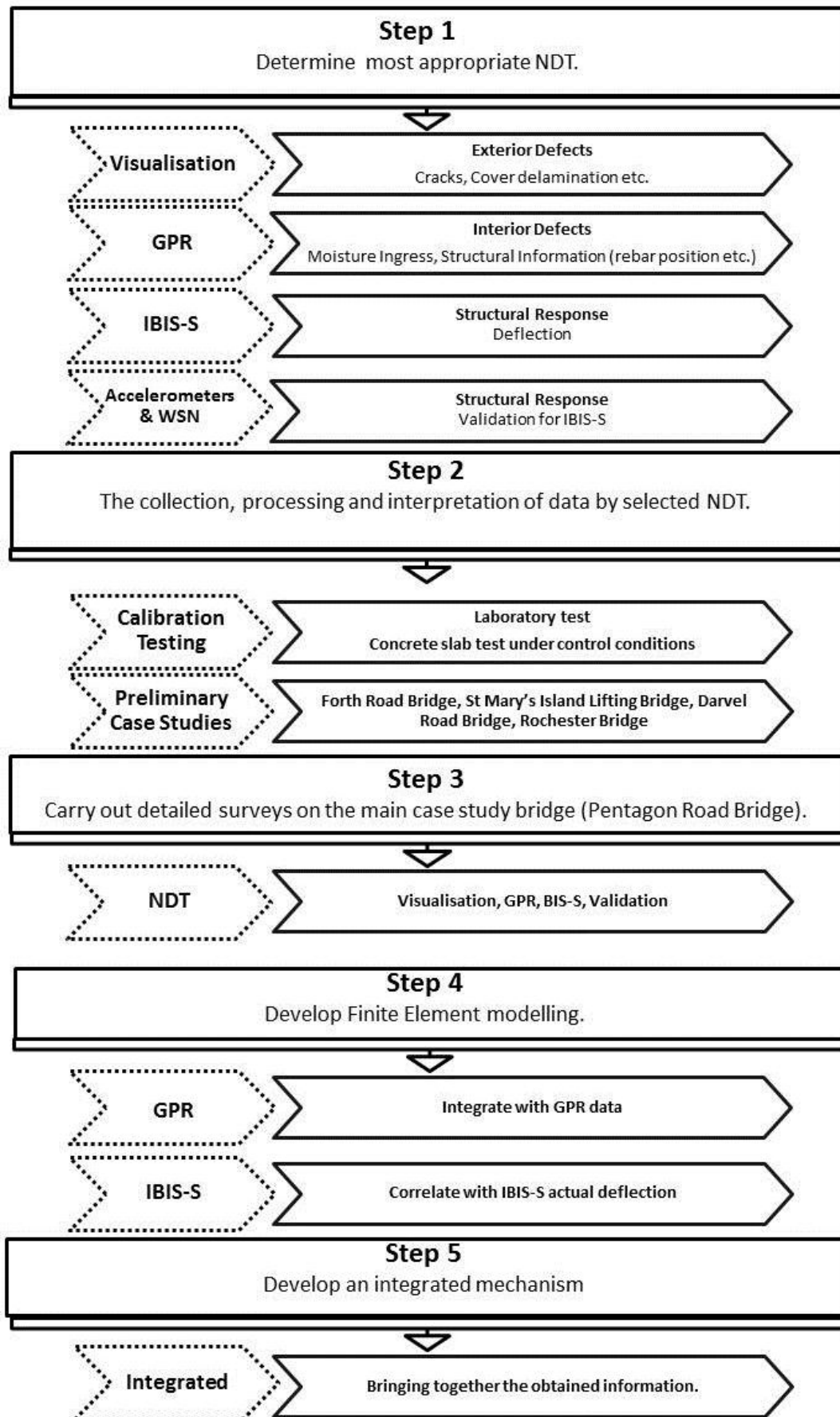


Figure 3.2 - Five Stage Research Design Framework

3.2 Step 1: Determine the most appropriate NDT for bridge health monitoring

An extensive literature review was undertaken in Chapter 2 encompassing a large number of important variables including time, cost and applicability (Highway Agency BA/8606 Section 3, 2006). This provided a solid base for the thesis by determining the most appropriate NDT for bridge health monitoring (see Figure 2.24).

These were found to be:

- **Visual Inspection:** This is an inexpensive and quick method of identifying any superficial structural problems such as moisture ingress and beam delamination. It does not give detailed results however, and must be combined with other techniques.
- **Ground Penetrating Radar (GPR):** GPR was chosen due to a number of factors such as the range of results, i.e. the presence of moisture and position of rebars (among others) which can be easily input into a finite element model. It is also easy to use and less time consuming than other techniques with a bridge deck survey for the main case study taking only half a day.
- **IBIS-S (Interferometric Radar):** GPR cannot show all structural response information for example deflection is not given, so another technique is required. IBIS-S gives results for the displacement of the bridge, which is an important health indicator. It is easy and quick to set up, which is an additional advantage.
- **Accelerometers and Wireless sensors:** These provide validation for IBIS-S to provide additional confidence in its measurements.

Other NDT such as laser scanning, infrared thermography and ultrasonic techniques etc. were disregarded as viable options due to reasons outlined in Section 2.8.

This helped fulfil objective one which aim was in part to identify appropriate NDT.

3.3 Step 2: The collection, processing and interpretation of data by selected NDT

The necessary knowledge of operation, collection, processing and interpretation of complex data was gathered for each of the NDT listed in the above section. The methods followed to achieve this step for each of the individual NDT are listed below.

3.3.1 Visual Inspection

Through the literature review identified main factors which should be present in all visual inspection (Highway Agency BA 86/06 Section 2.3, 2006). Jacobs, (2010) also created an independent report recording all the findings of their visual inspection which was referred to during the course of this work. Figure 3.3 shows the visual inspection procedure.

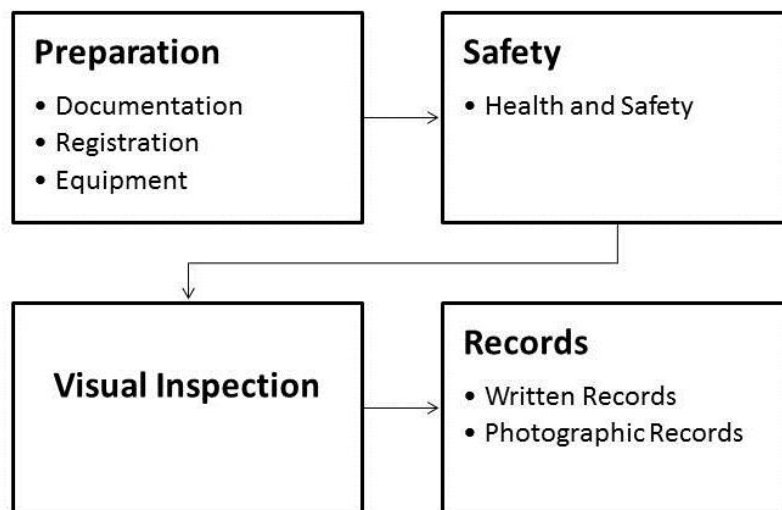


Figure 3.3 - Visual Inspection Procedure

Visual Inspection Procedure

- Preparation for Visual Inspections
 - Preparation relevant documentation (a copy of the previous inspections reports)
 - Registration (date, weather conditions, etc.)
 - Equipment (personal protective equipment (PPE) such as high visibility vest, safety boots; first aid kit; torch; binoculars; hammer; tape measure; camera; chalk and permanent marker)

- Operational Safety
 - Health and Safety
- Visual Inspection
 - Cracking
 - Scaling
 - Spalling
 - Delamination
 - Dampness
 - Surface Defects
 - Patching or Other Repairs
 - Alkali Aggregate Reaction
 - Corrosion of Reinforcement
 - Loose Connections
- Records
 - Written records
 - Photographic records

3.3.2 Ground Penetrating Radar

GPR operation and processing training was given by Kevin Banks of IDS limited, and further experience of GPR was gathered by applying it to both a concrete slab of known defects and the preliminary case studies. By doing this an understanding of the entire process of gathering, storing, processing and interpretation of the resultant data was achieved. Figure 3.4 shows GPR operation process.

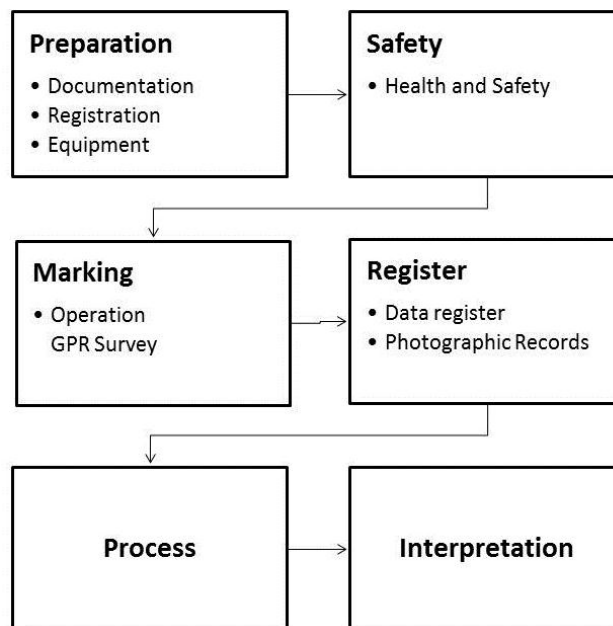


Figure 3.4 – GPR Survey Procedure

The main points to be considered during GPR operation are described below:

- Full access to the bridge was required during the survey (access to pedestrian zones, permission to interrupt the traffic flow, etc.);
- Any difficulties in accessing the site must be considered;
- The space available;
- The presence of parked cars;
- The level of traffic;
- Marking the reference system (Longitudinal and transverse markings on bridge deck).
- Operation GPR to register data
- Process the data for interpretation.

The first fundamental stage considered the accessibility of the bridge for the passage of the antenna trolley, and considering any architectural obstacles that could cause an obstacle to the data acquisition phase. The survey consisted of organising the health and safety and marking of the bridge deck. The marked features had to be clearly visible for the GPR survey and a reference system worked out during the preliminary investigation that best fits the operational conditions of the GPR equipment and maximises its productivity.

A full set of GPR equipment, including: 200-600MHz; 2GHz; and 1GHz antenna, was purchased by the University of Greenwich from IDS Ltd (an Italian ground radar development company based in the UK).

The RIS Hi BriT (High resolution Bridge Tomography) (2 GHz) antenna (see the Figure 3.5) is designed specifically for the inspection of bridge decks. This high frequency array is lightweight and manoeuvrable yet provides high quality, densely sampled data. Denser sampling produces higher quality tomography and 3D images which assist considerably in the interpretation of data. The RIS Hi Bright was specifically designed to work in conjunction with advanced software processing allowing the detection of shallow features and the condition of materials within structures. It was particularly intended for concrete assessment on bridges to detect; thickness of layers, shallow utilities and drainage, location and spacing of rebar, and moisture penetration and delamination.

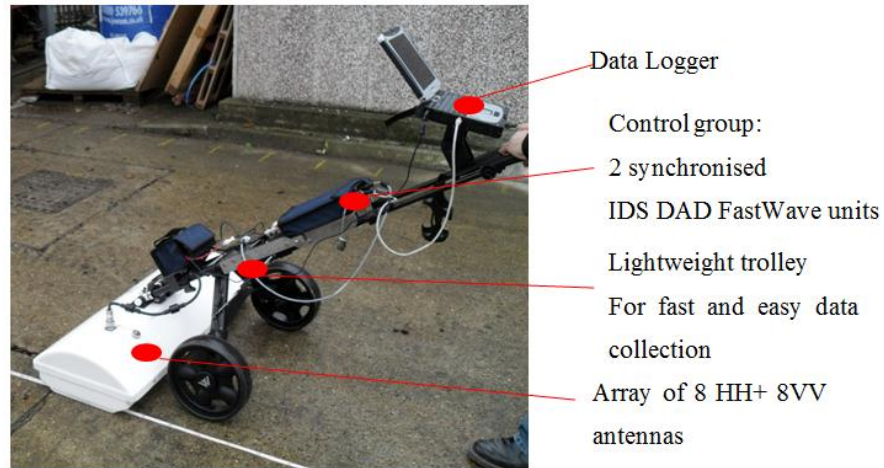


Figure 3.5 – GPR Hi BriT GPR Antenna (Photos from Gokhan Kilic, 2010)

The RISMF HI-MOD (200-600 MHz) GPR Antenna (see the Figure 3.6) uses a low frequency array, and is lightweight and manoeuvrable yet provides low quality but deeper densely sampled data.



Figure 3.6 – GPR Hi BriT GPR Antenna (Photos from Gokhan Kilic, 2010)

The system is composed of an array of one horizontally polarized 200 MHz and 600 MHz channels, mounted on a lightweight and highly manoeuvrable trolley and powered by a large, 24Ah 12V battery. The acquisition is controlled by K2 Fast-wave software, which runs on a standard ruggedized laptop.

The UTSI GPR antenna (see the Figure 3.7) is designed specifically for the inspection of bridge decks. The system is composed of an array of one horizontally polarized 1GHz, 1.5GHz and 4 GHz channels, mounted on a lightweight and highly manoeuvrable trolley on back of a vehicle. The acquisition is controlled by UTSI software, which runs on a standard ruggedized laptop.

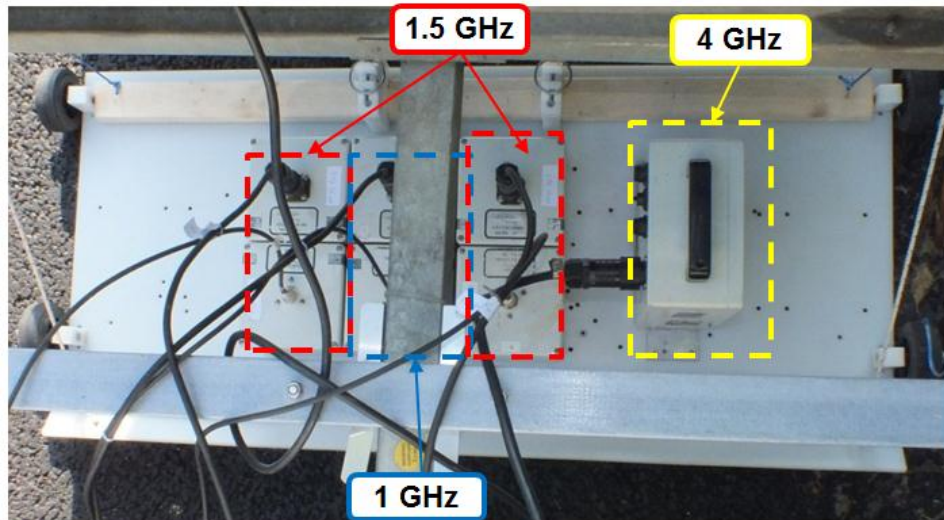


Figure 3.7 – UTSI GPR Antenna (Photos from Gokhan Kilic, 2010)

Four bridges of different design were chosen as preliminary case studies for this project. GPR surveys were carried out on all bridges and the results examined in order to obtain a realistic picture of both the health of the bridge and position of key features such as, rebar condition and location, delamination, moisture, thickness of layers, map drainage and other buried utilities.

- Preliminary Case study 1: Forth Road Bridge – Scotland
- Preliminary Case study 2: St Marys Island Bridge – Kent
- Preliminary Case study 3: Darvel Road Bridge – Glasgow
- Preliminary Case study 4: Historic Rochester Bridge –Kent

The purpose of the four preliminary case studies is to demonstrate non-destructive technology in structural monitoring, the assessment of bridge structures, and the processing and interpretation of the data collected.

3.3.3 IBIS-S Interferometric Radar

Training using the IBIS-S equipment was given under the supervision of IDS limited and all tests were also carried out under the supervision of representatives from this company (Figure 3.8). It was not possible to implement IBIS-S surveys on the preliminary case studies so to gain additional confidence in its measurements on the main case study bridge other methods were used to validate its results. These methods were accelerometer and wireless sensor networks.

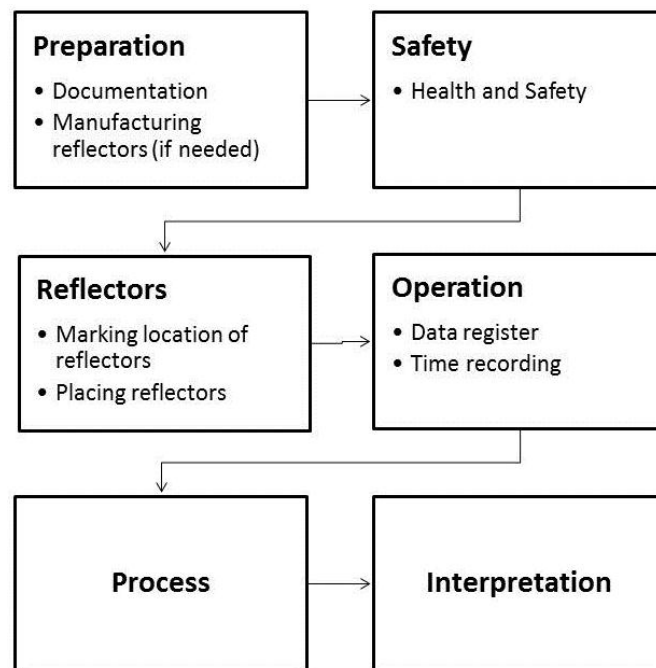


Figure 3.8 – IBIS-S Monitoring Procedure

IBIS-S monitoring procedure is described below:

- Full access to the bridge was required during the survey (access to bridge side to set up reflectors, permission to interrupt the traffic flow, etc.);
- Health and safety must be considered;
- Operation on both side;
- Save the data for processing;
- Interpret the data;

The IBIS-S system is an advanced non-destructive interferometric radar technique to remotely measure displacements with a sampling frequency up to 200 Hz with an accuracy as fine as a hundredth of a millimetre (see the Figure 2.14).

3.3.4 Validation IBIS-S

As it was not possible to use IBIS-S on the preliminary case study, another method was needed to ensure the validity of its results. Accelerometers were used for this purpose as they record different variables (vibration) from IBIS-S in order to calculate deflection.

Eight Wilcoxon Research model 775A accelerometers were used for the purpose of recording bridge deflection under dynamic loading. Before installation on the bridge deck they were calibrated using a Model 699A02 Hand Held Shaker. The shaker with a known vibrational frequency is applied to the accelerometer. The results from the accelerometer are then compared to this known frequency.

Following the calibration of each of the sensors, they were placed at intervals corresponding to the position of selected IBIS-S reflectors (see Figure 4.32). As there were significantly more reflectors than accelerometers it was decided to place the accelerometers at the positions that experienced the maximum deflection at the previous IBIS-S survey.

All the accelerometers were connected to one control panel to record their measurements. Full details of the process undertaken during the survey are available in Section 4.2.3.

The survey was completed in collaboration with XODUS GROUP (an international multidisciplinary energy consultancy company based in the UK). XODUS GROUP also provided necessary training in the data collection and interpretation process. They provided a full set of accelerometer sensors and survey for the main case study Pentagon Road Bridge. Accelerometer survey provided with necessary information for main case study bridge to validate the data collected by IBIS-S monitoring.

3.4 Step 3: Carry out detailed surveys on the main case study

In order to fulfil both objectives two and three which relate to demonstrating the effectiveness of NDT on bridges and establishing detail information about structural

defects and information respectively detailed surveys of the main case study bridge were carried out.

Two surveys using IBIS-S were carried out with a 15 month gap between them in order to examine the variation in wet and dry conditions. Also accelerometer surveys were carried out. By using this additional equipment, the IBIS-S data which was used as a comparison for the FEM was validated and also additional necessary information was provided by the other sensors. The surveys were carried out with an 18tonne lorry load moving across the main case study bridge to obtain dynamic loading results. This gave information regarding the behaviour i.e. the deflection in a real scenario.

Two surveys using IDS GPR equipment were carried out with a 10 month gap between them in order to examine the variation in wet and dry conditions. The information gathered included visual cracks, vibration, rebar location, deterioration and moisture ingress. The dedicated software's specifically designed for the above equipment and was used to process and analyse the data. The rebar position results gathered from GPR were input into a finite-element model in ANSYS (Section 5.5.1). The information gathered from the visual inspection and all GPR, IBIS-S and Accelerometer results indicated that a particular area of the bridge had a significant structural health problem. This correlated with the findings of the finite-element model developed and compared with the information given by the NDT from IBIS-S and Accelerometer.

In the final survey of the bridge additional GPR equipment from (Utsi electronics) was used in order to compare antenna from differing manufacturer. Utsi Electronics provided a full set of (200-600MHz; 2GHz) GPR for the survey. The results gathered were used to validate the data collected by IDS Ltd (200-600MHz; 2GHz) GPR Antenna.

For all the above surveys, health and safety working practices (Medway Council) were fully prepared and followed. After visual inspections were completed, IBIS-S, GPR and Accelerometer surveys were completed. From the results of these surveys detailed information was gathered about the actual structural defects and deflection of the main case study.

3.5 Step 4: Develop FEM

ANSYS and SAP2000 were chosen as they have been used worldwide in both research and industry for many decades. FEM are needed in order to determine the deflection of the case study bridge without defect and compare it with its current deflection (as given by IBIS-S). This can indicate deterioration in the bridge structure. Information given by GPR such as rebar position can also be input into these models for additional accuracy (see Figure 5.2).

Using the finite element software SAP2000 (Computers and Structures, 2011), which was provided by Computer and Structures (an incorporated company from the U.S.A) who also delivered online training and support. ANSYS (2011) software was also used to provide more accurate modelling of the main case study bridge in the study. A member of the supervision team was also available to offer help with SAP2000 and ANSYS.

An initial model of the main case study bridge was created using both ANSYS and SAP2000 with parameters gathered from the visual inspection and a number of assumptions such as rebar position, rebar parameters and concrete information. This model was created to understand the behaviour of the structural. The results from this model are detailed in Chapter 5.

This helped fulfil objective one which aim was in part to identify appropriate FE Software.

The first model of the bridge was developed in SAP2000 using the data provided by an external principal report obtained from Medway Council and visual inspection data. At this point, no defects were input into the model. This model was used to predict the deflection of the bridge under the same dynamic loading as the survey completed using the IBIS-S and Accelerometer equipment. This allows for a comparison between the results the modelled deflection of the bridge without defects and the actual deflection.

The second model of the main case study bridge was developed in SAP2000 and ANSYS utilising the data provided by GPR. This created an accurate finite element

model of the bridge utilising the information regarding rebar position obtained from GPR surveys which was used for further analyses and testing. This testing consisted of both applied a dynamic load identical to the cherry picker used in the IBIS-S tests.

Crack propagation was also modelled on areas of the main case study bridge deemed to be significant and the effect of these cracks on structural response predicted using the CRACK tool in ANSYS (Section 5.5.2).

The numerical model of the main case study bridge was developed for two reasons:

- To compare the idealised displacement of the bridge as a newly built structure with the IBIS-S results
- To define parametric sensitivity of the structural response of significant spans (section 5.6.2).

More is detailed on the results of this model in Chapter five and this has fulfilled objective four.

3.6 Step 5: Develop an Integrated approach for bridge health monitoring

This was achieved the data gathered by visual inspection GPR, IBIS-S, and Accelerometer during the assessment of the main case study. This data was analysed and used to identify key structural failings of the bridge. By comparing all the data gathered by both survey and parametric study, it was possible to pinpoint areas of the bridge which were in need of remedial action. This whole process was the integrated approach for bridge health monitoring mentioned in the objective five. This process is again clearly illustrated in the following Figure 3.9.

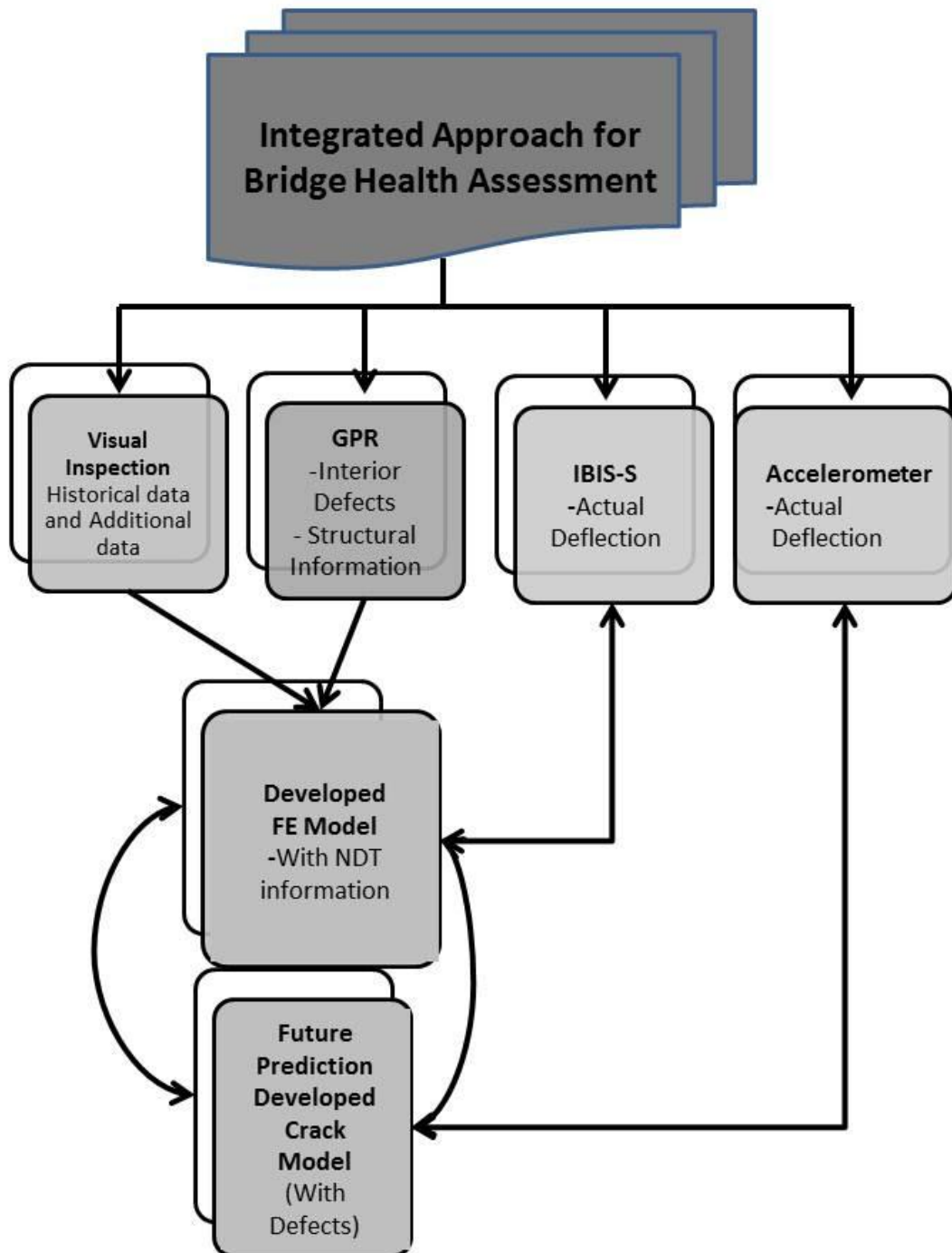


Figure 3.9– Integrated approach for bridge health assessment

This approach will have direct applications in planned and preventative maintenance systems of structures such as bridges, and will give both an enhanced knowledge of the actual bridge defects and also increased confidence when decisions have to be taken with regards to remedial action. This integrated approach is described in Chapter 6 and successfully fulfils the final objective of this thesis.

3.7 Summary

The following summaries of five stage research design framework were adopted for this thesis in order to ensure that all objectives were sufficiently completed:

- Step 1 used a literature review in order to identify and show understanding of the scope of research and identify the main non-destructive technologies such as Visualization, GPR, IBIS-S, Wireless sensor network and Accelerometer which were later applied in preliminary and main case studies.
- Step 2 discussed the operation, collection and interpretation of the data. The two main items of equipment (GPR and IBIS-S) were also tested or validated to ensure their validity.
- Step 3 involved several surveys of the main case study bridge using all NDT equipment. This proved that the NDT chosen were effective as bridge health monitoring techniques as they identified key structural information and defects of the bridge.
- Step 4 developed a finite element model using two different types of commercial software for parametric studies. The modified FE model to improve its accuracy, this was compared to IBIS-S and accelerometer results and a parametric assessment of the cracked zones was also modelled in this section.
- Step 5 combined the information gathered in steps 3 and 4 to create an integrated approach to assess bridge health. This approach will indicate if any further examination or remedial work is necessary.

In conclusion by completing these steps all the objectives of this thesis were met and the overall aim of creating an integrated bridge health approach was realised.

Chapter 4

Results and Analysis

In previous chapters the advanced NDT's for bridge health assessment have been described, along with illustrative examples to demonstrate certain procedures and compare the performance, advantage, disadvantage and limitation of different approaches. In this chapter applications of NDT are carried out on preliminary case studies “the Forth Road Bridge, the St Mary’s Island Lifting Bridge, the Darvel Road Bridge, and the Rochester Bridge” and on main case study “the Pentagon Road Bridge”. Velocity analysis is also carried out on main case study to ascertain the presence of moisture ingress. Finally, the integrated health mechanism approach is presented for the main case study.

4.1 GPR Trials

GPR trials were completed on a concrete slab 36 m^2 with known structural defects such as cracks, pits and metal pins (Figure 4.1). The GPR was moved both transversally and longitudinally across the whole slab. The results of these scans were then processed using the appropriate software (GRED). This gave both L and T scans, an example of an L scan is shown in Figure 4.2. The features identified on the surface of the slab (metal pin, pit) are clearly visible in the distorted hyperbole. The GPR data was found to give an accurate prediction of the locations of cracks and metal pins and also thickness of the slab itself. From the results of this trial it was determined that GPR is an accurate non-destructive technique and decided that it should be carried out on the preliminary case studies.

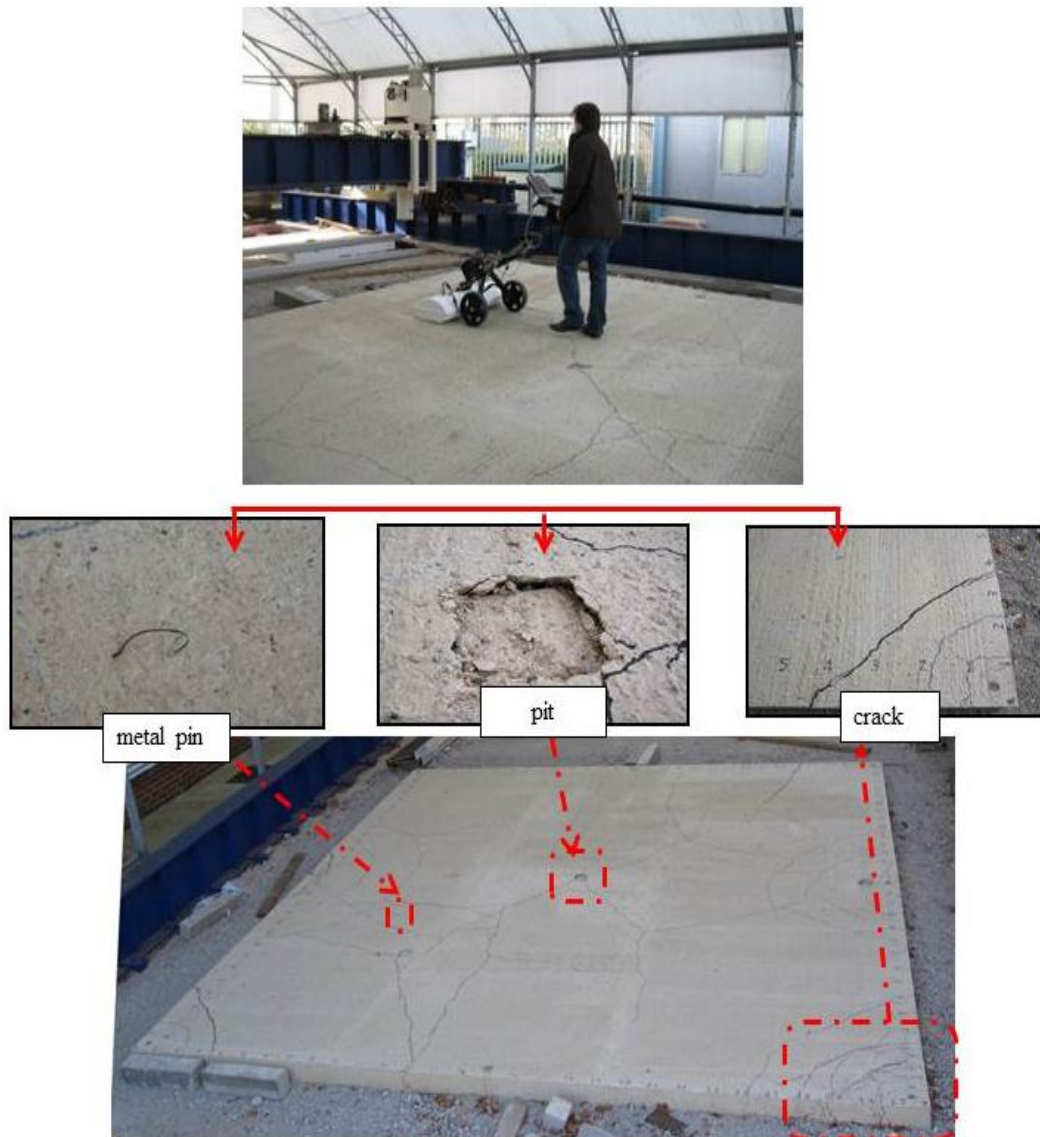


Figure 4.1 – GPR trials on a concrete slab

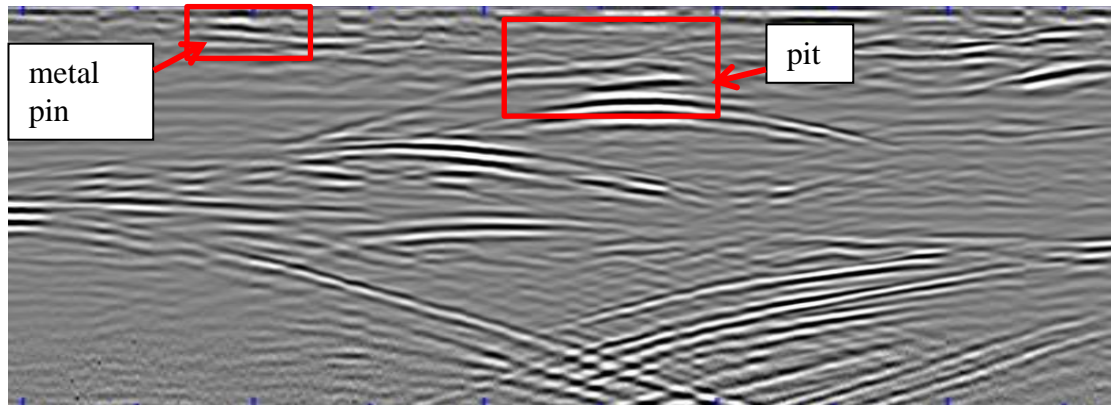


Figure 4.2 – GPR trials radargram

4.2 Preliminary Case Studies

In this section, appropriate bridges (Forth Road Bridge, St Marys Island Lifting Bridge, Darvel Road Bridge, and Rochester Bridge) were selected as preliminary case studies. This selection was based on a variety of different factors including accessibility, importance and also requests for health assessment by the relevant authorities. The main objective of these preliminary case studies was to increase the knowledge of operating, collecting, interpreting and processing the NDT data and validate their results.

Firstly, visual inspections were carried out on them. After these visual inspections were completed, a GPR survey was undertaken on all of the preliminary case study bridges. These surveys gave an opportunity to prove the accuracy of the GPR equipment as a non-destructive bridge health monitoring technique along with the slab test detailed in previous section.

Due to budgetary limitations, it was not possible to utilise the other forms of NDT examined for this study: IBIS-S and FEM. But as the main purpose of these case studies was to validate the NDT and learn about their operation, alternative methods needed to be found for two methods not utilised. This was accomplished by receiving training using IBIS-S from IDS Ltd. and validating its results using accelerometers. FEM training was received online and completed under the supervisory team. The FE models were validated by comparison between each other and against IBIS-S data.

4.2.1 Forth Road Bridge

Forth Road Bridge (Figure 4.4) is in east central Scotland (Figure 4.3). The bridge provides access to the capital city Edinburgh from North Queensferry.

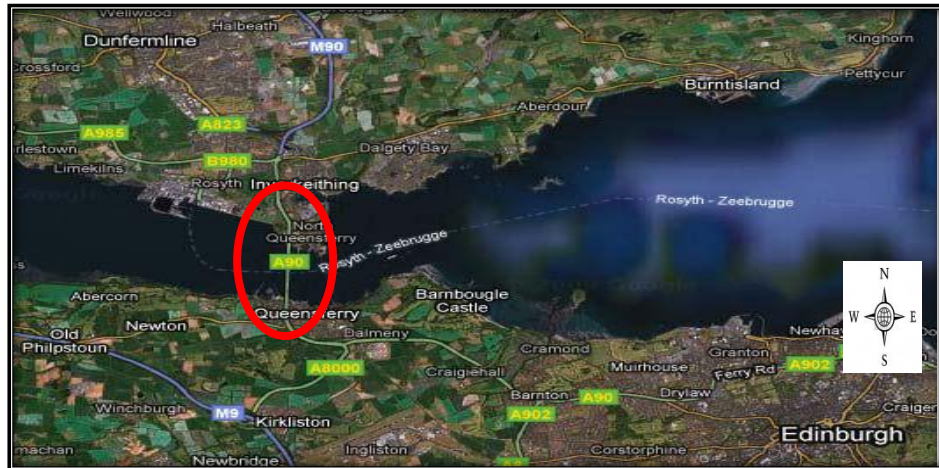


Figure 4.3 – Location of the Forth Road Bridge. (Google Maps, 2010)

The Forth Road Bridge opened in 1964 and it is a suspension bridge. Every year the bridge traffic has increased up to now from 4 million to 24 million vehicles. The Forth Road Bridge main span is 1006m, the two side spans are 408m, total length between abutments is 2517m, and tower height is 156m (Colford and Clark, 2008).



Figure 4.4 – General view of the Forth Road Bridge (Forth Estuary Transport Authority, 2010)

The visual inspection and GPR survey was carried out by IDS limited (the research industrial partner).

4.2.1.1 GPR Assessment

A GPR survey using the RIS Hi BriT (2 GHz) Antenna was performed by IDS limited (the research industrial partner) on three areas of the Forth Road Bridge (Figure 4.5). The GPR data for these three areas was processed and interpreted by the author and research team.



Figure 4.5 – Areas of Investigation of the Forth Road Bridge. (Google Maps, 2010)

The Radar data acquired from the GPR scans of the bridge was saved as raw data and then processed to recover the information required. After a standard processing has been performed, data for each channel was displayed as a ‘b-scan’. Each b-scan represents a vertical slice through the bridge, and is useful when identifying factors such as rebar positions and moisture.

The following radargram Figure 4.6 shows a b-scan that has been annotated to identify the features discovered during the radar survey of Area 1. By performing this interpretation on several b-scans side by side it is possible to build up a picture of the conditions inside the bridge.

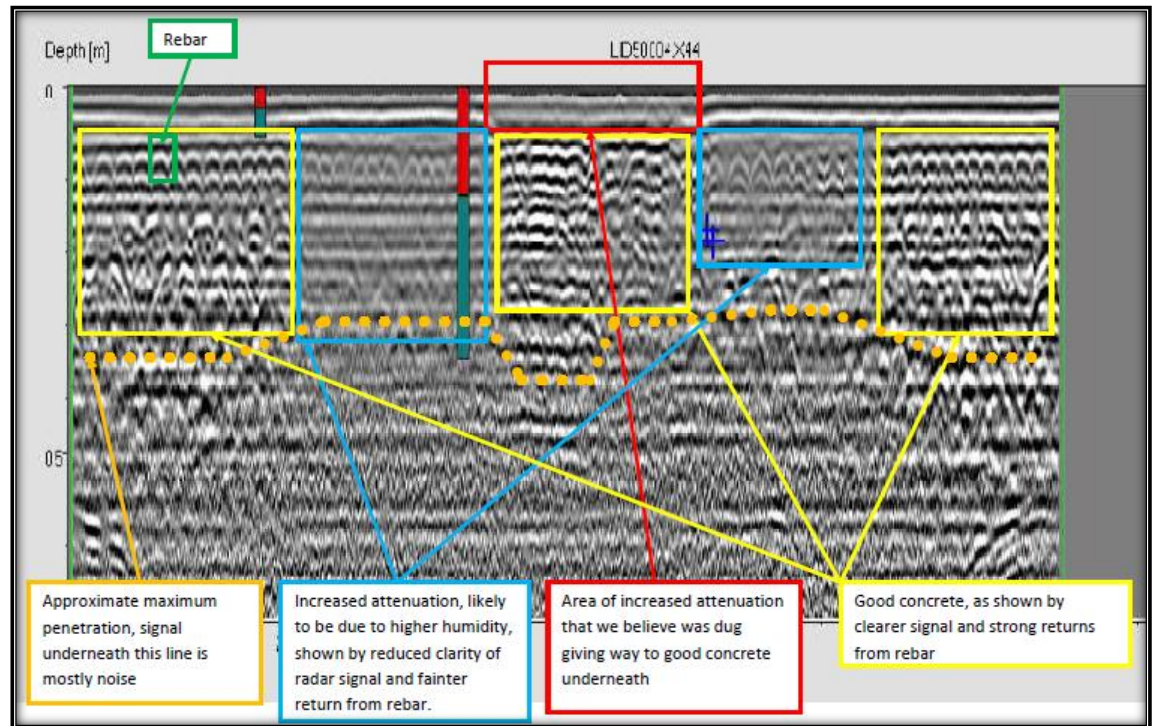


Figure 4.6 – The b-scan with identified section

The Figure 4.6 is a longitudinal section down the centre of the damaged area, identified by the red line in the horizontal section shown Figure 4.6.

4.2.1.2 Results

Using the processed and interpreted data from the GPR, by comparing the b-scans, it is possible to produce horizontal sections of the area surveyed as seen in Figure 4.7, which displays the expansion of the moisture affected area at lower depths; scans Area 1, these results were derived from the radar data and from them it was possible to determine the following information:

- The location and spacing of two separate layers of rebars which were the: top layer of rebars in both directions and the deeper layer of rebar in one direction only.
- The area of moisture penetration close to the surface.
- The larger area of moisture penetration underneath the surface damage.

The processed data was examined (at approximately 20cm depth), it is clear that the concrete is in good condition, which is represented by lighter contrast and the rebar can be clearly seen as illustrated in Figure 4.7. The area of moisture is also identified by a patch of reduced contrast, the size of this deteriorated area is highlighted in Figure 4.7(d).

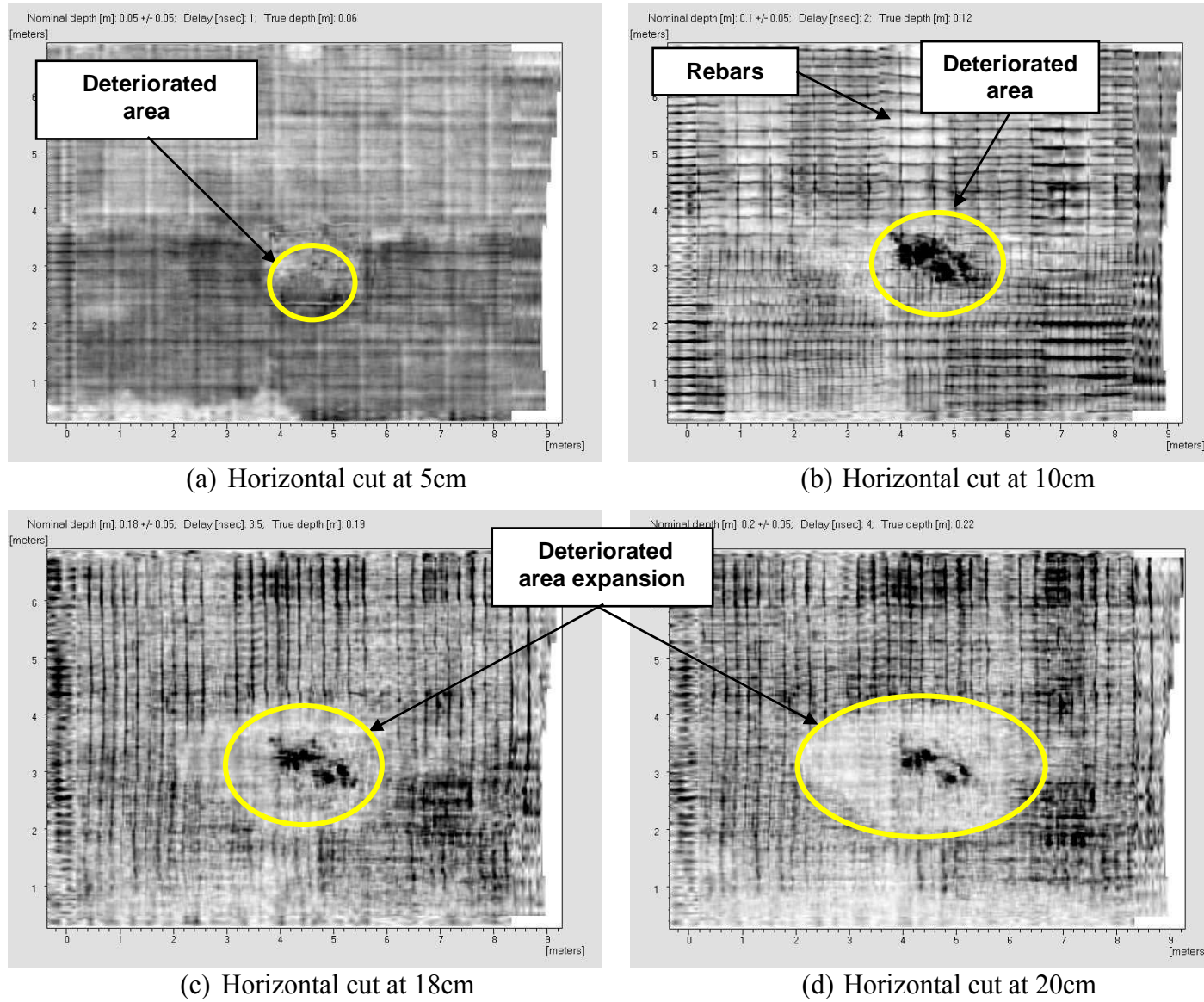


Figure 4.7 – Expansion of the moisture affected area 1 (Data processed by Gokhan Kilic, 2010)

One of the most important findings from the radar data on area 1 was an indication of an area of moisture at 20cm depth that surrounds the shallow area excavated, a core sample is recommended to verify this.

Due to the density of channels in the RIS Hi BriT (2 GHz) Antenna it is possible to recover large quantities of information during a radar acquisition. This gives a high level of confidence in the data acquired as well as enabling radargrams of exceptional quality to be produced, which aids data interpretation. It also allows more advanced processing techniques to be performed such as the mathematical calculation of the areas with higher than average attenuation (absorption of the radar signal), producing a 2D map of the moisture levels within the bridge.

This is proven by the following Figure 4.8 in which the present moisture ingress and the concrete was removed and shallow layer of rebar is visible.



Figure 4.8 – Area 1 of visible rebar (Photo from Kevin Banks, 2010)

The results from remedial works carried out by the Forth Road Bridge Authority so far confirm that:

- Location and spacing of two separate layers of rebar such as: top layer of rebar in both directions,
- Area of moisture ingress close to the surface.

This excavation took place on the damaged section of the bridge. The excavation ended when all the moisture damaged material had been removed and the diggers hit sound concrete at a shallow depth. These findings serve to further validate the use of GPR as a non-destructive bridge health monitoring technique.

4.2.2 St Marys Island Lifting Bridge

St Marys Island Lifting Bridge (Figure 4.9) was constructed in 1996 and is located on Pembroke Road between Gillingham and St Marys Island in Chatham (Figure 4.9). (Chatham Maritime House, 2010)



Figure 4.9 – Location of the St Marys Island Bridge. (Google Maps, 2010)

In 1994 St Marys Island Lifting Bridge (see Figure 4.10) project involved the removal of an existing bridge structure and construction of a new access bridge to St Marys and its approach embankments. (Chatham Maritime House, 2010)

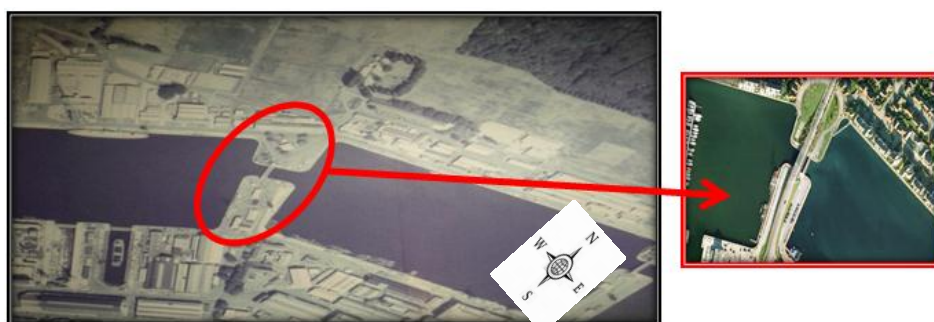


Figure 4.10 – The St Marys Island Bridge previous (left) and recent view (right). (Chatham Maritime House, 2010)

The St Marys Island Lifting Bridge is a three span construction comprising two concrete approach spans and a single leaf lifting bridge centre span. The bridge includes a 6.75m wide carriageway with a 3.0m combined footpath and cycleway on the west side and a

1.8m footpath of the east side. The two internal piers are connected to pile caps which are supported on bored piles.

A visual inspection was completed by the author and research team in collaboration with the industrial partner which showed no signs of structural defects and anomalies.

4.2.2.1 GPR Assessment

Subsequent to visual inspection a GPR pavement survey was carried out on a single side of the bridge and the collected data was processed and interpreted. The GPR survey using the RIS Hi BriT (2 GHz) Antenna was performed on a single side of the pavement (Figure 4.11).



Figure 4.11 – GPR Survey on the St Marys Island Lifting Bridge. (photo from Gokhan Kilic, 2010)

4.2.2.2 Results

This GPR Survey gave the measurements of the pavement, concrete slab thickness and the location of buried pipes and drainage patterns.

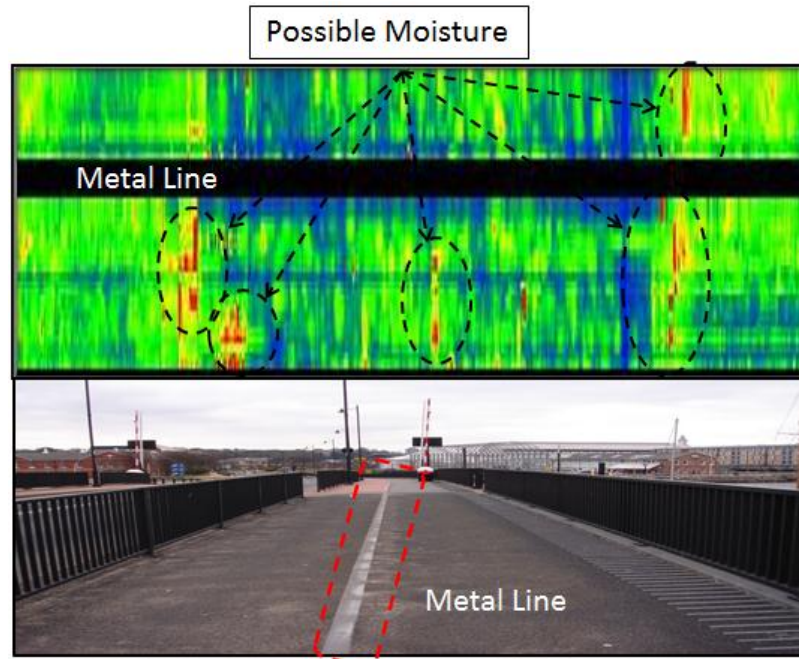


Figure 4.12 – Pavement GPR B-Scan 20cm depth Result (North view)

Figure 4.12 shows the b-scan which is a profile of the pavement at a depth of 20cm beneath the surface. The black line indicates the metal line which does not allow any reflection of electromagnetic waves. It is clear from this processed data that there are some anomalies in the results indicated by the red areas. These red areas could indicate moisture ingress in the pavement slab although it is impossible to verify these results without further excavation which is not appropriate in this case as the anomalies do not pose a risk to the bridge health.

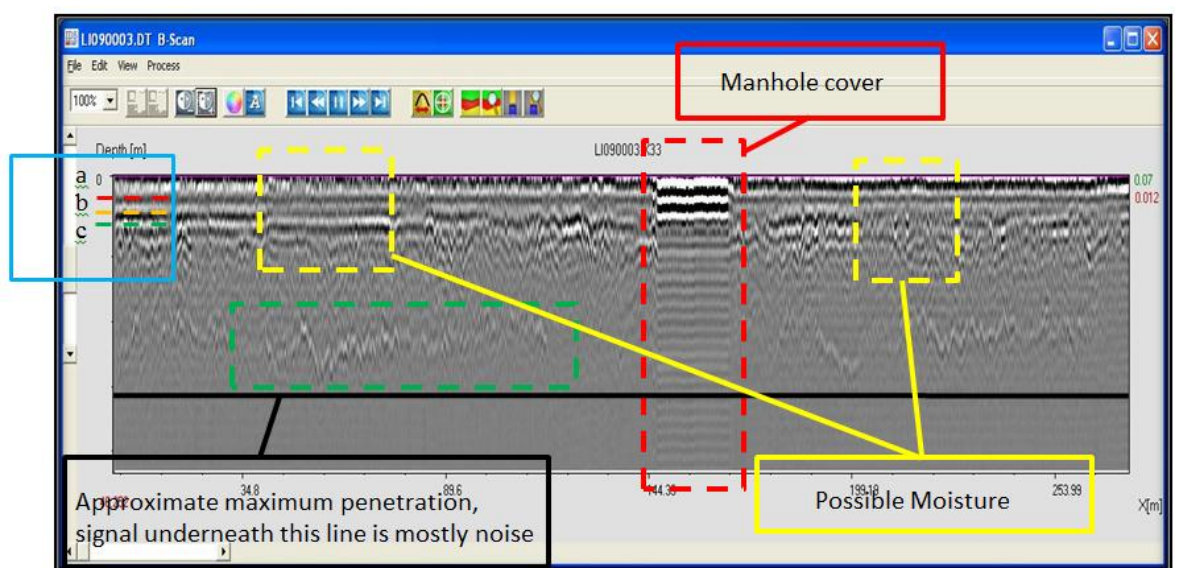


Figure 4.13 –GPR Radargram results

Figure 4.13 shows a radargram which illustrates the response from the pavement underlying constituents over a depth of 60cm. The depth was limited by the use of a RIS Hi BriT (2 GHz) Antenna which gave greater resolution at a cost to penetration depth. The layers of underlying pavement are indicated by the lines a, b and c. Moisture areas were identified by the lowering in resolution of the hyperbola which are close to the surface. Some distortion in the results is caused by the presence of a metal manhole cover; metal as stated in chapter two attenuates the electromagnetic waves and does not allow for radar reflection” which prevents an accurate radargram.

Figure 4.13 summarise the results from the GPR Survey as follows;

- Location and spacing of two separate layers.
- Area of moisture penetration close to the surface.

These results are important as they highlight the ability of the GPR scan to identify key factors in the health monitoring of a bridge. Both the position of the layers and moisture content were crucial factors in the decision to preform remedial work on the Forth Road Bridge so although St Marys Island Lifting Bridge is not in need of any renovation, it is still useful to identify aspects such as moisture which could change this assessment in the future. Moisture is generally present in bridges with cracks which allow transport of water through the concrete, thus newer bridges do not have excessive moisture ingress. Moisture in bridge decks can cause the corrosion of rebars and the degradation of concrete thus weakening the structural integrity which was found in the case of the Forth Road Bridge.

4.2.3 Darvel Road Bridge

The Darvel Road Bridge (Figure 4.14) is a beam bridge on the M74 Motorway connecting Glasgow and northern England.

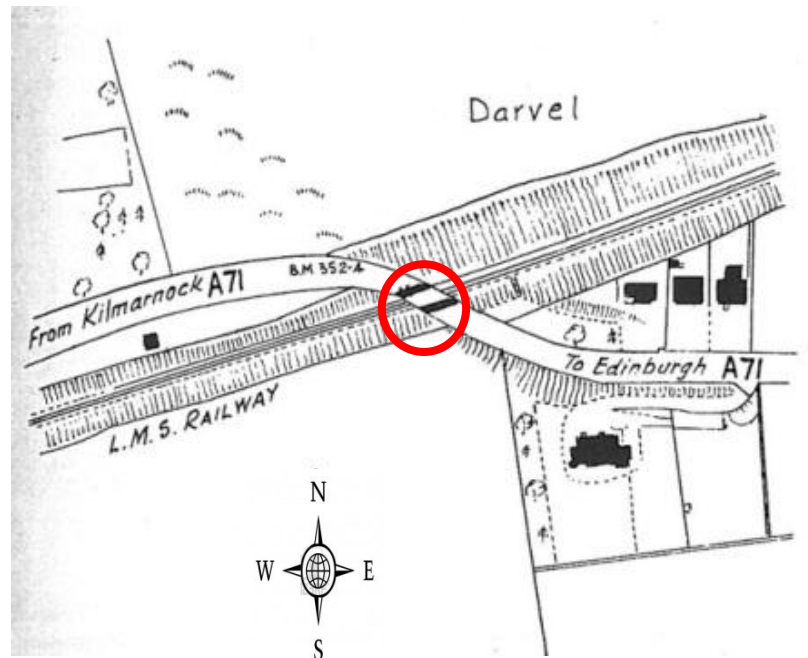


Figure 4.14 – Location of the Darvel Road Bridge. (Wikipedia, 2010)

Figure 4.15 (a) shows an historic view of the bridge, as it was built to span a railway track however this railway is now defunct and the track has been overgrown by plants and other natural events which will be detailed later. The bridge has seen an increase in traffic and use over the previous decades, with any such old structure continuous health monitoring is essential.



Figure 4.15 – Historic and recent view of the Darvel Road Bridge. (Wikipedia and Picture by Gokhan Kilic, 2010)

The visual inspection was completed which noted that heavy vegetation covered the steel parapet wall on south side of the bridge and the underneath area of the bridge (Figure 4.16). There was also water ponding on the north side of the bridge due to the blockage of a drainage pipe which needs to be investigated and eventually rectified (Figure 4.17).



Figure 4.16 – Heavy vegetation North side view of the bridge (photo taken by Gokhan Kilic, 2010)



Figure 4.17 – Water ponding on north side of the bridge (photo taken by Gokhan Kilic, 2010)

4.2.3.1 GPR Assessment

There is no existing plans or design information regarding this bridge due to its age, therefore surveys such as this are one of the only methods available to determine its properties such as beam position without the need for destructive techniques. The purpose of this survey was to determine the beam position as piling work needed to be completed on the bridge and the beam depths were not known.

Over the bridge deck, a total of 11 longitudinal and 50 transversal array scans with the RIS Hi BriT (2 GHz) Antenna and 9 longitudinal and 14 transversal array scans with the RISMFI-HI-MOD (200-600 MHz) Antenna were collected. The survey was performed on bridge deck which had an area of approximately 10 m x 35m (Figure 4.18).



Figure 4.18 – GPR Survey on the west view of the Darvel Road Bridge. (photo taken by Gokhan Kilic, 2010)

A GPR survey was performed by marking two different coloured grids on the ground using chalk. One grid had lines marked every 40cm for the RISMF HI-MOD (200-600 MHz) Antenna, the other had lines marked every 80cm for the RIS Hi BriT (2 GHz) Antenna. Next the radar was pushed across the grid in straight lines for each of the antenna. The location of the grid was referenced by recording the coordinates with respect to a fixed location. Due to the frequency of the antennas and the size of the array, surveys were performed covering moderate areas, rather than one large survey.

4.2.3.2 Results

The data from the GPR survey was collected, processed and interpreted and the position of the beams determined from the radargram.

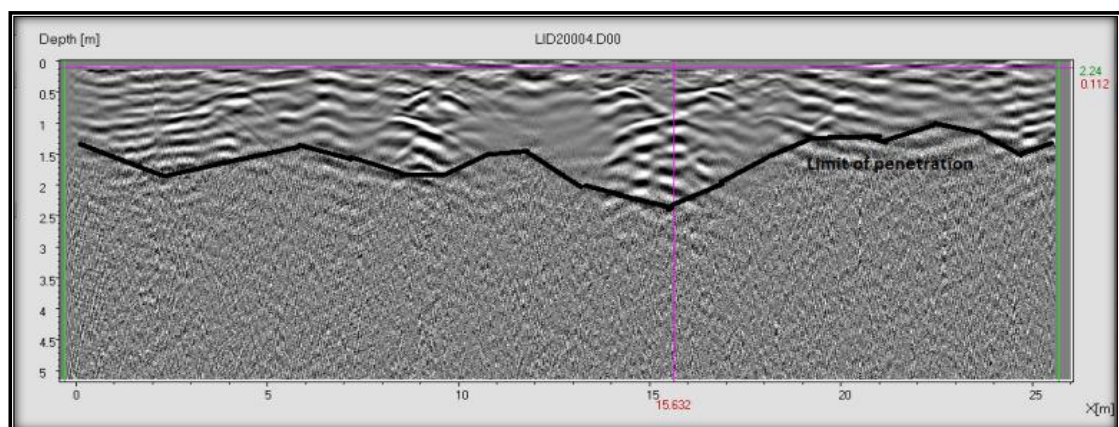


Figure 4.19 –GPR Radargram 600 MHz

On Figure 4.19, the limited penetration depth is clearly marked. The hyperbole indicate the position of the beams.

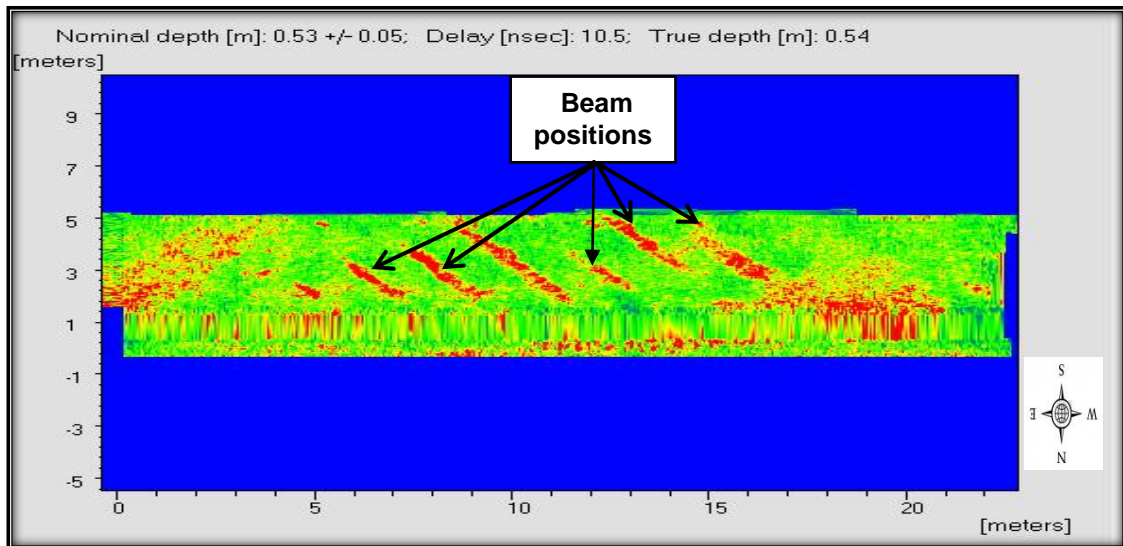


Figure 4.20 – Area 1 GPR b-Scan 20cm depth Result

In Figure 4.20, the red colour indicates the beam positions at a depth of 53cm. From the b-scan the position of the top of the beam can be identified and this is then transformed manually to an AutoCAD drawing (Figure 4.21) which shows the complete co-ordinates and the depth of the beams.

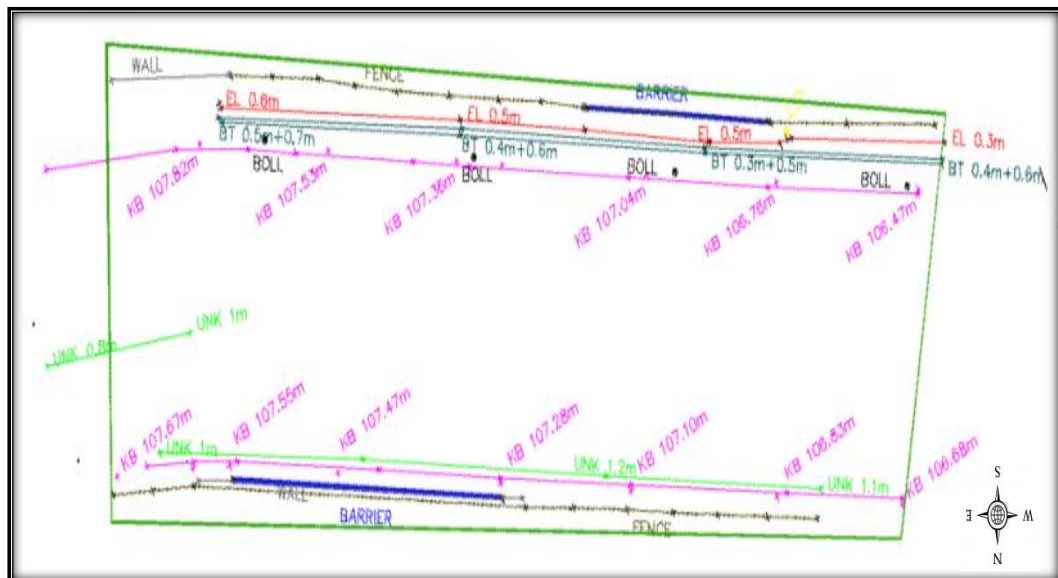


Figure 4.21 – Beams locations shown on an AutoCAD Plan

From Figure 4.21, it was possible for the excavations to be completed without damage to the beams.

4.2.4 Historic Rochester Bridge

The reconstruction of the Historic Rochester Bridge (Figure 4.22) “Old Bridge” was completed in 1914 (The Rochester Bridge Trust, 2010).



Figure 4.22 – Location of the Historic Rochester Bridge. (Google Maps, 2010)

The bridge has three arched steel truss spans and a plate girder approach span with ramps at each end. The Strood approach at the western end is constructed over brick arches. The carriageway, originally built for two tramway tracks and the third lane for overtaking traffic, is 7.93 metres wide. Today, it carries the two lanes of westward-bound traffic from Rochester to Strood (Figure 4.23).

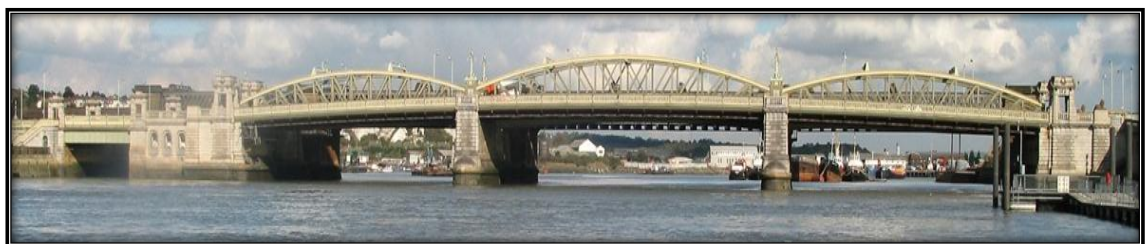


Figure 4.23 – Rochester Bridge (The Rochester Bridge Trust, 2010)

4.2.4.1 GPR Assessment

The GPR was survey performed (Figure 4.24) using the RIS Hi BriT (2 GHz) Antenna.

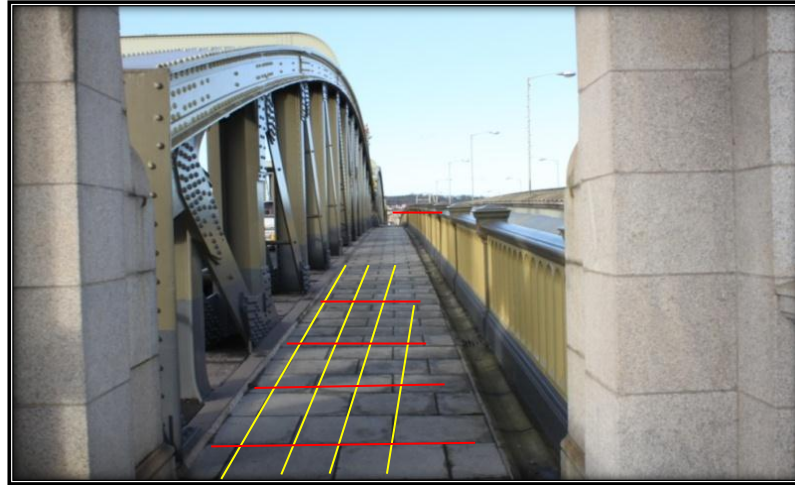


Figure 4.24 – Bridge deck to be surveyed by GPR (north view) (photos from Gokhan Kilic, 2010)

A GPR survey was performed by marking a grid (Figure 4.24) on the ground using chalk and pushing the radar across the grid in straight lines.

4.2.4.2 Results

Specified parts of the bridge pavement were surveyed using GPR (Figure 4.25). The data was divided into four parts for processing and interpretation. From this processed data it was clear that some part of this surveyed area had structural defects which needed further attention.

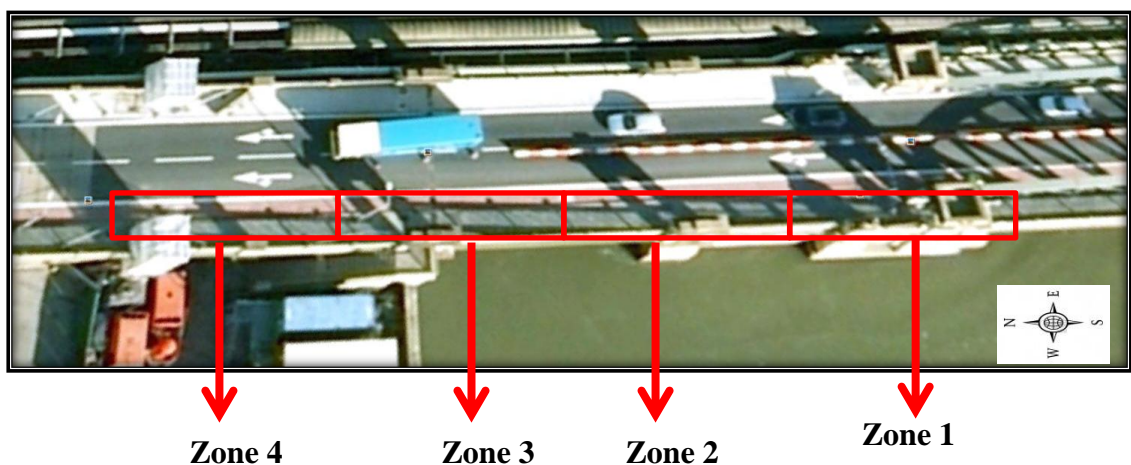
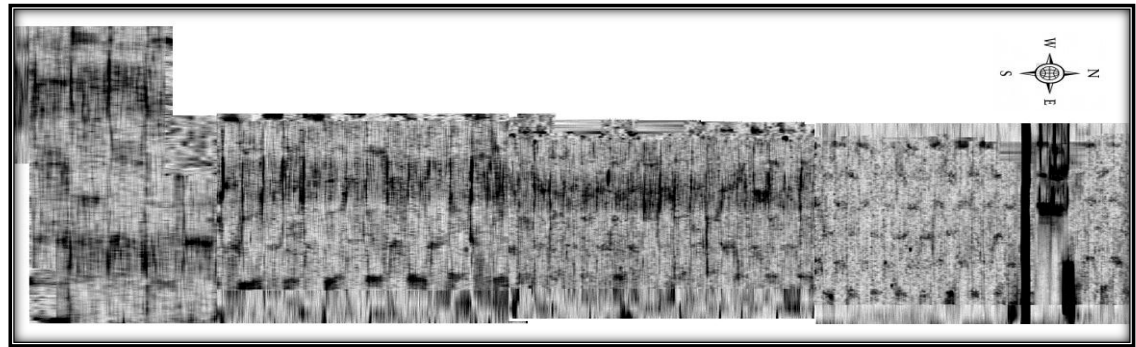
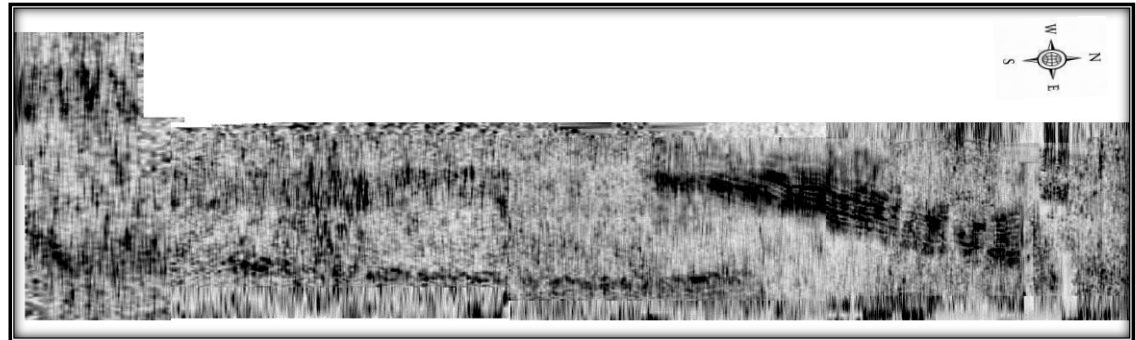


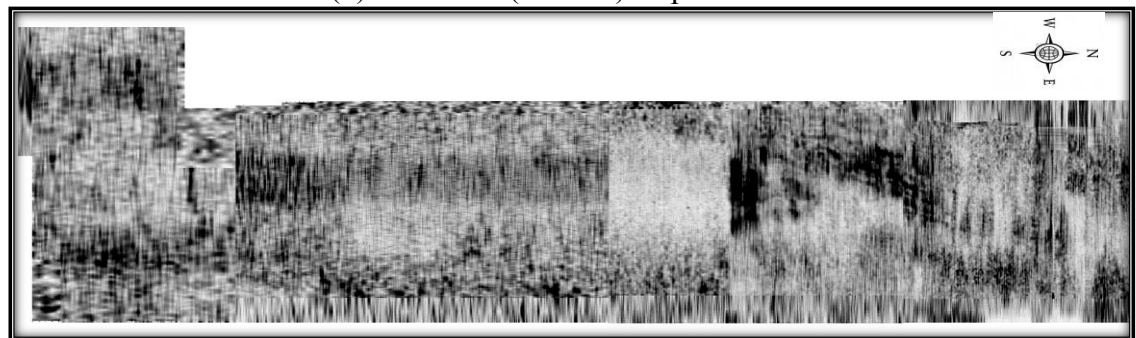
Figure 4.25 – GPR Survey areas



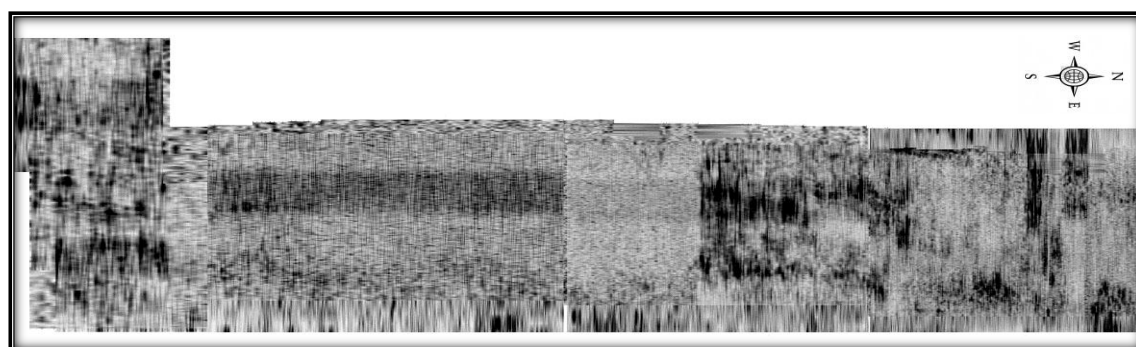
(a) All Zones (1-2-3-4) Depth =0cm



(b) All Zones (1-2-3-4) Depth = 15cm



(c) All Zones (1-2-3-4) Depth = 25cm



(d) All Zones (1-2-3-4) Depth = 45cm

Figure 4.26 – GPR Processed Data

Figure 4.26 shows the layers of the pavement structure at various depths. It is clear that as depth increases the area of moisture increases. Larger area of moisture penetration underneath indicates surface damage.

Also at a depth of 45cm shows previous remedial work which is confirmed by the site engineer.

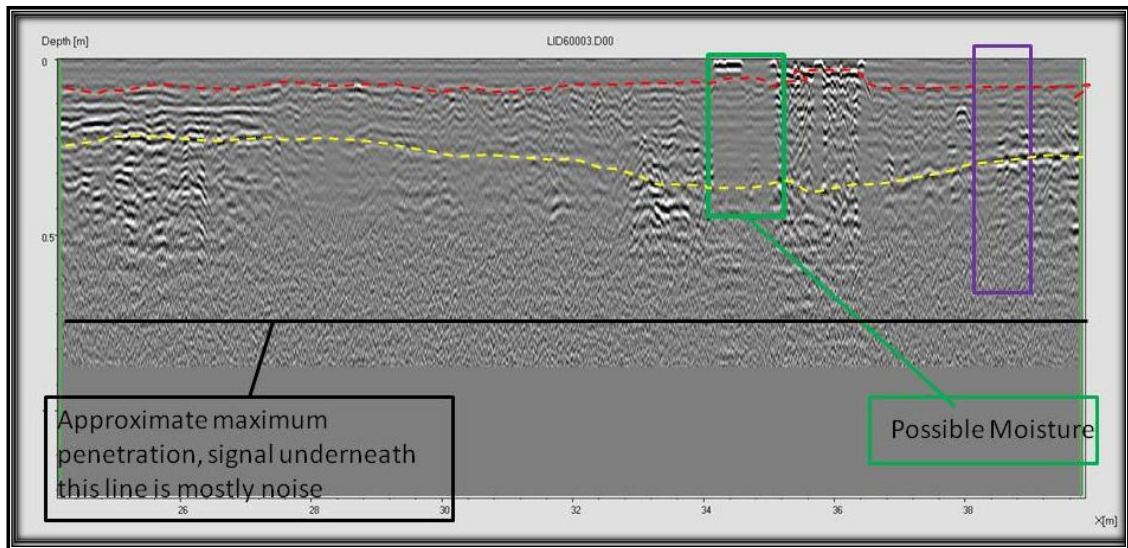


Figure 4.27 – GPR Radargram (zone 1)

Figure 4.27 shows maximum penetration, moisture area and layers of the underlying pavement slab.

A large amount of information was created and handled in order to tackle the fixed aims of this bridge assessment. A quantity of data has been selected to emphasize the value of GPR in the assessment of bridge structures in recognizing potential faults as is seen Figure 4.27 in the form of moisture that otherwise are not clearly identifiable by using other standard techniques. GPR is also useful in identifying structural properties such as rebar or beam position which may not be known especially in older structures.

4.2.5 Summary and Significant of Preliminary Case Studies

The GPR surveying along with visual inspection was carried out on the preliminary case study bridges. Data collected from these preliminary case studies (Forth Road Bridge, St Marys Island Lifting Bridge, Darvel Road Bridge and Historic Rochester Old Bridge) was used for data processing and interpretation. This proved to be vital to establish benchmarks and develop an effective methodology for the Pentagon Road Bridge assessment and monitoring. Similarly, its effectiveness and applicability as a non-destructive testing method was proven.

These Preliminary Case Studies surveys were very successful and the results obtained were significant in line with the first set objective of this thesis. These Preliminary Case Studies were composed of data collection, processing, analysis and interpretation by the author in order to understand the limitations and advantages of the GPR device. Secondly, the study investigated as listed below:

- Demonstrate technology in structural monitoring and assessment of bridge structures.
- Processing and interpretation of data collected.
- Measure pavement and concrete slab thickness
- Locate deck slab and protective concrete damage
- Map drainage and other buried pipes
- Determine reinforcement cover depth
- Detect moisture ingress

4.3 Main Case Study: PENTAGON ROAD BRIDGE

4.3.1 Introduction

Pentagon Road Bridge (Figure 4.28) carries an access road from Rope Walk to the Pentagon Shopping Centre with a four span simply supported concrete deck of beam and slab construction. The bridge was constructed in 1975 in Chatham. At the east, low end support is a leaf pier that is shared with the access road and the west, high end, the bridge links to the access road to the rooftop car park of the shopping centre. There are a number of known defects on the bridge with the rebar visible in some places due to concrete deterioration.



Figure 4.28 – View of Pentagon Road Bridge (Photos from Gokhan Kilic, 2010)

The Pentagon Road Bridge was chosen as the main case study as no detailed information was available on the bridge. This is similar to a large number of bridges throughout this country such as the Darvel Road Bridge which have no structural information recorded on them. Thus if it can be comprehensively proven that the integrated bridge health mechanism is appropriate for this bridge, there is no doubt that it can be used on all similar bridges.

The following Figure 4.29 illustrates the timeline under which the non-destructive testing was carried out.

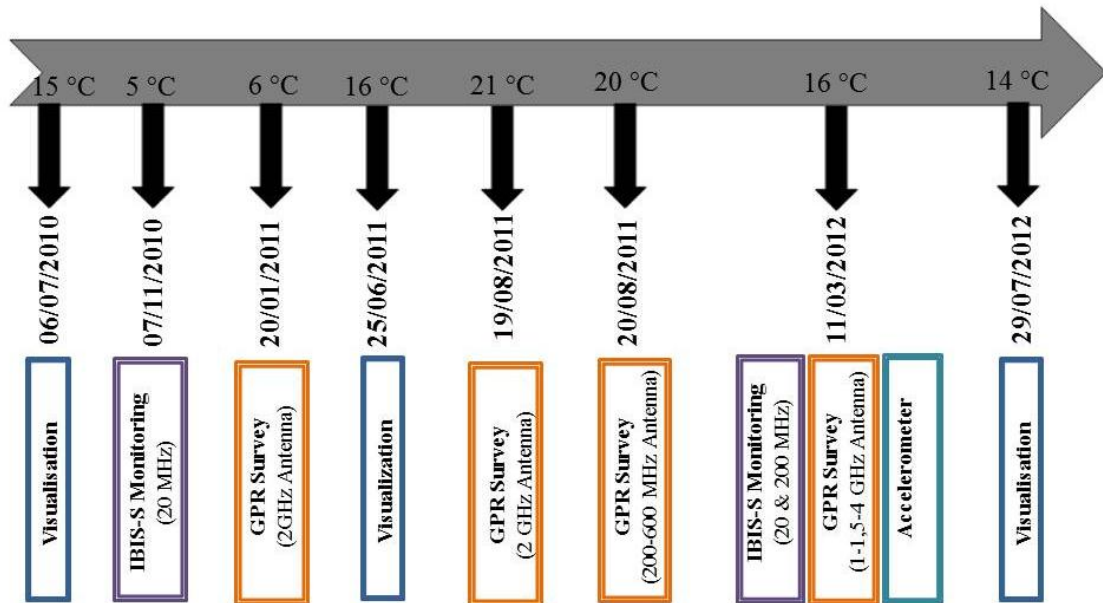


Figure 4.29 – Non-destructive testing timeline on Pentagon Road Bridge

Detailed records of the inspection of all visible component parts of the Pentagon Road Bridge are presented in Appendix D.

The following section contains results from the visual inspection (section 4.2.2); findings from IBIS-S monitoring (section 4.2.3) which was validated with accelerometers (section 4.2.4); results from the GPR Survey (section 4.2.5) and further GPR velocity analysis (section 4.2.6).

4.3.2 Visual Inspection

In this section, firstly the previous visual inspection by Jacobs Engineering U.K. Limited is introduced. Secondly, a visual inspection report detailing material defects, structural defects is provided. Finally, a health assessment and several common deficiencies distinguished of the bridge is summarised, and future study is identified.

Previously a visual inspection was carried out with a camera, Leica Disto laser height measuring instrument, crack gauge, hammer, torch, ladder, and 22m ascendant telescopic hoist in 2009 by Jacobs Engineering U.K. Limited (Denness et al., 2009). From the report, the faults and recommendations are a number of known defects on the bridge with the rebar visible in some places due to concrete deterioration. Concrete repairs are required to the West End Leaf Pier Support, Piers 1 and 2 and all of the deck

spans. The transverse beam at the west end of Span 4 is in very poor condition and required an assessment of its adequacy prior to any remedial works being carried out. The surfacing on the deck is nearing the end of its life with areas of reinstatement, some in poor condition, potholes and fretting. All of the bearings to the main spans that could be seen were in a poor condition. The fixed bearing at the east of the north deck of Span 1 has a broken bottom plate/shell and needs to be replaced. The report recommended that all of the bearings needs to be replaced. The transverse joints and the longitudinal joints have faults that indicate that there is leakage at each; concluding that the joints should be replaced. The parapets are damaged with areas of corrosion and required repair and painting.

4.3.2.1 Inspection

A visual inspection was carried out on 6th July 2010, 25th June 2011 and 29 July 2012 by Gokhan Kilic under the supervision team. A bridge inspection was performed and a health assessment was made of the structure presented in Table 4.1:

Table 4.1 – Visual Inspection

Visual Inspection	Dates	Temperature	Weather
1	6 July 2010	15 °C	The weather was sunny day.
2	25 June 2011	16 °C	The weather was sunny day.
3	29 July 2012	14 °C	The weather was sunny day.

There were structural defects visible to the naked eye which is not fully specified in this section. These included cracks which may lead to further deterioration in the form of efflorescence, discoloration, spalling and corrosion of rebars which could, in time result in structural collapse.

The Pentagon Road Bridges visual condition was categorised. This categorisation was based on the problems encountered such as: concrete and steel members, bearing and expansion joints, vibrations and the impact of vehicles. The problems that the bridge inspections investigate may cause many further technical and economical problems if left unchecked.

The visual inspection was carried out within touching distance of each element such as, the deck slab soffit which was inspected from the footway and carriageway below for cracking, spalling, exposed reinforcement, seepage and staining.



(a) – Asphalt potholes with visible rebar on Span 3 (b) –Expansion joint between span 3 and 4

Figure 4.30 – General Visual Inspection

Based on the Figure 4.30 (a) shown above, surfacing asphalt over the bridge deck can be seen, the asphalt also displays has signs of cracks, settlement, potholes, deformation, general deterioration and exposed reinforcement. Figure 4.30 (b) also shown above are expansion joints and display signs of cracking, debonding and leakage. These may indicate defects to the bridge deck. Also, the surfacing over the deck has areas requiring reinstatement, some in poor condition with potholes and fretting. Regrettably the bearings were not possible to inspect however; the ground level bearing shelves were inspected.

Starting from the south end of the bridge, the bridge deck in the first and second span, with a depth of 110 cm doesn't show any structural deterioration or problems. The third span is a 50 cm thick shell and the thickness of the last span is even reduced to 30 cm. The fourth span is supported by a grid of beams especially at the end in the vicinity of the third span where a cantilever zone is provided. The third and fourth spans are in very poor condition and require an assessment of their adequacy prior to any remedial works being carried out. The surfacing on the deck is nearing the end of its life with areas of reinstatement, some in poor condition, potholes and fretting. All of the bearings to the main spans that could be seen are in poor condition.

There are a number of known defects on the bridge with the rebar visible in some places due to concrete deterioration such as severe cracks between Spans three and four, deterioration of concrete (chemical reaction evident) and rebar (possible corrosion) with water seepage, cover delimitations and significant cracks. The Figures 4.31 below explain the findings based on the inspection conducted.

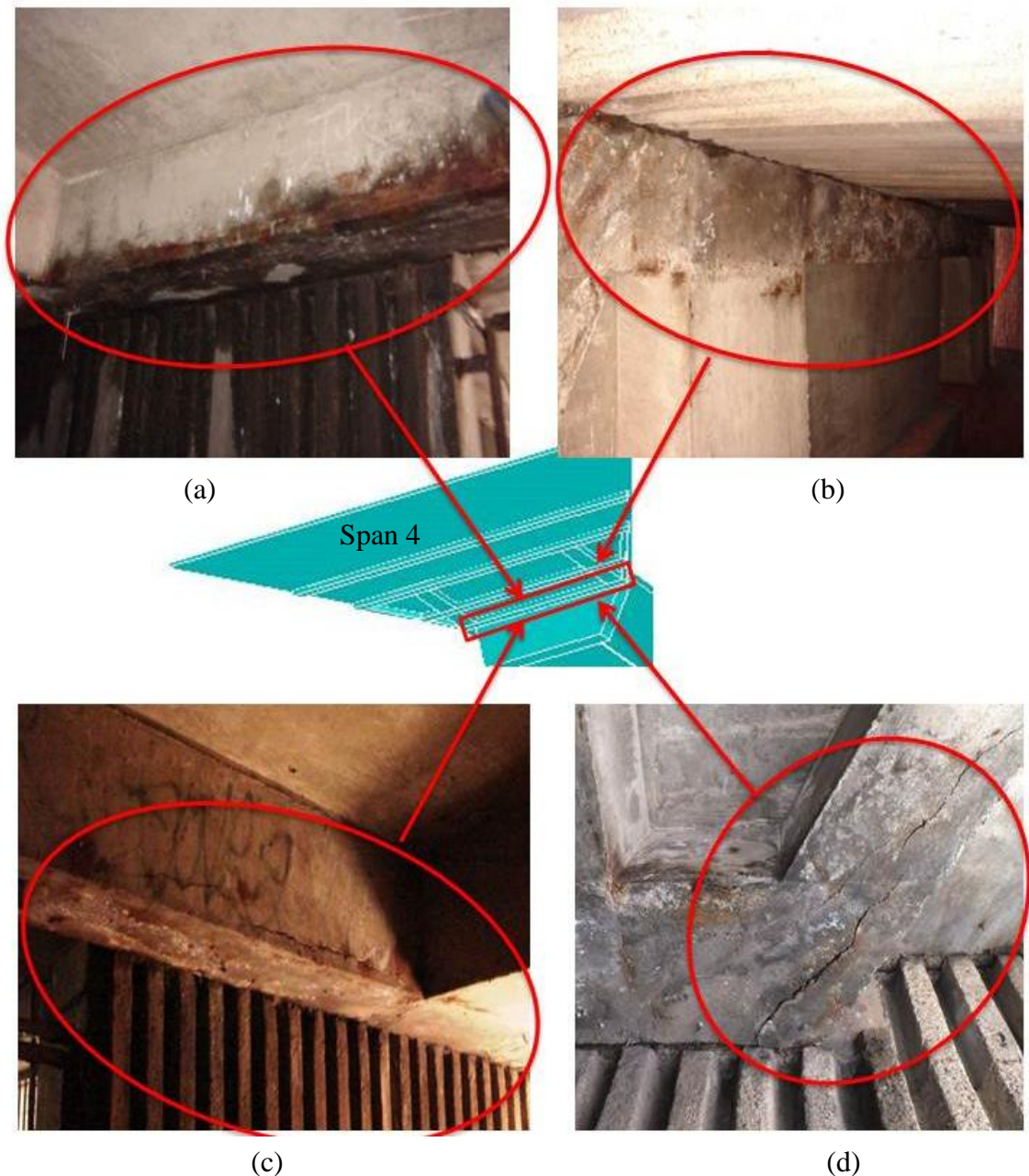


Figure 4.31 – Concrete deterioration between span three and four

Figure 4.31(a) shows efflorescence has occurred in this area and is present as a white deposit on the surface of concrete. This will be due to the reaction of calcium hydroxide

from cement which reacts with carbon dioxide to form calcium carbonate. This will have no significance towards the strength of concrete however, as reaction continues it may result in corrosion.

Figure 4.31(b) shows that water is easily seeping through the deteriorating concrete which is causing the concrete further damage. During the visual inspection, it was noted that the water was continually dripping through the concrete indicating underlying concrete deterioration and significant corrosion.

Figure 4.31(c) shown above, illustrates a horizontal crack. The reasons for this problem may be moisture inside the deck. This will directly reduce the strength of the beam. This problem is of utmost importance as reinforcements play an integral role by providing strength in the concrete.

Figure 4.31(d) displays longitudinal cracks which might be due to vehicle impact. The beam might have weakened in strength caused by dynamic loading from the bridge deck transmitted to the concrete. This is a serious problem as any weakening of the bridges support system should be taken seriously as it can result in further deterioration and eventually structural collapse. In the short term it may also lead to deterioration in the surface of concrete leading to efflorescence and staining.

During the course of this investigation the structure has undergone more deterioration in the form widening cracks and excessive cover delamination as illustrated in Figure 4.31(d). These widening cracks were observed during the visual inspection, however it was not possible to install sensors which would have quantified this growth. None the less the increase in crack size between 2010 (Figure 4.32a) and 2012 (Figure 4.32c) is clearly visible to the naked eye. This deterioration could be caused by number of factors such as seasonal changes. However the following conditions which could have an impact on these defects were observed to be elements such as the leaking water in the bridge body. These cause a weakening of the structural integrity of the bridge, especially between span three and four. It is important to continually monitor this deterioration in order to determine the safety of the bridge, which is of course of paramount concern. This will be achieved by combining the NDT to create an integrated bridge health monitoring mechanism.



(a) Visual Inspection on 06/07/2010



(b) Visual Inspection on 25/06/2011



(c) Visual Inspection on 29/07/2012

Figure 4.32 – Apparent cracks, Rebar deterioration and concrete degradation (Span 4)

4.3.2.2 Main Findings of Visual Inspection

Based on the inspections completed in this section, several areas of concern were highlighted. This included efflorescence, moisture ingress, delamination and most worryingly longitudinal cracks. These could be caused by the dynamic loading of vehicular impact on the bridge deck which may weaken the concrete strength and result in spalling occurring. Apart from vehicular impact, the moisture present may be due to insufficient asphalt cover caused by potholes. Inadequate concrete cover could also be to blame for delamination which eventually will lead to reinforcement exposure, accelerated corrosion at reinforcement, which will be exacerbated by the actions of moisture and oxygen from the air.

The cracks found between spans three and four are still in an early stage of propagation. However, if remedial treatment is not sought, it will further prolong these problems and cause distress in concrete especially towards its strength on the bridge and its ability to sustain load.

For this particular case, maintenance is highly required in order to solve the problems mentioned above and prevent their reoccurrence. The following are preventative actions which are recommended to reduce the distress in the concrete:

1. Pressure grouting applied to exposed reinforcements such as those seen in Figure 4.31(c) will increase concrete cover.
2. To reduce the occurrence of longitudinal cracks as seen in Figure 4.31(d) strengthening of the beam is recommended.
3. Another option for the cracking mentioned above is the use of an Epoxy resin injection.
4. To prevent the water seepage seen in Figure 4.31(b) the use of crack sealant is advised.

The above inspection and subsequent report did not cover any sub-surface investigation and assessment of the bridge structure. Subsequent examinations were deemed necessary to investigate these issues therefore the author and research team at the University of Greenwich, requested access to the bridge via the highway engineering

department of the Medway City Council (the owners of the bridge) in order to carry out a full survey of the bridge using their GPR system (see section 4.2.5). As the GPR survey will not cover the vibrations of the bridge. Due to the deteriorated sections which were identified by this visual inspection IBIS-S is also used. IBIS-S interferometric radar monitors the dynamic deformations of the bridge under loading (see section 4.2.3). For that purpose the following objectives were set:

- To locate the position of the upper rebar
- To estimate the depth of rebar cover throughout the bridge deck
- To locate the position of the lower rebar
- To identify possible areas of moisture ingress below the deck surface
- To identify any other structural features and / or defects
- To measures dynamic or static displacement

Currently there are no weight restrictions in place on this bridge with regards to the vehicles which cross it.

4.3.3 IBIS-S Monitoring

This section explains the IBIS-S interferometric monitoring for the main case study, Pentagon Road Bridge. This assessment uses two different frequencies in application, which are 20 MHz and 200 MHz. Corner reflectors for the IBIS-S monitoring were manufactured and set up by Medway Council's Highway division on the side of the bridge and they also provided a cherry picker (see section 5.4). IBIS-S monitored the deflection of the bridge while a cherry picker crossed it. The test was completed several times with two different dates to show the data repeatability. Processing, interpretation and analysis of collected data were supported by the IBISDV3412 software (IDS Ingegneria dei Sistemi). The results gathered were compared with the finite element model (see chapter 5).

4.3.3.1 Survey Procedure

The IBIS-S test was carried out on the 7th November 2010 and 11th of March 2012. The weather on both dates was sunny and the temperature was 5°C and 16°C respectively. Monitoring was carried out with the full support of the Medway Council's Highway health and safety division (Medway Council) and their subcontractors. The surveys were also carried out in collaboration with IDS-UK (IDS Ingegneria dei Sistemi). The IBIS-S monitoring criteria are presented in Table 4.2:

Table 4.2 – The IBIS-S Monitoring

IBIS-S Monitoring	Frequency	Dates	Temperature	Weather
1	20 MHz	7 th November 2010	5 °C	The weather was sunny day.
2	20 MHz 200 MHz	11 th of March 2012	16 °C	The weather was sunny day.

- **Health and Safety**

Health and safety is performed with the Medway Council's Highway division. Safe working practice was followed during the survey. The minimum PPE (Personal Protective Equipment) requirements for this job were provided such as hard hats, high visibility vests, safety boots, tethers (whilst working on the bridge pillars), harness (for working at height), and long trousers.

- **Reflectors**

Most structures have enough natural reflectors to make it possible to perform a measurement without the installation of corner reflectors; however the Pentagon Road Bridge is smooth concrete and offers few naturally reflective points; therefore fifteen corner reflectors were installed at approximately four metre intervals along one side. Due to the frequency of the IBIS-S and the size of the array, it is recommended that multiple surveys are performed covering moderate areas, rather than one survey monitoring the entire structure. For optimum results it is recommended to monitor the bridge from both sides. Figure 4.33 shows the corner reflectors which were manufactured by Metal Prefabrication Ltd (2012) with a 152.4x152.4x152.4 millimetre stainless steel square bar.

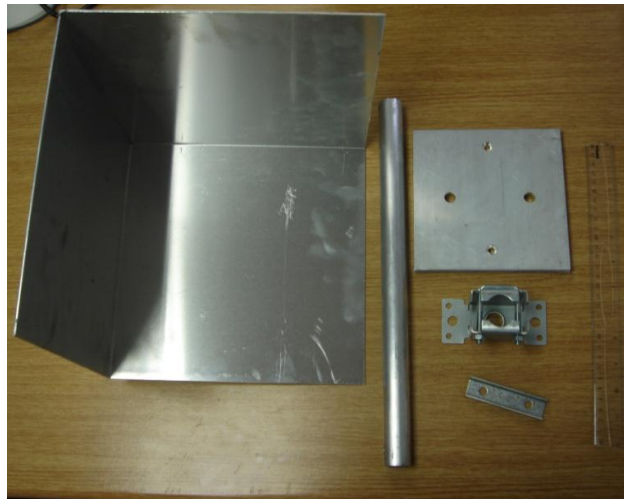


Figure 4.33 – Corner reflectors. (Photos from Gokhan Kilic, 2010)

The reflector positions were recommended by the collaborating partner IDS Ltd. and were based on the bridge size and angle. This type of spacing arrangement is also supported by literature (Gentile and Bernardini, 2008).

- **Operation**

IBIS-S is able to measure displacement under load. Corner reflectors are fixed to the edge of the bridge deck and the IBIS-S radar transceiver is set up in a location with which the majority of the reflectors can be seen (line of site); corner reflectors are used as they reflect any signal back towards its source. IBIS-S monitoring is performed with fifteen corner reflectors as seen in Figure 4.34. The location of the corner reflectors is referenced by recording the coordinates with respect to a fixed location.

When a load is applied to the deck, usually in the form of a vehicle of known weight passing over the deck, the radar is able to measure the deflection of the deck from the received signal by comparing this to the signal of the transmitted wave. By repeating the test with the deck loaded and unloaded comparisons between the two sets of data can be made and the structures behaviour under load can be assessed. It is possible to assess the structure under dynamic, live and static loads.



Figure 4.34 – Test Layout (Photos from Gokhan Kilic, 2010)

Figure 4.34 shows how IBIS-S was installed in two different locations (A and B) and from each position four measurements approximately, twenty minutes duration were performed. An 18 tonne cherry picker (see section 5.4) was driven across the bridge four times during each acquisition to excite the structure. The speed of the vehicle

remained constant at 25MPH which was confirmed using the speedometer and also IBIS-S results. Table 4.3 shows the time which the vehicle takes to cross the bridge for both position A and B of IBIS-S as shown by Figure 4.34.

Table 4.3 - Moving load crossing time (second)

	IBIS-S Position A	IBIS-S Position B	
1	8.06 second	7.02 second	
2	8.73 second	8.53 second	
3	7.53 second	7.54 second	
4	7.77 second	7.09 second	
5	8.07 second	7.95 second	
6	7.80 second	7.29 second	
7	7.57 second	7.10 second	
8	7.53 second	7.68 second	
Average	7.88 second	7.52 second	7.70 second

The IBIS-S survey results require processing and interpretation in order to produce data that can be used in order to determine the displacement of the bridge structure. A limitation of this method is that the transmitter can be obscured by non-removable clutter, therefore in order to tackle this data from two positions A and B, as shown in Figure 4.35, are combined in order to provide a more comprehensive set of results.

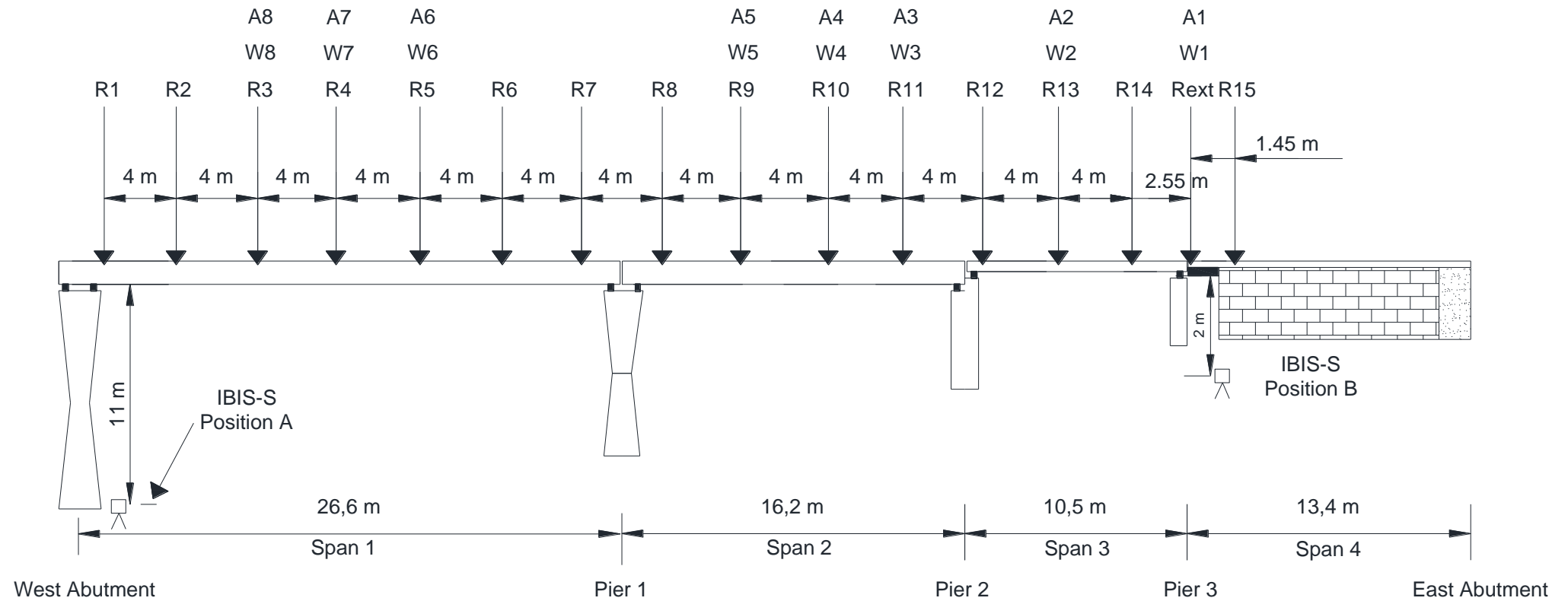


Figure 4.35 – Test Layout plan (not scaled) (Gokhan Kilic, 2010)

R = IBIS-S Reflector
A = Accelerometer
W = Wireless sensor

The processed and interpreted data provides, for each reflector, the maximum displacement observed as a moving load crosses the bridge structure. Comparing the maximum displacement for each reflector with parametric study results indicated potential areas of defects in the bridge structure.

4.3.3.2 IBIS-S Results

Following the initial survey in 2010, it was found that the maximum deflection took place in span 4, therefore in the subsequent survey it was decided to add additional reflectors to this area to accurately measure this (Figure 4.36).

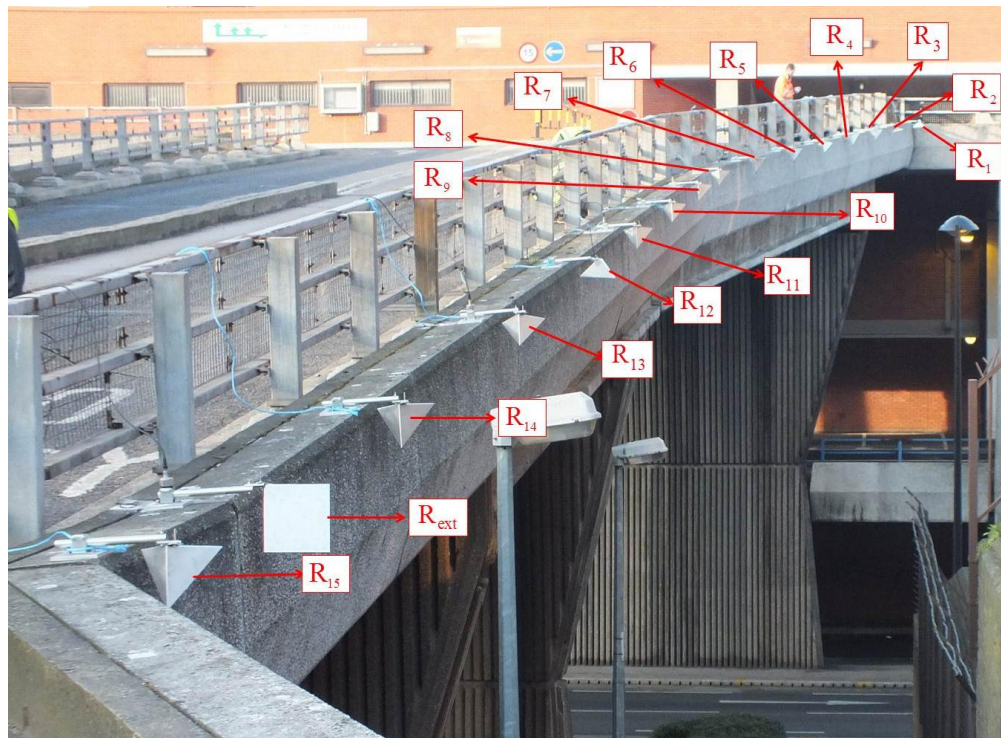


Figure 4.36 – View from IBIS-S Reflector Positions (Photos from Gokhan Kilic, 2010)

Figure 4.36 shows where reflectors are on the bridge. On the second survey an extra reflector (R_{ext}) was added between reflector 14 and 15 on top of the cantilever (see Appendix D). This is because in the first survey this region was the area which indicated the maximum deflection of the entire bridge structure. From both positions, A and B, it became evident that only R_4 or the R_{12} , and later R_{ext} , reflectors produced viable data, therefore the data from these reflectors are used. This still provides a

complete data set of the bridge structure however, it is recommended if obscuring structures can be avoided they are removed before performing an IBIS-S survey.

Figure 4.37 depicts a survey that was undertaken in November 2010 and reports a maximum deflection between span three and four cantilever zone of approximately -1.4mm. As this was undertaken in cold, hot conditions the deflections may be symptomatic of the weather conditions. In order to compare this case a second survey (Figure 4.38), in March 2012 under warmer, sunny conditions was undertaken. As the earlier study indicated a problem with deflection in the cantilever area a further reflector was positioned here in order to enhance the quantification of the deformation taking place. The results from the second survey reported a slight discrepancy, having a maximum deflection of approximately -1.5mm which may indicate that the weather condition can have an impact on the bridge deflection however, this is only to a minor extent (6 %). As can be seen from Figure 4.37 and 4.38 the direction of displacement can vary to negative axis.

Figure 4.38, 4.39, 4.42 and 4.43 depict two surveys during March 2012 however, these are from tests undertaken at both 20 MHz and 200 MHz respectively. Due to the increase in frequency the data from Figure 4.36 and 4.40 is taking more accurate results due to the increase in the number of readings. This accuracy is illustrated by the lack of distortion of the results which is apparent in Figure 4.40 and 4.44. The higher frequency readings also show a correlation in the results from all passes of the cherry picker showing the increased reliability of this antenna through its enhanced repeatability. The 200 MHz data follows the same trend as the 20 Hz readings however, this increase in the number of readings allows it to pick up the resultant impact of the bowing that occurs more effectively, hence the increase in the number of positive direction deflections measured. Comparing the results from the IBIS-S survey, as shown in Figures 4.40 and 4.44, there is an acceptable parity between three different monitoring, thus demonstrating the reliability of IBIS-S equipment.

The complete set of the data analyses is available in Appendix A.

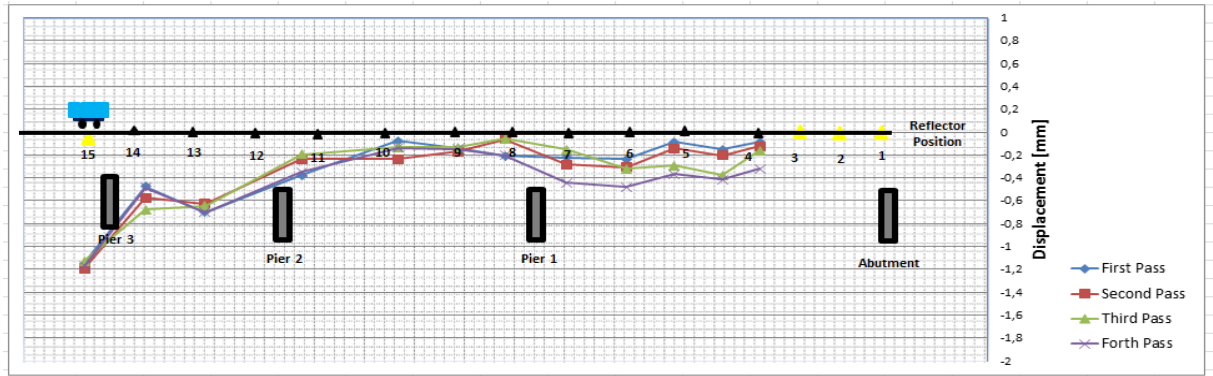


Figure 4.37 – IBIS-S 7th November 2010 20 MHz Monitoring Results

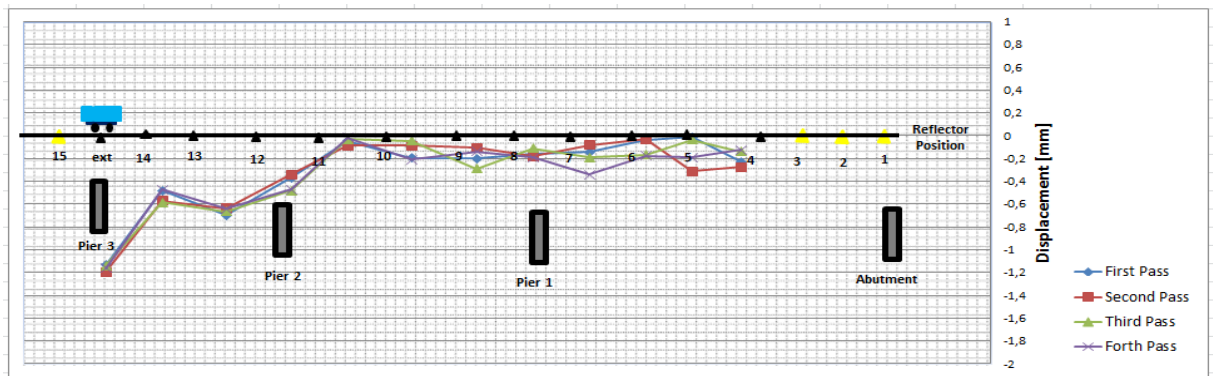


Figure 4.38 – IBIS-S 11th of March 2012 20 MHz Monitoring Results

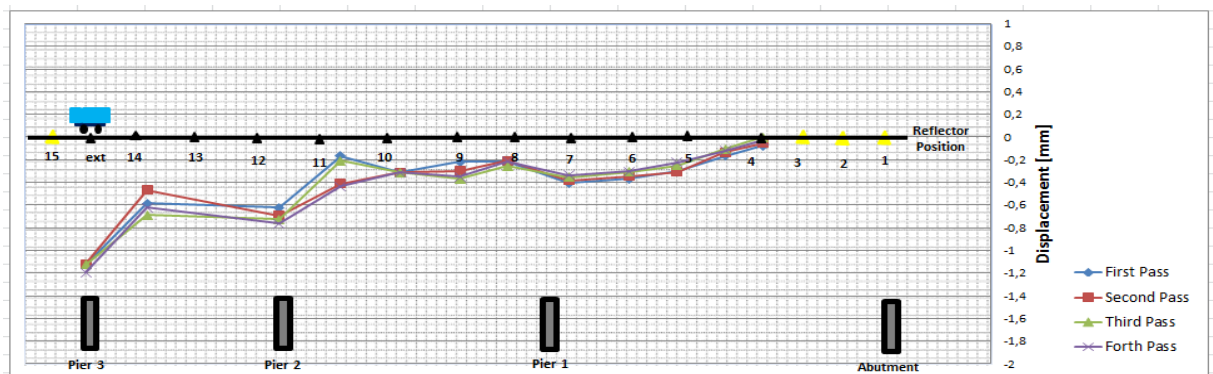


Figure 4.39 – IBIS-S 11th of March 2012 200 MHz Monitoring Results

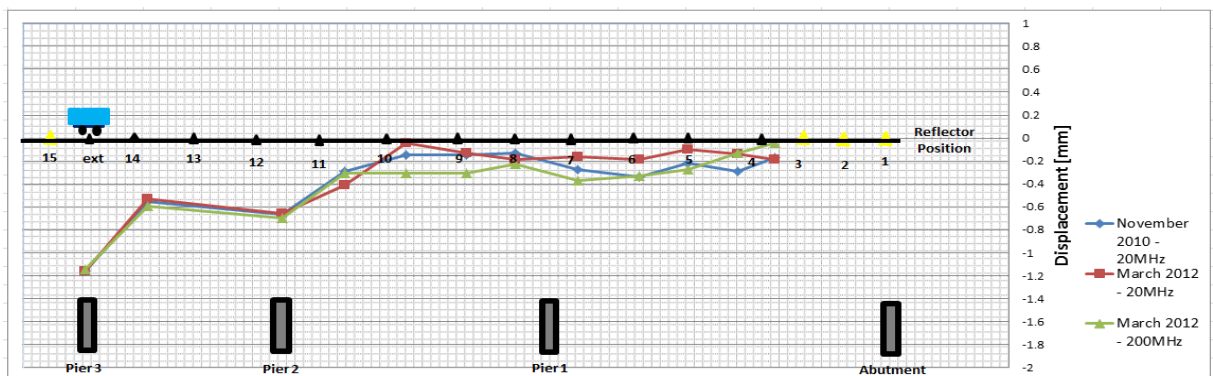


Figure 4.40 – Comparison of IBIS-S Monitoring Results (November 2010 – 20MHz, March 2012 – 20MHz, March 2012 – 200MHz)

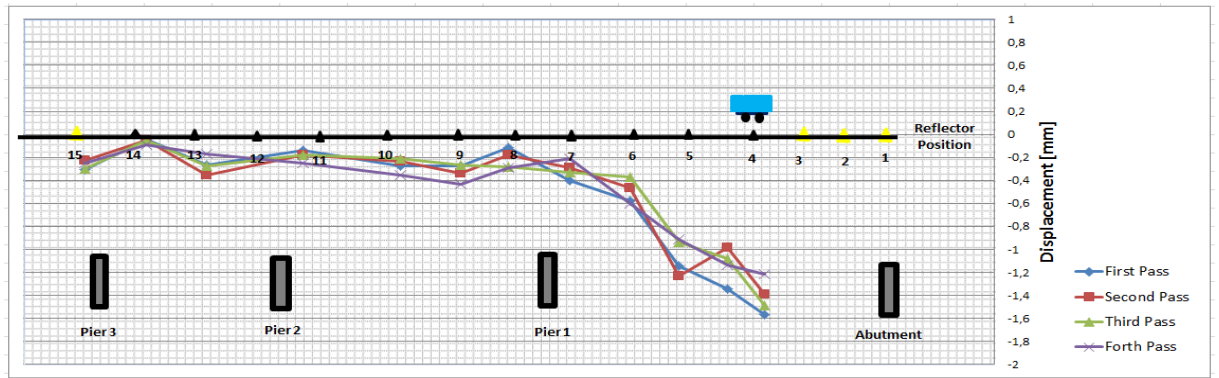


Figure 4.41 – IBIS-S 7th November 2010 20 MHz Monitoring Results

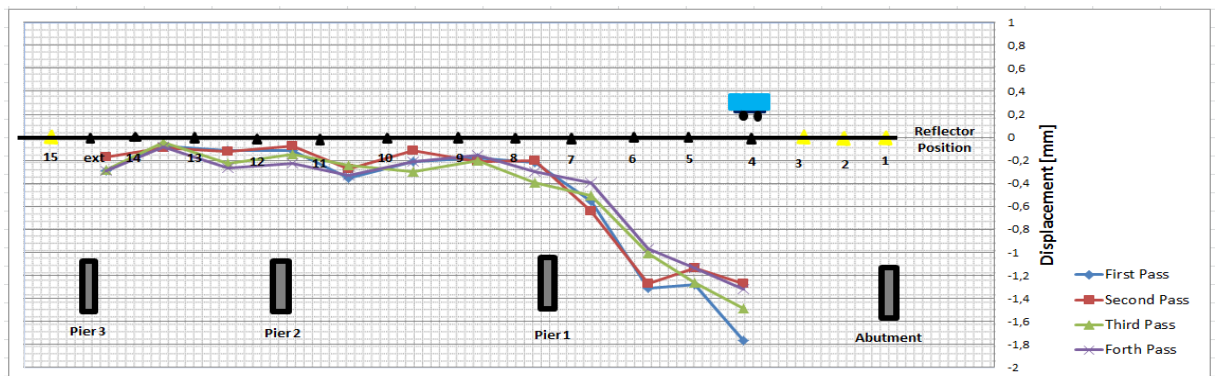


Figure 4.42 – IBIS-S 11th of March 2012 20 MHz Monitoring Results

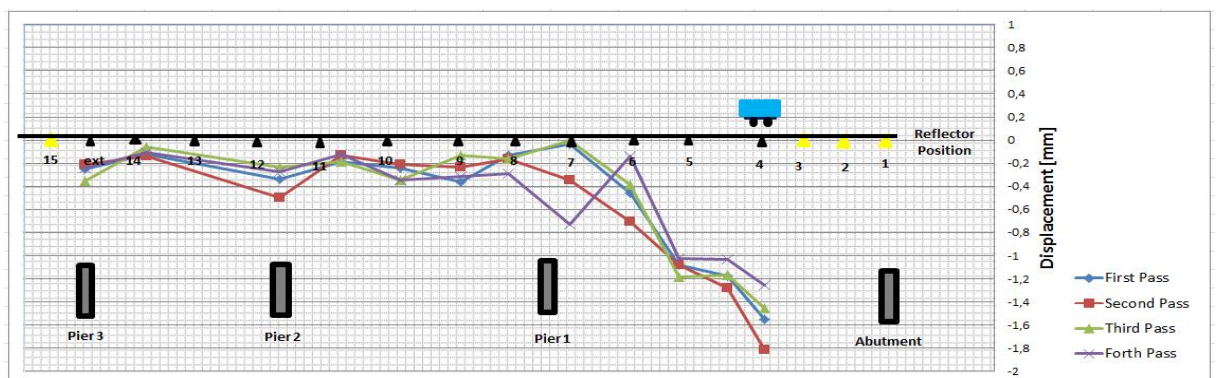


Figure 4.43 – IBIS-S 11th of March 2012 200 MHz Monitoring Results

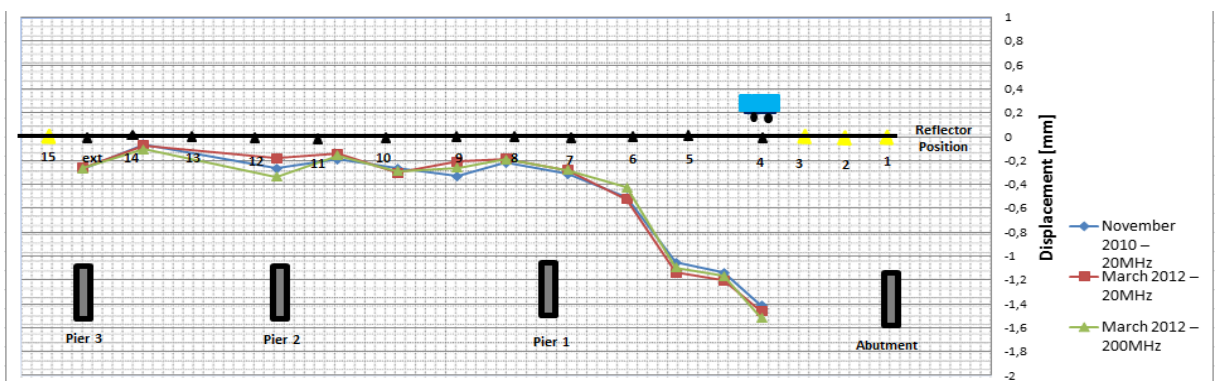


Figure 4.44 – Comparison of IBIS-S Monitoring Results (November 2010 – 20MHz, March 2012 – 20MHz, March 2012 – 200MHz)

4.3.3.3 Summary of IBIS-S Results

Following the visual inspections carried out on the Pentagon Road Bridge under examination in this project, structural cracks were found to exist throughout (with crack info Appendix D). The survey of the Pentagon Road Bridge by IBIS-S indicated maximum deflection of 1.4mm.

IBIS-S does not identify cracks, delamination or any other defect within the structure like the other NDT techniques however; it assesses the structures behaviour under load which is a characteristic of the structure, which relies on the faults within it. However IBIS-S is able to measure displacement under both a static and moving load. It can be used to identify points which require remedial action as it was used during investigations of the main case study.

The first of two surveys was carried out in November 2010 during cold weather conditions. The reflectors were positioned to obtain optimal results. The survey was then carried out with the dynamic load represented by a cherry picker (section 5.4). The results were processed and proven to illustrate the capability of IBIS-S to monitor the deflection of the bridge under both a static. The results were interpreted to prove the repeatability of the testing and further validate it. Furthermore the cantilever area between span three and four was found to undergo the maximum displacement out of the whole span of the bridge.

Figure 4.45 shows all the visible reflectors maximum and minimum displacement for the first passing of the moving load. It clearly shows that the bridge length between 40 and 50 meters, which is between span 3 and 4 has a maximum displacement of approximately 1.4 millimetres.

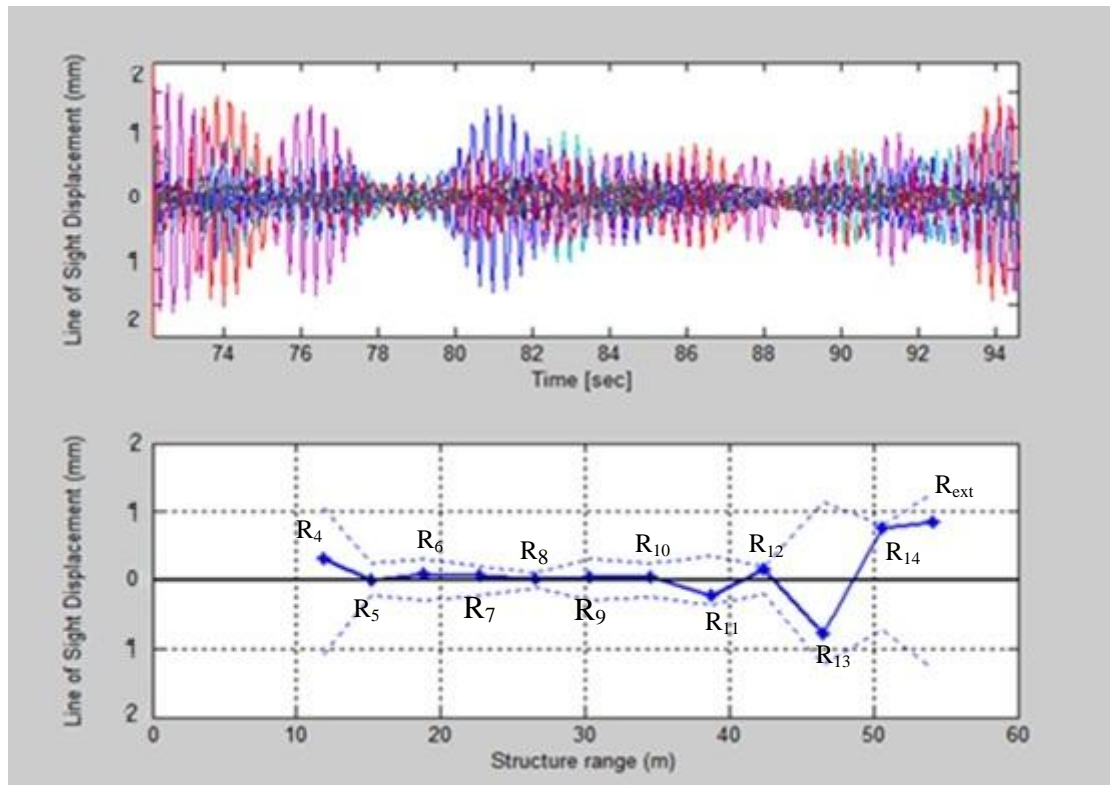


Figure 4.45 – Mode of Vibration of the Bridge (south view) for a given period of time

Further examination of this bridges displacement was undertaken during a sunny weather IBIS-S survey in March 2012. This survey served to examine the difference weather can have on results however only a very small discrepancy was found between the readings of both surveys. The second was carried out using two different frequencies of the IBIS-S antenna. This showed that the higher frequency antenna gave much more accurate results and increased the repeatability factor of these tests.

In conclusion, IBIS-S serves as an invaluable addition to this integrated bridge health monitoring approach as it further serves to increase confidence in making a decision to take remedial action. It does this IBIS-S further serving to validate the findings of the other health monitoring techniques of visual inspection and GPR survey. When using IBIS-S a lower frequency antenna will give an accurate reading for the position of the maximum deflection however for increased confidence and repeatability a higher frequency is always recommended.

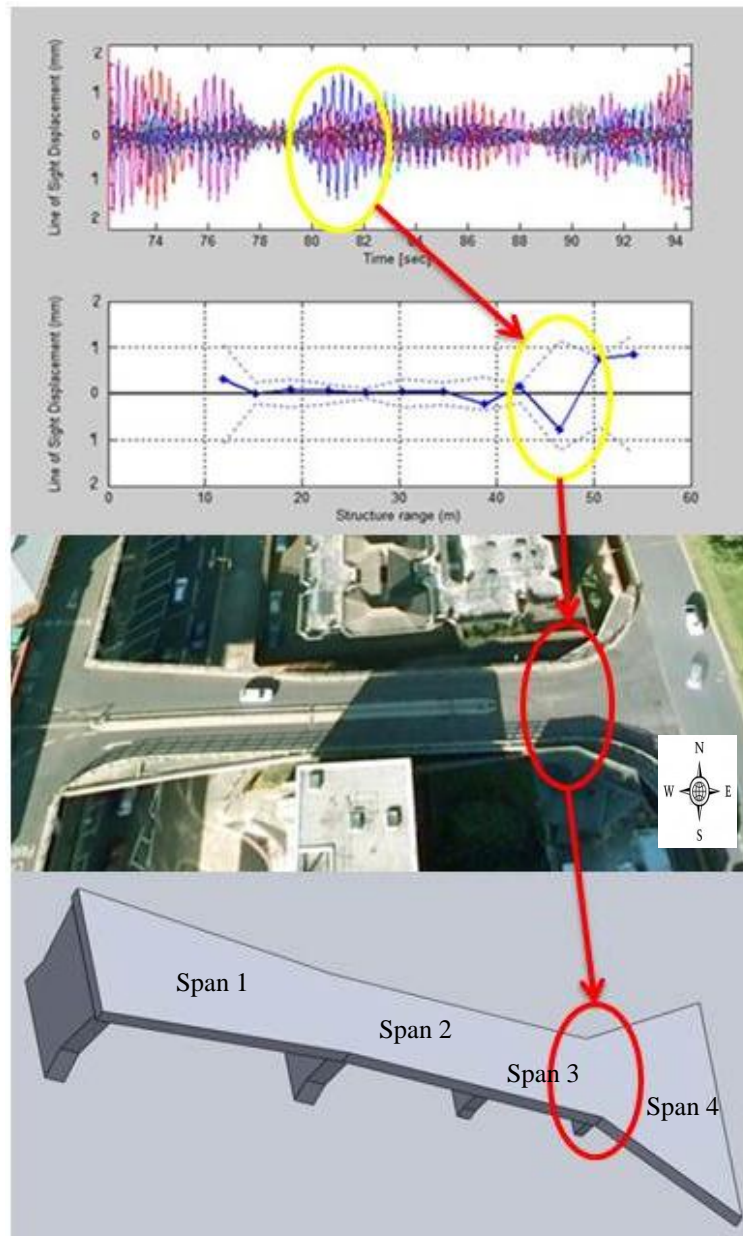


Figure 4.46 – Pointing the results in aerial and depiction view

The IBIS-S results further affirms that between span 3 and 4 should be the primary focus for future remedial action, as of the entire bridge structure it exhibits the greatest deflection (Figure 4.46). It also shows that variance can occur between both weather conditions and the frequency at which deflections are measured. This variance detailed is not significant enough to warrant concern however, this can show that there is value in undertaking multiple IBIS-S surveys in different weather conditions, and at different interferometric frequencies in case the variance measured is significant for a given structure.

4.3.4 Validation of the Measurements

The main goal of this section was to implement a wireless sensor network (WSN) and accelerometer sensors for monitoring the behaviour and integrity of the main case study: Pentagon Road Bridge. The results of the measurement setups are analysed and presented. The validation of the accelerometers and wireless sensor network (WSN) are addressed and relevant discussions are made. A set of eight nodes for the WSN monitoring and eight accelerometer sensors were set up by Medway Council's Highway division on the side of the bridge and they also provided a cherry picker. WSN and accelerometer sensors recorded the deflection of the bridge while a cherry picker crossed it. The test was completed with to validate the results. The results gathered were compared with the IBIS-S monitoring method and the finite element model (see chapter 5).

4.3.4.1 Introduction

The WSN and accelerometer sensors tests were carried out on the 11th of March 2012. The weather was sunny and the temperature was 16 °C. The aim of this study discussed previously was to obtain results which could be compared and validated against the IBIS-S monitoring equipment. For that purpose the following objectives were set:

- To identify the needed characteristics of accelerometer sensors, wireless communication adapters and the laptops they are use with.
- To calibrate the accelerometer sensors and wireless adapters appropriately to ensure that accurate results obtained.
- To install the accelerometer sensors and wireless equipment in the best manner, condition and place.
- To collect the data in appropriate manner.
- To interpret the results and compare with the results obtained from IBIS-S.

WSN and accelerometer monitoring enable many applications. WSN nodes can be imagined as small computers, extremely simple in terms of their interfaces and components. Figure 4.47 shows a wireless sensor node and Accelerometer sensor installed side of the Pentagon Road Bridge near the IBIS-S reflector.

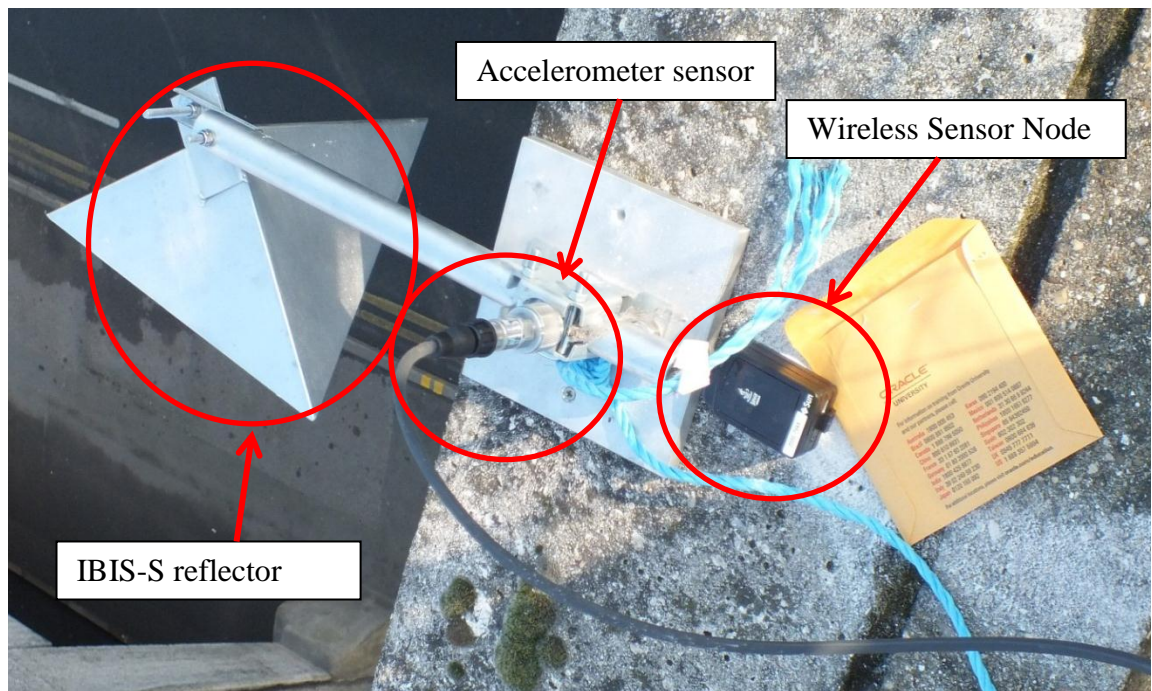


Figure 4.47– IBIS-S Reflector, Wireless Sensor Node and Accelerometer Sensor
(Photos from Gokhan Kilic, 2010)

The Wilcoxon Research model 775A accelerometers (Meggitt, 2012) were used. The Oracle WSN System were utilised with a sensor communication board which is designed based on IEEE 802.15.4 radio over the 2.4 GHz frequency band (Oracle, 2012) (see the Figure 4.47). For a more detailed explanation of the specifications and workings of both the wireless sensor network and the accelerometer sensors see Chapter 3.

Figure 4.48 shows the locations of IBIS-S reflectors (R) wireless sensor nodes (W) and accelerometer sensors (A) when a load is applied to the deck, usually in the form of a vehicle of known weight passing over the deck, the nodes is able to measure the deflection of the deck displacement. By repeating the test with the deck loaded and unloaded comparisons between the sixteen sets of data can be made and the structures behaviour under load can be assessed.

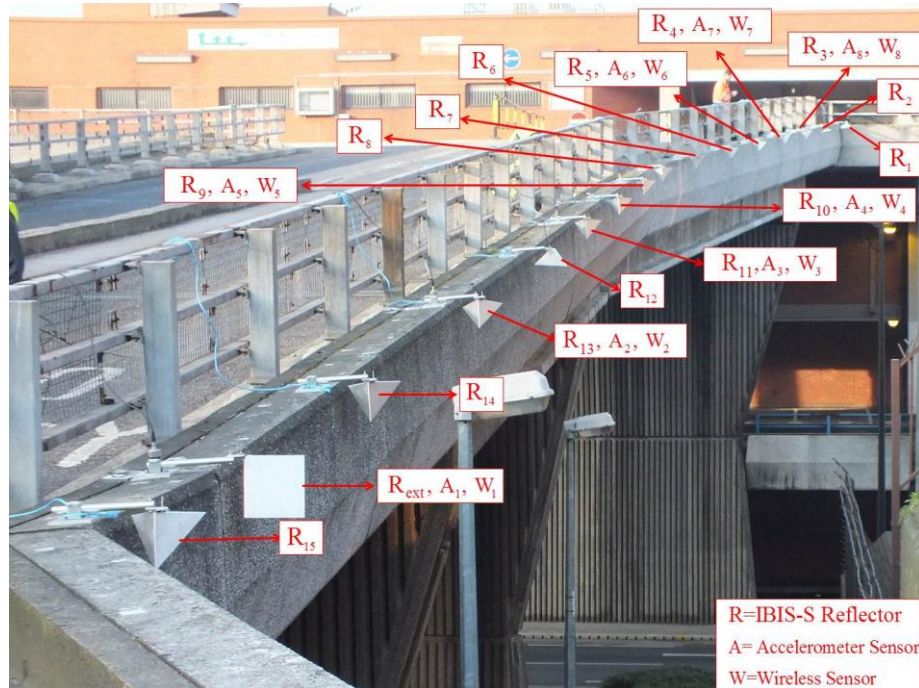


Figure 4.48 – Diagram of the system

Table 4.3 shows how IBIS-S was installed in two different locations (A and B) (Figure 4.35) and from each position, eight times, a measurement of, approximately, crossing duration was recorded. An 18 tonne vehicle was driven across the bridge four times during each acquisition to excite the structure. This monitoring ensures that the vehicle is moving at an almost constant speed to prove the repeatability of this survey (section 5.4) (Details of the procedure see page 138).

4.3.4.2 Wireless Sensor Network Monitoring

The wireless sensor system implemented includes a base station and eight wireless sensor nodes communicate each other, collect data and transmit to base station via a radio link. The base station is connected to a laptop via USB port and interfaces the wireless sensors nodes and a host. The base station gathered information such as collecting data, coordinate, communications with WS nodes. The key components of the WSN systems are the base station, wireless sensor nodes, software, and communication capability. The hardware design is optimized for structural monitoring applications.

One of the disadvantages discovered during the survey related to wireless sensor networks is the energy efficiency and power supply problem. The wireless sensors nodes were battery-powered and re-charged by using cables connect to a laptop. Each complete set of cherry picker movements took approximately 10-15 minutes to complete (a set comprised of 16 bridge crosses), during this time the wireless sensors often ran out of battery and needed to be restarted often. During the survey the solutions to this problem was minimize the power consumption of the wireless sensor nodes such as switch off the nodes if a waiting time needed for saving power.

4.3.4.3 Accelerometer Sensor Monitoring

Before survey the accelerometers were calibrated with a hand held shaker using the technique detailed in Chapter 3. The calibration was proven accurate, when the results given for the whole test were compared to the two monitoring techniques which have been detailed above.

The results from the accelerometer consist of readings for the acceleration $a(\tau)$ of the bridge on its vertical axis. These results can be transformed into displacement readings displacements $d_c(t)$ using the following equation 4.1:

$$d_c(t) = d_0 + v_0t + \int_0^t dt \int_0^\tau a(\tau) d\tau \quad (4.1)$$

where:

d_0 : initial displacement, $t = 0$

v_0 : initial velocity, $t = 0$

d_c : calculated displacement, t

Displacements from numerical integration of the digital acceleration and velocity signals (waveforms) can be calculated using several methods. However, all the techniques for integration calculated the area under the graph of the discrete function over time. A program was created using Matlab (MATLAB, 2010) to transform all the acceleration values to displacement.

4.3.4.4 Validation Results

The purpose of this accelerometer and WSN monitoring is to validate the IBIS-S results and to understand how structures perform under moving load conditions. It was found that the accelerometer provided very accurate results for the deflection of bridge deck when compare to IBIS-S. They also have advantages over IBIS-S with respect to time and cost. However, it was found that this type of WNS was not an appropriate method for measuring deflection as the battery life was not sufficient. Thus, no results were obtained from this WNS.

For the node Accelerometer 1 highlighted above, a detailed displacement graph is given below for both IBIS-S and accelerometer results (Figure 4.49). As can be clearly seen the when the load is located on this node the maximum displaced for both methods is seen. Also a good correlation is observed at all other times between the results. The comparison for further nodes can be found in Appendix C.

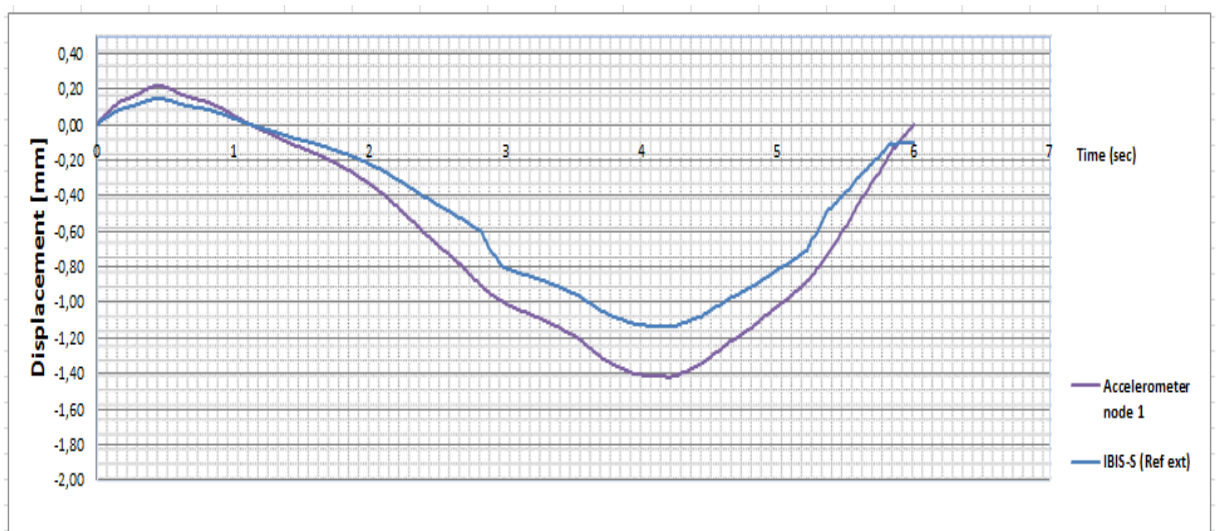


Figure 4.49 – Accelerometer node 1 and IBIS-S results

To further validate the IBIS-S results, Figure 4.50 and 4.51 is shown below detailing the behaviour of the bridge for several passes of the cherry picker. As is clear the results are very similar.

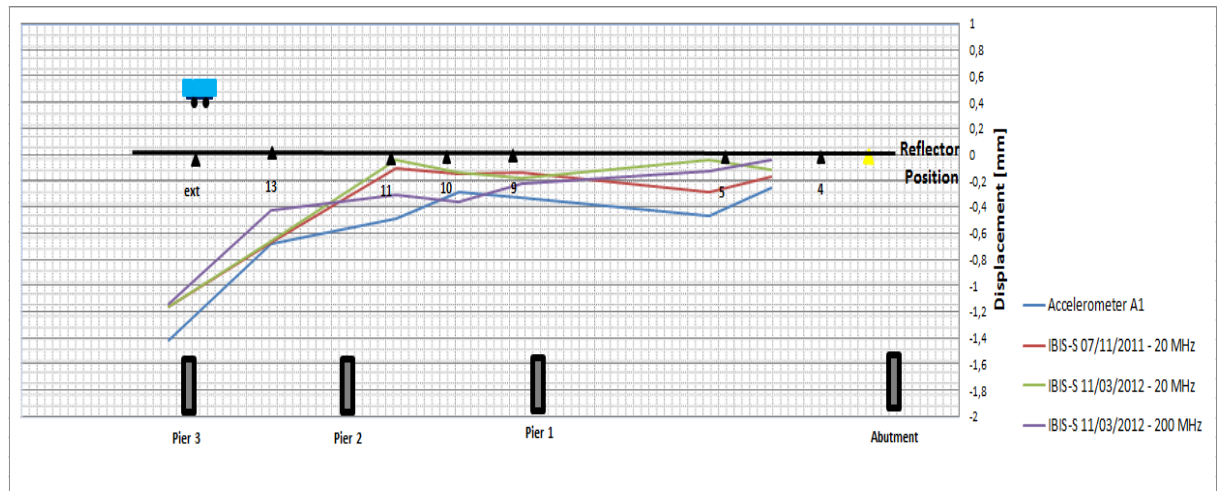


Figure 4.50 – IBIS-S 7th November 2010 20 MHz Monitoring and Accelerometer Results

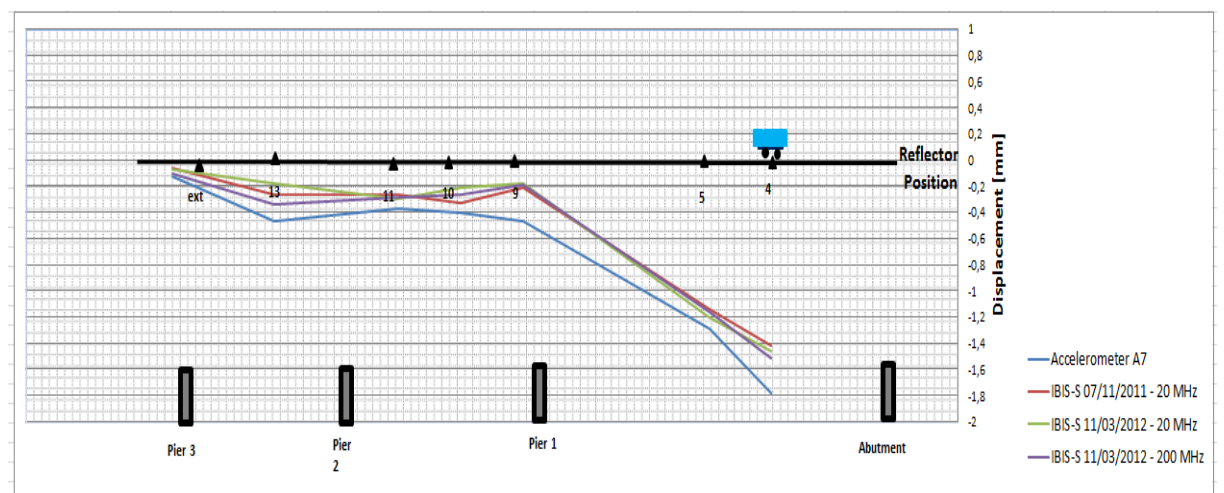


Figure 4.51 – IBIS-S 7th November 2010 20 MHz Monitoring and Accelerometer Results

The small discrepancy seen between the results could be owing to several different causes such as:

- The difference in horizontal positioning of the sensors.
- Completely different methods of calculating displacement. IBIS-S uses interferometric radar whereas accelerometers use a vibration technique.
- Small errors can occur while interpreting the data as mathematical equation like Equation 5 above cannot completely accurately quantify the translation of acceleration to displacement.
- IBIS-S can also be susceptible to external factors such as noise for passing vehicles which can minimally affect readings.

In conclusion, as is seen from the figures detailed in the results section, the accelerometer deflection measurements have successfully validated the IBIS-S findings (Figure 4.50 and 4.51). There are some minor discrepancies between the data but this can be attributed to the causes listed above.

The Oracle wireless network sensors were found to be inappropriate for use for this particular bridge scenario as their battery life was insufficient to record all the passes of the cherry picker. As such, this method is not recommended for in depth bridge health monitoring unless the battery life can be improved.

It was thus decided that the accelerometer and IBIS-S results be used to correlate the parametric study detailed in Chapter 5.

4.2.5 Ground Penetrating Radar (GPR) Survey

This section presents and discusses the applications of GPR in assessing the main case study (Pentagon Road Bridge), which is the structural integrity of a heavily used bridge. This assessment uses different antennae, in terms of frequency and method of application (2 GHz and 200-600 MHz IDS and 1-1,5-4 GHz UTSI) GPR antennas. Processing, interpretation and analysis of collected data were supported by the GRED software (IDS Ingegneria dei Sistemi); including its three-dimensional scanning capabilities. The results demonstrate the effectiveness of GPR mapping, providing information regarding the positions of rebar (upper and lower reinforcement), unknown structural features, as well as moisture ingress within the structure. Moisture ingress can cause corrosion of the rebars and deterioration of concrete as seen at the Forth Road Bridge preliminary case study. These effects can cause a weakening of the bridge structure causing excessive deflection and thus should be monitored so that remedial action can be taken if necessary. The results also highlight a possible phenomenon in identifying the presence of moisture within the bridge deck; confirming a similar finding in the preliminary case study of the Forth Road Bridge (see section 4.1.1).

4.3.5.1 Introduction

The visual inspection (section 4.2) and subsequent report did not cover any sub-surface investigation and assessment of the bridge structure. The thesis author, and the research team at the University of Greenwich requested access to the bridge via the highway engineering department of the Medway Council (the owners of the bridge) in order to carry out a full survey of the bridge using their GPR system. For that purpose the following objectives were set:

- To locate the position of the upper rebar.
- To estimate the depth of rebar cover throughout the bridge deck.
- To locate the position of the lower rebar.
- To identify possible areas of moisture ingress below the deck surface.
- To identify any other structural features and / or defects.

In order to acquire GPR operation, processing and interpretation data, the author was trained by Kevin Banks from IDS limited (IDS Ingegneria dei Sistemi).

The GPR survey was performed using the RIS Hi BriT (2 GHz) (IDS Ingegneria dei Sistemi), RISMFI HI-MOD (200-600 MHz) (IDS Ingegneria dei Sistemi) and UTSI (1-1,5-4 GHz) GPR antennas. The GPR assessment criteria are presented in Table 4.4:

Table 4.4 – The GPR assessments

GPR Assessment	Antenna	Dates	Temperature	Weather
1	RIS Hi BriT (2 GHz)	20 January 2011	6 °C	The weather was sunny day.
2	RIS Hi BriT (2 GHz)	19 August 2011	21°C	The weather was sunny day.
3	RISMFI HI-MOD (200-600 MHz)	20 August 2011	20°C	The weather was sunny day.
4	UTSI GPR (1-1,5-4 GHz)	11 March 2012	16°C	The weather was sunny day.

4.3.5.2 Setting out GPR Survey

Prior to carrying out any survey the Pentagon Road Bridge had to be prepared. The first fundamental stage considered the accessibility of the bridge for the passage of the antenna trolley, and considering any architectural obstacles that could cause an obstacle

to the data acquisition phase. The survey consisted of organising the health and safety and marking of the bridge deck. The marked features had to be clearly visible for the GPR survey and a reference system worked out during the preliminary investigation that best fits the operational conditions of the GPR equipment and maximises its productivity. Figure 4.52 shows 8 zones for GPR survey.

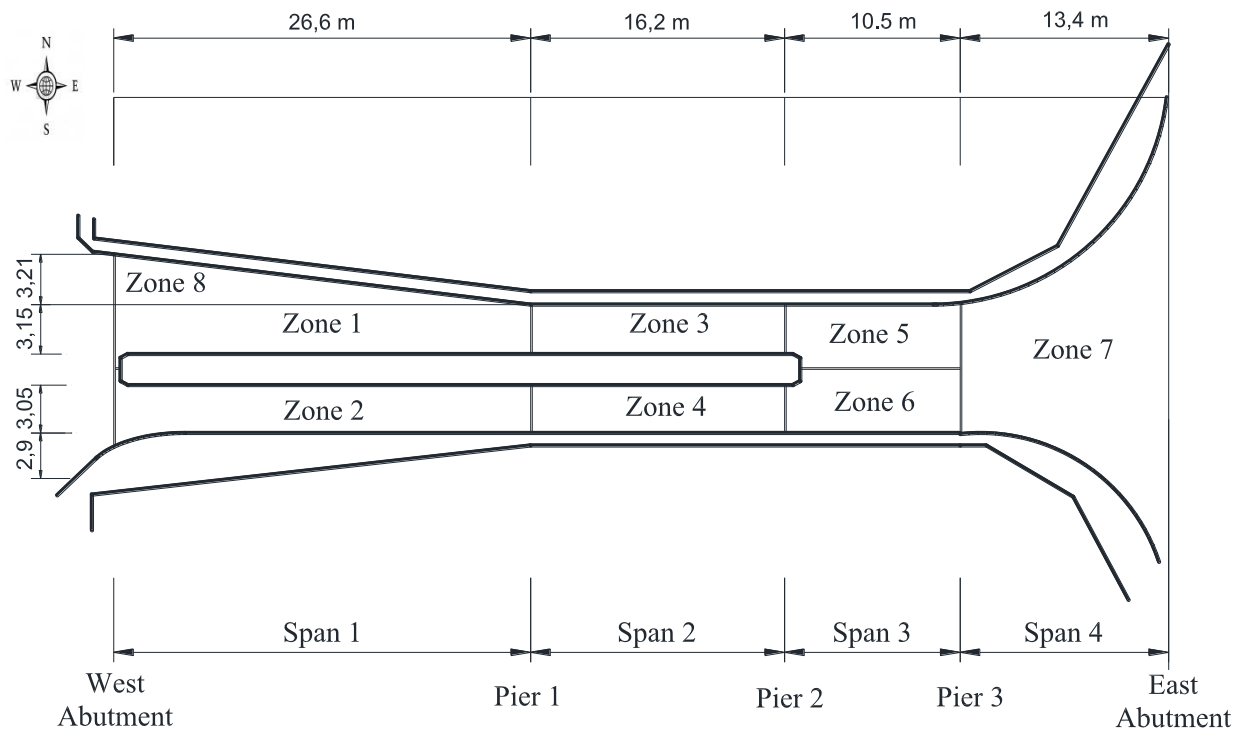


Figure 4.52 – GPR Survey zones

This survey was carried out with the full support of the Medway Council's Highway division and their subcontractors. This survey was also carried out in collaboration with IDS-UK and UTSI Electronics. It was necessary to introduce a traffic control system on the day as the bridge is heavily used by members of the public. Full access to the bridge was required during the survey.

The main points to be considered during this phase are described below:

- Full access to the bridge was required during the survey (access to pedestrian zones, permission to interrupt the traffic flow, etc.);
- Any difficulties in accessing the site must be considered;
- The space available;
- The presence of parked cars;

- The level of traffic;
- Positioning the reference system.

Having ensured adequate preparation is carried out any survey must be undertaken using a scientific method. The GPR technology was first veracity tested across four preliminary case studies (section 3.3.2.1), and tested in lab conditions (section 3.3.2). With these positive results steps were undertaken to ensure the validity of the data collection.

As the GPR surveys are to be undertaken at various levels of humidity, this meant other parameters for the survey had to be kept strictly the same; to ensure only one variable is modified. In order to achieve this: the GPR equipment, the referencing, and operator walking speed were the same in both instances of the RIS Hi BriT (2 GHz) and RISMF HI-MOD (200-600 MHz) (IDS Ingegneria dei Sistemi) surveys.

4.3.5.3 GPR Results

When the survey of the selected area has been completed, the data is taken off site for processing and interpretation. Once data has been processed it can then be rendered into a cross sectional image known as a B-scan, a plan of all acquired L or T scans known as a C-scan or it can be rendered into a 3D image (Figure 4.53), using all acquired data, which can be sliced in the x, y and z axes in order to identify defects.

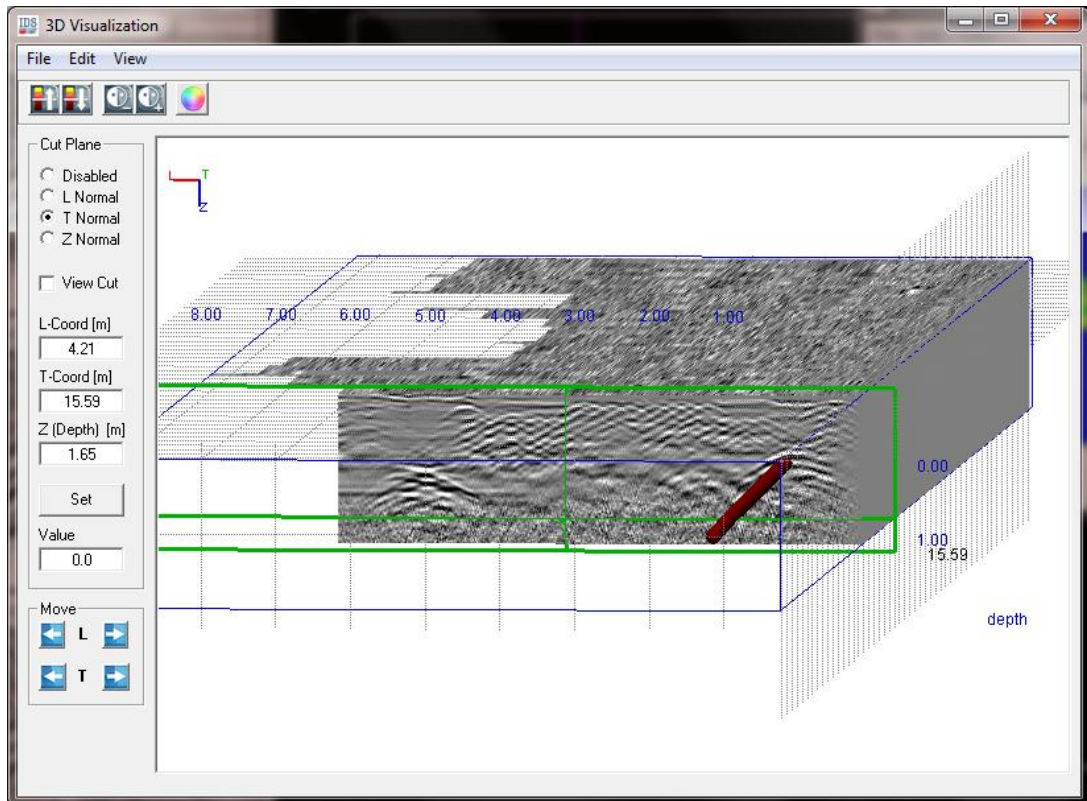


Figure 4.53 – 3D Volume processed data

Defects are identifiable in all of the scans however the C-scan and 3D scan provide the quickest method of identifying defects. For more accurate identification, the B-scan is used in conjunction with either the C or 3D scan to identify the exact location of the defect with regards to depth from the surface and location from the datum.

The GRED Software provides a 2D tomography of the underground layers and a 3D view of the surveyed volume. Thanks to the capability of merging on the same tomographic map of both datasets collected along longitudinal and transversal scans, it considerably increases the reliability of the results of the analysis due to the comparison between both B and C scans (2D tomography) with the 3D scan allowing for more accurate interpretation; as shown only Zone 5 in Figure 4.54.

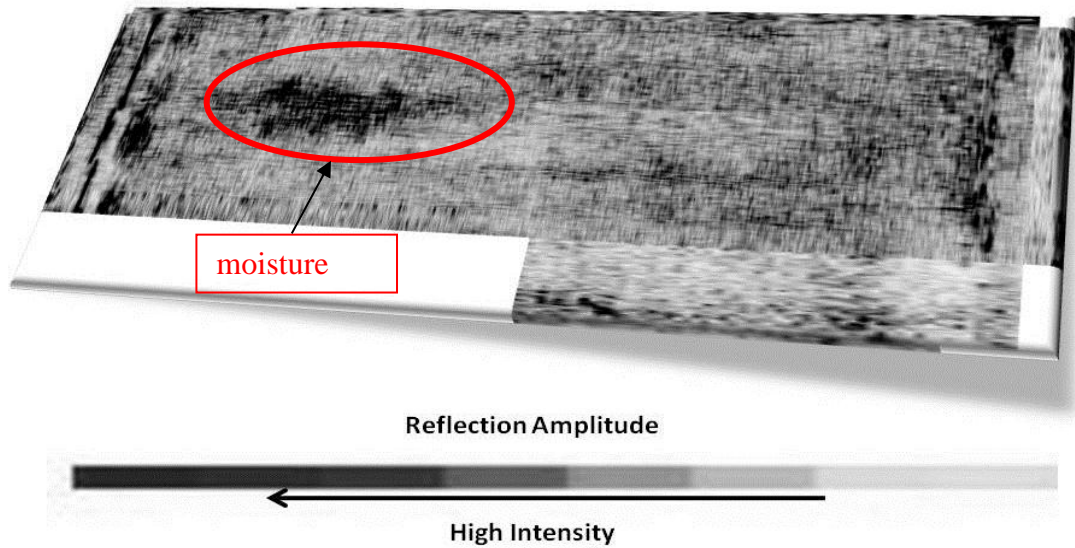
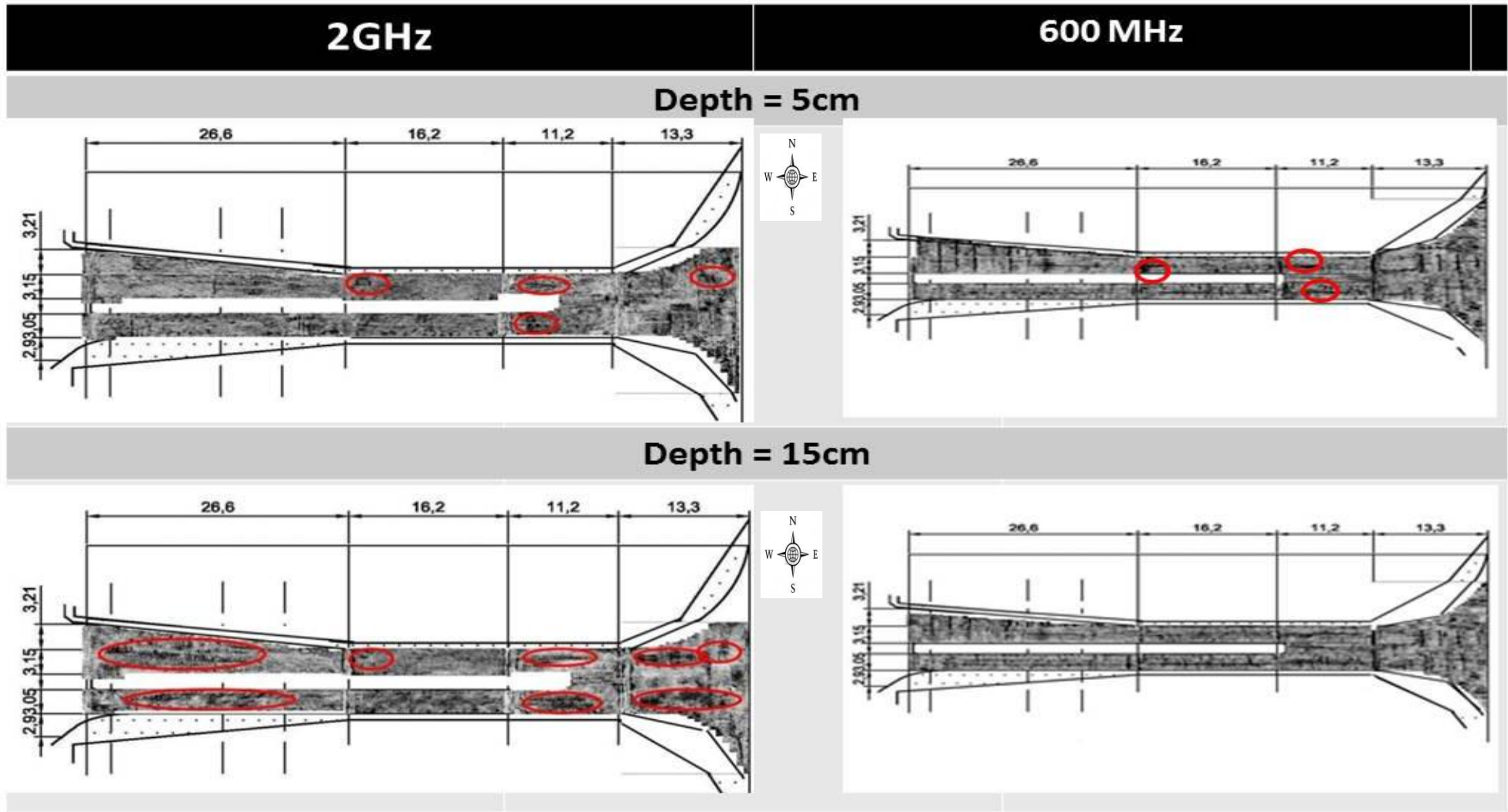


Figure 4.54 – Zone 5- 2D tomography data 40cm below the surface

The Figure 4.55 depicts a set of all zones vertical sliced data at depths 5, 15, 25, 35 and 50 cm with 2GHz and 600MHz antenna from the surface of the deck respectively. Certain consistent features and their respective appearance have also been highlighted (red circles). Moisture also becomes more visible at deeper penetrations and is clearly shown in Figure 4.55 as the high intensity darker area especially at 40 and 50cm depths (see Appendix D). The red circles denote areas of high moisture contents as identified by the author.



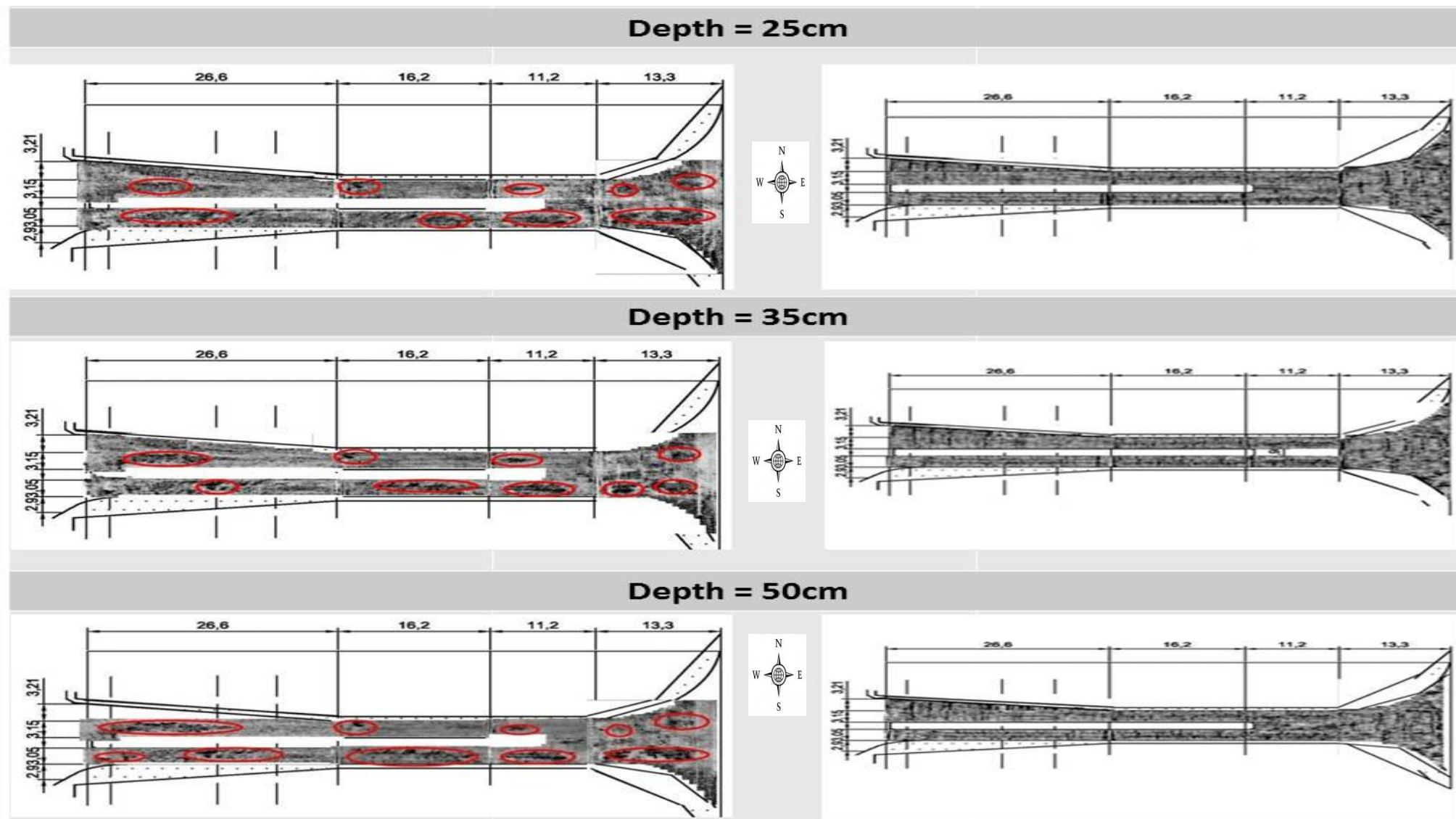


Figure 4.55 – 2GHz Horizontal Sliced processed data (left) and 600MHz Horizontal Sliced processed data (right)

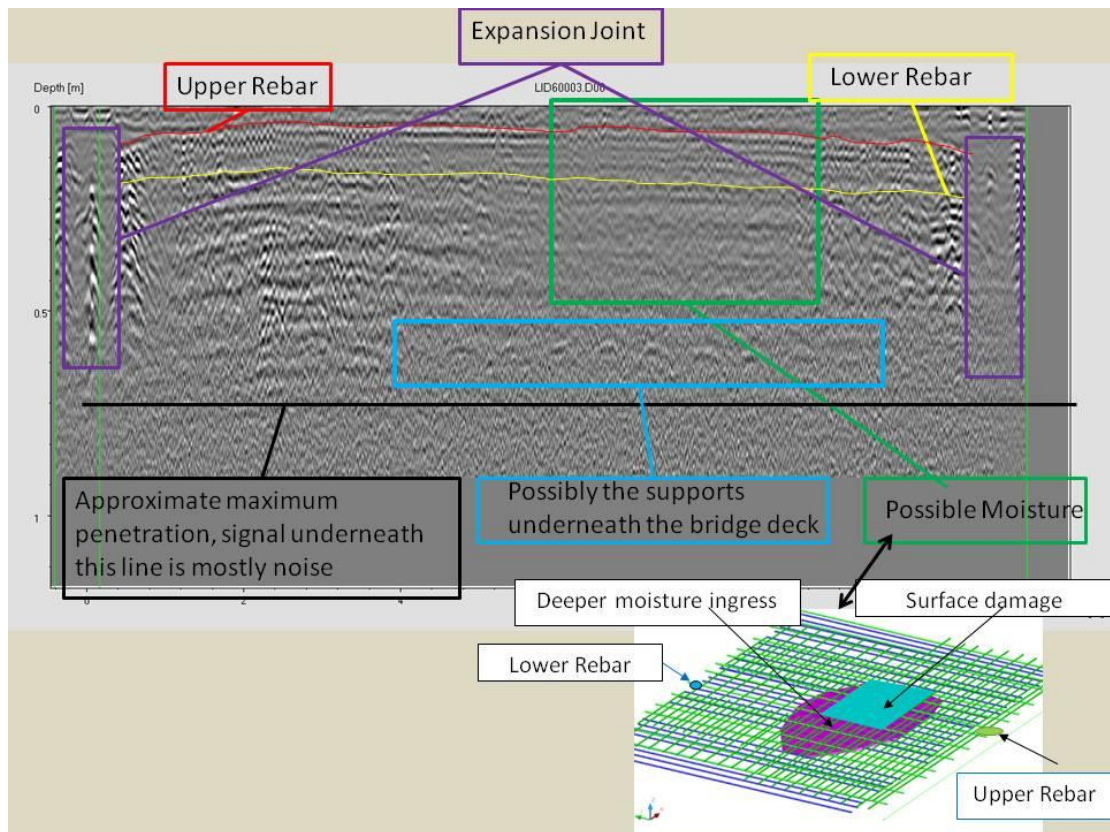


Figure 4.56 –GPR Zone 5 Radargram

The above Figure 4.56 shows a summary of all the information gathered from the radargram of zone 5. Therefore, the radargram gives the ability to identify and assess the following factors of bridge deck information:

- Location of two separate layers of rebar:
 - Top layer of rebar
 - Deeper layer of rebar.
- Area of moisture penetration close to the surface and the depth to which it infiltrates
- Position of expansion joints
- Position of possible supports within the bridge deck.

For further information regarding other zone of the bridge surveys completed refer to the Appendix B. All this information combines to give an accurate detailed map of the underlying bridge deck, which is crucial for developing a FEM and also a general understanding of the health of the bridge.

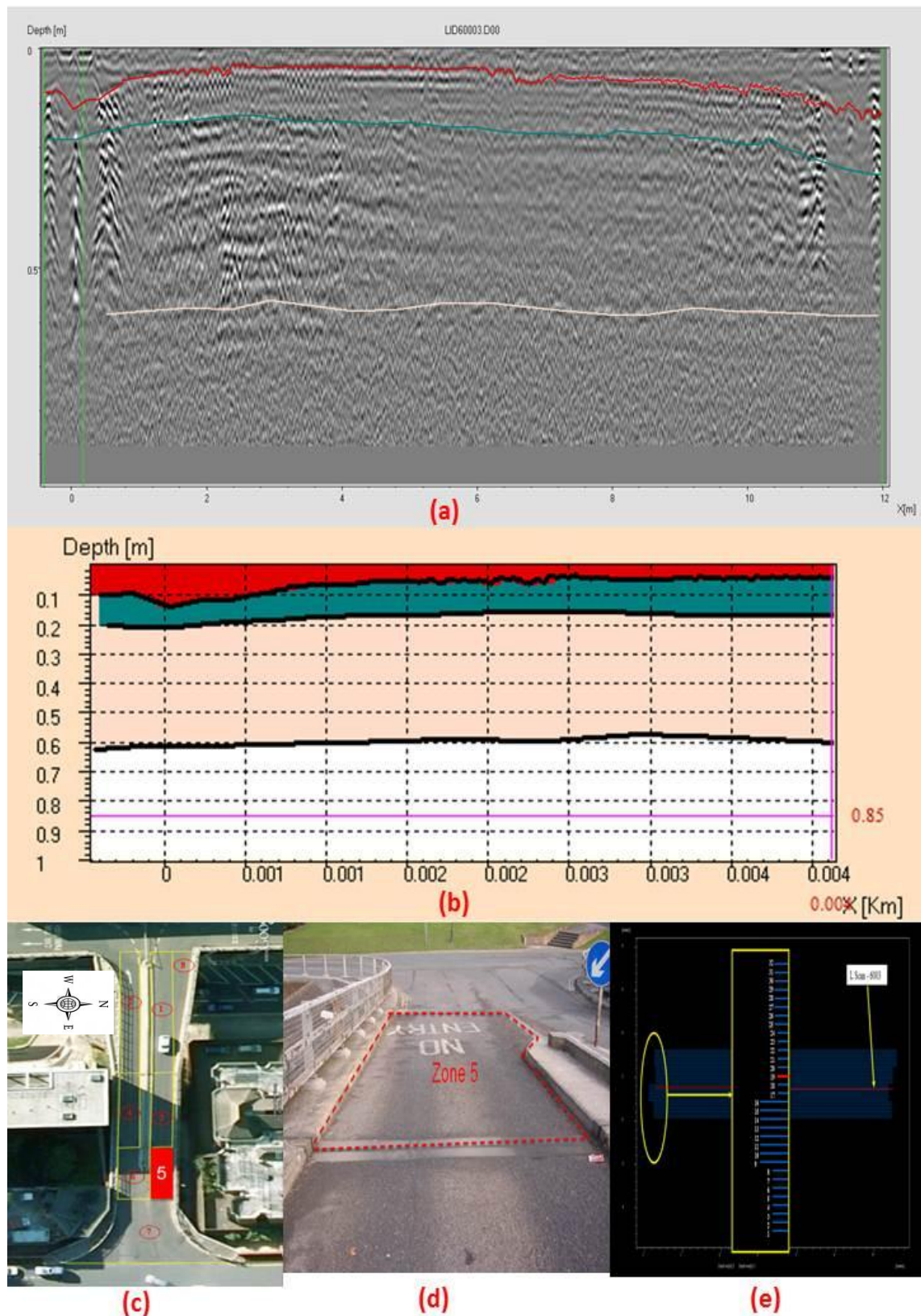
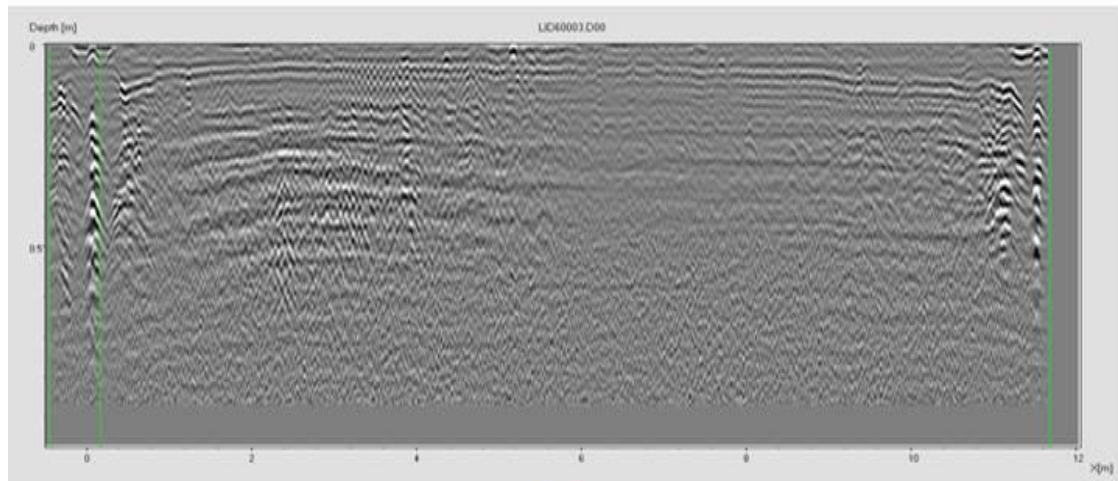
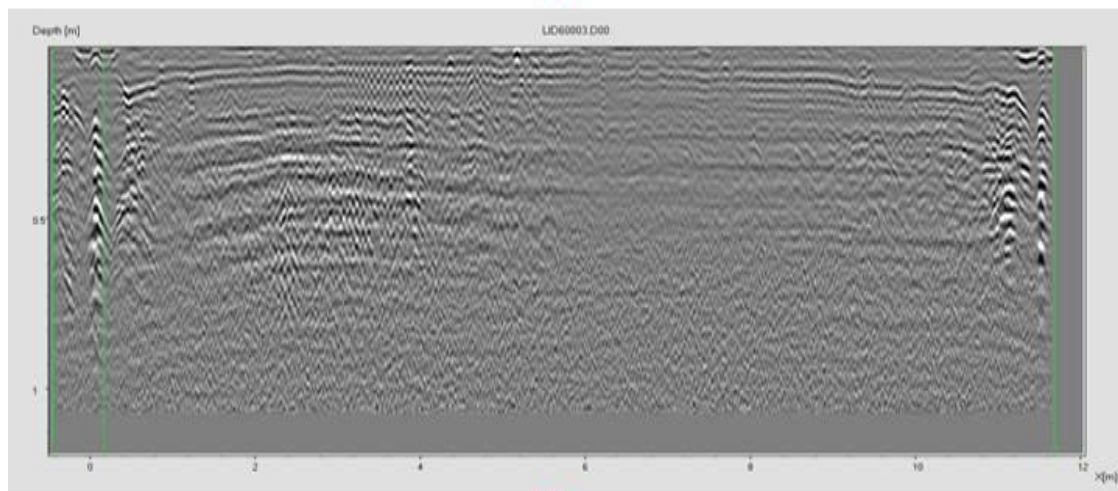


Figure 4.57 – (a) Radargram displays upper and lower rebars, (b) Upper and Lower rebar depth (d) zone 5 location, (e) view of zone 5, (f) the B-Scan slice position taken from zone 5.

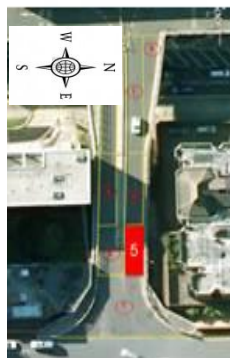
Figure 4.57 (e) demonstrates the B-Scan slice position taken from zone 5. For this B-Scan, having been processed, features of the structure can be extrapolated. Figure 4.57 (a) provides an interpretation demonstrating where the upper and lower rebars are within the structure; along with the limit of the scan. These can be further represented, as in Figure 4.57 (b) to more clearly indicate the depth of the rebars within the bridge deck. This demonstrates that the upper rebars are, in fact, not uniformly placed throughout the length of zone 5. This could be because of different settlement, how the structure was built, or due to construction error. Comparatively the lower rebars are relatively uniform in placement, which could indicate that defects have not penetrated to this depth; though could also be by design or construction error.



(a)



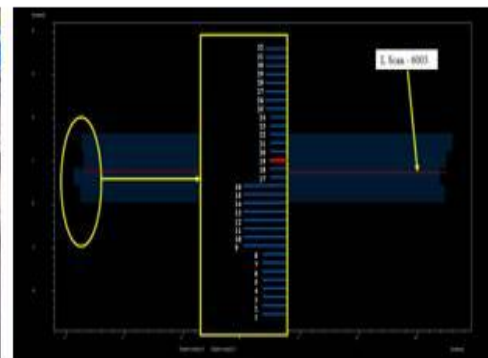
(b)



(c)



(d)



(e)

Figure 4.58 – (a) RIS Hi BriT (2 GHz) Radargram processed data, Winter 2011, (b) RIS Hi BriT (2 GHz) Radargram processed data, summer 2011, (c) zone 5 location, (d) view of zone 5, (e) the B-Scan slice position taken from zone 5.

The above Figure 4.58 shows a comparison of b-scans for Winter (Jan 2011) and Summer (Aug 2011). The second Summer reading was completed to ensure the repeatability of the equipment and to observe if the same equipment used in an identical manner. It is known that the interpretation of a radargram could be limited to only few factors: data processing and interpreter, thus as the data processing and interpretation would be the same on both occasions, the difference in results would be caused by external conditions. These external conditions could take the form of an increased degree of moisture in the Winter reading owing to cold weather. Both modelled bridge decks have provided the author with information on the effect that moisture ingress has on the transmitted wave. Dry and wet survey models were analysed and compared to the reference model as will be seen.

The differences between the radargram from different antennas are further examined in Figure 4.59. Two surveys were compared from two different manufacturers GPR antennas results. Figure 4.59 (a) shows the results from IDS GPR antenna suggest that there are supports underneath the bridge deck also, (Figure 4.59 (b)) these supports from UTSI GPR antenna are visible. Therefore similar results have been identified with two different manufacturer antennas.

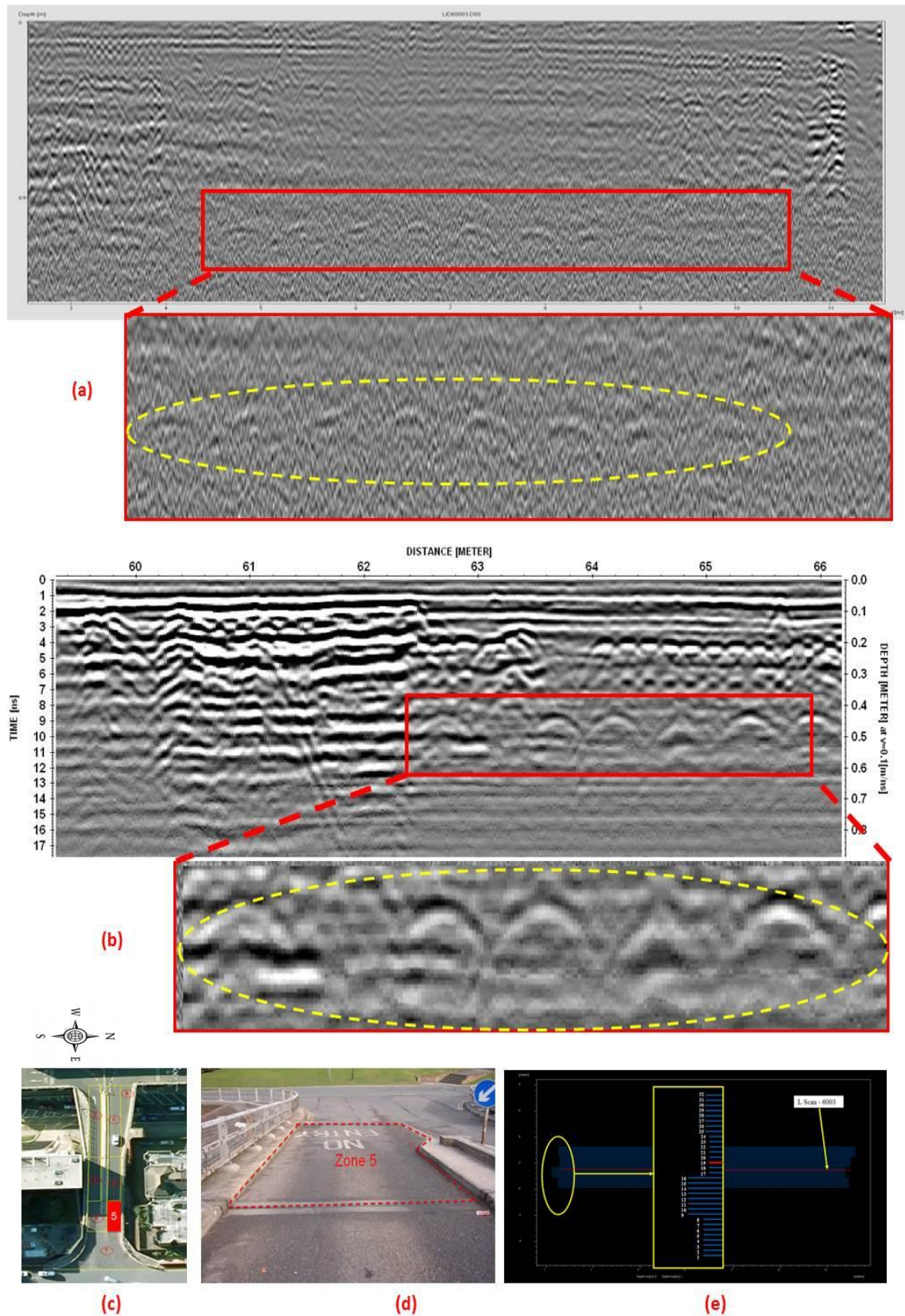


Figure 4.59 – (a) RIS Hi BriT (2 GHz) Radargram processed data, Winter 2011, (b) UTSI (1.5 GHz) Radargram processed data, summer 2011, (c) zone 5 location, (d) view of zone 5, (e) the B-Scan slice position taken from zone 5.

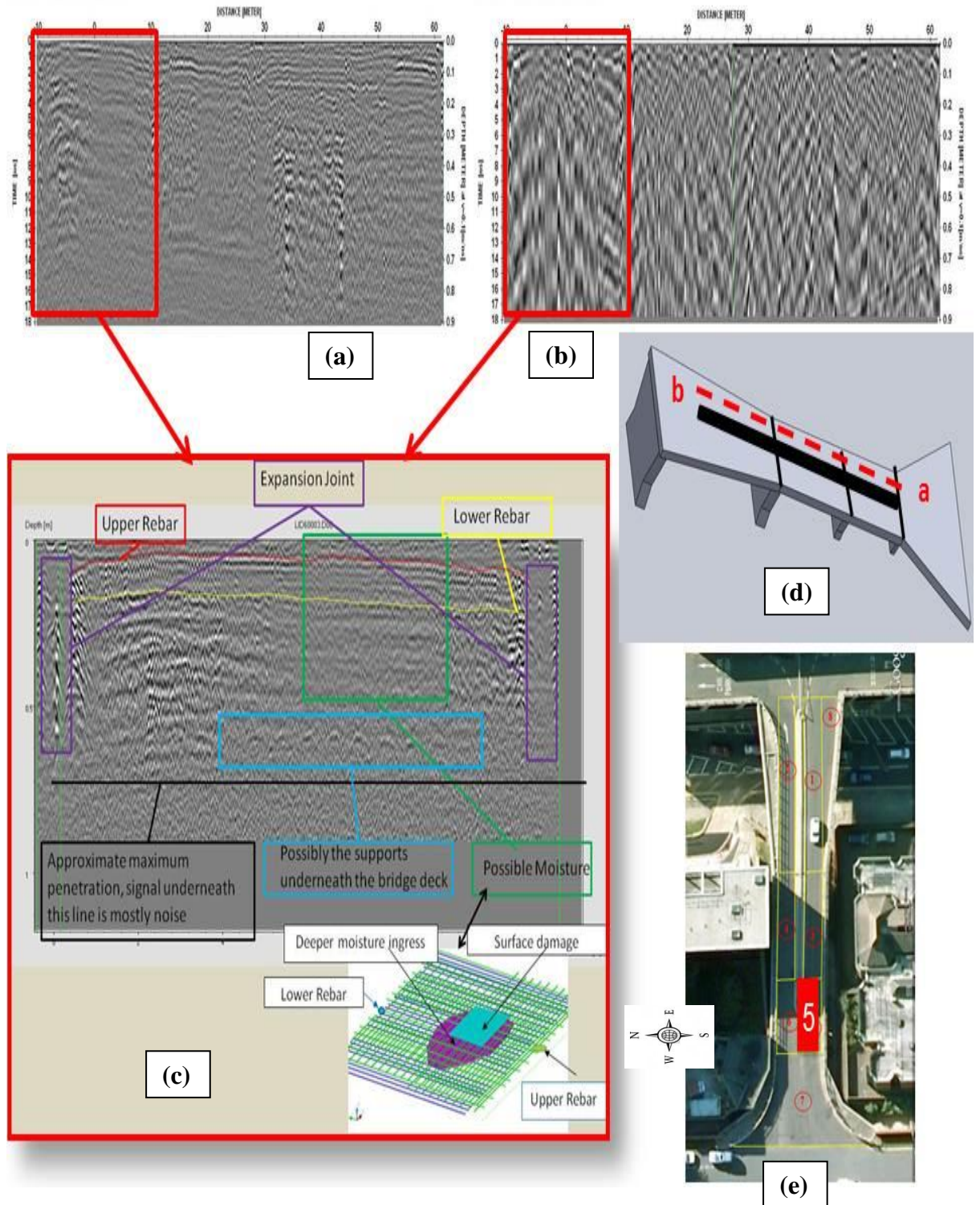


Figure 4.60 – (a) RIS Hi BriT (2 GHz) Radargram processed data, summer 2011, (b) RISMF HI-MOD (200-600 MHz) Radargram processed data (c) zoom output from identified area (red box), (d) surveyed line, (e) view of zone 5

The above Figure 4.60 is a comparison of the longitudinal radargrams given by a 2 GHz and a 600 MHz antenna respectively. Figure 4.60(a) and (b) are the radargrams for the B-scan (a-b shown in Figure 4.60 (d)) for the 2GHz and 600MHz antennas respectively.

It clearly shows that the maximum penetration depth of the 600 MHz antenna is much greater than the other. This penetration depth however comes at a cost to the resolution. This is apparent as in Figure 4.60 (a) the hyperbola (possible supports) are very clear and distinguishable in Figure 4.60 (b) after a depth of 70cm the hyperbola become distorted and unclear, it is therefore impossible to distinguish predominant features below a certain depth which confirms that the 2 GHz antenna is the optimum choice for bridge deck surveying. Figure 4.60 (c) shows zoom output from red box 2GHz antenna which identify and assess the bridge deck information factors such as: location of two separate layers of rebar (upper and lower rebar), area of moisture, position of expansion joints and position of possible supports within the bridge deck.

The differences between using different antennae in terms of frequency and method of application (2 GHz and 200-600 MHz IDS GPR antennae) and (1 GHz, 1,5 GHz and 4 GHz UTSI GPR antennae) are further examined respectively in Figure 4.62-66. Result are gathered middle of the zone 1,3 and 5 shown in Figure 4.61.

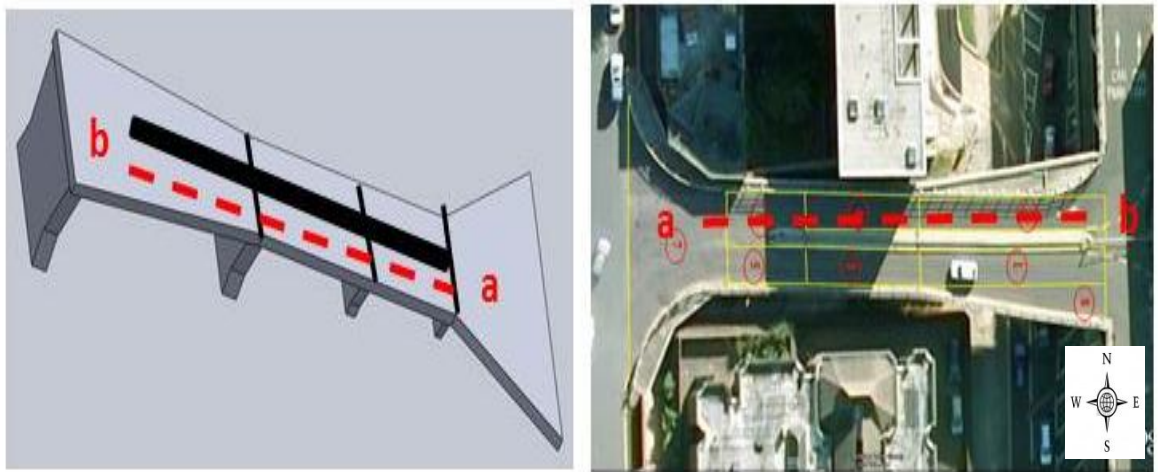


Figure 4.61 – Depiction and Aerial view of GPR a-b lane

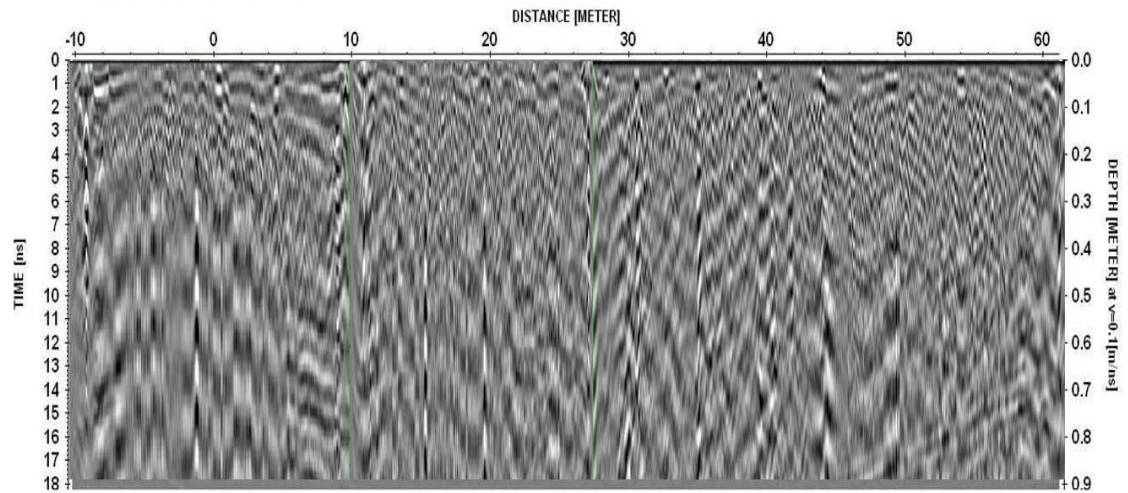


Figure 4.62 – 600MHz Antenna cross section a-b lane radargram

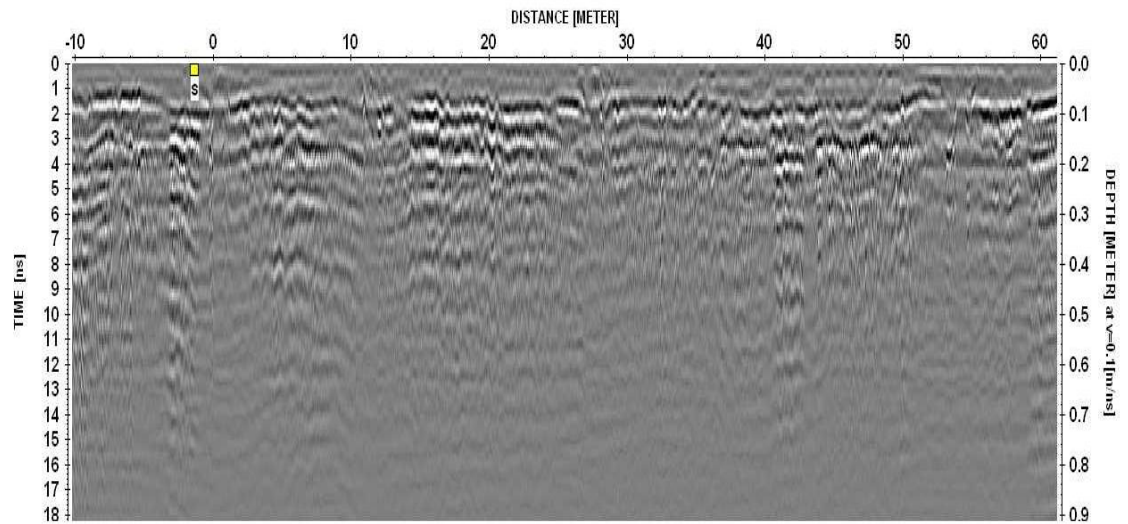


Figure 4.63 – 1GHz Antenna cross section a-b lane radargram

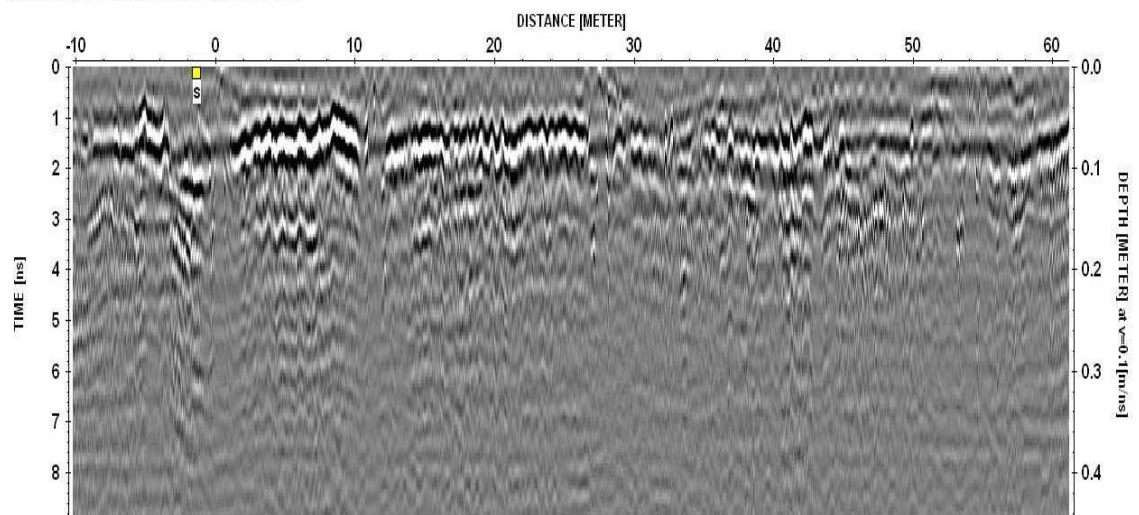


Figure 4.64 – 1.5 GHz Antenna cross section a-b lane radargram

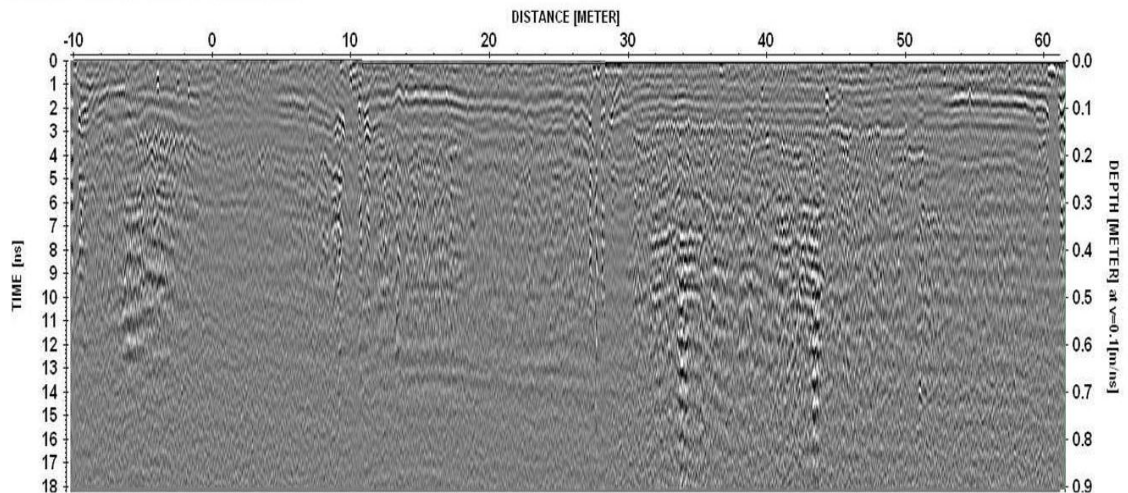


Figure 4.65 – 2GHz Antenna cross section a-b lane radargram

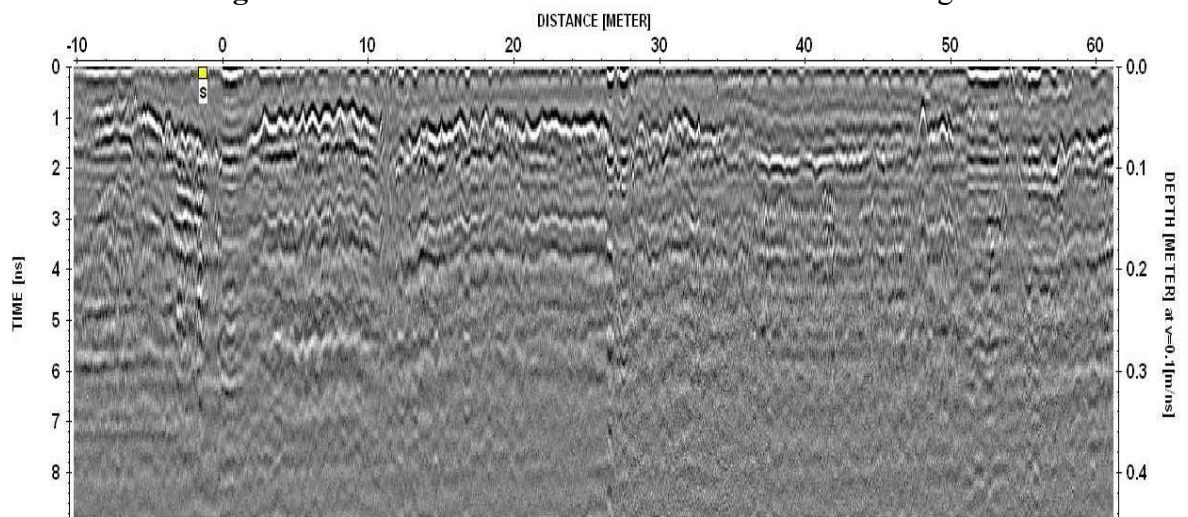


Figure 4.66 – 4GHz Antenna cross section a-b lane radargram

Figure 4.62-66 results illustrate the effectiveness of two different manufacturers and three different GPR antenna mapping providing information regarding the positions of rebar (upper and lower reinforcement), unknown structural features as well as moisture ingress within the structure. It clearly shows that the maximum resolution of the 4 GHz antenna is much greater than the others. This resolution however comes at a less penetration depth. The results also demonstrate a possible phenomenon in identifying the presence of moisture within the bridge deck confirming a similar finding in preliminary case study (Forth Road Bridge in Scotland). For further information regarding the other side of the bridge zone 2,4 and 6 surveys completed refer to the Appendix B.

4.3.5.4 Summary of GPR Results

A large quantity of data was created and processed in order to address the set objectives of this work was not possible to present them all in this section. However, for the purpose of this section selected number of data have been chosen to highlight the effectiveness of the GPR in assessment of Pentagon Road Bridge structures in identifying possible defects that otherwise are not easily identifiable by adopting conventional methods.

To summarise all the GPR surveys it can be concluded that:

- GPR gives information regarding internal structural defects such as moisture ingress which is not otherwise available (Figure 4.60). It also gives design information such as rebar positioning, which may not be readily accessible as in the case of the Pentagon Road Bridge zone 5 (Figure 4.67).

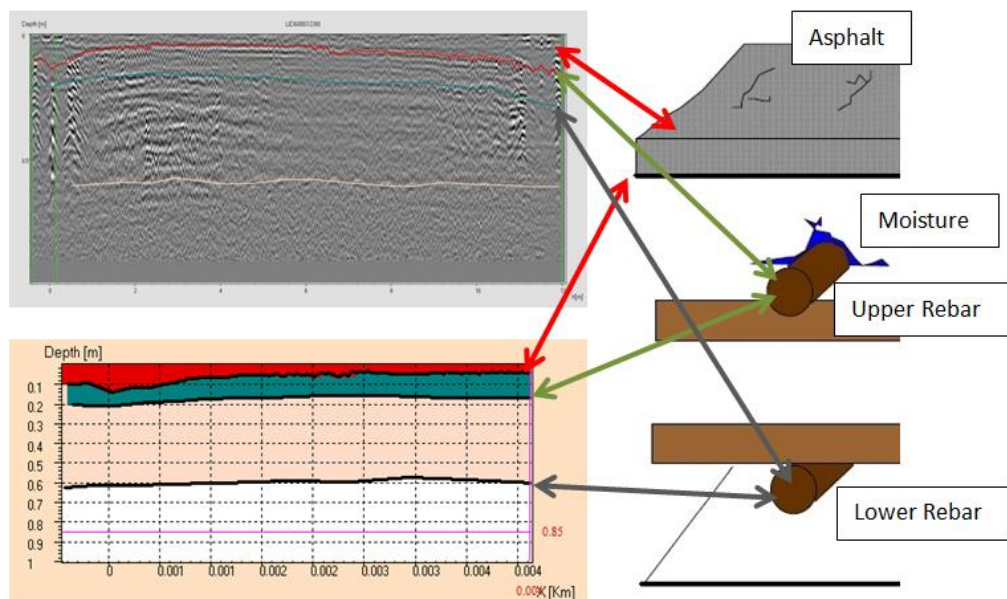


Figure 4.67 – Zone 5 GPR Radargram and Rebar Location

- As Figure 4.68 shows the GPR surveys have affirmed that zones 5 and 6 should be the main focus for further investigation. This is due to the defects detected, as well as the seasonal variation of its internal structure.

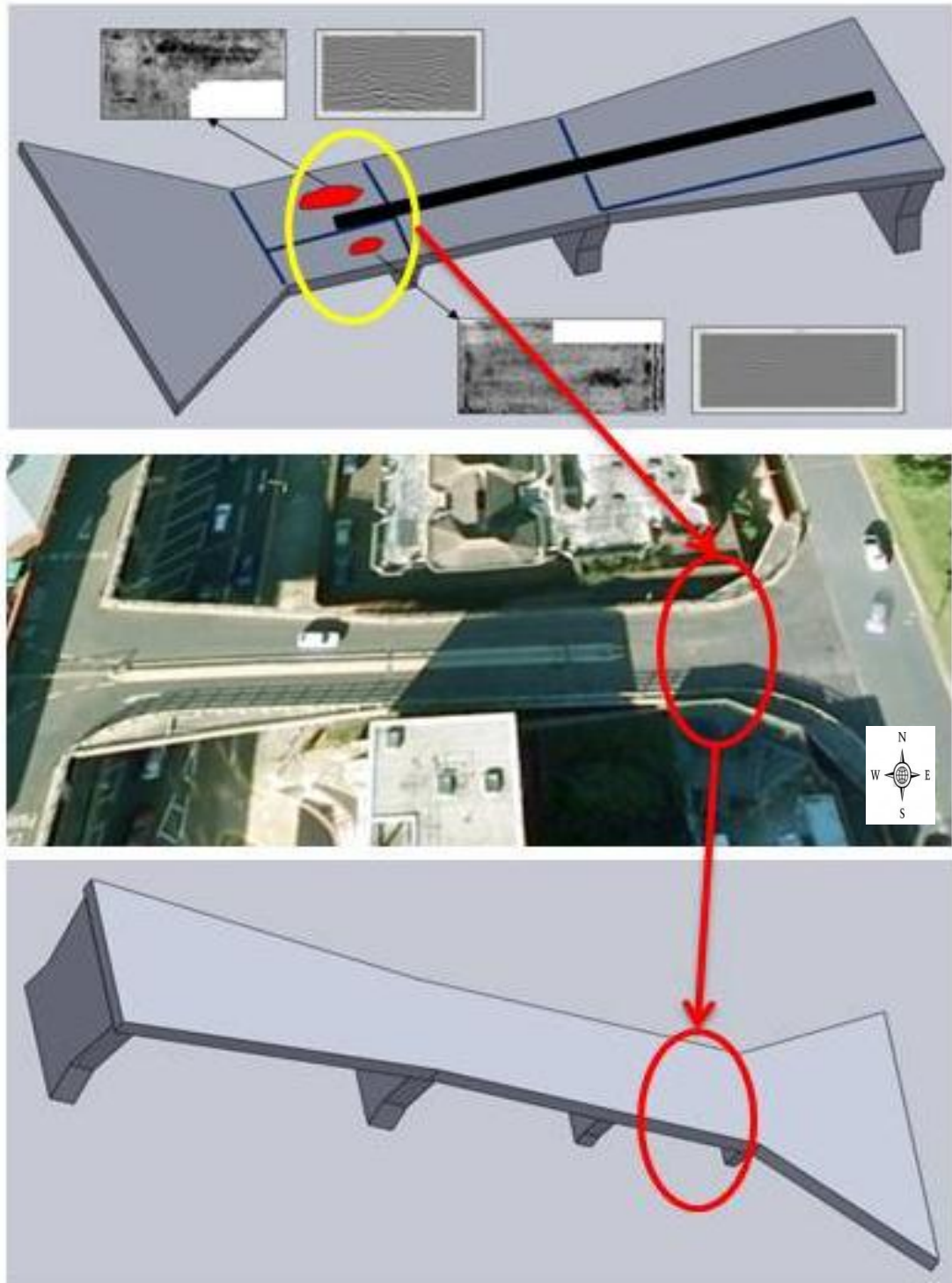


Figure 4.68 – Zone 5 and 6 GPR results

For further information regarding the surveys completed refer to the Appendix B which contains GPR survey results for all zones taken with five differing antennas at four varying days throughout the 2011 and 2012.

4.2.6 Analysis of GPR data: Wave Propagation Velocity Determination

This section presents and discusses the velocity analysis that was undertaken to validate the GPR investigation carried out as detailed in section 4.2.5. To carry out the velocity technique, the two-way travel time at the layer thickness location was recorded and the dielectric constant calculated and plotted along the Pentagon Road Bridge Zone 5 deck length.

4.3.6.1 Introduction

GPR assessment of the electromagnetic wave propagation velocity underground with a high resolution is essential to the effective imaging of the buried objects. One of the significant advantages of GPR in its use in engineering and environmental investigations is the ability to see and interpret the data as it is being collected.

GPR surveys have highlighted that zones 5 and 6 should be the main focus for further in. The velocity analysis is carried out for zone 5, owing to visual inspection indicated that this zone has more defects than zone 6. It has also been able to provide indicators as to potential seasonal changes within the internal bridge structure.

Figure 4.69 depicts how GPR operates when using the RIS Hi BriT (2 GHz) (transmitting) antenna which generates a 2GHz electromagnetic pulse that propagates into the material under investigation. The pulse is partially reflected by any internal structure and is detected by a receiving antenna. The amplitude and the time delay from transmission to reception are measured by the IDS GRED software (IDS Ingegneria dei Sistemi).

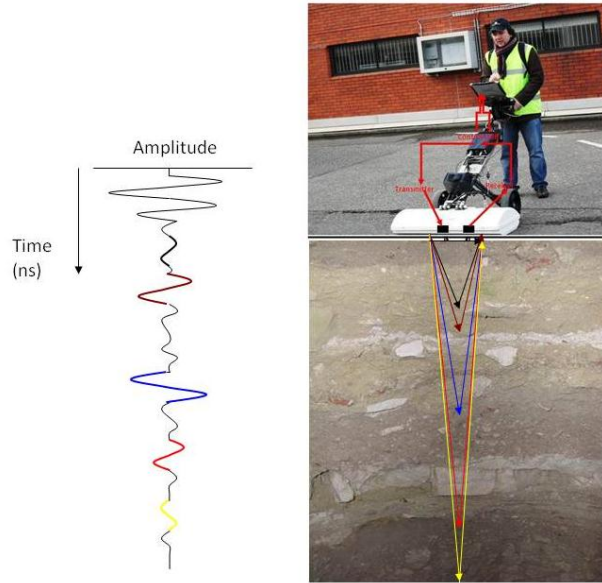


Figure 4.69 – Principle of GPR (Adopted from Gokhan Kilic, 2010)

The main interest is in the travel time and signal amplitude of the reflected pulse. The significance of travel time can be converted that to depth by knowing the propagation velocity of the EM pulse in the concrete. If the transmitter and receiver are coincident (point source), the velocity is calculated as equation (4.2) Jol (2009):

$$V_m = \frac{c}{\left(\frac{\epsilon_r \mu_r}{2} \left[\sqrt{1 + P^2} + 1 \right] \right)^{\frac{1}{2}}} \quad (mm / nano \text{ sec}) \quad (4.2)$$

where;

$$P = \frac{\sigma}{\omega \epsilon} = \text{loss factor } \sigma = \text{conductivity } \epsilon = \epsilon_r \epsilon_0$$

c = speed of light, ϵ_r = relative dielectric permittivity

μ_r = magnetic permeability

ϵ_R = dielectric constant (real part of the permittivity)

Velocity can be simplified for homogenous and isotropic material; the relative propagation velocity can be calculated from equation (4.3)

$$V_m = \frac{c}{\sqrt{\epsilon_R}} = \frac{11.8}{\sqrt{\epsilon_R}} (mm / nano \text{ sec}) \quad (4.3)$$

Equation (4.4) provides a dielectric constant. As the dielectric constant in concrete is directly connected to water content, the greater the water content, typically, the higher the dielectric constant.

$$\varepsilon_r = \frac{2}{\mu_r \left[\sqrt{1 + P^2} + 1 \right]} \left(\frac{c}{V_m} \right)^2 \quad (4.4)$$

4.3.6.2 Wave Propagation Velocity Determination Results

The IDS GRED software (IDS Ingegneria dei Sistemi) provides velocity, time delay and depth information from a radargram. Radargrams were processed using phase correlation, which matches the peak of the interpreted hyperbole with the rebar hyperbole at the same position. This provides velocity of the top of the hyperbole and gives the time delay and calculates depth; presented on the right side of the radargram as presented in Figure 4.70.

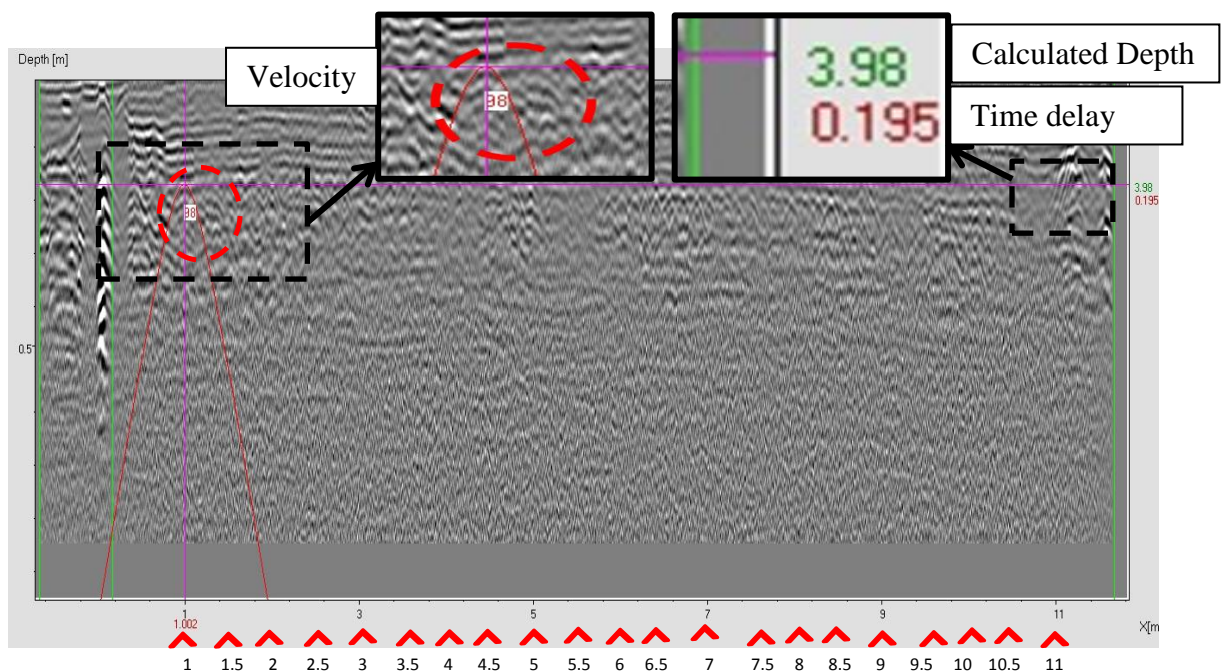


Figure 4.70 – Radargram velocity analyses

Figure 4.71 shows a highlighted lower rebar on a radargram of zone 5. The radargram enables the identification and assessment of velocity and depth in hot and cold weather conditions of bridge deck. The analysed information is presented in Figure 4.72 and 4.73.

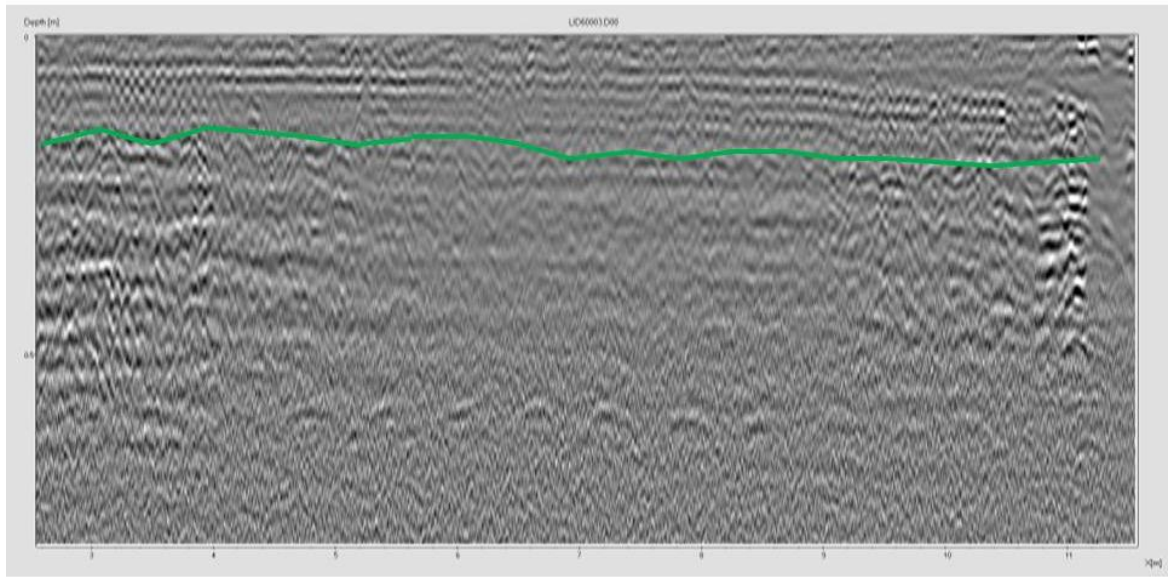


Figure 4.71 – Radargram lower rebar velocity analyses



Figure 4.72 – Calculated depth

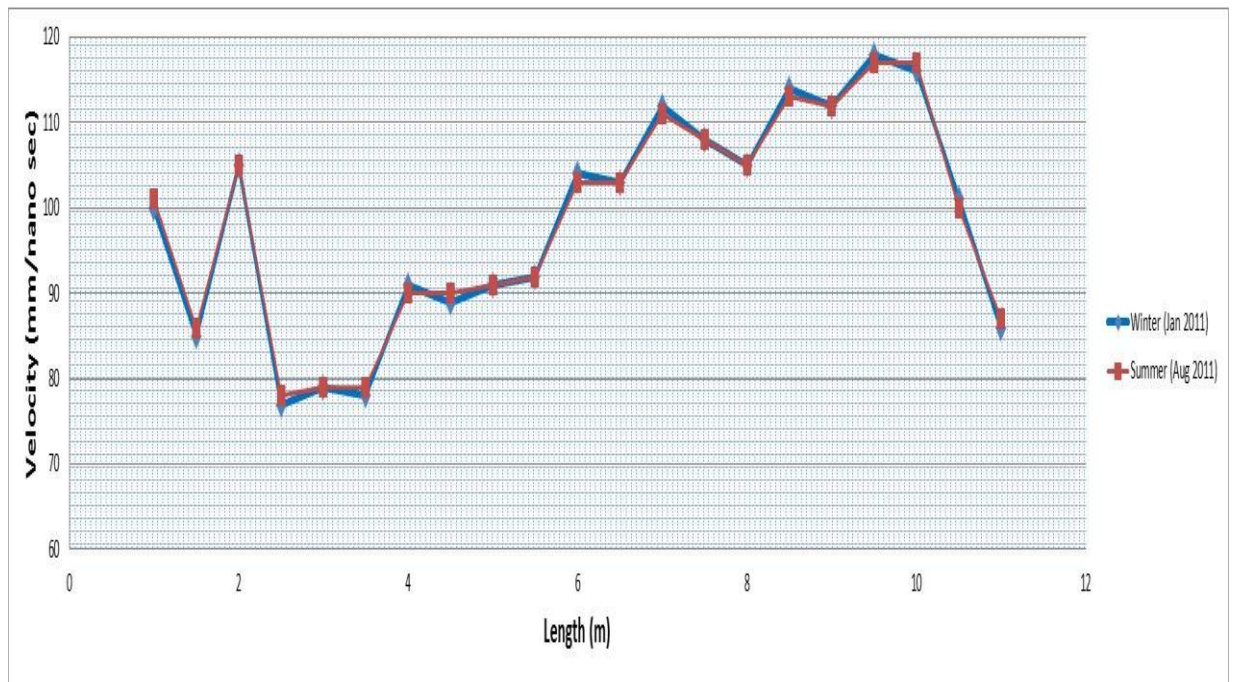


Figure 4.73 – Velocity

Figure 4.72 and 4.73 shows a comparison of velocity analyses and lower rebar positions for Winter (Jan 2011) and Summer (Aug 2011). The analyses was completed to ensure the repeatability of the GPR equipment and to ensure the same method was employed when carrying out the survey.

On the other hand, the velocity analyses of a radargram could be limited due to the external conditions. These external conditions such as degree of moisture in hot and cold surveys, which could affect the data processing and interpretation.

For further information regarding zone 5 the analysis of sixteen radargrams (Figure 4.74) were carried out using IDS GRED software (IDS Ingegneria dei Sistemi), where results were recorded every half-metre along the radargram. Figure 4.75 depicts the results of this velocity analysis, where the white marks indicate the peak of the interpreted hyperbole, across sixteen radargrams as indicated by the horizontal red lines.

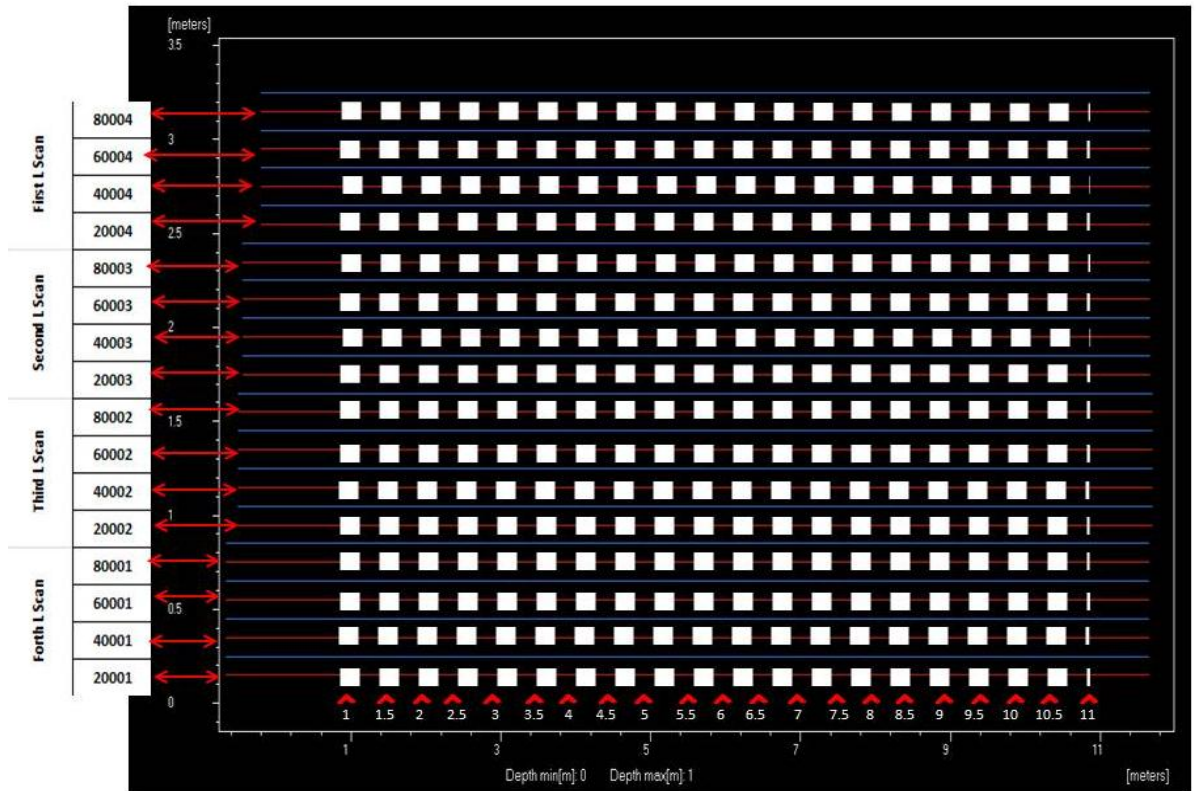


Figure 4.74 – Zone 5 plan

All radargrams were processed and analysed and the results are presented in Table 4.5.

Table 4.5 - Depth of the lower rebar

		Calculate Depth																				
		Distance [m]																				
		1	1,5	2	2,5	3	3,5	4	4,5	5	5,5	6	6,5	7	7,5	8	8,5	9	9,5	10	10,5	11
Forth L Scan	80004	0,144	0,14478	0,14589	0,1461	0,14453	0,147825	0,14444	0,14259	0,142615	0,14459	0,14872	0,14112	0,163775	0,16334	0,161735	0,15749	0,17096	0,175085	0,1842	0,18055	0,18318
	60004	0,14558	0,1486	0,16167	0,162225	0,1457	0,155035	0,15912	0,155035	0,15964	0,16473	0,1638	0,17819	0,16665	0,17054	0,1705	0,17391	0,173215	0,1925	0,206565	0,21008	0,18618
	40004	0,16585	0,18962	0,173225	0,161485	0,17098	0,155325	0,15325	0,15655	0,162225	0,15939	0,1616	0,17585	0,17872	0,17437	0,14091	0,16895	0,19491	0,20476	0,21944	0,20919	0,18318
	20004	0,18615	0,16821	0,18887	0,17493	0,1794	0,17312	0,16316	0,155	0,151515	0,16524	0,16632	0,187148	0,17472	0,18333	0,178095	0,18471	0,202905	0,21754	0,231	0,22329	0,18404
Third L Scan	80003	0,173225	0,12558	0,14647	0,1355	0,15631	0,132435	0,12846	0,16324	0,167475	0,183	0,17635	0,18921	0,1798	0,17136	0,17581	0,18788	0,16564	0,19998	0,20825	0,21896	0,1744
	60003	0,1534	0,133025	0,1596	0,11858	0,126005	0,13455	0,156975	0,14596	0,14742	0,15778	0,1898	0,17261	0,18104	0,17224	0,171625	0,18691	0,18944	0,19833	0,20852	0,19897	0,18404
	40003	0,132815	0,13927	0,13383	0,1265	0,14045	0,126245	0,14066	0,1568	0,14646	0,15515	0,15427	0,15416	0,15141	0,13528	0,16545	0,14529	0,1656	0,18838	0,1979	0,1701	0,18531
	20003	0,1368	0,141905	0,14017	0,13235	0,1495	0,142615	0,16416	0,141905	0,1473	0,14872	0,15043	0,1594	0,1624	0,1512	0,124155	0,1392	0,140175	0,16089	0,180545	0,19952	0,18275
Second L Scan	80002	0,13311	0,139965	0,15246	0,1495	0,15352	0,14656	0,17105	0,14787	0,14695	0,13925	0,164415	0,17748	0,1695	0,1765	0,1703	0,18631	0,177165	0,16768	0,20517	0,193465	0,1617
	60002	0,16118	0,1478	0,156848	0,15365	0,15582	0,14948	0,15878	0,16334	0,16796	0,17655	0,16119	0,17038	0,166	0,17152	0,17591	0,18074	0,18055	0,19175	0,20306	0,1962	0,161
	40002	0,1866	0,15271	0,146475	0,155925	0,13984	0,141405	0,15923	0,1676	0,168525	0,18198	0,197575	0,168025	0,16274	0,16856	0,17178	0,18083	0,2043	0,190025	0,201455	0,18308	0,1844
	20002	0,14368	0,12875	0,1279	0,107325	0,1482	0,103155	0,14194	0,14523	0,16219	0,171195	0,20758	0,1957	0,19055	0,18239	0,17003	0,17072	0,201507	0,21678	0,18146	0,19734	0,18876
First L Scan	80001	0,170085	0,14823	0,15065	0,18382	0,19005	0,18338	0,17289	0,15666	0,15785	0,173125	0,17121	0,171705	0,18178	0,18667	0,181525	0,20557	0,203595	0,21592	0,2014	0,20064	0,1984
	60001	0,1581	0,16368	0,16182	0,16192	0,165385	0,16611	0,17536	0,17725	0,15996	0,16184	0,19695	0,16469	0,16008	0,163601	0,1928	0,18045	0,187555	0,19366	0,212465	0,191555	0,15213
	40001	0,1577	0,15552	0,14924	0,15159	0,17278	0,16278	0,17187	0,1695	0,15664	0,177	0,17424	0,158895	0,159495	0,1416	0,16926	0,15169	0,177465	0,1706	0,18425	0,16185	0,19823
	20001	0,13795	0,1584	0,13795	0,15345	0,1515	0,151805	0,13167	0,15582	0,17289	0,14061	0,14255	0,16268	0,16176	0,14801	0,143605	0,15088	0,1547	0,1659	0,17696	0,16188	0,21

From Table 4.5 the depth of the lower rebar map can be presented as in Figure 4.75 which uses the MatLab program (The MathWorks, Inc., 2012) to generate a depth graph.

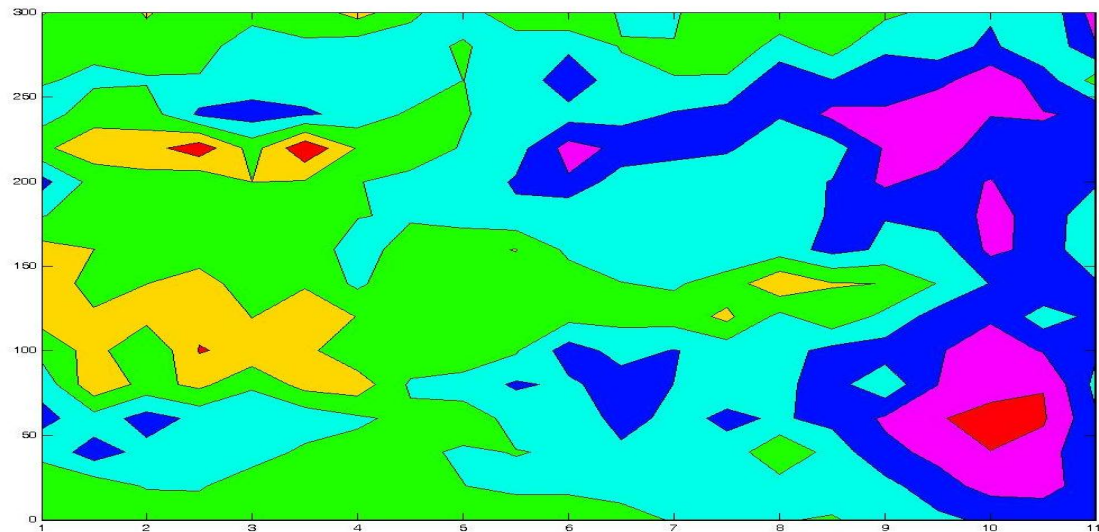


Figure 4.75 –Depth of the lower rebar

Figure 4.75 demonstrates the depth of the lower rebars within zone 5. This shows that the lower rebars are, in fact, not uniformly placed throughout the length of zone 5. This could be because of different settlement, design, construction error, or due to moisture.

In order to understand the effect of moisture on a radar signal and to identify the mechanisms behind the detection of moisture content at different layers, the velocity at which radar energy travels depends on the dielectric properties, ϵ , of the medium in which it is travelling. In particular, the velocity, ϵ_r , which is the dielectric constant; a misnomer as it is not a constant. Using equation 4.3 the characteristics of different materials are provided in Table 4.6.

Table 4.6 - Dielectric constant

		Dielectric Constant																				
		Distance [m]																				
		1	1,5	2	2,5	3	3,5	4	4,5	5	5,5	6	6,5	7	7,5	8	8,5	9	9,5	10	10,5	11
First L Scan	80004	8,978	9,606	9,516	9,875	9,067	9,606	9,337	8,798	9,965	9,786	9,965	11,491	10,324	9,696	9,606	9,516	10,055	8,708	10,594	9,247	7,721
	60004	6,195	8,080	9,157	9,247	8,439	9,067	9,157	9,067	9,337	9,157	9,337	9,247	9,067	9,157	8,978	9,157	9,067	8,978	10,145	9,067	7,811
	40004	9,426	11,581	9,426	9,965	9,247	8,529	9,875	9,067	9,247	8,888	9,337	9,426	9,696	8,439	6,913	5,476	10,683	10,414	9,337	10,683	7,721
	20004	9,875	7,990	9,067	8,798	9,337	9,786	9,337	8,978	8,170	9,157	8,888	9,965	8,619	8,708	8,349	8,439	9,786	9,965	9,426	10,145	7,721
Second L Scan	80003	9,426	7,003	8,708	6,284	8,798	7,272	6,105	9,516	9,426	8,978	9,426	9,157	9,965	9,337	9,606	9,157	7,362	8,888	9,875	10,414	7,182
	60003	8,978	7,631	9,426	6,913	7,092	7,003	8,170	7,990	8,170	8,259	9,337	9,247	10,055	9,696	9,426	10,234	10,055	10,594	10,414	9,067	7,721
	40003	9,067	10,594	11,402	10,414	9,516	10,234	10,414	10,055	10,414	9,606	9,965	9,696	8,798	7,990	9,875	7,811	8,080	10,953	9,875	8,080	7,811
	20003	8,529	9,067	10,234	9,875	9,875	9,965	10,234	9,067	9,875	9,337	10,234	9,875	10,055	9,426	7,990	8,619	7,990	8,349	10,504	10,055	7,721
Third L Scan	80002	7,811	8,349	8,888	8,978	9,067	9,247	9,875	8,349	9,516	8,798	8,708	9,157	8,978	9,875	9,875	10,953	8,349	6,374	10,504	9,606	6,284
	60002	9,696	8,978	11,132	10,324	9,516	9,067	10,773	9,696	9,337	9,875	9,516	10,234	8,978	10,055	10,594	9,157	9,247	9,875	9,516	8,080	6,284
	40002	10,773	10,234	8,349	8,888	9,965	10,504	11,402	9,965	9,606	9,696	10,324	10,324	11,132	10,414	10,234	12,389	10,773	9,426	9,965	8,259	7,182
	20002	10,145	8,978	8,978	7,272	10,234	6,195	8,439	8,439	8,798	9,067	9,606	9,247	9,247	9,516	9,157	7,900	9,606	8,798	7,721	8,259	7,900
Forth L Scan	80001	7,811	7,272	8,080	9,067	9,426	9,516	9,157	7,541	6,913	6,733	7,003	6,015	7,721	7,003	6,374	6,913	6,374	7,003	6,823	6,823	7,182
	60001	9,157	8,349	8,349	8,259	8,708	8,798	9,965	9,606	7,721	6,464	9,067	7,721	6,105	6,015	9,337	8,080	7,990	8,259	8,170	8,170	5,925
	40001	8,529	8,619	8,170	8,349	9,516	9,516	9,157	8,978	7,990	8,978	8,888	8,888	8,349	7,182	8,170	6,913	6,913	6,554	6,554	7,003	7,721
	20001	7,990	8,888	7,990	8,888	8,978	8,708	6,913	8,798	9,157	7,721	8,080	8,798	8,619	6,643	6,913	7,362	7,631	7,541	6,464	6,374	5,566

Figure 4.76 demonstrate the dielectric constant map within the zone 5 using MatLab program (The MathWorks, Inc., 2012).

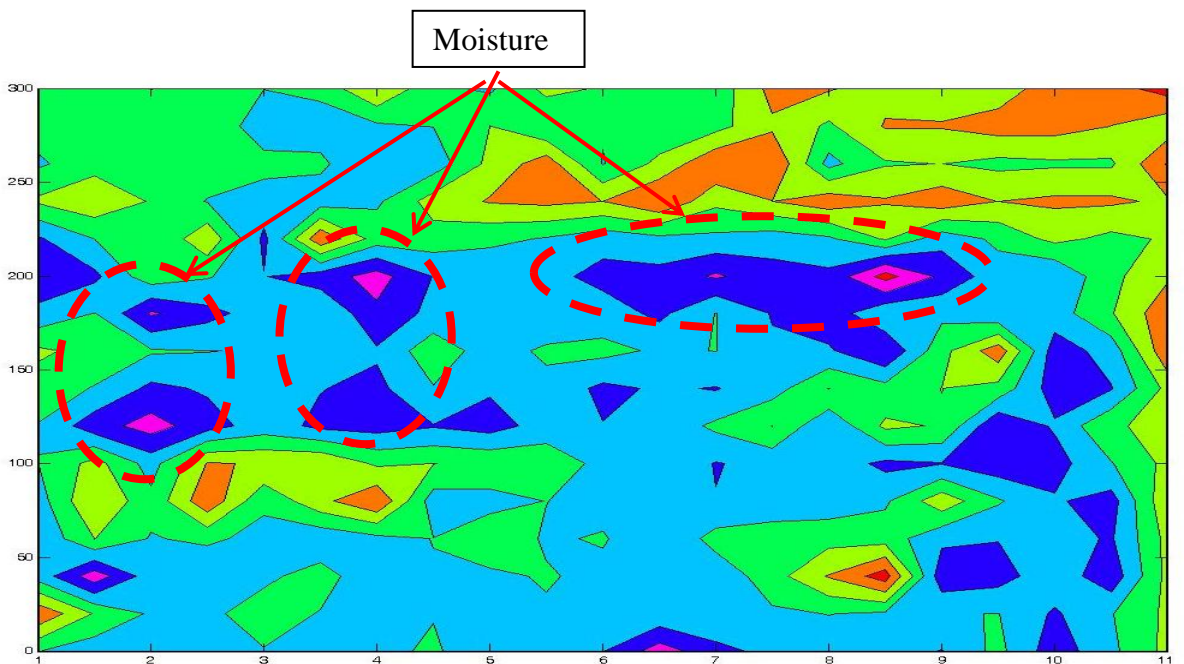


Figure 4.76 – Dielectric constant

Dielectric constant data was calculated in order to validate GPR results. However, for the purpose of this section a selected range of data has been chosen to highlight the effectiveness of the GPR in velocity analyses in identifying possible defects.

Figure 4.77 shows a processed 2D data, which generates a depth graph, from IDS GRED software (IDS Ingegneria dei Sistemi) which is constantly 20cm below the surface indicates the approximate lower-rebar depth.

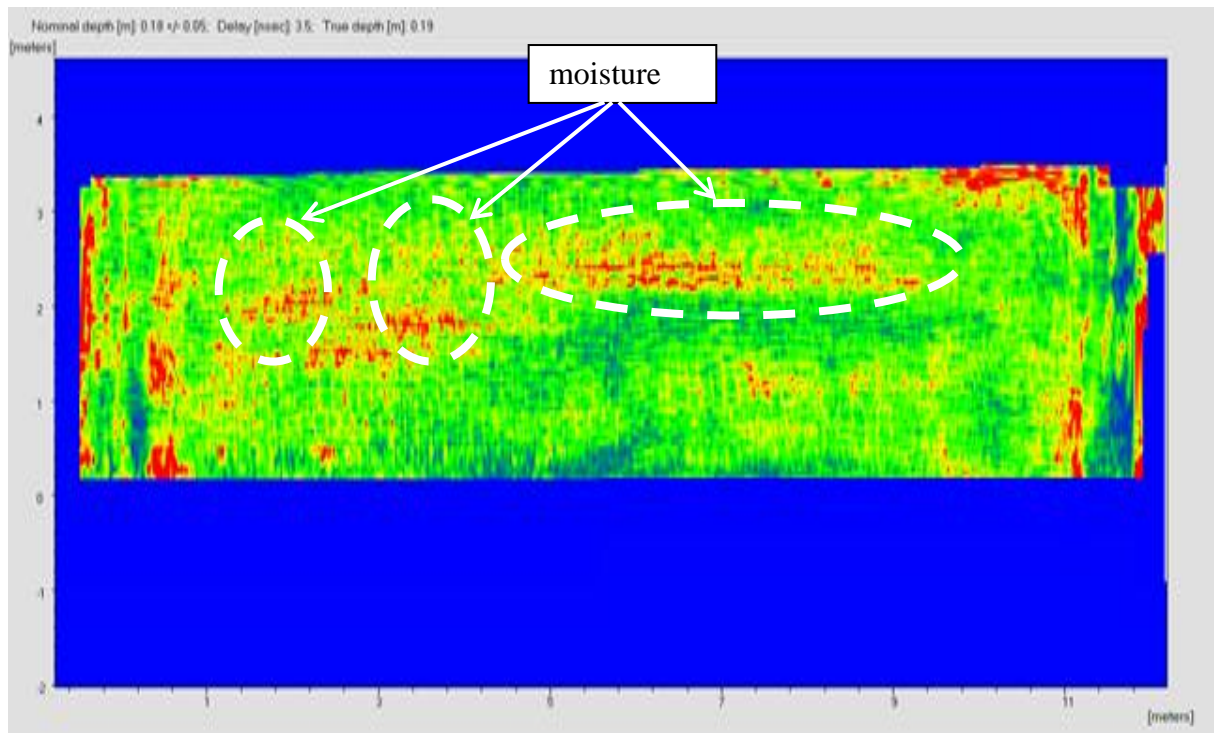


Figure 4.77 – GPR Output

4.3.6.3 Summary of Wave Propagation Velocity Determination

As was shown in the literature review the GPR signal travels slower through areas of moisture due to the change in the dielectric constant between dry and wet material. This anomaly was exploited in order to identify areas of moisture ingress in the bridge structure using velocity analysis. The velocity analysis was carried out by measuring the velocity at intervals and using this to calculate the dielectric constant. As concrete is a homogenous material of uniform construction higher dielectric constants are likely to indicate areas of higher moisture content.

The results obtained from this analysis compare favourably to the findings of the IDS GRED software (IDS Ingegneria dei Sistemi) and dielectric constant data which as stated previously showed the existence of a patch of moisture close to the surface. Both the position of the rebar and dielectric constant were crucial factors to understand the

health of the Pentagon Road Bridge. These findings serve to further validate the use of GPR as a non-destructive bridge health monitoring technique.

4.4 Summary

This chapter detailed the results of the NDT: visual inspection, GPR, IBIS-S and accelerometer. These results demonstrate the applicability and utility of these techniques for bridge health monitoring. This summary details each of the NDT used in terms of the structural information and results they provided.

- The result of visual inspection gives a very basic external understanding of the bridges health; it indicates superficial damage such as cracking and cover delamination which could denote more serious underlying structural defects. However it does not give detailed internal results. It is therefore appropriate as a NDT in order to provide a preliminary result as to the health of the bridge but a more detailed method is needed for further information. In the case of the Pentagon Road Bridge in provided information including defects such as moisture, cover delamination and cracks in span 4.
- The results of IBIS-S give the behavior of the bridge such as deflection which is of paramount concern when determining the safety of the bridge. Accelerometer results successfully validated the IBIS-S findings of the bridge deflection. On the other hand, Oracle WSN was found to be inappropriate for use for this particular bridge scenario due to their battery life. The results of IBIS-S and Accelerometers showed that a significant deflection occurred in the cantilever zone of span 4 which is unexpected compared to the results for the other spans. Also, the actual results obtained from IBIS-S surveys will be presented and compared with the Finite Element Model in next Chapter Five.
- GPR gives detailed results of internal structural defects and information. With regards to the Pentagon Road Bridge GPR showed a moisture presence particularly in span three and four. It also gave results for structural information such as the position of rebars which will be input into a FEM. The results of velocity analysis was carried out by measuring the velocity at intervals and using this to calculate the dielectric constant, since it a homogenous material of uniform construction (concrete) higher dielectric is likely to indicate an area of

more moisture. These findings serve to further validate the use of GPR as an appropriate non-destructive bridge health monitoring technique.

As can be seen from the below, the results given by GPR, IBIS-S, and visual inspection correlated to indicate a particular section of the bridge (cantilever zone) which needed further action is presented in Figure 4.78.

This combination of techniques has not been suggested previously and has distinct advantages over earlier bridge health monitoring approaches as it encompasses all aspects of structural design important to health and safety engineers such as cost effective and simple initial assessment (visual inspection), techniques which provide not only structural defects but also behaviour (GPR, and IBIS-S) and also a benchmark model with which these results can be compared to (FEM).

This combination mechanism, the author believes, has the strength to become a fundamental practice in bridge health engineering and in the future could become a popular step by step method of determining the health of bridge structures.

This approach will be further expanded on in the next section to include FEM and thus successfully fulfil the main aim of the thesis to create an integrated bridge health monitoring technique including all the aforementioned NDT.

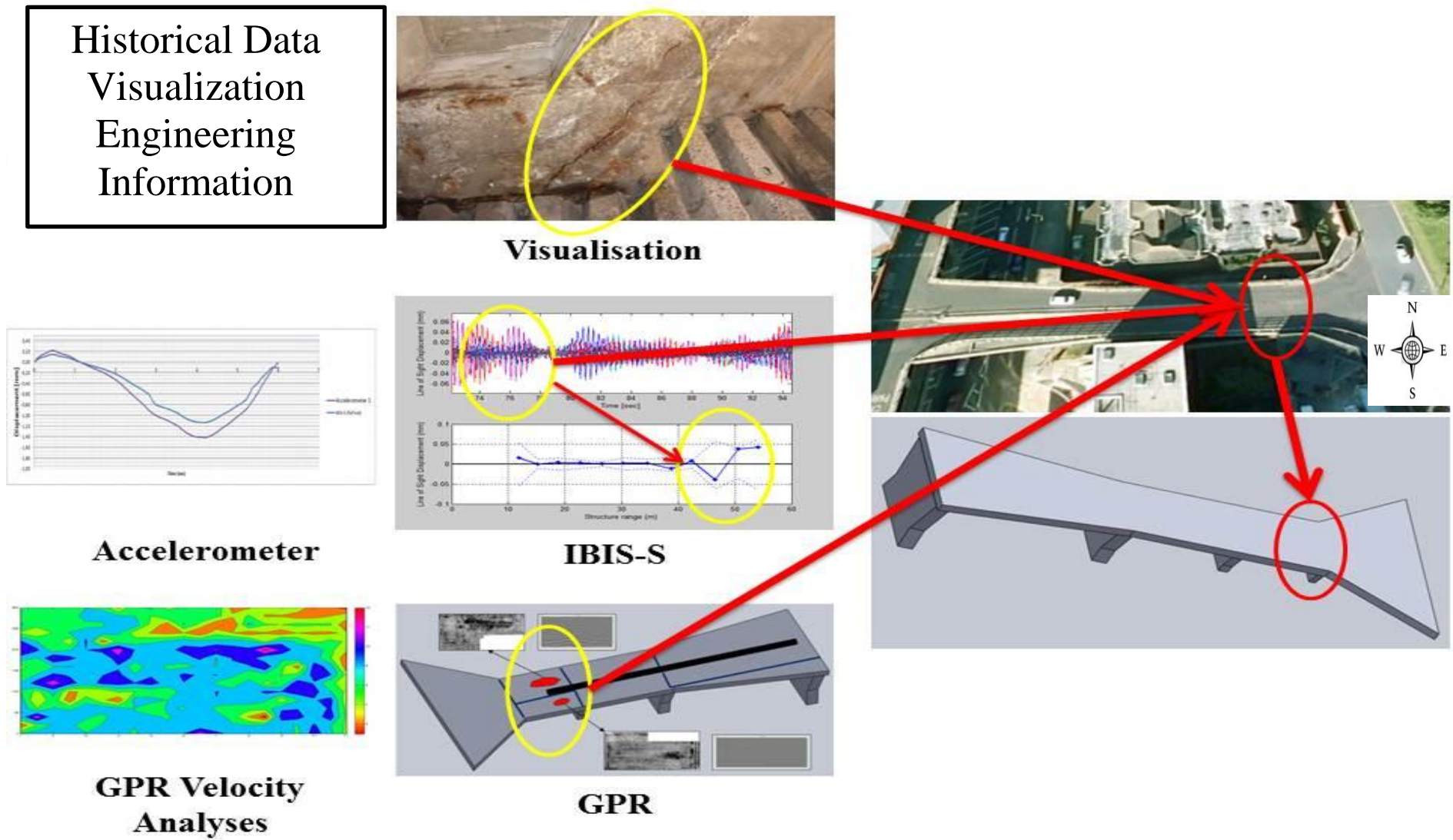


Figure 4.78 –Combination of Visualisation, IBIS-S, and GPR Results

Chapter 5

Parametric Study

The objectives of this chapter are to develop a numerical bridge model to be used for the main case study “Pentagon Road Bridge” to define parametric sensitivity, the effect on the level of structural response, and parametric assessment of the cracked zones.

5.1 Introduction

The main focus of this parametric study was to develop an FE model (in both SAP2000 (Computers and Structures, 2012) and ANSYS 12.1 (ANSYS, 2011)) based on the NDT results to compare with the actual behaviour of the bridge, in order to indicate deterioration in the bridge structure. This developed FE model gave a more accurate picture of how the bridge should behave which can be compared with the actual behaviour obtained from the other NDT. This parametric study also defines parametric sensitivity of the structural response to the width of cracks in the cantilever zone.

ANSYS and SAP2000 were chosen as they have been used worldwide in both research and industry for many decades. SAP2000 is easy to use software which enables the creation of preliminary models which can be used to gauge fundamental bridge behaviour. ANSYS is a more complex model which allows for detailed analysis of the bridge's deflection. Detailed information such as rebar position can be input to create an accurate model. It can also be used to predict the future behaviour of structures by utilising its CRACK modelling tool.

The first model of the Pentagon Road Bridge was developed in SAP2000 and ANSYS utilising the data provided by both an external principal report obtained from Medway Council and visual inspection. These models were used to predict the deflection of the bridge under the same dynamic loading (i.e. a cherry picker whose specifications were obtained from Medway Council) as the survey completed using the IBIS-S equipment and Accelerometer so that results could be compared. The second model of the Pentagon Road Bridge was developed in ANSYS utilising the data provided by GPR. This created an accurate FEM of the bridge utilising the information regarding rebar position obtained from the GPR surveys, which was used for further analyses and testing. Crack propagation was also modelled and the effect of these cracks on structural response predicted using the CRACK tool in ANSYS.

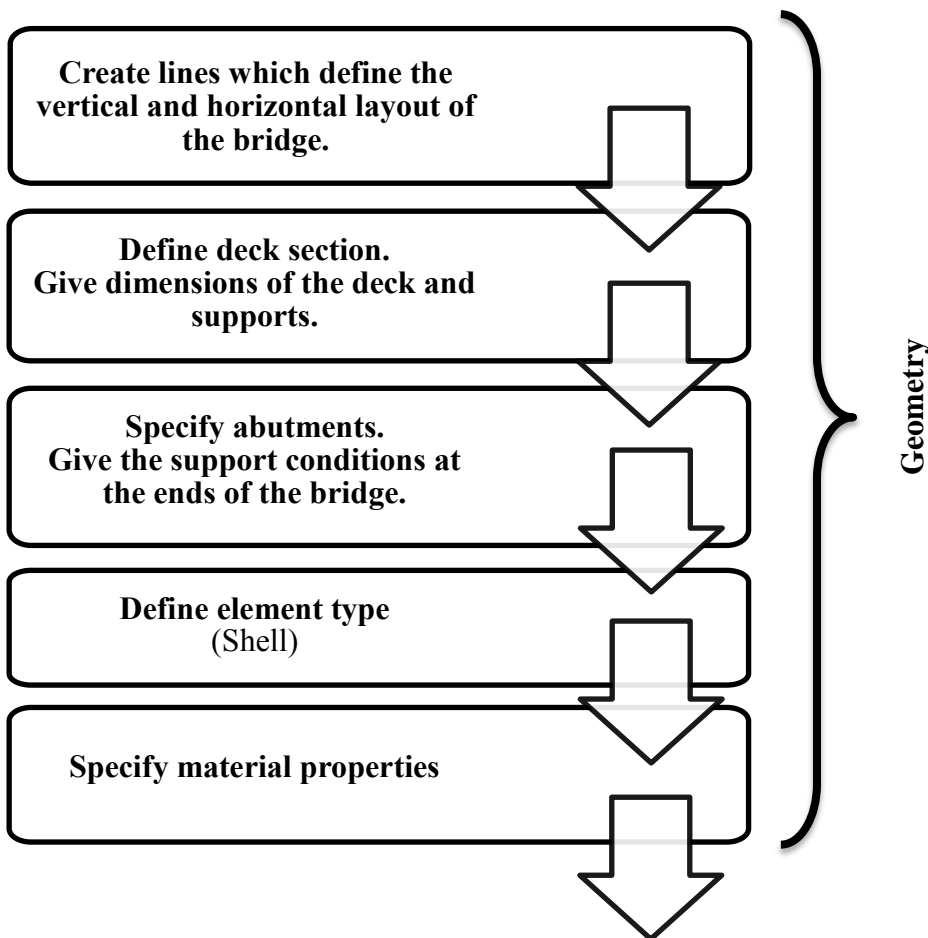
Only dynamic loading is considered by the FE model as this is deemed to be the worst case scenario for deflection, which is the main focus of this study. This choice was also due to the limited information available regarding the Pentagon Road Bridge.

The Pentagon Road Bridge model was developed using two different commercial FE software products (SAP2000 and ANSYS). The rest of this chapter is presented as follows: section 5.2 presents the procedure used when creating these FE models, section 5.3 details the assumptions made, section 5.4 presents the specification of moving load which was used in both of the FE models, section 5.5 discusses modelling with SAP2000, section 5.6 presents the modelling cracks with ANSYS and section 5.7 concludes the chapter.

5.2 Modelling Procedures

5.2.1 SAP2000 Modelling Procedure

Figure 5.1 details the procedure followed when creating the SAP2000 model (Computers and Structures, 2012).



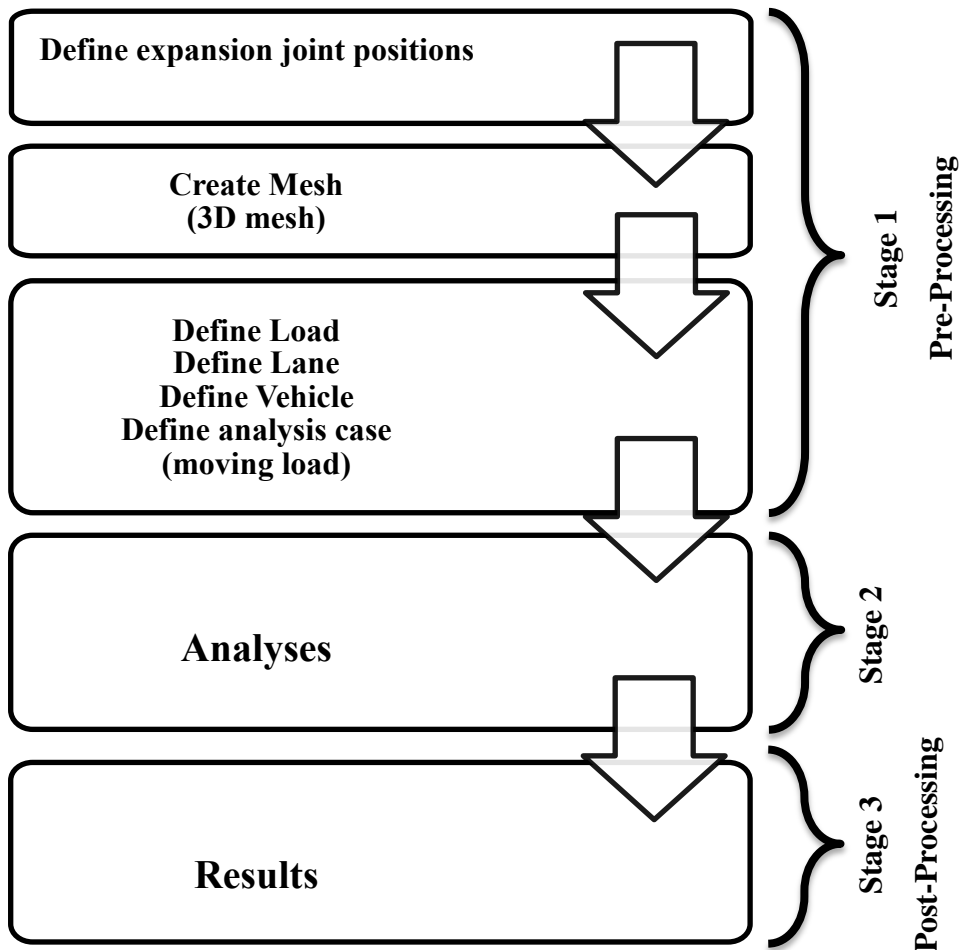
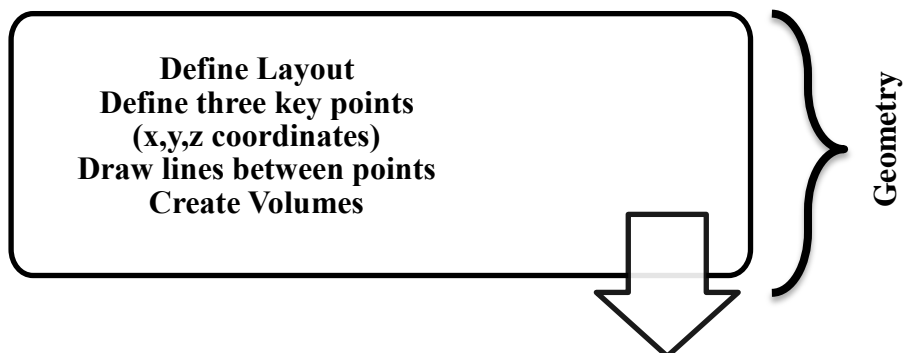


Figure 5.1 – SAP2000 modelling procedure

5.2.2 ANSYS Modelling Procedure

Figure 5.2 shows the procedure followed when developing the ANSYS model (ANSYS, 2011).



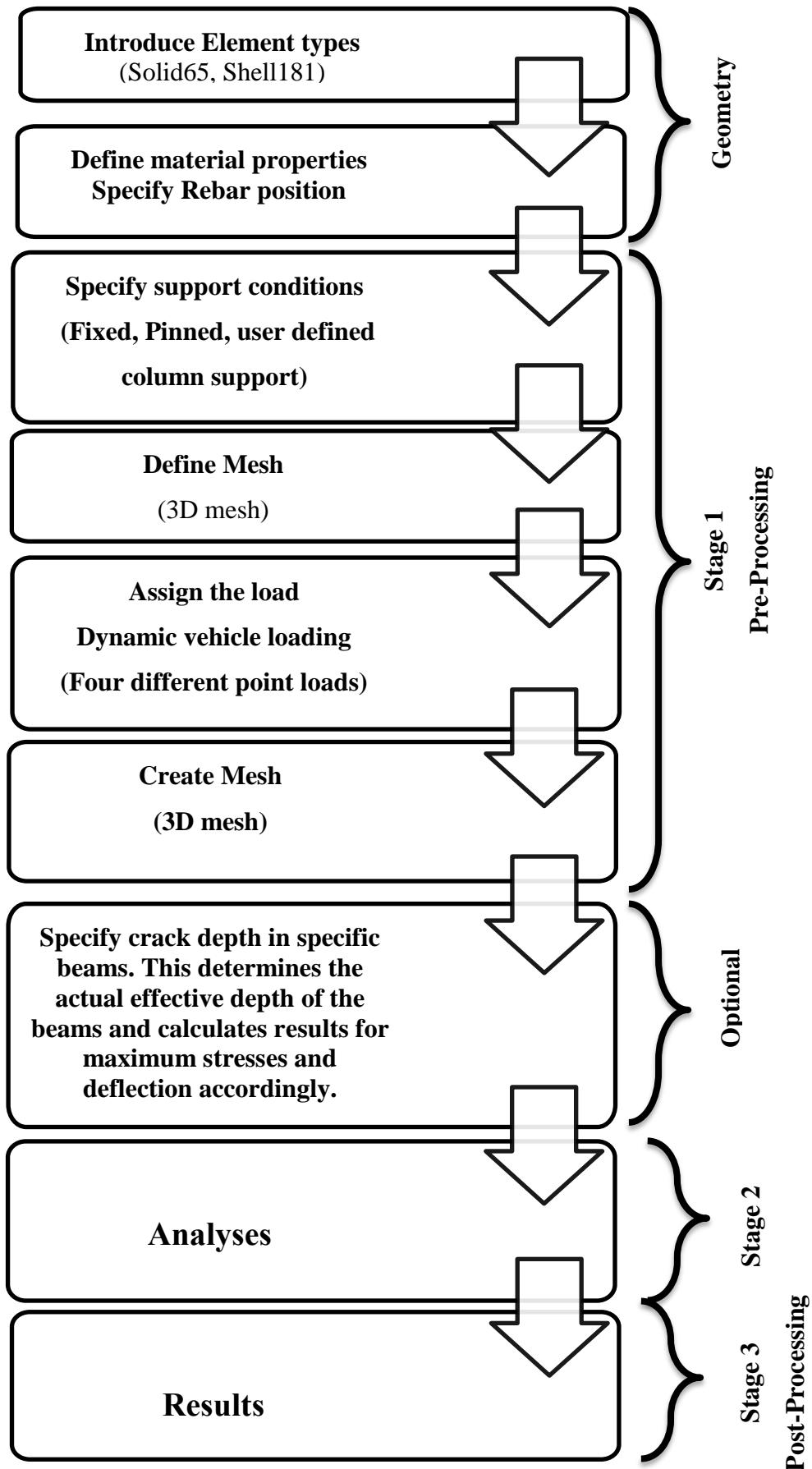


Figure 5.2 – ANSYS modelling procedure

5.3 FE Modelling Assumptions

Structural properties, such as specific concrete strength and connection details, are usually specified by the designer. There are two major cases in which these properties must be assessed based on the structure; first when there is doubt as to whether the structure conforms to the specified design properties, and second when the design assumptions and specifications are not accessible. In these cases, non-destructive or destructive tests are usually the best means to determine unknown factors. These both have their disadvantages: non-destructive testing is non-precise and depends on the interpretation of the user and destructive testing is not always viable as it causes damage to the structure. A combination of non-destructive evaluation techniques and the FE method is proposed here to find and evaluate the unknown structural properties of the Pentagon Road Bridge.

It was not viable to obtain core samples from the Pentagon Road Bridge, so it was not possible to determine the grade of steel and concrete used in construction. Therefore the parameters were determined from various literature sources as seen in Table 5.1.

Table 5.1 – Pentagon Road Bridge FE Modelling Assumptions

Concrete	$E_c = 21.53 \text{ GPa}$	$E_c = 4700\sqrt{f_c}$ (ACI / 343R-95, 2011)
	$f_c = 21 \text{ MPa}$	(Kosmatka et al, 2002)
	$\nu = 0.2$	EUROCODE 2-18
Steel	$E = 200 \text{ GPa}$	(AISC, 2006)
	$\gamma_s = 7800 \text{ kg/m}^3$	(AISC, 2006)
	$\nu = 0.3$	EUROCODE 3-22

Table 5.1 shows the initial assumptions made regarding material properties - these were then calibrated using IBIS-S data (see section 5.5).

The basic input data, such as geometrical properties of the Pentagon Road Bridge model to be developed are given in Appendix D. The data was obtained from visual inspection (see section 4.3.2) and a previous visual inspection report produced by Jacobs Eng. U.K. Limited (2009).

The following are the assumption made by the FE models:

- Temperature is uniform and constant in all models.
- Speed of the cherry picker (25 MPH) is constant throughout the loading period.
- Weight of the cherry picker is constant throughout the loading period (see Figure 5.8).
- All the models are three dimensional (3D) and all the nodes have degrees of freedom in all 3 dimensions.
- All bearings assumed to be at the same points as on Pier 3 (see Appendix D).
- No residual stresses applied to the model.
- The surface roughness was not considered.
- The damping ratio assumed as 5% (Chopra, 1995).
- Stiffness was calculated using the FE software.
- No boundary conditions were used in FE models.

The GPR results for rebar position were input into the ANSYS model when creating the mesh by specifying which areas were of steel composition (rebars ($A_s = A_s' = 7.68 \cdot 10^{-4} \text{ m}^2$)) and which areas were concrete (Figure 5.3).

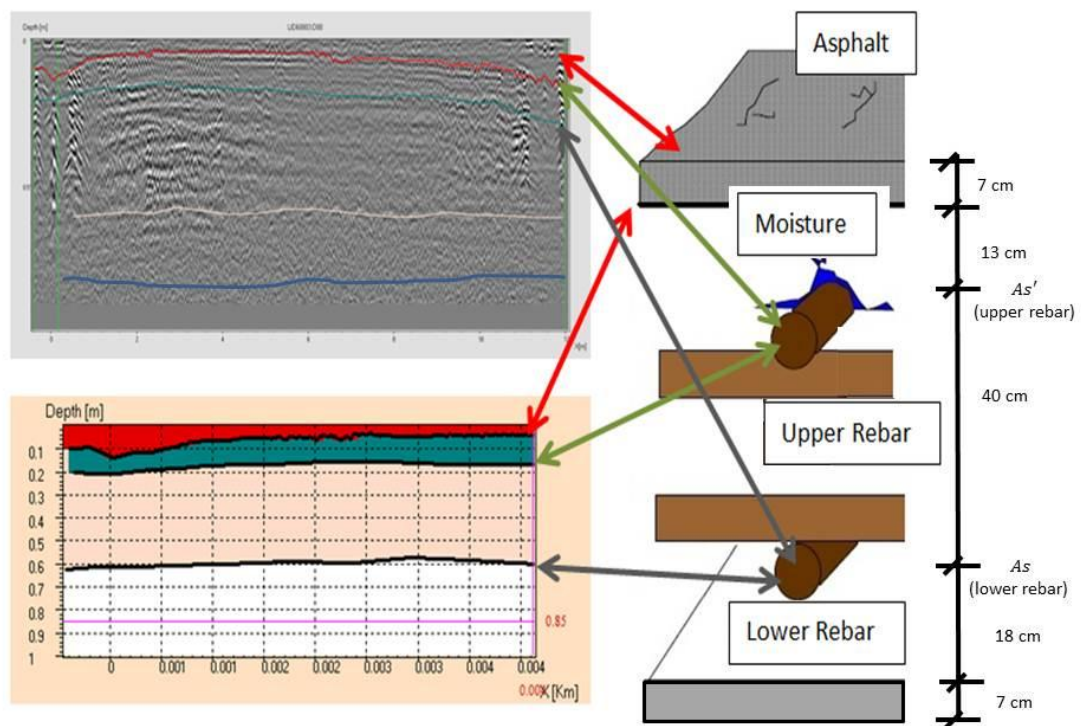


Figure 5.3 – Rebar position from GPR radargram

The rebar diameter was measured from a radargram as can be seen from Figure 5.4. The value of the diameter is the measurement from the top of the upper hyperbole to the top of the lower hyperbole.

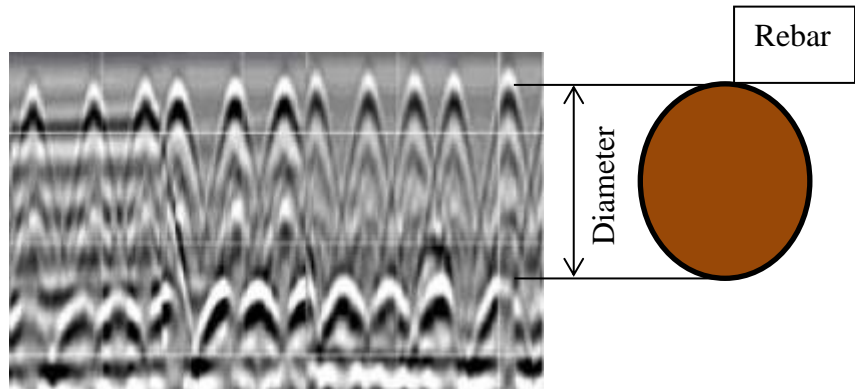


Figure 5.4 – Rebar diameter measurement from a radargram

The information from the GPR radargrams regarding rebar position was input into ANSYS by specifying which parts of the bridge deck were composed of steel and which parts of concrete. This is illustrated in Figure 5.5.

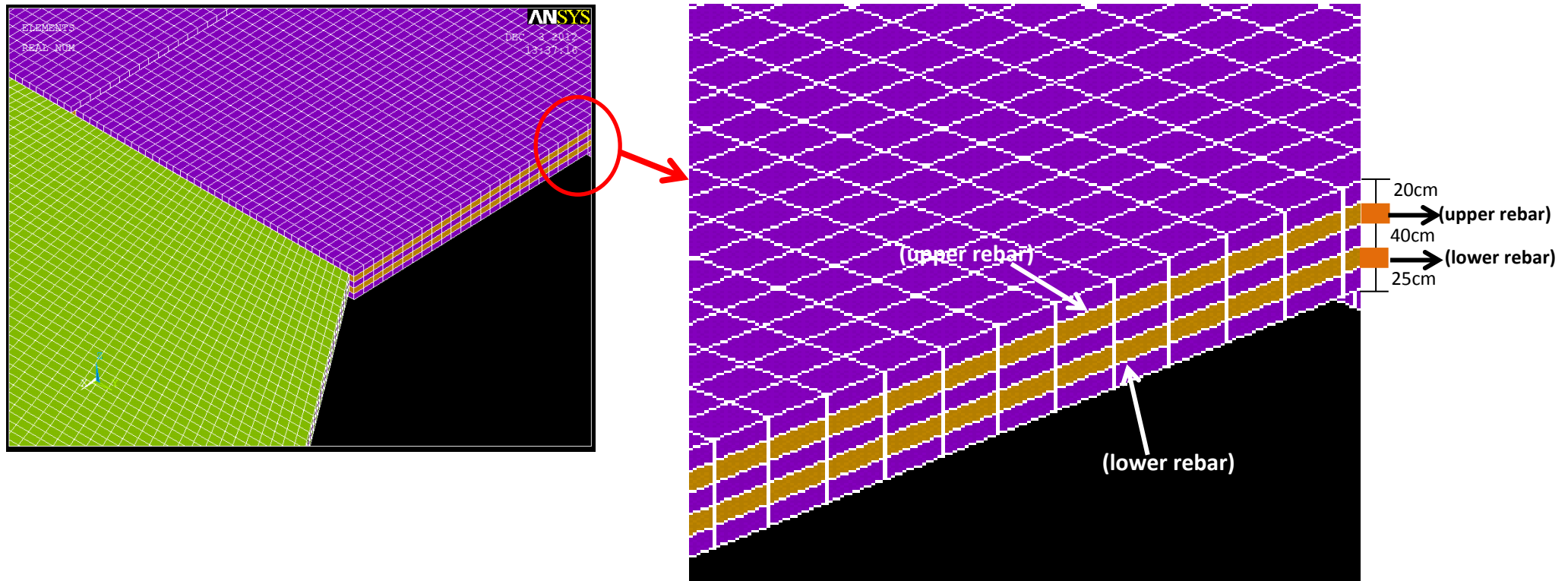


Figure 5.5 – Rebar position in ANSYS modelling

Shell 181, a system which can be used to interpret load stiffness effects of distributed pressures, was also applied to the Pentagon Road Bridge to model the decks, abutments and piers. An illustration of Shell 181's geometry, node locations and element coordinate system can be seen in Figure 5.6. This 4-node element has six degrees of freedom at each node: translations in the x, y, and z directions and rotations about the x, y, and z axes.

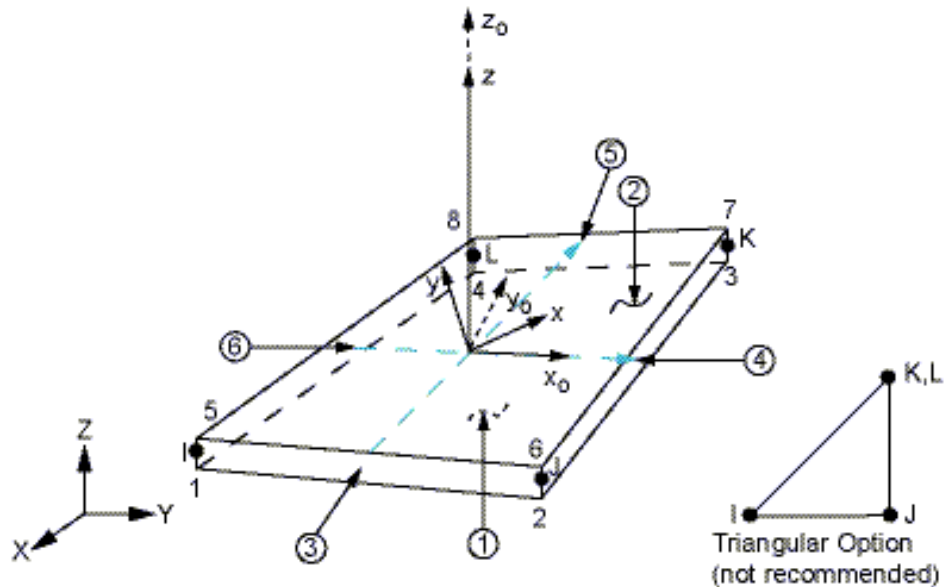


Figure 5.6 – Geometry of SHELL181 element in ANSYS

BEAM4, providing stress stiffening and large deflection capability, was applied to support concrete beams within the cantilever zone of zone 4 of the Pentagon Road Bridge. An illustration of BEAM4's geometry, node locations and coordinates can be seen in Figure 5.7. This uniaxial element with tension, compression, torsion, and bending capabilities has six degrees of freedom at each node: translations in the nodal x, y, and z directions and rotations about the nodal x, y, and z axes.

ANSYS works on the basis of assigning to each element its real constants, specifying its geometric properties, before modelling takes place. BEAM3 (the 2D beam element), for example, has real constants in area, moment of inertia, height, shear deflection constant, initial strain and added mass per unit length.

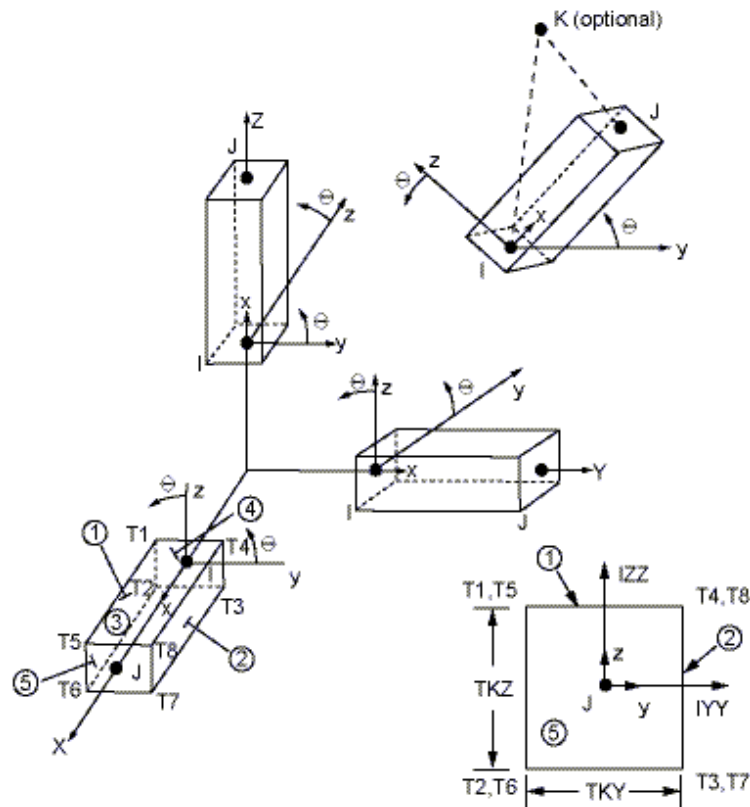


Figure 5.7 – Geometric detail of BEAM4 element in ANSYS

5.4 Moving Load

The load from the cherry picker front and rear axle point load was applied to the FE model. The cherry picker used in the IBIS-S survey is an 18 tonne two-axis lorry which passed over the bridge at an almost constant speed of 25 MPH. This was measured for all surveys using the vehicle's speedometer. Due to the limitations of this study, no additional form of testing (such as radar guns) was available to check the vehicle's speed. However, as the same vehicle was used for all tests, the speedometer was deemed to provide an accurate measurement of the velocity. Information relating to the cherry picker's weight of 18 tonnes was supplied by Medway Council. The rear axle bore 13 tonnes of the total weight of the lorry with the remainder imposed on the front axle. The distance between the two axles of the vehicle was 3.7m (Figure 5.8).

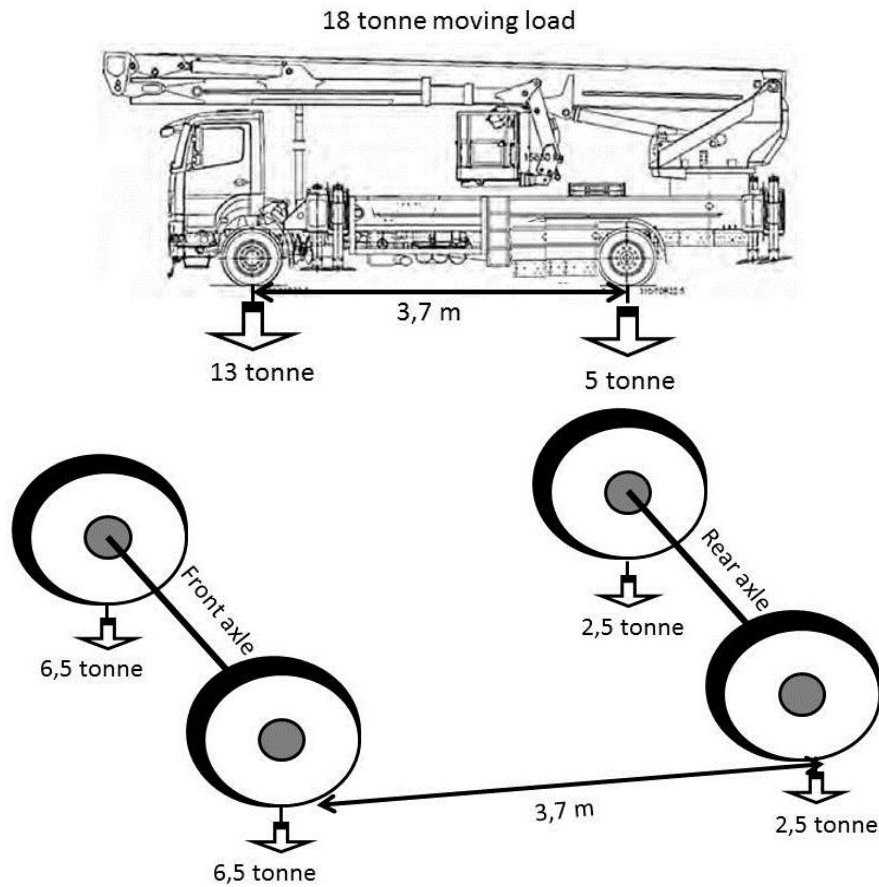


Figure 5.8 –Cherry Picker

The weight of the cherry picker was constant throughout the loading period and no damping characteristic of the vehicle was considered.

ANSYS (ANSYS, 2011) requires a set of data acquired from the weight of the cherry picker, in the form of a database, in order to derive a dynamic load. Fortunately, SAP2000 has the capability of modelling the variable load due to passing vehicles without this intermediary step. Thus the data was input into SAP2000 directly.

5.5 Modelling with SAP2000

5.5.1 Introduction

SAP2000 (Computers and Structures, 2012), structural analysis program, was used to model the structure. It is capable of modelling 3D structures under moving loads. The elements used in the model consist of thick shell and beam elements. The shell elements are used to model the decks, piers and abutment and the beam elements are intended to represent the beams in the last span of the bridge.

Figure 5.9 shows the plan and isometric 3D views of the model. The elements applied in modelling this bridge were shell 3D Solid elements. In the SAP2000 model, the nodes were defined on the mid-plane of the shell element.

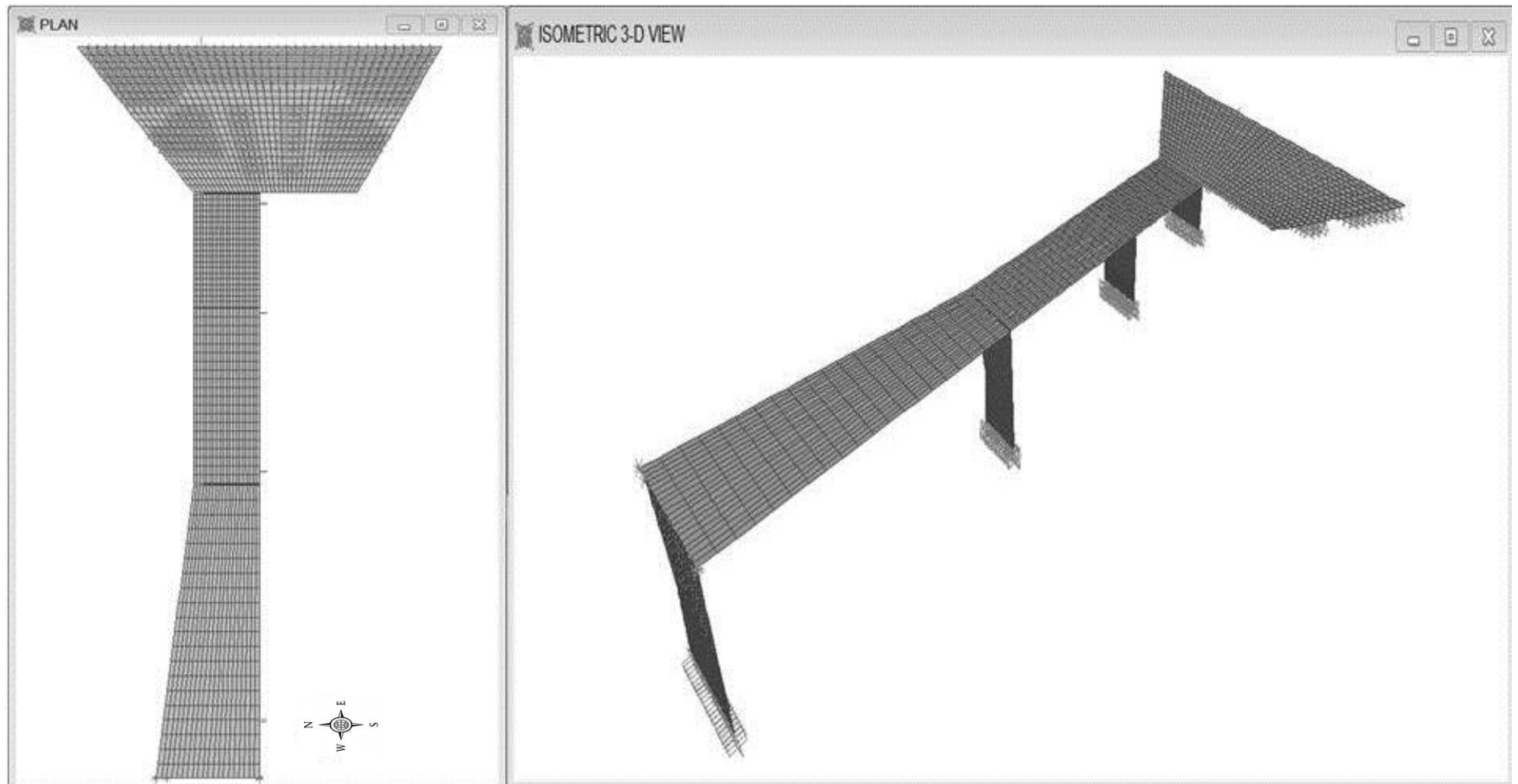


Figure 5.9 – Plan, Elevation and 3-D view of SAP model

5.5.2 Calibration of connections with IBIS-S monitoring results

The type of connection which formed the bond between the bridge deck and pier supports was unknown. This is because the nature of the bearings which made this connection could not be determined (see Appendix D, Figure D.5). Originally the connections of the bridge as new would have been simple; however this could have changed over the prevailing years due to numerous factors such as weather and constant use removing the lubrication of the bearings, creating a rigid connection. It is unknown whether this occurred however, and thus for the purpose of this study both connection types are examined and compared to actual deflection from IBIS-S as detailed in this section.

The material properties and the deck bearing support conditions are the two major parameters to be studied before any health assessment procedure starts. To find a good FE model for the deck support condition the connection condition was modelled in two extreme cases. Firstly it was assumed to be rigid and secondly it was assumed to be simple.

An inverse problem methodology was used in order to determine the structural parameters of the bridge (Figure 5.10). As part of this methodology, the following actions were undertaken:

- Measurement of the structural response parameters using NDT methods.
- A FE model of the bridge was developed.
- The FE models were calibrated with the actual structural response.
- The unknown structural information was found.
- The defects and cracks in the FE models were discussed.

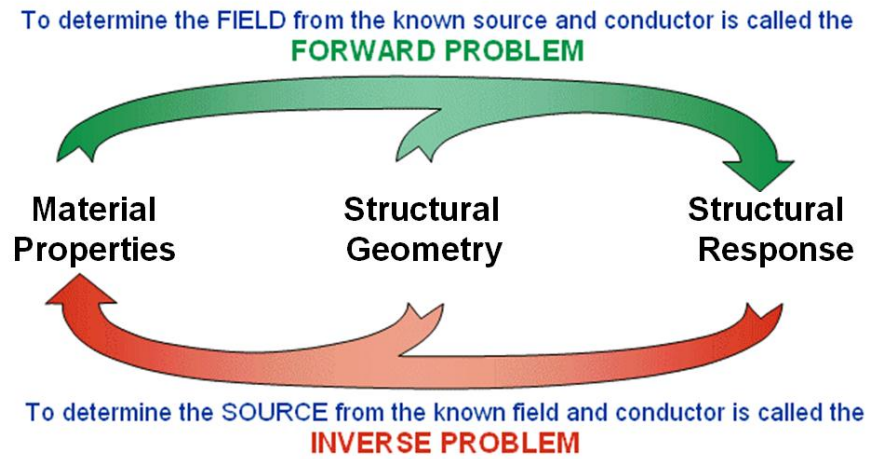


Figure 5.10 – Inverse Problem Methodology

Figure 5.11 illustrates the steps undertaken in analysing the structural response of the bridge, in order to solve the problem using an inverse method.

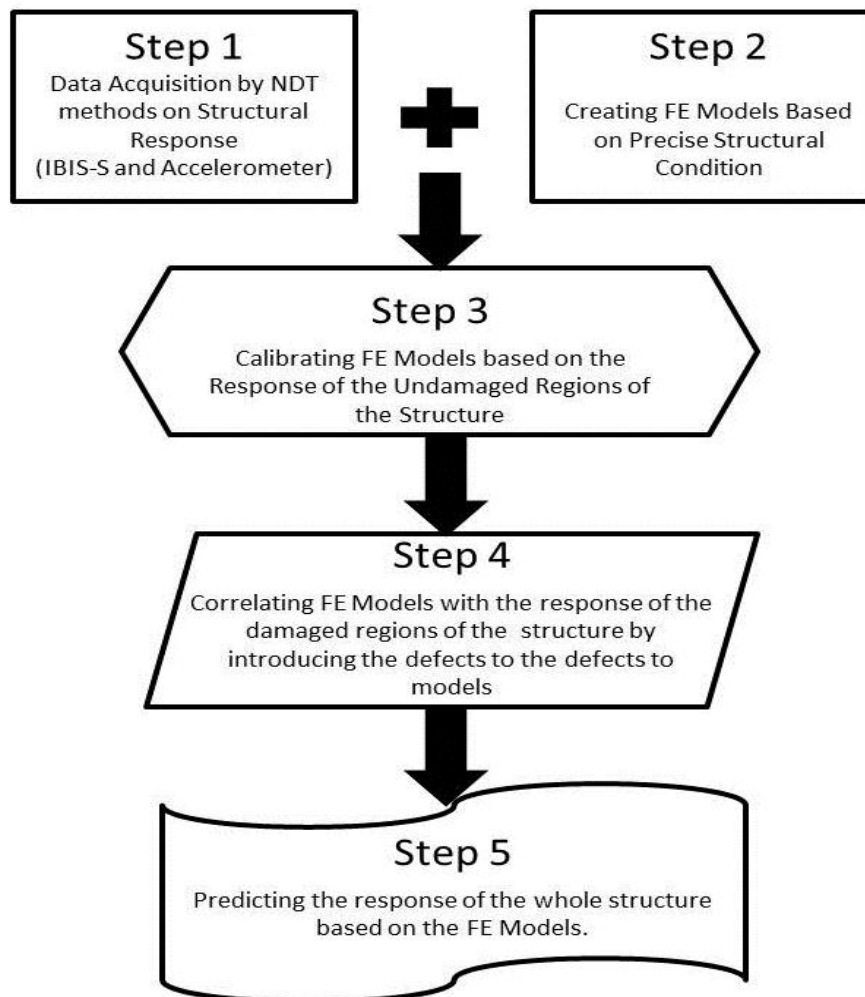


Figure 5.11 – Inverse problems flow chart

Figure 5.12 illustrates the presence and position of these bearings as modelled by SAP2000.

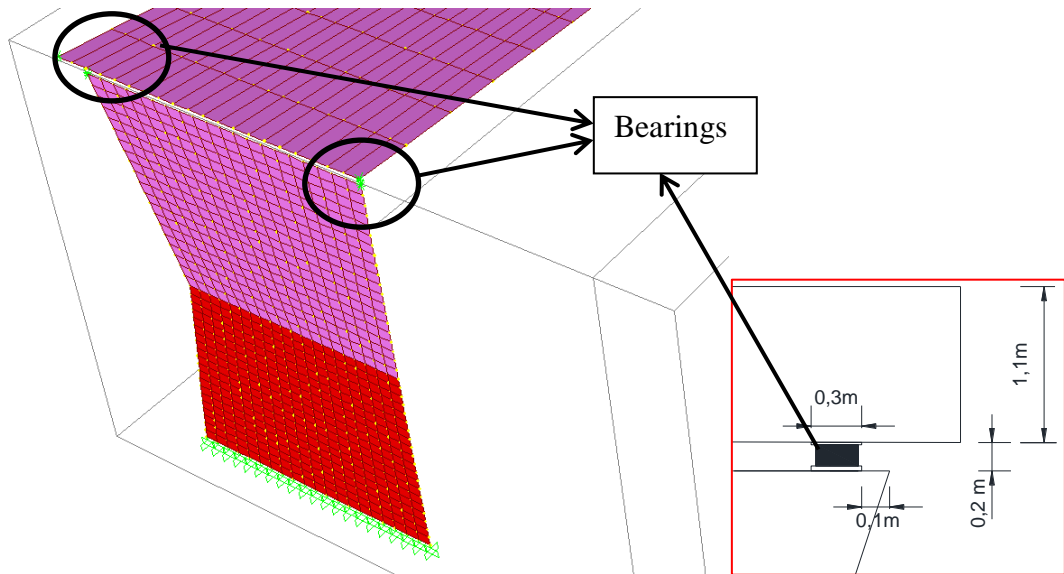


Figure 5.12 – View of Bearing Connections between Abutment and Bridge Deck

Figures 5.13 (a) and (b) illustrate the normalised deflection time history of the structure at Reflectors 4 and 10 at almost the midpoint of Spans 1 and 2 (see section 4.3.3, Figure 4.35), respectively. The results are normalised to a maximum of -1 so that the pattern of deflection between spans for all connection types can be accurately compared. For the results of Span 1 (Figure 5.13 (a)) the patterns for all connections are similar to the actual deflection - this is attributed to the long length of the span. On a shorter span such as Span 2 (Figure 5.13 (b)), it is clear that the simple connection assumption gives results much closer to the actual deflection. Thus simple connections are assumed throughout this model.

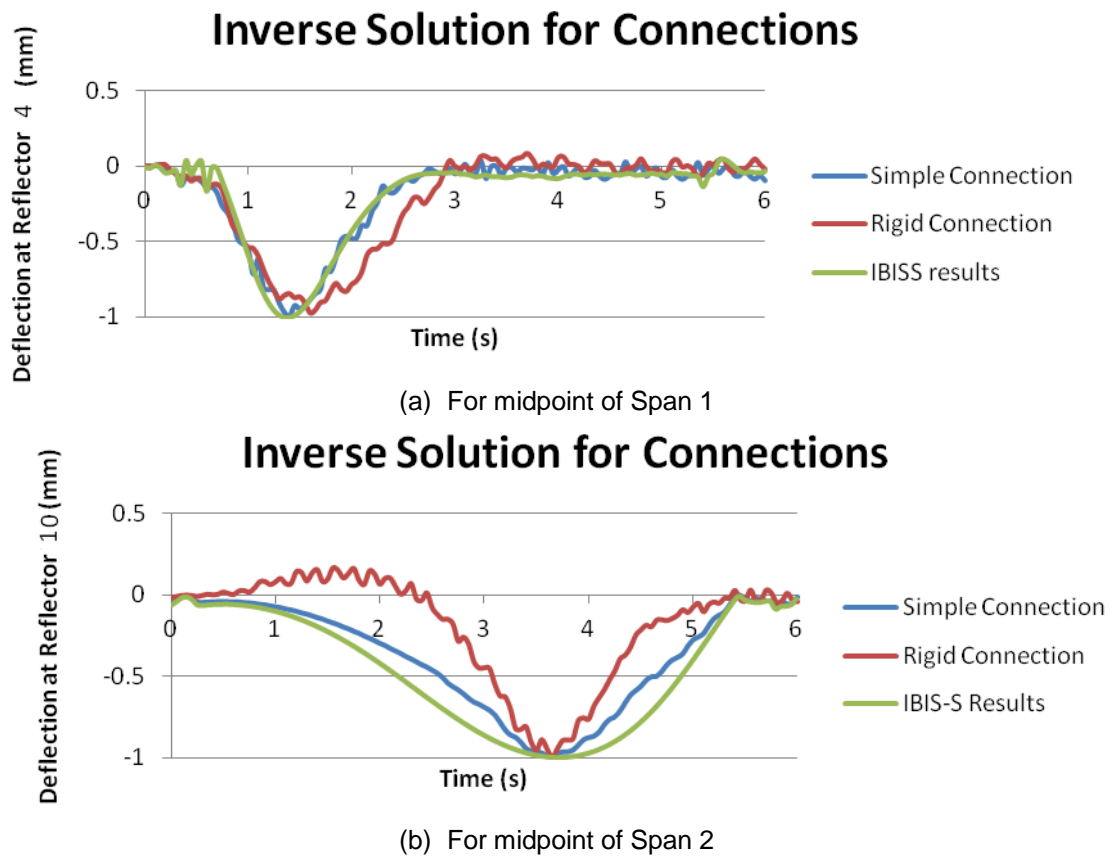


Figure 5.13 – Normalised deflections from rigid and simple connected bridge deck and IBIS-S monitoring

Figure 5.13 also clearly illustrates a better representation of the connection behaviour by the simple connections. Similar results have been found for the other two spans although the long Span 1 almost omits the effect of the end connection condition which is shown Figure 5.13 (a). So the simple connections will be used in the rest of the parametric studies.

The deflections from the FE models were normalised to omit the effect of the unknown material properties, and then were compared with corresponding deflections from IBIS-S surveys and proved the simple connection model has better correspondence with the IBIS-S results. The results of the study illustrated that the simple connection model can provide a better representation for the deck to pier/abutment connections.

The other unknown structural parameter to be calibrated using the IBIS-S monitoring results is the concrete modulus of elasticity. The modulus of elasticity of concrete in the FE models was set to 21.53GPa. Table 5.3 shows this comparison and the consequent

resulting Young's modulus for concrete must be equal to $21.53/1.092=19.72$ GPa where 1.902 is the average of the FE to IBIS-S maximum deflections.

Table 5.3 – Comparison of deflections from FE models to IBIS-S results to find actual Young's modulus

Reflector No.	Max. FE Deflection (mm)	Max. IBIS-S Deflection (mm)	FE/IBISS
4	-1.410	-1.18	1.194915
5	-1.462	-1.40	1.044286
6	-0.947	-0.92	1.029348
7	-0.877	-0.85	1.031765
8	-0.323	-0.23	1.404348
9	-0.612	-0.54	1.133333
10	-1.070	-0.98	1.091837
11	-0.540	-0.47	1.148936
12	-0.314	-0.28	1.121429
13	-0.322	-0.35	0.92
14	-0.592	-0.59	1.00339
15	-0.304	-0.31	0.980645
AVERAGE			1.092

To find a reasonable figure for the modulus of elasticity of concrete the maximum deflections of different nodes in FE model were found based preliminary value. These results were correspondingly compared with the deflections from the IBIS-S survey. The modulus of elasticity was then found for the bridge by dividing the preliminary value by the average of the results of IBIS-S monitored deflection and the FE outputs for the same nodes.

5.5.3 Results

A 'lorry' was modelled to use loading models with the same configuration as the actual cherry picker as a two axle truck with the front and rear axle loads equal to 50kN and 130kN respectively, with a 3.7m distance between them (Figure 5.5). Additionally, it would be desirable to use the load effects which are obtained from actual moving load data. The surface roughness was not considered and the damping ratio was assumed as 5% (Chopra, 1995). However, it is practically difficult to input all the actual truck configurations to software for the structure. The location of reflectors can be seen in section 4.3.3., Figure 4.35.

5.5.3.1 Moving Loading on Mid-point Span 1

After almost two seconds, as the lorry started to pass the bridge, it reached the mid-point of Span 1. This is the longest span, but fortunately defects are very rare in this part of the structure. It is possible that the thick deck has led to there being only minor defects, as shown in Figure 5.14.

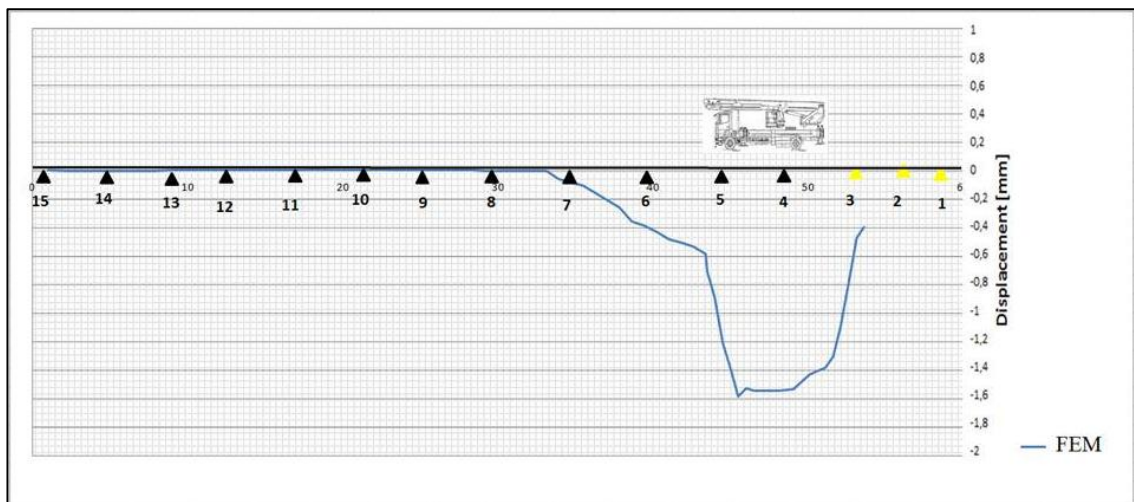


Figure 5.14 – SAP2000 - Mid-Point Span 1 Displacement Results

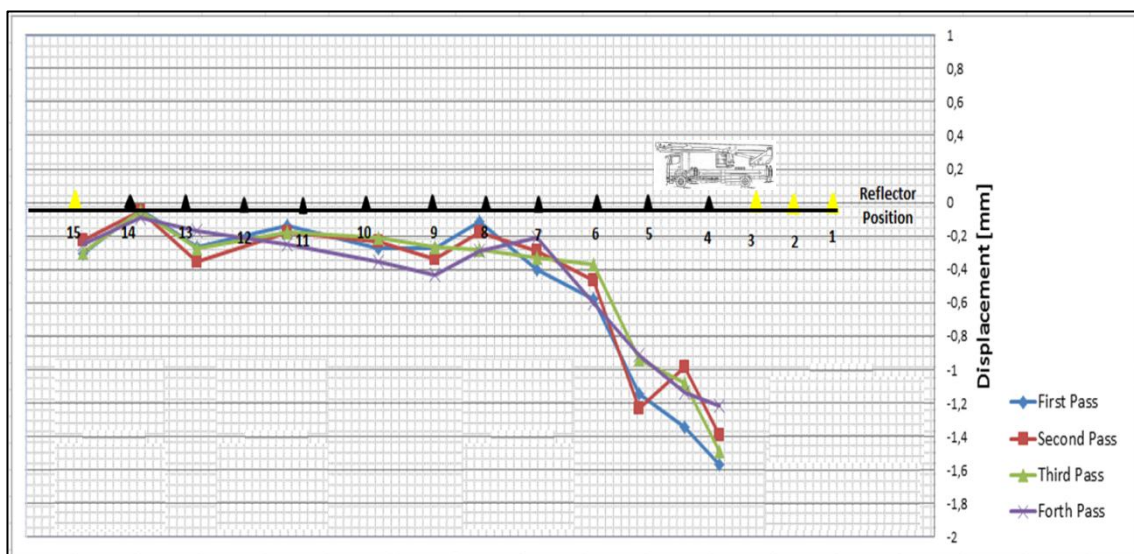


Figure 5.15 – IBIS-S Results - Mid-point Span 1 with four passes

Comparing the results from the IBIS-S survey (Figure 5.15) and the SAP2000 model, as shown in Figure 5.16, there is an acceptable parity between both, thus demonstrating the reliability of the SAP2000 model. This parity may be intuitive as the Young's modulus of concrete in the FEM has been calibrated using IBIS-S results. However this parity is

only seen in areas of the bridge without deterioration as will be discussed in greater detail in section 5.4.3.3.

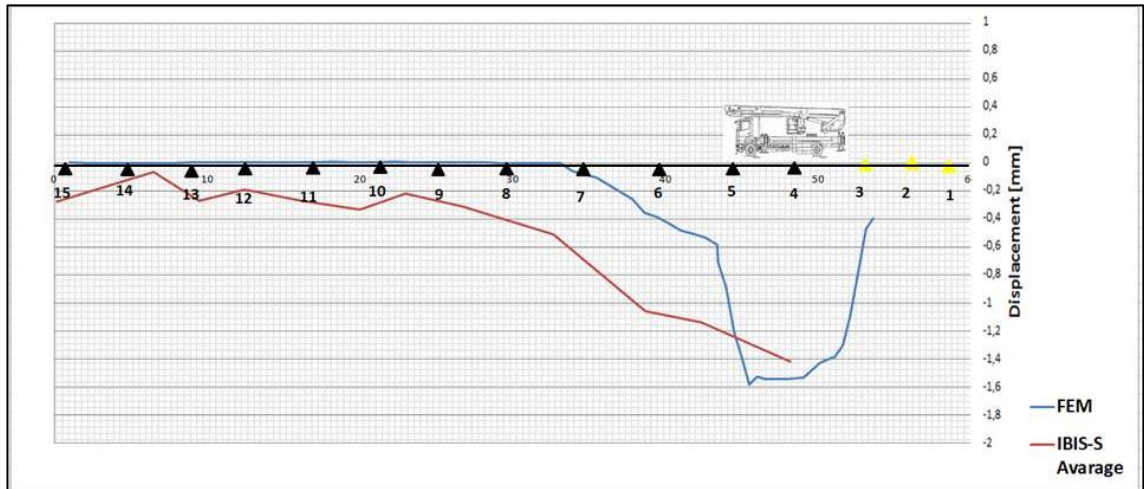


Figure 5.16 – IBIS-S and SAP2000 Span 1 Comparison (Lorry speed 25 MPH)

5.5.3.2 Moving Loading on Mid-point Span 2

Span 2 is considerably shorter than Span 1 and so it would be expected, given that it is simply supported, that the deflection present would be significantly less than that experienced in the previous span, as they are of the same deck thickness. This hypothesis is proven when the FEM results are viewed (see Figure 5.17) as, according to the model without any defects, the maximum deflection under the 18 tonne load of the cherry picker is approximately 0.65mm.

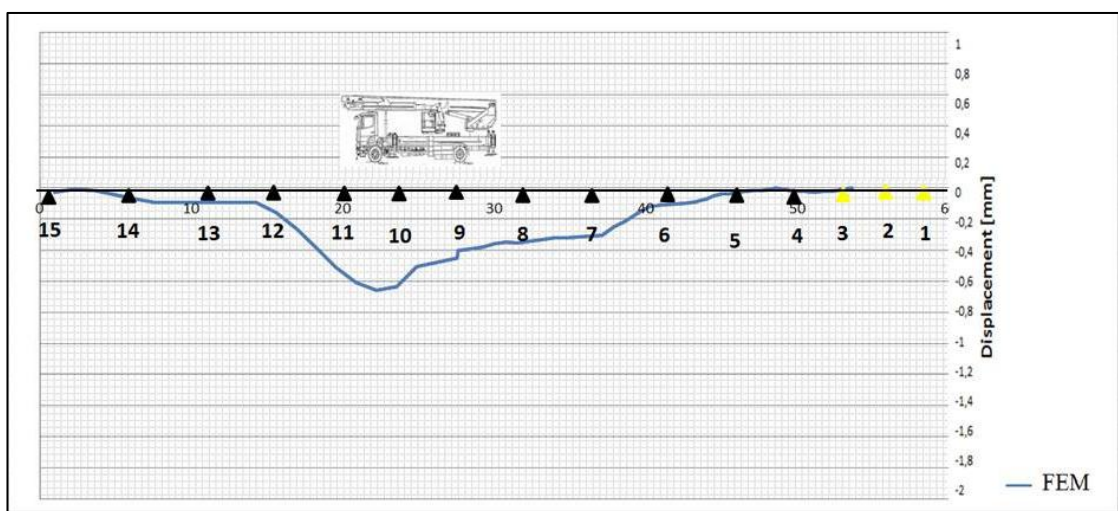


Figure 5.17 – SAP2000 - Mid-Point Span 2 Displacement Results

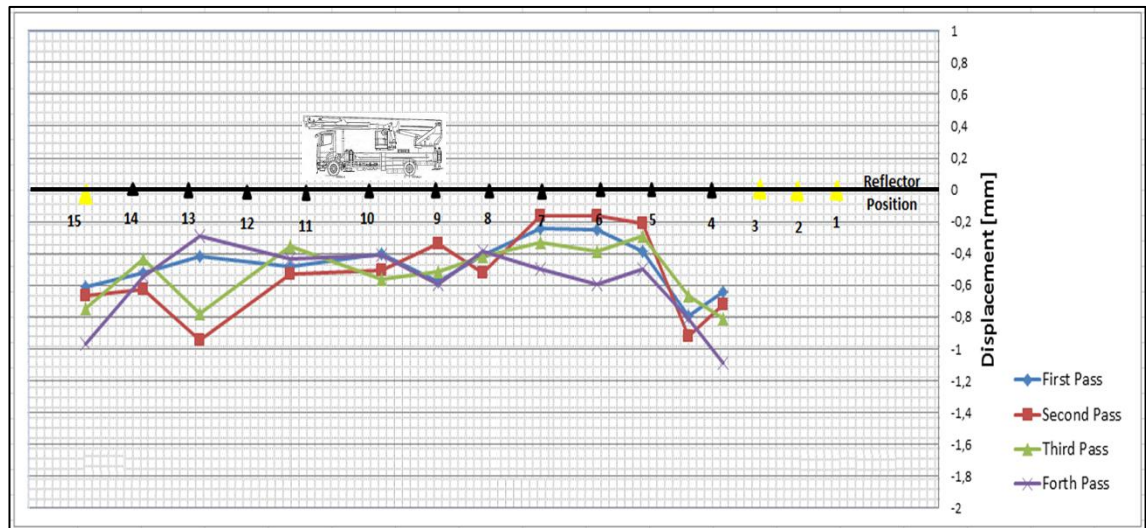


Figure 5.18 – IBIS-S Results - Mid-point Span 2 with four passes

Figure 5.19 shows an acceptable parity between both IBIS-S and FEM results and thus demonstrates the reliability of the SAP2000 model.

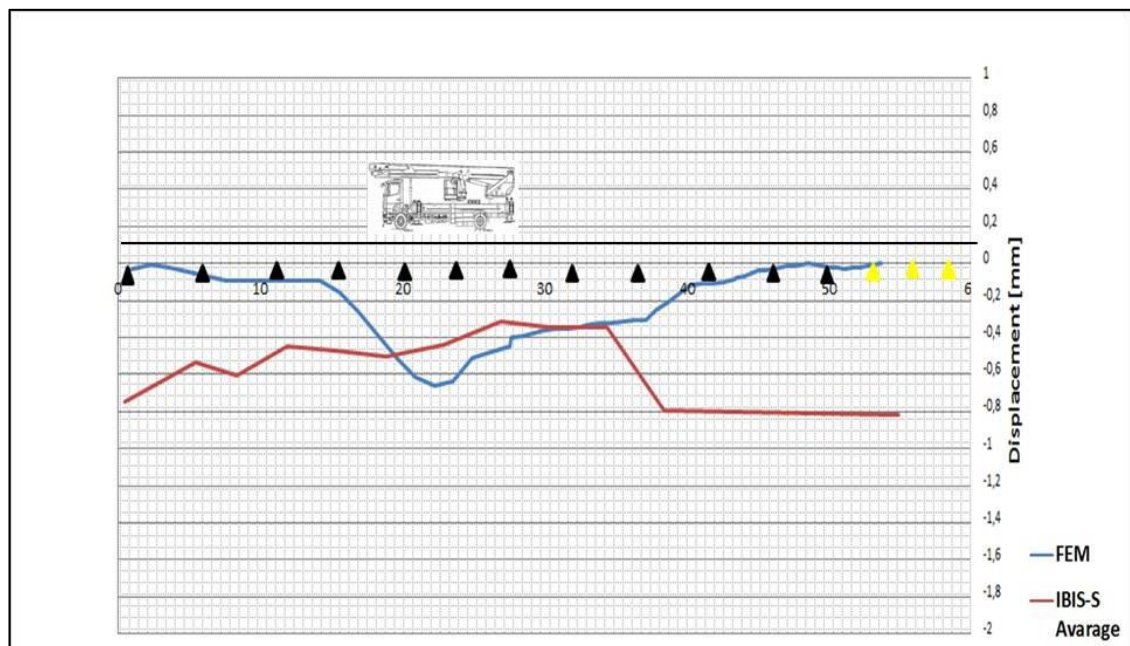


Figure 5.19 – IBIS-S and SAP2000 Span 2 Comparison (Lorry speed 25 MPH)

5.5.3.3 Moving Loading on Cantilever Zone

Span 3 is the shortest of this four span bridge and so it would be expected, given that it is simply supported, that the deflection present would be lesser than for the other two spans. This prediction of the cantilever zone is validated when the FEM results are

viewed (see Figure 5.20) as there is only approximately 0.40mm of deflection expected in the bridge as newly constructed.

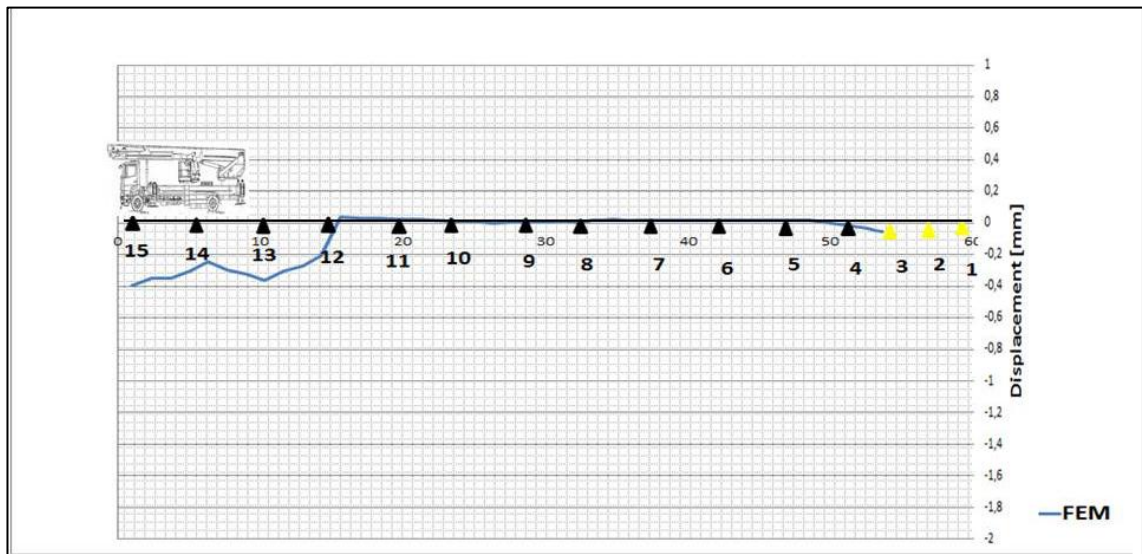


Figure 5.20 – SAP2000 – Cantilever Zone Displacement Results

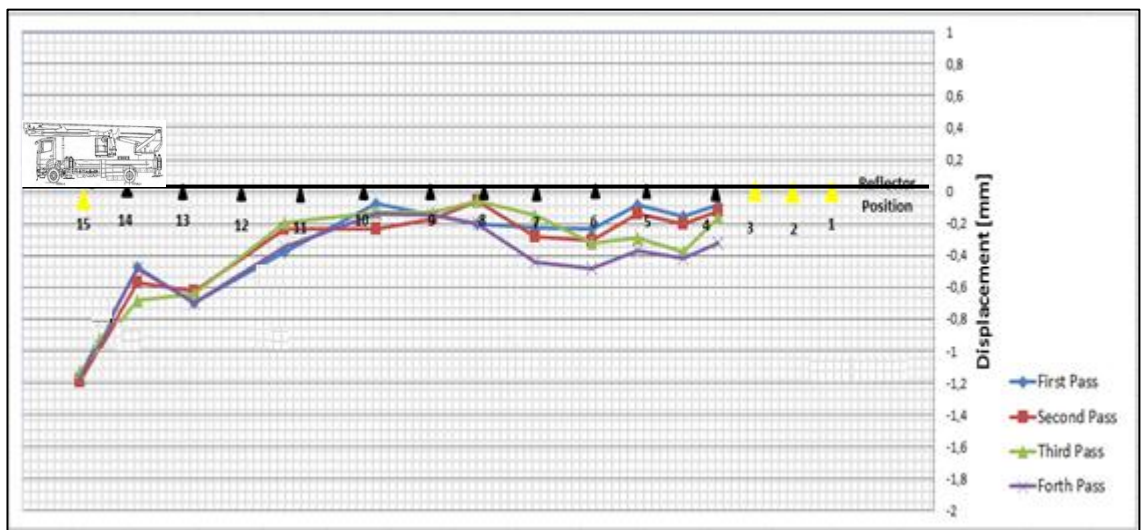


Figure 5.21 – IBIS-S Results - Cantilever Zone with four pass

However when this is compared to the deflection experienced by the actual bridge structure as measured by IBIS-S, major disparity is seen as shown in Figure 5.21. IBIS-S results show a significantly greater maximum deflection (1.4mm) as opposed to the 0.40mm predicted by the FEM, as shown in Figure 5.22.

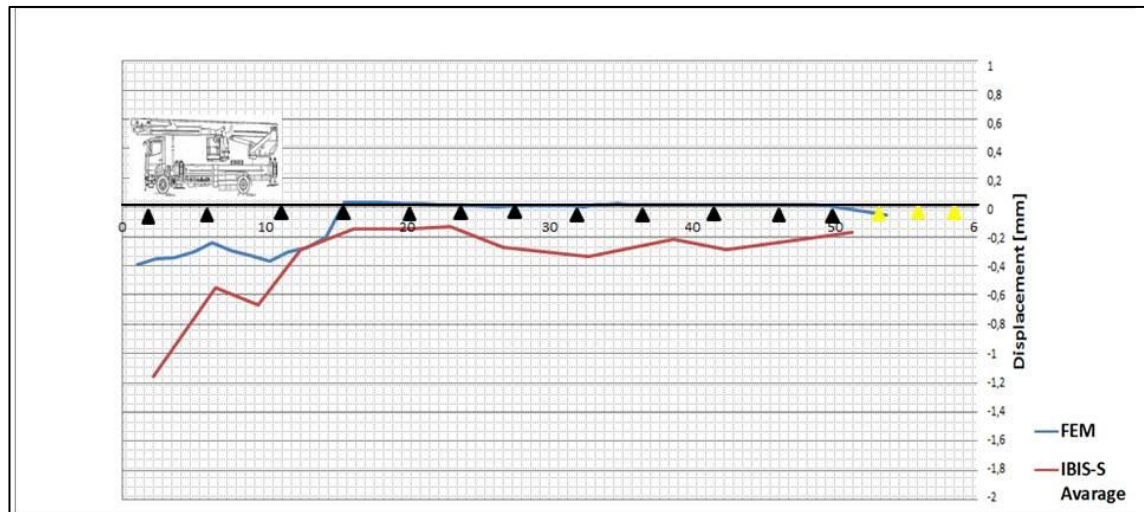


Figure 5.22 – IBIS-S and SAP2000 Comparison Cantilever Zone (Lorry speed 25 MPH)

This result is of no surprise however when compared to the findings of the other NDT which all indicate a problem in this area. This finding further lends importance to the development of an integrated bridge health monitoring mechanism to determine points of deterioration in a bridge structure.

In summary, it was seen that in the cantilever zone in Figure 5.22, the results of the SAP2000 model do not agree with those from the IBIS-S survey. The deflection shown by IBIS-S is, however, unusually high; this is due to the cracks in this zone, and this in combination with other defects is believed to be the main cause of this difference.

Unfortunately, IBIS-S was not able to monitor the deflection experienced by Span 4 due to both the angle of the bridge and to the positions of buildings which blocked the interferometric radar waves from reaching reflectors on the bridge deck (see Appendix D, Figure D.4).

In conclusion, by comparing the SAP2000 model predictions with the IBIS-S results a more comprehensive picture of the behaviour of the bridge deck can be achieved as areas of deterioration in the bridge structure can be identified. This is achieved as SAP2000 gives the deflection of the bridge without defects under the load of the cherry picker. This can then be compared to the actual deflection of the bridge under the same load recorded by IBIS-S. Thus any major difference between these two results can be attributed to deterioration of the bridge structure. These findings have shown that the

deflection in Span 4 (cantilever area) is significantly higher than that of a new bridge as predicted by SAP2000 suggesting structural problems within this area. This is further confirmed when compared to the results of the other NDT. The visual inspection showed large cracks and cover delamination in this span and GPR found moisture ingress in Span 4 also. This gives an overall indication that this area is in need of remedial work to decrease the deflection experienced and to prevent further deterioration. Figure 5.23 confirms the presence of cracks and defects.

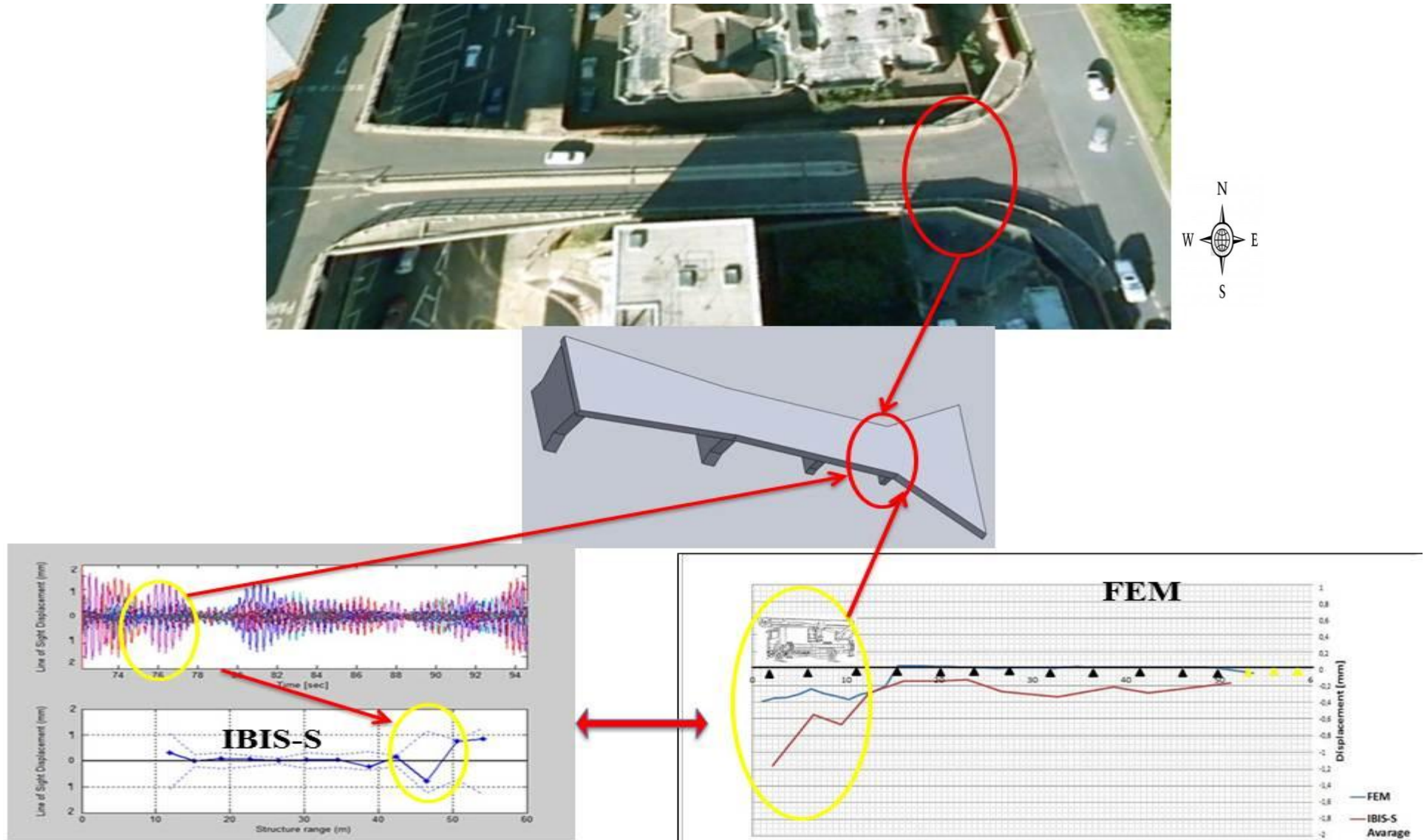


Figure 5.23 – IBIS-S and SAP2000 Conclusion

5.6 Modelling with ANSYS

5.6.1 Introduction

SAP2000 has provided an adequate model for an idealised structure. However, as has been indicated in section 5.5, the bridge structure has defects which include cracks. The ANSYS modelling software is able to include these defects along with dynamic load modelling which can be compared with SAP2000 and IBIS-S.

As illustrated in Figure 5.24, 40 cm depth slabs are constructed to support the cantilever zone of the bridge (see Appendix D, Figure D.9). The geometry of these beams has been measured precisely and modelled by SOLID65 elements in ANSYS. This demonstrates the ability to, as with SAP2000, utilise precise elements and implement an idealised structure in ANSYS. The degrees of freedom of the adjacent nodes of SOLID65 and Shells are coupled using the coupling capability of ANSYS.

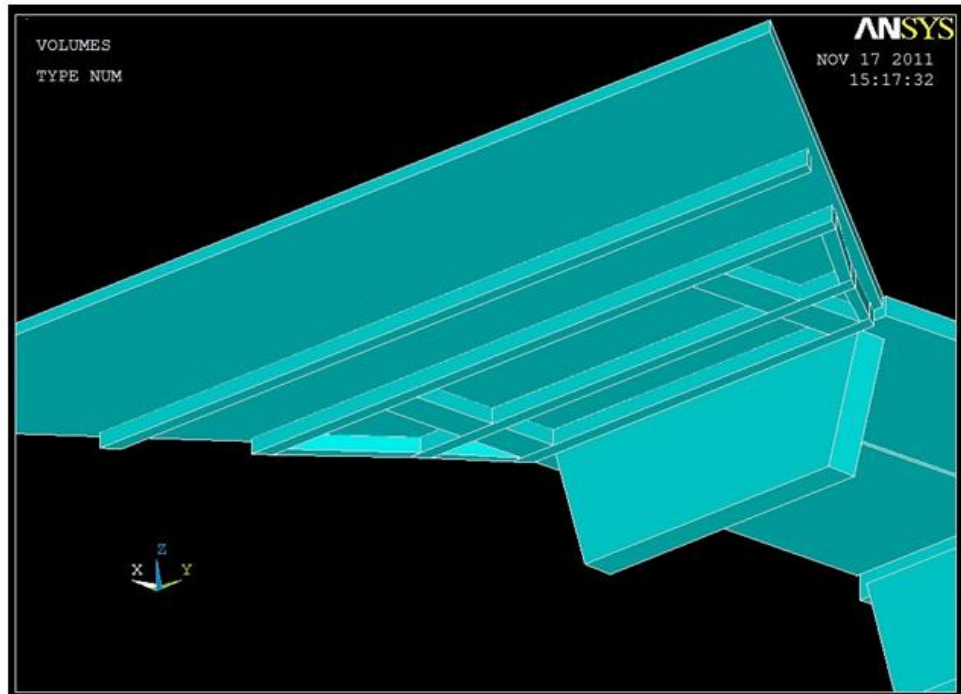


Figure 5.24 – ANSYS Beam Design

5.6.2 ANSYS Crack Modelling

The FE method has been employed here using the ANSYS package to model the Pentagon Road Bridge. Different aspects of load such as the lorry's gross weight and speed have been assumed as the investigated variables. The object of this study is to determine key indicators of the structural behaviour of the bridge, namely the displacements and stresses in the selected beam and Span 4 at critical positions.

Figure 5.25 illustrates the alignment of the beams in Span 4 and the selected beam for this FE investigation. This beam was selected as during the course of visual investigation significant cracks were observed (see section 4.3.2, Figure 4.32). The condition of this selected beam and its adequacy is the focus of this investigation. Also it is intended to clarify the effect of further decay and cracking in this beam.

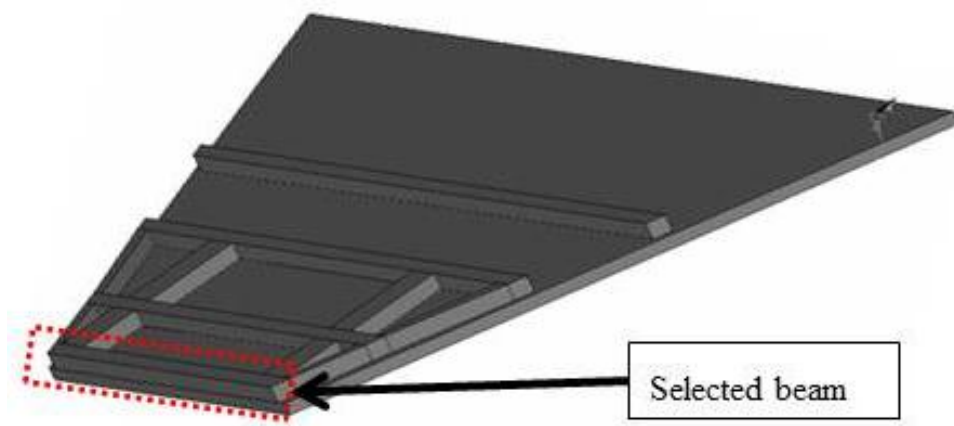


Figure 5.25 – Beam Alignment under Span 4.

The structure of Span 4 (see Appendix D, Figure D.4) is not connected to the last pier on the south end of the bridge and the cantilever section contains a grid of concrete beams (Figure D.9) with additional supports in the form of parapets (Figure D.10) which are designed to assist the dynamic behaviour of the thin shell.

During the course of this investigation the structure underwent further deterioration in the form of widening cracks and excessive cover delamination as illustrated in section 4.3.2, Figure 4.32. The widening of these cracks was visible to the naked eye and determined using visual inspection by both the author and the supervisory team. The apparent cracks in the Pentagon Road Bridge structure and the clear deteriorating

elements such as the leaking water in the bridge body are worsening the structural integrity of the bridge, especially Span 4 cantilever zone. The condition of the affected steel reinforcements can be predicted by the appearance of chemical stains near the cracks, indicating corrosion. It is important to predict the effect of this deterioration on the bridge structure in order to determine its safety. One method of achieving this is to examine the effects of crack width in FEM. This was accomplished by utilising the ANSYS crack modelling tool as will be discussed in this section.

5.6.3 Finite Element Model Specifications

The ANSYS software is a competent finite element-based tool that can be used to analyse a vast variety of structures. This package is equipped with numerous elements capable of modelling large or small strains and displacements, and concrete cracking under different loading conditions such as static and transient load cases.

Figure 5.26 illustrates the areas depicting the bridge deck and supporting abutments and piers. These areas are meshed using SHELL181 elements as presented in Figure 5.27. The thickness of each shell element is based on the actual thickness of the bridge deck to ensure accuracy. The beams are modelled meshing the lines in ANSYS. Each segment of the beam has the equivalent actual bridge dimension which specifies its geometric properties. The connections among the decks and the abutments and piers is modelled using the degrees of freedom-of-nodes coupling capability of the ANSYS software. Only the displacement degrees of freedom are coupled and the rotational degrees of freedom can behave separately. Similar to SAP2000, simple connections are assumed (see section 5.5.2). The supports are applied to the joints at the connections of the abutments and piers to the foundations. The load is a time history which represents the movement of a lorry along the bridge as a transient load.

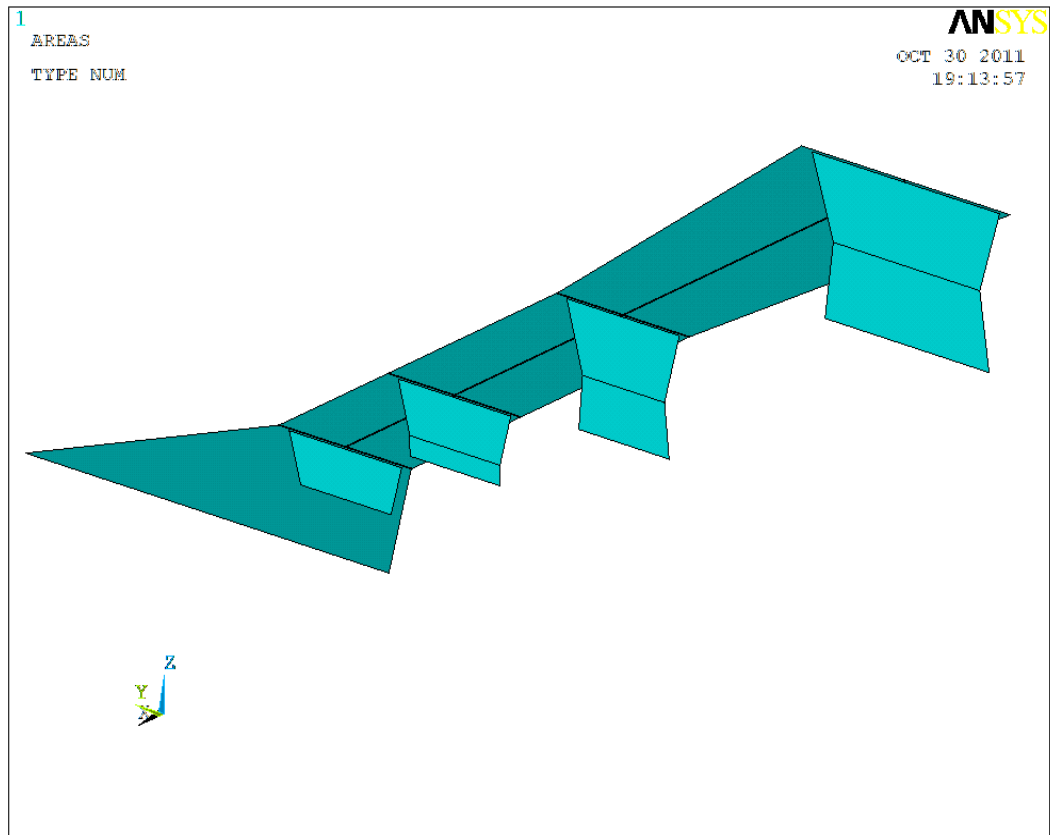


Figure 5.26 – Areas depicting the geometry of the bridge

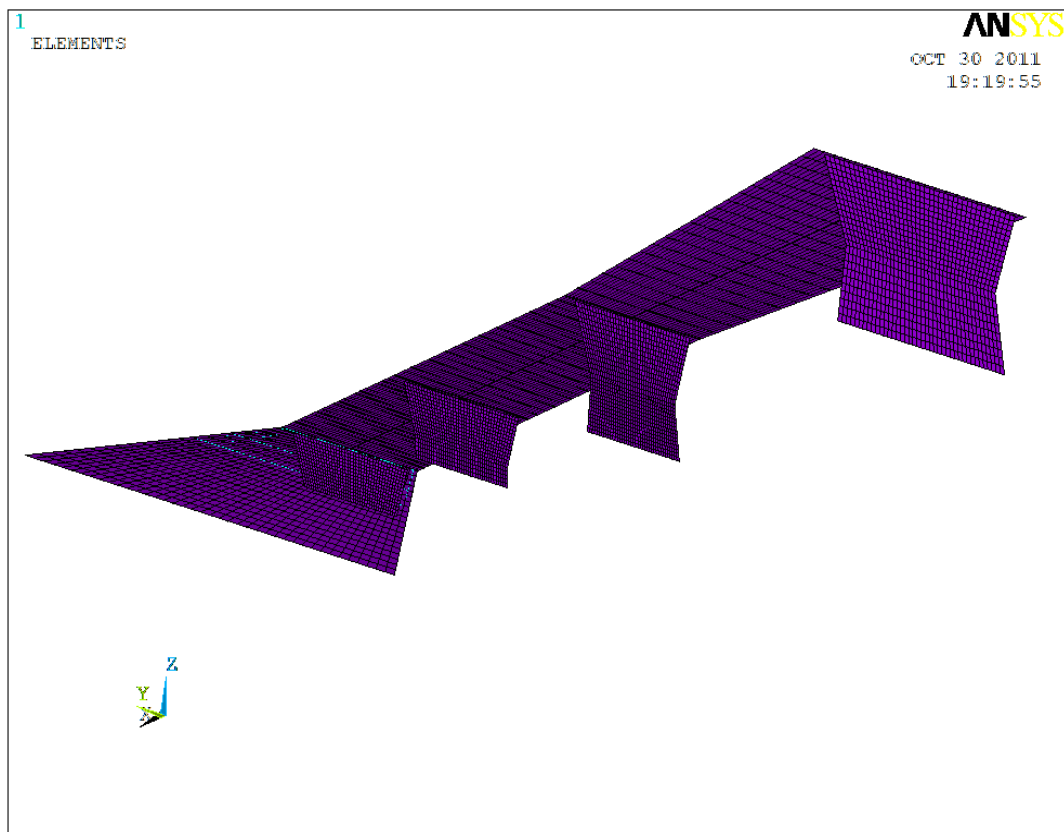


Figure 5.27 – Beam and Shell elements

5.6.4 Studied Parameters and Their Range of Change

The Pentagon Road Bridge has provided a satisfactory service for more than three decades. However, the bridge has not been looked after properly. The sewer leak has damaged the concrete and reinforcements, especially where the cracks have provided better access for it to precipitate into the interior parts of the structure (Figure 4.31). The covering asphalt layer has lost its quality and has not been repaired suitably. These have all led to serious concerns as to whether the bridge can maintain its serviceability in the long term.

If the degradation continues and the cracks advance, the deflections and stresses developed in the critical sections will increase considerably. This consequently increases the rate of degradation of the structure as more access will be provided for water leakage into the body of the structure, especially where the reinforcements are laid. The extra stress will make structural element damage more probable which may suddenly cause a brittle failure in the cantilever part of the bridge. To predict the behaviour of the bridge and prevent a catastrophic collapse in time, the FE method has been applied. Another matter that is not considered in this investigation, and might worsen the condition of the bridge, is the “fatigue” phenomenon. Based on the cyclic, dynamic nature of the thousands of loads applied to the bridge, fatigue is an inevitable part of the decaying scenario of the bridge and specific monitoring devices and schemes are needed. The data presently available is not sufficient for a fatigue analysis on the bridge or the supports and thus this factor is not considered in the research.

To predict structural response changes due to further crack development, different models are generated using the ANSYS package to which the cracks are applied stepwise. The selected beam under consideration has a cross section of 40 cm x 40 cm (Figure 5.25). The crack depth will be considered as the structural changing variable, and the effect of the lorry speed and weight on the structural response has been studied. The crack depth will vary from 0 cm up to 10 cm with a changing step of 5 cm (Table 5.4).

Table 5.4 – Selected beam for the parametric study

Wide (cm)	40	40	40
Depth (cm)	40	35	30

Also, the lorry weight will be altered from 18 tonnes to 46 tonnes which is the applicable range of passing traffic on this bridge with a step of 7 tonnes. The lorry speeds considered in this parametric study are mentioned in Table 5.5.

5.6.5 Numerical Results

Due to the cracks in the selected beam supporting the cantilever part of the Pentagon Road Bridge, the stress distribution in both the slab and the supporting beam will change before the cracks occur. The FE model is run under different loading conditions expressed in section 5.6.4 as a transient load and with different crack depths. The cracks caused by degradation may expand or lengthen during the lifecycle of the Pentagon Road Bridge. So, to consider the effect of these changes, the FE models were developed. These can be used to model the effects this cracking can have on bridge deflection. The resulted maximum deflections and stresses in the supporting beam, and also the maximum bending stresses in the slab in the cantilever zone, are extracted and tabulated in Table 5.5. The conclusions based on these results will be presented in section 5.5.6.

Table 5.5 – Maximum structural responses in the cantilever region

Lorry Speed (m/s)	Lorry Speed (MPH)	Lorry Weight (tonne)	Maximum Deflection (mm)			Maximum Beam Stress (MPa)			Maximum Slab Stress (MPa)		
			CD=0 cm	CD=5 cm	CD=10 cm	CD=0 cm	CD=5 cm	CD=10 cm	CD=0 cm	CD=5 cm	CD=10 cm
8.94	20	18	2.41	2.69	2.84	1.24	3.05	5.29	1.27	1.28	1.31
8.94	20	25	3.35	3.74	3.94	1.72	4.24	7.35	1.76	1.78	1.82
8.94	20	32	4.28	4.78	5.05	2.2	5.42	9.4	2.26	2.28	2.33
8.94	20	39	5.22	5.83	6.15	2.69	6.61	11.46	2.75	2.77	2.84
8.94	20	46	6.16	6.87	7.26	3.17	7.79	13.52	3.25	3.27	3.35
10	22.36	18	2.69	2.87	3.12	1.27	3.09	5.37	1.29	1.3	1.33
10	22.36	25	3.74	3.99	4.33	1.76	4.29	7.46	1.79	1.81	1.85
10	22.36	32	4.78	5.1	5.55	2.26	5.49	9.55	2.29	2.31	2.36
10	22.36	39	5.83	6.22	6.76	2.75	6.7	11.64	2.8	2.82	2.88
10	22.36	46	6.87	7.33	7.97	3.25	7.9	13.72	3.3	3.32	3.4
11.18	25	18	3.05	3.15	3.48	1.64	3.76	6.73	1.42	1.44	1.47
11.18	25	25	4.24	4.38	4.83	2.28	5.22	9.35	1.97	2	2.04
11.18	25	32	5.42	5.6	6.19	2.92	6.68	11.96	2.52	2.56	2.61
11.18	25	39	6.61	6.83	7.54	3.55	8.15	14.58	3.08	3.12	3.19
11.18	25	46	7.79	8.05	8.89	4.19	9.61	17.2	3.63	3.68	3.76
11.62	26	18	3.14	3.22	3.56	1.94	3.83	7.34	1.87	1.88	1.92
11.62	26	25	4.36	4.47	4.94	2.69	5.32	10.19	2.6	2.61	2.67
11.62	26	32	5.58	5.72	6.33	3.45	6.81	13.05	3.32	3.34	3.41
11.62	26	39	6.8	6.98	7.71	4.2	8.3	15.9	4.05	4.07	4.16
11.62	26	46	8.02	8.23	9.1	4.96	9.79	18.76	4.78	4.8	4.91
12	26.84	18	3.21	3.31	3.65	2.01	3.96	7.59	2.38	2.41	2.45
12	26.84	25	4.46	4.6	5.07	2.79	5.5	10.54	3.31	3.35	3.4
12	26.84	32	5.71	5.88	6.49	3.57	7.04	13.49	4.23	4.28	4.36
12	26.84	39	6.96	7.17	7.91	4.36	8.58	16.45	5.16	5.22	5.31
12	26.84	46	8.2	8.46	9.33	5.14	10.12	19.4	6.08	6.16	6.26
12.52	28	18	3.27	3.35	3.7	2.17	4.44	8.36	2.81	2.87	2.91
12.52	28	25	4.54	4.65	5.14	3.01	6.17	11.61	3.9	3.99	4.04
12.52	28	32	5.81	5.96	6.58	3.86	7.89	14.86	5	5.1	5.17
12.52	28	39	7.09	7.26	8.02	4.7	9.62	18.11	6.09	6.22	6.31
12.52	28	46	8.36	8.56	9.46	5.55	11.35	21.36	7.18	7.33	7.44
13.41	30	18	3.29	3.38	3.73	2.08	4.14	7.88	2.78	2.8	2.84
13.41	30	25	4.57	4.69	5.18	2.89	5.75	10.94	3.86	3.89	3.94
13.41	30	32	5.85	6.01	6.63	3.7	7.36	14.01	4.94	4.98	5.05
13.41	30	39	7.13	7.32	8.08	4.51	8.97	17.07	6.02	6.07	6.15
13.41	30	46	8.41	8.64	9.53	5.32	10.58	20.14	7.1	7.16	7.26

The results in Table 5.5 represent the maximum deflection and stress on selected beams and Span 4. In order to decrease computational and analytical time, it was decided that ANSYS provide maximum deflection and stress on Span 4 but not the location. The maximum deflection is of paramount importance as it is a key determining factor of bridge health and safety but the location of this deflection is not as important and therefore was not considered in this case.

5.6.6 Discussion on Numeric Results

The results can be interpreted by comparing the lorry speed against: deflection (Figure 5.28); selected beam bending stress (Figure 5.29); and slab bending stress (Figure 5.30). Only the results of the 18 tonne lorry weight have been presented, due to this being the weight of the cherry picker used in IBIS-S, and the weight of the load applied in SAP2000.

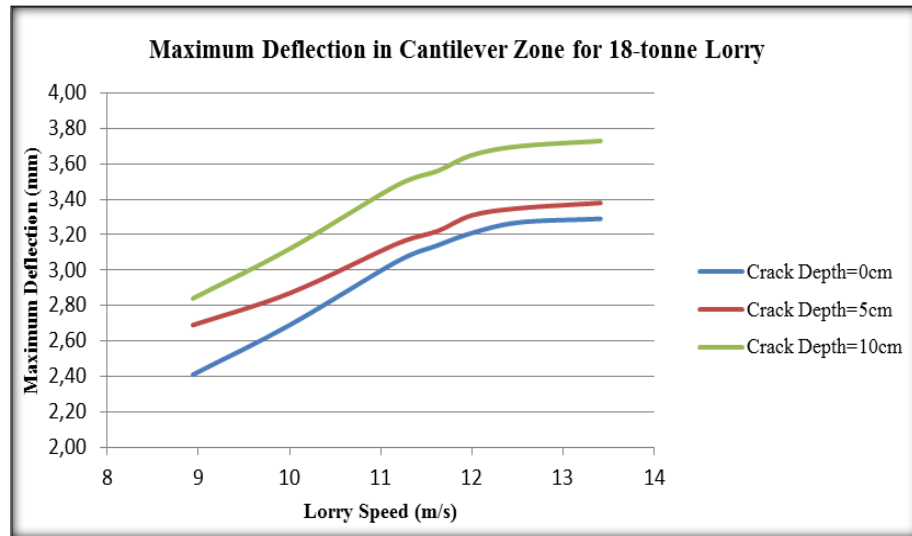


Figure 5.28 – Maximum deflection in the cantilever zone

Figure 5.28 illustrates the proportionality of the maximum deflection in the cantilever zone with both the lorry speed and the crack depth in the supporting beam. As the crack expands deeper into the supporting beam of the cantilever region, the stiffness will decrease and the deflections increase. Comparatively, this graph can prove that the lorry speed has a significant effect on the structural response. The greater deflection due to the increase of the lorry speed illustrates a dynamic effect that should be particularly regarded.

As the vehicles pass with different speeds on the bridge, a nonlinear combination of the effects of the loading condition and the natural frequencies of the bridge will determine the dynamic response of the structure. For slower and quicker passing speeds the rate of change of the structural response is less, which shows that the natural response of the cantilever section is more sensitive to medium speeds; around 25 MPH (11.18 m/s). This reality can also be proved by the graphs presented in Figures 5.29 and 5.30.

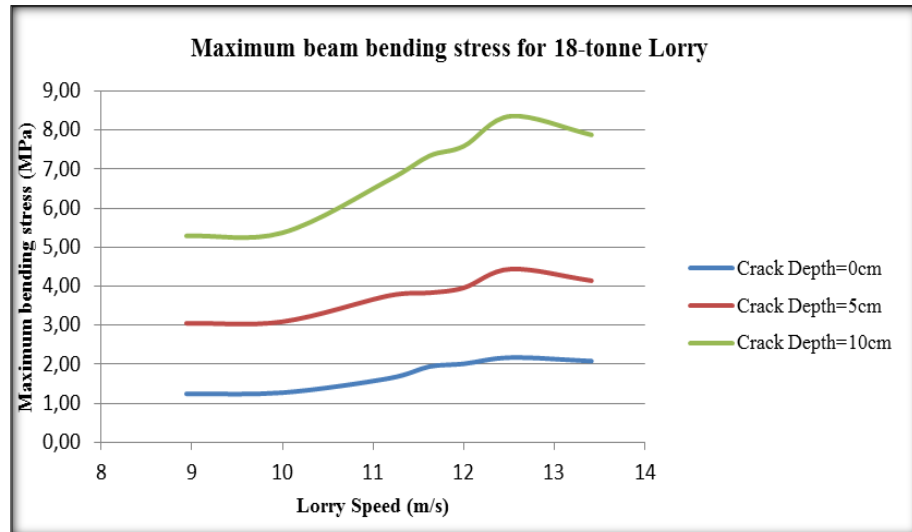


Figure 5.29 – Maximum bending stress in the beam supporting the cantilever slab

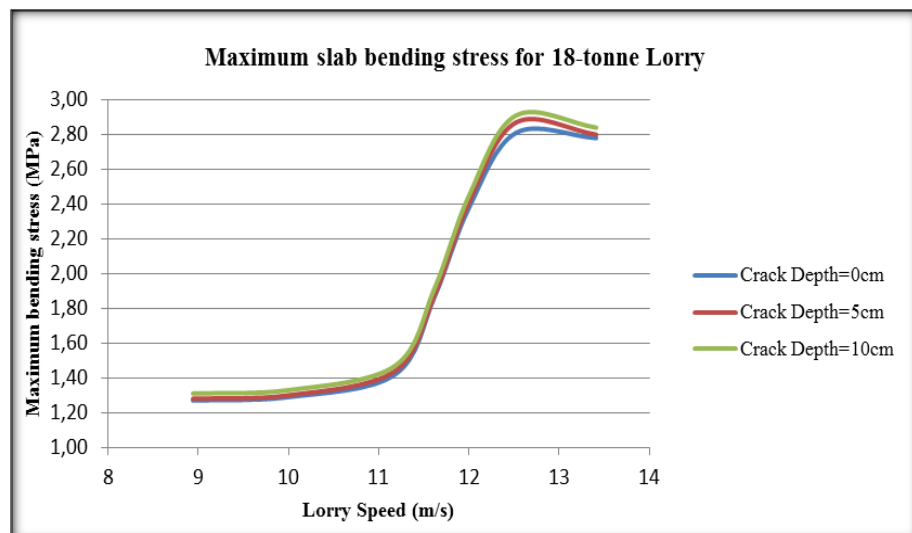


Figure 5.30 – Maximum bending stress in the cantilever slab zone

As shown in Figures 5.29 and 5.30 the maximum stresses in both the supporting beam and slab are developed as the lorry passes at a speed of 28 MPH (12.52 m/s). This shows an excited dynamic response at such a speed. The method of limiting the speed for all traffic on the bridge could lead to longer service if left in its current condition.

The most important result from Figures 5.28 and 5.29 is that the stress in the supporting beam increases considerably as the crack expands, but the size of the crack is insignificant. This contradiction is clarified by paying attention to the other beams

supporting the slab. As the beam at the cantilever zone end becomes weaker due to crack depth increase, its load carrying capacity and stiffness decrease considerably.

As reported earlier, the introduced assumed Modulus of Elasticity of concrete in the Finite Element models was 21.53GPa, corresponding to a concrete with specific compressive strength value of 3000psi. Table 5.3 defines this comparison in detail. From this it can be deduced that the actual Modulus of Elasticity value is equal to 19.72GPa with an average ratio value of 1.092 between the Finite Element model and the maximum deflections obtained by IBIS-S. This corresponds to an actual specific strength of 17.6 MPa using the following formula (ACI, 2011):

$$E_c = 4700\sqrt{f_c}$$

So, as can be seen from Table 5.5, where the beam will fail due to excessive loading ($18.76 > 17.6$), this is listed in Table 5.6 below.

Table 5.6 – Maximum beam stress in the cantilever region

Lorry Speed	Lorry Speed	Lorry Weight	Maximum Beam Stress (MPa)
(m/s)	(MPH)	(tonne)	CD=10 cm
12.52	26	46	18.76

The results indicate that if a lorry with a weight of more than 46 tonnes passes over the bridge at a speed greater than 26 MPH it will cause a catastrophic collapse (Figure 5.31).

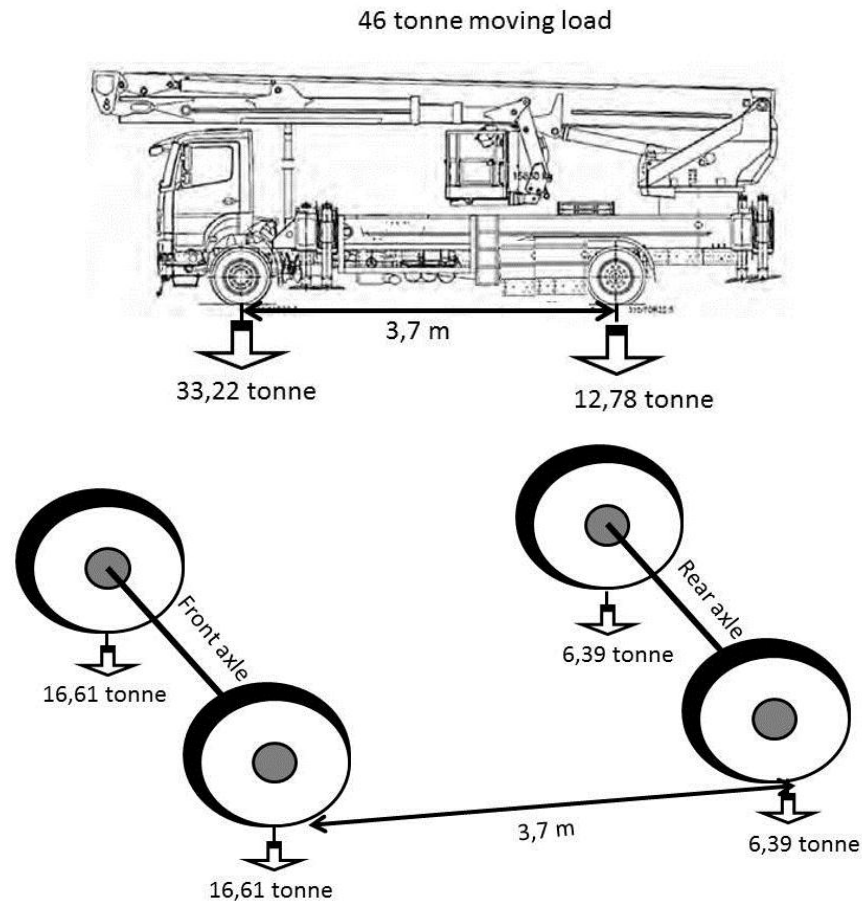


Figure 5.31 – 46 Tonne Moving Load

In summary, the purpose of an ANSYS FE investigation on the Pentagon Road Bridge is to assess its health condition, especially in the region where the cracked supporting beam has caused doubts about the structural adequacy of the structure.

The specifications of the lorry used in the IBIS-S monitoring were introduced to the ANSYS software and the results of the analyses were compared with the IBIS-S results to verify the FE approach. The parity of the FE results to the IBIS-S data proved the order of accuracy of the assumptions for the structural factors as well as the modelling method and approach.

Based on the results of the FE models illustrated in Figures 5.28, 5.29 and 5.30, it is evident that the bridge will not cease functioning in its present condition or in the very near future unless an extraordinary load case, such as a lorry weighing more than 46 tonnes passing at a speed of about 28 miles per hour, occurs. Also it must be regarded that as the cracks expand deeper into the end supporting beam of the cantilever zone the

load must be carried more by the longitudinal supporting beams because the tensile strength of the slab is reduced due the cracking. Consequently the cracking scenario might continue into these beams, which in turn will result in a disastrous event.

5.7 Summary

This research is a health assessment investigation on the Pentagon Road Bridge using field results and FE modelling software. However, the concept that makes it unique and innovative is the compensation for the lack of information about the material properties and support systems of the bridge. The use of these FEM has further illustrated the importance of an integrated bridge health mechanism.

In the case of the Pentagon Road Bridge, as with other bridges throughout the country, no information regarding structural parameters was available. Thus the FE models were generated with different conditions of connections; these were evaluated against the results of IBIS-S to choose the most appropriate type. The modulus of elasticity of concrete was found using an inverse approach. The positions of the rebars derived from GPR results were used as input data (Figure 5.4) to create a model which is more accurate, increasing confidence in its predictions. The model created predicts the behaviour of the bridge without defects.

The results of the models agree with those measured by IBIS-S monitoring except for the cantilever zone where the defects and cracks cause the structure to behave adversely. This has further proved that the bridge has undergone significant deterioration since it was built which was also indicated by the results of the visual inspection and GPR survey. These defects were added to the model and a parametric study was undertaken taking into account the speed of the lorry and the extent of the cracks. It is concluded that the stress in the beams of the cantilever zone will substantially increase if the crack expands but the sensitivity of the deflection is not as severe.

Therefore, a precise health assessment procedure and continuous monitoring of the bridge can be derived. Multiple NDT's can be applied in order to validate one another, as well as the addition of FE modelling analysis provided by software such as SAP2000 and ANSYS. These results indicate that although results can draw parity, it is in fact the

areas that show disparity and warrant further investigation that can provide insight into the health of bridge structures. This bridge health assessment experimentation can also be formulated into a method by which various different aspects of bridge structures can be investigated, which can then be used to assess whether, and to what extent, remedial action is warranted.

Chapter 6

Discussion

This chapter discusses the findings of the research presented in the previous chapters of this thesis. It commences by describing the framework of the integrated mechanism and then examines the individual components in detail in terms of their effectiveness and utility individually and as part of the mechanism. It highlights the advantages of this approach over others taken in the past and further underlines its importance as a bridge health monitoring technique for the future.

6.1 Discussion

Needs were identified based on research gaps found from a review of state-of-the-art research and industrial work. Too often individual techniques were being used in isolation resulting in an incomplete assessment of bridge health (Barnes et al., 2009, Sevim et al., 2011, Gentile and Bernardini, 2008). In recent times the approach of using multiple techniques has gathered pace although systematic linkage of data from all the techniques has not been achieved (Lubowieka et al., 2009). This is the gap which this thesis serves to rectify. Figure 6.1 describes the integrated mechanism used to fulfil this gap in research. This has been explained in detail in Chapter 3. In this chapter the individual components will be discussed in terms of the contribution they bring to the approach and also their applicability and utility as bridge health monitoring techniques. The method used to incorporate the results of GPR and IBIS-S into the FEM are discussed in detail in section 5.5.1.

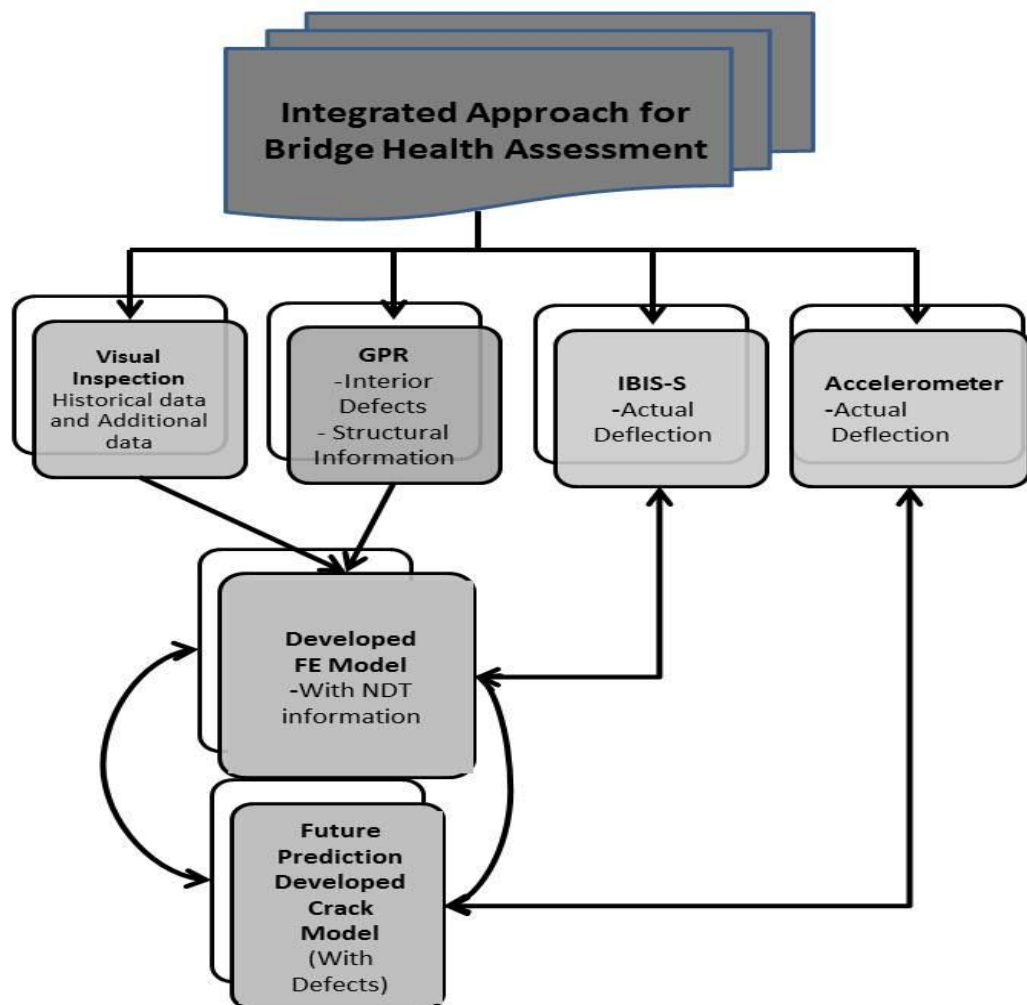


Figure 6.1 –Development Integrated Approach

6.1.1 Advanced Non-Destructive Testing

- **Visual Inspection**

Visual inspection is a useful practice for gathering basic information regarding a bridge's structural health as it is an inexpensive and quick method of identifying any superficial structural problems such as moisture ingress and beam delamination (Meng et al., 2011). However, it does not provide detailed information regarding the structural composition of the bridge or construction method (Abudayyeh et al., 2004). It was also unreliable in the case of the Pentagon Road Bridge as it did not yield the data required for development FE modelling; therefore it was necessary to make assumptions regarding the input parameters needed for the parametric study.

Visual inspection is a well-established practice in bridge health monitoring and provides a useful first step for the analysis of a structure; however much more detailed analysis of the structure is required before a health assessment is made.

- **Ground Penetrating Radar**

GPR was chosen as a technique as it is widely used in the bridge health monitoring industry as a means to identify hidden defects and their extent within the structure. It can also be used to discover the position of hidden features such as buried pipes and rebars which usually take very disruptive and destructive tests to unearth. There are a number of bridges which, similar to the Pentagon Road Bridge, have no detailed structural information available, which is needed to understand the behaviour of the structure for health monitoring and assessment. To increase the confidence of making a judgment it is recommended to use advanced NDT's such as GPR to identify the structural features needed for the development of an accurate FEM which can show whether remedial action is required. This thesis provides a novel approach of integrating rebar position from GPR to FE modelling (Section 5.5.1).

In order to fully understand the operation, collection and processing of GPR data training was undertaken along with a selection of preliminary case studies. Four bridges of different design were chosen as preliminary case studies (Forth Road Bridge, St Mary's Island Lifting Bridge, Darvel Road Bridge and Historic Rochester Old Bridge)

for this project. GPR surveys and visual inspections were carried out on all four bridges. The results provided a realistic picture of both the health of the bridge and the position of key features such as rebar condition and location, the measurement of pavement and concrete slab thickness, the location of deck slab and protective concrete damage, mapping of drainage and other buried pipes, delamination, reinforcement cover depth and moisture ingress (Parrello and Roberts, 2006), (Benmokrane et al., 2004), (Rhazi et al., 2003), (Lubowiecka et. al., 2009). Data collected from these preliminary case studies was used for data collection, processing, analysis and interpretation in order to understand the limitations and advantages of GPR.

Two different manufacturers and three different GPR antenna systems were used to provide valuable information regarding the positions of rebar (upper and lower reinforcement), unknown structural features and possible moisture ingress within the structure. Four different full GPR surveys were completed on the Pentagon Road Bridge with summer and winter environment conditions. More details are presented in section 4.2.5.

These antenna systems were used in order to gain a full range of knowledge regarding the structure at all depths, with higher frequencies utilized for more detailed radargrams and lower frequencies for greater penetrative depths. This gives both high quality radargrams in terms of resolution and internal composition at depth. By comparing all the radargrams it is possible to comprehensively establish the position of the rebars.

GPR results identified that possible deterioration has occurred in significant parts of the bridge decks. It was concluded that the identified areas could be interpreted as signs of delamination and serious moisture ingress within the structure. This indicated structural anomalies in certain parts of the bridge.

The significance of these results comes into force when the information that is acquired from GPR (rebar position in particular) is input into a FEM which provides greater accuracy to the model's findings. This results in greater confidence in the model when modelling for future deteriorations (Section 5.5.1).

- **IBIS-S and Accelerometer**

IBIS-S was chosen as it is one of the most trusted methods of determining movement/deflection of structures such as bridges. The magnitude of deflection is an important factor when determining bridge health as there is a maximum safe deflection limit as established by Eurocode (Eurocodes, 2007). IBIS-S is not able to establish the causes of excessive displacement and it is therefore important to compliment the process with a method such as GPR to identify defects in the bridge deck.

In order to verify the quality of results obtained by IBIS-S it was decided to adopt an independent set of field test (parallel to the IBIS-S test) (Gentile and Bernardini, 2008). For this purpose accelerometer sensors were used.

IBIS-S, according to the manufacturer, gives results in terms of 1/100 mm displacement accuracy allowing for a detailed comparison with the FEM. Pentagon Road Bridge deflection was monitored twice with IBIS-S equipment in different weather conditions and once with accelerometer validation, the results of which were presented in detail in section 4.2.3. These surveys were completed with a one year gap between tests. This allowed for possible secondary analysis to observe changes (deterioration) in the intervening year.

The IBIS-S and Accelerometer results are of great importance as they allow for a comparison between the behaviour of the bridge as new (FEM) and as is (IBIS-S and Accelerometer results). This has been attempted before by Bernardini et al. (2007) although the model they created was based on a project report. Often these reports are not available in cases of older bridges or infrastructure which highlights the importance of the application of NDT methods in monitoring and assessing structural features which are included in this thesis's FEM.

These results proved to be vital to establish benchmarks and develop an effective methodology for the assessment and monitoring of the Pentagon Road Bridge. The Pentagon Road Bridge exercise was considered successful as it provided vital additional information in relation to internal defects and anomalies of the bridge deck structure.

As a result, the effectiveness of the adopted non-destructive testing methods was evident in all cases, as a significant quantity of anomalies, defects and structural features were detected.

6.1.2 Analysis

- **Developed FE Model**

The aim of this developed Finite Element Model is to facilitate a “better” understanding of the conditions of the bridge structure. This will give a more realistic picture of the bridge condition, and increase confidence when making a judgment regarding remedial action. The quality of this model is more accurate than others previously developed and reported as it has the additional information provided by GPR (rebar positions) added to it. This is illustrated by comparisons between the initial FEM and the more detailed one, in which the detailed model shows a far higher accuracy owing to the greater amount of information input.

This model is significant as it is the first attempt to combine other NDT data (GPR) with a FEM in order to ascertain its behaviour as built. This was achieved by inputting the rebar position from GPR results into the FEM. This is then combined with IBIS-S which provides a measure of bridge deterioration in terms of its behaviour. This is a little known combination technique, attempted only once previously (without GPR data) outside this thesis.

From these results, it is clear that the developed FE model provides an invaluable tool for predicting the behaviour of the Pentagon Road Bridge without damage which provides a suitable benchmark for comparison with visual inspection, GPR, IBIS-S and Accelerometer results. This comparison indicates whether there is a significant health issue with the Pentagon Road Bridge and questions whether remedial action is needed.

6.1.3 Future Predictions

- **Developed Crack Model**

Pentagon Road Bridge parametric study results presented the proportionality of the maximum deflection in the cantilever zone with both the lorry speed and the crack depth in the supporting beam. It is clear that as the crack expands deeper into the supporting beam of the cantilever region, the stiffness will decrease and the deflections must increase. However, it is demonstrated that the lorry speed has a significant effect on the structural response. The greater deflection due to the increase of the lorry speed illustrates a dynamic effect that requires detailed study. As the vehicle passes the bridge at various speeds, a nonlinear combination of the effects of the loading condition and the natural frequencies of the bridge will determine the dynamic response of the structure (Kamaya, 2006).

The maximum stresses in both the supporting beam and slab are developed as the lorry passes at a speed of approximately 28 miles per hour. This shows an excited dynamic response at such a speed. The introduction of vehicular speed limitation could extend the service life of the bridge. Most importantly it was demonstrated that the stress in the supporting beam increases considerably as the crack expands but this increased stress is insignificant in the slab. This issue is clarified by paying attention to the other beams supporting the slab (Khennane and Kaci, 2010). As the beam at the cantilever zone end becomes weaker due to crack depth increase, its load carrying capacity and stiffness decrease considerably.

It was found that if a lorry with a weight in excess of 46 tonnes passes over the bridge at a speed of 28 miles per hour then the tensile stresses in the steel reinforcements will exceed the rebar tensile yield stress and, due to the poor condition of the reinforcements, a catastrophic collapse will ensue.

This possible failure illustrates the importance of undertaking such predictive modelling whose accuracy has been increased by both the inclusion (GPR data) and comparison with (IBIS-S data) NDT.

6.1.4 Integrated Health Mechanism

The developed integrated mechanism resulting from the above combination of techniques provides a valuable approach to bridge health assessment. It is unique as no other complete method which encompasses so many valuable techniques has ever been suggested. It offers a tailor-made solution to the problems faced by bridge engineers when selecting NDT for health assessments of concrete bridges.



















This technique could be used as part of a bridge health monitoring strategy. The whole mechanism can be applied every couple of years. The period between assessments is dependent on several factors including budgetary and time constraints. It is also dependent on the rate of deterioration of the structure, this can be determined by a visual inspection.



It is a valuable contribution which can be used by industry as an all-encompassing technique to evaluate the health of bridges which is often complicated by the myriad of equipment and techniques on offer to engineers. This integrated approach offers a solution to this confusion by identifying NDTs which can be used together to complement one another; thus a thorough assessment of the bridge health is achieved without the need for additional testing unless required.

The developed integrated mechanism carried out in this thesis is certainly feasible for the main case study - the Pentagon Road Bridge - and could be adopted for other structures, adding to the existing knowledge and understanding of bridge structures and their behaviour in terms of function and durability. The integrated model which was the ultimate aim of this thesis, provides ample knowledge for structural engineers and researchers in terms of long term functionality and stability of bridge structures.

Table 6.1 shows the impact of using additional NDT information in FEM on a variety of parameters. It concludes along with this thesis that, although NDT requires additional time and cost, the accuracy it gives in return is more than compensated for. This accuracy will no doubt save costs in the long term as well as more importantly people's lives.

Table 6.1 – Correlation of the FE models

FE Model with NDT information	FE Model without NDT information
 Time (assessment needs more time)	 Time (assessment needs less time)
 Accurate (more accurate information)	 Accurate (less accurate information)
 Expensive (Equipment costly)	 Cheaper (Equipment cheaper)
 Decision (More Confident)	 Decision (Less Confident)
 Safety (More safety)	 Safety (less safety)
 Assured (More assured)	 Assured (less assured)
 Subjectivity (Less subjectivity)	 Subjectivity (More subjectivity)
 Objectively (more real data)	 Objectively (less real data)
 Security More Safe	 Security Less Safe

 less  more

This developed integrated mechanism, the author believes, has the strength to become a fundamental practice in bridge health engineering and in the future could become a popular step by step method of determining the health of bridge structures.

In summary the significance of this study can be described as follows:

Importance of Training:

- Allowing utilisation of equipment (GPR, IBIS-S and Accelerometers) with confidence and ease.
- Understanding challenges during assessment/monitoring surveys, data processing and interpretation of results.
- Aids in the speed of operation and decision making.

Significance of GPR results in this study:

- Establishing invaluable information about structural and non-structural features of the bridge under study.
- Establishing possible defect positions within the bridge deck structure.
- Providing detailed information about extent of defect.
- Adding to the existing knowledge on GPR applications in general (valuable information for the GPR)

Significance of IBIS-S and Accelerometer results in this study:

- Providing invaluable information on the dynamic behaviour of the bridge structure (on a point-by-point scale).
- Allowing for a comparative study to be carried out (with FE Model).
- Validation of the obtained IBIS-S data (with accelerometers).

Significance of FE Modelling and parametric study results:

- Simulation of bridge structure under static and dynamic conditions.
- Allowing comparative study to be carried out (with field data).
- Pave the way for an accurate model to be developed for the prediction of bridge behaviour in the future.

Significance of this study:

- Contributed to existing knowledge by increasing our understanding on effective application of non-destructive testing methods in bridge structures' monitoring and assessment.

- Demonstrating how structural monitoring data can be used in developing reliable numerical models for bridge health monitoring.

6.2 Contribution to Knowledge

During the course of this research several key contributions to knowledge in this field of research were identified.

The first was to demonstrate effectively the applications of certain NDT methods in enhancing the accuracy of FE modelling of structures (bridges). This was achieved by integrating the results of the GPR survey (upper and lower rebar position) into the FEM of the bridge. To the authors knowledge this has not been attempted previously. This helped to ensure the inner composition of the bridge was accurately quantified. With regards to the other important factor needed by the FE software to calculate the stiffness matrix “Young’s modulus”, this was found by calibrating the model using the actual bridge deflection data obtained from IBIS-S system. This enabled an iterative approach when calculating Young’s modulus. It also created an additional confidence in the model as its results correlated well with IBIS-S for the spans where no significant deterioration had occurred. Together this has served to highlight the NDT which can be used to gather information that will create accurate FEM which can be used for future prediction. This is especially useful for bridges where no structural information is available such as the Pentagon Road Bridge.

Secondly, this thesis introduced a novel mechanism / approach for effective health monitoring and assessment of bridge structures. This was achieved by combining several NDT identified as the most beneficial for bridge health monitoring: visual inspection, GPR, IBIS-S and FEM. In the past these were often used singularly and thus a comprehensive bridge health assessment was not obtained (Maser, 2009). Other approaches such as Lubowieka et al. (2009) have evaluated a masonry bridge using GPR, Laser Scanner and FEM software however no structural response of the bridge was measured and thus a complete health assessment was not obtained. This thesis however included all the elements detailed by Lubowieka et al (2009) (Although the geometric data collection was achieved using an independent report and visual inspection not a laser scanner) and further information such as actual bridge deflection

(IBIS-S and accelerometer), detailed internal composition i.e. rebar position (GPR), and detail structural modelling i.e. crack propagation (ANSYS). This, therefore results in a far more accurate assessment of the bridge health than that found by Lubowieka et al (2009). By using all the detailed NDTs together, it is also possible to highlight key areas of the bridge in need of remedial action in this case Span 4 of the Pentagon Road Bridge. And as several independent techniques indicate the same deteriorated area of the bridge, additional confidence is gained when a decision needs to be made regarding areas in need of remedial action.

Finally, these contributions and findings have been disseminated to the larger research community through several international conferences and peer reviewed journals. A comprehensive list of publications with abstracts is shown in Appendix E.

Chapter 7

Conclusion and Further Work

This chapter examines the objectives provided in Chapter 1, in order to conclude to what extent they have been met. Having completed this conclusion, future work is identified.

7.1 Conclusion

In order to provide a comprehensive set of conclusions for this thesis, this chapter has been divided into sections which evaluate the findings of this research in terms of the contributions they have made to the main objectives of this thesis.

With respect to Objective One (acquire necessary knowledge of operation, collection, processing and interpretation of complex data compiled by advanced structural monitoring equipment):

An in-depth literature review was carried out which provided the necessary background knowledge for this project in terms of understanding the theory and practice (operation, data collection and processing and interpretation of results) of possible NDT methods that could be adopted in this study.

The literature review was extended to the study of bridge structures' behaviour under static and dynamic loading conditions. A significant number of articles and scientific papers were studied in order to understand the theory and design criteria for bridge structures. This study also provided an opportunity to identify the gaps in knowledge in this particular area.

The literature review identified certain NDT which would be suitable for the development of the integrated approach mechanism. These were identified as GPR, IBIS-S, Accelerometers and appropriate finite element modelling software. GPR enables the identification of defects and hidden structural supports of the bridge; IBIS-S gives results for deflection, validated with Accelerometers, and FEM provides an accurate method (when coupled with GPR results) of monitoring the deterioration of the bridge and modelling further degradation.

This successfully completed Objective One as all the appropriate NDT methods were identified and analysed.

With respect to Objective Two (demonstrate the effectiveness and applicability of non-destructive testing methods and technology in structural monitoring and assessment of bridge structures):

Following the identification of the appropriate NDT methods in Objective One, these methods were further analysed in terms of their applicability to bridge health monitoring.

Appropriate training sessions in the operation of GPR were undertaken, provided by the supervisor team, IDS Limited (manufacturer of the GPR and IBIS-S equipment) and UTSI Electronics (manufacturer of GPR). GPR surveying along with visual inspection was carried out on the preliminary case study bridges. Data collected from these preliminary case studies (Forth Road Bridge, St Mary's Island Lifting Bridge, Darvel Road Bridge and Historic Rochester Old Bridge) was used for data processing and interpretation. These case studies served as training exercises.

In the case of the Forth Road Bridge the GPR radargram indicated the presence of moisture, which was proven to be correct by means of destructive testing. The radargram's indication of rebar and beam positions was also shown to be accurate. This further demonstrated the effectiveness of GPR as a bridge health monitoring technique.

With respect to FEM, training was undertaken with the supervision team and by the use of online training sources. This succeeded in giving sufficient knowledge in the operation of both ANSYS and SAP2000 so that the main case study bridge could be modelled in both.

In collaboration with Medway Council Highway Engineering Department, the Pentagon Road Bridge was identified as the main case study in this thesis. After the first full visual inspection, which revealed the need for further investigation, and in association with an independent study that was carried out by Medway Council's contractors (Jacobs), it was agreed to carry out a full monitoring survey of the bridge using GPR, IBIS-S, Accelerometers and Wireless Network Sensors (WNS). Two full surveys using GPR and IBIS-S (with an interval of ten months) and one full survey using Accelerometers and WNS were carried out to

show the variability of results depending on meteorological/weather conditions. Several subsequent visual inspections were carried out in conjunction with these surveys. This case study was successful in terms of providing vital additional information in relation to internal defects and anomalies of the bridge deck structures.

The results produced by GPR, IBIS-S, and visual inspection together indicated a particular section of the bridge which needed further attention. In order to validate the results from IBIS-S, both WNS and Accelerometers were used to obtain further results for deflection. The results from Accelerometers correlated well with IBIS-S results. However, it was discovered that WNS is inappropriate for this type of bridge health monitoring owing to several factors, the most prominent of which being battery life. However, the results from Accelerometers were deemed appropriate to compare and hence validate the IBIS-S findings.

By completing these surveys on the bridge the appropriateness of NDT for bridge monitoring was proven. Advantages such as ease of use and cost levels uncovered within the literature review were proven in all cases, with the exception of the WNS.

From the training mentioned above, knowledge was acquired which could be used in the development of models for bridge health design. Using this knowledge, a preliminary model of the bridge was designed in both ANSYS and SAP2000. This model was formed using information from structural reports and visual inspections and was used to gain a preliminary insight into the movement of the bridge under dynamic and static loading before any NDT was completed. The utility of this model serves to prove the applicability of FEM as a suitable bridge health monitoring method when complemented by other NDT methods.

This completed Objective Two.

With respect to Objective Three (establish detailed monitoring data on the extension of structural defects and identification of structural and non-structural features which increases understanding of anomalies within the bridge structure):

Data relating to moisture damage, delamination, asphalt and concrete slab thickness measurement, deck slab and protective concrete damage location, rebar condition and depth measurement were determined by GPR. These defects were easily identifiable from the radargrams as extensive training had been given in their detection. Structural information relating to the rebar positions within the bridge deck was identified in the radargrams.

For the Pentagon Road Bridge, two different manufacturers with three different GPR antenna systems were again used to provide required data regarding the positions of rebar (upper and lower reinforcement), unknown structural features as well as possible moisture ingress within the structure. The RIS Hi BriT (2 GHz) Antenna proved the most appropriate for both these tasks, clearly showing moisture ingress increasing with depth and also the upper rebar position. However it was also noted that RISMF HI-MOD (200-600 MHz) and UTSI Electronics GPR Antennas identified possible lower supports but did not detect moisture below 10cm. Three different antennas produced radargrams which indicated possible rebar distortion. These radargrams also indicated areas of deterioration on the bridge; a possible explanation for the appearance of the highlighted features could be ingress of moisture through the surface of the deck. These features correlate with surface cracks that were observed during the visual assessment of the bridge. Recommendations have been made to the owners of the bridge to expose one of the highlighted areas in order to verify the suggested moisture presence and possible delamination of the concrete at lower levels of the bridge structure. However, permission was not granted by the bridge owner to perform such excavation works as the bridge is heavily used.

Thus another method was required to determine the presence of moisture - velocity analysis – the results of which were compared with the IDS GRED software results. The results of the dielectric constant map correlated well with the processed data, giving confidence in the judgement that moisture was present and is affecting the radargram hyperbole.

IBIS-S equipment was used to determine the deflection of the bridge and Accelerometers were used to validate the findings. The results of both monitoring methods indicated a certain degree of deflection but as no structural reports existed into the initial deflection of the bridge as new it was impossible to know whether this displacement was excessive. Hence FEMs were developed using the rebar positions determined by GPR to replicate the deflection of the bridge as new so a comparison can be made.

This successfully completed Objective Three.

With respect to Objective Four (develop Finite Element modelling of bridge structures using specialist software (SAP2000 and ANSYS) for simulation purposes):

After a preliminary investigation in terms of appropriateness of available software for modelling purposes, SAP2000 and ANSYS were identified as the most suitable software for modelling bridge structures under both static and dynamic loading conditions. Finite element models of the Pentagon Road Bridge were developed to predict the behaviour of the bridge as if it were completely free of any structural defects (using information obtained from an independent technical report and visual inspection). A simulation process was then carried out using a lorry of identical specifications to the one used in the IBIS-S surveys, thus allowing for the bridge's behaviour as brand new to be compared with the actual recorded behaviour from the IBIS-S surveys.

The results were as follows:

- Both the IBIS-S and the FE models illustrate considerable deflections (although permissible) on the Pentagon Road Bridge.
- Finite Element Analysis (Parametric Study) on the effects of dynamic loading of the deteriorated cantilever part of the bridge beams demonstrates possible serious damage in this particular section of the Pentagon Road Bridge.

From these results, it is clear that the FEM provides an invaluable tool for predicting the behaviour of a bridge without damage, providing a suitable benchmark for comparison with GPR and IBIS-S results. This comparison indicates whether there is a significant health issue with the bridge and questions whether remedial action is needed.

This successfully completed Objective Four.

With respect to Objective Five (develop an integrated mechanism bringing together the obtained knowledge and information about defects and mechanical behaviour of bridges within the context of health monitoring and integrity of structures):

The results presented in this thesis reveal valuable and “accurate” information about the internal structure of the bridge (including rebar position) and possible defects in terms of location and structural configurations. The results of all the NDT methods used indicate a specific area of the bridge (Figure 7.1) to be in urgent need of repair. These results were achieved by comparing where exterior and interior defects correlate with excessive deflection, resulting in a complete picture of bridge health. This increases confidence in a decision regarding remedial action in the indicated area.

The work carried out in this thesis is certainly feasible for the Pentagon Road Bridge and could be adopted for other structures. It will add to the existing knowledge and understanding of bridge structures’ behaviour in terms of function and durability. The integrated model which was the ultimate aim of this project provides ample knowledge for structural engineers and researchers in terms of long term functionality and stability of bridge structures.

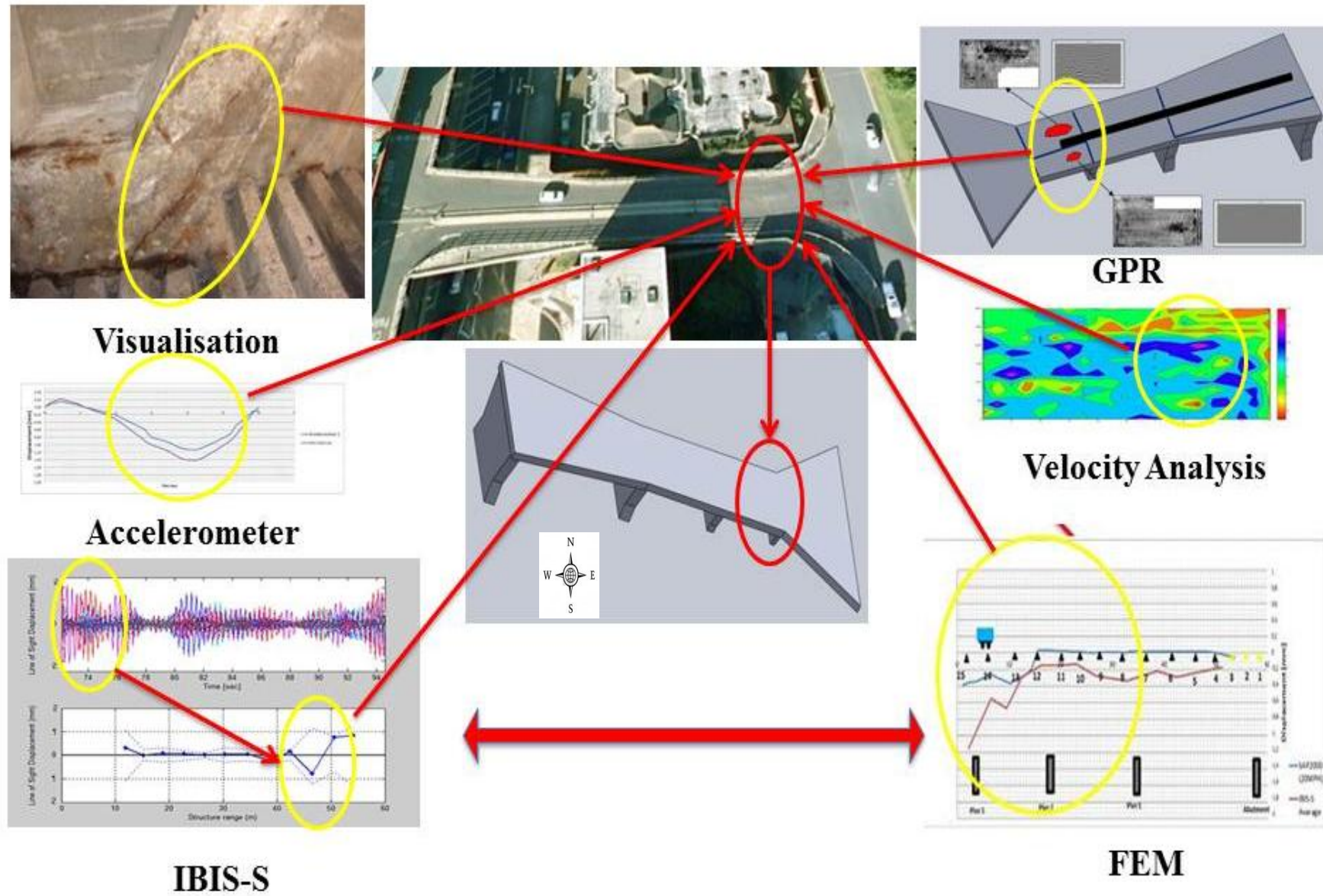


Figure 7.1 – Integrated approach on the Pentagon Road Bridge

From this approach, a modified integrated approach model with improved accuracy has been developed, as depicted in Figure 7.2.



Figure 7.2 – Development of Integrated Approach

First, the visual inspection gives a very basic external understanding of bridge health. If any damage such as cracking or cover delamination is seen, it is advised to further examine the health of the bridge through GPR and IBIS-S technologies.

This combination of techniques has not been suggested previously and has distinct advantages over earlier bridge health monitoring approaches as it encompasses all aspects of structural design important to health and safety engineers, i.e. cost efficiency and simple initial assessment (visual inspection). It is believed that this mechanism has the strength to become a fundamental practice in bridge health engineering and in the future could become a popular step-by-step method of determining the health of bridge structures.

7.2 Recommendations for Future Research

Research indicates that the acquisition of other NDT such as Laser Scanning would be highly advisable for this project (provided adequate training was undertaken). This is due to the fact that the parameters of the bridge were obtained from very rudimentary measurements using tape measures etc. A laser scanner would provide a detailed 3d image of the bridge which could then be input into a FEM. This could be used to develop a more accurate FEM which would give increased confidence in the predictions it makes.

In the future more bridges of various construction types (e.g. steel, suspension, masonry) should be examined using this integrated mechanism. This would help to determine the additional NDT needed for certain bridge structures such as the addition of fatigue monitoring for steel. This would increase the applicability of this method and prove its repeatability.

The bridge health monitoring approach proposed could be further expanded to encompass a computer model which, when input with the NDT assessment results and modelling information, would give an indication of possible areas of deterioration of any bridge. This computer model would decrease costs and eliminate the need for time consuming comparison between results from different surveys. It would continue to be evaluated with input from industry in order to further enhance understanding of the response of bridges to static and dynamic loading. The final output is the functional specifications for an integrated system design using the proposed methodology, and it will be verified and evaluated using industrial case studies. This model will give a better insight into planned and preventative maintenance systems and will prove a valuable tool in both the academic and industrial sectors.

References

- ABUDAYYEH, O., AL BATAINEH, M. & ABDEL-QADER, I. 2004. An imaging data model for concrete bridge inspection. *Advances in Engineering Software*, 35, 473-480.
- ACI, 2011 American Concrete Institute 343R-95, *Analysis & Design of Reinforced Concrete Bridge Structures*, 2011
- AISC, 2006, American Institute of Steel Construction, 13 Edition, ISBN 1-56424-055-X, 2006
- AGENCY, H. 2011. Available: <http://www.highways.gov.uk/>.
- AL-KHEDER, S., AL-SHAWABKEH, Y. & HAALA, N. 2009. Developing a documentation system for desert palaces in Jordan using 3D laser scanning and digital photogrammetry. *Journal of Archaeological Science*, 36, 537-546.
- ALBAA, M., BERNARDINIB, G., GIUSSANIA, A., RICCIB, P. P., RONCORONIA, A., VALGOIC, M. S. P. & ZHANGD, K. 2008. Measurement of dam deformations by terrestrial interferometric techniques.
- ALBARBAR, A., BADRI, A., SINHA, J. K. & STARR, A. 2009. Performance evaluation of MEMS accelerometers. *Measurement*, 42, 790-795.
- ASTM International, WWW.ASTM.ORG., 2010
- ARMESTO, J., ROCA-PARDIÑAS, J., LORENZO, H. & ARIAS, P. 2010. Modelling masonry arches shape using terrestrial laser scanning data and nonparametric methods. *Engineering Structures*, 32, 607-615.
- ÅKESSON, B. 2008. *Understanding Bridge Collapses*.

- ALTUNISIK AHMET CAN, ALEMDAR BAYRAKTAR, BARIS, SEVIM SEVKET ATEŞ, "Ambient vibration based seismic evaluation of isolated Gulburnu highway bridge" *Soil Dynamics and Earthquake Engineering* 31(2011)1496–1510
- ANDERSON, T.L., 2005. *Fracture Mechanics - Fundamentals and Applications*. 3rd ed. Boca Raton: CRC Press.
- ANON (1997) *Guidance on radar testing of concrete structures (Concrete Society Technical Report No 48)* 88 pp
- ANSYS, 2011, ANSYS 12.1 manual, Inc. (CSI), http://www1.ansys.com/customer/content/documentation/ans_cmd.pdf
- ASCE. 2011. Available: www.asce.org.
- AZARBAYEJANI, M. 2009. Optimal sensor placement in structural health monitoring (shm) with a field application on arc bridge.
- BALAKUMARAN, S. S. G. 2010. Influence of Bridge Deck Concrete Parameters on the Reinforcing Steel Corrosion.
- BARNES CHRISTOPHER L., JEAN-FRANC-OIS TROTTIER, Dean Forgeron, 2008, "Improved concrete bridge deck evaluation using GPR by accounting for signal depth– amplitude effects" *NDT&E International* 41 (2008) 427– 433
- BARNES CHRISTOPHER L., JEAN-FRANC-OIS TROTTIER, 2000, "Ground-Penetrating Radar for Network-Level Concrete Deck Repair Management, (ASCE)0733-947X(2000)126:3(257)
- BARTON MIKE AND RAJAN S. D., 2000, *Finite Element Primer for Engineers*, 2010
- BAPAT AMEY V., 2009, "Influence of bridge parameters on finite element modelling of slab on girder bridges" *Master of Science In Civil Engineering, Virginia Polytechnic Institute and State University*, 2009
- BASHARAT, A., CATBAS, N. & SHAH, M. A framework for intelligent sensor network with video camera for structural health monitoring of bridges. *Pervasive Computing and Communications Workshops, 2005. PerCom 2005 Workshops. Third IEEE International Conference on*, 8-12 March 2005 2005. 385-389.
- BENMOKRANE, B., EL SALAKAWY, E. F., EL RAGABY, A., DESGAGNÉ, G. & LACKEY, T. 2004. Design, construction and monitoring of four innovative concrete bridge decks using non corrosive FRP composite bars. *Annual Conference & Exhibition of the Transportation Association of Canada. Québec, Canada.*
- BERARD, B. A. & MAILLOL, J.-M. 2007. Multi-offset ground penetrating radar data for improved imaging in areas of lateral complexity -- Application at a Native American site. *Journal of Applied Geophysics*, 62, 167-177.
- BERGERON, J. 2003. Functional verification of HDL models.

- BERK, A. 2006. Development of a safety-inspection methodology for river bridges.
- BERNARDINI, G., DE PASQUALE, G., BICCI, A., MARRA, M., COPPI, F., RICCI, P. & PIERACCINI, M. 2007. Microwave interferometer for ambient vibration measurement on civil engineering structures: 1. Principles of the radar technique and laboratory tests. VACES'07 Experimental Vibration Analysis for Civil Engineering Structures. Porto, Portugal.
- BERGMEISTER, K. (2002): Vorgespannte Aramidbänder - Umwicklung eines Brückenpfeilers. Beton- und Stahlbetonbau, 97, 11, 599 - 600
- BERSEZIO, R., GIUDICI, M. & MELE, M. 2007. Combining sedimentological and geophysical data for high-resolution 3-D mapping of fluvial architectural elements in the Quaternary Po plain (Italy). *Sedimentary Geology*, 202, 230-248.
- BINDA, L., SAISI, A. & ZANZI, L. 2003. Sonic tomography and flat-jack tests as complementary investigation procedures for the stone pillars of the temple of S. Nicolò l'Arena (Italy). *NDT & E International*, 36, 215-227.
- BRIAUD, J.-L., HURLEBAUS, S., CHANG, K.-A., YAO, C., SHARMA, H., YU, O.-Y., DARBY, C., HUNT, B. E. & PRICE, G. R. 2010. Realtime monitoring of bridge scour using remote monitoring technology. <http://www.parallax.com/dl/docs/prod/compshop/SICMemsicTut.pdf>.
- BROOMFIELD, J. P. 2007. Corrosion of Steel in Concrete.
- BROSTEN, T. R., BRADFORD, J. H., MCNAMARA, J. P., GOOSEFF, M. N., ZARNETSKE, J. P., BOWDEN, W. B. & JOHNSTON, M. E. 2009. Estimating 3D variation in active-layer thickness beneath arctic streams using ground-penetrating radar. *Journal of Hydrology*, 373, 479-486.
- BRAIN INSTITUTE, WWW.BRAIN101.INFO/EMF.PHP., 2010
- BUNGEY, J. H. 2004. Sub-surface radar testing of concrete: a review. *Construction and Building Materials*, 18, 1-8.
- CAGNOLI, B. & RUSSELL, J. K. 2000. Imaging the subsurface stratigraphy in the Ubehebe hydrovolcanic field (Death Valley, California) using ground penetrating radar. *Journal of Volcanology and Geothermal Research*, 96, 45-56.
- CAGNOLI, B. & ULRYCH, T. J. 2001. Ground penetrating radar images of unexposed climbing dune-forms in the Ubehebe hydrovolcanic field (Death Valley, California). *Journal of Volcanology and Geothermal Research*, 109, 279-298.
- CANER, A., YANMAZ, A. M. & BERK, A. 2006. Remarks on Development of a Safetyinspection Algorithm for River Bridges. International Congress on Advances in Civil Engineering, Yıldız Technical University, Istanbul, Turkey.

-
- CAO, Y., DAI, S., LABUZ, J. F. & PANTELIS, J. 2007. Implementation of Ground Penetrating Radar. Minnesota Department of Transportation
- CARINO, N. J. 2001. The Impact-Echo Method: An Overview.
- CASSIDY, N. J. & HARRY, M. J. 2009. Chapter 5 - Ground Penetrating Radar Data Processing, Modelling and Analysis. Ground Penetrating Radar Theory and Applications. Amsterdam: Elsevier.
- CBDG, 2012, Concrete Bridge Development Group, <http://www.cbdg.org.uk/intro2.asp>
- CENTER, N. R. 2010. Available: <http://www.ndt-ed.org>.
- CERDEIRA, F., VÁZQUEZ, M. E., COLLAZO, J. & GRANADA, E. Applicability of infrared thermography to the study of the behaviour of stone panels as building envelopes. Energy and Buildings, In Press, Corrected Proof.
- CERDEIRA, F., VÁZQUEZ, M. E., COLLAZO, J. & GRANADA, E. 2011. Applicability of infrared thermography to the study of the behaviour of stone panels as building envelopes. Energy and Buildings, 43, 1845-1851.
- CHAE, M. J., YOO, H. S., KIM, J. Y. & CHO, M. Y. 2012. Development of a wireless sensor network system for suspension bridge health monitoring. Automation in Construction, 21, 237-252.
- CHANG., Y. CHANG, P.F. SUTHERS, C.D. Maranas "Identification of optimal measurement sets for complete flux elucidation in metabolic flux analysis experiments Biotechnol. Bioeng., 100 (2008), pp. 1039–1049
- CHAN T. H. T. Y. YU, K.Y. WONG, Z. X. LI, Condition-assessment-based finite element modelling of long-span bridge by mixed dimensional coupling method, 2011
- CHOPRA, A. K. (1995). Dynamics of Structures Theory and Applications to Earthquake Engineering, Prentice Hall, Upper Saddle River, NJ.
- CHEN, W. & DUAN, L. 2003. Bridge Engineering: Construction and Maintenance. CRC Press, Boca Raton, Fla.
- CHOWDHURY, M. R. & RAY, J. C. 2003. Accelerometers for bridge load testing. NDT & E International, 36, 237-244.
- COMPUTERS AND STRUCTURES, 2012, SAP2000 manual, Inc. (CSI), www.csiberkeley.com/sap2000
- CONCRETE SOCIETY, "Guidance on radar testing of concrete structures," Tech. Rep., Vol. 48, 88, 1997.
- COPE, R.J. (Robert J.), 1987 Concrete—Maintenance and repair. I. TG335.C57 1987
- CLARK, M. R., MCCANN, D. M. & FORDE, M. C. 2003. Application of infrared thermography to the non-destructive testing of concrete and masonry bridges. NDT & E International, 36, 265-275.

- CLOUDE, J., 2011, BEng (Hons) Civil Engineering Studies, University of Greenwich, 000395443, 2011
- DAHMANI, L., KHENNANE, A. AND KACI, S., 2010. Crack identification in reinforced concrete beams using ANSYS software. *Strength of Materials*. Vol. 42(2). 232-240.
- DANIELS, D. J. 1996. Surface-penetrating radar. *ELECTRONICS & COMMUNICATION ENGINEERING JOURNAL*, 165 - 182.
- DANIELS, D. J. 2007. *Ground Penetrating Radar*, 2nd Edition, The Institution of Engineering and Technology.
- DAVIS, J. L. & ANNAN, A. P. 1989. GROUND-PENETRATING RADAR FOR HIGH-RESOLUTION MAPPING OF SOIL AND ROCK STRATIGRAPHY1. *Geophysical Prospecting*, 37, 531-551.
- DEI, D., PIERACCINI, M., FRATINI, M., ATZENI, C. & BARTOLI, G. 2009. Detection of vertical bending and torsional movements of a bridge using a coherent radar. *NDT & E International*, 42, 741-747.
- DEPARIS, J., GARAMBOIS, S. & HANTZ, D. 2007. On the potential of Ground Penetrating Radar to help rock fall hazard assessment: A case study of a limestone slab, Gorges de la Bourne (French Alps). *Engineering Geology*, 94, 89-102.
- DEFENCETALK, WWW.DEFENCETALK.COM U.S. Army uses Ground Penetrating Radar., 2010
- DIAMANTI, N., GIANNOPOULOS, A. & FORDE, M. C. 2008. Numerical modelling and experimental verification of GPR to investigate ring separation in brick masonry arch bridges. *NDT & E International*, 41, 354-363.
- DIGEST 444 Part 1, 2000, Corrosion of steel in concrete Durability of reinforced concrete structures, BRE Centre for Concrete Construction, CI/SfB q4, February 2000
- DIGEST 449, 2000, Corrosion of steel in concrete, A review of the effect of humidity, G Sergi and A Dunster BRE Centre for Concrete Construction, 2000
- DIXIT, P.M., *Modelling of Metal Forming and Machining Process by Finite Element and Soft Computing Methods* (Springer, London, 2008)
- EMF, E. M. F. Available: <http://brain101.info/EMF.php> 14/04/2010].
- ÉKES, C. & HICKIN, E. J. 2001. Ground penetrating radar facies of the paraglacial Cheekye Fan, southwestern British Columbia, Canada. *Sedimentary Geology*, 143, 199-217.
- ELSENER, B. 2001. Half-cell potential mapping to assess repair work on RC structures. *Construction and Building Materials*, 15, 133-139.
- EUROGPR. www.eurogpr.org. 2010
- EUROCODE 2-18, *Structural Eurocodes, Design of concrete structures*, British Standards Institution, 2010

- EUROCODE 3-22, Structural Eurocodes, Design of steel structures, British Standards Institution, 2010
- EVANS, R. D., FROST, M. W., DIXON, N. & STONECLIFFE-JONES, M. 2008. The response of ground penetrating radar (GPR) to changes in temperature and moisture condition of pavement materials. TC3 Conference.
- FARRAR, C. R., DARLING, T. W., MIGLIORI, A. & BAKER, W. E. 1999. MICROWAVE INTERFEROMETERS FOR NON-CONTACT VIBRATION MEASUREMENTS ON LARGE STRUCTURES. *Mechanical Systems and Signal Processing*, 13, 241-253.
- FERNANDES, B. 2010. Nondestructive Evaluation of Deteriorated Prestressing Strands Using Magnetic Field Induction.
- FERRETTI, A., GUARNIERIA, M., C., P., F., R. & D., M. 2007. InSAR Principles: Guidelines for SAR Interferometry Processing and Interpretation.
- FITZPATRICK TONY, PAT DALLARD, SOPHIE LE BOURVA, ANGUS LOW, ROGER RIDSDILL SMITH AND MICHAEL WILLFORD, "Linking London: The Millennium Bridge", Royal Academy of Engineering, London, Paper ISBN 1 871634 99 7 (2001). An amended version of this paper with additional material was subsequently published as P. Dallard et al. "The London Millennium Footbridge", *The Structural Engineer*, 79, No. 22, 17-33 (2001).
- FLANNIGAN, J. C. 2005. Acoustic emission monitoring on fiber reinforced bridge panels.
- FORDE, M. C., MCCANN, D. M., CLARK, M. R., BROUGHTON, K. J., FENNING, P. J. & BROWN, A. 1999. Radar measurement of bridge scour. *NDT & E International*, 32, 481-492.
- GANGONE, M. V., WHELAN, M. J., JANOYAN, K. D., CROSS, K. & JHA, R. 2008. Performance Monitoring of a Bridge Superstructure Using a Dense Wireless Sensor Network.
- GARNIER, C., PASTOR, M.-L., EYMA, F. & LORRAIN, B. 2011. The detection of aeronautical defects in situ on composite structures using Non Destructive Testing. *Composite Structures*, 93, 1328-1336.
- GASTINEAU, A., JOHNSON, T. & SCHULTZ, A. 2009. Bridge Health Monitoring and Inspections – A Survey of Methods In: *TRANSPORTATION*, M. D. O. (ed.). University of Minnesota.
- GENTILE, C., BERNARDINI, G. & RICCI, P. P. 2008. A new interferometric radar for full-scale testing of bridges: 2. Ambient vibration tests and operational modal analysis. *Structural Faults & Repair* 2008. Edinburgh, U.K.
- GLOBALSPEC. 2010. Available: <http://www.globalspec.com/>.
- GONZÁLEZ, I. 2011. Study and Application of Modern Bridge Monitoring Techniques.

- GORDON, M. O., HARDY, M. S. A. & GIANNOPOULOS, A. 2001. Semi-intrusive determination of ground penetrating radar wave velocity. *NDT & E International*, 34, 163-171.
- GRANDJEAN, G., GOURRY, J. C. & BITRI, A. 2000. Evaluation of GPR techniques for civil-engineering applications: study on a test site. *Journal of Applied Geophysics*, 45, 141-156.
- GROS, X. E. 2001. *Applications of NDT Data Fusion*. Kluwer Academic Publishers.
- GU, P. & BEAUDOIN, J. J. 2009. Obtaining Effective Half-Cell potential Measurements in reinforced Concrete Structures.
- GUCUNSKI, N., ROMERO, F., KRUSCHWITZ, S., FELDMANN, R. & PARVARDEH, H. 2011. Comprehensive Bridge Deck Deterioration Mapping of Nine Bridges by Nondestructive Evaluation Technologies.
- GUOA. 2011. Optimal sensor placement in structural health monitoring (shm) with a field application on arc bridge.
- GÓMEZ-ORTIZ, D., MARTÍN-CRESPO, T., RODRÍGUEZ, I., SÁNCHEZ, M. J. & MONTOYA, I. 2009. The internal structure of modern barchan dunes of the Ebro River Delta (Spain) from ground penetrating radar. *Journal of Applied Geophysics*, 68, 159-170.
- HACKMANN, G., GUO, W., YAN, G., LU, C. & DYK, S. 2010. *Cyber-Physical Codesign of Distributed Structural Health Monitoring With Wireless Sensor Networks*.
- HADDAD, N. A. 2011. From ground surveying to 3D laser scanner: A review of techniques used for spatial documentation of historic sites. *Journal of King Saud University - Engineering Sciences*, 23, 109-118.
- HAN, Z., LUO, H., CAO, J. & WANG, H. 2011. Acoustic emission during fatigue crack propagation in a micro-alloyed steel and welds. *Materials Science and Engineering: A*, 528, 7751-7756.
- HARTMANN F, KATZ C (2007) *Structural analysis with finite elements*, 2nd edn. Springer, Berlin
- HE, X.-Q., ZHU, Z.-Q., LIU, Q.-Y. & LU, G.-Y. 2009. Review of GPR Rebar Detection. *PIERS Proceedings*. Beijing, China.
- HEJLL ARVID , 2007, "Civil Structural Health Monitoring Strategies, Methods and Applications", PhD Thesis, Luleå University of Technology Department of Civil and Environmental Engineering Division of Structural Engineering
- HIGHWAY, C. F. L. Available: www.cflhd.gov [Accessed 10/03/2010].
- HIGHWAYS AGENCY UK Highways Agency, design manual for roads and bridges, Part 7, BA86/06, Available: www.highways.gov.uk ,2011.

- HING, C. L. 2006. Nondestructive Evaluation of Fiber Reinforced Polymer Bridge Decks Using Ground Penetrating Radar and Infrared Thermography.
- HSIAO, C., CHENG, C.-C., LIOU, T. & JUANG, Y. 2008. Detecting flaws in concrete blocks using the impact-echo method. *NDT & E International*, 41, 98-107.
- HUGENSCHMIDT, J. 2002. Concrete bridge inspection with a mobile GPR system. *Construction and Building Materials*, 16, 147-154.
- HUGENSCHMIDT, J., KALOGEROPOULOS, A., SOLDVIERI, F. & PRISCO, G. 2010. Processing strategies for high-resolution GPR concrete inspections. *NDT & E International*, 43, 334-342.
- HUGENSCHMIDT, J. & MASTRANGELO, R. 2006. GPR inspection of concrete bridges. *Cement and Concrete Composites*, 28, 384-392.
- HUISMAN, J. A., SNEPVANGERS, J. J. J. C., BOUTEN, W. & HEUVELINK, G. B. M. 2002. Mapping spatial variation in surface soil water content: comparison of ground-penetrating radar and time domain reflectometry. *Journal of Hydrology*, 269, 194-207.
- HUSTON, D., HU, J. Q., MASER, K., WEEDON, W. & ADAM, C. 2000. GIMA ground penetrating radar system for monitoring concrete bridge decks. *Journal of Applied Geophysics*, 43, 139-146.
- IAEA 2002. International Atomic Energy Agency. In: SERIES, V. T. C. (ed.).
- IDS Manual, 2010, access: www.idscompany.it (http://www.idscompany.it/upload4/File/BRO_GEO_IBIS_FS_12_REV1.0_LR.pdf)
- IMRAN MUHAMMAD, 2005, Health Monitoring in Proactive Reliability Management of Deteriorating Concrete Bridges, University of Surrey, February 2005
- INTERNATIONAL, A. 1996. The human eye [Online].
- JACOBS LTD., 2010, "Pentagon Road Bridge Visual Inspection Report" 2010
- JASELSKIS, E. J., J, G. & A, B. 2003. Dielectric properties of asphalt pavement. *Journal of Materials in Civil Engineering*.
- JEONGYEUP, P., CHINTALAPUDI, K., GOVINDAN, R., CAFFREY, J. & MASRI, S. 2005. A Wireless Sensor Network for Structural Health Monitoring: Performance and Experience. *Embedded Networked Sensors*, 2005. EmNetS-II. The Second IEEE Workshop on, 1-10.
- JOL, H. M. 2009. *Ground Penetrating Radar: Theory and Applications*, Oxford, Elsevier.
- JUDD, B. 2008. Using Accelerometers in a Data Acquisition System. http://www.ueidaq.com/media/static/apps/appnote-029_accel.pdf.

- JU SHEN-HAW, LIN HUNG-TA, "A finite element model of vehicle–bridge interaction considering braking and acceleration", 2007
- KAZYS, R. & SVILAINIS, L. 1995. Analysis of adaptive imaging algorithms for ultrasonic non-destructive testing. *Ultrasonics*, 33, 19-30.
- KASZYNSKA, P., PARKINSON, J. & FOX, W., 2005. *Re-thinking Neighbourhood Planning*, London:
- RIBA.KEELING, D. J. 2009. Photojournal: Bridging Space and Time around the World. *Focus on Geography*, 52, 56-61.
- KAMAYA, M., 2006. Stress Intensity Factor of Surface Crack with Undulated Front. *JSME International Journal*, Vol. 49(4). 529-535.
- KESSLER, S. S. 2002. Piezoelectric-based in-situ damage detection of composite materials for structural health monitoring systems.
- KIJEWSKI-CORREA, T., DAME, N., HAENGGI, M., HALL, F., ANTSAKLIS, P. & HALL, F. 2006. *Wireless Sensor Networks for Structural Health Monitoring: A Multi-Scale Approach*.
- KIM & LYNCH 2012. Experimental analysis of vehicle–bridge interaction using a wireless monitoring system and a two-stage system identification technique.
- KIM, S., PAKZAD, S., CULLER, D., DEMMEL, J., FENVES, G., GLASER, S. & TURON, M. 2007. *Health Monitoring of Civil Infrastructures Using Wireless Sensor Networks*.
- KIM, W. 2005. *Ground penetrating radar application for non-destructive testing: Bridge deck inspection and dowel bar detection*. Ph.D. Thesis, University of Missouri-Rolla.
- KIMOTO, K., UENO, S. & HIROSE, S. 2006. Image-based sizing of surface-breaking cracks by SH-wave array ultrasonic testing. *Ultrasonics*, 45, 152-164.
- KOCIERZ, R., KURAS, P., OWERKO, T. & ORTY 2011. *Assessment of Usefulness of Radar Interferometer for Measuring Displacements and Deformations of Dams*.
- KOSMATKA, STEVEN H., KERKHOFF, BEATRIX, PANARESE, WILLIAM C., *Design and Control of Concrete Mixtures*, EB001, Portland Cement Association, 2002, 372 pages.
- KOWALIK, A. 2008. *Acoustic Monitoring on the Fred Hartman Bridge*. Bridge Division, Texas Department of Transportation.
- KRAUSE, H. J., WOLF, W., GLAAS, W., ZIMMERMANN, E., FALEY, M. I., SAWADE, G., MATTHEUS, R., NEUDERT, G., GAMPE, U. & KRIEGER, J. 2002. SQUID array for magnetic inspection of prestressed concrete bridges. *Physica C: Superconductivity*, 368, 91-95.

- KRÜGER, M. 2005. Scanning impact-echo techniques for crack depth determination.
- LAGARDE-FOREST, R. 2007. Ground penetrating radar applications in highway structures. passed, University of Portsmouth.
- LAGASSE, P. F., ZEVENBERGEN, L. W., SCHALL, J. D. & CLOPPER, P. E. 2001. HEC 23 Bridge Scour And Stream Instability Countermeasures.
- LAI, W. L., KOU, S. C., POON, C. S., TSANG, W. F. & LAI, C. C. 2010. Characterization of the deterioration of externally bonded CFRP-concrete composites using quantitative infrared thermography. *Cement and Concrete Composites*, 32, 740-746.
- LATASTE, J. F., SIRIEIX, C., BREYSSE, D. & FRAPPA, M. 2003. Electrical resistivity measurement applied to cracking assessment on reinforced concrete structures in civil engineering. *NDT & E International*, 36, 383-394.
- LAWA S.S., J.Q. BU B, X.Q. ZHU A, S.L. CHAN, 2004, " Vehicle axle loads identification using finite element method", 2004
- LECLERC, R. F. & HICKIN, E. J. 1997. The internal structure of scrolled floodplain deposits based on ground-penetrating radar, North Thompson River, British Columbia. *Geomorphology*, 21, 17-25, 29-38.
- LEE, J. W., KIM, J. D., YUN, C. B., YI, J. H. & SHIM, J. M. 2002. HEALTH-MONITORING METHOD FOR BRIDGES UNDER ORDINARY TRAFFIC LOADINGS. *Journal of Sound and Vibration*, 257, 247-264.
- LEE, R.-G., CHEN, K.-C., LAI, C.-C., CHIANG, S.-S., LIU, H.-S. & WEI, M.-S. 2007. A backup routing with wireless sensor network for bridge monitoring system. *Measurement*, 40, 55-63.
- LEELALERKIET, V., KYUNG, J.-W., OHTSU, M. & YOKOTA, M. 2004. Analysis of half-cell potential measurement for corrosion of reinforced concrete. *Construction and Building Materials*, 18, 155-162.
- LESTER, J. & BERNOLD, L. E. 2007. Innovative process to characterize buried utilities using Ground Penetrating Radar. *Automation in Construction*, 16, 546-555.
- LIMITED, I. 2010. Available: <http://www.idscompany.it>.
- LINDSAY, A. 2005. Accelerometer - Getting Started.
- LIU, M., FRANGOPOL, D.M., AND KIM, S. (2009). "Bridge safety evaluation based on monitored live load effects," *Journal of Bridge Engineering*, ASCE, 14(4), 257-269.
- LOIZOS, A. & PLATI, C. 2007. Accuracy of pavement thicknesses estimation using different ground penetrating radar analysis approaches. *NDT & E International*, 40, 147-157.

- LOULIZI, A. 2001. Development of Ground Penetrating Radar Signal Modeling and Implementation for Transportation Infrastructure Assessment.
- LUBOWIECKA, I., ARMESTO, J., ARIAS, P. & LORENZO, H. 2009. Historic bridge modelling using laser scanning, ground penetrating radar and finite element methods in the context of structural dynamics. *Engineering Structures*, 31, 2667-2676.
- LU Z.R., LIU J.K., 2011 "Identification of both structural damages in bridge deck and vehicular parameters using measured dynamic responses", 2011
- LYNCH, J. P. & LOH, K. J. 2006. A Summary Review of Wireless Sensors and Sensor Networks for Structural Health Monitoring.
- LYNCH, J. P., PARTRIDGE, A., LAW, K. H., KENNY, T. W., KIREMIDJIAN, A. S. & CARRYER, E. 2003. Design of Piezoresistive MEMS-Based Accelerometer for Integration with Wireless Sensing Unit for Structural Monitoring.
- MARTIN, J., BROUGHTON, K. J., GIANNOPOLOUS, A., HARDY, M. S. A. & FORDE, M. C. 2001. Ultrasonic tomography of grouted duct post-tensioned reinforced concrete bridge beams. *NDT & E International*, 34, 107-113.
- MAGIC DRAGON MULTIMEDIA WWW.MAGICDRAGON.COM.2010
- MANACORDA, GUIDO, Alessandro Simi1 and Mario Miniati "Mapping Underground Assets with Fully Innovative Gpr Hardware And Software Tools", 2009 Paper D-5-04
- MASER, K. R. 2009. Integration of Ground Penetrating Radar and Infrared Thermography for Bridge Deck Condition Evaluation. *NDTCE'09, Non-Destructive Testing in Civil Engineering*. Nantes, France.
- MAURYA, D. M., GOYAL, B., PATIDAR, A. K., MULCHANDANI, N., THAKKAR, M. G. & CHAMYAL, L. S. 2006. Ground Penetrating Radar imaging of two large sand blow craters related to the 2001 Bhuj earthquake, Kachchh, Western India. *Journal of Applied Geophysics*, 60, 142-152.
- MAYER, L., YANEV, B., OLSON, L. D. & SMYTH, A. 2009. Monitoring of the Manhattan Bridge for Vertical and Torsional Performance with GPS and Interferometric Radar Systems.
- MAWSON B R and LARK R J, 2009, Newport Transporter Bridge - An historical perspective, Institution of Civil Engineers, February 2009
- MALÅ Geoscience, WWW.MALAGS.COM.2010
- MCCANN, D. M. & FORDE, M. C. 2001. Review of NDT methods in the assessment of concrete and masonry structures. *NDT & E International*, 34, 71-84.

- MCMECHAN, G. A., LOUCKS, R. G., ZENG, X. & MESCHER, P. 1998. Ground penetrating radar imaging of a collapsed paleocave system in the Ellenburger dolomite, central Texas. *Journal of Applied Geophysics*, 39, 1-10.
- MEHTA, K. P. 2005. *Concrete: Microstructure, Properties, and Materials*.
- MENG, X., GOGOI, N., DODSON, A. H., ROBERTS, G. W. & BROWN, J. 2011. Using Multi-constellation GNSS and EGNOS for Bridge Deformation Monitoring.
- MINES, W. A. Ground penetrating Radar [Online]. Available: <http://www.wiki-against-mines.org> [Accessed 05/03/2010].
- MISTRASGROUP. 2011. Total Asset Protection Solutions for Structural Testing & Monitoring of Bridges [Online]. Available: www.mistrasgroup.com.
- MEGGITT SENSING SYSTEMS, WWW.WILCOXON.COM.,2012
- MISTRAS Group, WWW.PACNDT.COM. 2010
- MONDORF, P. E. 2006. *Concrete Bridges*, London and New York, Taylor & Francis.
- MORGANTI, F., CARASSA, A. & GEMINIANI, G. 2007. Planning optimal paths: A simple assessment of survey spatial knowledge in virtual environments. *Computers in Human Behavior*, 23, 1982-1996.
- MORI, K., SPAGNOLI, A., MURAKAMI, Y., KONDO, G. & TORIGOE, I. 2002. A new non-contacting non-destructive testing method for defect detection in concrete. *NDT & E International*, 35, 399-406.
- MOSCHAS, F. & STIROS, S. 2011. Measurement of the dynamic displacements and of the modal frequencies of a short-span pedestrian bridge using GPS and an accelerometer. *Engineering Structures*, 33, 10-17.
- NAGAYAMA, T., USHITA, M. & FUJINO, Y. 2011. Suspension Bridge Vibration Measurement Using Multihop Wireless Sensor Networks. *Procedia Engineering*, 14, 761-768.
- NASA, WWW.NASA.GOV.,2010
- NAIR, A. & CAI, C. S. 2010. Acoustic emission monitoring of bridges: Review and case studies. *Engineering Structures*, 32, 1704-1714.
- NARAYANAN, R. M., JAKUB, J. W., LI, D. & ELIAS, S. E. G. 2004. Railroad track modulus estimation using ground penetrating radar measurements. *NDT & E International*, 37, 141-151.
- NEAL, A. 2004. *Ground-penetrating radar and its use in sedimentology: principles, problems and progress*. *Earth-Science Reviews*, 66, 261-330.
- NEILD, S. A. (2001). *Using non-linear vibration techniques to detect damage in concrete bridges*. DPhil. University of Oxford., 2001

- NEWMAN, J. C., JR., AND RAJU, I. S., 1979. Analysis of Surface Cracks in Finite Plates under Tension or Bending Loads. NASA Technical Paper 1578. National Aeronautics and Space Administration.
- NDT Education Resource Center, WWW.NDT-ED.ORG., 2010
- NIXON, R. D. V., SWEENEY, L., ERICKSON, D. B., & Touyz, S. W. (2003). Parent-child interaction therapy: a comparison of standard and abbreviated treatments for oppositional defiant preschoolers. *Journal of Consulting and Clinical Psychology*, 71, 251-260.
- NGUYEN, D.A. (2006), Bridge aeroelastic analysis in the frequency domain (no submission)
- OLHOEFT, G. R. 2000. Maximizing the information return from ground penetrating radar. *Journal of Applied Geophysics*, 43, 175-187.
- OLHOEFT, G. R. & SMITH III, S. S. 2000. Automated processing and modeling of GPR data for pavement thickness and properties. In: GOLD COAST, A., MAY, D. A. N., G. F. STICKLEY & D. LONGSTAFF (eds.) GPR2000, Proc. Of the 8th Int'l Conference on Ground Penetrating Radar. North Salem, NH, USA.
- PADMARAJAIAH, S.K. AND RAMASWAMY, A., 2002. A finite element assessment of flexural strength of pre-stressed concrete beams with fiber reinforcement, *Cement and Concrete Composites*, Vol. 24. 229-241.
- PAN, N.-F., LIN, T.-C. & PAN, N.-H. 2009. Estimating bridge performance based on a matrix-driven fuzzy linear regression model. *Automation in Construction*, 18, 578-586.
- PARK, H. S., LEE, H. M., ADELI, H. & LEE, I. 2007. A New Approach for Health Monitoring of Structures: Terrestrial Laser Scanning. *Computer-Aided Civil and Infrastructure Engineering*, 22, 19-30.
- PARRILLO, R. & ROBERTS, R. 2006. Bridge Deck Condition Assessment using Ground Penetrating Radar. ECNDT Geophysical Survey Systems. North Salem, NH, USA.
- PARAMESWARAN, LAKSHMY; RAM KUMAR; AND G. K. SAHU, 2008, Effect of Carbonation on Concrete Bridge Service Life, ASCE1084-0702, 2008
- PEARSON-KIRK, D., CROKE, K. S. & CAIRNS, R. J. M. 2005. Cost Effective condition monitoring of concrete bridges. *Current and future trends in bridge design, construction and maintenance 4*. London: Thomas Telford.
- PHARES, B. M., D.D.ROLANDER, B.A.GRAYBEAL & G.A.WASHER 2000. Studying the Reliability of Bridge Inspection. *National Bridge Inspection Standards*.
- PIERACCINI, M., FRATINI, M., PARRINI, F., ATZENI, C. & BARTOLI, G. 2008. Interferometric radar vs. accelerometer for dynamic monitoring of large structures: An experimental comparison. *NDT & E International*, 41, 258-264.

- PORTO, F. D., VALLUZZI, M. R. & MODENA, C. 2003. Use of sonic tomography for the diagnosis and the control of intervention in historic masonry buildings.
- PRINE, D. W. 2008. Application of Acoustic, Strain, and Optical Sensors to NDE of Steel Highway Bridges. Sensors Expo Conference, 16 May 1995, BIRL Industrial Research Laboratory, Northwestern University.
- PÉREZ-GRACIA, V., CASELLES, O., CLAPÉS, J., OSORIO, R., CANAS, J. A. & PUJADES, L. G. 2009a. Radar exploration applied to historical buildings: A case study of the Marques de Llió palace, in Barcelona (Spain). *Engineering Failure Analysis*, 16, 1039-1050.
- PÉREZ-GRACIA, V., DI CAPUA, D., GONZÁLEZ-DRIGO, R. & PUJADES, L. 2009b. Laboratory characterization of a GPR antenna for high-resolution testing: Radiation pattern and vertical resolution. *NDT & E International*, 42, 336-344.
- R.J.COPE 1987. CONCRETE BRIDGE ENGINEERING Performance and Advances.
- RADAR(GPR), M. G. L. I. G. P. Available: www.malags.com [Accessed 12/04/2010].
- RASHIDI, MARIA; PETER GIBSON, 2011, Proposal of a Methodology for Bridge Condition Assessment Australasian Transport Research Forum 2011
- REN, W. X., AND CHEN, H. B. (2010). "Finite element model updating in structural dynamics by using response surface method." *Eng. Struct.*, 32(8), 2455–2465.
- RHAZI, J., DOUS, O., BALLIVY, G., LAURENS, S. & BALAYSSAC, J. P. 2003. Non destructive health evaluation of concrete bridge decks by GPR and half cell potential techniques. 6th International Conference on Nondestructive Testing in Civil Engineering. Berlin.
- RHEE H. C. AND SALAMA, M. M., 1987. Mixed-Mode Stress Intensity Factor Solutions of a Warped Surface Flaw by Three-Dimensional Finite Element Analysis. *Engineering Fracture Mechanics*. Vol. 28-2. 203-209.
- RIVEIRO, B., MORER, P., ARIAS, P. & DE ARTEAGA, I. 2011. Terrestrial laser scanning and limit analysis of masonry arch bridges. *Construction and Building Materials*, 25, 1726-1735.
- RATEDESI, WWW.RATEDESI.COM. ,2010
- ROBERTS, G. W., MENG, X., BROWN, C. J. & DALLARD, P. 2006. GPS Measurements on the London Millennium Bridge. *ICE Bridge Engineering Journal*, 159(BE4), 153-161.
- RON BONNER. (7th of November 2010 and 11th of March 2012). Structural Engineer, from IBIS-S Survey. Medway City Council, Medway, Kent, [7th of November 2010 and 11th of March 2012].
- ROMERO, F. & ROBERTS, R. 2004. Data Collection and Analysis Challenges – GPR Bridge Deck Deterioration Assessment of Two Unique Bridge Deck Systems.

- RYALL, M. J.; G. A. R. PARKE, J. E. HARDING (2000). The Manual of Bridge Engineering. Thomas Telford. pp. 15. ISBN 0-7277-2774-5.
- SAARENKETO, T. 2006. Electrical properties of road materials and subgrade soils and the use of ground penetrating radar in traffic infrastructure surveys.
- SAARENKETO, T. & SCULLION, T. 2000. Road evaluation with ground penetrating radar. Journal of Applied Geophysics, 43, 119-138.
- SARKAR, T. K., MAILLOUX, R. J., OLINER, A. A., SALAZAR-PALMA, M. & SENGUPTA, D. L. 2006. Historical German Contributions to Physics and Applications of Electromagnetic Oscillations and Waves, John Wiley & Sons, Inc.
- SEVIM BARIS- ALEMDAR BAYRAKTAR, AHMET CAN ALTUNISIK, SEZER ATAMTURKTUR, FATMABIRINCI, 2011, Finite element model calibration effects on the earthquake response of masonry arch bridges, Finite Elements in Analysis and Design, 2011
- SCHLUNE HENDRIK, MARIO PLOS, KENT GYLLTOFT, Improved bridge evaluation through finite element model updating using static and dynamic measurements, 2009
- SCHROTT, L. & SASS, O. 2008. Application of field geophysics in geomorphology: Advances and limitations exemplified by case studies. Geomorphology, 93, 55-73.
- SCOTT, M., REZAIZADEH, A., DELAHAZA, A., SANTOS, C. G., MOORE, M., GRAYBEAL, B. & WASHER, G. 2003. A comparison of nondestructive evaluation methods for bridge deck assessment. NDT & E International, 36, 245-255.
- SCOTT, M. L. 1999. Automated Characterization of Bridge Deck Distress Using Pattern Recognition Analysis of Ground Penetrating Radar Data. State University.
- SCHLUNE, H., PLOS, M. & GYLLTOFT, K. (2011) Safety formats for nonlinear analysis tested on concrete beams subjected to shear forces and bending moments. Engineering Structures, 33, 8. pp. 2350-2356.
- SHIN, H. & GRIVAS, D. 2003. How Accurate is Ground Penetrating Radar (GPR) for Bridge Condition Assessment.
- SISON, M., J.C. DUKE, J., CLEMENÁ, G. & LOZEV, M. G. 2008. Acoustic Emission: A Tool for the Bridge Engineer. The American Society for Non-Destructive Testing.
- SPENCER, F. W. 1996. Visual Inspection Research Project Report on Benchmark Inspections.
- SRITHARAN S., M.J. NIGEL PRIESTLEY", Frieder Seible, Nonlinear Finite element analyses of concrete bridge joint systems subjected to seismic actions Finite Elements in Analysis and Design 36 (2000) 215}233

- SUSSMANN, T. R., SELIG, E. T. & HYSLIP, J. P. 2003. Railway track condition indicators from ground penetrating radar. *NDT & E International*, 36, 157-167.
- TAYLOR, R. L., BERESFORD, P. J. AND WILSON, E. L., 1976. A Non-Conforming Element for Stress Analysis. *International Journal for Numerical Methods in Engineering*. Vol. 10. 1211-1219.
- TANG, P. & AKINCI, B. 2012. Formalization of workflows for extracting bridge surveying goals from laser-scanned data. *Automation in Construction*, 22, 306-319.
- THUMM, M. 2006. HISTORICAL GERMAN CONTRIBUTIONS TO PHYSICS AND APPLICATIONS OF ELECTROMAGNETIC OSCILLATIONS AND WAVES. Forschungszentrum Karlsruhe, Association EURATOM-FZK, 1-23.
- TRADER, B. 2011. Pile restoration of the lake pontchartrain causeway world's longest bridge.
- UPPAL, A. S. 2000. Monitoring Bridge Components Using Acoustic Emissions. *Railway Track and Structures*.
- U.S. Department of Transportation, WWW.CFLHD.GOV., 2010
- VANDENBERGHE, J. & VAN OVERMEEREN, R. A. 1999. Ground penetrating radar images of selected fluvial deposits in the Netherlands. *Sedimentary Geology*, 128, 245-270.
- VAGHEFI KHATEREH; RENEE C. OATS; DEVIN K. HARRIS, A.M.ASCE; THERESA (TESS) M. AHLBORN, M.ASCE; COLIN N. BROOKS; K. ARTHUR ENDSLEY; CHRISTOPHER ROUSSI; ROBERT SHUCHMAN; JOSEPH W. BURNS; AND RICHARD DOBSON¹, 2012, Evaluation of Commercially Available Remote Sensors for Highway Bridge Condition Assessment, 10.1061/(ASCE)BE.1943-5592.0000303. , 2012 American Society of Civil Engineers.
- WADE, J. D. 2010. Magnetic Sensor for Nondestructive Evaluation of Deteriorated Prestressing Strand.
- WANG XIANG QIU, ZHI GUO ZHOU, YU HONG ZHANG, 2010, " Non-Linear FEM Analysis for the Layered Rock-Mass Tunnel Based on the Twin Shear Strength Criterion" *Advanced Materials Research (Volumes 168 - 170)*
- WILSON, E. L., TAYLOR, R. L., DOHERTY, W. P., AND GHABOUSSI, J., 1973. Incompatible Displacement Models. *Numerical and Computer Methods in Structural Mechanics*. Edited by S. J. Fenves, et al. Academic Press, Inc. N. Y. and London. 43-57.
- WILLAM, K. J. AND WARNKE, E. D. (1975), Constitutive Model for the Triaxial Behavior of Concrete, *Proceedings, International Association for Bridge and Structural Engineering*, Vol. 19, ISMES, Bergamo, Italy, p. 174.
- WALKER, R. (2010) "Issues current UK bridges, Seminar on Assessment and Maintenance of Concrete Highway Bridges, UK, April, 2000

-
- WHELAN, M. J., GANGONE, M. V. & JANOYAN, K. D. 2009. Highway Bridge Assessment Using an Adaptive Real-Time Wireless Sensor Network. *Sensors Journal, IEEE*, 9, 1405-1413.
- WHELAN, M. J., GANGONE, M. V., JANOYAN, K. D., CROSS, K. & JHA, R. 2007. Reliable High-Rate Bridge Monitoring using Dense Wireless Sensor Arrays.
- WOODWARD, R. J. 1989. Non destructive testing methods for concrete bridges. In: 25, T. R. R. (ed.).
- WORLDWIDE, A. I. S. Available: www.astm.org [Accessed 10.02.2010].
- XIA, J., FRANSEEN, E. K., MILLER, R. D. & WEIS, T. V. 2004. Application of deterministic deconvolution of ground-penetrating radar data in a study of carbonate strata. *Journal of Applied Geophysics*, 56, 213-229.
- YU, J., ZIEHL, P., ZÁRATE, B. & CAICEDO, J. 2011a. Prediction of fatigue crack growth in steel bridge components using acoustic emission. *Journal of Constructional Steel Research*, 67, 1254-1260.
- YU, L., SEPANDARMAZMOMENI, GODINEZ, V., GIURGIUTIU, V., ZIEHL, P. & YU, J. 2011b. Dual Mode Sensing with Low-Profile Piezoelectric Thin Wafer Sensors for Steel Bridge Crack Detection and Diagnosis.
- YUYAMA, S., YOKOYAMA, K., NIITANI, K., OHTSU, M. & UOMOTO, T. 2007. Detection and evaluation of failures in high-strength tendon of prestressed concrete bridges by acoustic emission. *Construction and Building Materials*, 21, 491-500.
- ZHOU X., Rheological behaviors of the fresh SFRCC extrudate: experimental, theoretical and numerical investigations, Ph.D. thesis, Hong Kong University of Science and Technology, Hong Kong, 2004.
- ZHU, Z., GERMAN, S. & BRILAKIS, I. 2010. Detection of large-scale concrete columns for automated bridge inspection. *Automation in Construction*, 19, 1047-1055.

APPENDIX A

IBIS-S INTERFEROMETRIC MONITORING RESULTS

This appendix presents the complete set of the data analyses of the IBIS-S interferometric monitoring results for the main case study, Pentagon Road Bridge under the dynamic loading of a cherry picker. These assessments were undertaken in November 2010 with 20 MHz antenna and March 2012 where two different frequencies of antenna 20 MHz and 200 MHz were applied.

Below the Figures A.1 to A.36 present the results for the maximum deflection under dynamic loading of the surveys which were undertaken.

As can be seen from figures A.3 to A.38 the direction of displacement has been normalized to the negative direction only for ease of comparison. Initially, the displacement took place in two directions both the negative and the positive.

Both antenna show similar results for deflection across the bridge deck increasing the confidence in the reliability of this antenna through enhanced reliability.

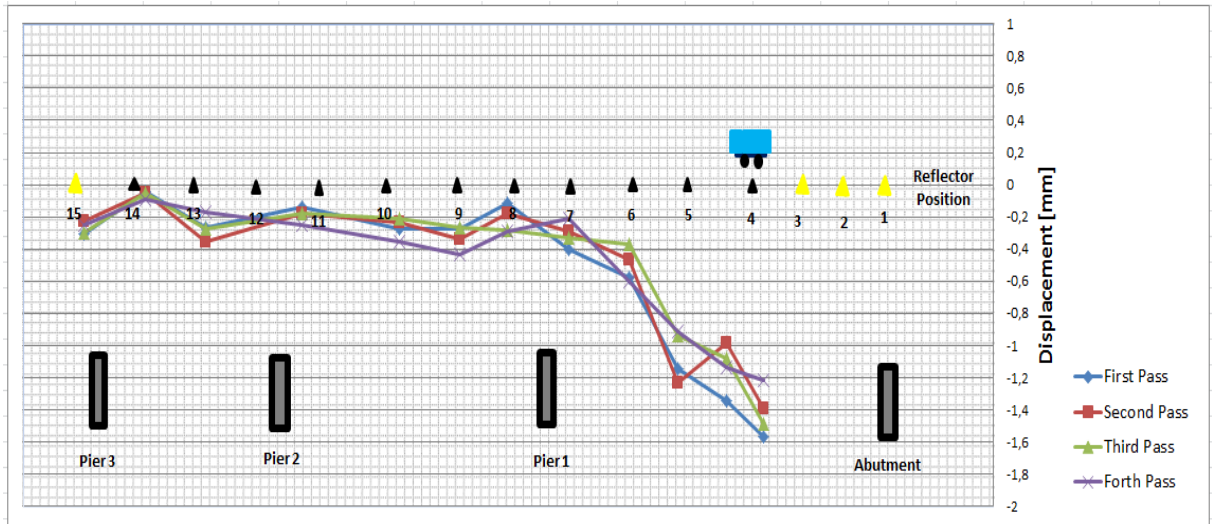


Figure A.1 – IBIS-S 7th November 2010 20 MHz Monitoring Results

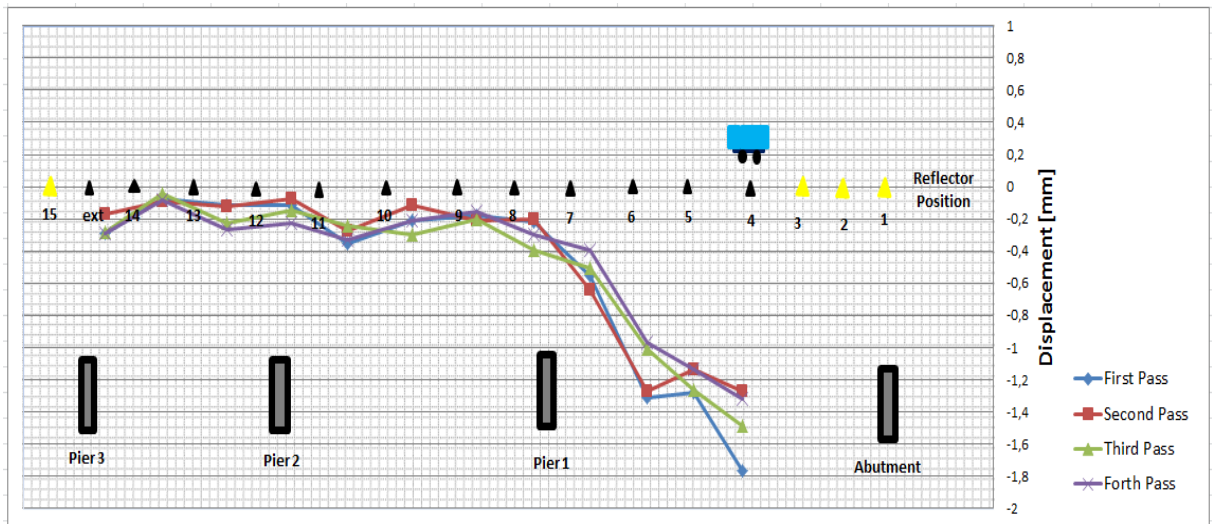


Figure A.2 – IBIS-S 11th of March 2012 20 MHz Monitoring Results

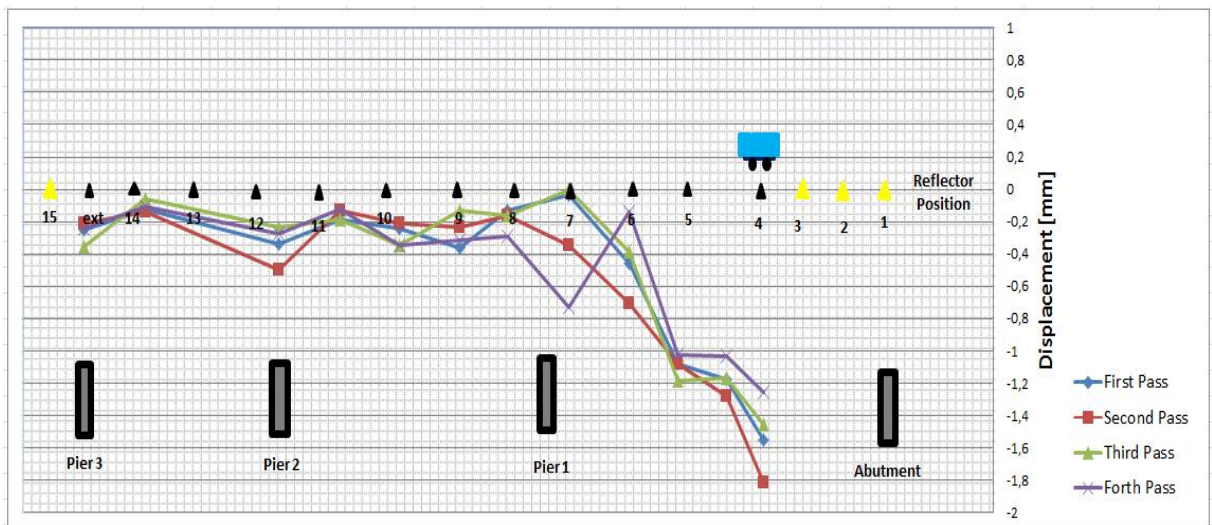


Figure A.3 – IBIS-S 11th of March 2012 200 MHz Monitoring Results

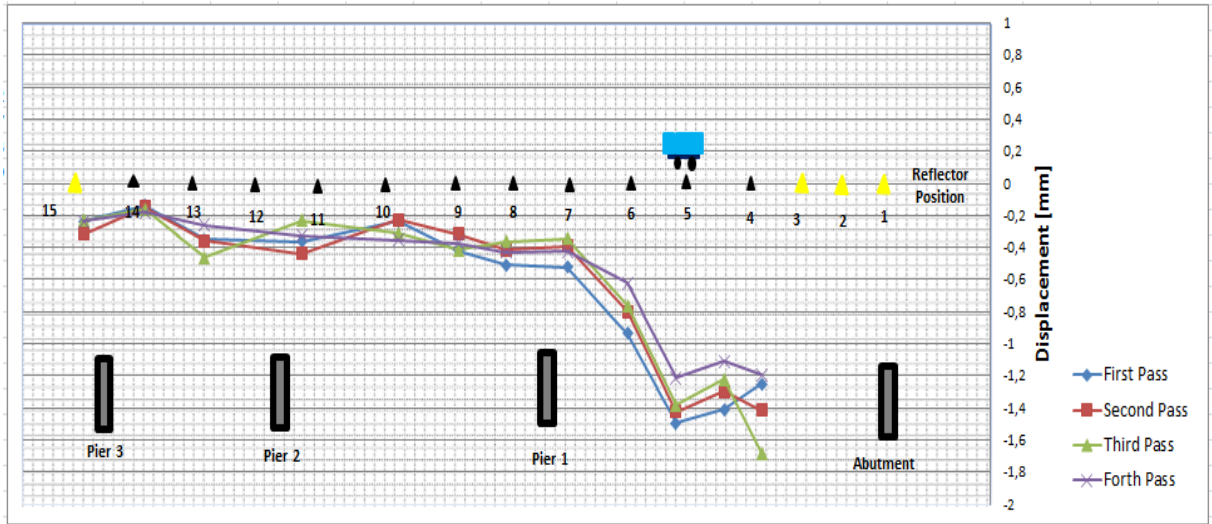


Figure A.4 – IBIS-S 7th November 2010 20 MHz Monitoring Results

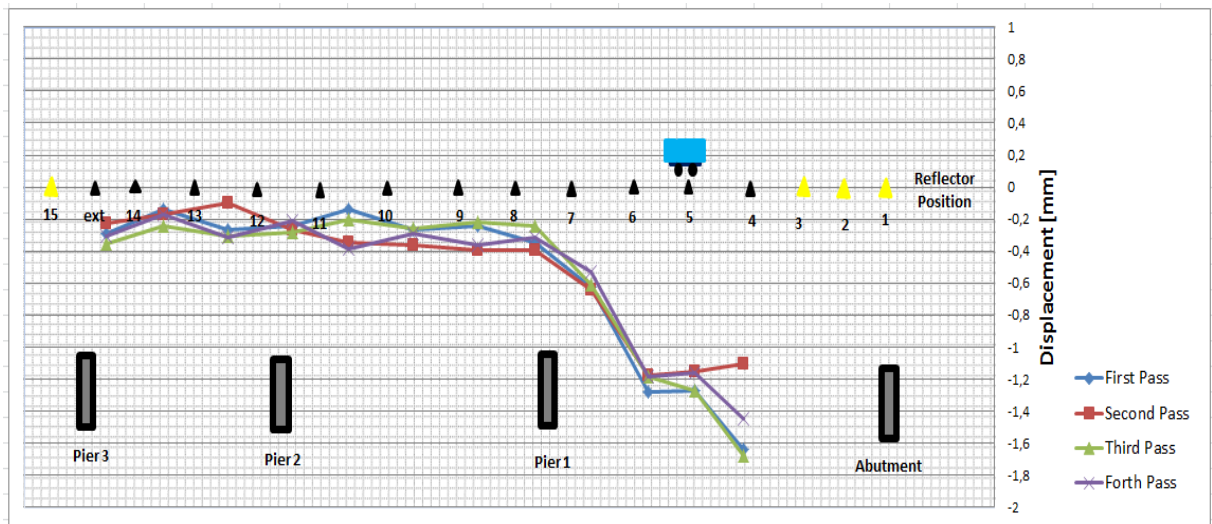


Figure A.5 – IBIS-S 11th of March 2012 20 MHz Monitoring Results

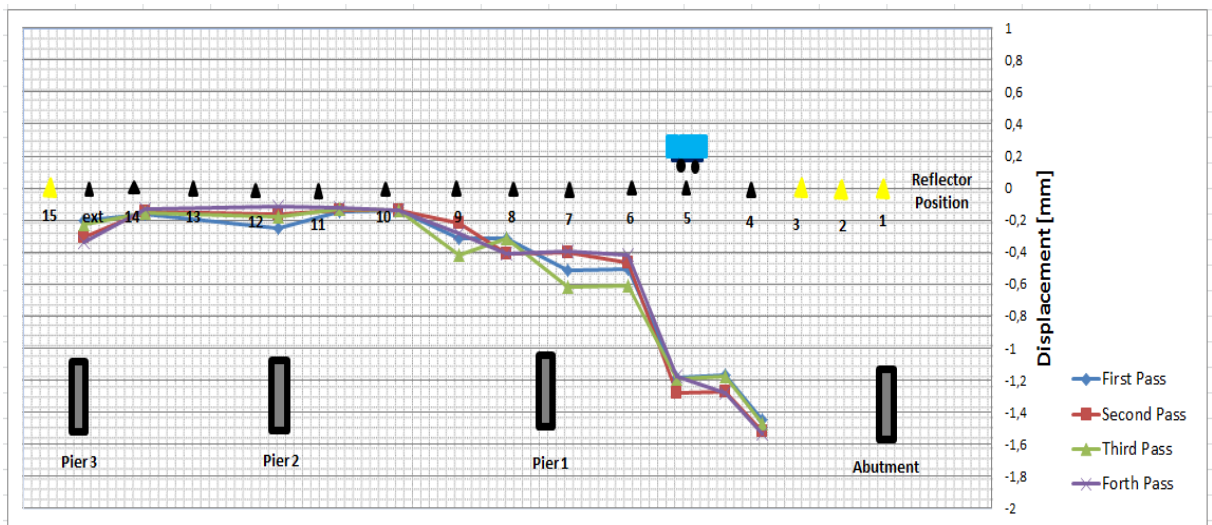


Figure A.6 – IBIS-S 11th of March 2012 200 MHz Monitoring Results

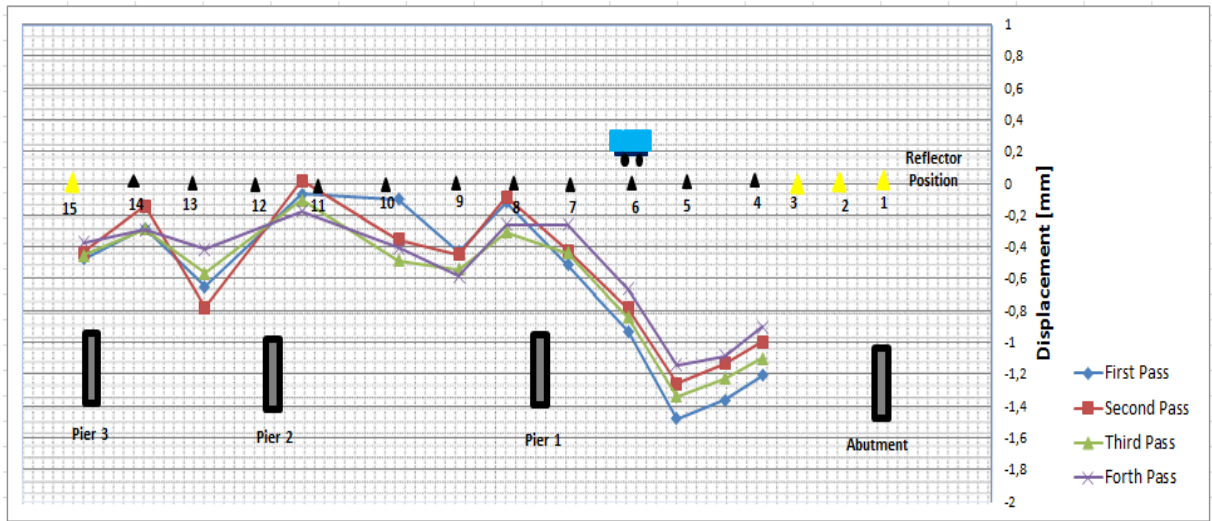


Figure A.7 – IBIS-S 7th November 2010 20 MHz Monitoring Results

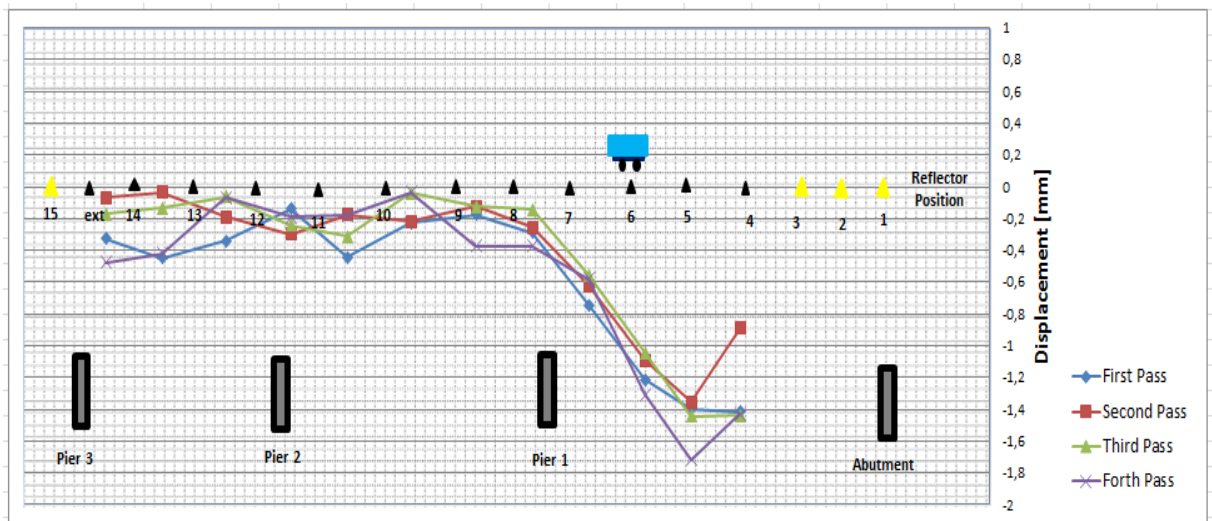


Figure A.8 – IBIS-S 11th of March 2012 20 MHz Monitoring Results

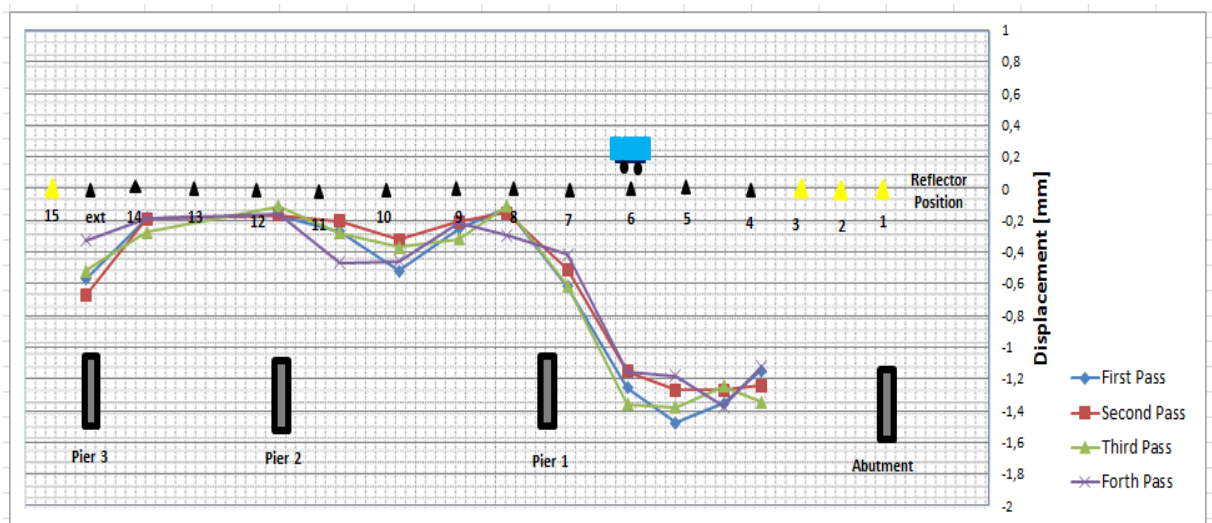


Figure A.9 – IBIS-S 11th of March 2012 200 MHz Monitoring Results

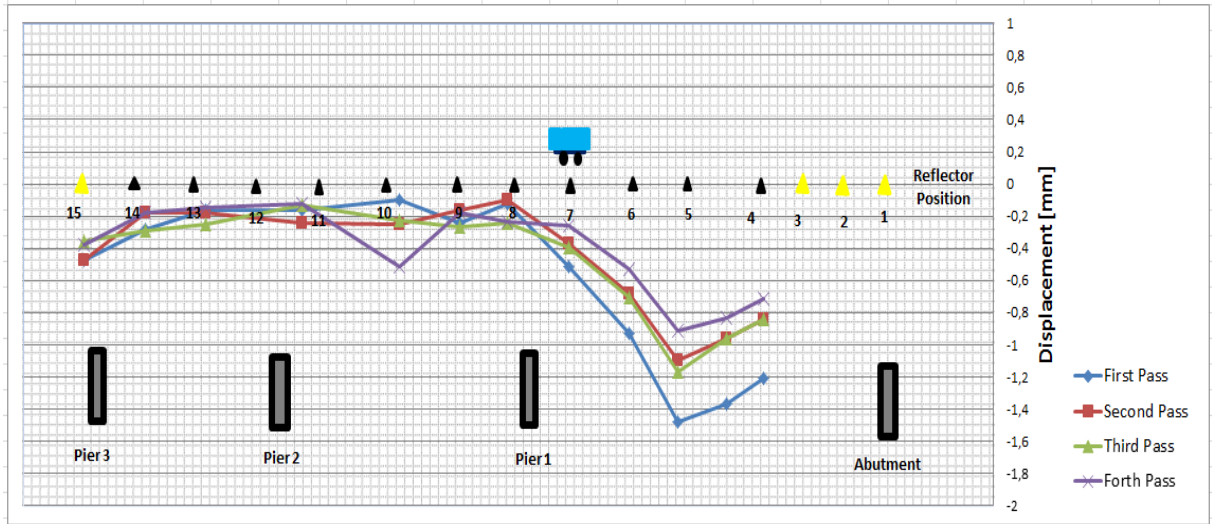


Figure A.10 – IBIS-S 7th November 2010 20 MHz Monitoring Results

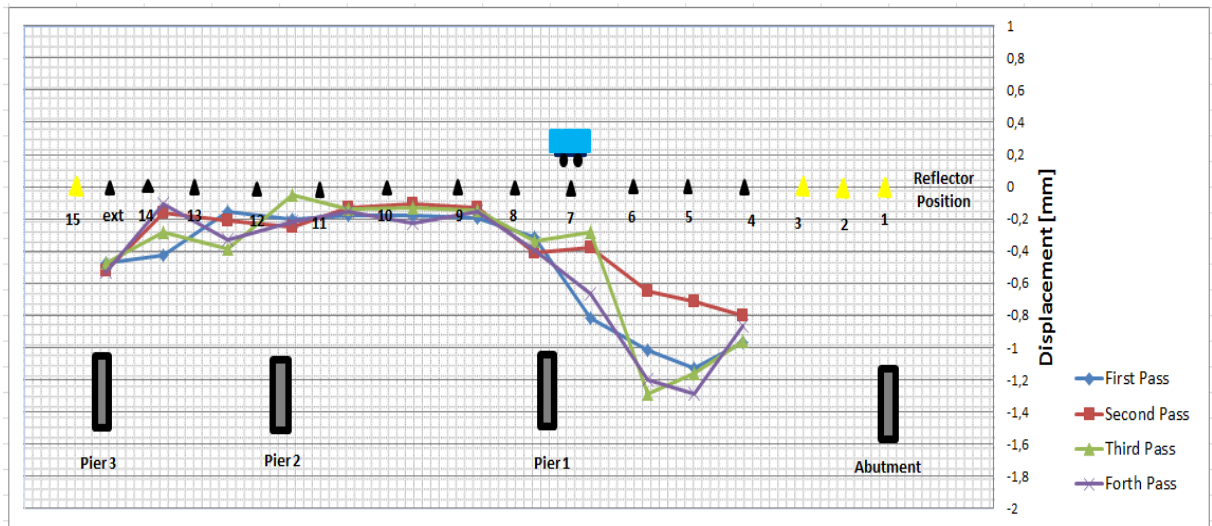


Figure A.11 – IBIS-S 11th of March 2012 20 MHz Monitoring Results

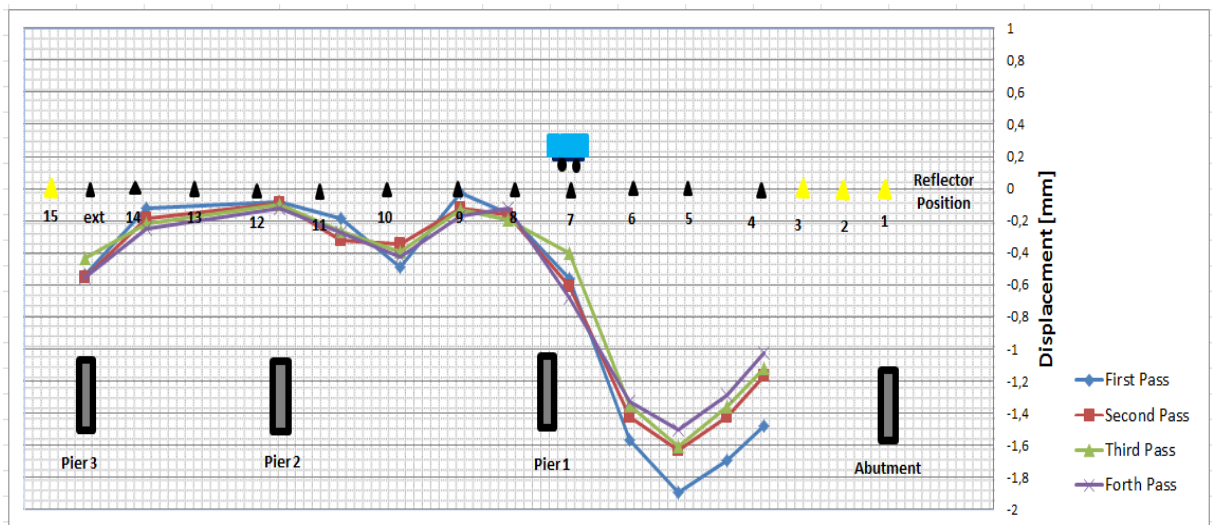


Figure A.12 – IBIS-S 11th of March 2012 200 MHz Monitoring Results

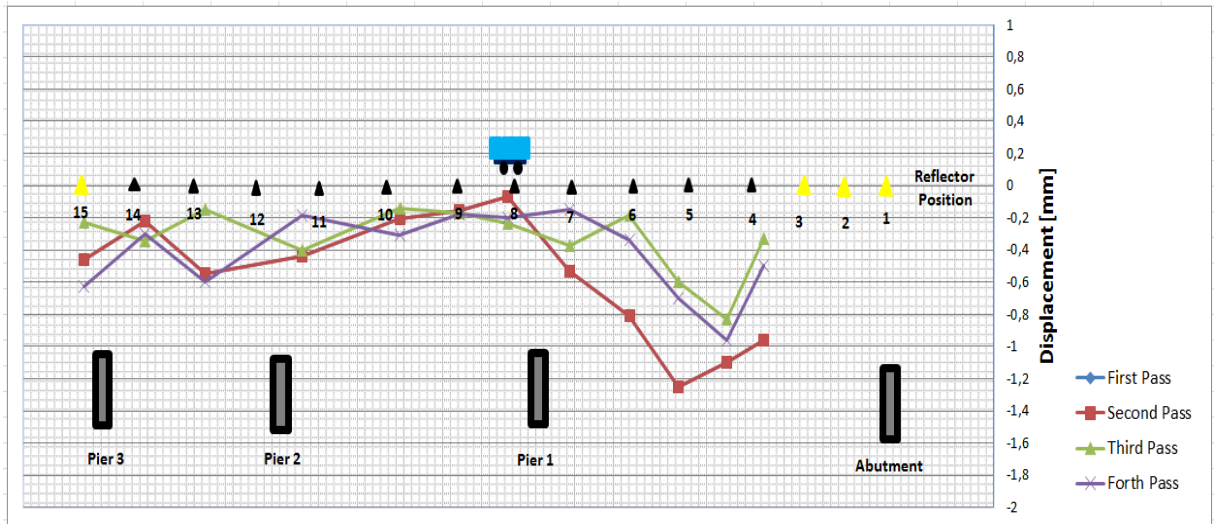


Figure A.13 – IBIS-S 7th November 2010 20 MHz Monitoring Results

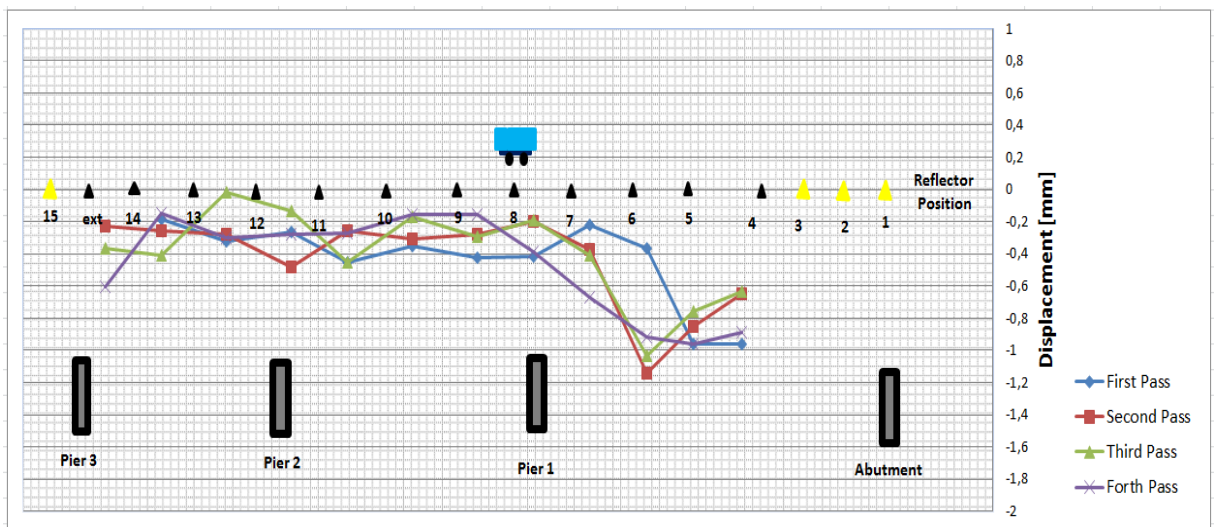


Figure A.14 – IBIS-S 11th of March 2012 20 MHz Monitoring Results

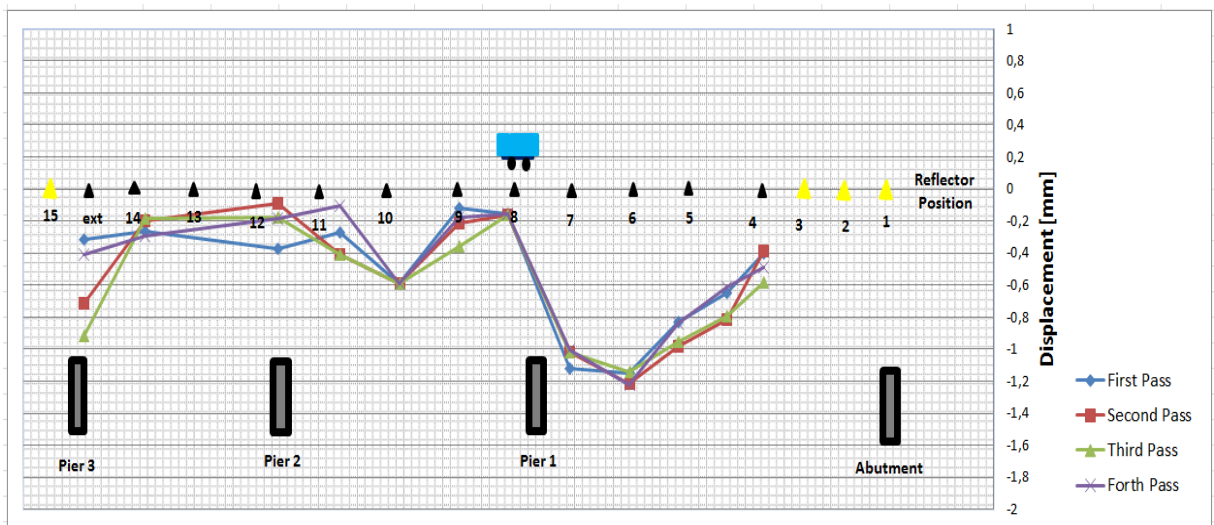


Figure A.15 – IBIS-S 11th of March 2012 200 MHz Monitoring Results

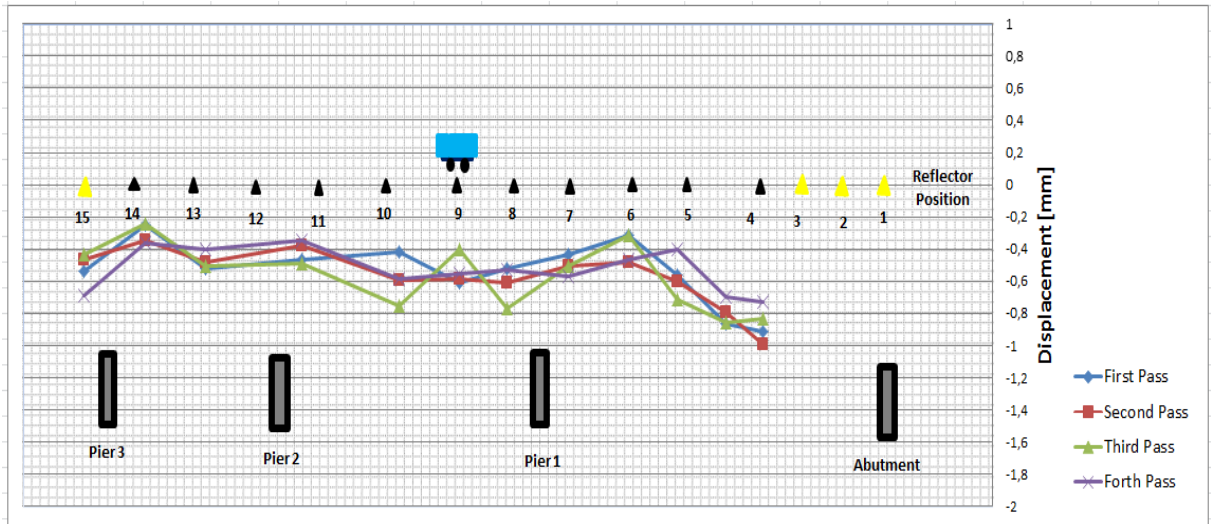


Figure A.16 – IBIS-S 7th November 2010 20 MHz Monitoring Results

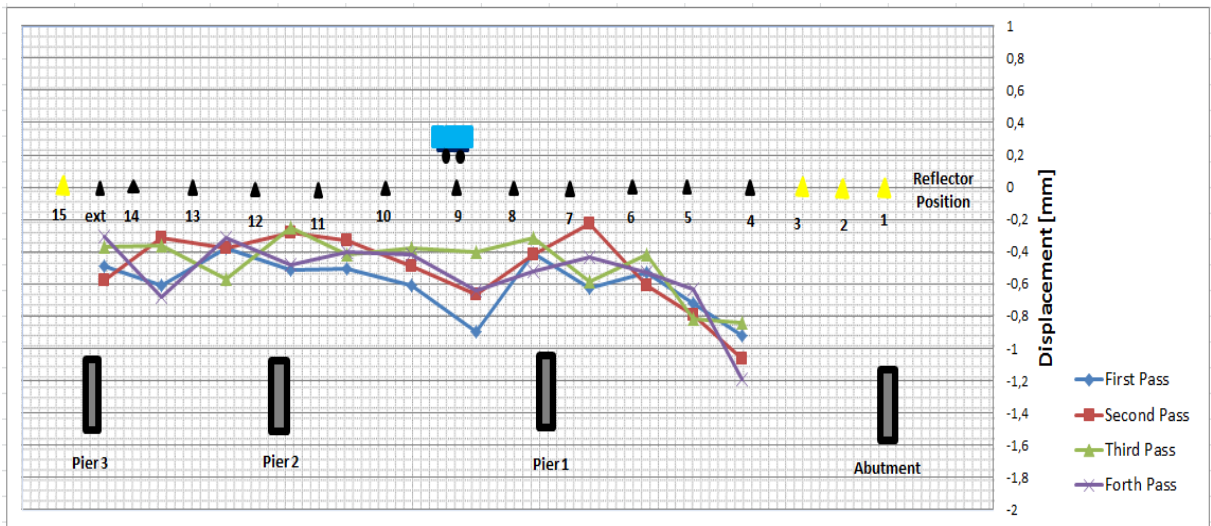


Figure A.17 – IBIS-S 11th of March 2012 20 MHz Monitoring Results

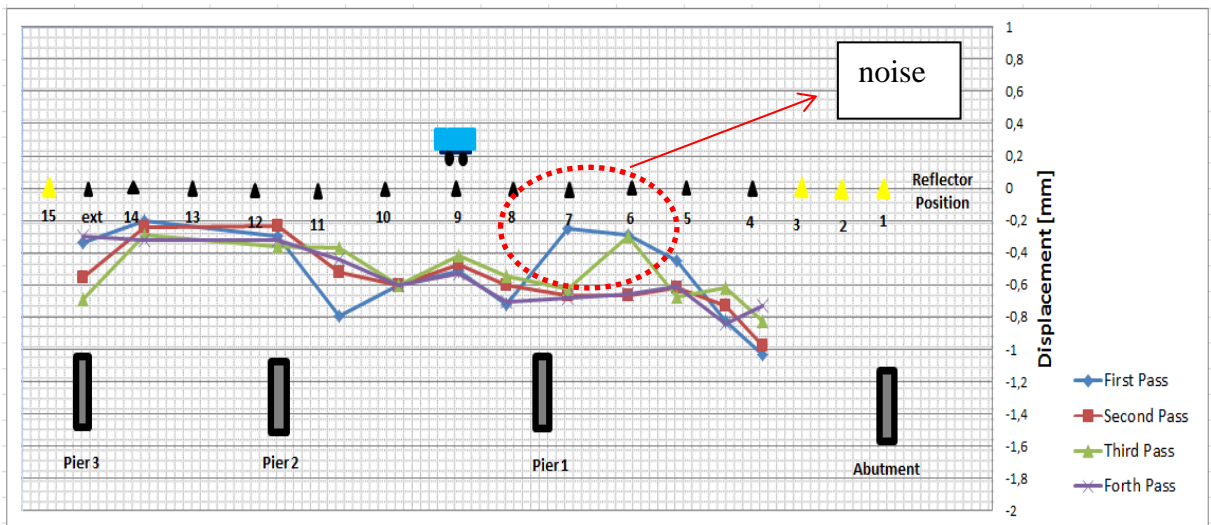


Figure A.18 – IBIS-S 11th of March 2012 200 MHz Monitoring Results

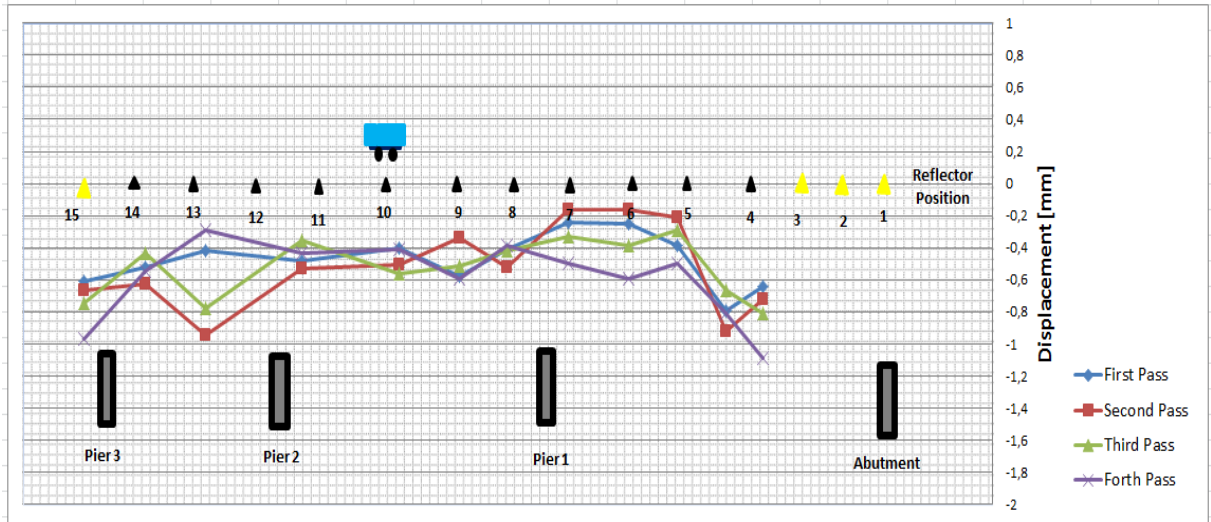


Figure A.19 – IBIS-S 7th November 2010 20 MHz Monitoring Results

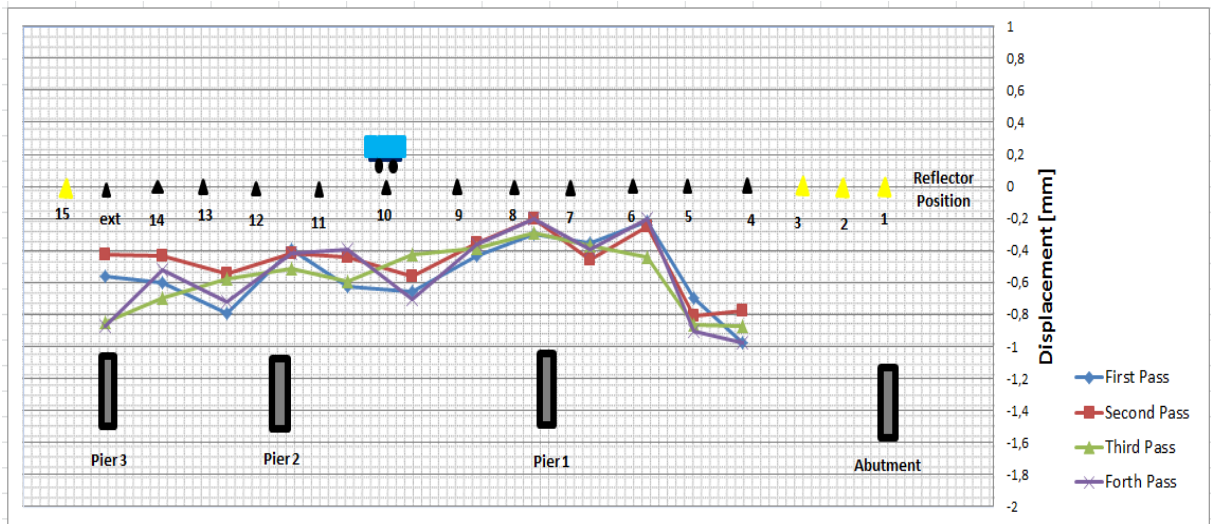


Figure A.20 – IBIS-S 11th of March 2012 20 MHz Monitoring Results

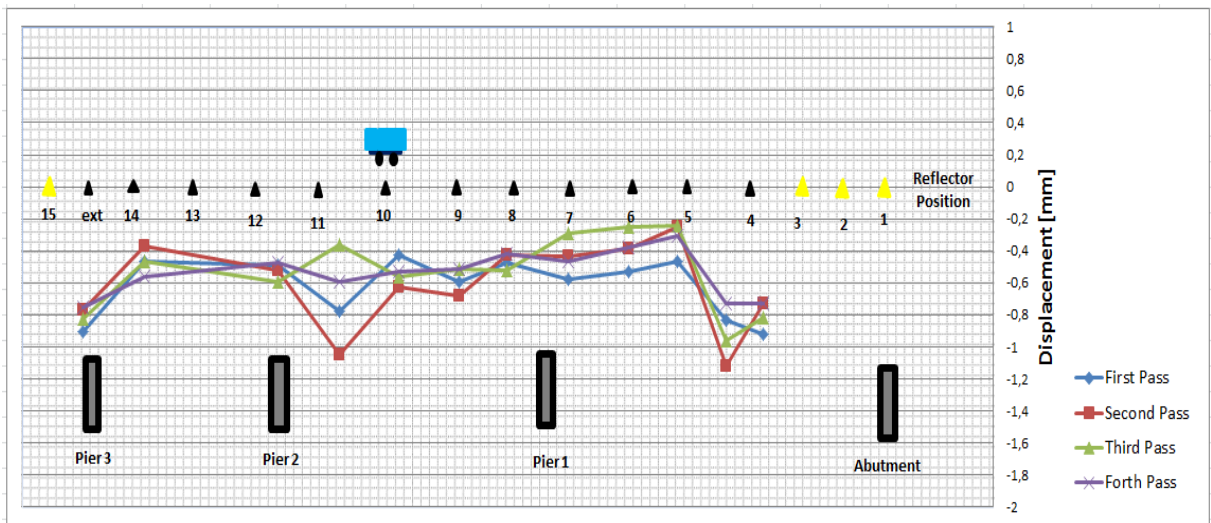


Figure A.21 – IBIS-S 11th of March 2012 200 MHz Monitoring Results

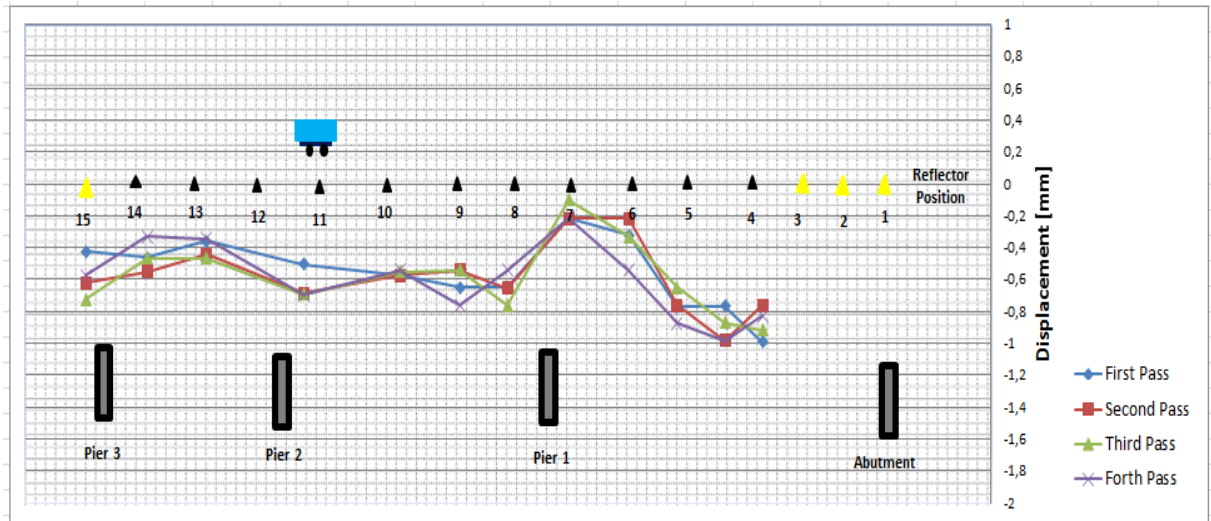


Figure A.22 – IBIS-S 7th November 2010 20 MHz Monitoring Results

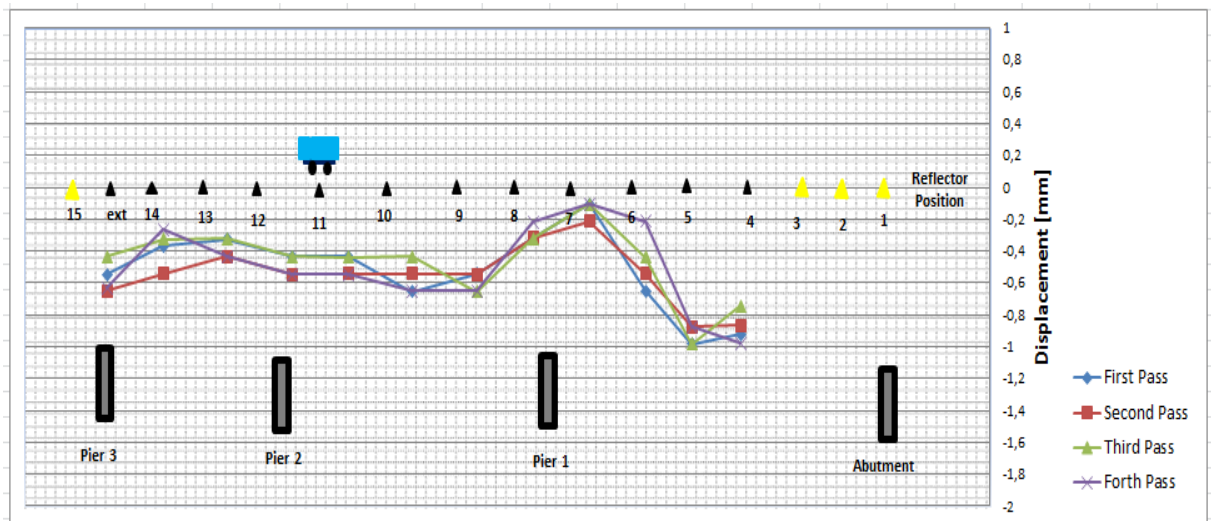


Figure A.23 – IBIS-S 11th of March 2012 20 MHz Monitoring Results

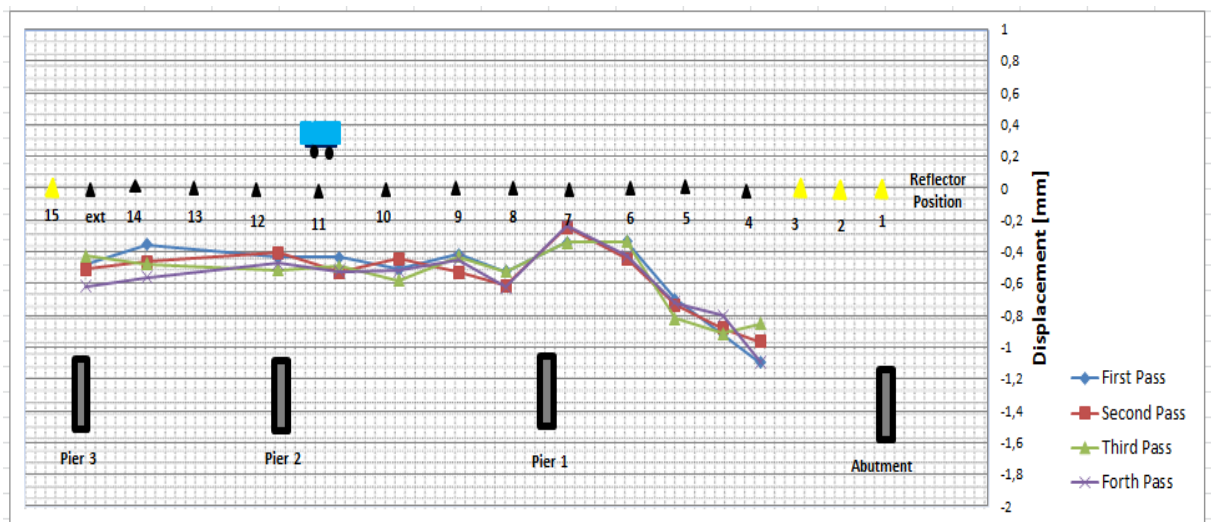


Figure A.24 – IBIS-S 11th of March 2012 200 MHz Monitoring Results

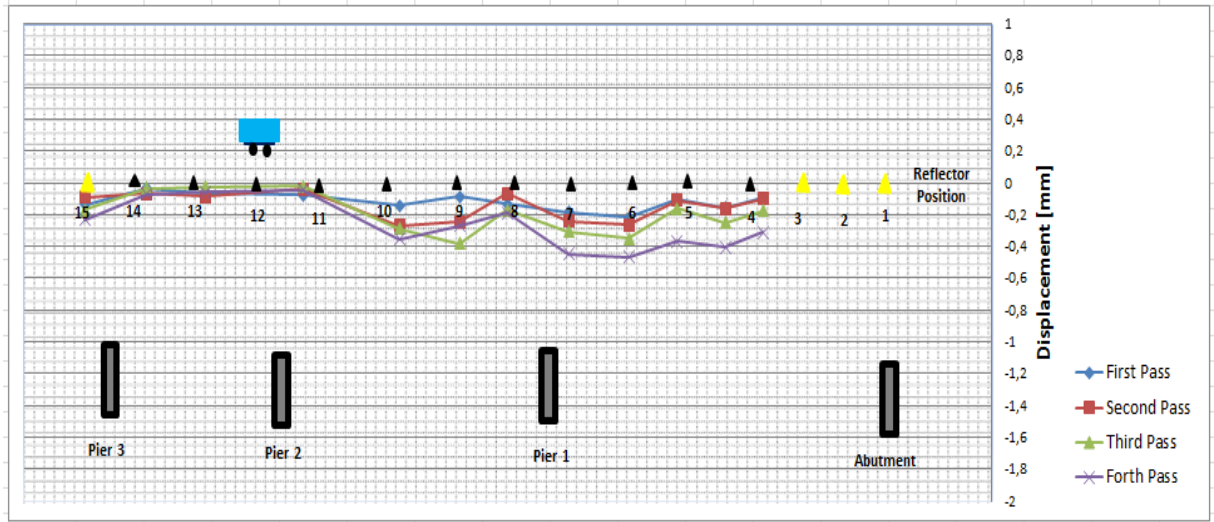


Figure A.25 – IBIS-S 7th November 2010 20 MHz Monitoring Results

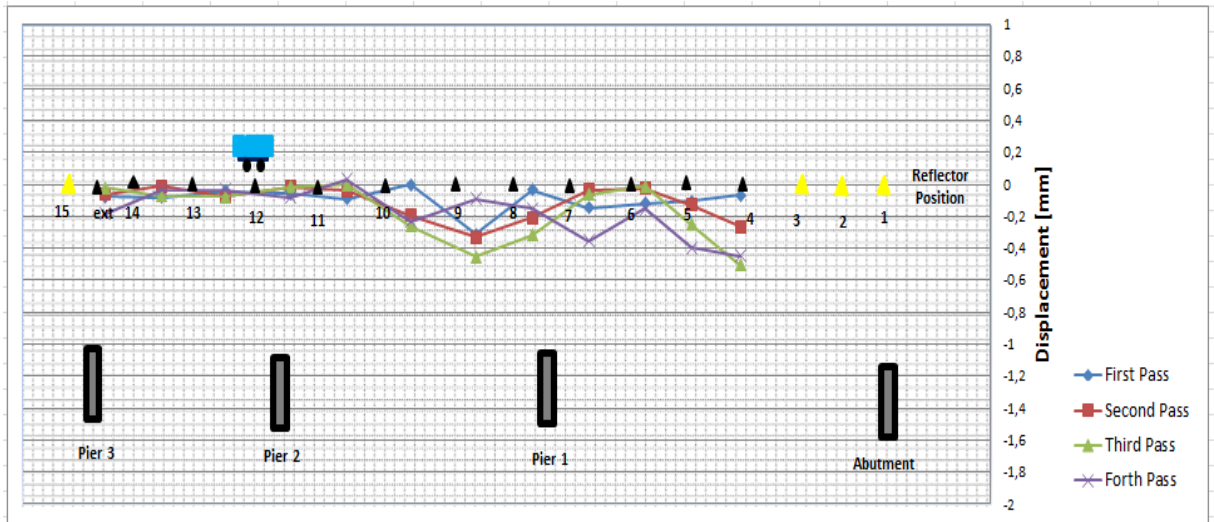


Figure A.26 – IBIS-S 11th of March 2012 20 MHz Monitoring Results

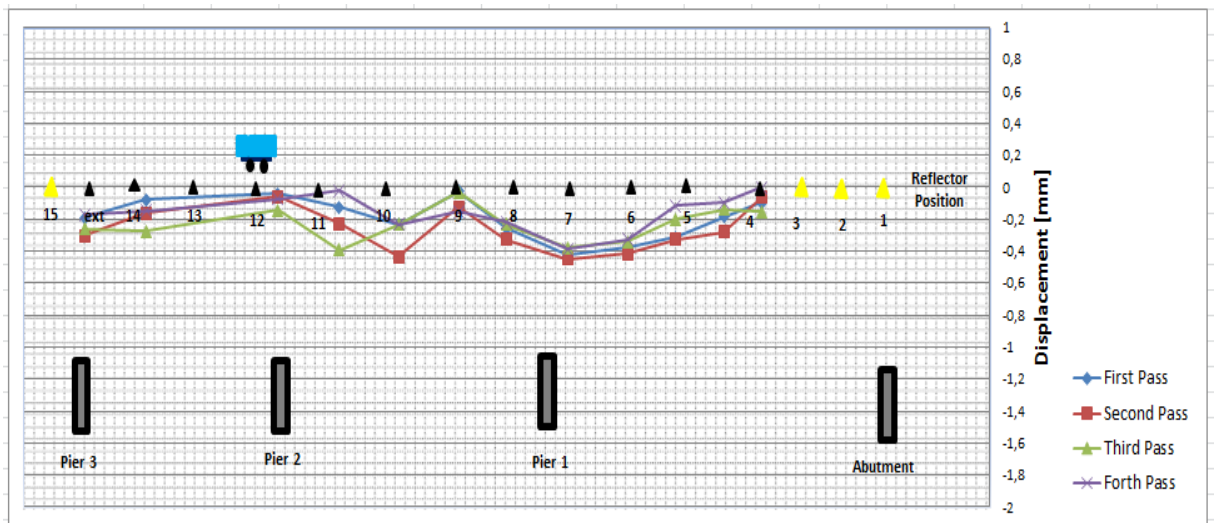


Figure A.27 – IBIS-S 11th of March 2012 200 MHz Monitoring Results

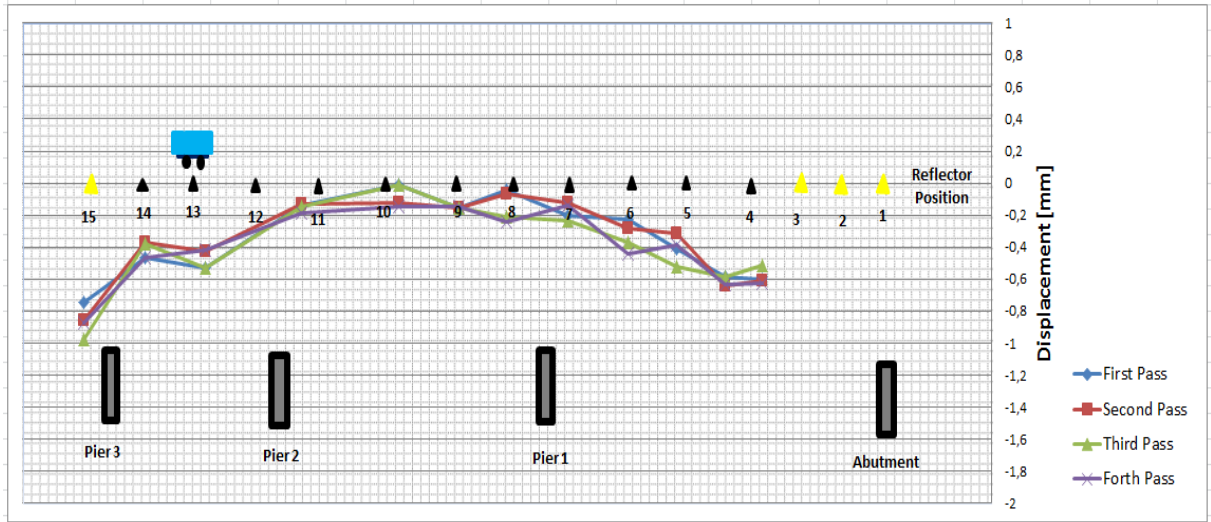


Figure A.28 – IBIS-S 7th November 2010 20 MHz Monitoring Results

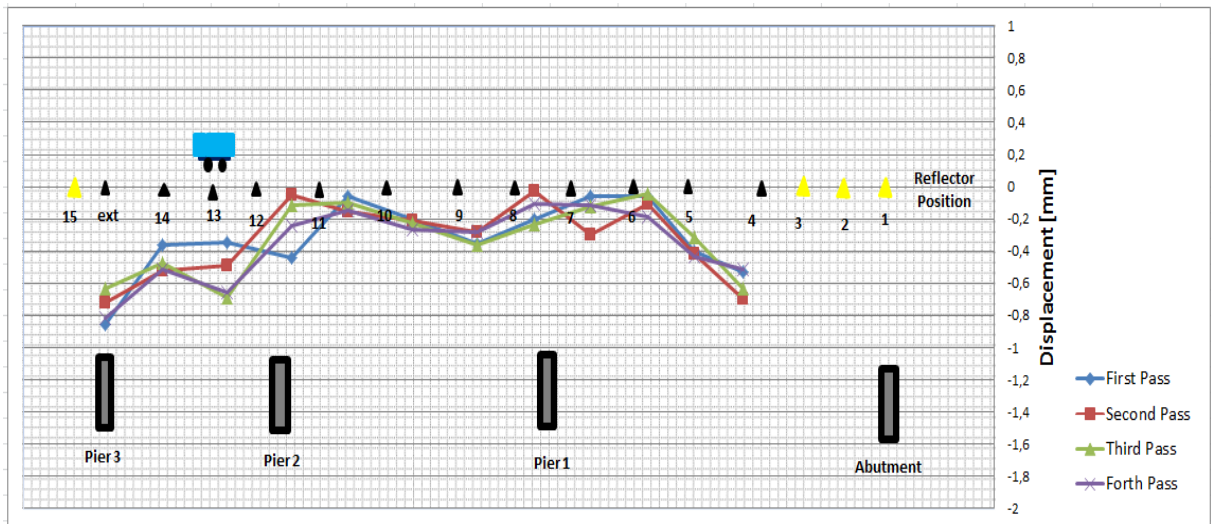


Figure A.29 – IBIS-S 11th of March 2012 20 MHz Monitoring Results

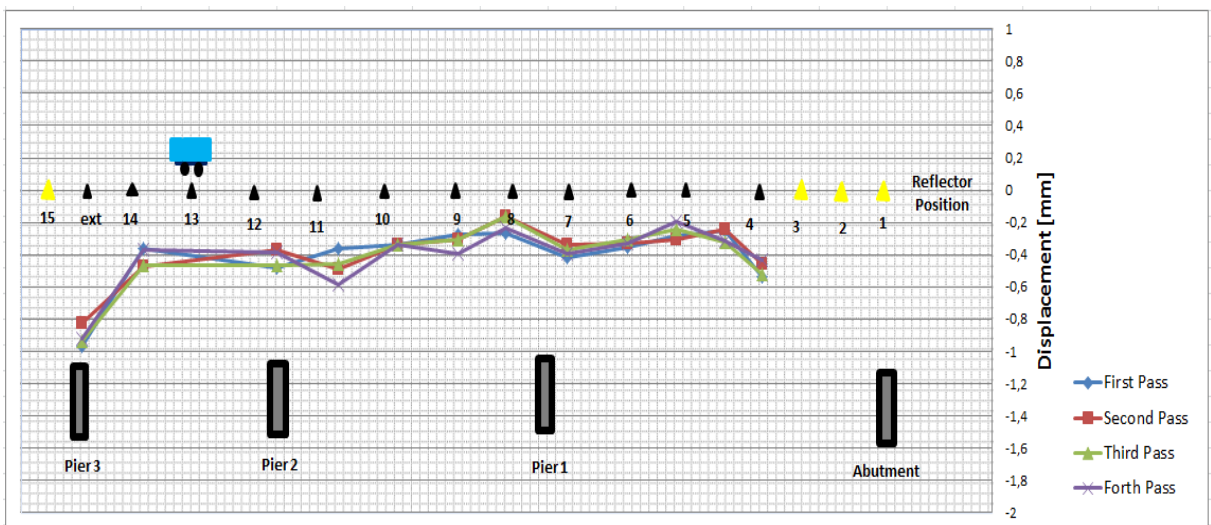


Figure A.30 – IBIS-S 11th of March 2012 200 MHz Monitoring Results

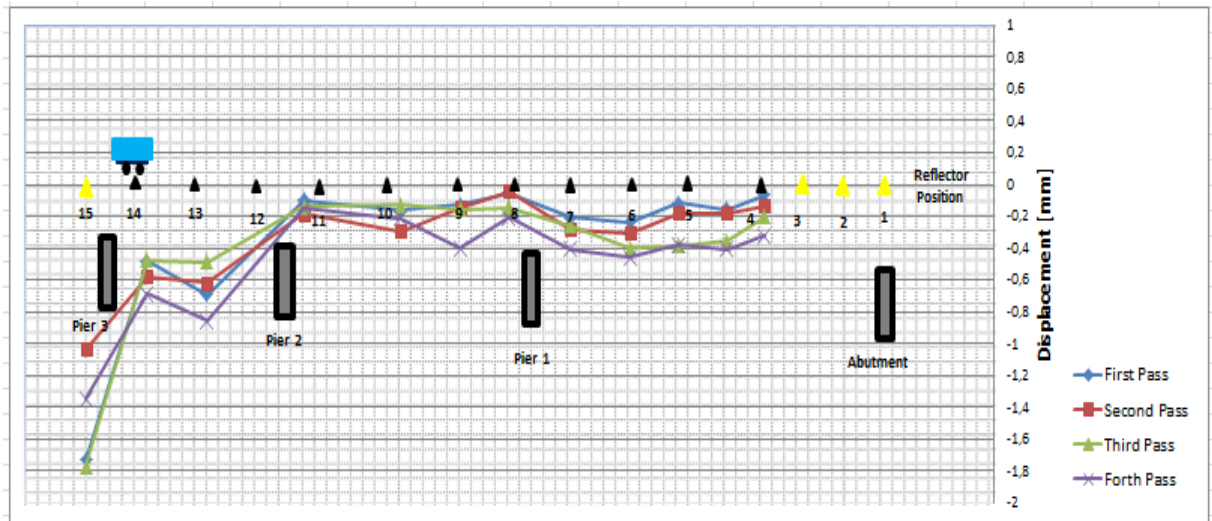


Figure A.31 – IBIS-S 7th November 2010 20 MHz Monitoring Results

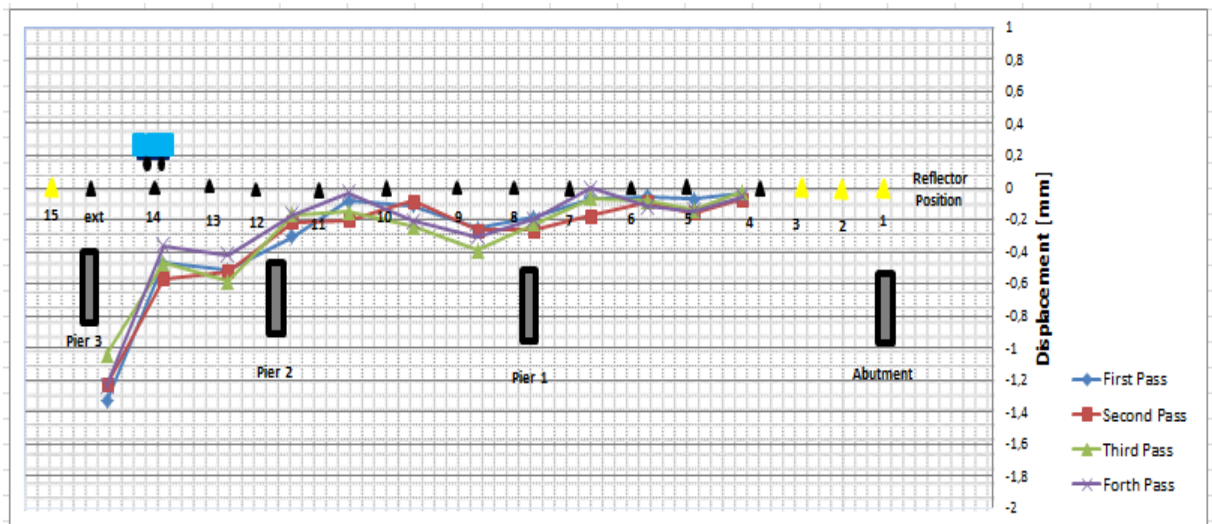


Figure A.32 – IBIS-S 11th of March 2012 20 MHz Monitoring Results

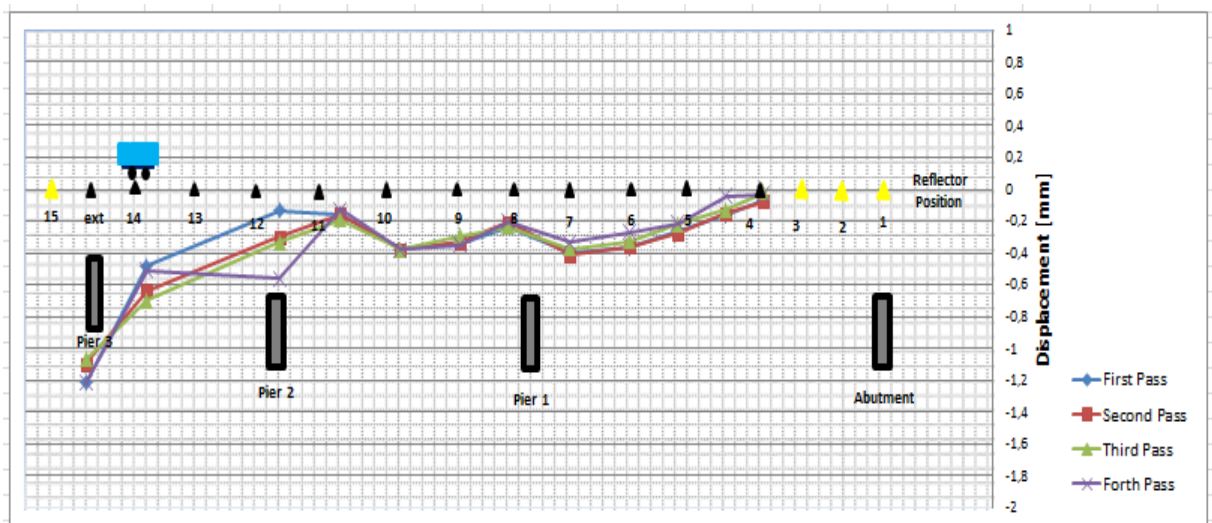


Figure A.33 – IBIS-S 11th of March 2012 200 MHz Monitoring Results

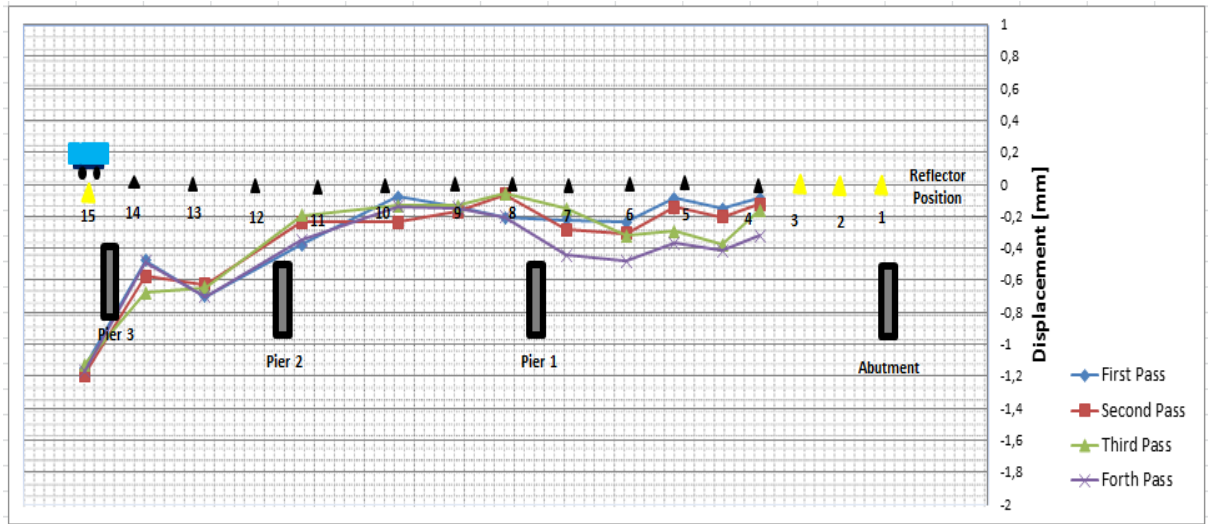


Figure A.34 – IBIS-S 7th November 2010 20 MHz Monitoring Results

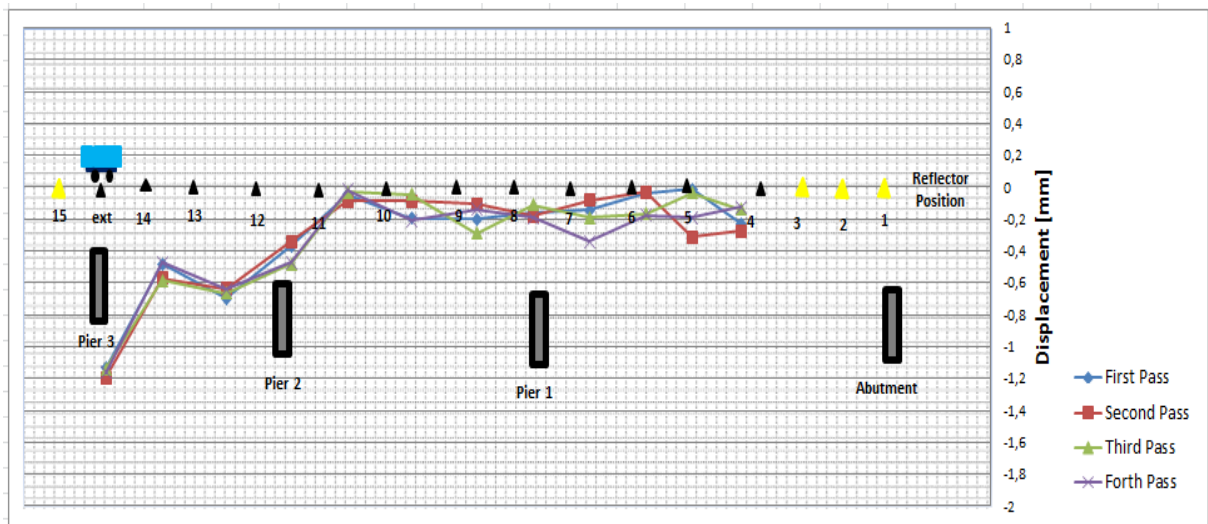


Figure A.35 – IBIS-S 11th of March 2012 20 MHz Monitoring Results

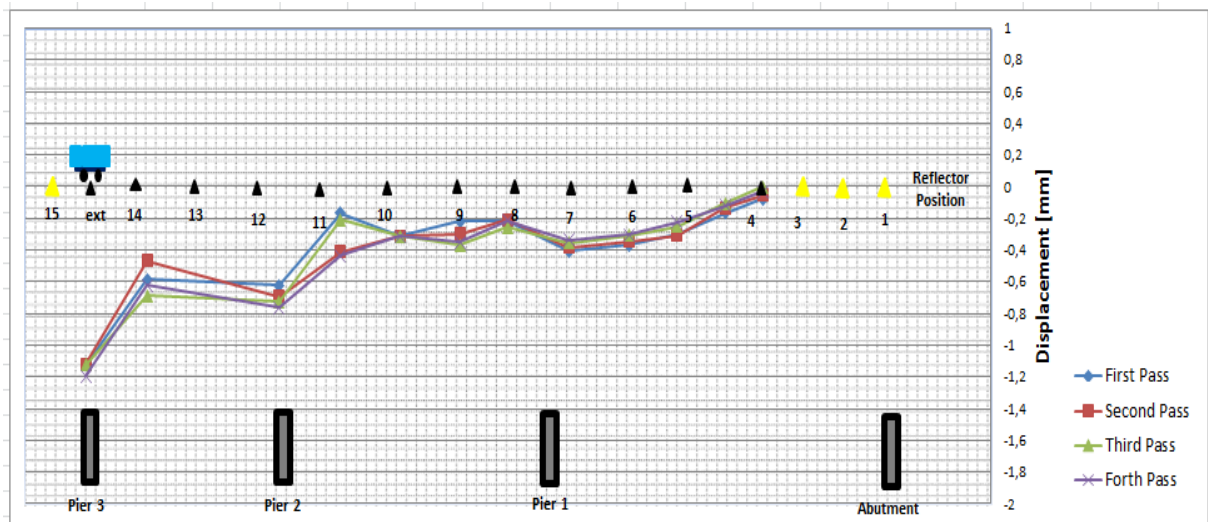


Figure A.36 – IBIS-S 11th of March 2012 200 MHz Monitoring Results

APPENDIX B

GPR SURVEY RESULTS

This appendix presents GPR survey results for all zones taken with five different antennas on four separate days throughout 2011 and 2012 for the main case study (Pentagon Road Bridge). This assessment uses different antennae, in terms of frequency and method of application (2 GHz and 200-600 MHz IDS and 1-1,5-4 GHz UTSI) GPR antennas. Processing, interpretation and analysis of collected data were supported by the GRED software (IDS Ingegneria dei Sistemi).

The radargrams produced by processing the GPR data demonstrate the effectiveness of two different manufacturers and three different GPR antenna mapping and providing valuable information regarding the positions of rebar (upper and lower reinforcement), unknown structural features as well as possible moisture ingress within the structure. An example of the identification of these features is shown by Figure B.1. Figure B.3 to B.38 illustrate other radargrams produced by these surveys. It is clear even to the untrained eye that the maximum resolution of the 4 GHz antenna is much greater than the others. This resolution however comes at a decreased penetration depth.

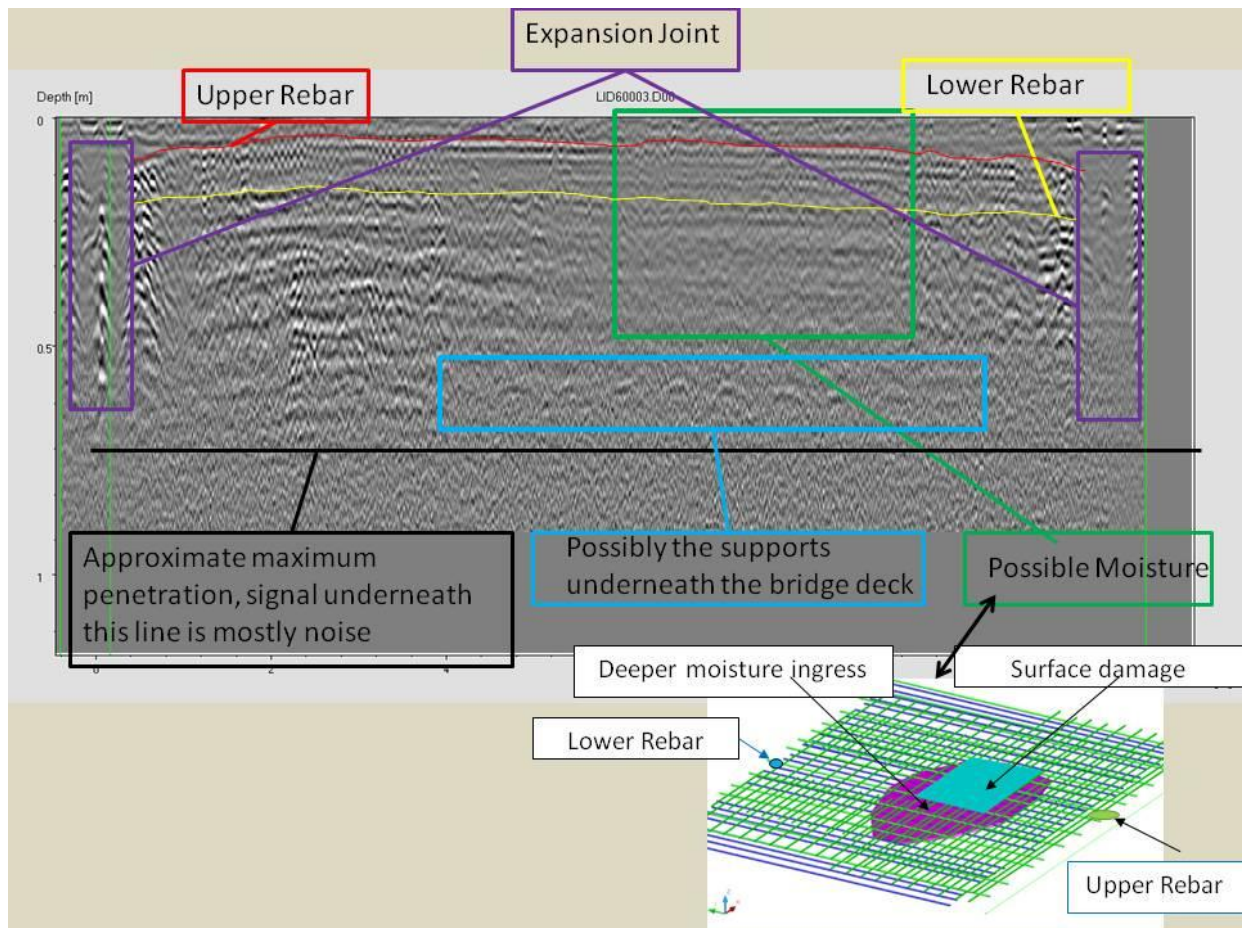


Figure B.1 – GPR Zone 5 Radargram

The results from the time slices shown in Figure B.38 also highlight the presence of moisture within the bridge deck.

The differences between using different antennae in terms of frequency and method of application (2 GHz and 200-600 MHz IDS GPR antennae) and (1 GHz, 1.5 GHz and 4 GHz UTSI GPR antennae) are further examined respectively in Figure B.3 to B.38. Results are gathered from zone 1, 2, 3, 4, 5 and 6 shown in Figure B.2.

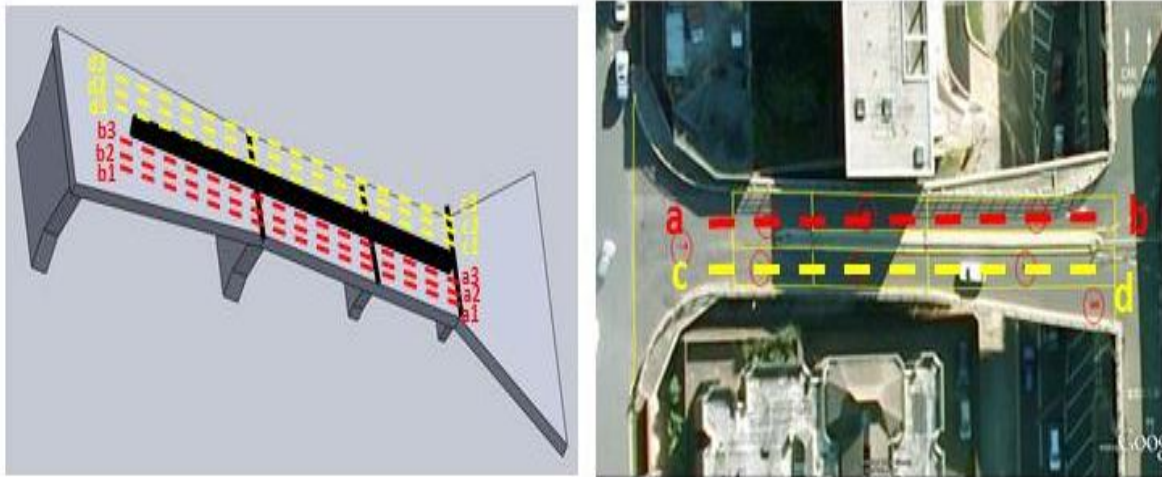


Figure B.2– Depiction and Aerial view of GPR Survey Map

A1B1 Lane Radargrams

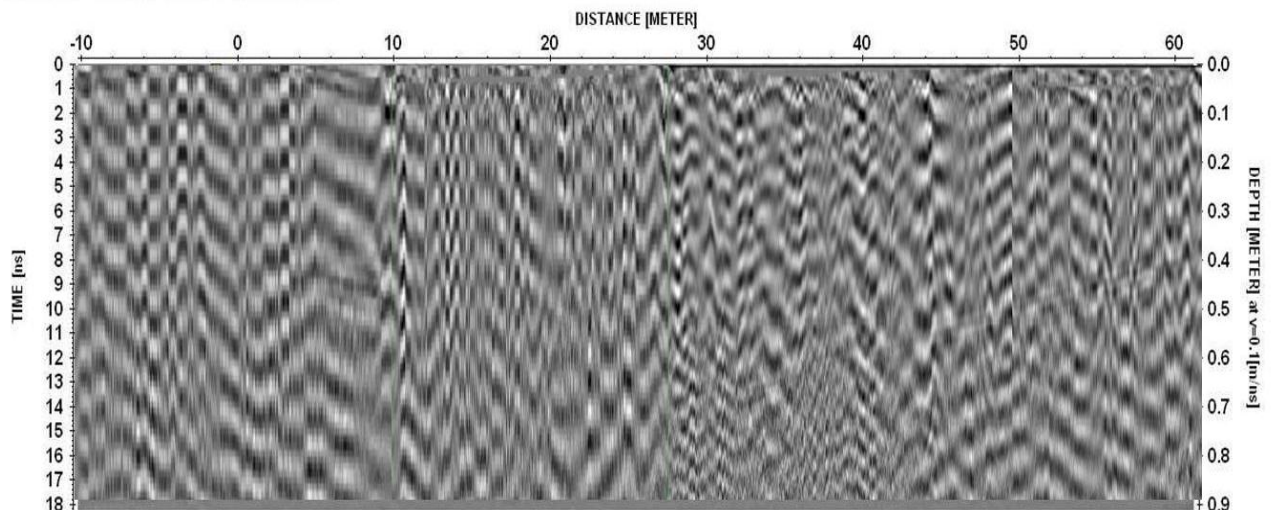


Figure B.3 – 600MHz Antenna cross section A1-B1 lane radargram

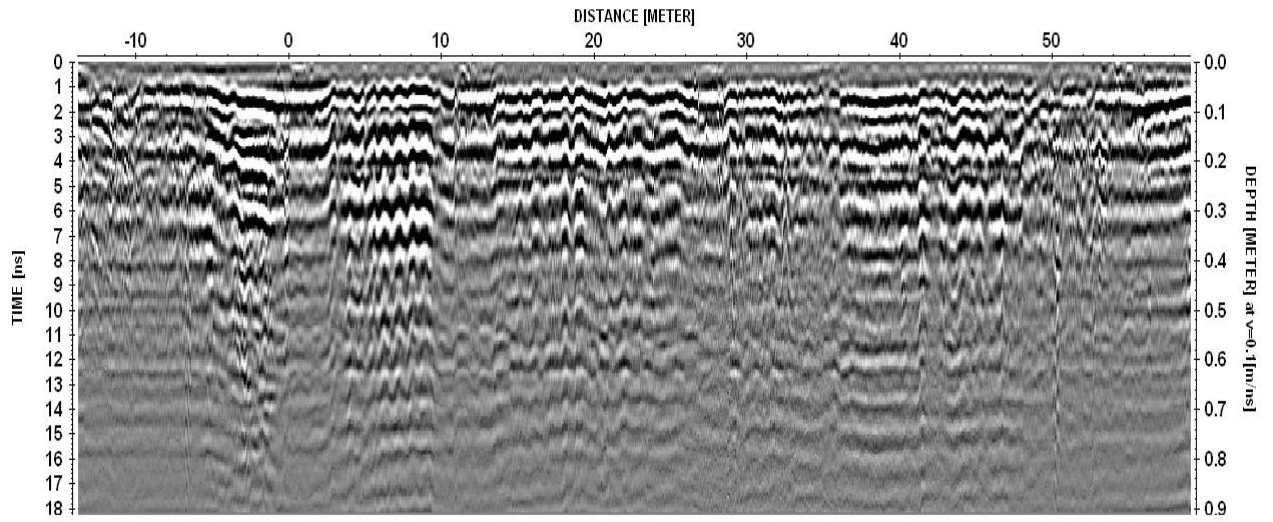


Figure B.4 – 1GHz Antenna cross section A1-B1 lane radargram

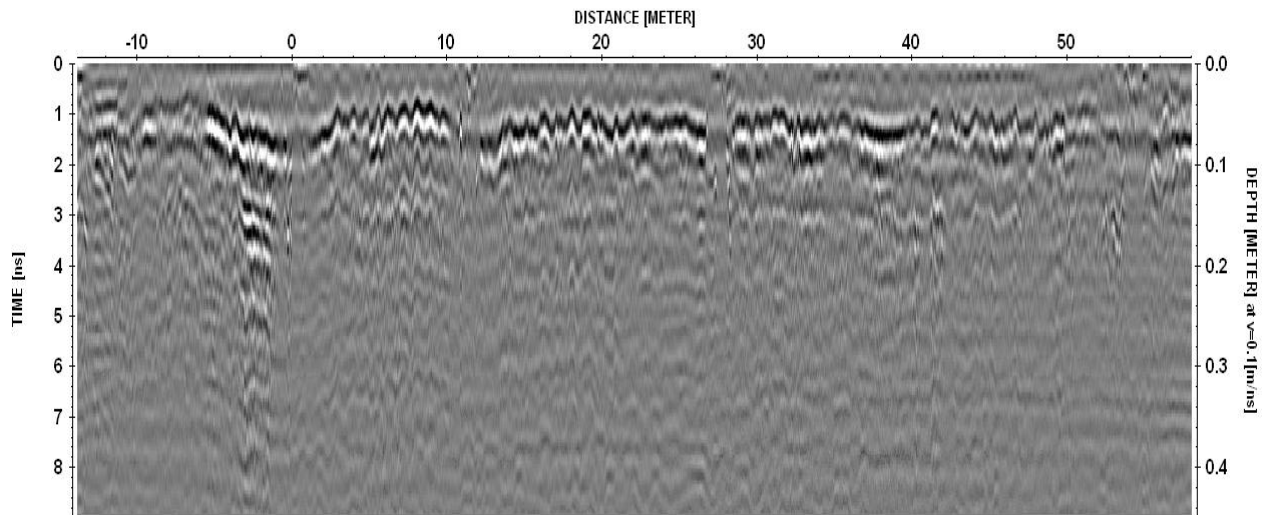


Figure B.5 – 1.5 GHz Antenna 1 cross section A1-B1 lane radargram

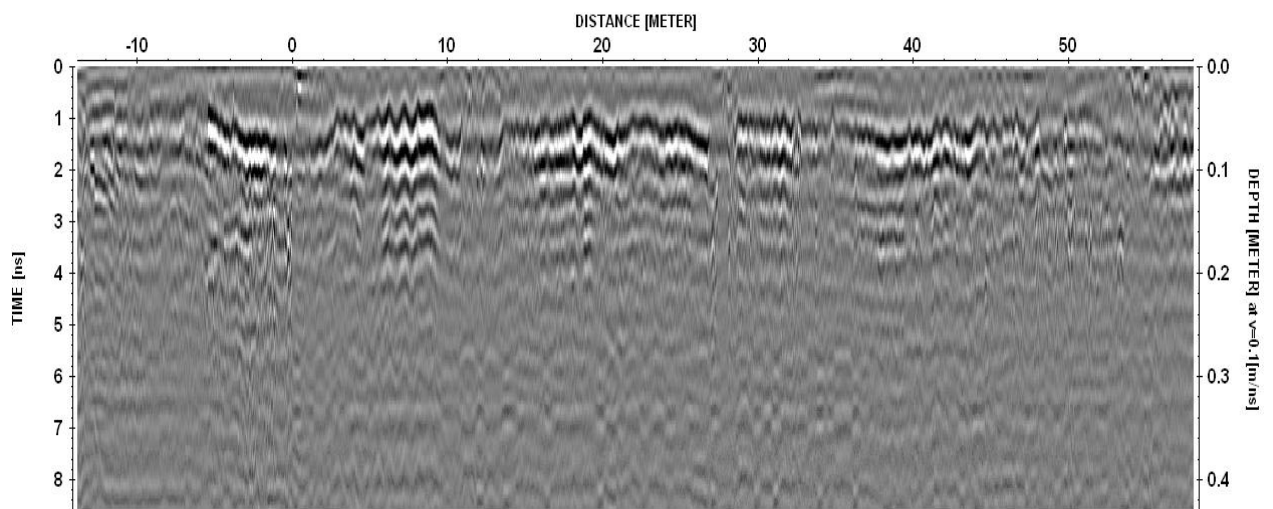


Figure B.6 – 1.5 GHz Antenna 2 cross section A1-B1 lane radargram

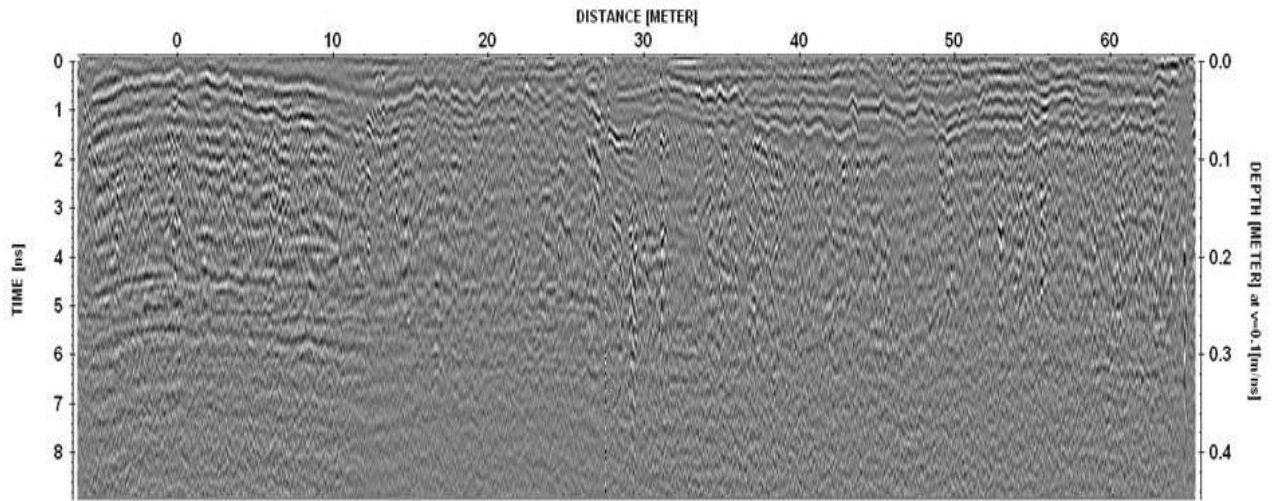


Figure B.7 – 2 GHz Antenna2 cross section A1-B1 lane radargram

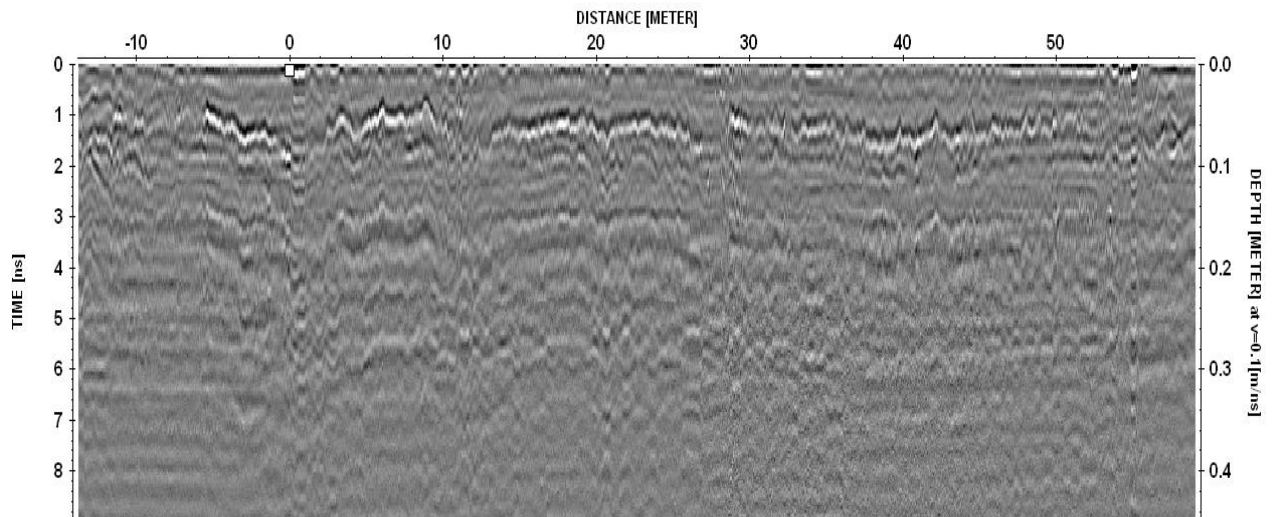


Figure B.8 – 4 GHz Antenna cross section A1-B1 lane radargram

A2B2 Lane Radargrams

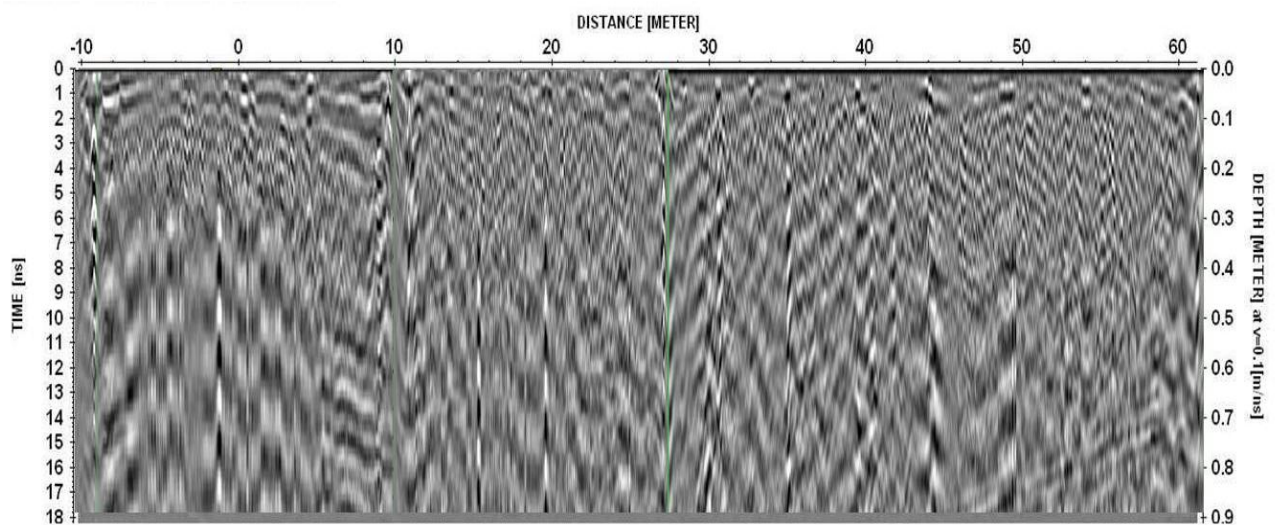


Figure B.9 – 15: 600MHz Antenna cross section A2-B2 lane radargram

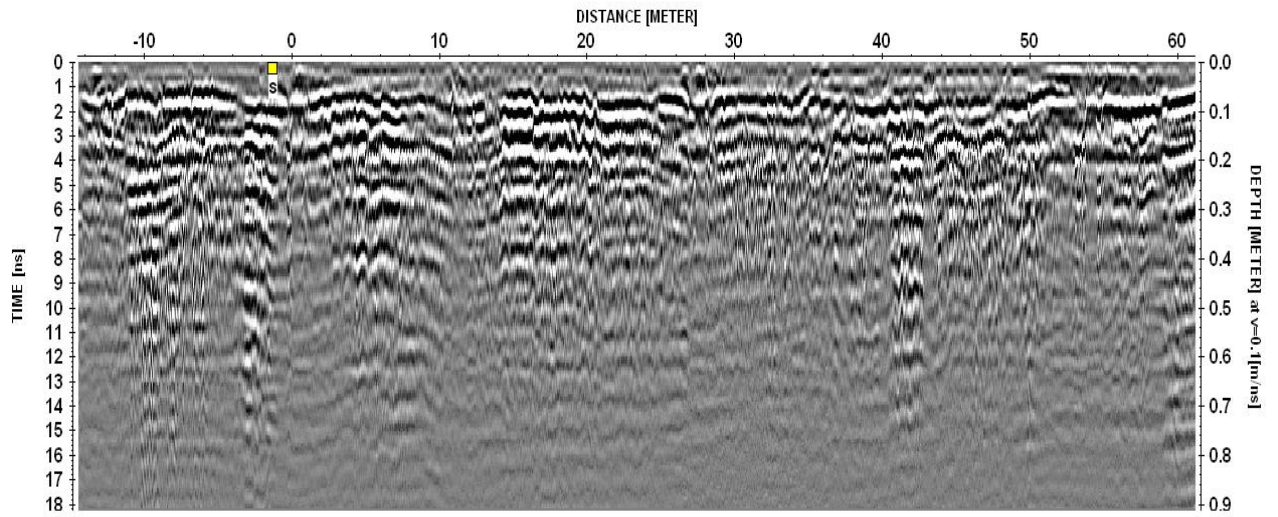


Figure B.10 – 1GHz Antenna cross section A2-B2 lane radargram

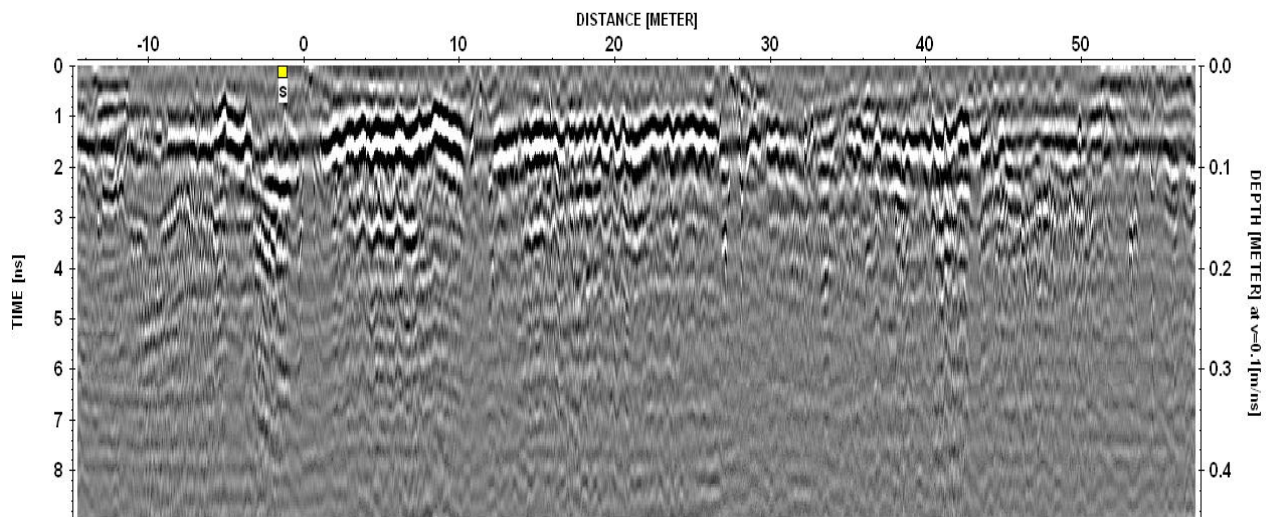


Figure B.11– 1.5 GHz Antenna1 cross section A2-B2 lane radargram

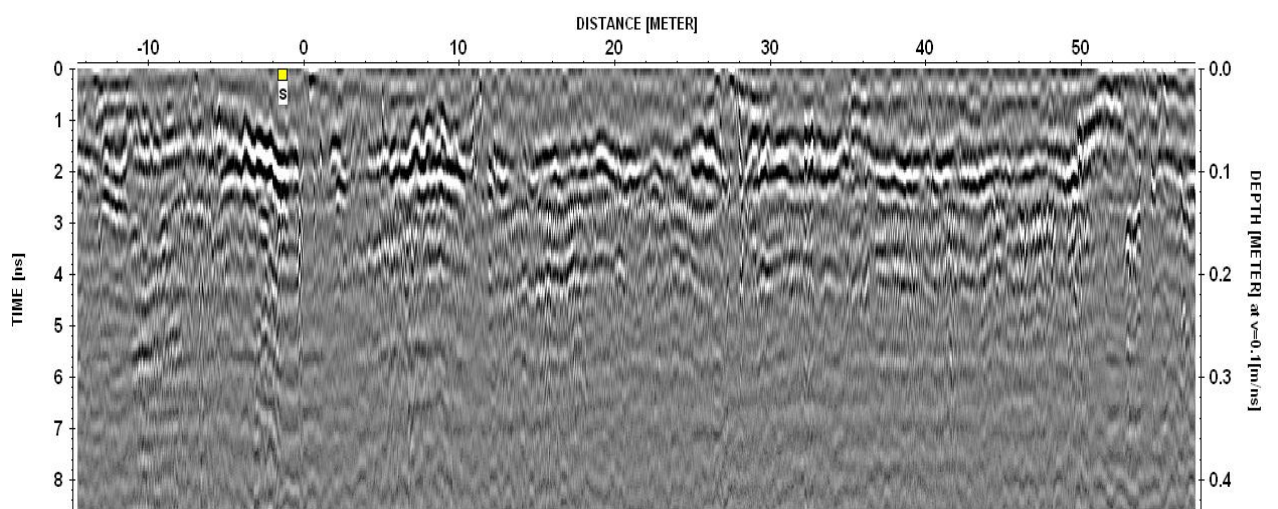


Figure B.12– 1.5 GHz Antenna2 cross section A2-B2 lane radargram

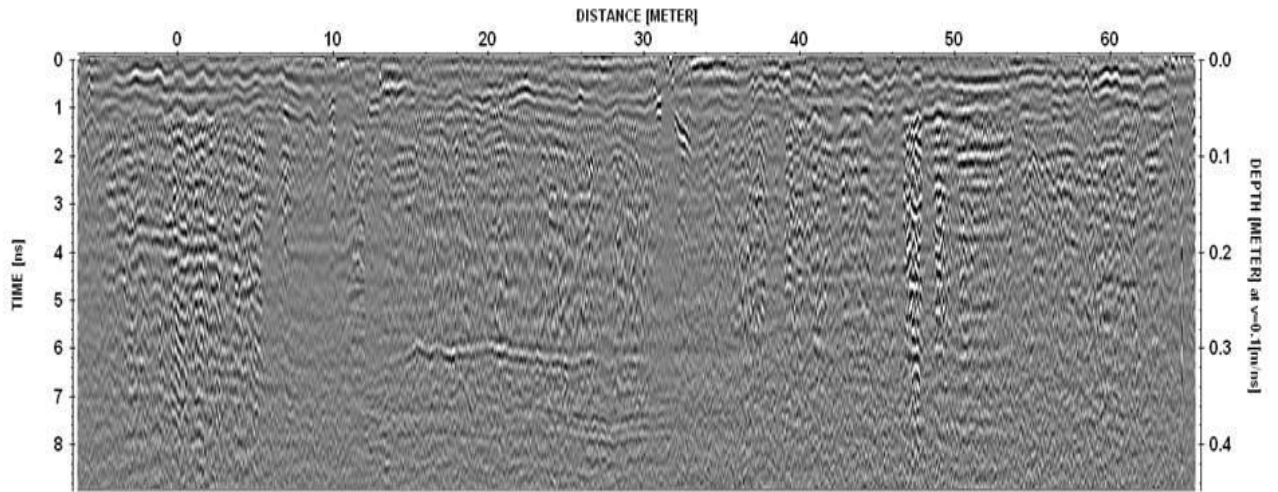


Figure B.13– 2 GHz Antenna2 cross section A2-B2 lane radargram

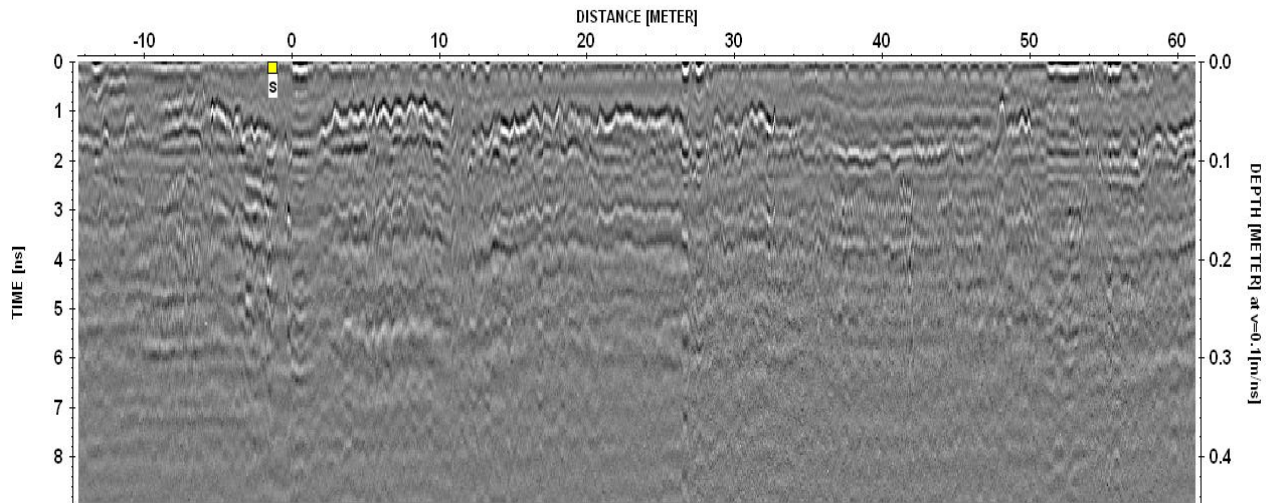


Figure B.14 – 4 GHz Antenna cross section A2-B2 lane radargram

A3B3 Lane Radargrams

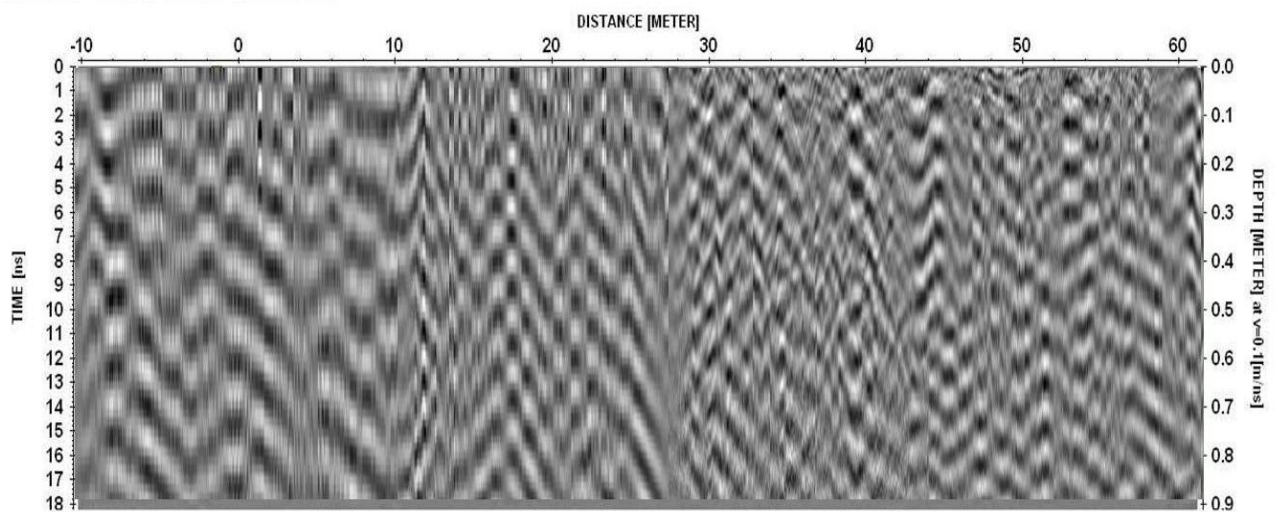


Figure B.15– 600MHz Antenna cross section A3-B3 lane radargram

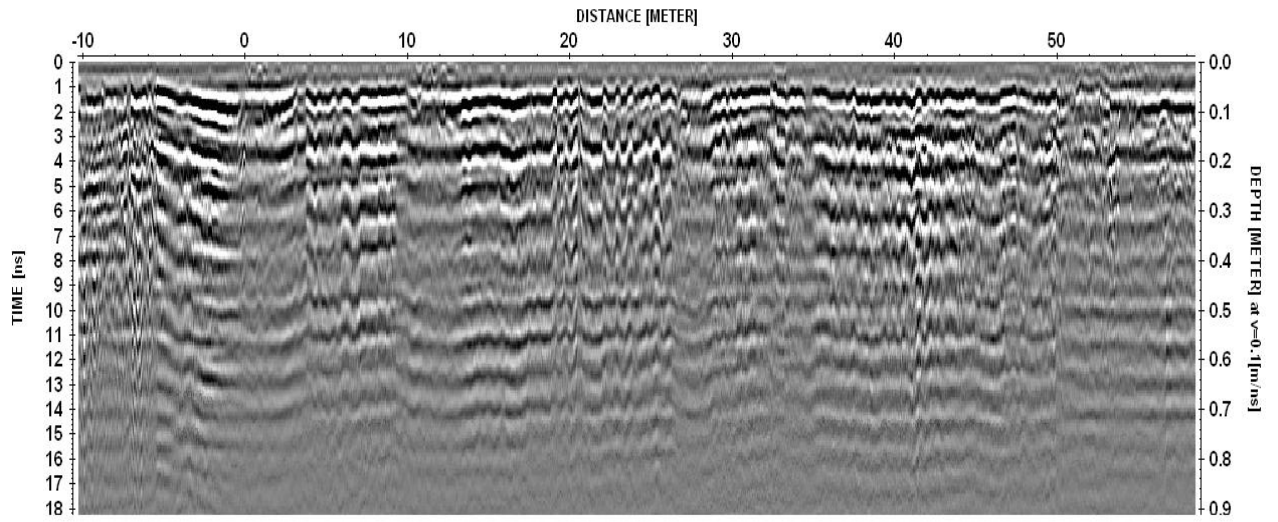


Figure B.16– 1GHz Antenna cross section A3-B3 lane radargram

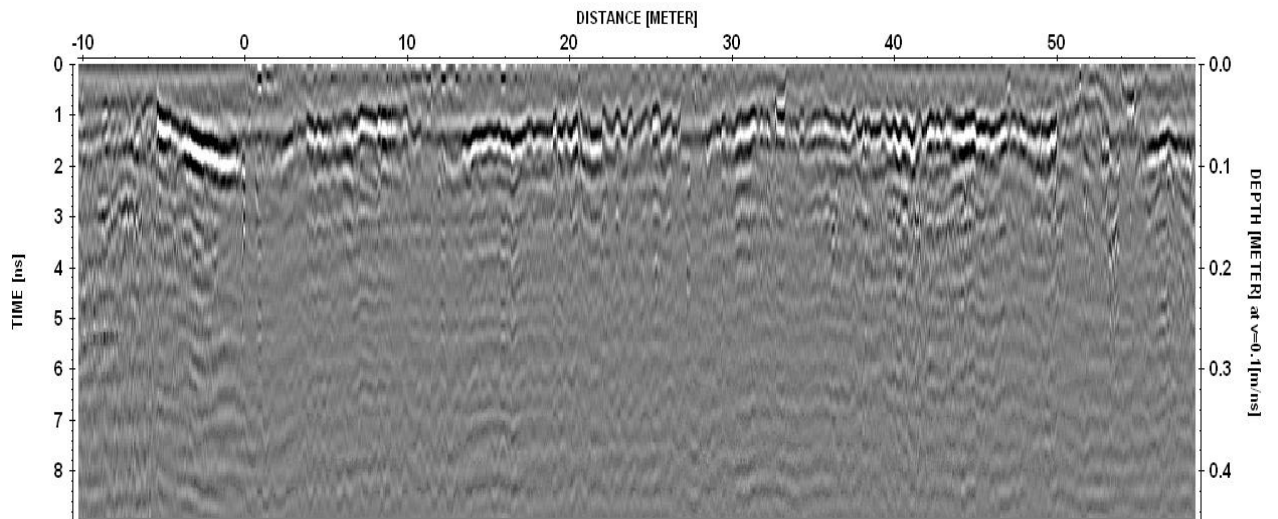


Figure B.17 – 1.5 GHz Antenna1 cross section A3-B3 lane radargram

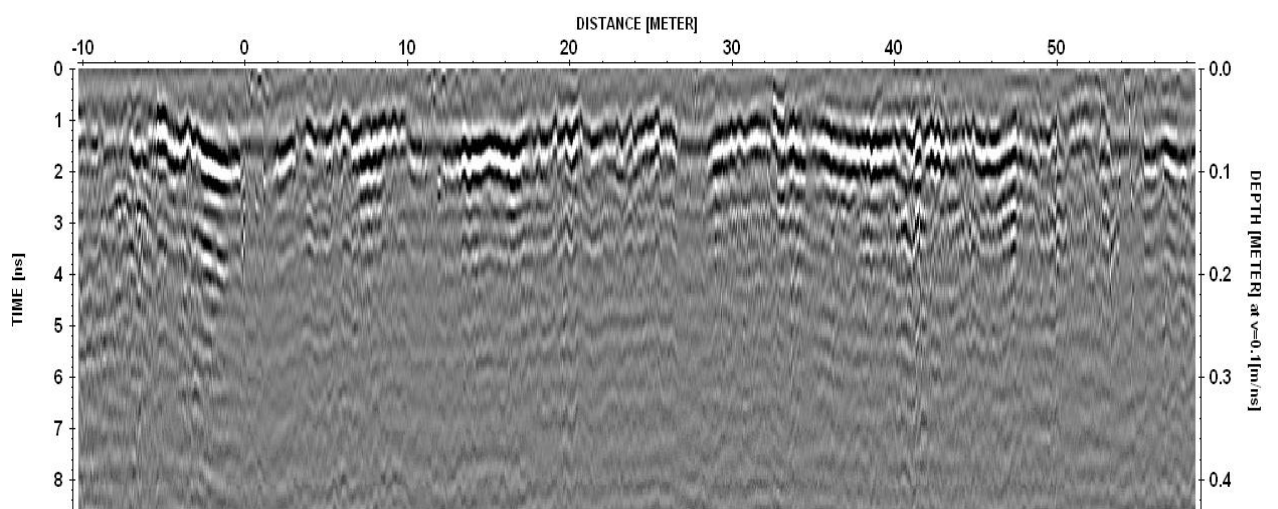


Figure B.18 – 1.5 GHz Antenna2 cross section A3-B3 lane radargram

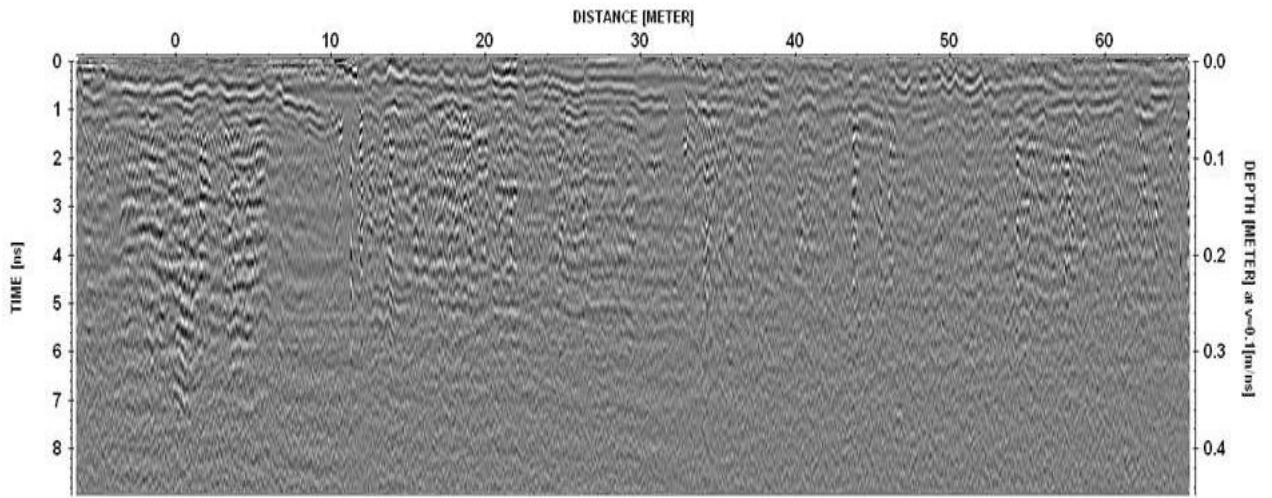


Figure B.19 – 2 GHz Antenna2 cross section A3-B3 lane radargram

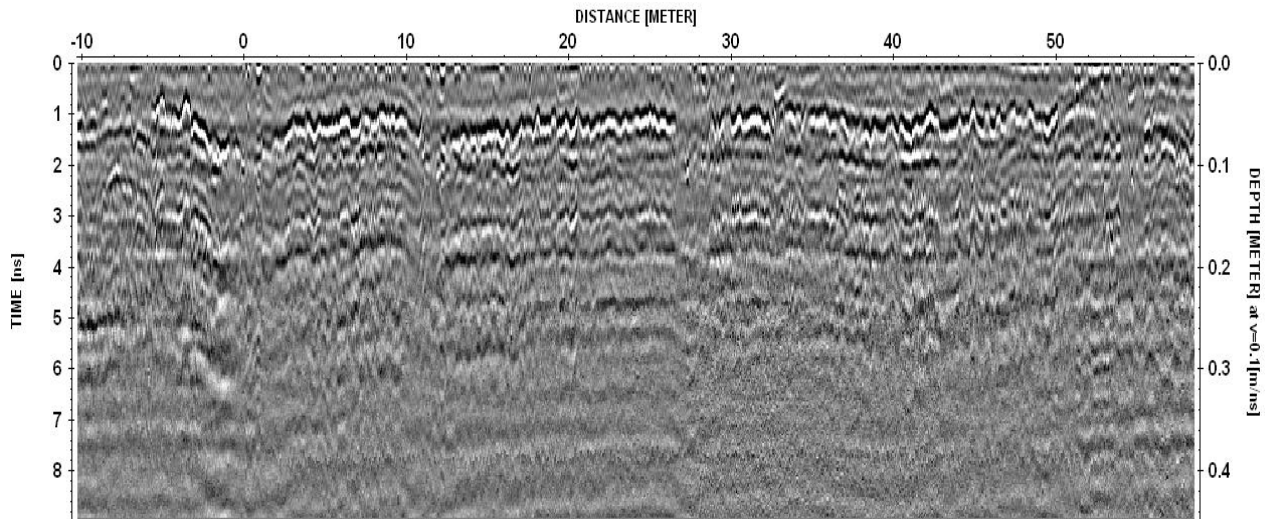


Figure B.20 – 4 GHz Antenna cross section A3-B3 lane radargram

C1D1 Lane Radargrams

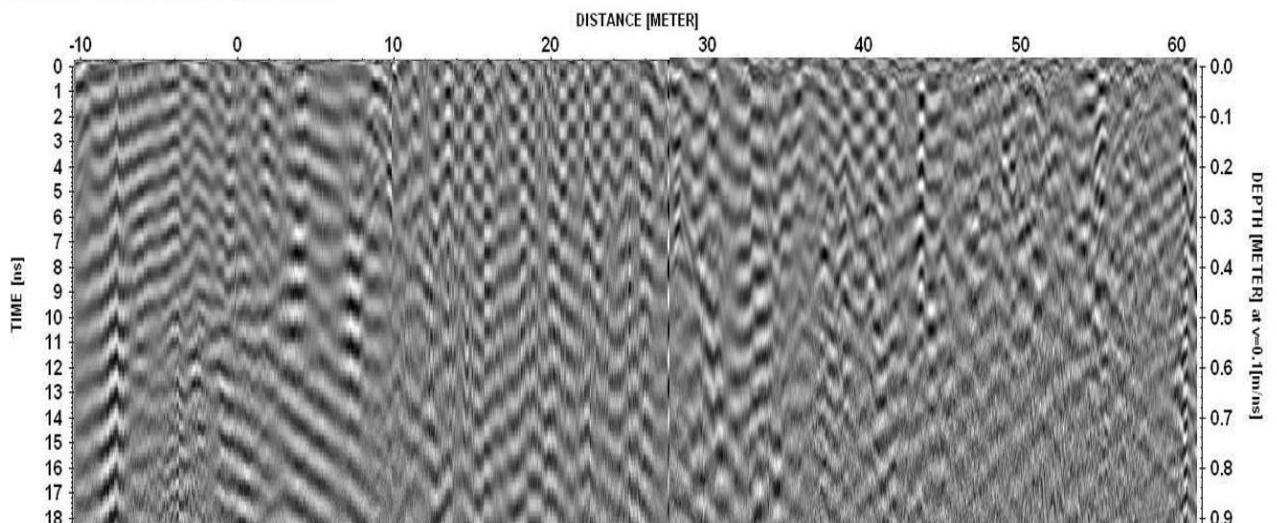


Figure B.21– 600MHz Antenna cross section C1-D1 lane radargram

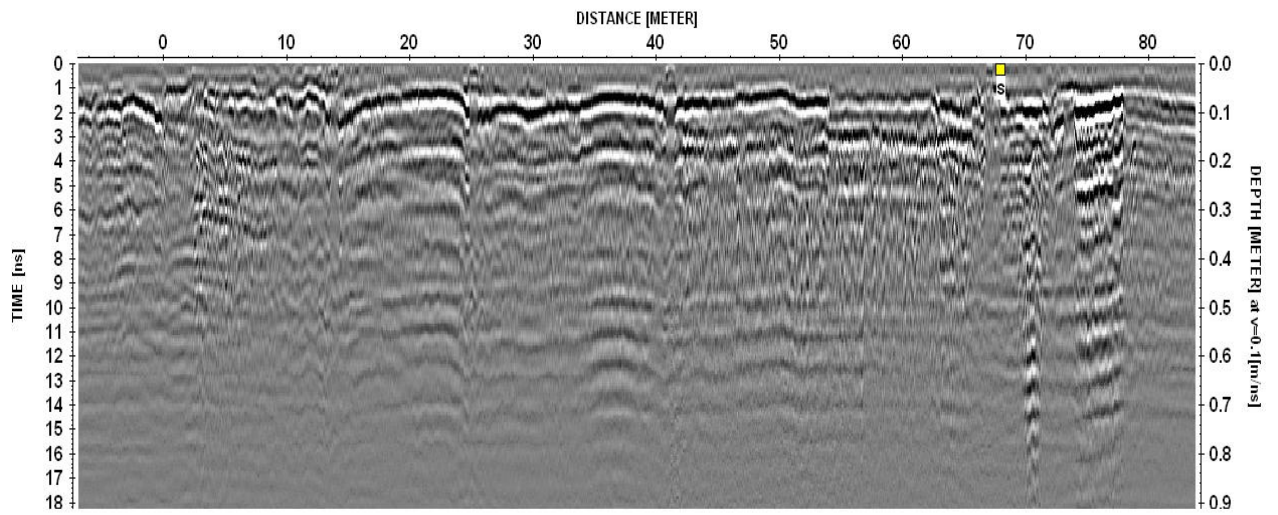


Figure B.22– 1GHz Antenna cross section C1-D1 lane radargram

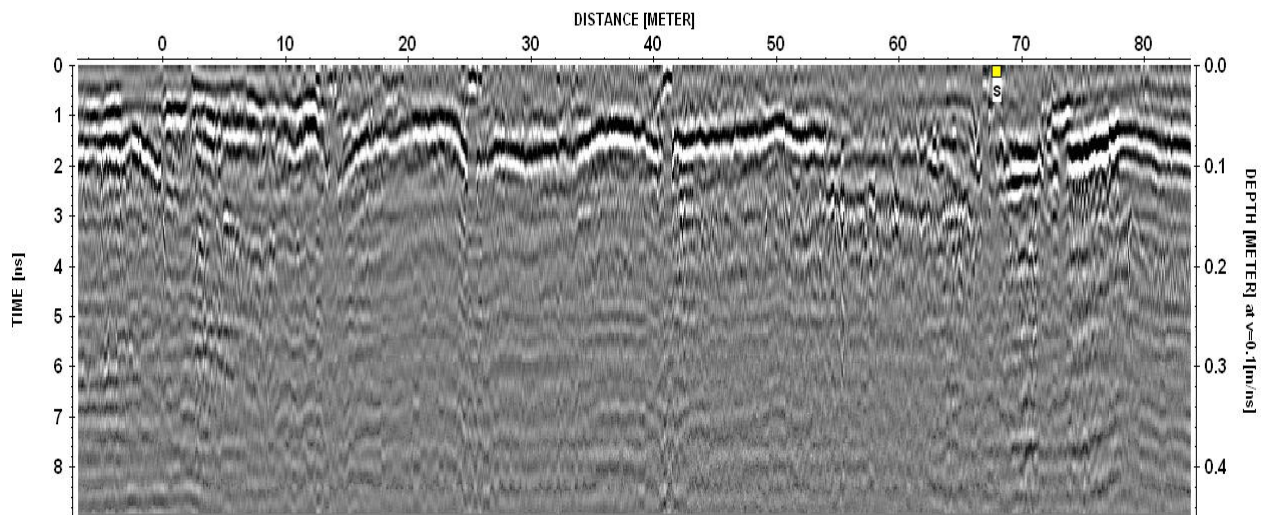


Figure B.23 – 1.5 GHz Antenna1 cross section C1-D1 lane radargram

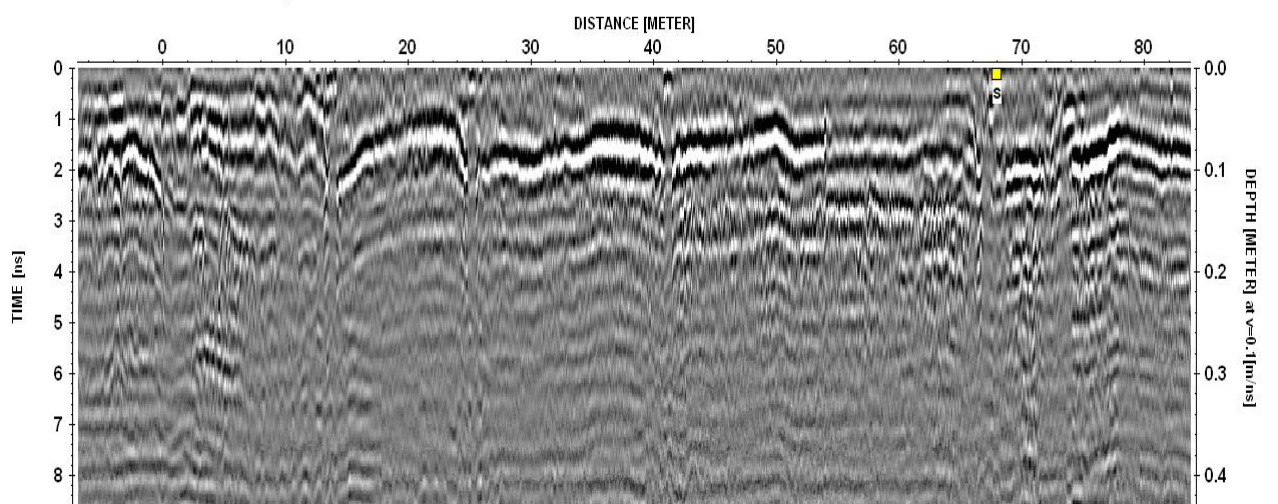


Figure B.24 – 1.5 GHz Antenna2 cross section C1-D1 lane radargram

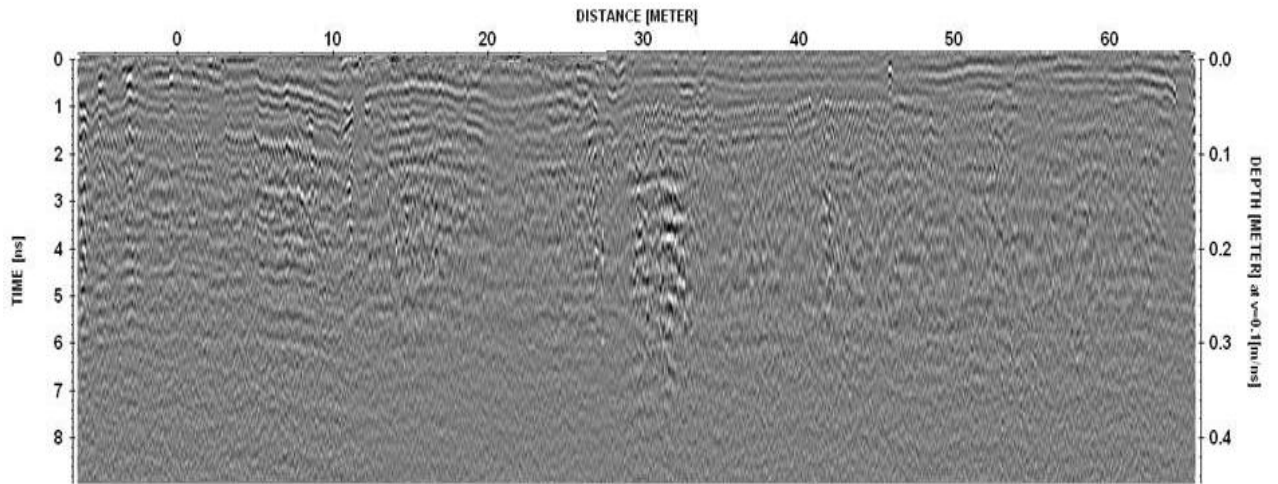


Figure B.25– 2 GHz Antenna2 cross section C1-D1 lane radargram

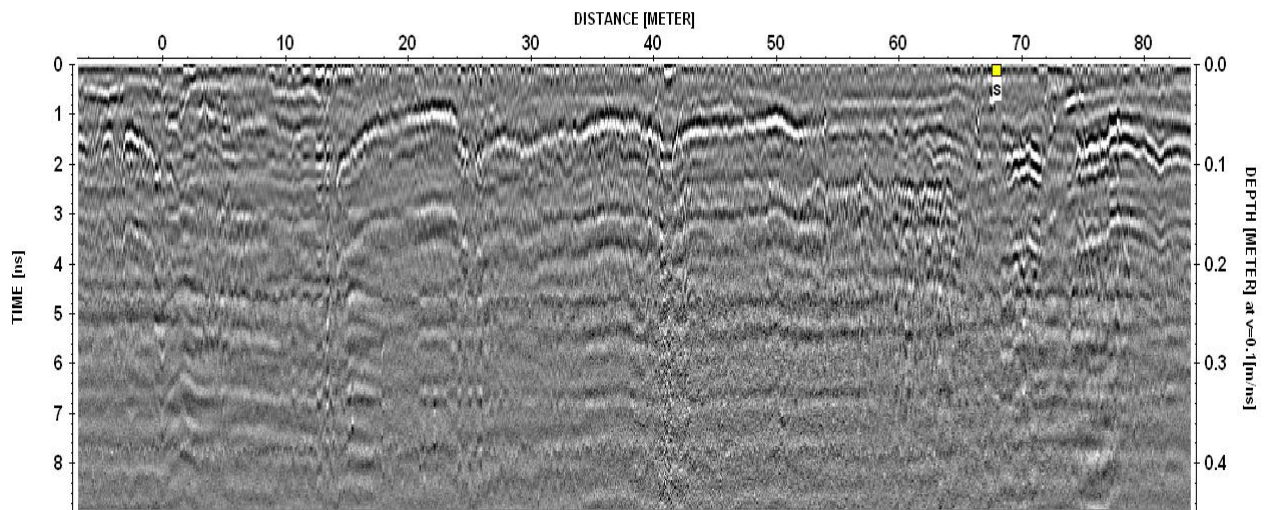


Figure B.26 – 4 GHz Antenna cross section C1-D1 lane radargram

C2D2 Lane Radargrams

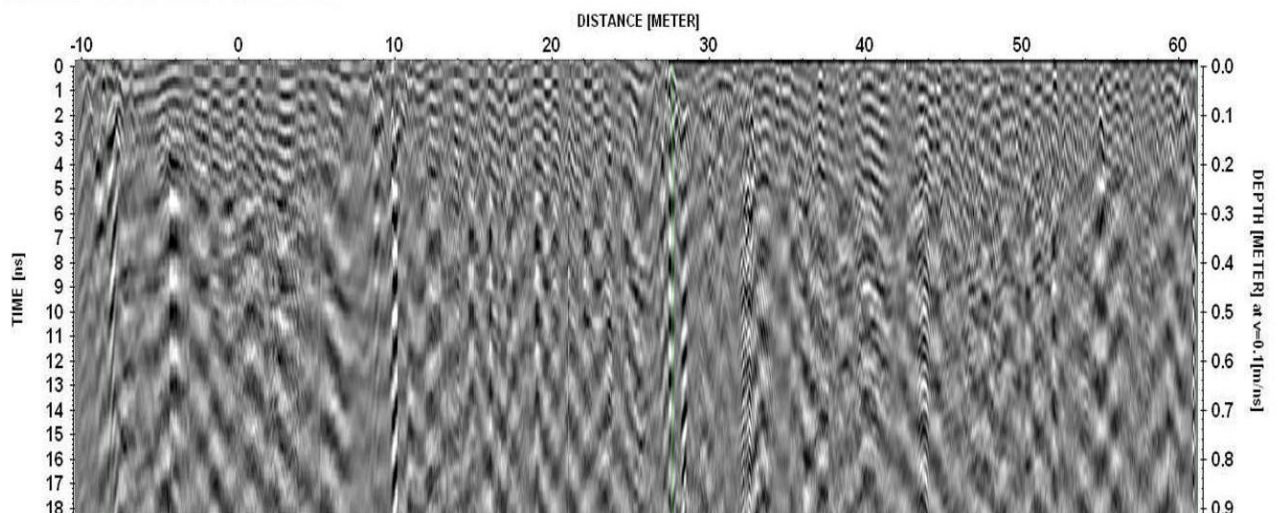


Figure B.27– 600MHz Antenna cross section C2-D2 lane radargram

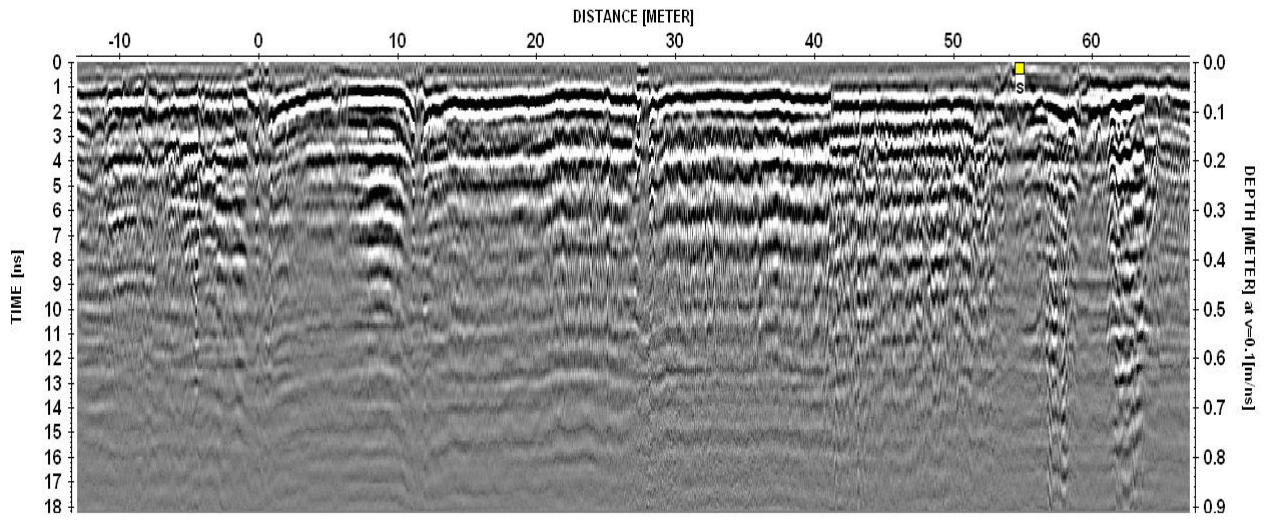


Figure B.28 – 1GHz Antenna cross section C2-D2 lane radargram

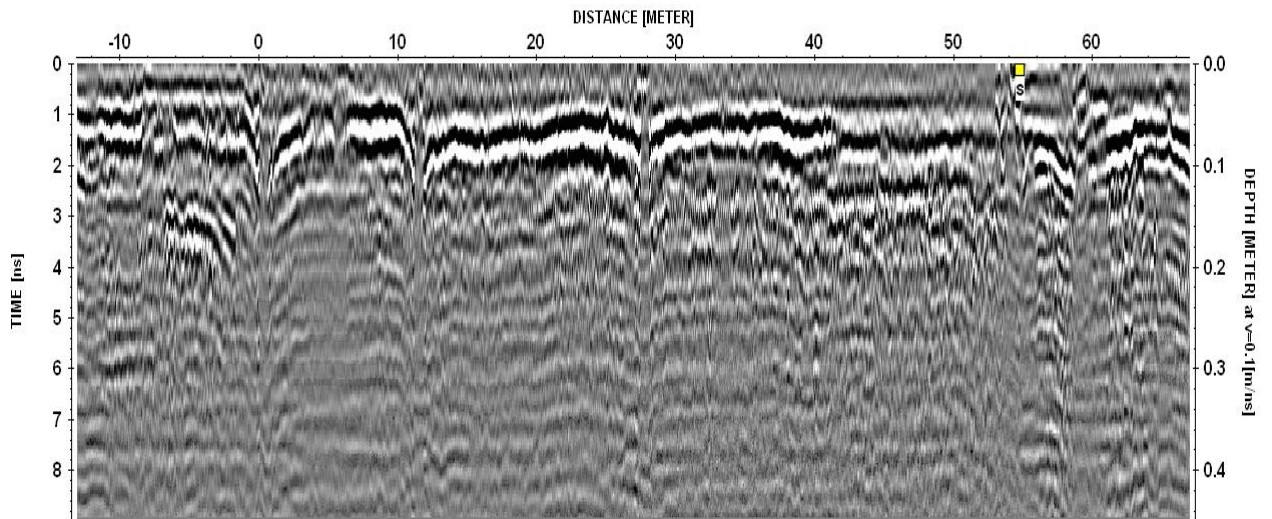


Figure B.29 – 1.5 GHz Antenna1 cross section C2-D2 lane radargram

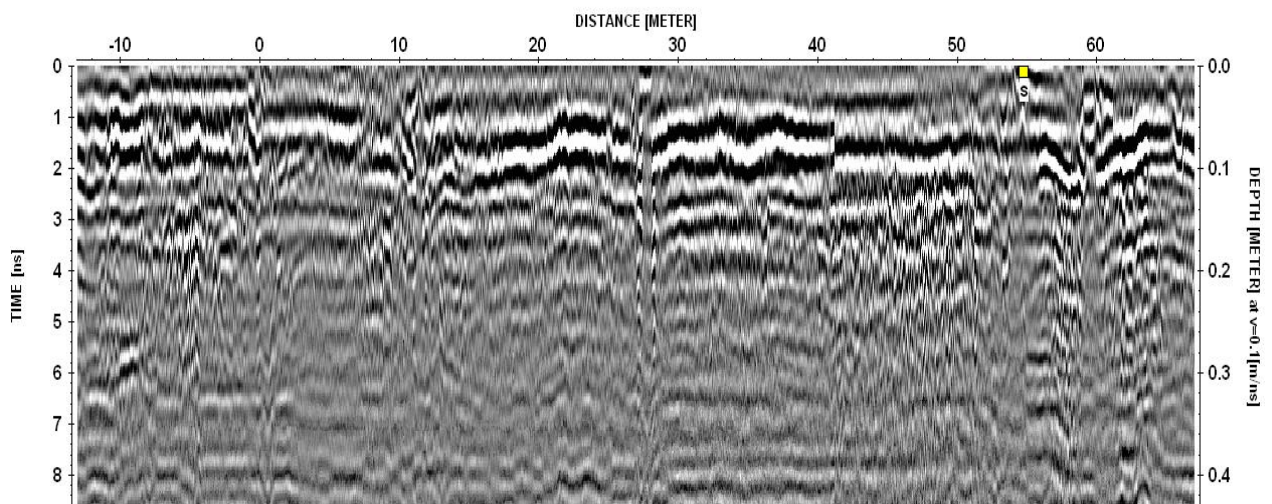


Figure B.30 – 1.5 GHz Antenna2 cross section C2-D2 lane radargram

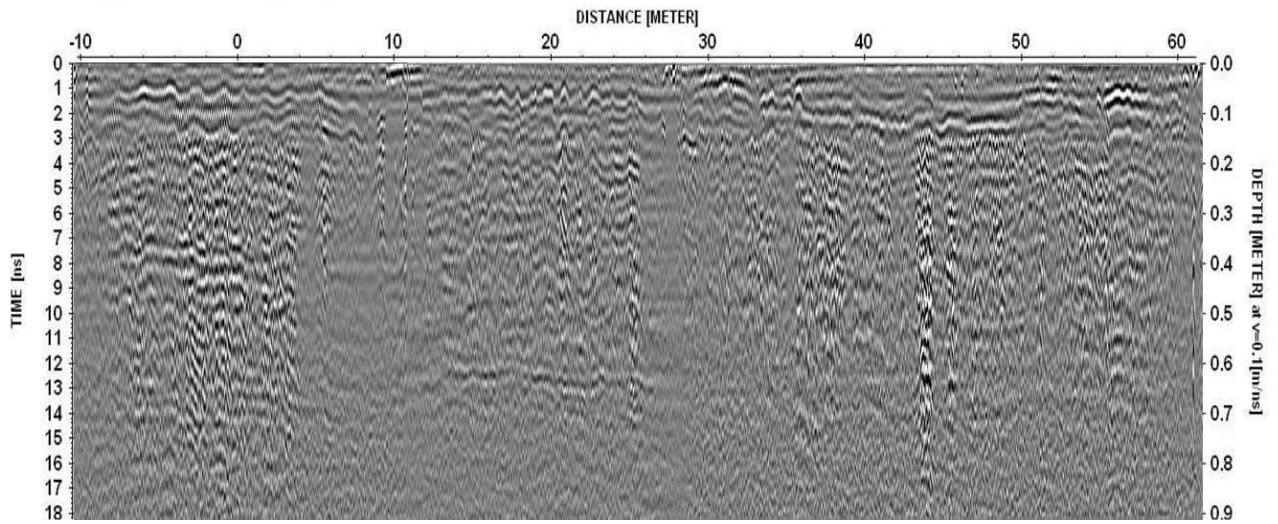


Figure B.31– 2GHz Antenna cross section C2-D2 lane radargram

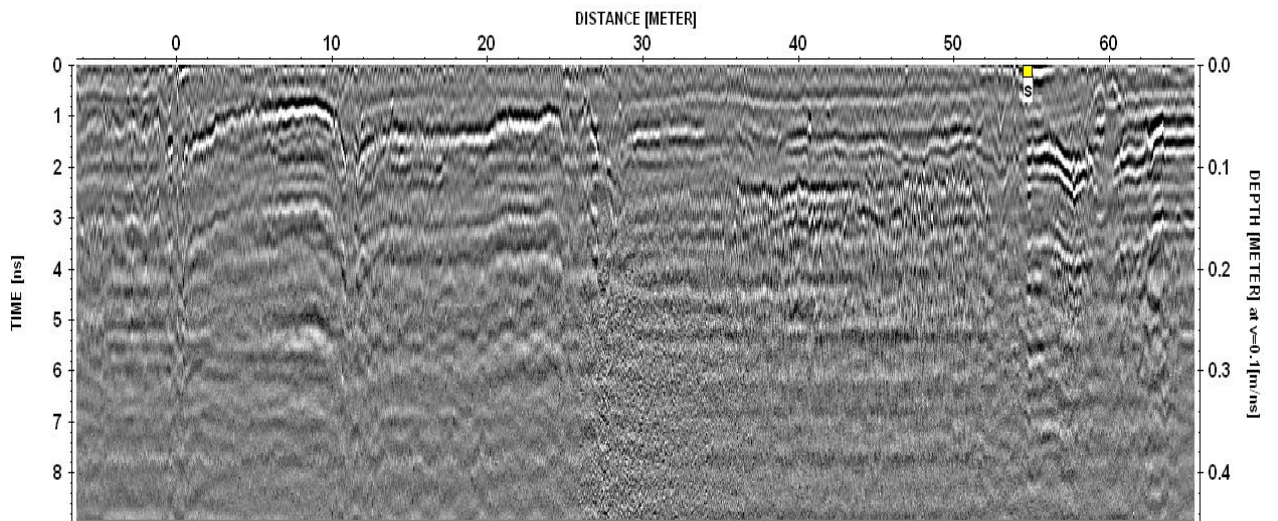


Figure B.32– 4 GHz Antenna cross section C2-D2 lane radargram

C3D3 Lane Radargrams

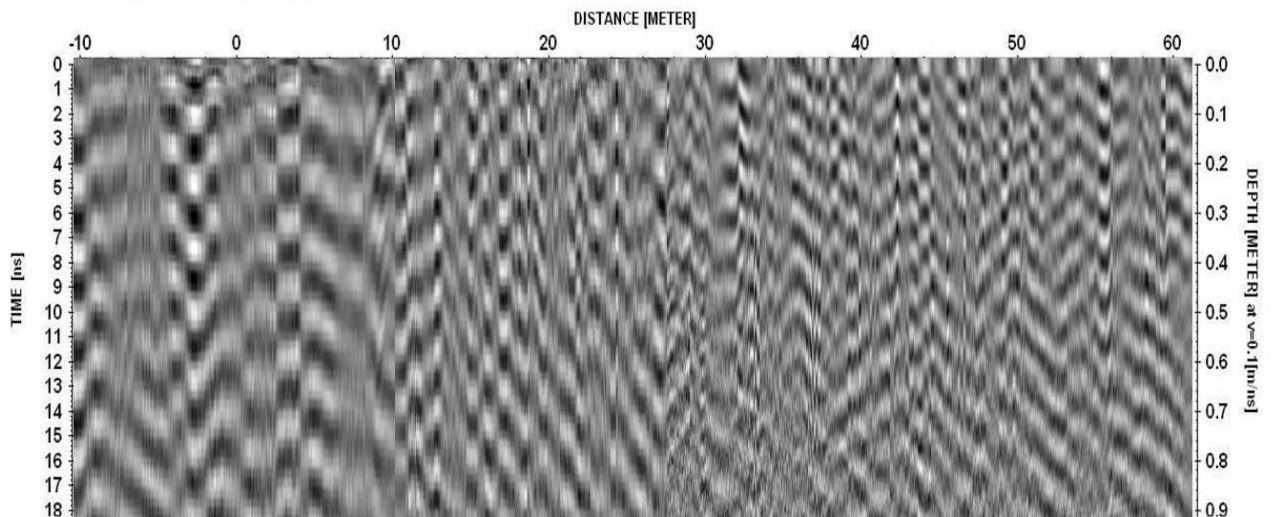


Figure B.33– 600MHz Antenna cross section C3-D3 lane radargram

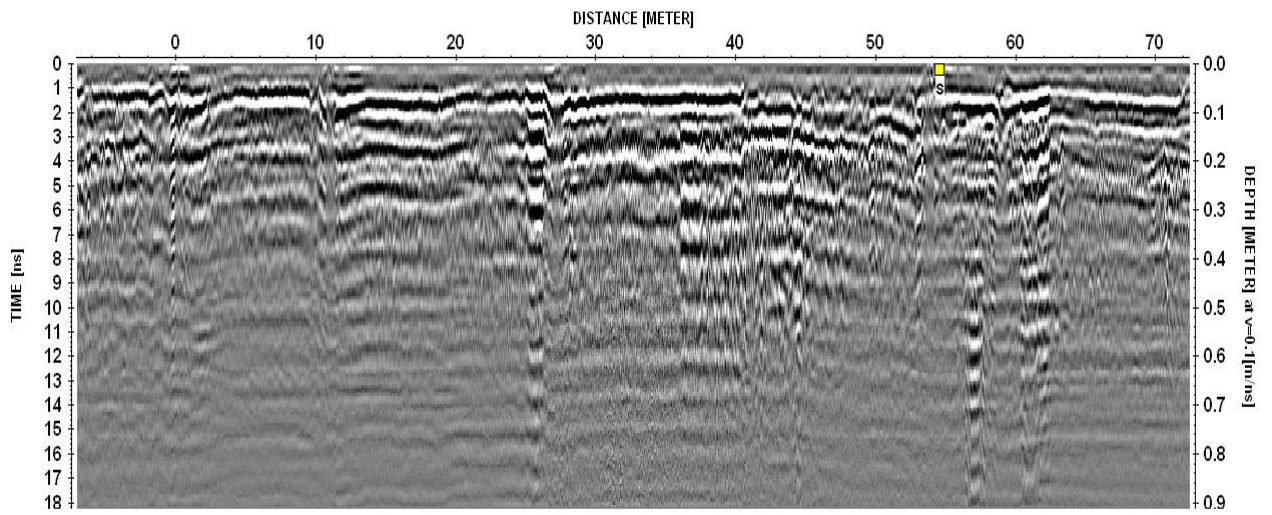


Figure B.34 – 1GHz Antenna cross section C3-D3 lane radargram

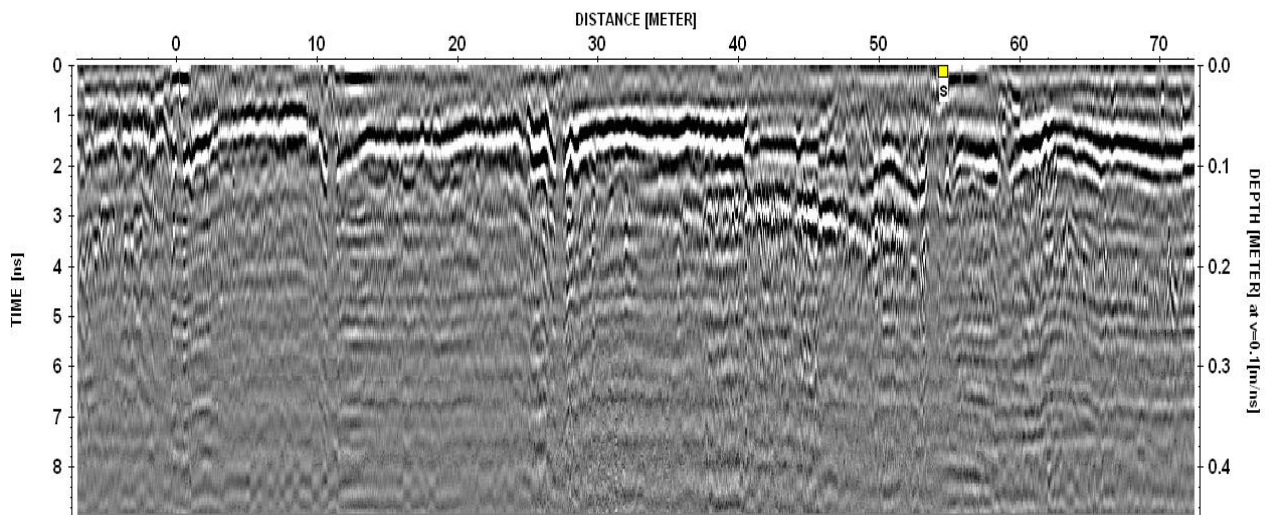


Figure B.35 – 1.5 GHz Antenna1 cross section C3-D3 lane radargram

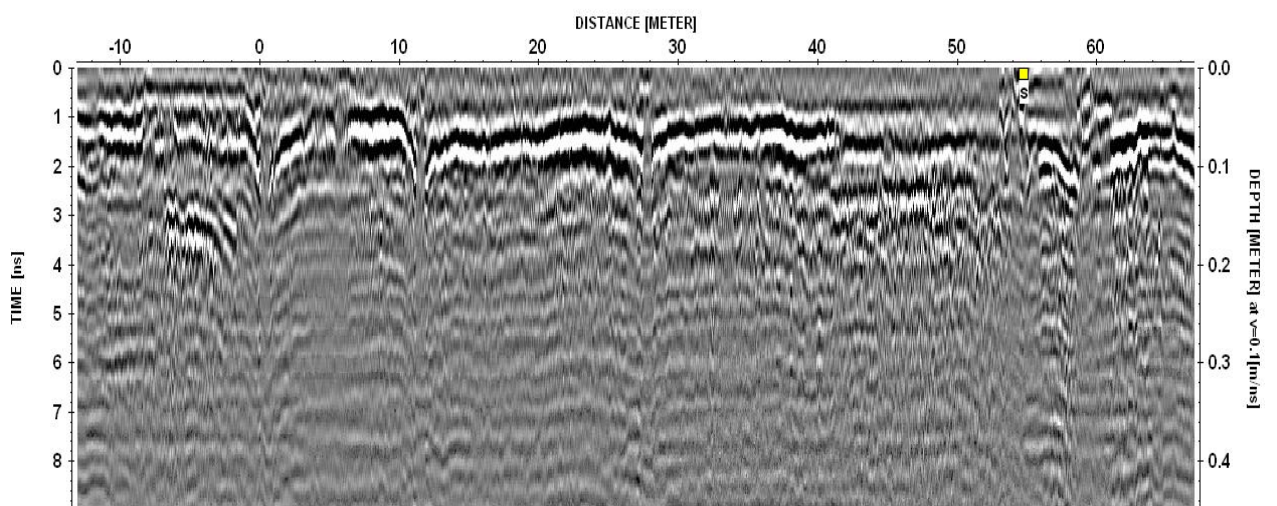


Figure B.36 – 1.5 GHz Antenna2 cross section C3-D3 lane radargram

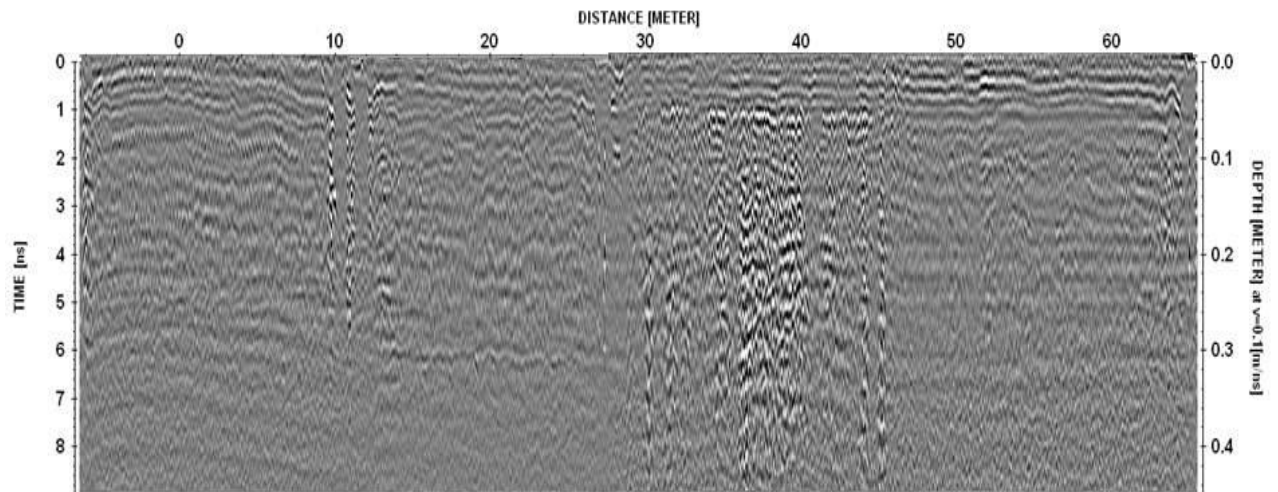


Figure B.37– 2 GHz Antenna2 cross section C3-D3 lane radargram

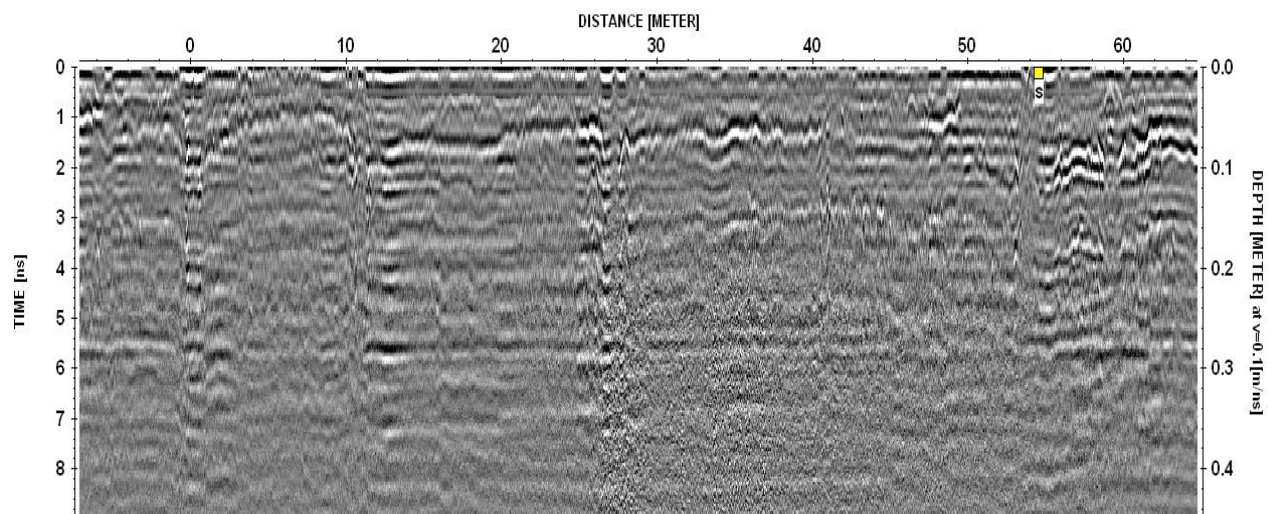


Figure B.38 – 4 GHz Antenna cross section C3-D3 lane radargram

As shown in Figure B.39, slices of the 3D volume are displayed as a 2D image allowing for identification of moisture ingress. The upper and lower rebars which were previously identified in Chapter 4 from the 3D volume and radargram are apparent in the slices. Moisture also becomes more visible at deeper penetrations and is clearly shown in each Figure B.38 to B.45 as the high intensity darker area especially at 40 and 50cm depths.

Figure B.39 depicts a set of vertical sliced data at depths 5, 15, 25, 35 and 50 cm from the surface of the deck respectively. Certain consistent features and their respective appearance have also been highlighted (red circles).

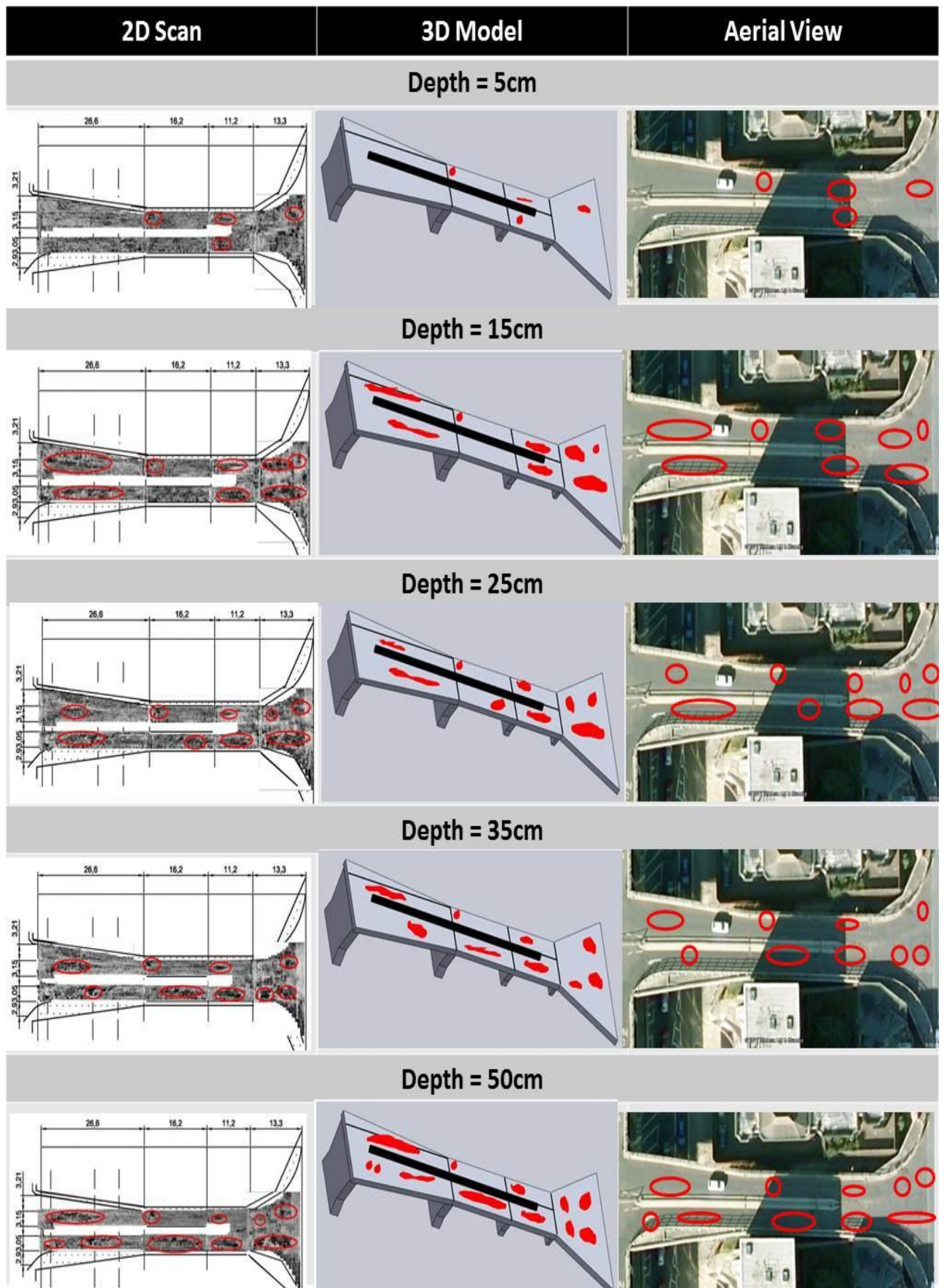


Figure B.39– Vertical sliced processed data (left), Moisture location (right) and computer modelled depiction of moisture ingress (middle)

APPENDIX C

VALIDATION RESULTS

This appendix presents the complete set of the data analyses of the Accelerometer and IBIS-S interferometric monitoring results for the main case study, Pentagon Road Bridge while under the dynamic loading of a cherry picker.

Below the Figure C.1 to C.14 show the results of the survey which was undertaken in March 2012. These figures show the maximum deflection as a function of time and give a comparison between accelerometer and IBIS-S monitoring while a cherry picker crossed it.

As can be seen from figures C.1 to C.14 the results have been normalized to negative direction only in a similar fashion to the data correction applied to the results in Appendix A.

The variation in readings between the IBIS-S and accelerometer can be attributed to a number of different factors. These factors are discussed in detail in main text and may include:

- The difference in installation horizontal position.
- The different methods of calculating displacement. IBIS-S uses interferometric radar whereas accelerometers use a vibration technique.
- Minor errors can occur while interpreting the data as mathematical equation cannot completely accurately quantify the translation of acceleration to displacement.
- IBIS-s can also be susceptible to external factors such as noise for passing vehicles which can minimally affect readings.

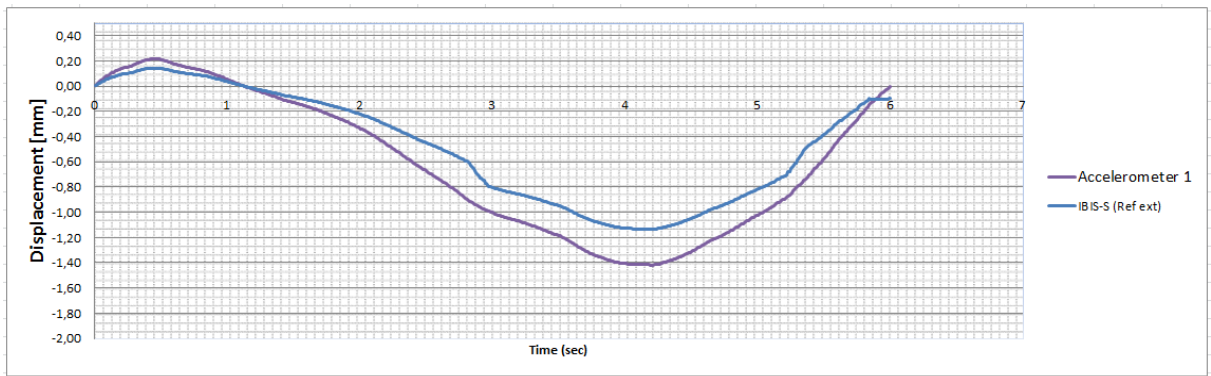


Figure C.3 – Accelerometer node 1 and IBIS-S 200 MHz Monitoring Results

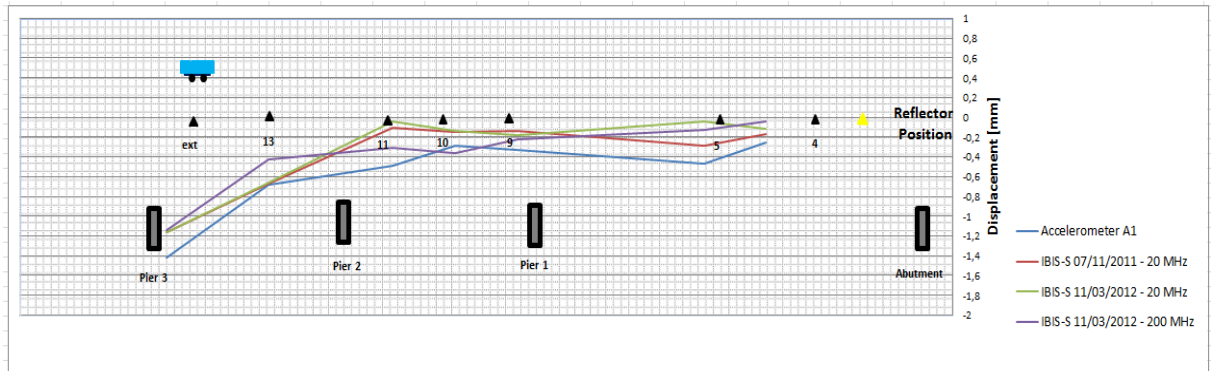


Figure C.4 – Accelerometer node 1 and IBIS-S Monitoring Results

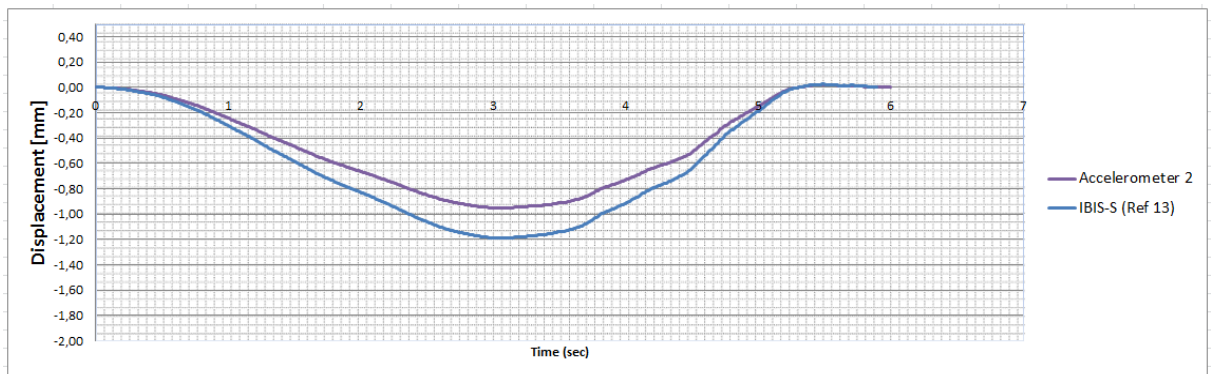


Figure C.5 – Accelerometer node 2 and IBIS-S 200 MHz Monitoring Results

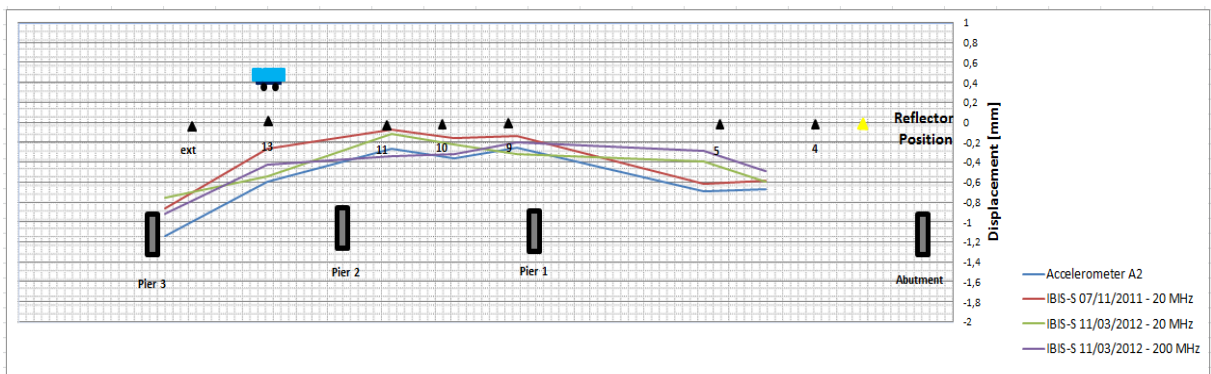


Figure C.6 – Accelerometer node 2 and IBIS-S Monitoring Results

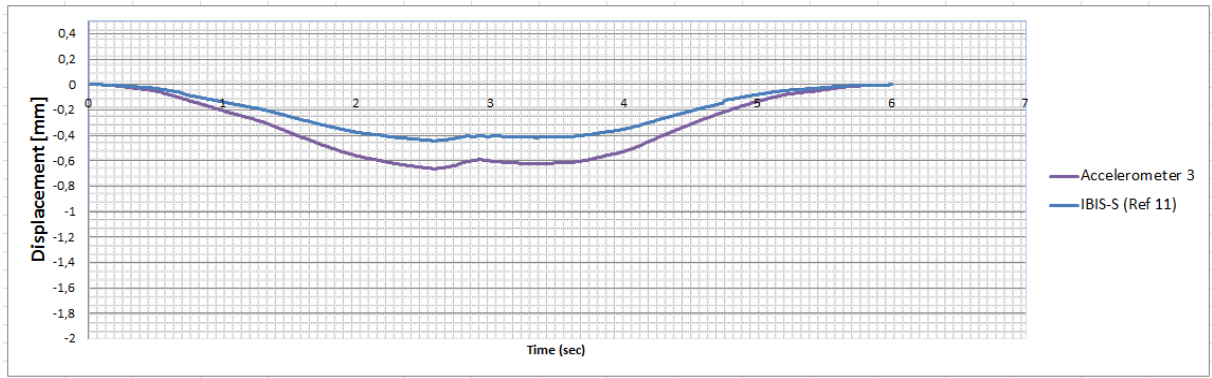


Figure C.7 – Accelerometer node 3 and IBIS-S 200 MHz Monitoring Results

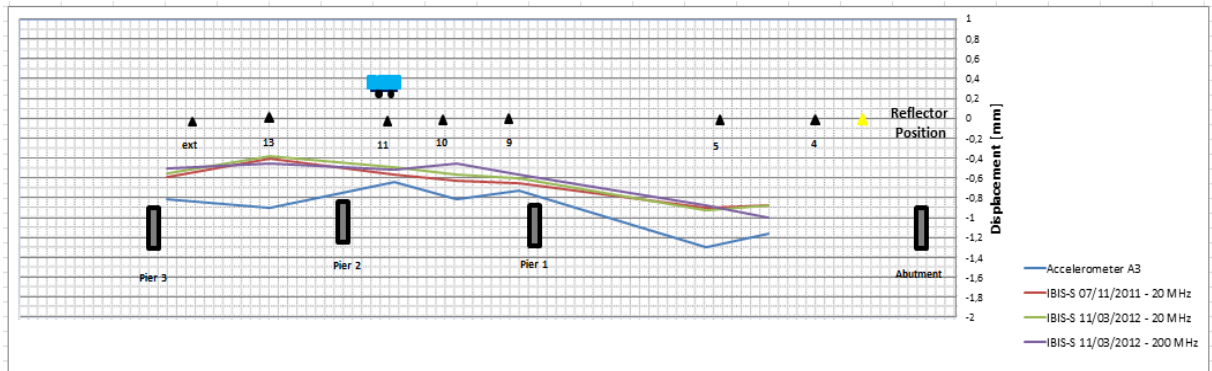


Figure C.8 – Accelerometer node 3 and IBIS-S Monitoring Results

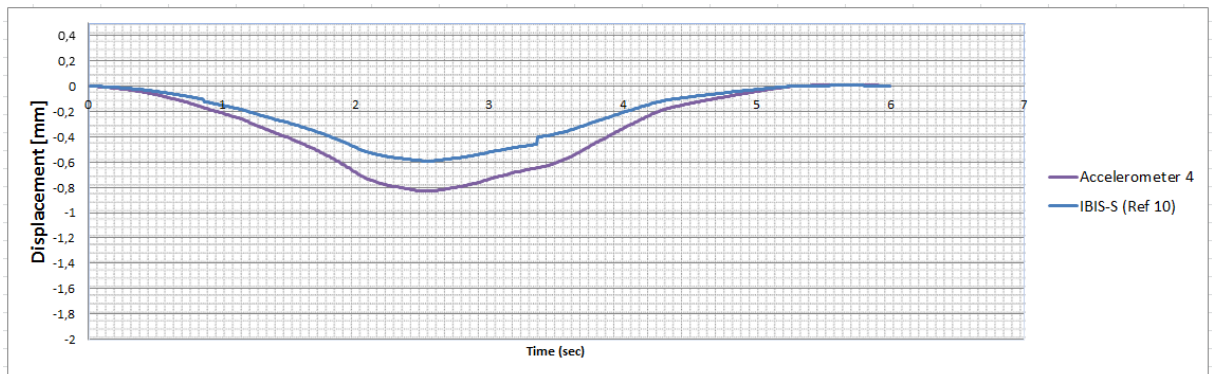


Figure C.9 – Accelerometer node 4 and IBIS-S 200 MHz Monitoring Results

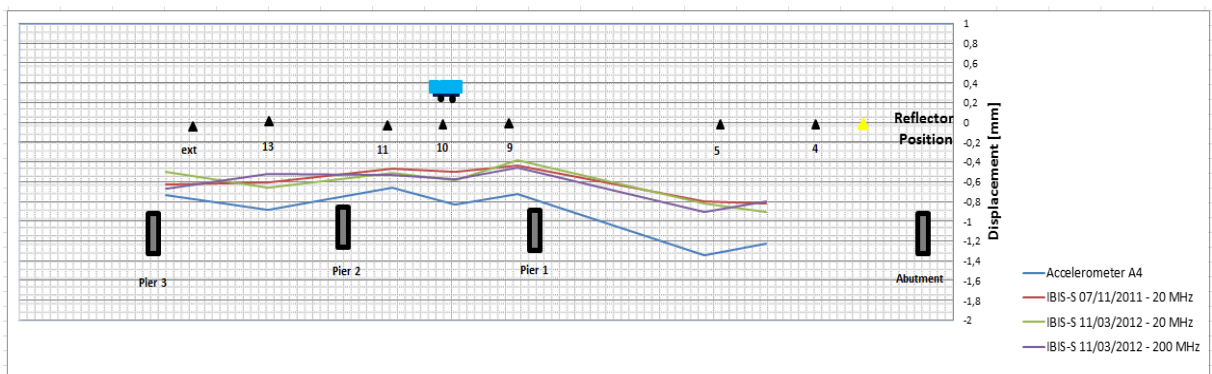


Figure C.10 – Accelerometer node 4 and IBIS-S Monitoring Results

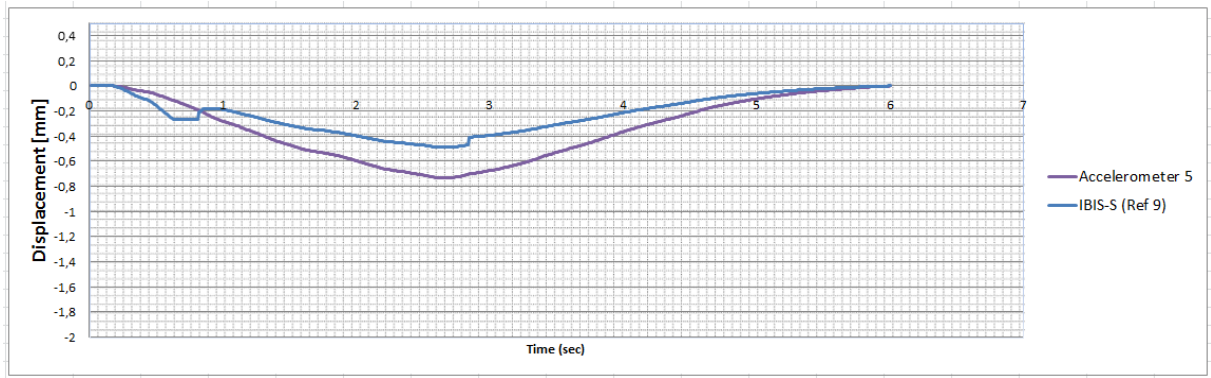


Figure C.11 – Accelerometer node 5 and IBIS-S 200 MHz Monitoring Results

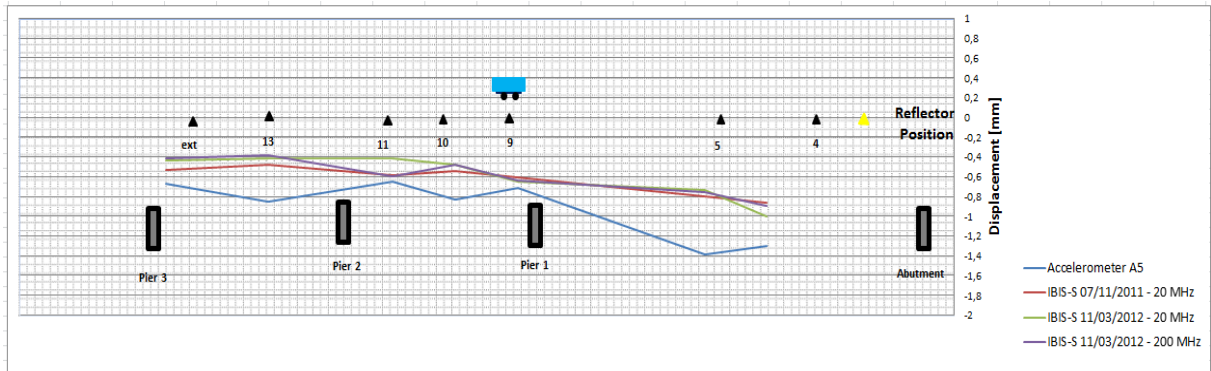


Figure C.12 – Accelerometer node 5 and IBIS-S Monitoring Results

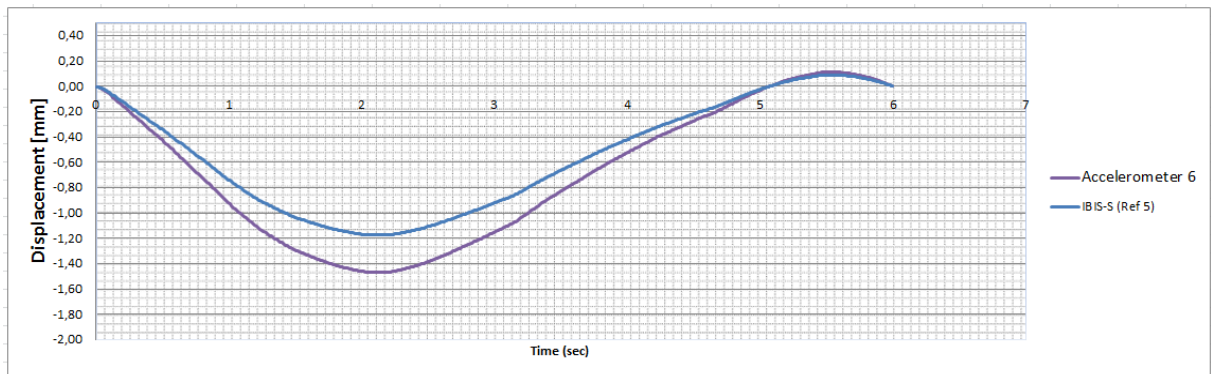


Figure C.13 – Accelerometer node 6 and IBIS-S 200 MHz Monitoring Results

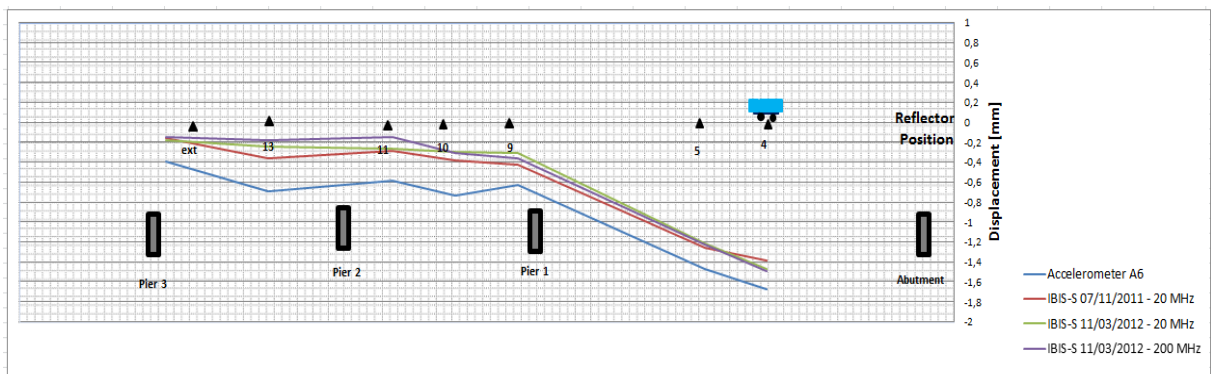


Figure C.14 – Accelerometer node 6 and IBIS-S Monitoring Results

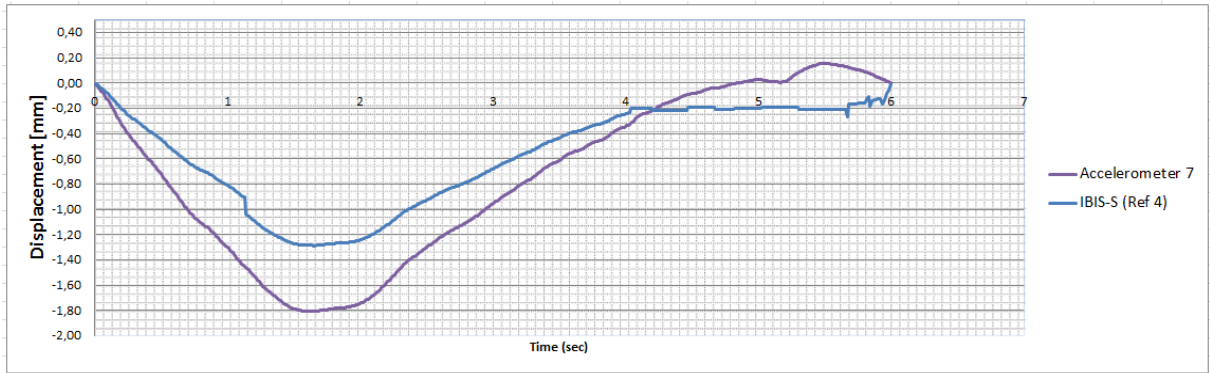


Figure C.15 – Accelerometer node 7 and IBIS-S 200 MHz Monitoring Results

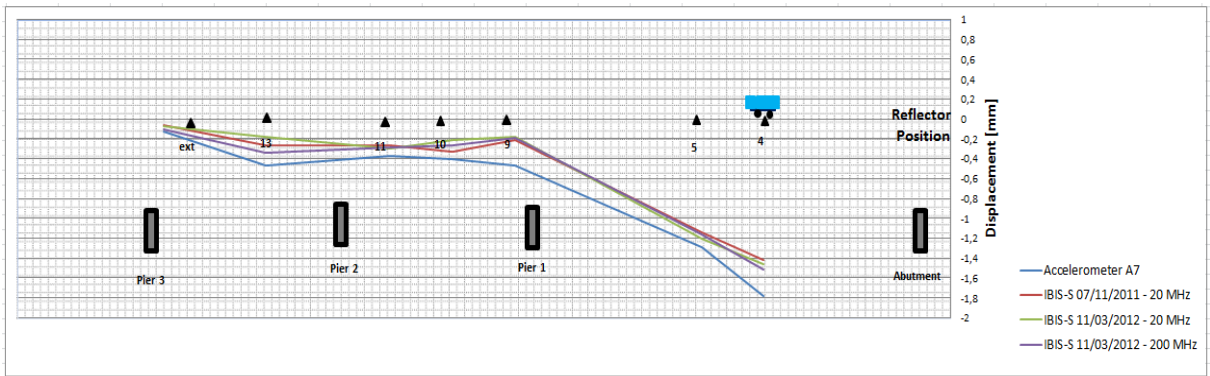


Figure C.16 – Accelerometer node 7 and IBIS-S Monitoring Results

APPENDIX D

PENTAGON ROAD BRIDGE

This appendix presents a detailed record of the inspection of all visible component parts of the Pentagon Road Bridge.

Table of Contents

1	Introduction	301
2	Structural Elements	305
2.1	Foundations	305
2.2	Bearings.....	305
2.3	Piers/ Abutments/End Supports	308
2.4	Supports beneath Span 4	310
2.5	Decks.....	313
2.6	Expansion Joints.....	314
3	Visual Inspection.....	315

1. Introduction

Pentagon Road Bridge (Figure D.1) was constructed in 1975 and carries an access road from Rope Walk to the Pentagon Shopping Centre in Chatham, Kent.



Figure D.1 - General view of the Pentagon Road Bridge (North Elevation)

The Pentagon Road Bridge consists of a four span approximately 8 % slope and simply supported concrete deck of beam and slab construction. At the west, high end, the bridge links to the access road to the rooftop car park of the shopping centre. The end-support is a leaf pier (pier 3) that is shared with the access road. There is a lower access road for buses, which is a brick faced concrete abutment at the east, low end of the bridge. At the east end there used to be a pedestrian walkway beneath the deck but it has been removed. The bridge foundations are spread footings (Jacobs Engineering UK Limited, 2009).

As illustrated in Figure D.2, the location of Pentagon Road Bridge is in Chatham Medway, south east of the UK.

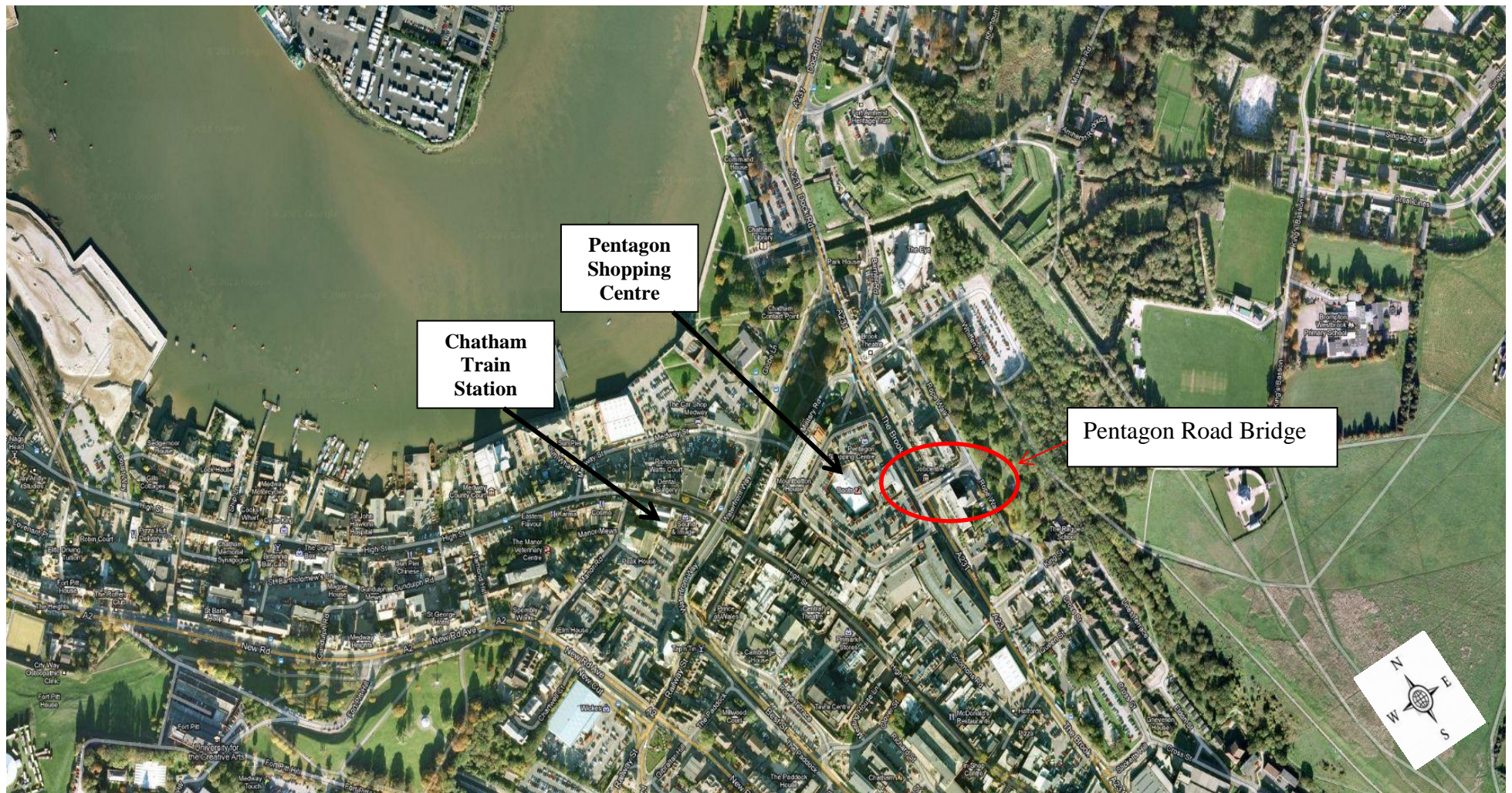


Figure D.2 - Location of the Pentagon Road Bridge (Google Maps, 2012).

There were no drawings available for the Pentagon Road Bridge. The construction details of the structure are not known. The only drawing available was a deck plan (Figure D.3 and D.4).

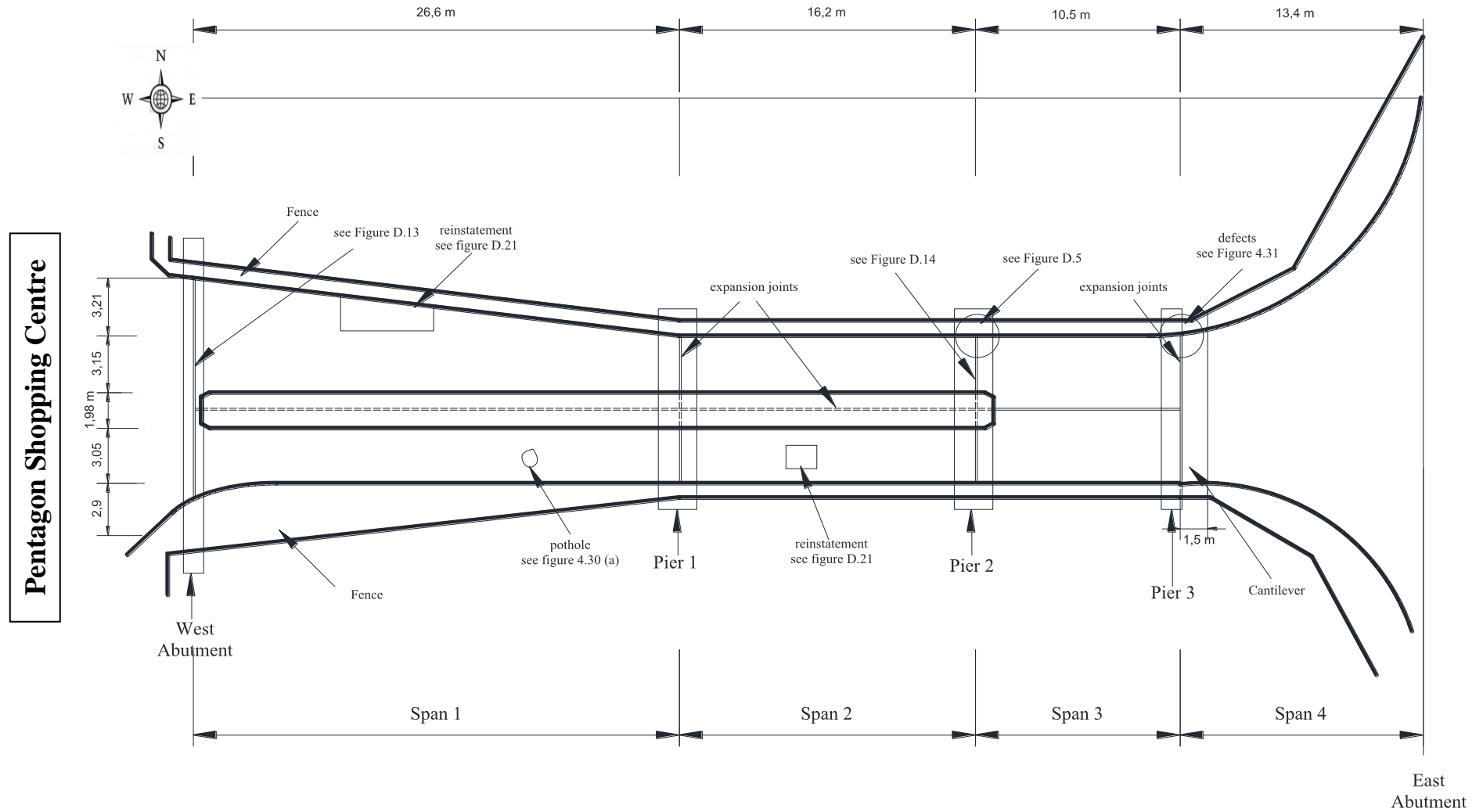


Figure D.3 – Pentagon Road Bridge plan view (see Figure D.4)

There was no other information regarding the structural composition of the bridge or construction method and the visual inspections did not yield the data required, therefore it was necessary to make assumptions regarding the input parameters needed for the parametric study (see chapter 5).

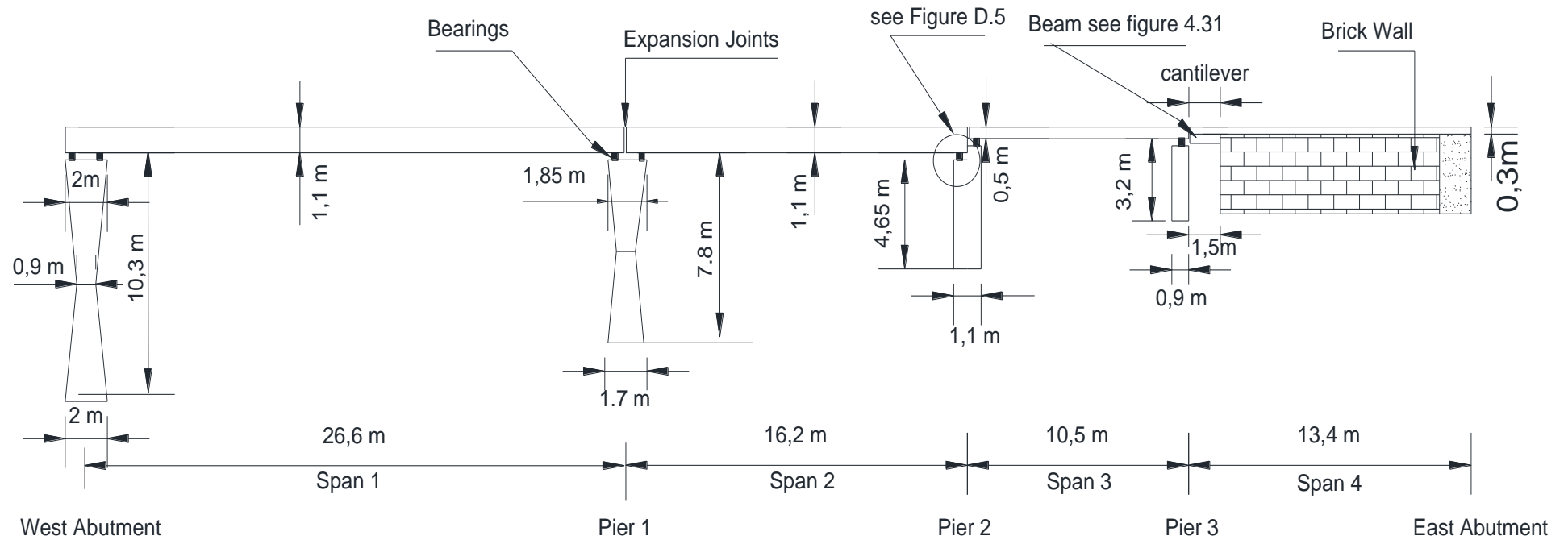


Figure D.4– South Elevation of the Pentagon Road Bridge.

2. Structural Elements

2.1 Foundation

According to Jacobs Report (2009) foundations are reinforced concrete spread footings to piers, abutments and discrete supports beneath span 4. There were no details available and the foundations were not visible for inspection. There were no indications of settlement or movement, which would indicate the foundations are inadequate.

2.2 Bearings

The nature of the bearings could not be determined. Because of the size of the bridge and the amount of the vehicular and pedestrian traffic it was not possible to carry a full detail survey. However, Pier 2 was accessible to pedestrians via an underpass and thus could be examined. It was visible inspected and it was found that the bearings were located close to the sides of the deck (Figure D.5). It was thus assumed that the bearings for all the piers and abutments were located at the same points as on Pier 3 for the purpose of FEM.



Figure D.5– Pier 2 Bearing

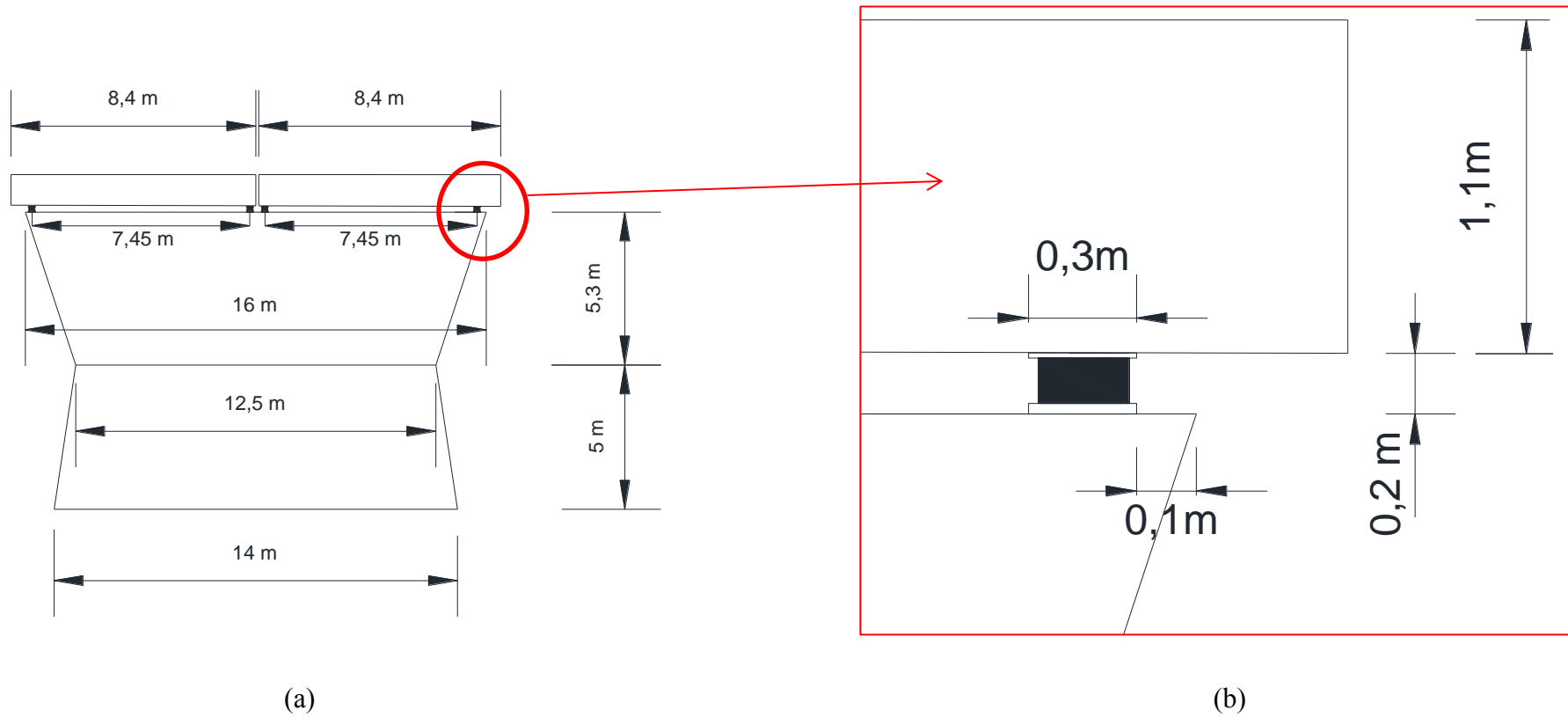


Figure D.6– (a) West Face Abutment (b) enlarged detail of bearing (not scaled)

2.3 Piers, Abutments and End Supports

The dimension of the piers, abutments and end supports cross section was shown in Figure D.7 and D.8.

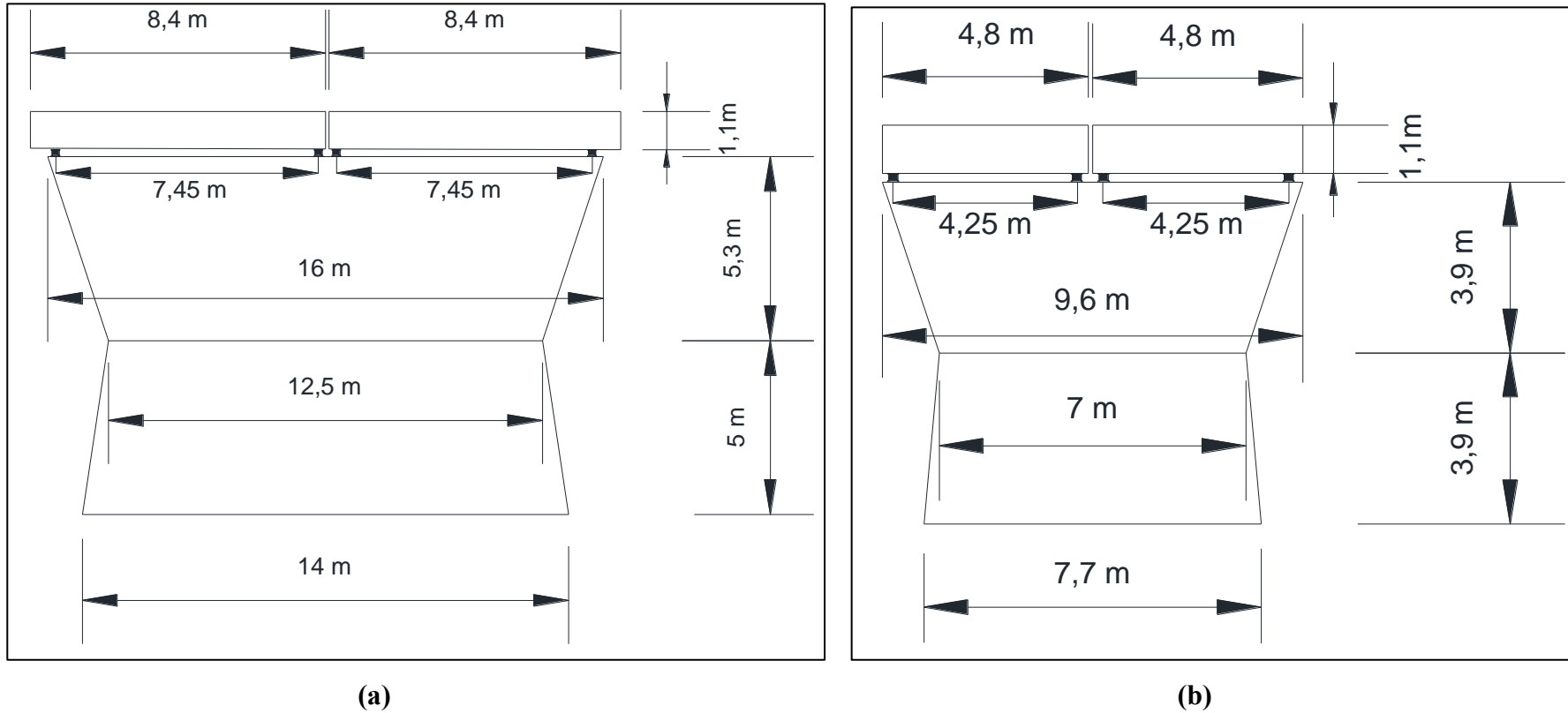
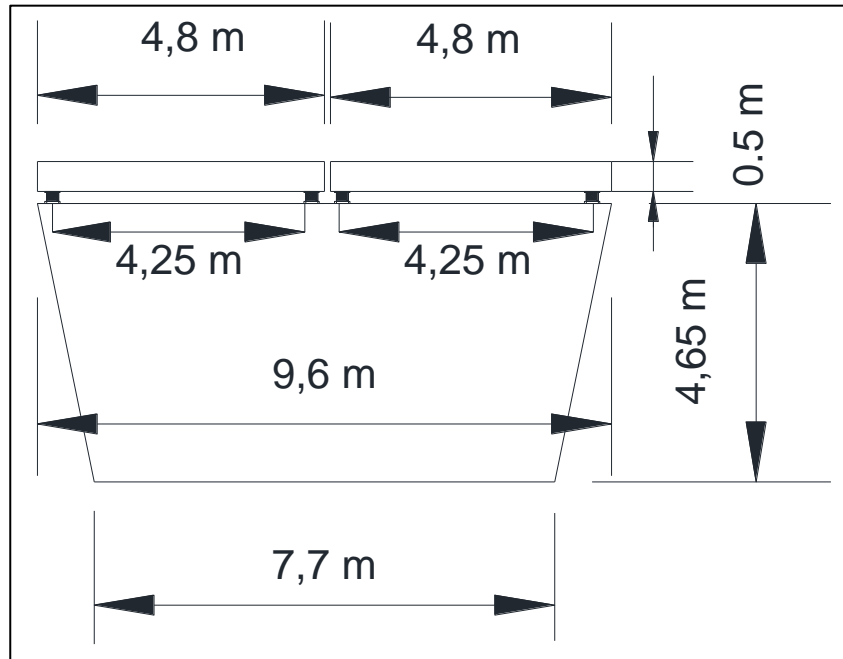
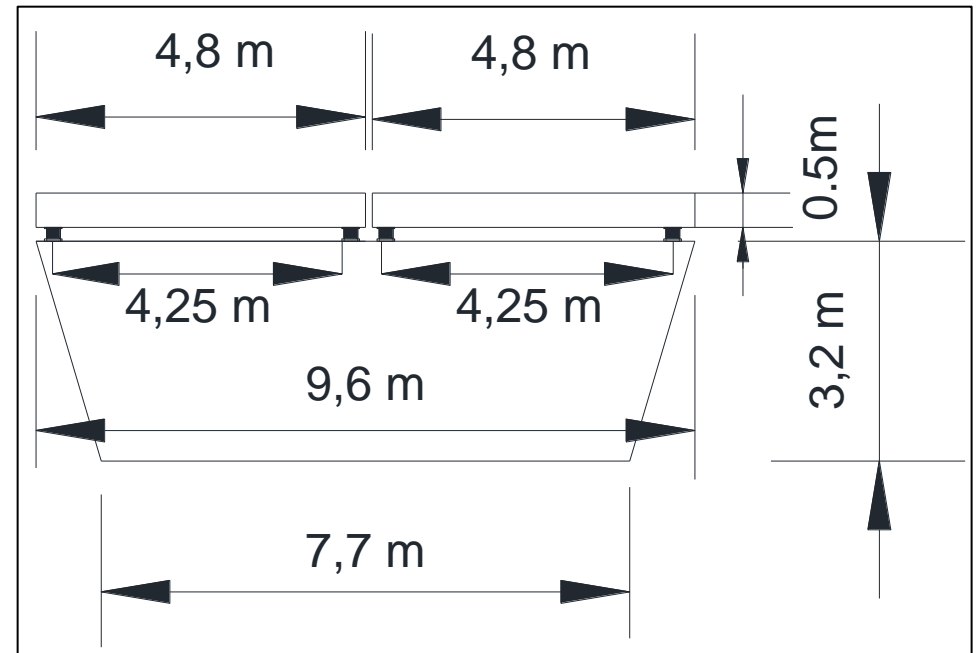


Figure D.7– (a) West Face Abutment (b) West Face Pier 1(not scaled)



(a)



(b)

Figure D.8– (a) West Face Pier 2 (b) West Face Pier 4(not scaled)

2.4 Supports beneath Span 4

The span 4 is supported by a grid of beams that support a cantilever. Under visual inspection (see section 4.2.2) it is evident that the third and fourth spans are in very poor condition, and require an assessment of their adequacy prior to any remedial works being carried out. The dimension of the supports beneath span 4 with beam plan and brick wall plan views was shown in Figure D.9, D.10 and D.11.

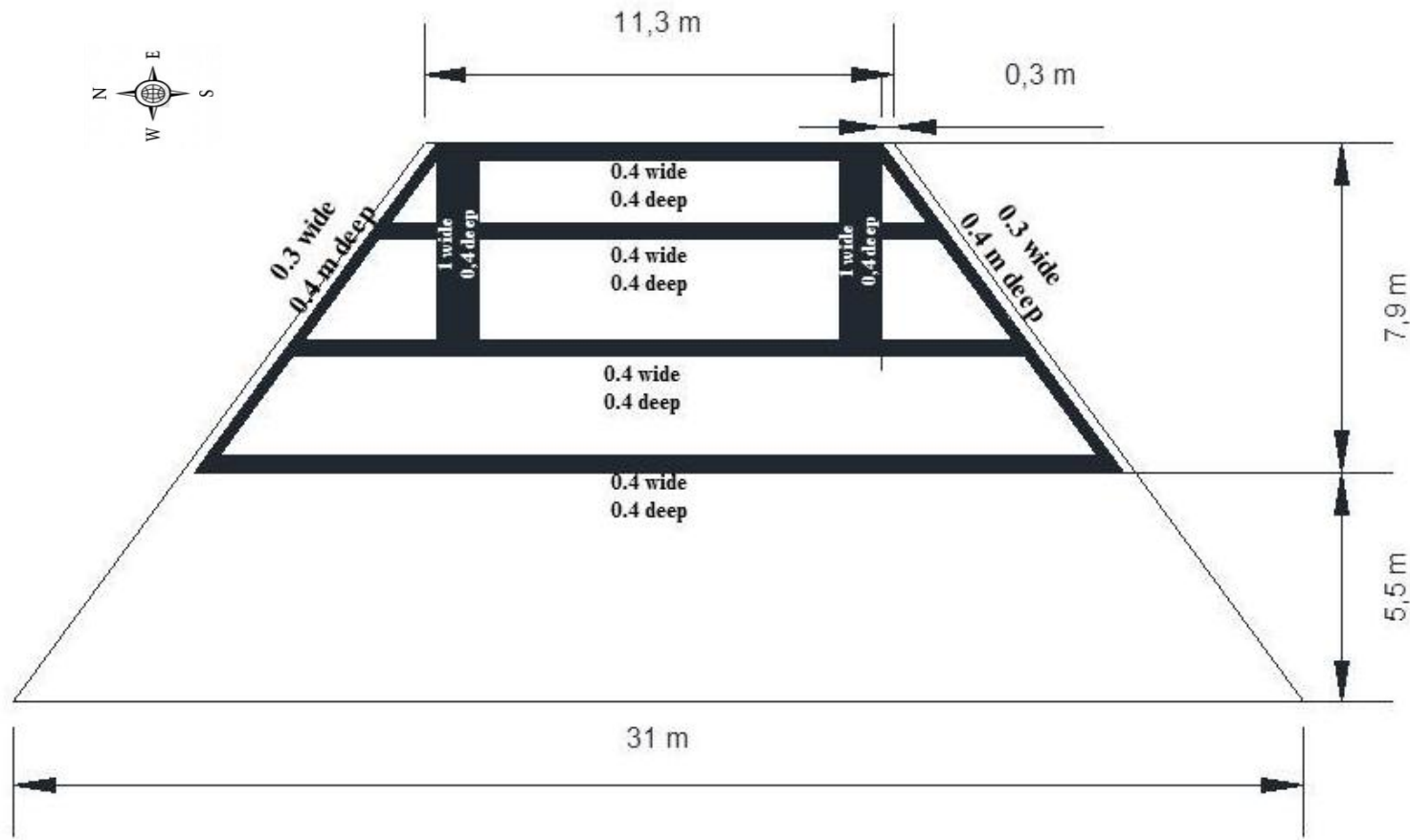


Figure D.9 – Pentagon Road Bridge Span 4 beam plan view

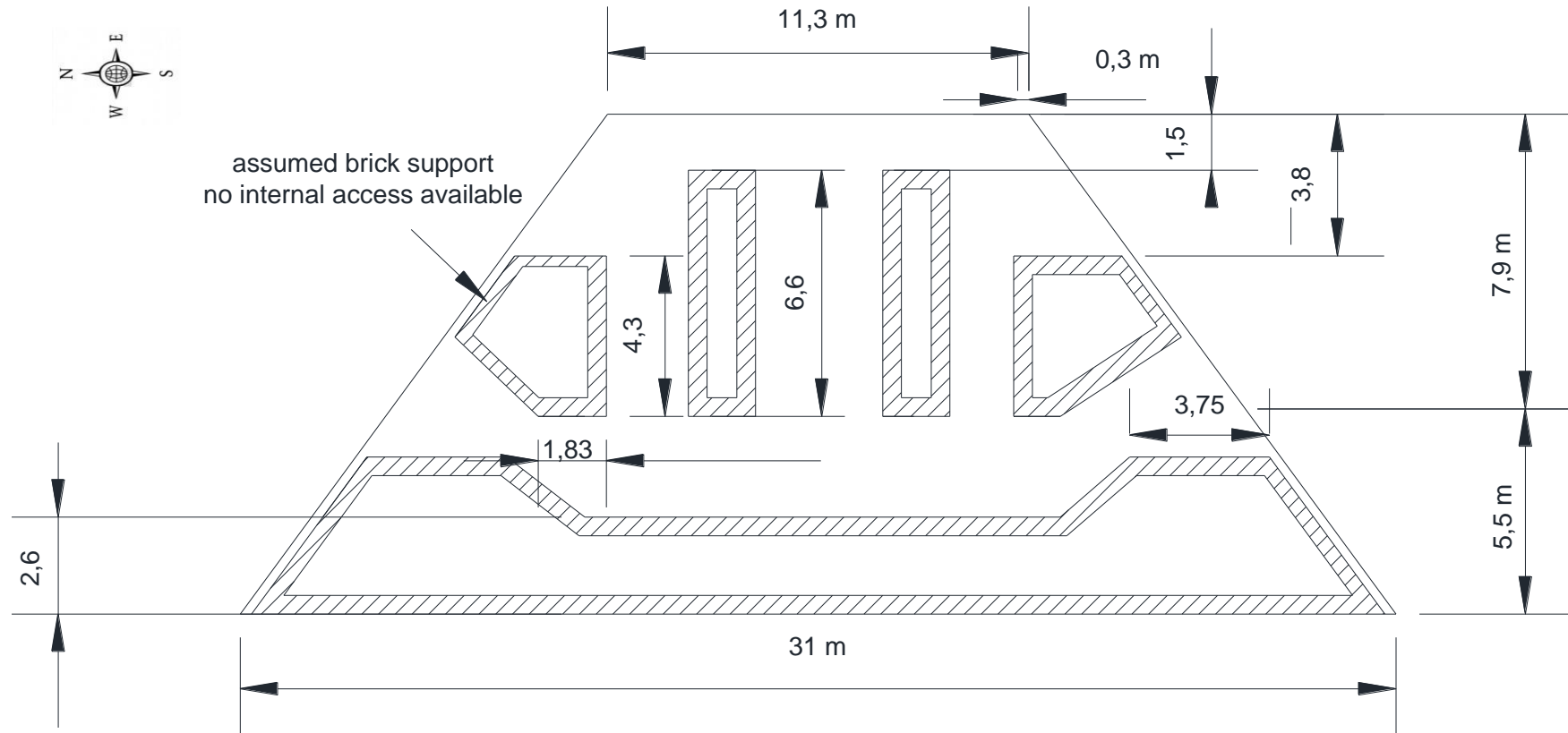


Figure D.10 – Pentagon Road Bridge Span 4 Brick wall plan view

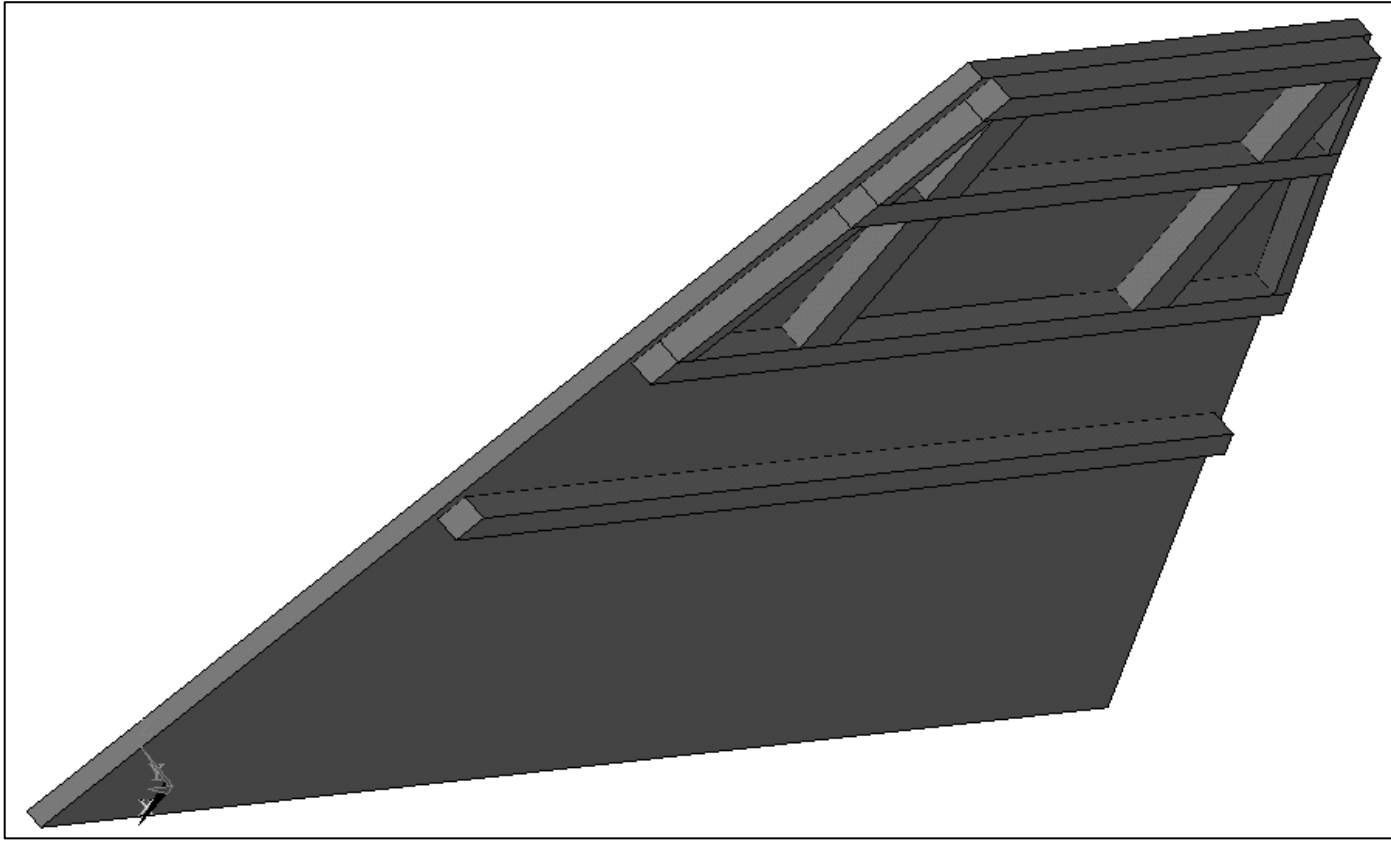


Figure D.11 – Pentagon Road Bridge Span 4 3D view

2.5 Decks

Starting from the west end of the bridge, the bridge deck in the first and second span, with a depth of 110cm does not display any structural deterioration or problems after visual inspection. The depth in the third span is decreased to 50cm while the slab depth of the fourth span is only 30cm (Figure D.12).

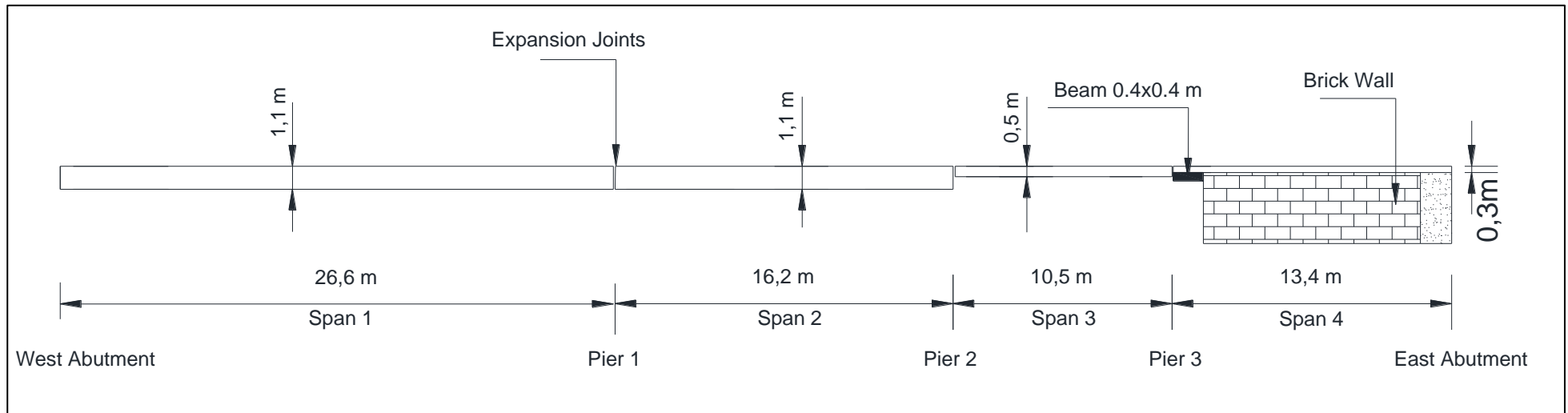


Figure D.12 – Pentagon Road Bridge Decks Cross Section View

2.6 Expansion joints

Expansion joints gaps measured on 25th June 2011 at 12:00 am at 16 °C (Table D.1). Expansion joints have got signs of cracking, debonding, leakage and loss of material from nosings. (see Figure D.13 and D.14)

Table D.1 – Expansion joints gaps

	West	East
West end – Span 1	86 mm	86 mm
Span 1 – Span 2	80 mm	81 mm
Span 2 – Span 3	86 mm	85 mm
Span 3 – Span 4	88 mm	85 mm



Figure D.13 – Expansion span 1 and 2



Figure D.14 – Expansion joints between span 3 and 4

3. Visual Inspection

Following Figures D.15-16 shows general views of the structure.



Figure D.15 – South view of Span 1



Figure D.16 – North view of Span 1

Figure D.17 and D.18 shows that the Pentagon Bridge forms the entrance to the Pentagon Shopping Centre car park.



Figure D.17 – West View of structure



Figure D.18 – East view of structure

Figure D.19 and D.20 shows south and north view of the Pentagon Road Bridge.



Figure D.19 – South Edge Beam and Parapet



Figure D.20 – North Edge Beam and Parapet

Figure D.21 and D.22 shows reinstatement view on the Pentagon Road Bridge.



Figure D.21 – Span 1 reinstatement view



Figure D.22 – Span 4 reinstatement view

APPENDIX E

LIST OF PUBLICATIONS

The following publications were accomplished during the author's PhD studies in University of Greenwich.

Journals

- Gökhan Kılıç, Amir M. Alani, Morteza Aboutalebi "Damage Detection and Health Monitoring of Pentagon Road Bridge Using IBIS-S and Finite Element Method" *Journal of Structural Concrete*, 2012, (ISSN 1464-4177) (Submitted)
- Amir M. Alani, Morteza Aboutalebi, Gökhan Kılıç "A Parametric Assessment of the Cracked Pentagon Road Bridge Using the Finite Element Method" *The Baltic Journal of Road and Bridge Engineering*, 2012, (no-no1747-1567) (Submitted).
- Morteza Aboutalebi, Amir M. Alani, Gökhan Kılıç "FE Modelling For Bridge Assessment Based On Actual and Simulated Data" *Journal of Structure and Infrastructure Engineering*, 2012, (ISSN 1744-8980) (Accepted).
- Amir M. Alani, Morteza Aboutalebi, Gökhan Kılıç "Applications of Ground Penetrating Radar (GPR) in Bridge Deck Monitoring and Assessment", *Journal of Applied Geophysics*, 2012, (ISSN 0926-9851), (Submitted).

Conferences

- Amir M. Alani, Gökhan Kılıç, Morteza Aboutalebi "Applications of Ground Penetrating Radar in Bridge Health Monitoring Using Different Frequency Antennae Systems" *EGU GA - Civil Engineering Applications of Ground Penetrating Radar*, 22-27 April 2012, Wien, Austria
- Amir M. Alani, Morteza Aboutalebi, and Gökhan Kılıç. 2012. Health Assessment of Bridge Structures Adopting Inverse Parametric Approach. *XXII International Scientific and Technical Conference STARODUBOVSKIY CHTENIYA*, 19–20 April 2012, Prydniprov's'ka State Academy, Dnipropetrovs'k, Ukraine.
- Gökhan Kılıç, Amir M. Alani, Pentagon Road Bridge Health Assessment and Analysis, University of Greenwich, School of Engineering, 10th School Research Conference (2011) (Oral / poster).
- Amir M. Alani, Gokhan Kilic, Kevin Banks, "Applications of Ground Penetrating Radar in Bridge Health Monitoring and Assessment, XXI International Scientific and Technical Conference – Starodubov's Reading, PSACEA ,Dnepropetrovsk, Ukraine 19-21 April 2011.
- Gökhan Kılıç, Amir M. Alani, Application of Advanced Non-Destructive Testing Methods on Bridge Health Assessment and Analysis, University of Greenwich, School of Engineering, 10th School Research Conference (2010) (Oral / poster).



Damage Detection and Health Monitoring of Pentagon Road Bridge Using IBIS-S and Finite Element Method

Journal:	<i>Structural Concrete</i>
Manuscript ID:	Draft
Wiley - Manuscript type:	Technical Paper
Date Submitted by the Author:	n/a
Complete List of Authors:	KILIÇ, Gökhan; University of Greenwich, Civil Engineering Alani, Amir; University of Greenwich, Civil Engineering Aboutalebi, Morteza; University of Greenwich, Civil Engineering
Subject codes:	building maintenance/refurbishment, analysis and design methods, testing experiments
Keywords:	Finite Element Modelling, Bridge Health Monitoring, IBIS-S Sensor, ANSYS
Abstract:	<p>The main objective of this investigation is to provide an alternative method for damage detection and assessment of bridge structures based on comparisons between Finite Element (FE) modelling/analysis and field data. The field data reported in this paper refers to the application of a non-destructive structural testing method (IBIS S sensor system– displacement/movement detecting sensors with interferometric capabilities) and inspections by visualisation. The developed FE models presented in this study demonstrate certain degrees of reliability in terms of predicting mechanical behaviour of the bridge structure under investigation. The FE models were developed using the ANSYS software package. This investigation also provides a detailed report on application of the field survey that was carried out on a rather heavily used bridge located in Chatham, Kent, UK. The reported field data concerning the IBIS-S sensors correspond to subjecting the bridge to different static and dynamic loading conditions. The static and dynamic structural responses of the bridge were created by driving a lorry up and down the bridge. Then the same loading conditions were simulated using the developed FE model verifying the sensitivity of the model. This FE model was then used to study the response of the bridge to other loading conditions. It is believed that the proposed method could potentially be utilised in assessing bridge structures within the context of the health monitoring of structures.</p>

ASSESSMENT OF BRIDGE STRUCTURES – FINITE ELEMENT APPLICATION

Amir M Alani¹, Morteza Aboutalebi², Gokhan Kilic³

¹Head of Department of Civil Engineering and the Bridge Wardens' Chair in Bridge and Tunnel Engineering, University of Greenwich, Chatham, ME4 4TB, UK, m.alani@gre.ac.uk

²Senior Researcher, Department of Civil Engineering, University of Greenwich, aboutalebi@greenwich.ac.uk

³Ph.D. Candidate, Department of Civil Engineering, University of Greenwich, G.Kilic@greenwich.ac.uk

Abstract

The main focus of this study is on providing a new approach for damage detection and health assessment of bridge structures. In this alternative method the identified defects of the bridge are introduced into the developed Finite Element (FE) models and the results are compared with field data. The field data containing the dynamic response of the bridge is obtained using radar based non-destructive tests (NDT). These models can accurately predict the structural behaviour under any loading and structural conditions. The critical condition of the Pentagon Road Bridge (in Chatham, Kent, England) is assessed by this approach, both to give a better understanding of the present damage level and to provide a suitable basis for future rehabilitation studies. The models prove that the bridge is able to perform safely under current circumstances, but if the deterioration continues at the present rate, the possibility of failure will increase significantly.

Keywords: Bridge; Deterioration; Non-destructive testing; Structural Health Monitoring; Structural Modelling.

Nomenclature:

B : frequency bandwidth

c : light speed in free space

R_{max} : maximum distance to be observed

T_{pulse} : duration of each single pulse

τ : pulse duration

Δf : frequency step

Δr : range resolution

Proposed Finite Element Model for Bridge Structures with Applications of Non-destructive Testing Method (IBIS-S Sensor System)

Morteza Aboutalebi, Post-doctoral Fellow, Department of Civil Engineering, University of Greenwich, Chatham Maritime, ME4 4TB, UK, aboutalebi@greenwich.ac.uk

Amir Morteza Alani, Head of Department of Civil Engineering and the Bridge Wardens' Chair in Bridge and Tunnel Engineering, University of Greenwich, Chatham Maritime, ME4 4TB, UK, m.alani@gre.ac.uk

Gokhan Kilic, Ph.D. Candidate, Department of Civil Engineering, University of Greenwich, Chatham Maritime, ME4 4TB, UK, G.Kilic@greenwich.ac.uk

Abstract

A “new” approach to assessing the structural response of bridges without access to substantial information relating to structural properties is the main focus of this study. The complex structure of the Pentagon Road Bridge in Chatham, Kent in the UK in parallel with the lack of access to structural details of the bridge have led the health monitoring of the bridge into a sophisticated problem. The dynamic structural response of the bridge in this study was instigated by a moving lorry with enforced full traffic control. The magnitude of deflection due to vibration was measured by a non-destructive monitoring system (IBIS-S system with interferometric capabilities) and compared with deflections obtained numerically. The modified numerical model was then enhanced by introducing structural cracks simulating the actual condition of the bridge. This development hence proposes a reliable method of assessment of bridge structures with limited availability of structural details.

Keywords: *Assessment, Bridges, Concrete Structures, Non-destructive Tests, Structural Health Monitoring, Structural Modelling.*

Applications of Ground Penetrating Radar (GPR) in Bridge Deck Monitoring and Assessment

Professor Amir M Alani, Head of Department of Civil Engineering and Professor of Bridge and Tunnel Engineering, University of Greenwich, Chatham, UK, m.alani@gre.ac.uk

Dr Morteza Aboutalebi, Research Fellow, Department of Civil Engineering, University of Greenwich, UK

Gokhan Kilic, PhD Research Assistant, Department of Civil Engineering, University of Greenwich, UK

Abstract

This paper presents the essence of two case studies by the authors on two major bridges in the UK. The first case study reports on the applications of GPR and associated work carried out on the Forth Road Bridge near Edinburgh, Scotland, with the main objective of identifying possible structural defects including damaged rebar and moisture ingress at specific locations of the bridge deck. The second case study focuses on a full assessment of the Pentagon Road Bridge, in Chatham, Kent, England with particular emphasis on the identification of possible defects including structural cracks within the deck structure and establishing the layout of the upper and lower rebar positions throughout the bridge. These studies present interesting results in terms of locations of rebar and an accurate estimate of cover materials as well as reporting on a remarkable similarity in the processed data concerning areas affected by ingress of moisture within the deck structures of the two bridges under investigation. It is believed that this paper will be of particular interest to bridge engineers and structural engineering practitioners with enthusiasm for adopting non-destructive testing methods such as GPR in the health monitoring and assessment of bridge structures. The observed similarities in the processed data between the two reported case studies present an interesting concept within the general context of the interpretation of GPR data, with the potential for use in many other forthcoming cases. The paper also reports on the adopted method for the GPR survey with emphasis on difficulties and challenges encountered during the actual survey. The presented results benefit from advanced processing and presentation techniques.

Key Words: Bridge Structures, Health Monitoring and Assessment, GPR and Data Processing



Applications of Ground Penetrating Radar in Bridge Health Monitoring Using Different Frequency Antennae Systems

A. Alani, G. Kilic, and M. Aboutaleb

Department of Civil Engineering, University of Greenwich, Chatham Maritime, Kent, UK (M.Alani@greenwich.ac.uk)

Inspection and assessment of bridge structures within the context of health monitoring of structures as well as the life cycle of structures is of paramount importance for structural engineers and bridge owners. No doubt the early detection of structural defects in particular internal structural elements such as bridge deck delamination, formation of cracks and corrosion of rebar will enable engineers to remedy the imperfection and prolong the serviceability of the structure. Applications of Ground Penetrating Radar (GPR) have proved to be effective in detecting such imperfections if utilised correctly.

This paper presents and discusses the applications of GPR in assessing the structural integrity of a heavily used bridge in a town centre position (Pentagon Road Bridge, Chatham, Kent, UK) using different antennae in terms of frequency and method of application (2 GHz and 200-600 MHz GPR antennae). The paper focuses on the effectiveness of using the 'correct' tool and data processing in terms of better understanding possible structural defects. Processing, interpretation and analysis of collected data were supported by GRED software, with three-dimensional scanning capabilities. Reported results illustrate the effectiveness of GPR mapping providing valuable information regarding the positions of rebar (upper and lower reinforcement), unknown structural features as well as possible moisture ingress within the structure.

The results also demonstrate a possible phenomenon in identifying the presence of moisture within the bridge deck confirming a similar finding in an earlier case (Forth Road Bridge in Scotland).

Keywords: Bridge; Structure; Health Monitoring; Moisture Ingress.

Applications of Ground Penetrating Radar in Bridge Health Monitoring and Assessment

Amir M Alani, Head of Department of Civil Engineering and Professor of Bridge and Tunnel Engineering, University of Greenwich, Chatham, UK, m.alani@gre.ac.uk

Gokhan Kilic, Research assistant, Department of Civil Engineering, University of Greenwich, Chatham, UK, g.kilic@gre.ac.uk

Kevin Banks, Radar Application Engineer, IDS-UK is the trading name of IDS Ingegneria Dei Sistemi (UK) Limited, Fareham, UK, kevinbanks@idsuk-ltd.co.uk

Abstract

The development of bridge systems is an area of significant engineering investment and has been a feature of human progress. This is primarily because any failure in bridge and highway maintenance is likely to lead to increased deterioration with known consequences such as accidents and closures with a significant economical impact. Bridges are constantly subject to different loading conditions (dynamic and static loading) as well as being susceptible to receive the full impact of natural and environmental events such as flooding and earthquakes. They are also subject to a natural process of deterioration of construction materials as well as. In one short sentence bridges are an important part of the infrastructure asset and the heritage of any society. They require care and should be the subject of any planned maintenance mechanism adopted by the owners. Employment of new technology in bridge health monitoring and assessment has taken momentum in recent years. Applications of Ground Penetrating Radar systems have proved to be effective in detecting certain aspects of a bridge's structural components. This paper presents and discusses the adopted methodology and the results and of a case that GPR was used in monitoring and assessing a bridge in Chatham, Kent. It focuses on the effectiveness of using the "correct" tool and data processing in understanding of possible defects on a very busy bridge.

Keywords: GPR; IBIS-S; Bridge; Monitoring; Non-destructive

Introduction

Bridges are assets and vital to the human life in terms of economy, mobility, environment and development of communities. No doubt assets should be harnessed and looked after, but not in a dispersive and disorganised manner. It should be part of a robust planned monitoring and maintenance mechanism within the context of life cycle of structures. In this day and age, it is imperative that any assessment and monitoring method adopted should be "cost effective", efficient and fit for purpose.

Depending on types and needs of bridge, different approaches should be adopted in order to generate relevant and useful information (data) accordingly. Most bridge health assessment theories emphasise that it is important to know how each technique and method works and is applied. What exactly is anticipated to achieve and how it is achieved.

Different types of NDT (non-destructive testing) techniques are commercially available within the context of bridge health monitoring and assessment. Naming a few, accelerometers, smart total station, vibration measurement sensors, wireless network systems, and GPR have proved to be of great service to the industry if and when they have been adopted appropriately. It is known